Stem Cells International

Mesenchymal Stem Cells as Promoters, Enhancers, and Playmakers of the Translational Regenerative Medicine

Lead Guest Editor: Andrea Ballini
Guest Editors: Salvatore Scacco, Dario Coletti, Stefano Pluchino, and Marco Tatullo

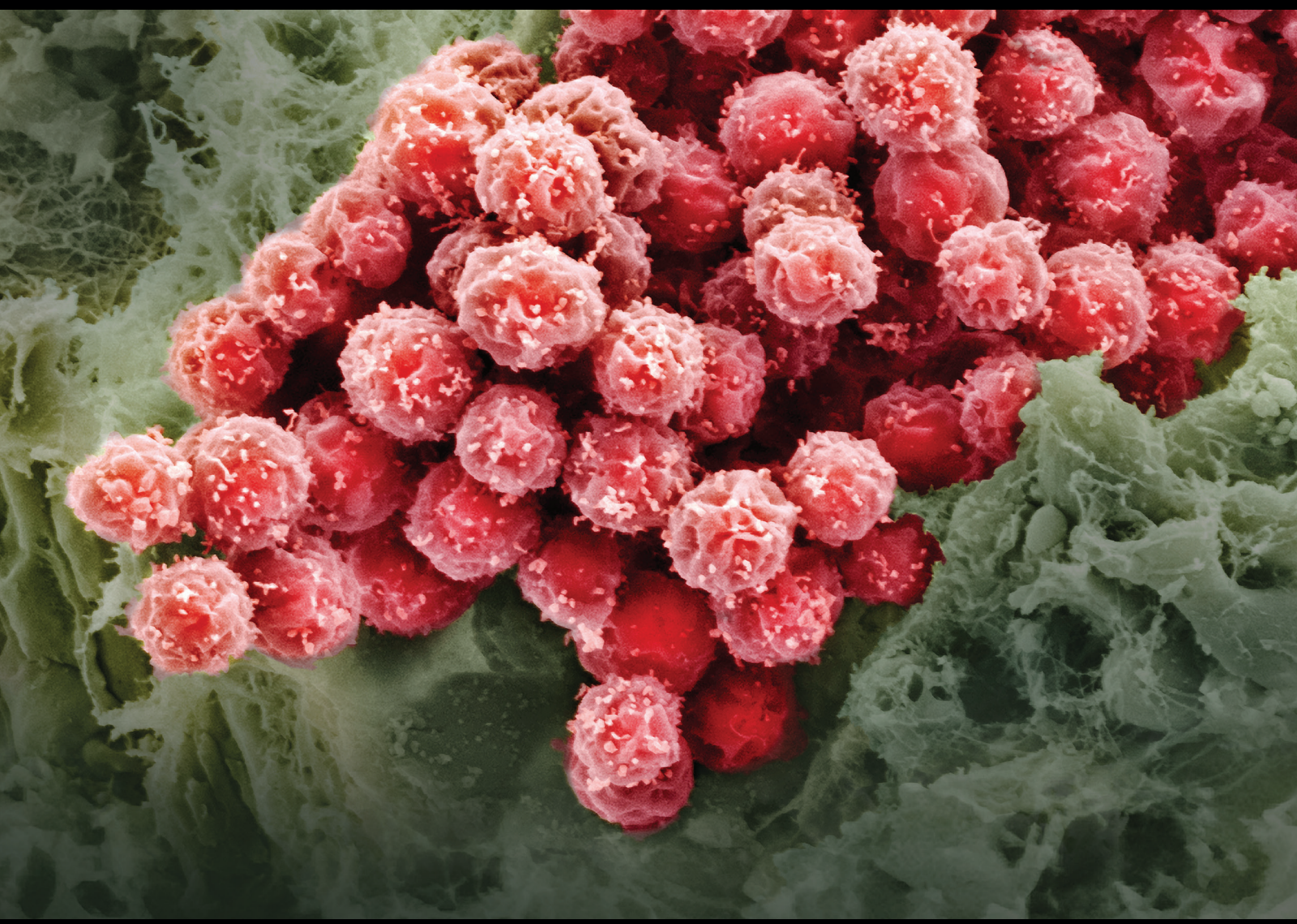

Mesenchymal Stem Cells as Promoters, Enhancers, and Playmakers of the Translational Regenerative Medicine

Stem Cells International

Mesenchymal Stem Cells as Promoters, Enhancers, and Playmakers of the Translational Regenerative Medicine

Lead Guest Editor: Andrea Ballini
Guest Editors: Salvatore Scacco, Dario Coletti, Stefano Pluchino, and Marco Tatullo

Editorial Board

Contents

Contents

Hindawi
Stem Cells International
Volume 2017, Article ID 3292810, 2 pages
https://doi.org/10.1155/2017/3292810

Editorial

Mesenchymal Stem Cells as Promoters, Enhancers, and Playmakers of the Translational Regenerative Medicine

Andrea Ballini,[1] Salvatore Scacco,[1] Dario Coletti,[2] Stefano Pluchino,[3] and Marco Tatullo[4]

[1]*Department of Basic Medical Sciences, Neurosciences and Sense Organs, University of Bari "Aldo Moro", Bari, Italy*
[2]*Institut de Biologie-Biology of Adaptation and Aging (B2A), Université Pierre et Marie Curie Paris 6, Paris, France*
[3]*Department of Clinical Neurosciences-Division of Stem Cell Neurobiology, Wellcome Trust-Medical Research Council Stem Cell Institute and NIHR Biomedical Research Centre, University of Cambridge, Cambridge, UK*
[4]*Biomedical Section, Tecnologica Research Institute, Crotone, Italy*

Correspondence should be addressed to Andrea Ballini; andrea.ballini@uniba.it

Received 4 April 2017; Accepted 6 April 2017; Published 22 June 2017

Since their first isolation and characterization by Friedenstein et al. in 1974 [1], mesenchymal stem cells (MSCs) were proven essential for tissue regeneration and homeostasis.

Over the years, thanks to a better understanding of the molecular mechanisms underlying the therapeutic effects of MSCs, several approaches with MSC-based therapies have been proposed, in order to treat different human diseases [2].

In this light, MSCs are currently being tested in preclinical in vivo settings as well as in early-stage clinical trials for their ability to modulate immune responses, fostering wound healing and tissue regeneration of various tissue types and organs, including the skin, bone, cartilage, brain, muscle, and tendons [3].

As defined by the International Society for Cellular Therapy (ISCT) in 2006, culture-expanded MSCs [4], harvested from bone marrow, adipose tissue, umbilical cord, dental tissues, and other sources, are being studied in clinical trials across evidence-based practice and numerous regulatory jurisdictions worldwide [5–9].

Recent reports have demonstrated therapeutic effects by MSCs on animal models, explained by the ability of MSCs to be activated by signals from injured tissues: in these damaged areas, MSCs showed regenerative behaviour, with the promotion of the tissue healing, and paracrine activities, with the secretion of anti-inflammatory factors [10].

Experimental in vivo models showed that the direct administration of the same factors secreted by MSCs replicated the local anti-inflammatory effects, highlighting the double role of MSCs as players of tissue regeneration and as regulators of the local environment in many pathological conditions [10–12].

Actually, several clinical trials focused on the role of MSCs in the treatment of the autoimmunity are currently in progress, with the aim to verify new therapeutic approaches for the most common and severe diseases, such as Crohn's disease, type 1 diabetes, and systemic lupus erythematosus (see www.clinicaltrials.gov) [10, 11].

Despite the numerous barriers to their clinical use, MSCs have shown sufficient promise to garner a primary place in the field of regenerative medicine. MSC-based cell therapies have significant implications for human health: clinical studies are greatly needed to confirm or to stimulate the basic and translational researches aimed to reach cutting-edge results.

The key deliverable for the scientific community involved in developing MSC clinical applications could be to better understand the mechanisms underlying the MSC commitment and behaviour, by creation of MSC-based platforms which could provide a useful guidance on selection of proper clinical trial subjects based on hypothesis-driven mechanistic predictors of response [13].

Although all are such promising results, there are still severe limitations that currently delay the implementation of stem cell models in practice assays. The articles published in this special issue make use of MSC application for translational regenerative medicine and try to address some of these

limitations. The original research articles as well as the review articles collected in this special issue will support the research community in approaching the goal of obtaining models for the lab that can better mimic the in vivo conditions.

Various methodologies have been employed to improve the cell phenotype generated from MSCs, for example, by modulation of biochemical activity, creation of scaffolds, and addition of growth factors to the culture medium. Furthermore, several topics regarding molecular mechanisms controlling MSC differentiation are covered.

Significant findings have been made in clinical research on application of MSCs for translational regenerative medicine: the reviews and original articles in this special issue highlight new methodological paradigms that challenge current thinking in clinical research and boost the development of clinical-grade MSCs under good manufacturing practice protocols and conditions, an essential step towards clinical applications.

The special issue has reported articles on MSCs used as therapeutic aid in clinical and surgical applications. The topics mainly reported have been the MSC therapy for spinal cord injuries (A. Zadroga et al. and F. Salamanna et al.) and the cell therapy as promising aid for retinal injuries due to ischemic damage (L. Li et al.), as well as for the proper management of stroke (C. Tan et al.).

The most reported translational use of MSC therapy is related to bone tissue regeneration: in fact, many authors have investigated about the osteogenic ability of different stem cell types, with several scaffolds as support to regeneration (Y. Kim et al.), as well as about the use of MSCs to treat osteonecrosis in the maxillofacial region (T. Lombard et al.); the dental-derived MSCs used for bone tissue engineering seem to be still the most used by the S.I. authors (F. Posa et al.), even if bone marrow cells have been used both in bone regeneration (A. Scarano et al. and D. C. Bonfim et al.) and also in the therapy of acute liver diseases (C. O. Kieling et al.).

A special attention has been paid also to umbilical cord stem cells, due to their large application on translational medicine (I. Arutyunyan et al.) and due to their ability to produce exosomes with interesting abilities (B. Zhang et al.).

Some authors have focused their researches on the influence of growth factors and proteins of ECM on MSCs (A. Youssef et al. and M. Moslem et al.) as well as the ability by MSCs to release GFs during their specific stage of life (C. G. Pfeifer et al.) or in combination with adipose-derived stem cells in bone regenerative protocols (F. Mussano et al.).

An interesting general view has been also given on topics related to MSCs of general interest, topics regarding the innovative ways to manage and store the stem cells for therapeutic uses in most different tissues (A. Bissoyi et al. and R. Rohban and T. R. Pieber).

Finally, some authors have also reported interesting aspects on regulatory and quality requirements in MSC research (P. Galvez-Martin et al.).

In this special issue, the editors together with the involved authors have well described the MSCs in their different but fundamental roles as promoters, enhancers, and playmakers of the translational regenerative medicine. Starting from the contents of our issue, the scientific community will be stimulated to experiment new ideas, to improve the knowledge of the MSCs, and to speed up their clinical application, so to improve the future therapies.

Andrea Ballini
Salvatore Scacco
Dario Coletti
Stefano Pluchino
Marco Tatullo

References

[1] A. J. Friedenstein, R. K. Chailakhyan, N. V. Latsinik, A. F. Panasyuk, and I. V. Keiliss-Borok, "Stromal cells responsible for transferring the microenvironment of the hemopoietic tissues. Cloning in vitro and retransplantation in vivo," *Transplantation*, vol. 17, pp. 331–340, 1974.

[2] B. Parekkadan and J. M. Milwid, "Mesenchymal stem cells as therapeutics," *Annual Review of Biomedical Engineering*, vol. 12, pp. 87–117, 2010.

[3] C. Lechanteur, A. Briquet, O. Giet, O. Delloye, E. Baudoux, and Y. Beguin, "Clinical-scale expansion of mesenchymal stromal cells: a large banking experience," *Journal of Translational Medicine*, vol. 14, no. 1, p. 145, 2016.

[4] J. Galipeau, M. Krampera, J. Barrett et al., "International Society for Cellular Therapy perspective on immune functional assays for mesenchymal stromal cells as potency release criterion for advanced phase clinical trials," *Cytotherapy*, vol. 18, no. 2, pp. 151–159, 2016.

[5] R. Fazzina, P. Iudicone, D. Fioravanti et al., "Potency testing of mesenchymal stromal cell growth expanded in human platelet lysate from different human tissues," *Stem Cell Research & Therapy*, vol. 7, no. 1, p. 122, 2016.

[6] T. Squillaro, G. Peluso, and U. Galderisi, "Clinical trials with mesenchymal stem cells: an update," *Cell Transplantation*, vol. 25, no. 5, pp. 829–848, 2016.

[7] M. Marrelli, F. Paduano, and M. Tatullo, "Human periapical cyst-mesenchymal stem cells differentiate into neuronal cells," *Journal of Dental Research*, vol. 94, no. 6, pp. 843–852, 2015.

[8] F. Paduano, M. Marrelli, L. J. White, K. M. Shakesheff, and M. Tatullo, "Odontogenic differentiation of human dental pulp stem cells on hydrogel scaffolds derived from decellularized bone extracellular matrix and collagen type I," *PloS One*, vol. 11, no. 2, article e0148225, 2016.

[9] A. Di Benedetto, G. Brunetti, F. Posa et al., "Osteogenic differentiation of mesenchymal stem cells from dental bud: role of integrins and cadherins," *Stem Cell Research*, vol. 15, no. 3, pp. 618–628, 2015.

[10] A. Uccelli and D. J. Prockop, "Why should mesenchymal stem cells (MSCs) cure autoimmune diseases?" *Current Opinion in Immunology*, vol. 22, pp. 768–774, 2010.

[11] D. J. Prockop and J. Y. Oh, "Mesenchymal stem/stromal cells (MSCs): role as guardians of inflammation," *Molecular Therapy*, vol. 20, no. 1, pp. 14–20, 2012.

[12] Y. Shi, G. Hu, J. Su et al., "Mesenchymal stem cells: a new strategy for immunosuppression and tissue repair," *Cell Research*, vol. 20, no. 5, pp. 510–518, 2010.

[13] S. V. Boregowda and D. G. Phinney, "Quantifiable metrics for predicting MSC therapeutic efficacy," *Journal of Stem Cell Research & Therapy*, vol. 6, no. 11, 2016.

Hindawi
Stem Cells International
Volume 2017, Article ID 6202783, 11 pages
https://doi.org/10.1155/2017/6202783

Research Article

Cytokine, Chemokine, and Growth Factor Profile Characterization of Undifferentiated and Osteoinduced Human Adipose-Derived Stem Cells

F. Mussano,[1] T. Genova,[1,2] M. Corsalini,[3] G. Schierano,[1] F. Pettini,[3] D. Di Venere,[3] and S. Carossa[1]

[1]*CIR Dental School, Department of Surgical Sciences, UNITO, Via Nizza 230, 10126 Turin, Italy*
[2]*Department of Life Sciences and Systems Biology, UNITO, Via Accademia Albertina 13, 10123 Turin, Italy*
[3]*Dipartimento Interdisciplinare di Medicina, Università di Bari, Piazza Giulio Cesare 11, 70124 Bari, Italy*

Correspondence should be addressed to F. Mussano; federico.mussano@unito.it

Received 18 September 2016; Revised 8 January 2017; Accepted 28 February 2017; Published 10 May 2017

Academic Editor: Dario Coletti

Bone is the second most manipulated tissue after blood. Adipose-derived stem cells (ASCs) may become a convenient source of MSC for bone regenerative protocols. Surprisingly, little is known about the most significant biomolecules these cells produce and release after being osteoinduced. Therefore, the present study aimed at dosing 13 candidates chosen among the most representative cytokines, chemokines, and growth factors within the conditioned media of osteodifferentiated and undifferentiated ASCs. Two acknowledged *osteoblastic* cell models, that is, MG-63 and SaOs-2 cells, were compared. Notably, IL-6, IL-8, MCP-1, and VEGF were highly produced and detectable in ASCs. In addition, while IL-6 and IL-8 seemed to be significantly induced by the osteogenic medium, no such effect was seen for MCP-1 and VEGF. Overall SaOS-2 had a poor expression profile, which may be consistent with the more differentiated phenotype of SaOs-2 compared to ASCs and MG-63. Instead, in maintaining medium, MG-63 displayed a very rich production of IL-12, MCP-1, IP-10, and VEGF, which were significantly reduced in osteogenic conditions, with the only exception of MCP-1. The high expression of MCP-1 and VEGF, even after the osteogenic commitment, may support the usage of ASCs in bone regenerative protocols by recruiting both osteoblasts and osteoclasts of the host.

1. Introduction

Unlike the majority of adult tissues, bone is capable to self-repair without forming scars, as most fractures demonstrate by healing spontaneously [1] or through mild surgery. Notwithstanding this inherent regenerative capacity of bone, at least one tenth of the more than 6.2 million fractures [2] occurring yearly suffer from impaired healing. In addition, inborn malformations, alveolar resorption, and critical-size bone defects resulting from severe trauma or malignant tumor resection [3] make bone the second most *transplanted* tissue after blood [4]. Treatments include grafting with both autogenous and allogenic bone, which are not without limitations [5].

Autogenous bone is widely considered the gold standard of bone grafting materials. Nevertheless, there are still some limits to the use of autogenous bone due to the donor site morbidity, the difficulty in obtaining it, and the prolonged healing time [6, 7]. Recently, autologous bone has been used for the regeneration of bony structures and defects [8]. However, autologous bone administration has been highly associated with the risk of disease transmission and immune reaction [9]. Furthermore, synthetic bone grafting materials have been produced to mimic the bone structure and to promote osteoconduction. However, fabricating and manufacturing these graft materials preclude their extensive application due to the involved primary expenses [7, 10].

One of the major goals of tissue engineering [11] is to overcome the pitfalls traditional techniques face when applied to treat large bone defects [12]. Among the three key components of each regenerative protocol, besides scaffolds and signaling molecules, cells play a paramount role. To this end, primary multipotent stem cells, along with several immortalized cell lines, have been widely used for cytocompatibility testing and osteogenic potential evaluation of biomaterials in regenerative medicine [13]. However, the heterogeneity of these cells, too often simply defined as *osteoblasts* or *osteblastic precursors*, should be carefully considered.

Albeit easy to obtain and handle, tumor-derived cell lines may present peculiar nonphysiological features [14]. For instance, osteosarcoma cell lines (SaOs-2, MG-63, and U-2 OS) differ significantly from primary osteoblasts as for immunocytochemical markers and matrix produced [15]. The most used human cell line SaOs-2 cells display a mature osteoblast phenotype and form a calcified matrix resembling woven bone [16]. SaOs-2 cells share with primary human osteoblasts a similar expression profile of cytokines, growth factors, and receptors for parathyroid hormone [17]. MG-63 cell line represents an immature osteoblast phenotype. Despite the inconsistencies about their mineralization capabilities [14], MG-63 cells have been used in long-term studies concerning cell behavior on biomaterials [18]. Notwithstanding the abovementioned pitfalls, SaOs-2 and MG-63 cells are the most studied osteoblasts.

On the other hand, primary stem cells are characterized by higher variability and are usually available in smaller amounts [19]. Although, mesenchymal stem cells deriving from bone marrow are somehow archetypic [20, 21], more recently, adipose-derived stem cells (ASCs) [22] have emerged as a viable alternative source of mesenchymal cells. As it has been exhaustively reviewed [23], ASCs are relatively abundant and easy to access and may therefore become the elective source of mesenchymal stem cells for bone regenerative protocols. Surprisingly, however, little is known about the most significant biomolecules osteo-committed cells produce and release. Therefore, the present study aimed at dosing 13 candidates chosen among the most representative cytokines, chemokines, and growth factors within the conditioned media of osteodifferentiated and undifferentiated ASCs. As a complimentary analysis, two acknowledged "osteoblastic" cell models were compared, based on their different maturation stage.

2. Materials and Methods

2.1. Cell Culture. ASCs were isolated from fat tissue obtained from three different donors as described previously [22] and maintained in Dulbecco's minimum essential medium enriched with sodium pyruvate and supplemented with 10% foetal bovine serum (FBS, Gibco Life Technologies), 100 U/ml penicillin, 100 μg/ml streptomycin, and 250 ng/ml amphotericin B. The nonadherent cell population was removed after 48 h, and the adherent cell layer was washed twice with fresh medium; cells were then continuously cultured since their harvest until sixth passage. SaOs-2 (ATCC number: HTB-85) and MG-63 (ATCC number: CRL-1427) cells were, respectively, cultured in McCoy'5A (Gibco, Life Technologies) with 15% FBS (Benchmark, Gemini Bio-Products) and in Dulbecco's modified eagle's medium (DMEM, Gibco, Life Technologies) with 10% FBS. Both media were supplemented with 1% penicillin-streptomycin (MD Biomedicals, Thermo Fisher Scientific). Cells were always passaged at subconfluency to prevent contact inhibition and were kept under a humidified atmosphere of 5% CO2 in air, 37°C.

2.2. Detection of Interleukins, Chemokines, and Growth Factors Using Bio-Plex System. To analyze the profile of the biomolecules, cells were seeded in 96-well plates (10^3 cells/well) in their own maintaining medium for 1 day. Afterwards, cells were incubated in RPMI in the presence of 2% FBS and 2% FBS + osteogenic factors (50 μM ascorbic acid, 10 mM beta glycerophosphate, and 100 nM dexamethasone) either for 7 (T1) and 14 (T2) in the case of SaOs-2 or for 21 (T1) and 28 (T2) days in the case of MG-63 and ASCs. At the day of harvest, media were removed, cells washed twice in PBS, and fresh starving medium (RPMI 0.5% bovine serum albumin) was incubated for 2 hours. Conditioned media thus obtained were characterized, without adding any activation substances, by measuring the concentration of the following specific biomolecules: interleukin-2 (IL-2), interleukin-6 (IL-6), interleukin-8 (IL-8), interleukin-10 (IL-10), interleukin-12 (IL-12), granulocyte-colony stimulating factor (G-CSF), interferon-gamma (INF-γ), tumor necrosis factor-α (TNF-α), monocyte chemoattractant protein-1 (MCP-1) (CCL-2), CXCL10 chemokine (IP-10), platelet-derived growth factor (PDGF), basic-fibroblastic growth factor (bFGF), and vascular endothelial growth factor (VEGF). The flexible Bio-Plex system (Bio-Rad Laboratories, Hercules, CA, USA) was employed as previously described [24]. All samples were analyzed following the manufacturer's protocol. At least two independent repetitions in duplicate were made per sample. Concentrations of the analytes were expressed in pg/ml. A standard curve ranging on average from 0.15 pg/ml to 3700 pg/ml (High Photomultiplier Tube Setting—PMT setting) was prepared and then fitted by Bio-Plex Manager software.

2.3. In Vitro Osteogenic Differentiation Tests. In vitro osteogenic differentiation was performed at the same conditions described above to run a series of assays aiming at revealing established bone markers, as described elsewhere [25, 26].

2.3.1. Alkaline Phosphatase (ALP) Activity Assay. Alkaline phosphatase (ALP) activity was determined using a colorimetric end point assay [27, 28], which measures the conversion of the colorless substrate p-nitrophenol phosphate (PNPP) by the enzyme ALP to the yellow product p-nitrophenol. To measure ALP activity, cells were lysed with 0.05% Triton X-100 and incubated with the reagent solution containing phosphatase substrate (Sigma-Aldrich, Milan, Italy) at 37°C for 15 min. The rate of color change corresponds to the amount of enzyme present in solution. Optical density was measured at a wavelength of 405 nm (reference

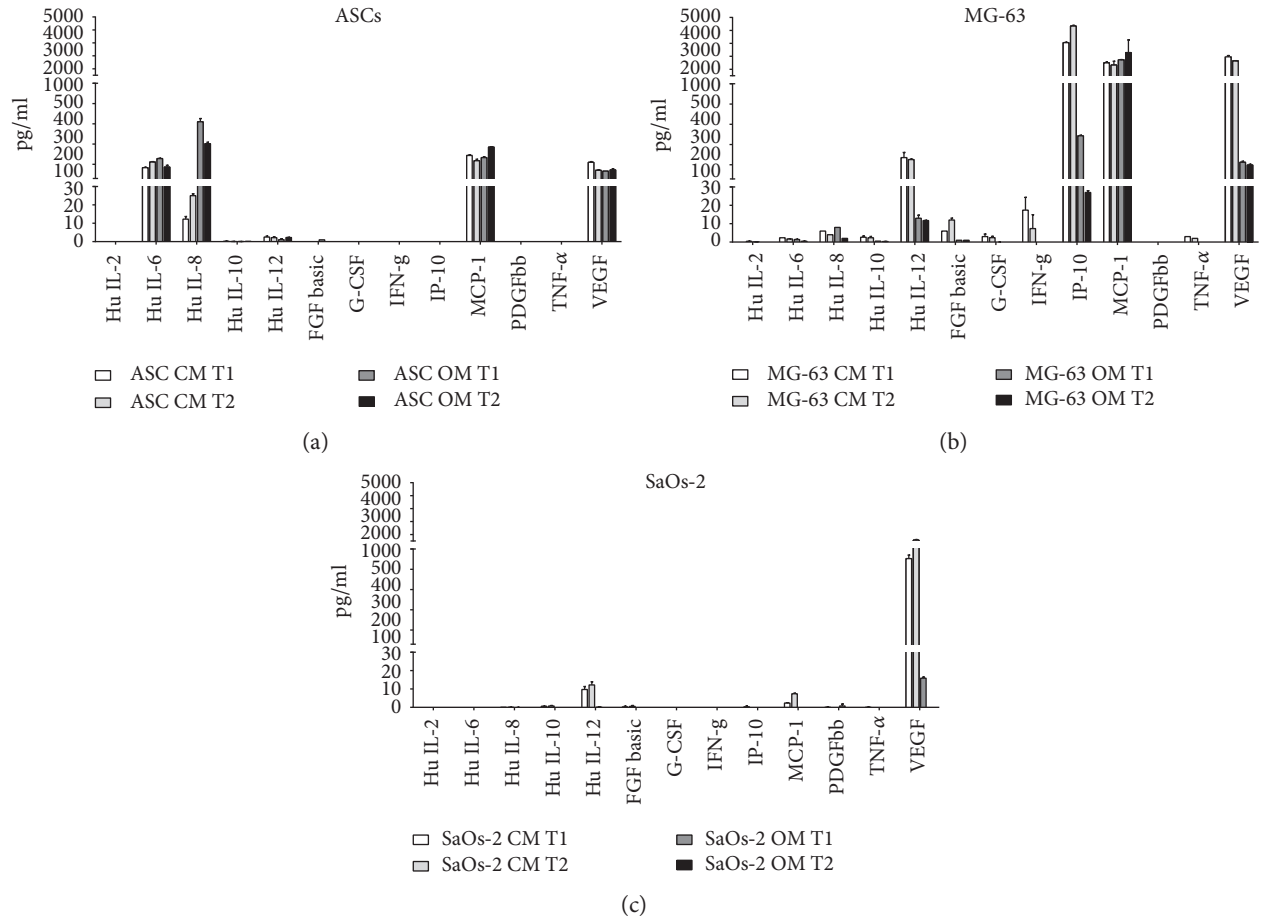

Figure 1: Cytokine quantification. Cytokine levels of ASCs (a), MG-63 (b), and SaOS-2 (c) measured by Bio-Plex analysis are shown. Two times (T1, T2) and two conditions (CM, OM) were considered for each cell line. For ASCs and MG-63, T1 = 21 days and T2 = 28 days; for SaOs-2, T1 = 7 days and T2 = 14 days. CM = control medium (DMEM 2% FBS); OM = osteogenic medium (see Materials and Methods).

620 nm). Samples were compared against the calibration curve of p-nitrophenol standards. The final alkaline phosphatase concentration was adjusted per total protein content, to avoid biases due to the cell number. Therefore, part of the cell lysates obtained for ALP quantification was incubated with BCA™ (Thermo Fisher Scientific, Waltham, MA, USA) protein assay, following to the manufacturer's instructions. Optical density was measured at a wavelength of 570 nm, and results were adjusted to a calibration curve made by known number of cells. ALP values were determined and normalized on whole protein content at day 3 in SaOs-2 and at day 7 in MG-63 and ASCs.

2.3.2. Calcium Content Assay. Cell calcium content was determined at day 14 for SaOs-2 and at day 21 for MG-63 and ASCs by Calcium colorimetric assay kit (BioVision Research Products, Mountain View, CA, USA), according to the manufacturer's protocol. The OD was measured at 575 nm within 20 minutes since preparation. A calibration curve was always made.

2.3.3. Collagen and Calcium Staining. At the established time points, cells grown in six-plate wells were washed once with PBS and fixed with 4% paraformaldehyde for 10 min at room temperature. The solution was removed and cells were washed with PBS. To stain collagen, Sirius Red dye (Direct Red 80, Sigma-Aldrich) dissolved (1 mg/ml) in a saturated aqueous solution of picric acid (Sigma-Aldrich), was added to the fixed cell cultures. After kept under mild shaking for 2 hours, samples were quickly rinsed in acid water (0.5% acetic acid in pure water) and then abundantly washed with distilled water. Calcium salts were stained after von Kossa following published protocols [15]. For both picro-Sirius Red and von Kossa stains, the cultures were observed under light microscopy and representative pictures captured by an Olympus camera.

2.4. Statistical Analysis. Data were analysed by GraphPad Prism6 (GraphPad Software, Inc., La Jolla, CA, USA). Each experiment was repeated at least three times. Statistical analysis was performed by using the nonparametric test Wilcoxon–Mann–Whitney test. A p value of <0.05 was considered significant.

3. Results

3.1. Detection of Interleukins, Chemokines, and Growth Factors. The concentrations of interleukin-2 (IL-2),

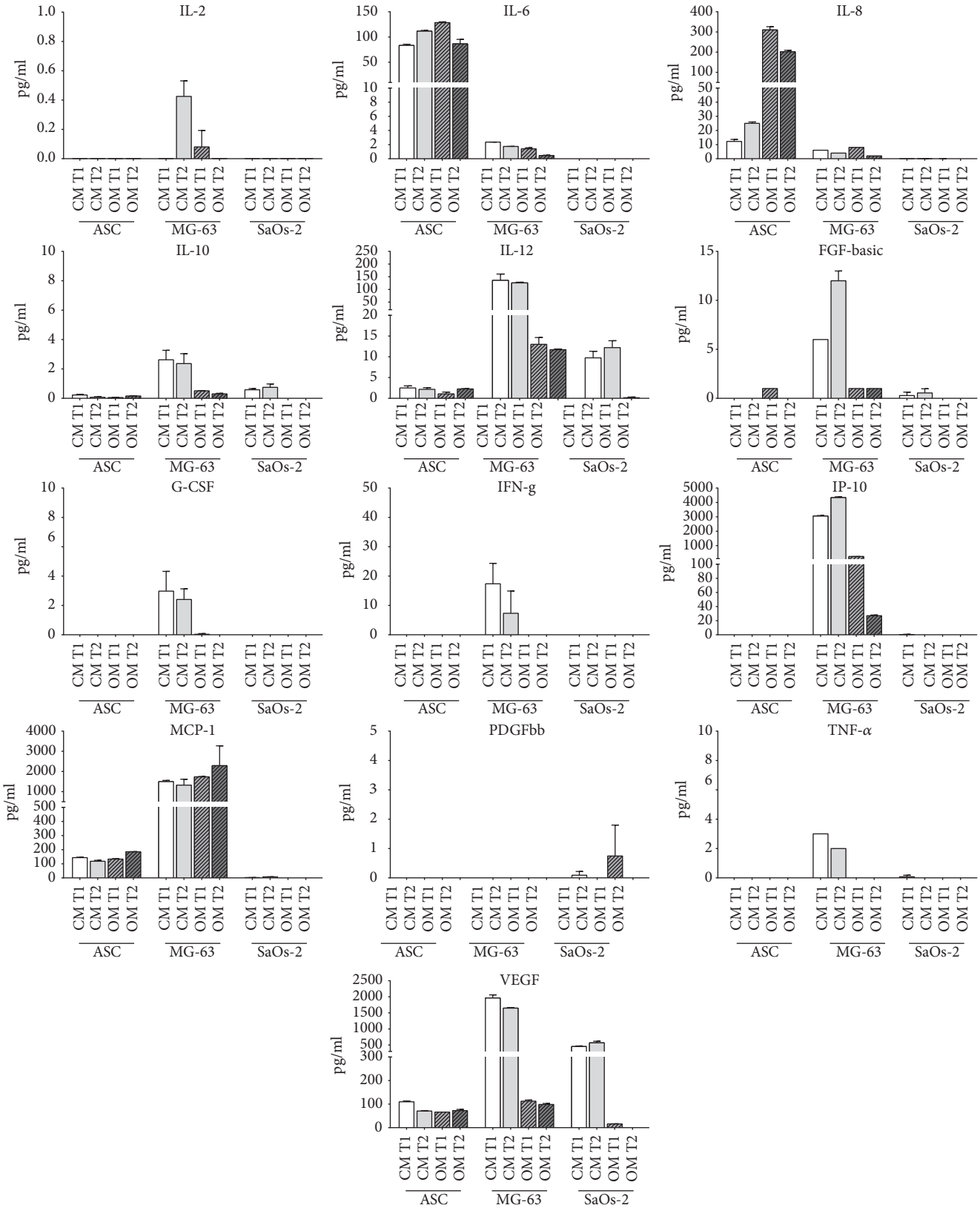

Figure 2: Cytokine quantification 2. Data from Bio-Plex analysis are reported as different histograms for each cytokine. In particular, the quantification of each molecule in ASCs, MG-63, and SaOs-2 is shown at T1 and T2 and in CM and OM conditions. For ASCs and MG-63, T1 = 21 days and T2 = 28 days; for SaOs-2, T1 = 7 days and T2 = 14 days. CM = control medium (DMEM 2% FBS); OM = osteogenic medium (see Materials and Methods).

interleukin-6 (IL-6), interleukin-8 (IL-8), interleukin-10 (IL-10), interleukin-12 (IL-12), granulocyte-colony stimulating factor (G-CSF), interferon-gamma (INF-γ), tumor necrosis factor-α (TNF-α), monocyte chemoattractant protein-1 (MCP-1) (CCL-2), CXCL10 chemokine (IP-10), platelet-derived growth factor (PDGF), basic-fibroblastic growth factor (bFGF), and vascular endothelial growth factor (VEGF) are reported in Figure 1 for ASCs, MG-63, and SaOs-2 cells that were kept both under maintaining and differentiation media.

Interestingly, there is a big difference in the expression pattern of interleukins, chemokines, and growth factors among different cells. ASCs produce a considerable level of IL-6, IL-8, MCP-1, and VEGF without particular variations between osteodifferentiated and control condition (with the exception of IL-8). MG-63 shows high levels of expression of IL-12, IP-10, MCP-1, and VEGF. Importantly, in osteodifferentiating conditions, the expression of IL-12, IP-10, and VEGF decreases. SaOs-2 cells show very low expression levels of the considered molecules, except for the VEGF. Notably, the osteodifferentiating medium inhibits the expression of IL-12 and VEGF in SaOs-2, similarly to MG-63 cells. To further highlight the differential expression of the considered molecules among ASCs, MG-63, and SaOs-2 cells, a panel showing the expression values for each biomolecule is reported in Figure 2.

3.2. In Vitro Osteogenic Differentiation Tests. The osteogenic potential of the cells has been assessed at the early stage by quantifying ALP activity (Figure 3) and staining the collagen matrix through Sirius Red (Figure 4). Interestingly, the osteodifferentiating condition significantly increased the level of ALP activity for each cell type. At later stages, the extracellular calcium content was determined colorimetrically (Figure 5) and with the Von Kossa method (Figure 6). In osteodifferentiating condition, a significant increase of extracellular calcium content was found for each cell type. Collectively, the differentiating condition appeared more performing than the undifferentiated control, proving the effectiveness of the osteogenic medium.

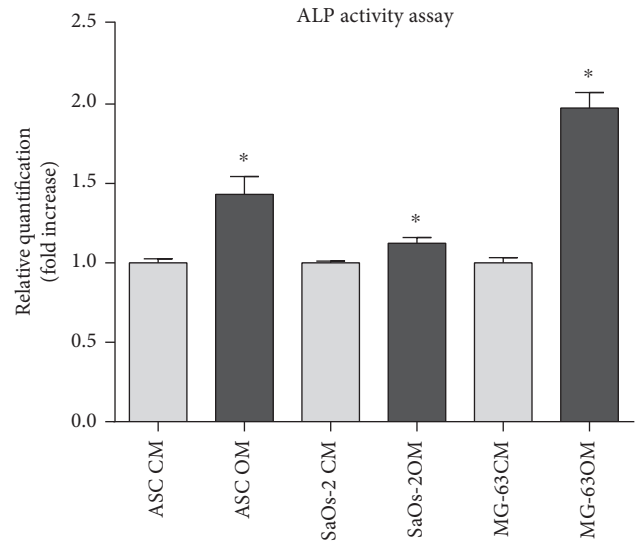

Figure 3: ALP activity quantification. ALP activity was evaluated recurring to a colorimetric assay. Values were normalized on whole protein content at day 3 in SaOs-2 and at day 7 in MG-63 and ASCs. For each cell type, data were normalized on control condition (CM) set as 1. OM condition significantly increase the ALP activity in each cell type. CM = control medium (DMEM 2% FBS); OM = osteogenic medium (see Materials and Methods). Statistical analysis was performed by using the Wilcoxon–Mann–Whitney test. A p value of <0.05 was considered significant.

4. Discussion

In the present study, the differential expression of signaling molecules among three different cell types under both osteodifferentiating and control conditions is shown for the first time. To achieve this, a highly sensitive method was used. In particular, the cellular models considered in this work are the ASC, the MG-63, and the SaOs-2 cells. Notably, the ASCs represent a particular type of mesenchymal stem cells of great potential applications in the context of bone regeneration. On the other hand, despite their ineligibility for clinical use owing to their tumor derivation [29–31], MG-63 and SaOs-2 cells were chosen to this study as they are a widely diffused and accepted in vitro model, in the field of bone biology [16, 17, 32–37]. This paper underlines also the differences in the expression variations of signaling molecules during differentiation among cells.

In 2001, Zuk et al. [22] described a putative population of multipotent stem cells isolated through the enzymatic digestion of the stromal vascular fraction of adipose tissue. Cultured over time, these adherent cells display features of multipotency; specifically, they tend to become relatively homogenous trough passages and are capable to undergo differentiation toward adipocytes, osteoblasts, and chondrocytes, under proper conditions [38]. Since this is true even when expanded from a single clone, these cells have been termed "adipose-derived stem cells" (ASCs) based on a consensus reached by the Second Annual Meeting of the International Fat Applied Technology Society [39].

Notwithstanding the huge amount of research at the in vitro and in vivo levels, the clinical usage of ASCs for bone reconstruction has been limited. It is worth mentioning the successful, although almost anecdotal, treatment of critical bone defects in humans by the seeding of ASCs into poly lactic-co-glycolic acid (PLGA) scaffolds [40] and beta-tricalcium phosphate granules [41]. Bone restoration efforts may profit from the combination with traditional techniques such as grafts and ex vivo expansion under GMP techniques [42]. Increasing interest has been focused on the biomaterials used as carriers, as described, for instance, by Mellor et al., who proposed stacked electrospun polylactic acid nanofibrous scaffolds containing tricalcium phosphate nanoparticles [43].

The actual efficacy of ASCs is, however, not solely restricted to their differentiation capacity, but it owes also a great deal to the delivery and localized secretion of signaling molecules promoting, eventually, tissue recovery. Following this research route, recent studies [43, 44] have explained

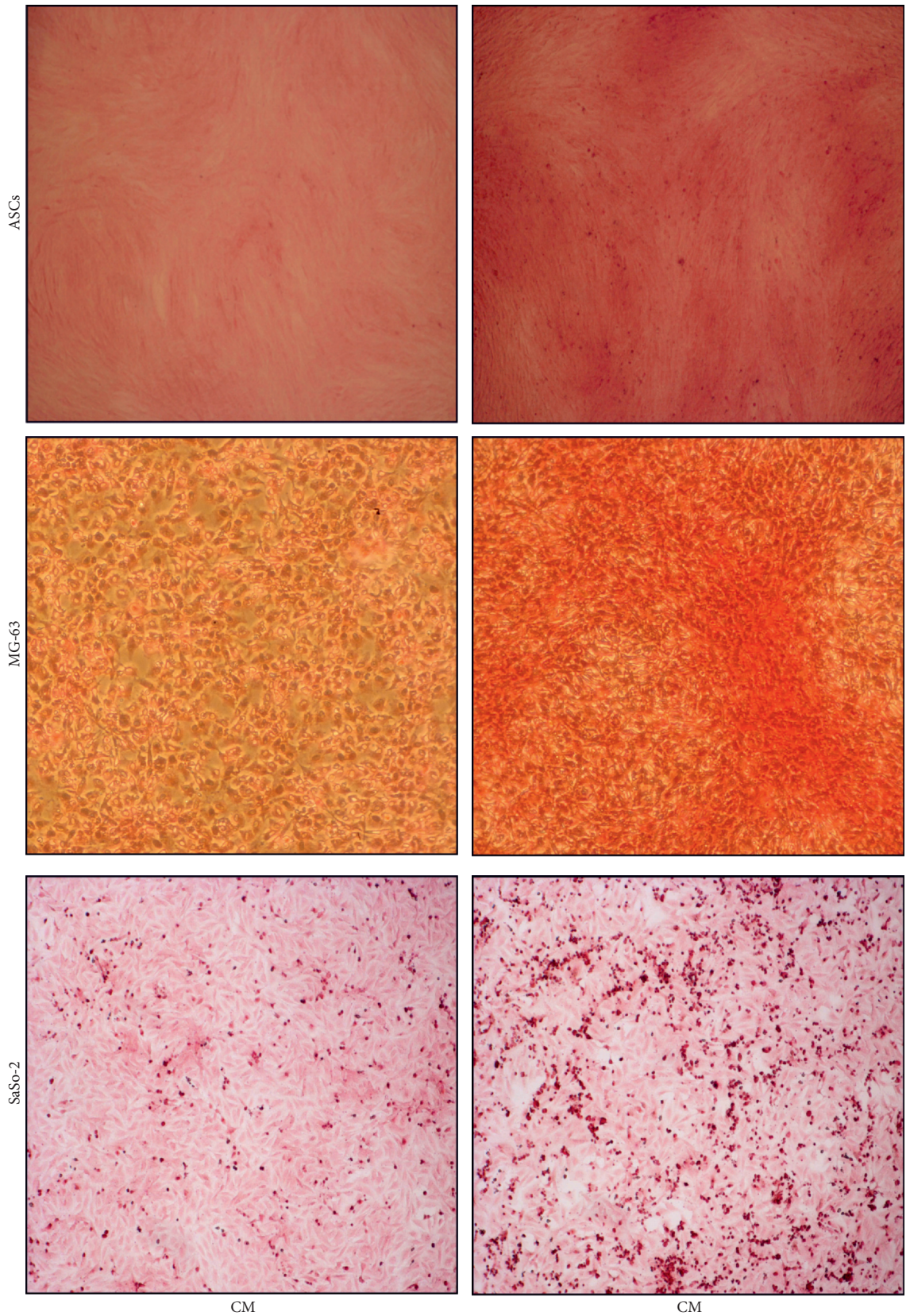

Figure 4: Collagen staining. Sirius Red dye staining was performed in order to show collagen deposition at day 3 in SaOs-2 and at day 7 in MG-63 and ASCs. In OM condition, the staining is more intense for each cell type. CM = control medium (DMEM 2% FBS); OM = osteogenic medium (see Materials and Methods). Images were taken at 100x magnification.

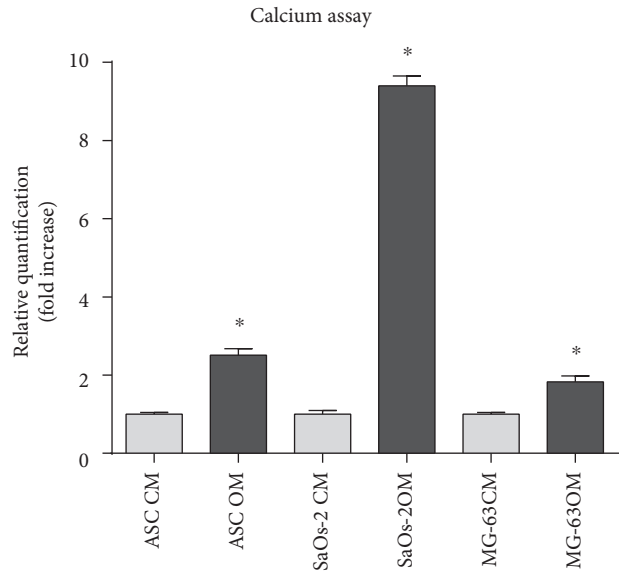

Figure 5: Calcium quantification. Cell calcium content was determined kit recurring to a colorimetric assay. Evaluation was performed at day 14 for SaOs-2 and at day 21 for MG-63 and ASCs. For each cell type, data were normalized on control condition (CM) set as 1. OM condition significantly increases the calcium content in each cell type with a particularly high level in SaOs-2. CM = control medium (DMEM 2% FBS); OM = osteogenic medium (see Materials and Methods). Statistical analysis was performed by using the Wilcoxon–Mann–Whitney test. A p value of <0.05 was considered significant.

the therapeutic effect of ASCs in ischemic models as a result of the release of angiogenic factors such as HGF and VEGF. Human ASCs were proven to secrete both factors constitutively [45]. Kilroy et al. [46] reported that ASCs produce angiogenic (HGF and VEGF), proinflammatory (IL-6, IL-8, IL-11, LIF, and TNF alpha), and hematopoietic-supportive cytokines (G-CSF, M-CSF, GM-CSF, and IL-7) following exposure to common inductive factors including LPS. Ribeiro and colleagues characterized the secretome of ASCs with neurologic implications [47], while Succar and coworkers profiled and compared different formulations for cell therapy of osteoarthritis [48]. Nevertheless, to the authors' surprise, the scientific literature has lacked up to now a comprehensive description of a significant range of biomolecules secreted by ASCs subjected to osteogenic differentiation, the great interest being more focused on the intracellular dynamics.

Therefore, this study focused on the detection of a representative panel of signaling molecules that ASCs, SaOs-2 cells, and MG-63 cells produce when cultured in either maintaining or osteogenic medium. Each cell type behaved differently. It is noteworthy that IL-6, IL-8, MCP-1, and VEGF were highly produced and detectable in ASCs even in the absence of any stimulus. In addition, while IL-6 and IL-8 seemed to be significantly induced by the osteogenic medium, no such effect was seen for MCP-1 and VEGF. The multiplex immunological system here adopted called Luminex® is capable to simultaneously detect and quantify up to several hundreds of analytes across multiple samples, reducing time, cost, and sample requirements in comparison to ELISA assays [49]. The capture antibodies of Luminex recognise specific analytes and are attached to microbeads with defined spectral address. The technique sensitivity thus reaches concentrations even lower than 1 pg/ml, which explains, for instance, why we report on the presence of IL-12 in ASCs contradicting Kilroy and colleagues' outcomes based on ELISA kits [46].

Overall SaOS-2 cells had a poor expression profile (only IL-12 and VEGF resulted greater than 10 pg/ml), which may be consistent with the more differentiated phenotype of SaOs-2 cells compared to ASCs and MG-63, as thoroughly reviewed elsewhere [14]. Instead, when kept in maintaining medium, MG-63 cells displayed a very rich production of IL-12, MCP-1, IP-10, and VEGF. This remarkable secretory activity was inhibited by the osteogenic conditions, except for MCP-1, a chemokine pivotal for macrophage activation and thus bone remodeling. Notably, MCP-1, which is known to be constitutively expressed in osteoblasts [50], was herein enhanced in osteodifferentiated MG-63 cells.

The high level of IP-10 quantified in MG-63 cells may be correlated to the tumor origin of the cell line [50, 51]. IP-10 was possibly produced in response to IFN-g, which was detected only in MG-63 (as shown in Figures 1 and 2). Compared to ASCs and SaOs-2, MG-63 produced also more FGF-b, although the overall level is generally low. Considering these results, it could be interesting to investigate the related TGF-b expression [52].

As noted above, contrary to MG-63 and SaOs-2 cells, VEGF did not trend downward when ASCs were osteoinduced, even though the inhibitory effect of dexamethasone, present in the osteogenic medium, is well known for endothelial and tumoral cells [53, 54]. Along with the constitutive high expression of MCP-1, the steady release of VEGF may underpin the usage of ASCs for bone regenerative protocols, where these biomolecules could contribute to recruit bone cells within the host [55–58]. Very interestingly, Hu and Olsen [55] studied bone repair in mice with a monocortical defect within the tibial cortex. Osteoblast-derived VEGF was proven to stimulate crosstalk between osteoblastic, endothelial, and hematopoietic cells in a paracrine manner, while directly affecting osteoblasts via autocrine mechanisms. The role of MCP-1 was instead investigated as for the PTH-induction during osteoclastogenesis by Li et al. [58], providing a rationale for increased osteoclast activity to initiate greater bone remodeling.

On these premises, it will be of great interest to study ASCs in a more physiologic context so as to provide more reliable and predictive results. A possible approach might consist in elucidating the behavior of ASCs in coculture systems, with endothelial cells that are known to be key players in bone formation and regeneration [5].

5. Conclusion

Currently, the amount of proposals for the use of ASCs in tissue repair and regeneration is impressive. The number of clinical trials evaluating the efficacy and safety of ASCs in the reconstruction and regeneration of tissues increases

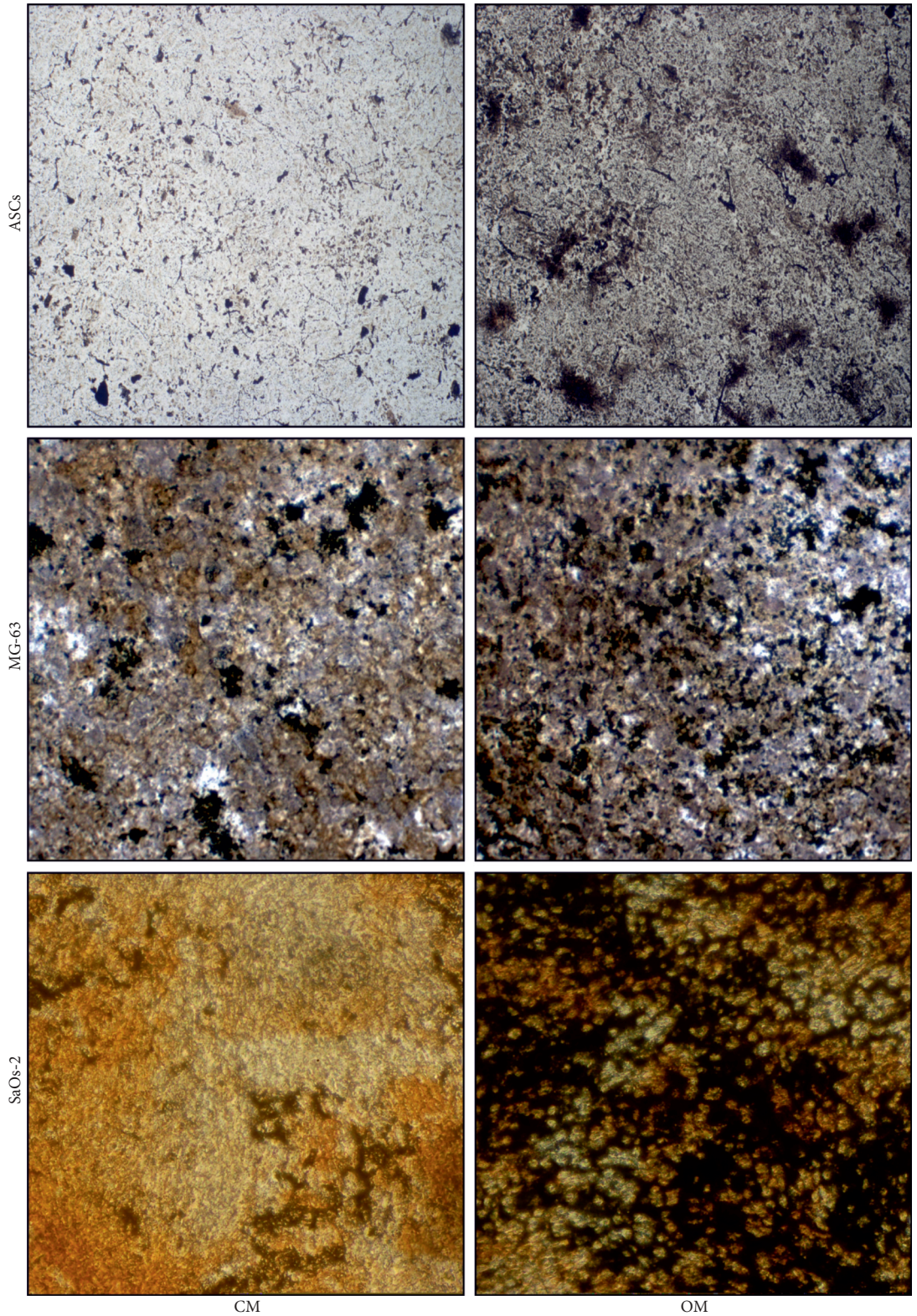

Figure 6: Calcium staining. Von Kossa staining was performed in order to show calcium deposition at day 14 for SaOs-2 and at day 21 for MG-63 and ASCs. In OM condition, the staining is more intense for each cell type. CM = control medium (DMEM 2% FBS); OM = osteogenic medium (see Materials and Methods). Images were taken at 100x magnification.

significantly every year. According to the clinical trials database (ClinicalTrials.gov database 2015), 122 studies are currently using ASCs [59, 60].

In particular, positive results have been obtained using autologous ASCs in clinical trials for craniofacial bone reconstruction by producing new, mature, vital, and vascularized

bone [40–42, 61–63]. To date, bone regeneration is the most promising field for clinical translation of experimental ASC protocols [62]. This study supports, once more, the viability of ASCs in bone tissue engineering based on the cytokines, chemokines, and growth factors detected.

Disclosure

No involvement is to be reported at any stage of the study or while preparing the paper.

Conflicts of Interest

The authors declare that there are no competing interests regarding the publication of this paper.

Authors' Contributions

F. Mussano and T. Genova equally contributed to this work.

Acknowledgments

This research was partly funded by the Piedmont Region with the POLI D'INNOVAZIONE-III Annualità (research project acronym: BIOBONE).

References

[1] T. A. Einhorn, "The science of fracture healing," *Journal of Orthopaedic Trauma*, vol. 19, no. 10, pp. S4–S6, 2005, August 2016, http://www.ncbi.nlm.nih.gov/pubmed/16479221.

[2] American Academy of Orthopaedic Surgeons, *Musculoskeletal Injuries Report: Incidence, Risk Factors and Prevention*, AAOS, Rosemont, IL, USA, 2000.

[3] M. D. McKee, "Management of segmental bony defects: the role of osteoconductive orthobiologics," *The Journal of the American Academy of Orthopaedic Surgeons*, vol. 14, no. 10, pp. S163–S167, 2006, August 2016, http://www.ncbi.nlm.nih.gov/pubmed/17003191.

[4] P. Giannoudis, H. Dinopoulos, and E. Tsiridis, "Bone substitutes: an update," *Injury*, vol. 36, Supplement 3, pp. S20–S27, 2005.

[5] T. Genova, L. Munaron, S. Carossa, and F. Mussano, "Overcoming physical constraints in bone engineering: "the importance of being vascularized"," *Journal of Biomaterials Applications*, vol. 30, no. 7, pp. 940–951, 2016.

[6] M. E. Aichelmann-Reidy and R. A. Yukna, "Bone replacement grafts. The bone substitutes," *Dental Clinics of North America*, vol. 42, no. 3, pp. 491–503, 1998, December 2016, http://www.ncbi.nlm.nih.gov/pubmed/9700451.

[7] G. Fernandes and S. Yang, "Application of platelet-rich plasma with stem cells in bone and periodontal tissue engineering," *Bone Research*, vol. 4, article 16036, 2016.

[8] M. A. Brunsvold and J. T. Mellonig, "Bone grafts and periodontal regeneration," *Periodontology 2000*, vol. 1, no. 1, pp. 80–91, 1993, December 2016, http://www.ncbi.nlm.nih.gov/pubmed/8401863.

[9] C. Delloye, "Bone grafts using tissue engineering," *Bulletin et Mémoires de l'Académie Royale de Médecine de Belgique*, vol. 156, no. 7-9, pp. 418–425, 2001, December 2016, http://www.ncbi.nlm.nih.gov/pubmed/11995186.

[10] W. Li, L. Xiao, and J. Hu, "The use of enamel matrix derivative alone versus in combination with bone grafts to treat patients with periodontal intrabony defects," *Journal of the American Dental Association (1939)*, vol. 143, no. 9, pp. e46–e56, 2012.

[11] R. Langer and J. P. Vacanti, "Tissue engineering," *Science*, vol. 260, no. 5110, pp. 920–926, 1993.

[12] C. Szpalski, F. Sagebin, M. Barbaro, and S. M. Warren, "The influence of environmental factors on bone tissue engineering," *Journal of Biomedical Materials Research. Part B, Applied Biomaterials*, vol. 101, no. 4, pp. 663–675, 2013.

[13] V. Kartsogiannis and K. W. Ng, "Cell lines and primary cell cultures in the study of bone cell biology," *Molecular and Cellular Endocrinology*, vol. 228, no. 1, pp. 79–102, 2004.

[14] E. M. Czekanska, M. J. Stoddart, R. G. Richards, and J. S. Hayes, "In search of an osteoblast cell model for in vitro research," *European Cells and Materials*, vol. 24, no. 4, pp. 1–17, 2012, November 2015, http://www.ncbi.nlm.nih.gov/pubmed/22777949.

[15] C. Pautke, M. Schieker, T. Tischer et al., "Characterization of osteosarcoma cell lines MG-63, Saos-2 and U-2 OS in comparison to human osteoblasts," *Anticancer Research*, vol. 24, no. 6, pp. 3743–3748, 2004, February 2015, http://www.ncbi.nlm.nih.gov/pubmed/15736406.

[16] S. B. Rodan, Y. Imai, M. A. Thiede et al., "Characterization of a human osteosarcoma cell line (Saos-2) with osteoblastic properties," *Cancer Research*, vol. 47, no. 18, pp. 4961–4966, 1987, January 2015, http://www.ncbi.nlm.nih.gov/pubmed/3040234.

[17] G. Bilbe, E. Roberts, M. A. Birch, and D. B. B. Evans, "PCR phenotyping of cytokines, growth factors and their receptors and bone matrix proteins in human osteoblast-like cell lines," *Bone*, vol. 19, no. 5, pp. 437–445, 1996.

[18] J. Lincks, B. D. Boyan, C. R. Blanchard et al., "Response of MG63 osteoblast-like cells to titanium and titanium alloy is dependent on surface roughness and composition," *Biomaterials*, vol. 19, no. 23, pp. 2219–2232, 1998, January 2015, http://www.ncbi.nlm.nih.gov/pubmed/9884063.

[19] C. Li, G. Wei, Q. Gu et al., "Donor age and cell passage affect osteogenic ability of rat bone marrow mesenchymal stem cells," *Cell Biochemistry and Biophysics*, vol. 72, no. 2, pp. 543–549, 2015.

[20] M. F. Pittenger, A. M. Mackay, S. C. Beck et al., "Multilineage potential of adult human mesenchymal stem cells," *Science*, vol. 284, no. 5411, pp. 143–147, 1999, July 2014, http://www.ncbi.nlm.nih.gov/pubmed/10102814.

[21] N. Jaiswal, S. E. Haynesworth, A. I. Caplan, and S. P. Bruder, "Osteogenic differentiation of purified, culture-expanded human mesenchymal stem cells in vitro," *Journal of Cellular Biochemistry*, vol. 64, no. 2, pp. 295–312, 1997.

[22] P. A. Zuk, M. Zhu, H. Mizuno et al., "Multilineage cells from human adipose tissue: implications for cell-based therapies," *Tissue Engineering*, vol. 7, no. 2, pp. 211–228, 2001.

[23] U. D. Wankhade, M. Shen, R. Kolhe et al., "Advances in adipose-derived stem cells isolation, characterization, and application in regenerative tissue engineering," *Stem Cells International*, vol. 2016, Article ID 3206807, p. 9, 2016.

[24] F. Mussano, T. Genova, L. Munaron, S. Petrillo, F. Erovigni, and S. Carossa, "Cytokine, chemokine, and growth factor profile of platelet-rich plasma," *Platelets*, vol. 27, no. 5, pp. 467–471, 2016.

[25] F. Mussano, K. J. Lee, P. Zuk et al., "Differential effect of ionizing radiation exposure on multipotent and differentiation-restricted

bone marrow mesenchymal stem cells," *Journal of Cellular Biochemistry*, vol. 111, no. 2, pp. 322–332, 2010.

[26] F. Mussano, A. Bartorelli Cusani, A. Brossa, S. Carossa, G. Bussolati, and B. Bussolati, "Presence of osteoinductive factors in bovine colostrum," *Bioscience, Biotechnology, and Biochemistry*, vol. 78, no. 4, pp. 662–671, 2014.

[27] H. L. Holtorf, N. Datta, J. A. Jansen, and A. G. Mikos, "Scaffold mesh size affects the osteoblastic differentiation of seeded marrow stromal cells cultured in a flow perfusion bioreactor," *Journal of Biomedical Materials Research. Part a*, vol. 74, no. 2, pp. 171–180, 2005.

[28] F. Mussano, T. Genova, P. Rivolo et al., "Role of surface finishing on the in vitro biological properties of a silicon nitride–titanium nitride (Si3N4–TiN) composite," *Journal of Materials Science*, vol. 52, no. 1, pp. 467–477, 2017.

[29] H. Masuda, C. Miller, H. P. Koeffler, H. Battifora, and M. J. Cline, "Rearrangement of the p53 gene in human osteogenic sarcomas," *Proceedings of the National Academy of Sciences*, vol. 84, no. 21, pp. 7716–7719, 1987.

[30] E. Murray, D. Provvedini, D. Curran, B. Catherwood, H. Sussman, and S. Manolagas, "Characterization of a human osteoblastic osteosarcoma cell line (SAOS-2) with high bone alkaline phosphatase activity," *Journal of Bone and Mineral Research*, vol. 2, no. 3, pp. 231–238, 1978.

[31] H. Heremans, A. Billiau, J. J. Cassiman, J. C. Mulier, and P. De Somer, "In vitro cultivation of human tumor tissues II. Morphological and virological characterization of three cell lines," *Oncologia*, vol. 35, no. 6, pp. 246–252, 1978.

[32] R. J. Fernandes, M. A. Harkey, M. Weis, J. W. Askew, and D. R. Eyre, "The post-translational phenotype of collagen synthesized by SAOS-2 osteosarcoma cells," *Bone*, vol. 40, no. 5, pp. 1343–1351, 2007.

[33] L. G. Rao, M. K. Sutherland, G. S. Reddy, M. L. Siu-Caldera, M. R. Uskokovic, and T. M. Murray, "Effects of 1alpha, 25-dihydroxy-16ene, 23yne-vitamin D3 on osteoblastic function in human osteosarcoma SaOS-2 cells: differentiation-stage dependence and modulation by 17-beta estradiol," *Bone*, vol. 19, no. 5, pp. 621–627, 1996, January 2017, http://www.ncbi.nlm.nih.gov/pubmed/8968029.

[34] J. Clover, R. A. Dodds, and M. Gowen, "Integrin subunit expression by human osteoblasts and osteoclasts in situ and in culture," *Journal of Cell Science*, vol. 103, Part 1, 1992.

[35] R. Olivares-Navarrete, P. Raz, G. Zhao et al., "Integrin alpha2beta1 plays a critical role in osteoblast response to micron-scale surface structure and surface energy of titanium substrates," *Proceedings of the National Academy of Sciences of the United States of America*, vol. 105, no. 41, pp. 15767–15772, 2008.

[36] A. Kumarasuriyar, S. Murali, V. Nurcombe, and S. M. Cool, "Glycosaminoglycan composition changes with MG-63 osteosarcoma osteogenesis in vitro and induces human mesenchymal stem cell aggregation," *Journal of Cellular Physiology*, vol. 218, no. 3, pp. 501–511, 2009.

[37] L. Saldaña, F. Bensiamar, A. Boré, and N. Vilaboa, "In search of representative models of human bone-forming cells for cytocompatibility studies," *Acta Biomaterialia*, vol. 7, no. 12, pp. 4210–4221, 2011.

[38] P. A. Zuk, M. Zhu, P. Ashjian et al., "Human adipose tissue is a source of multipotent stem cells," *Molecular Biology of the Cell*, vol. 13, no. 12, pp. 4279–4295, 2002.

[39] "Stem Cells From Fat Focus Of International Fat Applied Technology Society," in *Second Annual Meeting of the International Fat Applied Technology Society*, Pittsburgh, PA, 2004.

[40] S. Lendeckel, A. Jödicke, P. Christophis et al., "Autologous stem cells (adipose) and fibrin glue used to treat widespread traumatic calvarial defects: case report," *Journal of Cranio-Maxillo-Facial Surgery*, vol. 32, no. 6, pp. 370–373, 2004.

[41] T. Thesleff, K. Lehtimäki, T. Niskakangas et al., "Cranioplasty with adipose-derived stem cells and biomaterial: a novel method for cranial reconstruction," *Neurosurgery*, vol. 68, no. 6, pp. 1535–1540, 2011.

[42] K. Mesimäki, B. Lindroos, J. Törnwall et al., "Novel maxillary reconstruction with ectopic bone formation by GMP adipose stem cells," *International Journal of Oral and Maxillofacial Surgery*, vol. 38, no. 3, pp. 201–209, 2009.

[43] A. Miranville, C. Heeschen, C. Sengenès, C. A. Curat, R. Busse, and A. Bouloumié, "Improvement of postnatal neovascularization by human adipose tissue-derived stem cells," *Circulation*, vol. 110, no. 3, pp. 349–355, 2004.

[44] V. Planat-Benard, J.-S. Silvestre, B. Cousin et al., "Plasticity of human adipose lineage cells toward endothelial cells: physiological and therapeutic perspectives," *Circulation*, vol. 109, no. 5, pp. 656–663, 2004.

[45] J. Rehman, D. Traktuev, J. Li et al., "Secretion of angiogenic and antiapoptotic factors by human adipose stromal cells," *Circulation*, vol. 109, no. 10, pp. 1292–1298, 2004.

[46] G. E. Kilroy, S. J. Foster, X. Wu et al., "Cytokine profile of human adipose-derived stem cells: expression of angiogenic, hematopoietic, and pro-inflammatory factors," *Journal of Cellular Physiology*, vol. 212, no. 3, pp. 702–709, 2007.

[47] C. A. Ribeiro, J. S. Fraga, M. Grãos et al., "The secretome of stem cells isolated from the adipose tissue and Wharton jelly acts differently on central nervous system derived cell populations," *Stem Cell Research & Therapy*, vol. 3, no. 3, p. 18, 2012.

[48] P. Succar, E. J. Breen, D. Kuah, and B. R. Herbert, "Alterations in the secretome of clinically relevant preparations of adipose-derived mesenchymal stem cells cocultured with hyaluronan," *Stem Cells International*, vol. 2015, Article ID 421253, p. 16, 2015.

[49] H. Kupcova Skalnikova, "Proteomic techniques for characterisation of mesenchymal stem cell secretome," *Biochimie*, vol. 95, no. 12, pp. 2196–2211, 2013.

[50] D. T. Graves, Y. Jiang, and A. J. Valente, "The expression of monocyte chemoattractant protein-1 and other chemokines by osteoblasts," *Frontiers in Bioscience*, vol. 4, pp. D571–D580, 1999, August 2016, http://www.ncbi.nlm.nih.gov/pubmed/10393126.

[51] P. Proost, C. De Wolf-Peeters, R. Conings, G. Opdenakker, A. Billiau, and J. Van Damme, "Identification of a novel granulocyte chemotactic protein (GCP-2) from human tumor cells. In vitro and in vivo comparison with natural forms of GRO, IP-10, and IL-8," *Journal of Immunology*, vol. 150, no. 3, pp. 1000–1010, 1993.

[52] T. Sobue, T. Gravely, A. Hand et al., "Regulation of fibroblast growth factor 2 and fibroblast growth factor receptors by transforming growth factor β in human osteoblastic MG-63 cells," *Journal of Bone and Mineral Research*, vol. 17, no. 3, pp. 502–512, 2002.

[53] S.-H. Shim, J. H. Hah, S.-Y. Hwang, D. S. Heo, and M.-W. Sung, "Dexamethasone treatment inhibits VEGF production via suppression of STAT3 in a head and neck

cancer cell line," *Oncology Reports*, vol. 23, no. 4, pp. 1139–1143, 2010, August 2016, http://www.ncbi.nlm.nih.gov/pubmed/20204302.

[54] J. J. Logie, S. Ali, K. M. Marshall, M. M. S. Heck, B. R. Walker, and P. W. F. Hadoke, "Glucocorticoid-mediated inhibition of angiogenic changes in human endothelial cells is not caused by reductions in cell proliferation or migration," *PloS One*, vol. 5, no. 12, article e14476, 2010.

[55] K. Hu and B. R. Olsen, "Osteoblast-derived VEGF regulates osteoblast differentiation and bone formation during bone repair," *The Journal of Clinical Investigation*, vol. 126, no. 2, pp. 509–526, 2016.

[56] Y.-Q. Yang, Y.-Y. Tan, R. Wong, A. Wenden, L.-K. Zhang, and A. B. M. Rabie, "The role of vascular endothelial growth factor in ossification," *International Journal of Oral Science*, vol. 4, no. 2, pp. 64–68, 2012.

[57] M. Ishikawa, H. Ito, T. Kitaori et al., "MCP/CCR2 signaling is essential for recruitment of mesenchymal progenitor cells during the early phase of fracture healing," *PloS One*, vol. 9, no. 8, article e104954, 2014.

[58] X. Li, L. Qin, M. Bergenstock, L. M. Bevelock, D. V. Novack, and N. C. Partridge, "Parathyroid hormone stimulates osteoblastic expression of MCP-1 to recruit and increase the fusion of pre/osteoclasts," *The Journal of Biological Chemistry*, vol. 282, no. 45, pp. 33098–33106, 2007.

[59] A. Bajek, N. Gurtowska, J. Olkowska, L. Kazmierski, M. Maj, and T. Drewa, "Adipose-derived stem cells as a tool in cell-based therapies," *Archivum Immunologiae et Therapiae Experimentalis (Warsz)*, vol. 64, no. 6, pp. 443–454, 2016.

[60] B. Péault, G. Asatrian, D. Pham, W. R. Hardy, and A. W. James, "Stem cell technology for bone regeneration: current status and potential applications," *Stem Cells and Cloning: Advances and Applications*, vol. 8, p. 39, 2015.

[61] G. K. Sándor, V. J. Tuovinen, J. Wolff et al., "Adipose stem cell tissue–engineered construct used to treat large anterior mandibular defect: a case report and review of the clinical application of good manufacturing practice–level adipose stem cells for bone regeneration," *Journal of Oral and Maxillofacial Surgery*, vol. 71, no. 5, pp. 938–950, 2013.

[62] M. Barba, C. Cicione, C. Bernardini, F. Michetti, and W. Lattanzi, "Adipose-derived mesenchymal cells for bone regereneration: state of the art," *BioMed Research International*, vol. 2013, Article ID 416391, p. 11, 2013.

[63] B. E. Grottkau and Y. Lin, "Osteogenesis of adipose-derived stem cells," *Bone Research*, vol. 1, no. 2, pp. 133–145, 2013.

Hindawi
Stem Cells International
Volume 2017, Article ID 9082869, 9 pages
https://doi.org/10.1155/2017/9082869

Research Article

Bone Regeneration Induced by Bone Porcine Block with Bone Marrow Stromal Stem Cells in a Minipig Model of Mandibular "Critical Size" Defect

Antonio Scarano,[1] Vito Crincoli,[2] Adriana Di Benedetto,[3] Valerio Cozzolino,[1] Felice Lorusso,[1] Michele Podaliri Vulpiani,[4] Maria Grano,[5] Zamira Kalemaj,[6] Giorgio Mori,[3] and Felice Roberto Grassi[7]

[1]*Department of Medical, Oral and Biotechnological Sciences and CeSI-Met, University of Chieti-Pescara, Chieti, Italy*
[2]*Interdisciplinary Department of Medicine, University of Bari "A. Moro", Bari, Italy*
[3]*Department of Clinical and Experimental Medicine, Medical School, University of Foggia, Foggia, Italy*
[4]*Department of Animals Sperimentation, Istituto Zooprofilattico Sperimentale dell'Abruzzo e del Molise "G. Caporale", Teramo, Italy*
[5]*Department of Emergency and Organ Transplantation, University of Bari "A. Moro", Bari, Italy*
[6]*Department of Surgical Sciences, Dental School, University of Turin, Torino, Italy*
[7]*Department of Basic and Medical Sciences, Neurosciences and Sense Organs, University of Bari, Bari, Italy*

Correspondence should be addressed to Antonio Scarano; ascarano@unich.it

Received 21 July 2016; Revised 2 September 2016; Accepted 19 March 2017; Published 2 May 2017

Academic Editor: Dario Coletti

Introduction. Adding stem cells to biodegradable scaffolds to enhance bone regeneration is a valuable option. Different kinds of stem cells with osteoblastic activity were tested, such as bone marrow stromal stem cells (BMSSCs). *Aim*. To assess a correct protocol for osteogenic stem cell differentiation, so BMSSCs were seeded on a bone porcine block (BPB). *Materials and Methods*. Bone marrow from six minipigs was extracted from tibiae and humeri and treated to isolate BMSSCs. After seeding on BPB, critical-size defects were created on each mandible of the minipigs and implanted with BPB and BPB/BMSSCs. After three months, histomorphometric analysis was performed. *Results*. Histomorphometric analysis provided percentages of the three groups. Tissues present in control defects were 23 ± 2% lamellar bone, 28 ± 1% woven bone, and 56 ± 4% marrow spaces; in BPB defects were 20 ± 5% BPB, 32 ± 2% lamellar bone, 24 ± 1% woven bone, and 28 ± 2% marrow spaces; in BPB/BMSSCs defects were 17 ± 4% BPB/BMSSCs, 42 ± 2% lamellar bone, 12 ± 1% woven bone, and 22 ± 3% marrow spaces. *Conclusion*. BPB used as a scaffold to induce bone regeneration may benefit from the addition of BDPSCs in the tissue-engineered constructs.

1. Introduction

1.1. Bone Regeneration with Stem Cells. A common problem facing the dental community is the rehabilitation of oral functions in patients with edentulous atrophic alveolar process. Improvement of successful methods to induce bone regeneration is a continuous challenge in dentistry [1]. In recent years, the use of biomaterials to enhance bone regeneration has greatly developed because of their capacity to mimic the natural environment of the extracellular matrix [2]. To increase the effectiveness of this methodology, the use of biomaterials, or scaffolds, in association with stem cells with osteoblast-like activity has been introduced [3, 4]. In 1968, Friedenstein et al. first published works demonstrating the osteogenic property of bone marrow transplants in different tissues and the possibility of cultivating, cloning, and retransplanting in vivo [5]. A number of stem cell studies have followed [6, 7]. Adult mesenchymal stem cells can be obtained

from many sources. In particular, they can successfully be differentiated in osteoblast-like cells originating from different dental tissues [8–11].

1.2. BMSSC. Among the stem cells with the desired osteoblastic activity, BMSSCs have proved effective in inducing new bone formation in critical-size defects of animal models [12–14]. Indeed, the ability of those cells to enhance bone formation can even be found in scaffold-type constructions, tridimensional shapes, and the culturalization of cells. In recent years, several matrices have been used, from nonresorbable biomaterials, such as hydroxyapatite, in different relationships with BMSSCs, including layers encapsulated in hydrogel [15] or calcined bovine bone [16], to resorbable ones such as beta-tri-calcium phosphate (β-TCP) or calcium phosphate (CP) [17]. When comparing matrices, one study found a better response in vivo and in vitro from calcium phosphate rather than hydroxyapatite on increased trabecula formation, cell density, and decreased fibrosis [18]. Regardless of the results, there is still no universally accepted scaffold and each one has to be tested individually.

On those scaffolds, BMSSCs are cultured in situ improving bone healing and matrix reabsorption with an osteogenic effect. In a recent experiment, BMSSCs with an enriched chitosan scaffold produced bone, more than CP alone in rat muscle [19]. BMSSCs are the nonhematopoietic elements of the bone marrow (BM). This cluster of cells comprises less than 0.01% of the overall cell population residing in the BM [20]. The nonhomogeneous nature of BMSSCs is clearly evident when examining individual colonies. Different cell morphologies include spindle cells, fibroblast-like cells, or colonies of large and flat-shaped cells. Furthermore, if such cultures are allowed to develop for up to 20 days, phenotypic heterogeneity is also noted. Some colonies are highly positive for alkaline phosphatase (ALP), while others are negative, and a third type is positive in the central region and negative in the periphery [21]. Some colonies form nodules of mineralized matrix which can be identified by alizarin red or von Kossa staining for calcium. Yet others accumulate fat, identified by oil red O staining [22], while some colonies form cartilage as identified by alcian blue staining [23]. In a recent study [24] on mice mesenchymal stem cells derived from dental pulp and periosteum, a difference in bone regeneration was found, confirming the hypothesis of enhancing regeneration with mesenchymal stem cells. It was measured as a percentage of bone volume on the total defect area, when seeded with scaffold block deproteinized porcine bone (BDPB) alone and with dental pulp and periosteal stem cells. Qualitative observations on bone histomorphometry classify the nature of bone elements as either lamellar or woven. The presence of residual biomaterial and inflammatory mediators within the defects was also observed. A similar model has been adopted in this study to evaluate different degrees of bone regeneration using bone porcine block with bone marrow stromal stem cells (BPB/BMSSCs).

The aim of this study is to assess a correct protocol for osteogenic stem cell differentiation of an osteoblastic phenotype on an appropriate substrate: BMSSCs seeded on a bone porcine block (BPB) in order to increase performance in bone regeneration using scaffold from the block and inducing a qualitative superior regeneration with BMSSCs.

2. Materials and Methods

2.1. Animals. Six adult minipigs of a mean age of 2 years were used in the present study. The mean of weight was 29 kg ± 4 kg. The study protocol was approved by the Italian National Health (protocol number 7326-26/06/2013).

The animals were maintained according to the guidelines for ethical conduct developed by the European Communities Council Directive of November 24, 1986 (86/609/EEC). All efforts were made to minimize pain or discomfort of the animals. In each emi-mandibula, 3 defects (5 mm wide and 5 mm deep) were created. The defects were then filled in the following way: one defect with a bone porcine block (BPB) (OsteoBiol, Tecnoss, Coazze, Italy) with BMSSCs was inserted, one filled with bone porcine block left without BMSSCs empty, and one defect was left blank as control. A total of 36 critical-size circular defects (5 mm diameter; 5 mm thickness) were created.

2.2. In Vitro Cell Culture. Bone marrow was harvested according to the following surgical technique.

In the minipigs, the bone marrow was harvested from the proximal tibiae and humeri. The volume of blood circulating in pigs is 65–75 ml/kg. The animals used for the experiments were about ~30 kg of body weight; thus, a total volume of 20 ml of bone marrow per animal was safely collected, specifically 5 ml per bone segment considering the two humeri and the two tibias, obtaining approximately 2×10^9 bone marrow mononuclear cells (BMMNCs) per pig [25–27]. The pigs were anesthetized as previously described. The technique was performed in an aseptic environment and using sterile gloves and instruments, after shaving and a thorough disinfection of the skin in the harvesting site. The procedure was realized with a needle specifically built to harvest the bone marrow, 11 gauges × 110 mm, which has a cutting edge and a spindle. The harvesting site was in correspondence with the medial tibia and the proximal humerus of both limbs, where the compact bone is more compliant having this area a relatively thin cortical bone. The pigs were placed in the lateral decubitus position. The bone marrow aspiration needle was passed through the skin with the spindle in position. In the the cortical bone, the spindle was removed, and the bone marrow, in the volume of 5 ml for skeletal segment, was aspirated into a sterile syringe containing 0.2 ml of heparin (1000 units/ml). The samples were quickly transferred to the laboratory for the subsequent steps of isolation and stem cell differentiation.

2.3. BMSSC Isolation, Culture, and Scaffold Preparation. In order to obtain BMSSCs, bone marrow aspirates were processed as previously described briefly [28, 29]: samples were subjected to Histopaque 1077 density gradient (Sigma-Aldrich, St. Louis, MO, USA). The buffy coat cell fraction was entirely harvested and incubated in a humidified atmosphere of 5% CO2 at 37°C to obtain the BMNCs: after 24 hours, the nonadherent cell fraction was discarded while

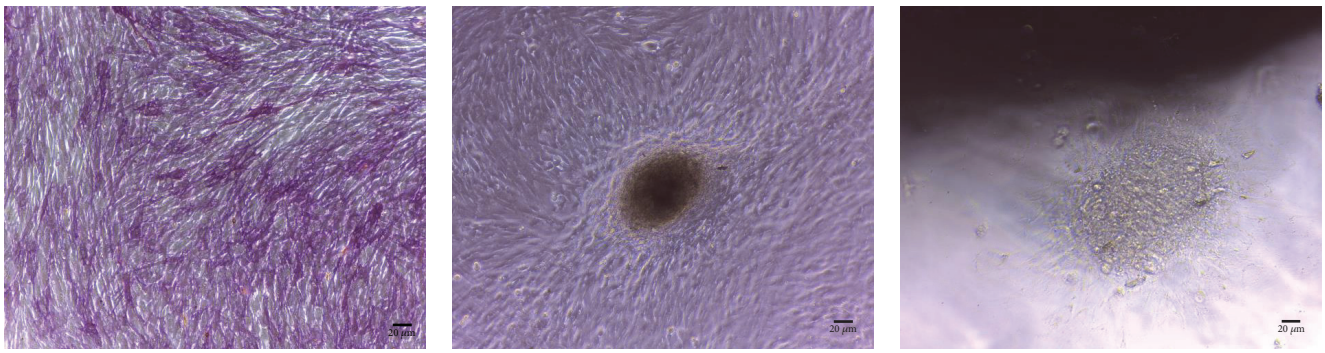

(a) (b) (c)

Figure 1: (a) In vitro appearance of BMSSCs forming a matrix nodule after two weeks of culture in the presence of osteoblast differentiation medium. (b) Cultures of BMSSCs stained for ALP expression. (c) In vitro appearance of BMSSCs forming a matrix nodule in proximity of BPB before grafting.

the adherent cell fraction was cultured for 48–72 hours until it reached a semiconfluent status (Figure 1(a)).

The BMSSC cultures, thus obtained, were trypsinized, counted, and used to be tested and then integrated in the scaffolds. To control the osteogenic differentiation, a cell fraction was cultured in the presence of ascorbic acid 50 ng/ml for ten days and then stained for alkaline phosphatase (ALP) expression as previously described (Figure 1(b)). From each animal, 1×10^6 BMSSCs were used for flow cytometric assay that demonstrated mesenchymal stem cell marker expression. The bone porcine block scaffold used presented a cylindrical shape, 5 mm in diameter, and 5 mm in length. They were rigid cancellous blocks and thus are able to maintain in time the original graft volume, which is particularly important in cases of large regenerations.

Before being integrated with the cells, the scaffolds were hydrated in alpha-MEM and incubated three times for 30 min in a humidified atmosphere of 5% CO2 at 37°C. Prior to cell seeding, the volume of medium contained in the tridimensional structure of the scaffolds was removed by absorption using sterile cotton balls. Then 100 μl BMSSC suspension (5×10^5 cells) was slowly dripped onto the scaffolds to avoid overflow. The scaffolds seeded with BMSSCs were incubated in a humidified atmosphere of 5% CO2 at 37°C for 2 h, after which the additional culture medium was added to fully cover the scaffolds. To ensure that cells can successfully attach to the scaffolds, the cultures were incubated in a humidified atmosphere of 5% CO2 at 37°C for 3 days. After 3 days, 50 μg/ml ascorbic acid was added and the media was changed every 2 days for two weeks in order to obtain, before scaffold grafting, BMSSC osteogenic differentiation on the cells integrated into the scaffolds (Figure 1(c)).

2.4. In Vivo Mandibular Defect. Surgery was performed under general anesthesia with induction of Zoletil 100 (tiletamine hydrochloride + zolazepam hydrochloride) at a dosage of 6 mg/kg IM. Maintenance with isoflurane at 2/2.5% in oxygen. Three bilateral critical-size circular defects (5 mm diameter; 5 mm thickness) were created using a hand drill and trephine bit in the mandibular body (Figure 2). Posterior region of the mandible was chosen because of the presence of regular thickness of the vestibular cortical plate; defects

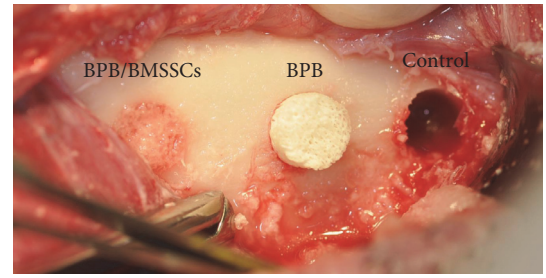

Figure 2: Three critical-size circular defects. Clinical situation during surgery.

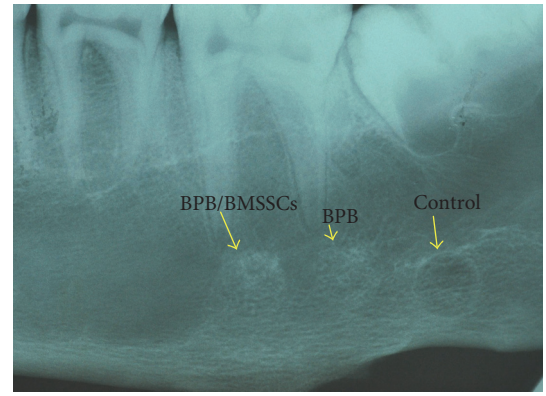

Figure 3: Standard RX 55 × 75 mm films have been performed on retrieved mandibulae to find the perfect position and alignment of biomaterial scaffolds with the bone itself.

were created with those specific measures to better place the cylindrical bone porcine blocks, perfectly adapted, into the defects. Each defect was filled randomly by the surgeon. During the procedure, sterile saline was dripped over the drilling site in order to avoid extensive heating and to protect surrounding bone.

Treatment of postoperative pain with flunifen (flunixin meglumine) at a dosage of 2.2 mg/kg IM once (for all) or twice depending on whether or not the animal showed pain. Antibiotic treatment with Repen (Benzilpenicillina

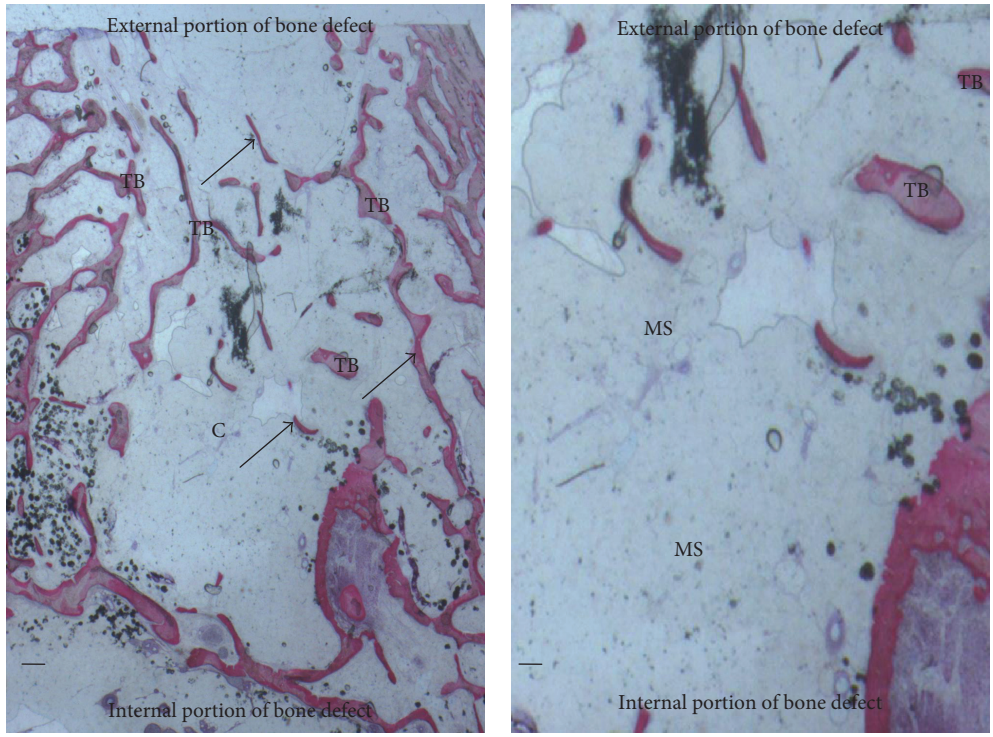

(a) (b)

FIGURE 4: (a) Control group. Trabecular bone (TB) was present in the central portion of the bone defects (c). New bone (arrows) extended to the basal third from the margin of the bone defect. Acid fuchsin and toluidine blue. Bar = 200 μ. (b) Previous image at higher magnification. Isolated trabecular bone (TB was seen throughout the medullary space (MS). Acid fuchsin and toluidine blue. Bar = 200 μ.

dihydrostreptomycin) at a dosage of 20.000 IU of Benzil-penicillina and 12.5 mg of dihydrostreptomycin/kg for 5 days IM.

2.5. Histomorphometry. The specimens were washed in saline solution and immediately fixed in 4% paraformaldehyde and 0.1% glutaraldehyde in 0.15 M cacodylate buffer at 4°C and pH 7.4, to be processed for histology. Cone beam computed tomography (CBCT) (Vatech Ipax 3D PCH-6500, Fort Lee, NJ USA) and standard RX 55 × 75 mm films (Figure 3) were performed on retrieved mandibulae. DICOM data were elaborated with Ez3D Plus Software (EZ3D Plus, VATECH Global Fort Lee, NJ USA) to elaborate 3D model specimens and find the perfect position and alignment of biomaterial scaffolds with the bone itself. CBCT analysis also permits to evaluate interface between the scaffold and the surrounding native bone. After scaffold position identification by CBCT, the posterior region of mandibulae was processed with a band saw to obtain thin ground sections with the Precise Automated System (Assing, Roma, Italy) The specimens were dehydrated in an ascending series of alcohol rinses and embedded in a glycolmethacrylate resin (Technovit 7200 VLC, Kulzer, Wehrheim, Germany). After polymerization, the specimens were sectioned in mesiodistal direction with 50 μm of distance from one slide to the subsequent one, with a high-precision diamond disc at about 150 μm and ground down to about 30 μm with a specially designed grinding machine. A total of 3 slides were obtained for each specimen. The slides were stained with acid fuchsin and toluidine blue, and they were observed in normal transmitted light under a Leitz Laborlux microscope (Leitz, Wetzlar, Germany).

Histomorphometry was carried out using a light microscope (Laborlux S, Leitz, Wetzlar, Germany) connected to a high-resolution video camera (3CCD, JVC KY-F55B, JVC®, Santa Clara, CA, USA) and interfaced to a monitor and PC (Intel Pentium III 1200 MMX, Intel®, Yokohama, Japan). This optical system was associated with a digitizing pad (Matrix Vision GmbH, Oppenweiler, Germany), and a histometry software package with image capturing capabilities (Image-Pro Plus 4.5, Media Cybernetics Inc., Immagini & Computer Snc Milano, Italy). Evaluation of the percentages of residual biomaterial, new bone formation, and marrow space was performed in the mandibular defects of the three experimental groups. Each section was examined at at least 6x magnification, and the entire area of the section was evaluated. Digital images of each section were acquired and used to trace the areas identified as new bone, residual particle, and marrow spaces. Image manipulation software was used to create individual layers of new bone, residual particles, and marrow spaces. These layers were then converted to a binary (black and white) form, and the area by percentage of each of the three layers was digitally calculated, based on the number of pixels, using image analysis software.

2.6. Statistical Analysis. A power analysis was performed using clinical software, freely available on the site http://clincalc.com/stats/samplesize.aspx, for determining the number of bone defects needed to achieve statistical significance

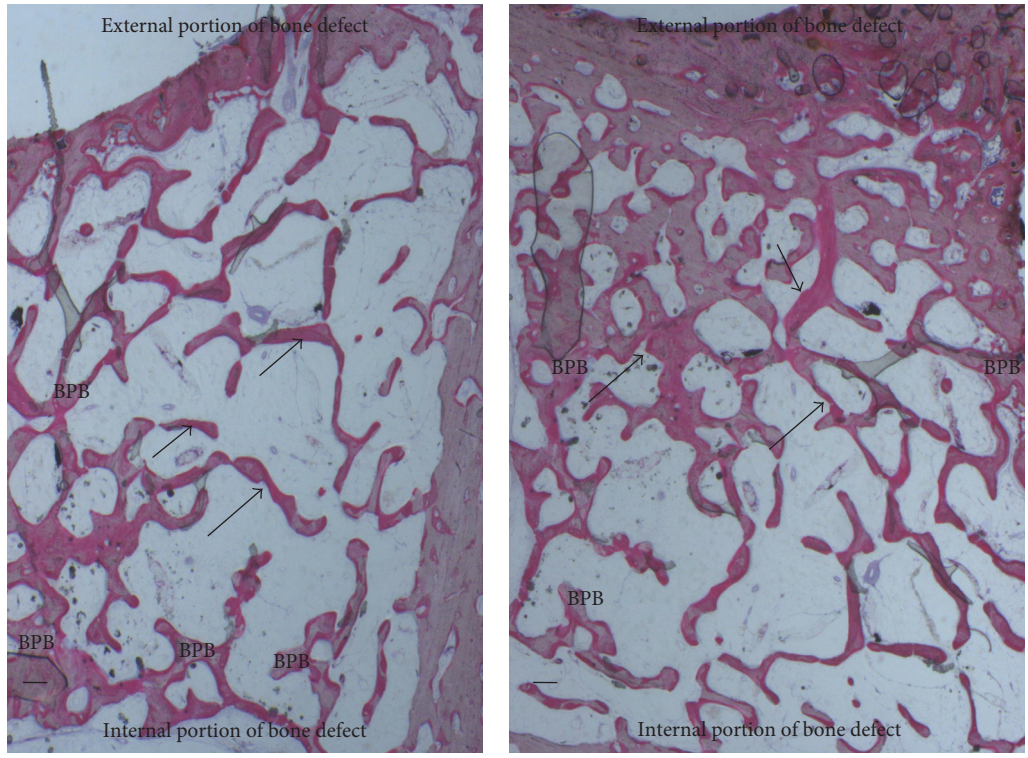

(a) (b)

Figure 5: (a) BPB group. New bone surrounded the block material (BPB). New bone (arrows) extended also in the central part of the bone defects. Acid fuchsin and toluidine. Bar = 200 μ. (b) BPB/BMSSCs group. New bone (arrows) was deposited in the block material (BPB). No fibrous tissue was observed in the defect area. Acid fuchsin and toluidine. Bar = 200 μ.

for quantitative analyses of histomorphometry. A calculation model was adopted for dichotomous variables (yes/no effect) by putting the effect incidence designed to caution the reasons at 20% for controls and 95% for treated. The optimal number of bone defects for analysis is 10, whereas in the present study, 12 defects were created per group.

Analysis of variance was used to determine the statistical significance of the differences between the three examined groups. The percentages of new bone formation, marrow spaces, and residual biomaterial were expressed as means ± standard deviations. The significance of the differences observed was evaluated using the Bonferroni test for multiple comparisons: threshold for statistical significance was set at $P < .05$.

3. Results

Histomorphometric results after analysis showed difference in bone regeneration between the BPB and BPB/BMSSC groups evaluated measuring percentages of the lamellar bone, woven bone, marrow spaces, and residual BPB. The control group showed a regular healing pattern. No macroscopic defects were found after three months.

3.1. Controls. Bone tissue was evident with well-differentiated cells and mineralized matrix: osteoid, osteoblasts, osteocytes, and blood vessels. Regenerating osseous tissue extending from the margin of the axial walls was observed. Fibrous tissue still occupied little space in the defect area (Figure 4). Traces of new bone from the periosteum were observed, overlying the superficial portion of the bone defect. The tissues present in the defect were composed of 23 ± 2% of the lamellar bone, 28 ± 1% of the woven bone, and 56 ± 4% of the marrow spaces.

3.2. Bone Porcine Block (BPB). At low magnification, it was possible to observe that almost all the block materials were surrounded by the mature bone: only around some fields was it possible to observe the presence of the osteoid material. The material particles were near marrow spaces in only a few areas. In all specimens, no acute inflammatory cell infiltrate or foreign body reactions were present around the particles or at the interface with the bone. All blocks were colonized and surrounded by the newly formed bone (Figure 5(a)). This bone was woven or lamellar. Inside the BPB, there was always the presence of newly formed bone. No epithelial cells or connective tissues were observed at the interface. The regenerated bone tissue extended to approximately all of the bone defects except in the central area, where the fibrous tissue still occupied a part of the interparticular spaces. Prominent lamination of the mature bone was observed. The periphery and central portion of the experimental cavities showed mineralized new bone formation (Figure 6(a)). The bone defects were not completely healed, and many particles or BPB were visible. The tissues present in the defects were composed of 20 ± 5% of BPB, by 32 ± 2% of the lamellar

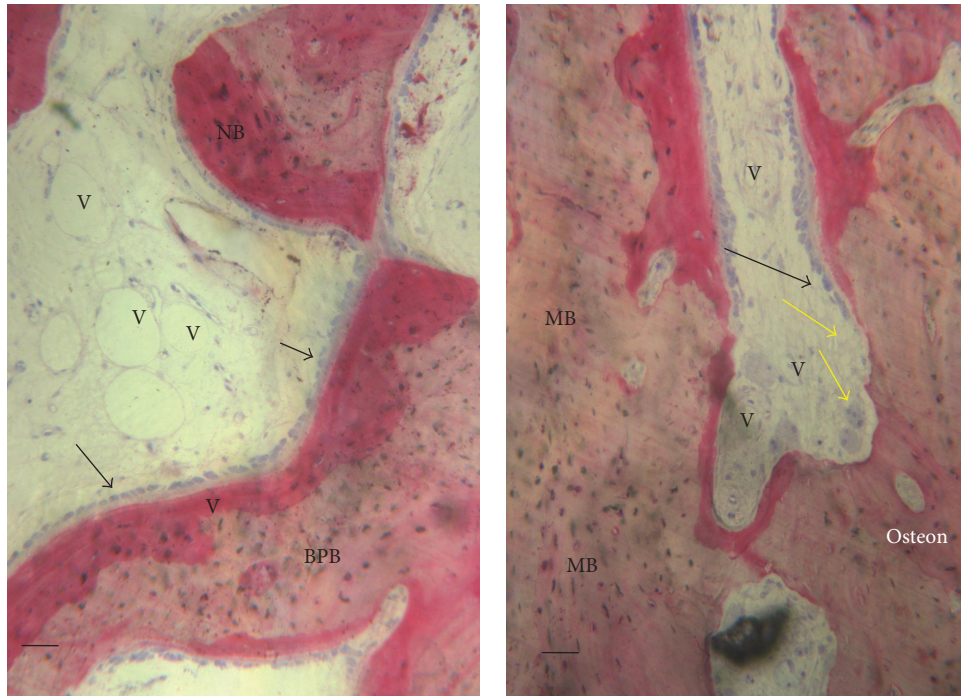

(a) (b)

Figure 6: (a) BPB group. Bone tissue was deposited in the block material (BPB). No fibrous tissue was observed in the defect area. Vessels (V) were present in the central part of the bone defects. New bone (NB) and osteoblasts in close contact with the block material acid fuchsin and toluidine blue. Bar = 100 μ. (b) BPB/BMSSCs group. Mature bone (MB) in the bone defect. Bone morphology was more mature and well organized, presenting a primary osteon. A basic multicellular unit of osteoclasts cells (yellow arrows) that dissolves an area of the bone surface and then fills it with new bone by osteoblasts (white arrows) to form haversian systems or osteons. A vessels (V) were present in the central part of the bone defects. Acid fuchsin and toluidine blue. Bar = 100 μ.

bone, 24 ± 1% of the woven bone, and by 28 ± 2% of the marrow spaces.

3.3. Bone Porcine Block with Bone Marrow Stromal Stem Cells (BPB/BMSSCs). Regenerating osseous tissue was observed surrounding some BPB extending from the margin of the axial walls. Bone tissue was deposited in the block (Figure 5(b)). New bone extended to the basal third from the margin of the bone defect and partially surrounded the BPB block. New bone extended also in the central part of the bone defects (Figure 5(b)). No fibrous tissue was observed in the defect area. Traces of new bone from the periosteum were seen overlying the superficial portion of the bone defect. Bone morphology was more mature and well organized presenting a lamellar pattern compared with bone around defect. Higher magnification of the bone tissue around the block showed that no gaps were present at the bone-biomaterial interface, and the bone seemed to always be in close contact with the block (Figure 6(b)). In some fields, osteoblasts were observed in the process of apposing bone directly on the block surface. No acute inflammatory cells infiltrate, or foreign body reactions were present around the particles or at the interface with the bone. All defects were filled with newly formed dense bone and bone marrow. The tissues present in the defects were composed of 17 ± 4% of BPB/BMSSCs, by 42 ± 2% of the lamellar bone, 12 ± 1% of the woven bone, and by 22 ± 3% of the marrow spaces.

3.4. Statistical Evaluation. Statistically significant differences were found in the percentage of the marrow space and lamellar bone between the three groups ($P < .001$). In detail, between BPB and BMSSCs/BPB, the difference of the lamellar and woven bones was found to be statistically significant with $P < .001$ and $P < .01$ considering marrow spaces, while no difference was found in biomaterial percentage between the two test groups (Figure 7).

4. Discussion

This study found a relevant difference in bone regeneration using a bone porcine block scaffold seeded with bone marrow stromal stem cells when compared with bone porcine block without any kind of treatment. Literature presents a variety of enriching stem/progenitor cells for use in cell-based bone regeneration. They have been explored both clinically and experimentally with varying degrees of success. Bone porcine block scaffolds are promising for a variety of tissue engineering applications. BPB scaffolds have a hard structure which prevents defects and creates the correct environment for bone regeneration without the risk of soft tissue colonization. BPB scaffolds are perfect material for local bone regeneration due to their biocompatibility, osteoconductivity [30], and porosity which allows for efficient BMSSC seeding and growth [31]. BPB biodegradation analysis was not the aim of this study, so the relationship between scaffold biodegradation

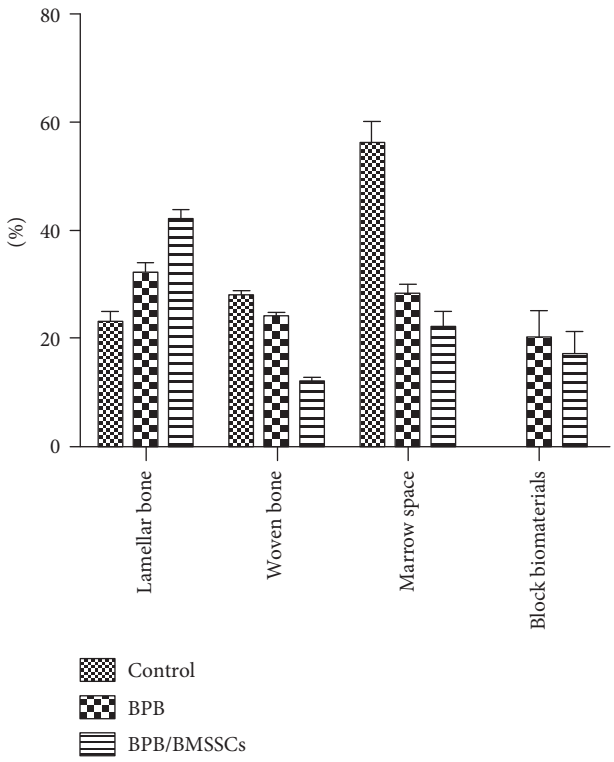

Figure 7: Percentage bar graphic showing difference between site compositions in three groups: control, bone porcine block, and bone marrow stromal stem cells/bone porcine block.

and bone formation has not been studied in detail, only measured as a percentage in histological evaluations.

In the present study, a 3D software analysis of CBCT was performed and histological images were acquired in which BPB implants were well positioned and induced a higher amount of BMD and SUV within the mandibular defects as compared to BPB without BMSSCs. Despite the contribution of BMSSCs, bone formation is visible in both groups. This study aimed to further characterize bone regeneration induced by BMSSCs in these scaffold-based implants by using histological parameters. The percentages of residual biomaterial, new bone formation, and marrow spaces in the mandibular defects filled with BPB alone or in combination with BMSSCs were evaluated. Histomorphometry was carried out individually for bone, marrow spaces, and residual graft material with a measure error, and the sum will never give 100. Moreover, a qualitative description of the histomorphology of the mandibular defects was provided. The description included the characterization of newly formed bone, the presence of inflammatory cell infiltrate, and the position of bone formation within the defects. The histomorphometric results showed that, at the observed time, the amount of marrow spaces and residual graft material more than new bone formation are always quite different from 100%, this is due to the fact that the three measurements are carried out individually with a margin of error and then the sum of the error is inclusive of the measurement performed in the BPB, lamellar bone, or woven bone and marrow spaces. The results showed that although the percentage of residual biomaterial was similar among the experimental groups, the percentage of formation of new bone and marrow space was different. The present study showed that the BPB/BMSSC group resulted in a significantly greater bone formation in alveolar bone defects in the minipig mandible than BPB groups alone. This suggests that BPB can produce synergic effect with BMSSCs. The minipig was chosen as an animal model because of its similarities to humans in terms of platelet count, clotting parameters, metabolic rate, bone structure, and characteristics of their MSCs [32]. An alveolar defect model offers several advantages for the histologic evaluation of bone tissue-engineered constructs. The surgical procedure is simple, with a limited risk of infection, and a similar intervention by grafting is advocated clinically. A true critical-sized mandibular defect in the minipig model is more than 5 mm [33]. Recently, the synergic effect of MSCs and platelet-rich plasma incorporated into a scaffold on fluorohydroxyapatite and bone formation in surgical bone defects in the edentulous mandible of minipigs has been reported [34]. These results suggest that MSCs show a positive effect on bone formation when combined with autologous growth factors [34]. In fact, the platelet growth factors and biomaterial combination were used with success for bone regeneration [35] and soft tissue augmentation [36, 37]. In the present study, a mandibular defect model was chosen to determine the potential ability of BPB to enhance bone formation when it was supplemented by BMSSCs. Each minipig served as its own control. In our study, BPB alone was used as a scaffold material for testing BMSSC bone induction. The reason for selecting this particular biomaterial was that BPB has been proven to be a suitable carrier for osteoblast-like cells, bone morphogenic proteins, and growth factors. This particular biomaterial has been proven to be a suitable carrier for osteoblast in vertical ridge augmentation of atrophic posterior mandible [38]. This biomaterial has a hard consistency and can be used to block the fragments of the osteotomized segments. When BPB was placed in the surgically created defects, it became properly integrated in the newly lamellar bone during healing [39]. This indicates that the material was osteoconductive and acted as a natural scaffold for new bone formation. Biocompatibility of BPB was confirmed by histological analysis [40]. The formation of a fibrous capsule around the particles did not occur in any section. In this respect, the current findings are consistent with observations made in human histologic studies. These studies indicate that an intimate contact is always established between BPB particles and newly formed mineralized bone [40]. The present findings show that the superior contribution of BMSSCs to bone regeneration is due to the formation of mature (lamellar) bone. Moreover, the contribution of stem cells is evident when analyzing the percentage of woven bone. Qualitative histomorphometry also showed that seeding of stem cells into the scaffolds resulted in greater bone formation in BPB/BMSSCs construct. This is evidenced by the presence of bone tissue in the periphery and in the central area of the defect. Most notably, osteogenesis was observed in the absence of inflammatory processes which may interfere with the process of regeneration [41].

5. Conclusion

This study demonstrates that BPB when used as a scaffold to induce bone regeneration may benefit from the addition of BMSSCs in the tissue-engineered constructs. Our data shows the healing pattern in a minipig model, but further research is needed for human applications.

Abbreviations

BMMNC: Bone marrow mononuclear cell
BMSSC: Bone marrow stromal stem cell
BPB: Bone porcine block.

Additional Points

Research Highlights. Bone marrow stromal stem cells (BMSSCs) were obtained from 6 minipigs. BMSSCs are suitable to be seeded and cultured on a biomaterial such as bone porcine block (BPB). BMSSCs on BPB showed better results in bone regeneration than those on the control and BPB alone groups.

Conflicts of Interest

The authors declare no conflicting financial or other competing interests.

Authors' Contributions

Giorgio Mori and Felice Roberto Grassi contributed equally to this work.

Acknowledgments

This work was partially supported by the Ministry of Education, University, Research (M.I.U.R.), PRIN 2009 Protocol no. 20098M9R_001, Rome, Italy.

References

[1] J. D. Bashutski and H. L. Wang, "Periodontal and endodontic regeneration," *Journal of Endodontia*, vol. 35, no. 3, pp. 321–328, 2009.

[2] J. E. Davies, R. Matta, V. C. Mendes, and P. S. Perri de Carvalho, "Development, characterization and clinical use of a biodegradable composite scaffold for bone engineering in oro-maxillo-facial surgery," *Organogenesis*, vol. 6, no. 3, pp. 161–166, 2010.

[3] F. M. Chen, H. H. Sun, H. Lu, and Q. Yu, "Stem cell-delivery therapeutics for periodontal tissue regeneration," *Biomaterials*, vol. 33, no. 27, pp. 6320–6344, 2012.

[4] P. Bianco and P. Robey, "Stem cells in tissue engineering," *Nature*, vol. 414, no. 6859, pp. 118–121, 2001.

[5] A. Friedenstein, "Stromal mechanisms of bone marrow: cloning in vitro and retransplantation in vivo," *Haematology and Blood Transfusion*, vol. 25, pp. 19–29, 1980.

[6] A. J. Friedenstein, R. K. Chailakhyan, and U. V. Gerasimov, "Bone marrow osteogenic stem cells: In vitro cultivation and transplantation in diffusion chambers," *Cell and Tissue Kinetics*, vol. 20, no. 3, pp. 263–272, 1987.

[7] A. J. Friedenstein, K. V. Petrakova, A. I. Kurolesova, and G. P. Frolova, "Heterotopic of bone marrow. Analysis of precursor cells for osteogenic and hematopoietic tissues," *Transplantation*, vol. 6, no. 2, pp. 230–247, 1968.

[8] G. Mori, G. Brunetti, A. Oranger et al., "Dental pulp stem cells: osteogenic differentiation and gene expression," *Annals of the new York Academy of Sciences*, vol. 1237, no. 1, pp. 47–52, 2011.

[9] A. Di Benedetto, G. Brunetti, F. Posa et al., "Osteogenic differentiation of mesenchymal stem cells from dental bud: role of integrins and cadherins," *Stem Cell Research*, vol. 15, no. 3, pp. 618–628, 2015.

[10] G. Mori, A. Ballini, C. Carbone et al., "Osteogenic differentiation of dental follicle stem cells," *International Journal of Medical Sciences*, vol. 9, no. 6, pp. 480–487, 2012.

[11] G. Mori, M. Centonze, G. Brunetti et al., "Osteogenic properties of human dental pulp stem cells," *Journal of Biological Regulators and Homeostatic Agents*, vol. 24, no. 2, pp. 167–175, 2010.

[12] Y. Yamada, M. Ueda, T. Naiki, M. Takahashi, K. Hata, and T. Nagasaka, "Autogenous injectable bone for regeneration with mesenchymal stem cells and platelet rich plasma: tissue-engineered bone regeneration," *Tissue Engineering*, vol. 10, no. 5-6, pp. 955–964, 2004.

[13] L. Meinel, R. Fajardo, S. Hofmann et al., "Silk implants for the healing of critical size bone defects," *Bone*, vol. 37, no. 5, pp. 688–698, 2005.

[14] M. H. Mankani, S. A. Kuznetsov, R. M. Wolfe, G. W. Marshall, and P. G. Robey, "In vivo bone formation by human bone marrow stromal cells: reconstruction of the mouse calvarium and mandible," *Stem Cells*, vol. 24, no. 9, pp. 2140–2149, 2006.

[15] A. Sarker, J. Amirian, Y. K. Min, and B. T. Lee, "HAp granules encapsulated oxidized alginate-gelatin-biphasic calcium phosphate hydrogel for bone regeneration," *International Journal of Biological Macromolecules*, vol. 81, pp. 898–911, 2015.

[16] Y. Liu, L. Ming, H. Luo et al., "Integration of a calcined bovine bone and BMSC-sheet 3D scaffold and the promotion of bone regeneration in large defects," *Biomaterials*, vol. 34, no. 38, pp. 9998–10006, 2013.

[17] Y. Wang, X. Bi, H. Zhou et al., "Repair of orbital bone defects in canines using grafts of enriched autologous bone marrow stromal cells," *Journal of Translational Medicine*, vol. 12, no. 1, p. 123, 2014.

[18] F. Özdal-Kurt, I. Tuğlu, H. S. Vatansever, S. Tong, and S. I. Deliloğlu-Gürhan, "The effect of autologous bone marrow stromal cells differentiated on scaffolds for canine tibial bone reconstruction," *Biotechnic & Histochemistry*, vol. 90, no. 7, pp. 516–528, 2015.

[19] Y. He, Y. Dong, X. Chen, and R. Lin, "Ectopic osteogenesis and scaffold biodegradation of tissue engineering bone composed of chitosan and osteo-induced bone marrow mesenchymal stem cells in vivo," *Chinese Medical Journal*, vol. 127, no. 2, pp. 322–328, 2014.

[20] C. M. Kolf, E. Cho, and R. S. Tuan, "Mesenchymal stromal cells. Biology of adult mesenchymal stem cells: regulation of niche, self-renewal and differentiation," *Arthritis Research & Therapy*, vol. 9, no. 1, p. 204, 2007.

[21] A. J. Friedenstein, N. W. Latzinik, A. G. Grosheva, and U. F. Gorskaya, "Marrow microenvironment transfer by heterotopic transplantation of freshly isolated and cultured cells in porous sponges," *Experimental Hematology*, vol. 10, no. 2, pp. 217–227, 1982.

[22] A. Herbertson and J. E. Aubin, "Cell sorting enriches osteogenic populations in rat bone marrow stromal cell cultures," *Bone*, vol. 21, no. 6, pp. 491–500, 1997.

[23] L. Berry, M. E. Grant, J. McClure, and P. Rooney, "Bone-marrow derived chondrogenesis in vitro," *Journal of Cell Science*, vol. 101, no. 2, pp. 333–342, 1991.

[24] S. Annibali, R. Quaranta, A. Scarano et al., "Histomorphometric evaluation of bone regeneration induced by biodegradable scaffolds as carriers for dental pulp stem cells in a rat model of calvarial," *Critical Size Defect Journal of Stem Cell Research and Therapy*, vol. 6, pp. 1–8, 2016.

[25] M. M. Swindle, *Surgery, Anesthesia and Experimental Techniques in Swine*, Iowa State University Press, Ames, IA, 1998.

[26] C. M. Fraser, J. A. Bergeron, A. Mays, and S. E. Aiello, *Merck Veterinary Manual*, Merck, Rahway, NJ, 1991.

[27] L. R. Pennington, F. Opitz, K. Sakamoto, M. D. Pescovitz, and D. H. Sachs, "Bone marrowtransplantation in miniatureswine in Tumbleson ME (ed)," in *Swine in Biomedical Research*, vol. 1, pp. 377–385, Plenum Publishers, NY, 1986.

[28] G. Brunetti, R. Rizzi, A. Oranger et al., "LIGHT/TNFSF14 increases osteoclastogenesis and decreases osteoblastogenesis in multiple myeloma-bone disease," *Oncotarget*, vol. 5, no. 24, pp. 12950–12967, 2014.

[29] S. Colucci, G. Brunetti, G. Mori et al., "Soluble decoy receptor 3 modulates the survival and formation of osteoclasts from multiple myeloma bone disease patients," *Leukemia*, vol. 23, no. 11, pp. 2139–2146, 2009.

[30] S. H. Kim, J. W. Shin, S. A. Park et al., "Chemical, structural properties, and osteoconductive effectiveness of bone block derived from porcine cancellous bone," *Journal of Biomedical Materials Research. Part B, Applied Biomaterials*, vol. 68, no. 1, pp. 69–74, 2004.

[31] S. A. Park, J. W. Shin, Y. I. Yang et al., "In vitro study of osteogenic differentiation of bone marrow stromal cells on heat-treated porcine trabecular bone blocks," *Biomaterials*, vol. 25, no. 3, pp. 527–535, 2004.

[32] B. Saka, A. Wree, L. Anders, and K. K. Gundlach, "Experimental and comparative study of the blood supply to the mandibular cortex in Göttingen minipigs and in man," *Journal of Cranio-Maxillo-Facial Surgery*, vol. 30, no. 4, pp. 219–225, 2002.

[33] B. Ruehe, S. Niehues, S. Heberer, and K. Nelson, "Miniature pigs as an animal model for implant research: bone regeneration in critical-size defects," *Oral Surgery, Oral Medicine, Oral Pathology, Oral Radiology, and Endodontics*, vol. 108, no. 5, pp. 699–706, 2009.

[34] F. Pieri, E. Lucarelli, G. Corinaldesi et al., "Effect of mesenchymal stem cells and platelet-rich plasma on the healing of standardized bone defects in the alveolar ridge: a comparative histomorphometric study in minipigs," *Journal of Oral and Maxillofacial Surgery*, vol. 67, no. 2, pp. 265–272, 2009.

[35] L. Ohayon, S. Taschieri, S. Corbella, and M. Del Fabbro, "Maxillary sinus floor augmentation using biphasic calcium phosphate and a hydrogel polyethylene glycol covering membrane: an histological and histomorphometric evaluation," *Implant Dentistry*, vol. 25, no. 5, pp. 599–605, 2016.

[36] A. Scarano, L. Valbonetti, M. Marchetti, F. Lorusso, and M. Ceccarelli, "Soft tissue augmentation of the face with autologous platelet-derived growth factors and tricalcium phosphate. Microtomography evaluation of mice," *The Journal of Craniofacial Surgery*, vol. 27, no. 5, pp. 1212–1214, 2016.

[37] A. Scarano, M. Ceccarelli, M. Marchetti, A. Piattelli, and C. Mortellaro, "Soft tissue augmentation with autologous platelet gel and β-TCP: a histologic and histometric study in mice," *BioMed Research International*, vol. 2016, Article ID 2078104, 2016.

[38] A. Scarano, F. Carinci, B. Assenza, M. Piattelli, G. Murmura, and A. Piattelli, "Vertical ridge augmentation of atrophic posterior mandible using an inlay technique with a xenograft without miniscrews and miniplates: case series," *Clinical Oral Implants Research*, vol. 22, no. 10, pp. 1125–1130, 2011.

[39] A. Scarano, F. Lorusso, L. Ravera, C. Mortellaro, and A. Piattelli, "Bone regeneration in iliac crestal defects: an experimental study on sheep," *BioMed Research International*, vol. 2016, Article ID 4086870, p. 6, 2016.

[40] A. Scarano, A. Piattelli, B. Assenza et al., "Porcine bone used in sinus augmentation procedures: a 5-year retrospective clinical evaluation," *Journal of Oral and Maxillofacial Surgery*, vol. 68, no. 8, pp. 1869–1873, 2010.

[41] Y. Liu, L. Wang, T. Kikuiri et al., "Mesenchymal stem cell-based tissue regeneration is governed by recipient T lymphocytes via IFN-γ and TNF-α," *Nature Medicine*, vol. 17, no. 12, pp. 1594–1601, 2011.

Hindawi
Stem Cells International
Volume 2017, Article ID 5270527, 8 pages
https://doi.org/10.1155/2017/5270527

Research Article

Paracrine Effects of Bone Marrow Mononuclear Cells in Survival and Cytokine Expression after 90% Partial Hepatectomy

Carlos Oscar Kieling,[1,2] Carolina Uribe-Cruz,[1,2,3] Mónica Luján López,[3,4] Alessandro Bersch Osvaldt,[5] Themis Reverbel da Silveira,[1,2] and Ursula Matte[3,4,6]

[1]*Experimental Laboratory of Gastroenterology and Hepatology, HCPA, Ramiro Barcelos 2350, 90035-903 Porto Alegre, RS, Brazil*
[2]*Post-Graduation Program on Medicine: Sciences in Gastroenterology, UFRGS, Ramiro Barcelos 2350, 90035-903 Porto Alegre, RS, Brazil*
[3]*Gene Therapy Center, HCPA, Ramiro Barcelos 2350, 90035-903 Porto Alegre, RS, Brazil*
[4]*Post-Graduation Program on Genetics and Molecular Biology, UFRGS, Av. Bento Gonçalves 9500, 91501-970 Porto Alegre, RS, Brazil*
[5]*Post-Graduation Program in Surgery, UFRGS, Ramiro Barcelos 2350, 90035-903 Porto Alegre, RS, Brazil*
[6]*Post-Graduation Program in Child and Adolescent Health, UFRGS, Ramiro Barcelos 2350, 90035-903 Porto Alegre, RS, Brazil*

Correspondence should be addressed to Ursula Matte; umatte@hcpa.edu.br

Received 23 September 2016; Revised 30 November 2016; Accepted 10 January 2017; Published 23 February 2017

Academic Editor: Dario Coletti

Acute liver failure is a complex and fatal disease. Cell-based therapies are a promising alternative therapeutic approach for liver failure due to relatively simple technique and lower cost. The use of semipermeable microcapsules has become an interesting tool for evaluating paracrine effects in vivo. In this study, we aimed to assess the paracrine effects of bone marrow mononuclear cells (BMMC) encapsulated in sodium alginate to treat acute liver failure in an animal model of 90% partial hepatectomy (90% PH). Encapsulated BMMC were able to increase 10-day survival without enhancing liver regeneration markers. Gene expression of *Il-6* and *Il-10* in the remnant liver was markedly reduced at 6 h after 90% PH in animals receiving encapsulated BMMC compared to controls. This difference, however, was neither reflected by changes in the number of CD68+ cells nor by serum levels of IL6. On the other hand, treated animals presented increased caspase activity and gene expression in the liver. Taken together, these results suggest that BMMC regulate immune response and promote apoptosis in the liver after 90% PH by paracrine factors. These changes ultimately may be related to the higher survival observed in treated animals, suggesting that BMMC may be a promising alternative to treat acute liver failure.

1. Introduction

Acute liver failure is a complex and fatal disease, characterized by jaundice, coagulopathy, and hepatic encephalopathy [1]. The etiology varies from viral hepatitis, drug-induced hepatotoxicity, and metabolic liver disease to uncertain causes [1, 2]. Liver transplantation remains the only proven treatment for end-stage liver failure but is limited by the availability of donor organs [1, 3].

Cell-based therapies are a promising alternative therapeutic approach for liver failure due to relatively simple technique and lower cost [3, 4]. Several preclinical and clinical experiments have been reported on the safety and efficacy of bone-marrow-derived mononuclear cells to treat liver disorders [5–8].

Recently, one of the best studied mechanisms of action for these cells is the release of paracrine factors cells [9]. However, the pathway in which they act has still not been fully clarified mainly by the difficulty of in vivo studies. The use of semipermeable microcapsules has become an interesting tool for evaluating paracrine effects in vivo. These microcapsules can immune-isolate xenogeneic cells allowing the exchange of low-molecular-weight nutrients and oxygen across the membranes [10]. In this study, we aimed to

assess the paracrine effect of bone marrow mononuclear cells (BMMC) encapsulated in sodium alginate to treat acute liver failure in an animal model of 90% partial hepatectomy.

2. Materials and Methods

2.1. Animals. Two-month-old male Wistar rats (298 ± 60 g) were kept under controlled temperature (between 18 and 22°C) in 12 h light-dark cycles with free access to water and standard chow at Experimental Animal Unit at Hospital de Clínicas de Porto Alegre (HCPA). Handling, care, and processing of animals were carried out according to regulations approved by our local Ethics Committee and complied with the National Guidelines on Animal Care.

2.2. Experimental Design. Rats were randomly divided into two groups. Treated group received encapsulated bone marrow mononuclear cells (BMMC, $n = 39$) and control group ($n = 41$) received empty capsules (EC). Survival was observed for up to 10 days after 90% PH.

To evaluate the early effects of treatments an additional set of animals were randomly divided into two groups (BMMC and EC) and euthanized at 6, 12, 24, 48, and 72 hours after 90% PH ($n = 6$–8/group/time point). For mononuclear bone marrow cells 5 animals were used as donors and another 5 animals without liver injury were used as normal controls.

2.3. Isolation of BMMC. Five naïve male Wistar rats were used as BMMC donors as described by Matte et al. [11]. Briefly, in a sterile environment, the femurs and tibias were isolated and whole bone marrow was flushed with complete medium: DMEM (Dulbecco's Modified Eagle Medium, LGC, Brazil) supplemented with 10% fetal bovine serum (Gibco, USA), 1% penicillin/streptomycin (Gibco, USA) and centrifuged at 800 g for 5 minutes. The pellet was diluted in complete medium and then placed onto a Ficoll Histopaque (GE-Healthcare, USA) layer and centrifuged at 800 g for 30 min. The interface was separated using a pipette, and cells were rinsed with PBS three times. Cells were counted using the Neubauer chamber and Trypan Blue exclusion test to verify cell viability.

2.4. Cell Encapsulation. Cell encapsulation was performed according to our laboratory protocol, previously described [12]. Briefly, BMMC were mixed with 1.5% sodium alginate (Sigma-Aldrich, USA) in complete medium and extruded through a Encapsulation Unit, type J1 (Nisco, Switzerland), attached to JMS Syringe Pump. Droplets were sheared off with an air flow of 5 L/min delivered to the tip of a 27 G needle and the rate of infusion was 40 mL/h. The droplets fell into a bath of 125 mM $CaCl_2$ and ionically cross-linked with $Ca_2{}^+$ to form solid spherical hydrogel beads containing embedded BMMC. In each well capsules were produced from a volume of 2 mL of alginate suspension, containing 1×10^6 BMMC/animal. BMMC encapsulation was carried out under sterile conditions. For control group, 2 mL of empty capsules was produced using the same approach, although without cells. The resulting capsules were maintained under normal cell culture conditions with complete medium at 37°C and 5% CO_2 for 24 h prior to administration.

2.5. Animal Model of 90% Partial Hepatectomy and Capsules Transplantation. Hepatectomy was carried out under isoflurane (Forane®, Abbott SA, Argentina) anesthesia [13]. An abdominal midline incision was made to expose the liver. Ninety percent hepatectomy was performed by a single operator as described by Gaub and Iversen (1984) [14]. In brief, the left lateral (30%), left median (40%), and right superior lobes (20%) were removed, leaving only the caudate lobes. Immediately after 90% PH, as well as before complete suture, microcapsules (either empty or containing BMMC) were placed into the peritoneal cavity and glucose was supplemented i.p. (5% of body weight). The incision was then closed. After the rats recovered from anesthesia, animals were given i.p. glucose (5% of body weight) until day seven and received 20% glucose in their drinking water and standard chow ad libitum until euthanasia.

2.6. Euthanasia. Euthanasia was performed in CO_2 chambers at the 6, 12, 24, 48, and 72 h or at 10 days after 90% PH. Immediately after euthanasia blood was collected and the serum was kept at −80°C until analysis; the liver was removed and weighed and part was flash-frozen in liquid nitrogen and the rest was placed in 10% buffered formalin. At each time point and every day until day 10 animals were weighed.

2.7. Liver Regeneration Rate. The liver regeneration rate [15] was calculated as follows: liver regeneration rate (%) $= 100 \times [C - (A - B)]/A$, where A is the estimated liver weight before PH, B is the excised liver weight at the time of PH, and C is the weight of the regenerated liver at the time of euthanasia.

2.8. Histology and Immunohistochemistry. Paraffin-embedded liver specimens were cut in 4 μm sections and stained with hematoxylin and eosin (H-E). Mitotic index was performed by counting the number of hepatocytes undergoing mitosis in 10 high power fields (HPF) at each time point until 72 h after 90% PH [6].

To assess the rate of hepatocyte proliferation, the number of hepatocytes undergoing mitosis was counted in 10 HPF. In addition, 5-bromo-2′-deoxyuridine (BrdU) immunostaining was done using BrdU staining kit (Invitrogen, USA). Two hours before sacrifice, rats ($n = 3$/group) were injected with BrdU (1 mL/g). Thereafter, liver sections were incubated with BrdU antibody and the number of positive hepatocytes was counted in 5 HPF.

2.9. Serum Cytokine Levels. Serum level of IL-6 was quantified by enzyme-linked immunosorbent assay (ELISA) using commercial kits (R&D Systems®, Minneapolis, Minnesota, EUA) in accordance with the manufacturer's instructions.

2.10. Quantitative Real-Time PCR. Total RNA was extracted from liver tissue (~50 mg) using TRIzol reagent (Invitrogen, USA) according to the manufacturer's instructions and 2 μg was reverse-transcribed using High Capacity cDNA Reverse

Transcription Kit (Life Technologies, USA). The expression of genes involved in inflammation pathway (Interleukins 6 and 10) and apoptosis (Caspase 3) were measured using TaqMan® assays (Life Technologies, USA). The percentage of a test RNA to that of β-actin was calculated by subtracting the cycle to reach the threshold (CT) for that gene from the CT for β-actin to determine the ΔCT, and the formula is percent β-actin = (100) × 2ΔCT [12]. The percent β-actin for hepatectomized animals was divided by the percent β-actin in normal animals to determine the ratio of gene expression in both treatments after 90% PH to normal rats. Livers of animals without injury were used as calibrator group (normal values = 1).

2.11. Immunohistochemistry Analysis. Paraffin-embedded liver specimens were cut in 4 μm sections and Kupffer cells were quantified by immunostaining for CD68. For that, liver sections were incubated overnight at 4°C with the primary antibody rabbit IgG-CD68 (1 : 800, Abcam, USA) and washed with phosphate buffer Tween 20; then universal biotinylated link and streptavidin-HRP were added (Dako, USA) and revealed with DAB kit (Dako, USA). The slides were counterstained with hematoxylin. The number of $CD68^+$ cells was counted in 5 randomly selected HPF (×400) per slide.

2.12. Caspase 3 Activity. Fluorometric Caspase 3 activity (Sigma-Aldrich, USA) assays were performed according to the manufacturer's instructions. Briefly, 15 μL of liver homogenate in PBS was placed in an opaque 96-well plate and 200 μL of mixture reaction solution (containing Acetyl-Asp-Glu-Val-Asp-7-amido-4-methylcoumarin) was added to each well. The plate was incubated in dark at 25°C and every 10 minutes the fluorescence was read at 360 nm of excitation and 460 of emission. Caspase activity was normalized by protein measured by Lowry method [16].

2.13. Statistical Analysis. Results were expressed as means ± standard deviation (SD) or medians when required. Statistical differences were assessed by Student's t-test and for nonparametric variables Mann–Whitney test was used. The survival rate was analyzed by Kaplan-Meier curve. The comparison of survival rates in different groups was tested by the log rank test. P values less than 0.05 were considered statistically significant.

3. Results

3.1. BMMC Increase Survival Rate in Rats with 90% Partial Hepatectomy. Survival rate was accompanied during 10 days after 90% PH. The survival rate in BMMC group was higher (54.5%) than EC group (5%; $P = 0.003$; Figure 1). Interestingly, the peak of death in BMMC group occurred within the first three days after PH. In contrast, animals in EC group died over time. Thus, the next analyses were performed until 72 hours after 90% PH to address the beneficial effect of encapsulated BMMC.

3.2. BMMC Do Not Enhance Liver Regeneration. To address if the increase of survival rate in BMMC was a consequence of a higher liver regeneration, we calculated liver regeneration rate until 72 hours after PH. Liver size increased over time in both groups and at 72 h the BMMC group reached 39% of the original liver weight, whereas EC group reached 46% (Figure 2(a)). In addition, the number of mitosis (Figure 2(b)) and positive hepatocytes for BrdU (Figures 2(c) and 2(d)) was also similar between groups. Therefore, BMMC do not seem to enhance liver regeneration after 90% PH.

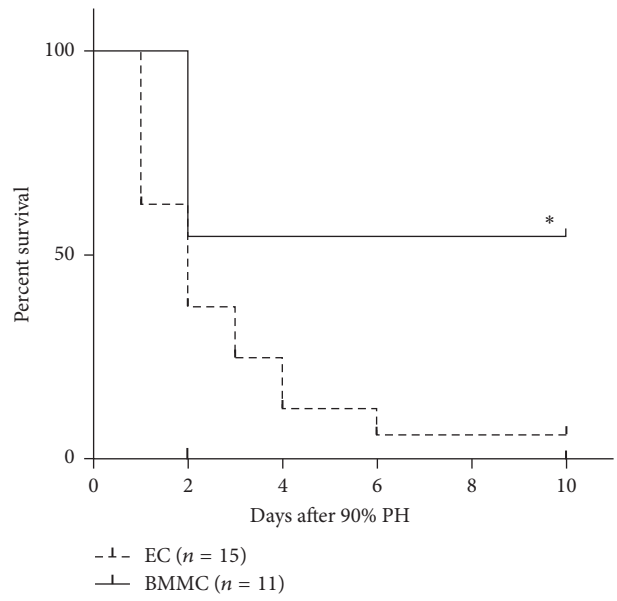

Figure 1: Survival rate for 10 days after 90% partial hepatectomy (PH). BMMC increase survival rate in rats submitted to PH ($^*P = 0.003$, log rank test). EC: empty capsules, BMMC: encapsulated bone marrow mononuclear cells.

3.3. BMMC Modulate Cytokines. It is well known that BMM have immunomodulatory properties [17]. Thus, in order to investigate the impact of immunomodulation on survival, we studied serum level of Interleukin-6 (IL-6) and its gene expression in the remnant livers. Serum IL-6 levels were increased in both groups at 6 h after 90% PH (268 pg/mL for EC group and 298 pg/mL for BMMC group, $P = 0.9$), but it decreased to normal range from 12 h in both groups equally (see Supplementary Figure 1 of the Supplementary Material available online at https://doi.org/10.1155/2017/5270527). However, in the remnant livers, we observed an increase in *Il-6* expression in both groups until 24 hours after 90% PH compared to normal values. However, in BMMC group, this increase is lower (5-fold increase) at 6 hours when compared to EC group (25-fold increase, $P = 0.03$). From 12 h after PH, the expression in EC group decreased to about 2-fold normal values, whereas in BMMC it remained around 3–6 times higher than normal, albeit this difference is not statistically significant (Figure 3(a)).

On the other hand, for *IL-10* liver gene expression a diverse outcome was observed. At 6 h after 90% PH BMMC group showed near to normal expression values, whereas EC group showed a 12-fold increase compared to normal animals (Figure 3(b), $P < 0.001$ comparing BMMC versus

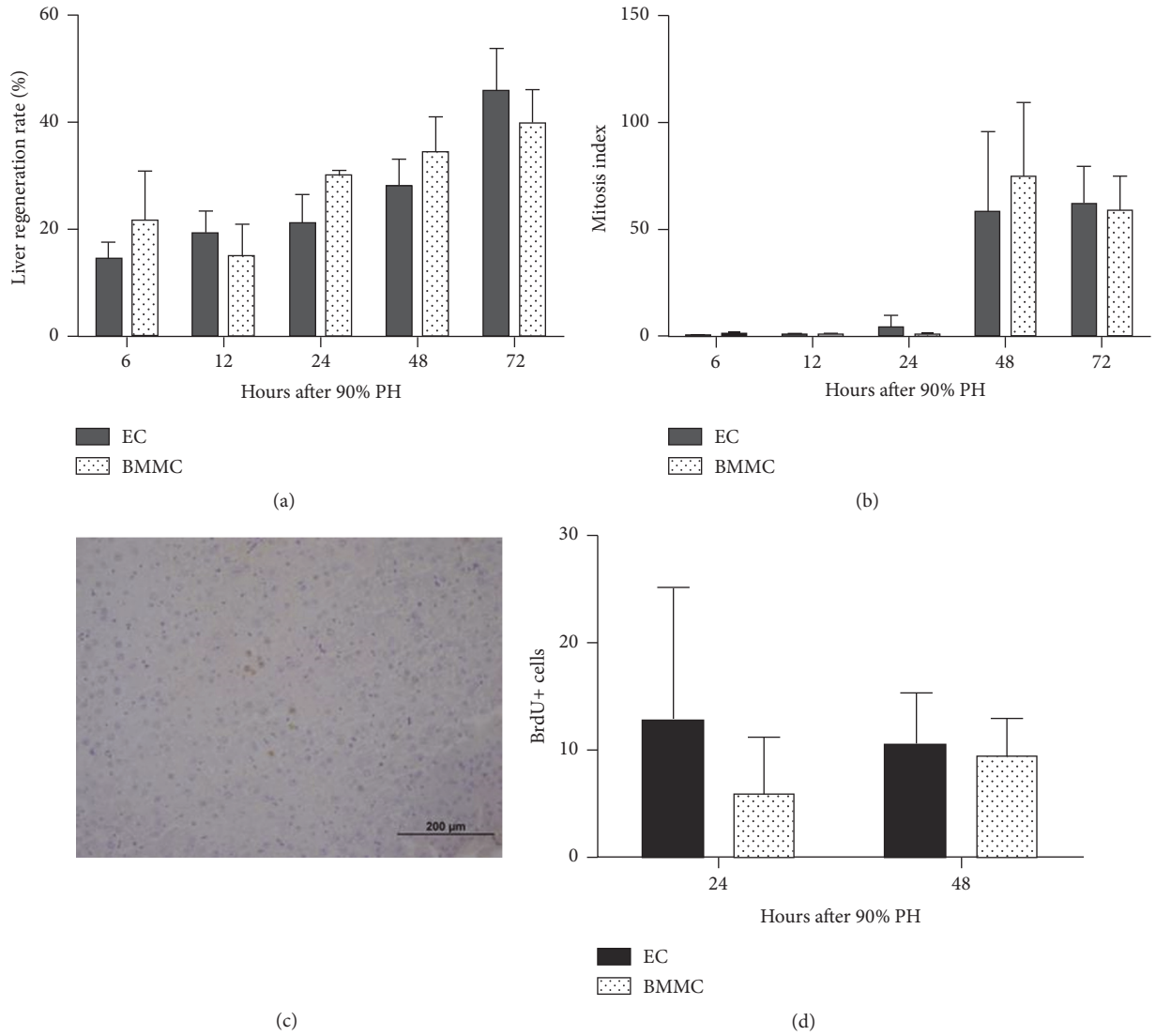

Figure 2: (a) Liver regeneration rate at 6, 12, 24, 48, and 72 hours after 90% partial hepatectomy (PH). (b) Mitotic index at 6, 12, 24, 48, and 72 hours after 90% PH. (c) BrdU immunohistochemistry, BMMC 48 hours after 90% partial hepatectomy (20x). (d) Positive hepatocytes for BrdU, EC, and BMMC 24: 12.72 ± 12.38 and 5.9 ± 5.3, respectively; EC and BMMC 48: 10.34 ± 5.03 and 9.46 ± 3.49, respectively. Values are expressed as means ± SD. Student's *t*-test. EC: empty capsules, BMMC: encapsulated bone marrow mononuclear cells.

EC groups). In the following hours (12 and 24 h after 90% PH) BMMC group remains close to normal values, whereas in EC group a sharp reduction in *IL-10* expression is observed ($P < 0.001$ and $P = 0.02$, resp.). At 48 and 72 h, though, BMMC show a reduction in expression.

3.4. Cytokine Modulation Is Not Related to the Number of Kupffer Cells. Kupffer cells (KC) are the macrophages resident in the liver and have an essential role in liver injuries by secreting cytokines and priming hepatocytes for division. To address if the expression of cytokines in the liver were was related to the number of KC, we assessed the number of CD68+ cells in liver sections. We note that in general there is no difference in the amount of KC cells between the groups except at 12 hours, when BMMC group showed an increase when compared to EC group ($P = 0.003$; Figure 4).

3.5. BMMC Benefits Apoptosis. In a previous study [12], we showed that encapsulated whole bone marrow cells increase apoptosis after 90% PH. Therefore, we analyzed Caspase 3 activity and its expression in the remnant liver. It was observed that BMMC group showed more Caspase 3 activity mainly at 24, 48, and 72 h after 90% PH ($P < 0.05$; Figure 5(a)). This result is consistent with the gene expression data, which also was high in BMMC group compared to EC group ($P < 0.05$; Figure 5(b)).

4. Discussion

The use of BMMC in cell therapy is a suitable approach due to its easy standardized protocol for cell collection and promising benefits in the treatment of liver disease [5, 18]. However, before this therapy can be widely accepted in the

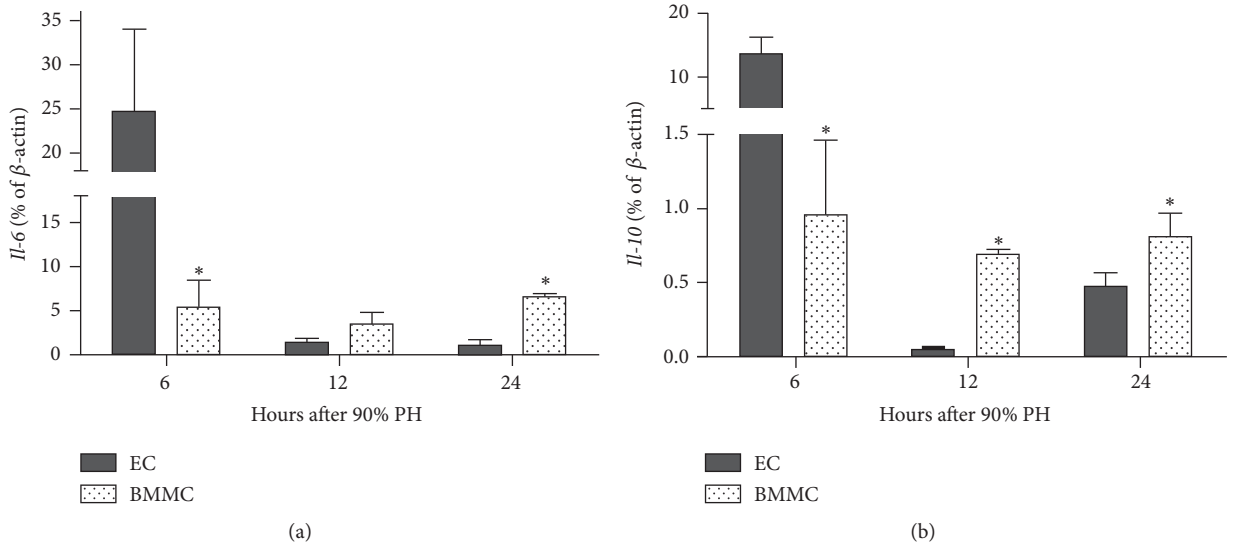

FIGURE 3: BMMC modulate liver cytokines. Liver gene expression of *Il-6* (a) and *Il-10* (b) at 6, 12, and 24 hours after 90% partial hepatectomy (PH). Values are expressed as means ± SD in log scale. Student's *t*-test, $^{*}P < 0.05$. EC: empty capsules, BMMC: encapsulated bone marrow mononuclear cells.

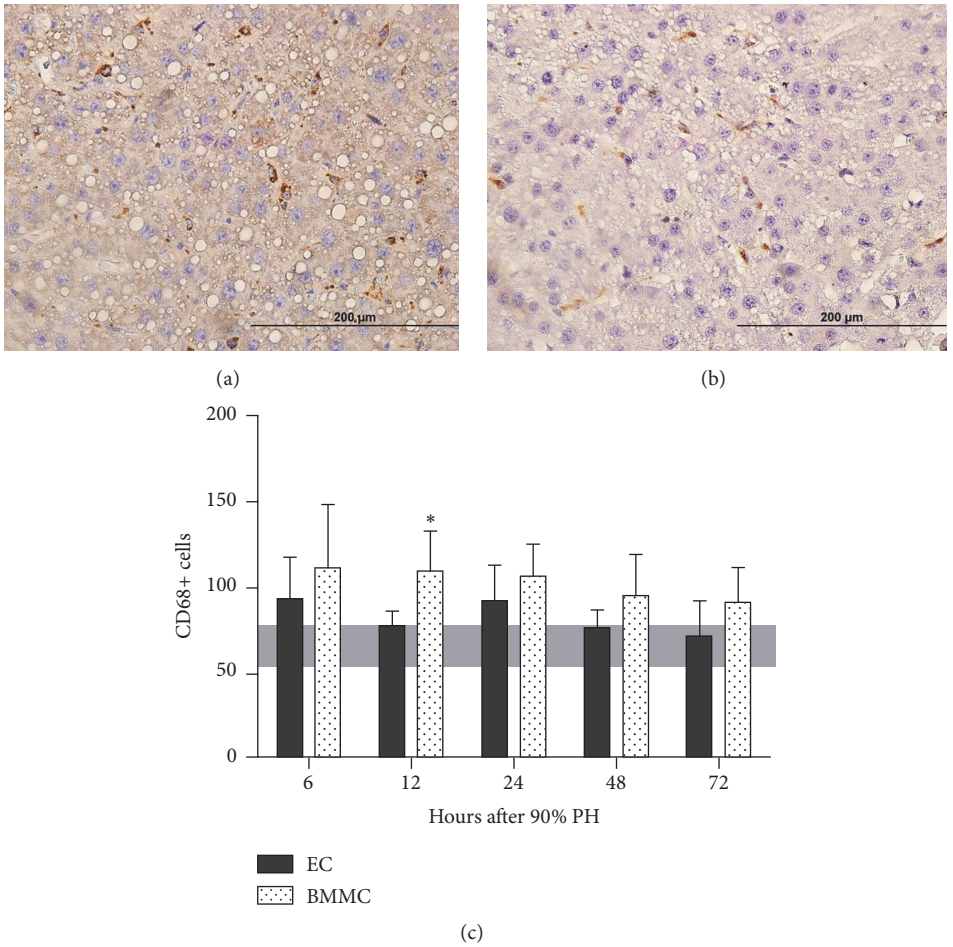

FIGURE 4: CD68+ cells in liver sections, EC, and BMMC 72 hours after 90% partial hepatectomy ((a) and (b), resp.). (c) CD68 + cell quantification at 6, 12, 24, 48, and 72 hours after 90% partial hepatectomy (PH). Values are expressed as means ± SD. Student's *t*-test, $^{*}P = 0.003$. EC: empty capsules, BMMC: encapsulated bone marrow mononuclear cells. Horizontal bar indicates normal values.

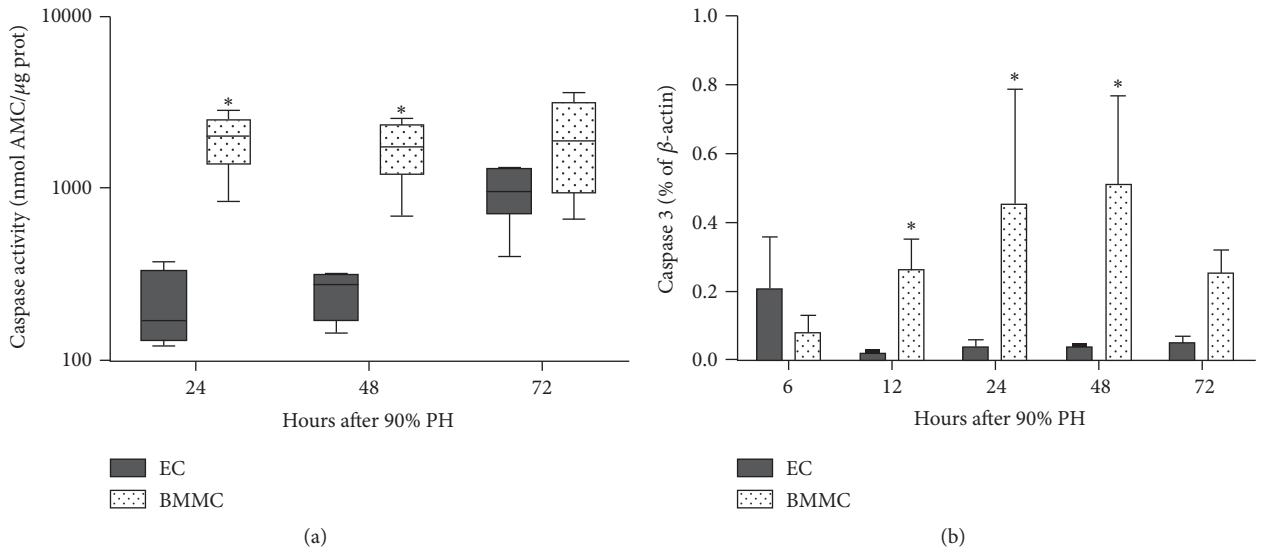

Figure 5: BMMC enhance apoptosis. (a) Caspase 3 activity and (b) liver gene expression of *Caspase 3* after 90% partial hepatectomy. Values are expressed as means ± SD. Student's *t*-test, $^{*}P < 0.05$. EC: empty capsules, BMMC: encapsulated bone marrow mononuclear cells.

clinic, its mechanisms of action must be better elucidated. Several studies have shown that BMMC have immunomodulatory properties [17, 19], focusing the attention of researchers on their paracrine effect [9]. In this sense, the use of microcapsules allows the communication between the cell entrapped within the capsule and the environment where they are implanted without cell-to-cell interaction [20]. In this study we evaluate the paracrine effect of BMMC using semipermeable microcapsules in rats with 90% PH, a suitable model for analyzing induced acute liver damage [21, 22].

The first result of our study showed a marked increase in survival rate in BMMC group which is consistent with other studies of cell therapy for acute liver disease using toxic models [6, 7, 23]. Other studies, using surgical models of 90% PH, such as Liu and Chang (2006) [24] and Uribe-Cruz et al. (2016) [12], also observed an increase in survival in animals treated with encapsulated cells, but both groups used encapsulated whole bone marrow cells, without separation of mononuclear cells.

In order to study the reasons for increased survival in BMMC group, we analyzed liver regeneration, which is a widely used method to assess recovery after partial hepatectomy [25, 26]. Liver regeneration rate, assessed either by liver weight, mitotic index, or BrdU, was similar in both groups suggesting that the increase in survival is not related to tissue regeneration. One must note that this is a 90% partial hepatectomy and not a classical liver regeneration model, such as 70% PH. So, although liver regeneration is essential for survival, different works point to other factors that influence recovery, including the pace of regeneration [27]. In addition, other studies from our group also point to a positive impact in survival that is not directly linked to hepatocyte regeneration [12, 28]. Thus, it is suggested that BMMC improve survival through mechanisms other than enhancing hepatocyte proliferation.

Acute liver failure promotes a shock septic response by the immune system [27, 28], leading to a disequilibrium in the levels of pro- and anti-inflammatory cytokines [29]. It is well recognized that IL-6 and IL-10 have an important role in improving recovery after acute liver failure [29, 30]. Thus, we analyzed the paracrine effect of BMMC on hepatic gene expression of *Il-6* and *Il-10* after liver injury. We observed that both experimental groups showed an increase in *Il-6* expression at 6 h after 90% PH; however in BMMC group this increase was much lower than in EC group. On the other hand, in BMMC-treated animals *Il-6* expression remains slightly elevated until 24 h after 90% PH. The expression of *Il-10* in BMMC group was also closer to normal levels, whereas in EC group it was increased at 6 h and greatly reduced at 12 hours after 90% PH. It is important to notice that *Il-6* is a major inducer of hepatic acute phase response and its expression plays a central role in restoring normal hepatic function following liver injury [31]. On the other hand, *Il-10* is a potent anti-inflammatory cytokine and selectively blocks proinflammatory genes in the liver after PH and reduces the number of macrophages and monocytes in the liver [32]. Moreover, the prevalence of an anti- or proinflammatory response results in the loss of immunohomeostasis and death [33]. So it can be suggested that the effect of BMMC is maintaining the balance between pro- and anti-inflammatory cytokines.

To address if the expression of cytokines in the liver was related to the number of KC, we assessed the number of CD68+ cells in liver sections. Normal Wistar rats have between 50 and 70 CD68+ cells, and this number does not increase significantly after 90% PH, except at 12 h, when BMMC show an average of 110 CD68+ cells. This lack of statistical difference may be due to the high variability observed among animals in both groups at any time point.

There are some works showing that these cytokines stimulate apoptosis in liver cells [34]. Our results show

an increase in Caspase 3 activity and gene expression in BMMC group when compared to EC group at 24 and 48 hours. These results are in agreement with the suggestion that apoptosis eliminates unwanted or harmful cells to maintain homeostasis and normal tissue functioning [35]. It is a pathophysiological beneficial process that regulates growth and proliferation, thus ensuring proper organ size and function [36]. We are suggesting that the death of damaged hepatocytes by apoptosis may be a positive effect. There are studies showing that caspases can induce proliferation of neighboring surviving cells to replace dying cells in a process referred to as "apoptosis-induced proliferation" that may be critical for stem cell activity and tissue regeneration [35]. It is possible that such impact on proliferation occurred at later times, that is, after 72 hours, and therefore was not detected in our study. In addition, the death of damaged cells by apoptosis involves less cell leakage and recruitment of inflammatory cells [37] and the therapeutic modulation of apoptosis may represent a valid strategy for the treatment of human liver diseases [38]. Thus, the paracrine effect of BMMC induces Caspase 3, which may result in proper balance between cell death and division during liver regeneration.

5. Conclusions

In summary, BMMC regulate immune response and promote apoptosis in the liver after 90% PH by paracrine factors. These changes ultimately may be related to the higher survival observed in treated animals. Therefore BMMC are a promising alternative to treat acute liver failure.

Competing Interests

The authors have no conflict of interests to declare.

Authors' Contributions

Carlos Oscar Kieling and Carolina Uribe-Cruz contributed equally to this work.

Acknowledgments

This work was supported by FIPE/HCPA and PRONEX/FAPERGS 10/0039-3.

References

[1] W. Lee, "Acute liver failure," *Seminars in Respiratory and Critical Care Medicine*, vol. 33, no. 1, pp. 36–45, 2012.

[2] A. Rutherford and R. T. Chung, "Acute liver failure: mechanisms of hepatocyte injury and regeneration," *Seminars in Liver Disease*, vol. 28, no. 2, pp. 167–174, 2008.

[3] K. Sun, X. Xie, J. Xie et al., "Cell-based therapy for acute and chronic liver failures: distinct diseases, different choices," *Scientific Reports*, vol. 4, article 6494, 2014.

[4] S. J. Forbes, S. Gupta, and A. Dhawan, "Cell therapy for liver disease: from liver transplantation to cell factory," *Journal of Hepatology*, vol. 62, no. 1, pp. S157–S169, 2015.

[5] M. Mohamadnejad, M. Vosough, S. Moossavi et al., "Intraportal infusion of bone marrow mononuclear or CD133+ cells in patients with decompensated cirrhosis: a double-blind randomized controlled trial," *Stem Cells Translational Medicine*, vol. 5, no. 1, pp. 87–94, 2016.

[6] G. Baldo, R. Giugliani, C. Uribe et al., "Bone marrow mononuclear cell transplantation improves survival and induces hepatocyte proliferation in rats after CCl_4 acute liver damage," *Digestive Diseases and Sciences*, vol. 55, no. 12, pp. 3384–3392, 2010.

[7] M. C. Belardinelli, F. Pereira, G. Baldo et al., "Adult derived mononuclear bone marrow cells improve survival in a model of acetaminophen-induced acute liver failure in rats," *Toxicology*, vol. 247, no. 1, pp. 1–5, 2008.

[8] C.-H. Park, S. H. Bae, H. Y. Kim et al., "A pilot study of autologous CD34-depleted bone marrow mononuclear cell transplantation via the hepatic artery in five patients with liver failure," *Cytotherapy*, vol. 15, no. 12, pp. 1571–1579, 2013.

[9] S. Otsuru, P. L. Gordon, K. Shimono et al., "Transplanted bone marrow mononuclear cells and MSCs impart clinical benefit to children with osteogenesis imperfecta through different mechanisms," *Blood*, vol. 120, no. 9, pp. 1933–1941, 2012.

[10] Y. Yu, J. E. Fisher, J. B. Lillegard, B. Rodysill, B. Amiot, and S. L. Nyberg, "Cell therapies for liver diseases," *Liver Transplantation*, vol. 18, no. 1, pp. 9–21, 2012.

[11] U. Matte, C. Uribe Cruz, M. L. López, L. Simon, F. Q. Mayer, and R. Giugliani, "Bone marrow-derived mononuclear cells differentiate into hepatocyte-like cells within few Hrs without fusion," *Journal of Cell Science & Therapy*, vol. 5, no. 3, article no. 163, 2014.

[12] C. Uribe-Cruz, C. O. Kieling, M. L. López et al., "Encapsulated whole bone marrow cells improve survival in wistar rats after 90% partial hepatectomy," *Stem Cells International*, vol. 2016, Article ID 4831524, 9 pages, 2016.

[13] C. O. Kieling, A. N. Backes, R. L. Maurer et al., "The effects of anesthetic regimen in 90% hepatectomy in rats," *Acta Cirurgica Brasileira*, vol. 27, no. 10, pp. 702–706, 2012.

[14] J. Gaub and J. Iversen, "Rat liver regeneration after 90% partial hepatectomy," *Hepatology*, vol. 4, no. 5, pp. 902–904, 1984.

[15] B. Zhang, M. Inagaki, B. Jiang et al., "Effects of bone marrow and hepatocyte transplantation on liver injury," *Journal of Surgical Research*, vol. 157, no. 1, pp. 71–80, 2009.

[16] O. H. Lowry, N. J. rosebrough, A. L. Farr, and R. J. Randall, "Protein measurement with the Folin phenol reagent," *The Journal of Biological Chemistry*, vol. 193, no. 1, pp. 265–275, 1951.

[17] P. Mattar and K. Bieback, "Comparing the immunomodulatory properties of bone marrow, adipose tissue, and birth-associated tissue mesenchymal stromal cells," *Frontiers in Immunology*, vol. 6, article no. 560, 2015.

[18] T. Itoh and A. Miyajima, "Liver regeneration by stem/progenitor cells," *Hepatology*, vol. 59, no. 4, pp. 1617–1626, 2014.

[19] T. Yi and S. U. Song, "Immunomodulatory properties of mesenchymal stem cells and their therapeutic applications," *Archives of Pharmacal Research*, vol. 35, no. 2, pp. 213–221, 2012.

[20] U. Matte, V. L. Lagranha, T. G. De Carvalho, F. Q. Mayer, and R. Giugliani, "Cell microencapsulation: a potential tool for the treatment of neuronopathic lysosomal storage diseases," *Journal of Inherited Metabolic Disease*, vol. 34, no. 5, pp. 983–990, 2011.

[21] P. N. A. Martins, T. P. Theruvath, and P. Neuhaus, "Rodent models of partial hepatectomies," *Liver International*, vol. 28, no. 1, pp. 3–11, 2008.

[22] M.-A. Aller, M. Mendez, M.-P. Nava, L. Lopez, J.-L. A. Arias, and J. Arias, "The value of microsurgery in liver research," *Liver International*, vol. 29, no. 8, pp. 1132–1140, 2009.

[23] S. Terai, I. Sakaida, H. Nishina, and K. Okita, "Lesson from the GFP/CCl4 model—translational research project: the development of cell therapy using autologous bone marrow cells in patients with liver cirrhosis," *Journal of Hepato-Biliary-Pancreatic Surgery*, vol. 12, no. 3, pp. 203–207, 2005.

[24] Z. C. Liu and M. S. Chang, "Transdifferentiation of bioencapsulated bone marrow cells into hepatocyte-like cells in the 90% hepatectomized rat model," *Liver Transplantation*, vol. 12, no. 4, pp. 566–572, 2006.

[25] H. Amemiya, H. Kono, and H. Fujii, "Liver regeneration is impaired in macrophage colony stimulating factor deficient mice after partial hepatectomy: the role of M-CSF-induced macrophages," *Journal of Surgical Research*, vol. 165, no. 1, pp. 59–67, 2011.

[26] F. Teixeira-Clerc, M.-P. Belot, S. Manin et al., "Beneficial paracrine effects of cannabinoid receptor 2 on liver injury and regeneration," *Hepatology*, vol. 52, no. 3, pp. 1046–1059, 2010.

[27] M. Ninomiya, K. Shirabe, T. Terashi et al., "Deceleration of regenerative response improves the outcome of rat with massive hepatectomy," *American Journal of Transplantation*, vol. 10, no. 7, pp. 1580–1587, 2010.

[28] M. L. López, C. O. Kieling, C. Uribe Cruz et al., "Platelet increases survival in a model of 90% hepatectomy in rats," *Liver International*, vol. 34, no. 7, pp. 1049–1056, 2014.

[29] Z. Wu, M. Han, T. Chen, W. Yan, and Q. Ning, "Acute liver failure: mechanisms of immune-mediated liver injury," *Liver International*, vol. 30, no. 6, pp. 782–794, 2010.

[30] W. Bernal, G. Auzinger, A. Dhawan, and J. Wendon, "Acute liver failure," *The Lancet*, vol. 376, no. 9736, pp. 190–201, 2010.

[31] D. Schmidt-Arras and S. Rose-John, "IL-6 pathway in the liver: from physiopathology to therapy," *Journal of Hepatology*, vol. 64, no. 6, pp. 1403–1415, 2016.

[32] M. Wang, X. Zhang, X. I. Xiong et al., "Bone marrow mesenchymal stem cells reverse liver damage in a carbon tetrachloride-induced mouse model of chronic liver injury," *In Vivo (Athens, Greece)*, vol. 30, no. 3, pp. 187–193, 2016.

[33] C. G. Antoniades, P. A. Berry, J. A. Wendon, and D. Vergani, "The importance of immune dysfunction in determining outcome in acute liver failure," *Journal of Hepatology*, vol. 49, no. 5, pp. 845–861, 2008.

[34] A. Dangi, C. Huang, A. Tandon, D. Stolz, T. Wu, and C. R. Gandhi, "Endotoxin-stimulated rat hepatic stellate cells induce autophagy in hepatocytes as a survival mechanism," *Journal of Cellular Physiology*, vol. 231, no. 1, pp. 94–105, 2016.

[35] H. D. Ryoo and A. Bergmann, "The role of apoptosis-induced proliferation for regeneration and cancer," *Cold Spring Harbor Perspectives in Biology*, vol. 4, no. 8, Article ID a008797, 2012.

[36] K. Wang and B. Lin, "Pathophysiological significance of hepatic apoptosis," *ISRN Hepatology*, vol. 2013, Article ID 740149, 14 pages, 2013.

[37] S. Elmore, "Apoptosis: a review of programmed cell death," *Toxicologic Pathology*, vol. 35, no. 4, pp. 495–516, 2007.

[38] M. E. Guicciardi and G. J. Gores, "Apoptosis: a mechanism of acute and chronic liver injury," *Gut*, vol. 54, no. 7, pp. 1024–1033, 2005.

Hindawi
Stem Cells International
Volume 2017, Article ID 3978595, 6 pages
https://doi.org/10.1155/2017/3978595

Review Article

Therapeutic Potential of Olfactory Ensheathing Cells and Mesenchymal Stem Cells in Spinal Cord Injuries

Zadroga Anna,[1] Jezierska-Woźniak Katarzyna,[2] Czarzasta Joanna,[1] Monika Barczewska,[2] Wojtkiewicz Joanna,[1,3,4] and Maksymowicz Wojciech[2]

[1]*Department of Pathophysiology, Faculty of Medical Sciences, University of Warmia and Mazury in Olsztyn, Olsztyn, Poland*
[2]*Department of Neurology and Neurosurgery, Faculty of Medical Sciences, University of Warmia and Mazury in Olsztyn, Olsztyn, Poland*
[3]*Laboratory for Regenerative Medicine, Faculty of Medical Sciences, University of Warmia and Mazury, Olsztyn, Poland*
[4]*Foundation for the Nerve Cells Regeneration, Olsztyn, Poland*

Correspondence should be addressed to Wojtkiewicz Joanna; joanna.wojtkiewicz@uwm.edu.pl

Received 21 September 2016; Revised 27 November 2016; Accepted 25 December 2016; Published 16 February 2017

Academic Editor: Dario Coletti

Spinal cord injury (SCI) is a devastating neurological condition that affects individuals worldwide, significantly reducing quality of life, for both patients and their families. In recent years there has been a growing interest in cell therapy potential in the context of spinal cord injuries. The present review aims to discuss and compare the restorative approaches based on the current knowledge, available spinal cord restorative cell therapies, and use of selected cell types. However, treatment options for spinal cord injury are limited, but rehabilitation and experimental technologies have been found to help maintain or improve remaining nerve function in some cases. Mesenchymal stem cells as well as olfactory ensheathing cells seem to show therapeutic impact on damaged spinal cord and might be useful in neuroregeneration. Recent research in animal models and first human trials give patients with spinal cord injuries hope for recovery.

1. Introduction

Spinal cord injury (SCI) is debilitating and devastating condition, considered as a major global issue affecting both young and elderly populations. Worldwide, the estimated amount of people living with SCI is about 2.5 million, with more than 130,000 new injuries reported each year. This disorder has a significant impact on life quality and expectancy and is economically burdensome, with considerable costs associated with primary care and loss of income [1]. SCI leads to primary partial or complete loss of motor, sensory and autonomic functions and secondary impairments below the injury level, due to the local spinal cord vasculature damage and the interruption of ascending and descending neural pathways. SCIs are broadly classified into two groups: traumatic and nontraumatic SCI (NTSCI). Patients with NTSCI state minority among the spinal cord population. NTSCI can be a consequence of multiple etiologies including infection, spinal stenosis, vascular impairment, transverse myelitis, syringomyelia, malignant and benign tumors [2]. Traumatic spinal cord injury results from contusion, compression, and stretch of the spinal cord. Trauma related injury is the most prevalent among SCI cases primarily involving road traffic accidents, especially in case of young adults between age group of 15 and 29 years and accidental falls in case of aged people (>65 years) [3]. Nerve cells in the injured segment exhibit necrosis and apoptosis. The necrotic and degenerated tissues are removed by phagocytes and replaced by neuroglial cells, leading to the formation of cystic, melanotic and colloidal lesions at the injured site within 6 weeks after the injury. Then, the physical separation and neural demyelination interrupt the physiological signal transduction pathway, which is marked clinically by a partial or total loss of sensory, motor, urine, and voluntary control of urination and defecation. Physiological neural regeneration is not possible because of injured central nerve axons.

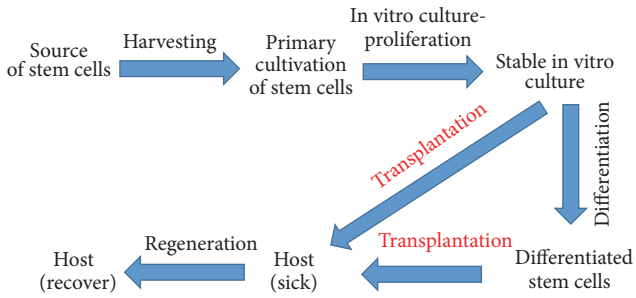

Figure 1: Scheme: therapy of stem cells.

Functional reconstruction after spinal cord injury has been a challenging clinical problem [4].

Following surgical interventions that include early spinal decompression and stabilization surgery [5], current treatments used for SCI have mainly neuroprotective or neuroregenerative effect. Neuroprotective therapies focus on impeding or preventing further progression of the secondary injury, whereas neuroregenerative therapies lay emphasis on recovering the lost or impaired functionality by repairing the broken neuronal circuitry of the spinal cord [6, 7]. Preclinical research has revealed that many elements of the secondary injury cascade occur over a prolonged period of time after injury, providing an opportunity for neuroprotective exogenous treatments to be effective if applied within this time period [8, 9]. The evaluation of patient's condition is based on classification of spinal cord injury severity using American Spinal Injury Association (ASIA) Impairment Scale. The main categories of the Impairment Scale are as follows: (A) total lack of sensory and motor function below level of injury, (B) some sensation below level of injury, (C) >50% of muscles below level of injury cannot move against gravity, (D) >50% of muscles below level of injury can move against gravity, and (E) all neurologic function has returned. In general, the effectivity of therapy in spinal cord injuries is established using ASIA scale [10].

Due to the complex nature of injury, several therapeutic strategies are combined to treat various aspects of the trauma. Neuroprotection pertains to the preservation of the spared neurons and their processes immediately following the injury, since the events that occur during the secondary injury or expansion phase harm the spared, once fully functional neurons. Neuroregeneration aims to modulate the lesion site environment to promote axonal regrowth by removing inhibitory growth substances and providing a growth supportive environment. Consequently, intraspinal transplants enrich the lesion site by replacing lost cells with new neurons and/or glial cells to create and restore functional connections or provide a more permissible medium for regenerating axons. Neurorehabilitation in a form of exercise/physical training has demonstrated beneficial effects at the cellular and molecular levels and may translate into recovery of function [11].

So far, a few approaches have been performed to increase the rate of improvement in nerve regeneration applications. One of them is a stem cell-based strategy, which is a very promising therapy for repairing the SCI (a general scheme of stem cell-based therapy is shown in Figure 1). Various types of stem cells from different sources were tested in the regeneration of damaged neural cells. Different cell sources for transplantation might be required for optimal clinical improvement, depending on type of the pathophysiology of the injury [12]. Grafting of somatic cells and tissues such as olfactory ensheathing cells (OECs), Schwann cells, fetal tissues, and peripheral nerves has made the SCI microenvironment more favorable for neural regeneration. On the other hand, neural progenitor/stem cells, embryonic stem cells, induced pluripotent stem cells, mesenchymal stem cells (MSCs), fibroblast-derived stem cells, and others are all exploited for their pluripotent differentiation ability to replace neuronal lineage cells, enhance axonal regeneration, and restore interneuron communications [13]. Following our literature studies we concluded that optimal adjuvant therapies for patients who suffered from SCI should have three main properties: (1) neurotrophic abilities to stimulate axonal growth from regular, existing cells; (2) immunomodulation to stop cell death; and (3) the competence to replace injured cells. The source of cells with regenerative potential should be discussed before the choice for particular therapy (classification based on the source of those cells is shown in Figure 2). This review is focused on therapies applying olfactory ensheathing cells, which are proved to act as stimulating axonal growth factors [14] and mesoderm derived mesenchymal stem cells (mainly derived from bone marrow) and their implantation in patients with SCI which are believed to occur through regulation of the immune system, leading to decreased cell death [15].

2. Olfactory Ensheathing Cells and Mesenchymal Stem Cells as Promising/Potential Candidates for Therapy of Patients with Spinal Cord Injuries

2.1. Olfactory Ensheathing Cells

2.1.1. Characteristic and Research. OECs are unique cells that are responsible for the expression of various neurotrophic factors, which are important for the extension and guidance of axons. They are a population of glial cells residing both in the peripheral and central nervous systems. Together with their accompanying envelope of olfactory nerve fibroblasts (ONFs), they enfold the bundles of olfactory nerve fibers in their path from the nasal mucosa to make synaptic connections in the olfactory bulb [16–19]. OECs share properties with astrocytes and Schwann cells [20]. The key ability of OECs from the perspective of neural regeneration is their migration from peripheral to the central nervous system. As a consequence the enhancement of axonal extension after injury is possible and can help neural regeneration. During embryonic olfactory system development, neural cell adhesion molecule (NCAM) and L1/neuron-glia cell adhesion molecule (L1/Ng-CAM) in the membrane of OECs enable the olfactory axons to take the glial cell surfaces as a substratum on which they grow, and the secreted laminin and nexin from OECs provide other adhesive substrates for the olfactory axons as the neuron-promoting agents [21]. OECs

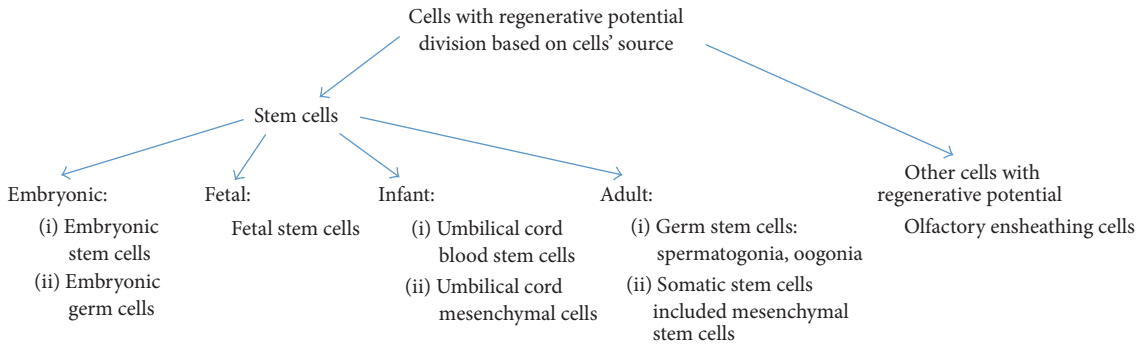

Figure 2: Classification of cells with regenerative potential.

migrate into the injury site, enhance the axon growth due to permissive OEC environment during neural regeneration [22]. Because of mentioned OECs properties for continuous regeneration and their stimulation of axonal growth, an increasing number of studies have attempted to transplant OECs into injured spinal cord for potential therapeutic use in neural regeneration.

In the last decade, the research on animals have shown that transplantation of OECs and ONFs cultured from the olfactory bulb mediate regeneration and functional reconnection of severed axons in spinal cord injuries [23–28]. In particular, Barbour and coauthors have demonstrated significant increase of neuronal cell survival after olfactory ensheathing cell transplantation in the rat model. Additionally, in the mouse model, Witheford et al. observed the ability of OECs to secrete adhesion molecule L1. Subsequently, those cells have stimulated axonal growth through the L1 activity. In another research, the functioning axons were identified at the injury site after OECs transplantation to the injured rat spinal cord [26]. Similarly, functional challenge was observed: three of nine rats with OECs treatment after SCI start to move their hind legs while 12 controls did not show any improvement.

To date, preliminary clinical trials seem to be inconsistent, but multiple small studies demonstrated benefits and safety of using OECs in humans. For example, Lima et al. [29] observed 55% effectiveness in ASIA grade improvement. During this study, 11 of 20 patients noticed an improvement after such treatment, including five patients who recovered voluntary bowel control and one who recovered bladder control. In another clinical trial only one of six patients with chronic SCI had any neurologic improvement [30]. The results obtained by Wu et al. [31] demonstrated safety of therapy with fetal olfactory ensheathing glia transplantation in patients with SCI. In this clinical trial, the olfactory bulb was harvested from 16-week-old fetuses following strict ethical guidelines. All eleven patients had no complication of neurological conditions. Three of five patients with low cervical cord injury had improvement of muscle strength below the level of injury: in patients with thoracic injury, the motor improvement was not observed, even though five of six patients had improved sensation to gentle touch and pinprick [31].

Recently, Tabakow et al. [32] have reported clinical trials using cells taken from the olfactory bulb and olfactory mucosa in human SCI patients. In this clinical trial, six patients received autologous OEC transplantation in a Phase I clinical trial, of whom three patients showed signs of improvement of SCI, and two demonstrated improvement according to ASIA scale (ASIA (A) to (C) and (B)). Researchers concluded after one year observations that the obtaining, culture and intraspinal transplantation of autologous OECs is safe. Furthermore, they considered that transplantation of OECs was the main factor contributing for the neurological improvements in the three patients with transplants. Study of this research group suggested the improvement is a consequence of transplanted OECs which may mediate some restitution of efferent and afferent long white matter tracts in three treated patients [32].

The latest results indicate that the transplantation of autologous bulbar cells in 38-year-old patient has been successful. Using MRI, it was found that grafts had braided the left side of the spinal cord, where the majority of these nerve grafts were implanted, and neurophysiological examinations confirmed the restitution of the integrity of the corticospinal tracts and the voluntary character of recorded muscle contractions [33].

2.2. Mesenchymal Stem Cells

2.2.1. Characteristic and Research. Mesenchymal stem cells are an umbrella term for adult stem cells originating from mesoderm. These cells could be harvested from multiple tissues, such as bone marrow, umbilical cord, adipose and pancreatic tissue [34]. The bone marrow-derived MSCs (BM-MSCs; the best known source of MSCs) belong to the multipotent somatic cells. In the process of cell isolation and in vitro culture, MSCs must be separated from hematopoietic stem cells before implantation. The benefit of allogenic transplantation relies on the lack of the class II major histocompatibility complex expression in those cells [15]. BM-MSCs are an innovative therapeutic tool in the treatment of a number of diseases through their neuroprotective and paracrine ability [35]. In the last decade, research focused on cell activity demonstrated significant neurotrophic properties of BM-MSCs. Those cells secrete nerve growth factor and neurotrophin-3, which support axonal growth [36]. In addition, MSCs offer the advantages of (1) being an easily obtainable source; (2) possessing the ability for expansion

in vitro; (3) lacking a requirement for immunosuppressive therapy to prevent rejections; and (4) having a reduced risk of malignant transformation [37]. The recent experiment of [37] research team demonstrated induction of MSCs to secrete neurotrophic factors (MSC-NTF cells) and implementing the cells in clinic for therapy of patients with amyotrophic lateral sclerosis. In the procedure, using a medium-based differentiation process, they have induced MSCs to become MSC-NTF cells, with markedly enhanced secretion of NTFs such as GDNF, brain-derived NTF, vascular endothelial growth factor (VEGF), and hepatocyte growth factor (HGF) [38].

The motor function recovery through an axonal regeneration after MSCs transplantation to the spinal cord was confirmed in animal studies. A lot of cytokines and growth factors such as neurotrophins, colony-stimulating factor (SCF), interleukins, stem cell factor (SCF), NGF, BDNF, HGF, and VEGF are expressed in MSCs. In rodent, the effect of MSCs transplantation was depending on time of grafting cells: the positive impact was noticed when cells were transplanted one week after injury (BBB scores), while transplantation of MSCs four months after SCI had no effect on examined parameters (BBB scores). It is generally proposed that this window spans between three days and three weeks after SCI [39]. In another rat model of SCI, increase in axonal growth factor levels as demonstrated in rats treated with MSCs compared to control rats. Additionally, new axons were oriented in the proper way and inhibition mechanism of T-cell activation has proven to preserve host neurons and myelin in rodents treated with MSCs compared with controls [40].

The hypothetical ability of MSCs to replace cells of the central nervous system has not been proven, even though some studies showed their ability to at least temporarily function as replacement cells. Firstly, Hofstetter et al. [41] observed that MSCs expressed neural markers and were tightly associated with immature astrocytes five weeks after SCI. However, the research team concluded that these cells could not perform the astrocytes function. In another animal study, 85% of MSCs transplanted into injured spinal cords of rats expressed neural cell markers two weeks after procedure. However, twelve weeks after surgery, only 10% of MSCs stayed positive for neural markers [42].

Some clinical trials which showed beneficial results and safety of using MSCs in humans have been conducted. However, the effects of these trials which certainly are very complex and require the highest precision of neurosurgeons are still ambiguous. In the research of Bhanot et al. [43] 13 patients with chronic SCI (class A of ASIA scale) were treated with laminectomy, followed by implantation of autologous MSCs into the spinal lesion. Three of these patients demonstrated some reaction: one of them had a slight improvement in motor function and two of them expressed pinprick sensation below the level of injuries. Another research team has been implemented autologous MSCs in patients with acute and subacute SCI [44]. Approximately 30% of these patients had at least one neurological improvement on ASIA scale, even though it is hard to estimate whether it was not the effect of the natural process of acute SCI [44].

3. Perspectives

3.1. Possibilities of OECs and MSCs Injection to Injured Spinal Cord. Considering the above mentioned specific characteristics of OECs and MSCs, these cells may influence the outcomes of therapeutic strategy for spinal cord injuries. Previously described preclinical and clinical studies also confirm their positive effective impact on the toxic environment in the injured spinal cord. However, there are no clear guidelines for a method of cell delivery to the damaged area of the spinal cord. It is necessary to conduct further research and establish an effective injection system. Scientists are looking to design a microinjection system, which will be mounted to the patient's spine for optimal stability and electronically controlled administration of OECs and MSCs to the injured spinal cord. The injection will be immobilized relative to the spine with percutaneous mounts attached to vertebral pedicles flanking the injection site. The spine mounts will allow the injection system to move with the patient during ventilation and in the event of inadvertent patient movement. The stabilized platform also would allow for accurate landmark-based targeting with the adjustable microinjector attached to the platform. This injection system will use an outer rigid cannula for accurate targeting and an inner flexible or floating cannula for cell delivery. Hopefully, these innovations will reduce the procedural risks associated with direct intraspinal cord injection and improve targeting capability.

4. Conclusion

A presented review attempted to discuss and compare the restorative approaches based on the current knowledge about available spinal cord restorative cell therapies and use of selected cell types. We believe that there is a strong need to help people suffering from spinal cord injuries to recover and come back to normal life. SCIs have a significant impact on life quality and expectancy and are economically burdensome, with considerable costs associated with primary care and loss of income. Treatment options for spinal cord injuries are limited, but rehabilitation and experimental technologies have been found to help maintain or improve remaining nerve function in some cases. Regenerative abilities of OECs and MSCs are still not enough understood and therefore the effective treatment of SCI has not been developed yet. However, recent development of stem cell approaches has highlighted their usefulness in treatment and give hope for patients with spinal cord injuries. A novel strategy that combines several disciplines such as neurology, neurosurgery, bioengineering, and stem cell therapy, which focus on therapeutic treatment of children and adults with spinal cord injuries, should be quickly implemented to improve patients' quality of life.

Competing Interests

The authors declare that they have no competing interests.

References

[1] International Campaign for Cures of Spinal Cord Injury Paralysis, http://www.campaignforcure.org/.

[2] S. Gabison, M. C. Verrier, S. Nadeau, D. H. Gagnon, A. Roy, and H. M. Flett, "Trunk strength and function using the multidirectional reach distance in individuals with non-traumatic spinal cord injury," *Journal of Spinal Cord Medicine*, vol. 37, no. 5, pp. 537–547, 2014.

[3] V. Sabapathy, G. Tharion, and S. Kumar, "Cell therapy augments functional recovery subsequent to spinal cord injury under experimental conditions," *Stem Cells International*, vol. 2015, Article ID 132172, 12 pages, 2015.

[4] Y. J. Rao, W. X. Zhu, Z. Q. Du et al., "Effectiveness of olfactory ensheathing cell transplantation for treatment of spinal cord injury," *Genetics and Molecular Research*, vol. 13, no. 2, pp. 4124–4129, 2014.

[5] M. G. Fehlings, A. Vaccaro, J. R. Wilson et al., "Early versus delayed decompression for traumatic cervical spinal cord injury: results of the surgical timing in acute spinal cord injury study (STASCIS)," *PLoS ONE*, vol. 7, no. 2, Article ID e32037, 2012.

[6] B. K. Kwon, W. Tetzlaff, J. N. Grauer, J. Beiner, and A. R. Vaccaro, "Pathophysiology and pharmacologic treatment of acute spinal cord injury," *Spine Journal*, vol. 4, no. 4, pp. 451–464, 2004.

[7] S. Hamid and R. Hayek, "Role of electrical stimulation for rehabilitation and regeneration after spinal cord injury: an overview," *European Spine Journal*, vol. 17, no. 9, pp. 1256–1269, 2008.

[8] O. N. Hausmann, "Post-traumatic inflammation following spinal cord injury," *Spinal Cord*, vol. 41, no. 7, pp. 369–378, 2003.

[9] S. Thuret, L. D. F. Moon, and F. H. Gage, "Therapeutic interventions after spinal cord injury," *Nature Reviews Neuroscience*, vol. 7, no. 8, pp. 628–643, 2006.

[10] S. C. Kirshblum, S. P. Burns, F. Biering-Sorensen et al., "International standards for neurological classification of spinal cord injury (revised 2011)," *Journal of Spinal Cord Medicine*, vol. 34, no. 6, pp. 535–546, 2011.

[11] K. Fouad and W. Tetzlaff, "Rehabilitative training and plasticity following spinal cord injury," *Experimental Neurology*, vol. 235, no. 1, pp. 91–99, 2012.

[12] W. Maksymowicz, J. Wojtkiewicz, H. Kozlowska, A. Habich, and W. Lopaczynski, "The perspectives of stem cell-based therapy in neurological diseases," in *Stem Cells and Human Diseases*, pp. 23–60, Springer, 2012.

[13] D. Y. Park, R. E. Mayle, R. L. Smith, I. Corcoran-Schwartz, A. I. Kharazi, and I. Cheng, "Combined transplantation of human neuronal and mesenchymal stem cells following spinal cord injury," *Global Spine Journal*, vol. 3, no. 1, pp. 1–6, 2013.

[14] M. Witheford, K. Westendorf, and A. J. Roskams, "Olfactory ensheathing cells promote corticospinal axonal outgrowth by a L1 CAM-dependent mechanism," *GLIA*, vol. 61, no. 11, pp. 1873–1889, 2013.

[15] V. Mundra, I. C. Gerling, and R. I. Mahato, "Mesenchymal stem cell-based therapy," *Molecular Pharmaceutics*, vol. 10, no. 1, pp. 77–89, 2013.

[16] J. R. Doucette, "The glial cells in the nerve fiber layer of the rat olfactory bulb," *The Anatomical Record*, vol. 210, no. 2, pp. 385–391, 1984.

[17] S. L. Lindsay, J. S. Riddell, and S. C. Barnett, "Olfactory mucosa for transplant-mediated repair: a complex tissue for a complex injury?" *GLIA*, vol. 58, no. 2, pp. 125–134, 2010.

[18] G. Raisman, "Specialized neuroglial arrangement may explain the capacity of vomeronasal axons to reinnervate central neurons," *Neuroscience*, vol. 14, no. 1, pp. 237–254, 1985.

[19] A. Ramón-Cueto and M. Nieto-Sampedro, "Glial cells from adult rat olfactory bulb: immunocytochemical properties of pure cultures of ensheathing cells," *Neuroscience*, vol. 47, no. 1, pp. 213–220, 1992.

[20] G. Gudiño-Cabrera and M. Nieto-Sampedro, "Schwann-like macroglia in adult rat brain," *GLIA*, vol. 30, no. 1, pp. 49–63, 2000.

[21] R. Doucette, "Glial influences on axonal growth in the primary olfactory system," *Glia*, vol. 3, no. 6, pp. 433–449, 1990.

[22] F. Chehrehasa, L. C. E. Windus, J. A. K. Ekberg et al., "Olfactory glia enhance neonatal axon regeneration," *Molecular and Cellular Neuroscience*, vol. 45, no. 3, pp. 277–288, 2010.

[23] N. Keyvan-Fouladi, G. Raisman, and Y. Li, "Functional repair of the corticospinal tract by delayed transplantation of olfactory ensheathing cells in adult rats," *Journal of Neuroscience*, vol. 23, no. 28, pp. 9428–9434, 2003.

[24] Y. Li, P. Decherchi, and G. Raisman, "Transplantation of olfactory ensheathing cells into spinal cord lesions restores breathing and climbing," *Journal of Neuroscience*, vol. 23, no. 3, pp. 727–731, 2003.

[25] Y. Li, P. M. Field, and G. Raisman, "Regeneration of adult rat corticospinal axons induced by transplanted olfactory ensheathing cells," *Journal of Neuroscience*, vol. 18, no. 24, pp. 10514–10524, 1998.

[26] A. Ramón-Cueto, M. I. Cordero, F. F. Santos-Benito, and J. Avila, "Functional recovery of paraplegic rats and motor axon regeneration in their spinal cords by olfactory ensheathing glia," *Neuron*, vol. 25, no. 2, pp. 425–435, 2000.

[27] A. Ramón-Cueto, G. W. Plant, J. Avila, and M. B. Bunge, "Long-distance axonal regeneration in the transected adult rat spinal cord is promoted by olfactory ensheathing glia transplants," *Journal of Neuroscience*, vol. 18, no. 10, pp. 3803–3815, 1998.

[28] H. R. Barbour, C. D. Plant, A. R. Harvey, and G. W. Plant, "Tissue sparing, behavioral recovery, supraspinal axonal sparing/regeneration following sub-acute glial transplantation in a model of spinal cord contusion," *BMC Neuroscience*, vol. 14, article no. 106, 2013.

[29] C. Lima, P. Escada, J. Pratas-Vital et al., "Olfactory mucosal autografts and rehabilitation for chronic traumatic spinal cord injury," *Neurorehabilitation and Neural Repair*, vol. 24, no. 1, pp. 10–22, 2010.

[30] A. Mackay-Sim, F. Féron, J. Cochrane et al., "Autologous olfactory ensheathing cell transplantation in human paraplegia: a 3-year clinical trial," *Brain*, vol. 131, no. 9, pp. 2376–2386, 2008.

[31] J. Wu, T. Sun, C. Ye, J. Yao, B. Zhu, and H. He, "Clinical observation of fetal olfactory ensheathing glia transplantation (OEGT) in patients with complete chronic spinal cord injury," *Cell Transplantation*, vol. 21, no. 1, pp. S33–S37, 2012.

[32] P. Tabakow, W. Jarmundowicz, B. Czapiga et al., "Transplantation of autologous olfactory ensheathing cells in complete human spinal cord injury," *Cell Transplantation*, vol. 22, no. 9, pp. 1591–1612, 2013.

[33] P. Tabakow, G. Raisman, W. Fortuna et al., "Functional regeneration of supraspinal connections in a patient with transected spinal cord following transplantation of bulbar olfactory ensheathing cells with peripheral nerve bridging," *Cell Transplantation*, vol. 23, no. 12, pp. 1631–1655, 2014.

[34] L. da Silva Meirelles, P. C. Chagastelles, and N. B. Nardi, "Mesenchymal stem cells reside in virtually all post-natal organs and tissues," *Journal of Cell Science*, vol. 119, no. 11, pp. 2204–2213, 2006.

[35] A. Uccelli, L. Moretta, and V. Pistoia, "Mesenchymal stem cells in health and disease," *Nature Reviews Immunology*, vol. 8, no. 9, pp. 726–736, 2008.

[36] P. Lu and M. H. Tuszynski, "Can bone marrow-derived stem cells differentiate into functional neurons?" *Experimental Neurology*, vol. 193, no. 2, pp. 273–278, 2005.

[37] D. Karussis, C. Karageorgiou, A. Vaknin-Dembinsky et al., "Safety and immunological effects of mesenchymal stem cell transplantation in patients with multiple sclerosis and amyotrophic lateral sclerosis," *Archives of Neurology*, vol. 67, no. 10, pp. 1187–1194, 2010.

[38] P. Petrou, Y. Gothelf, Z. Argov et al., "Safety and clinical effects of mesenchymal stem cells secreting neurotrophic factor transplantation in patients with amyotrophic lateral sclerosis," *JAMA Neurology*, vol. 73, no. 3, pp. 337–344, 2016.

[39] E. Syková, P. Jendelová, L. Urdzíková, P. Lesný, and A. Hejčl, "Bone marrow stem cells and polymer hydrogels—two strategies for spinal cord injury repair," *Cellular and Molecular Neurobiology*, vol. 26, no. 7-8, pp. 1111–1127, 2006.

[40] D. P. Ankeny, D. M. McTigue, and L. B. Jakeman, "Bone marrow transplants provide tissue protection and directional guidance for axons after contusive spinal cord injury in rats," *Experimental Neurology*, vol. 190, no. 1, pp. 17–31, 2004.

[41] C. P. Hofstetter, E. J. Schwarz, D. Hess et al., "Marrow stromal cells form guiding strands in the injured spinal cord and promote recovery," *Proceedings of the National Academy of Sciences of the United States of America*, vol. 99, no. 4, pp. 2199–2204, 2002.

[42] A. R. Alexanian, M. G. Fehlings, Z. Zhang, and D. J. Maiman, "Transplanted neurally modified bone marrow-derived mesenchymal stem cells promote tissue protection and locomotor recovery in spinal cord injured rats," *Neurorehabilitation and Neural Repair*, vol. 25, no. 9, pp. 873–880, 2011.

[43] Y. Bhanot, S. Rao, D. Ghosh, S. Balaraju, C. R. Radhika, and K. V. S. Kumar, "Autologous mesenchymal stem cells in chronic spinal cord injury," *British Journal of Neurosurgery*, vol. 25, no. 4, pp. 516–522, 2011.

[44] H. Y. Seung, S. S. Yu, H. P. Yong et al., "Complete spinal cord injury treatment using autologous bone marrow cell transplantation and bone marrow stimulation with granulocyte macrophage-colony stimulating factor: phase I/II clinical trial," *Stem Cells*, vol. 25, no. 8, pp. 2066–2073, 2007.

Hindawi
Stem Cells International
Volume 2017, Article ID 9453108, 12 pages
https://doi.org/10.1155/2017/9453108

Review Article

The Roles of Insulin-Like Growth Factors in Mesenchymal Stem Cell Niche

Amer Youssef,[1,2,3,4] Doaa Aboalola,[3,4,5,6] and Victor K. M. Han[1,2,3,4,5]

[1]*Department of Biochemistry, Western University, London, ON, Canada*
[2]*Department of Paediatrics, Schulich School of Medicine and Dentistry, Western University, London, ON, Canada*
[3]*Children's Health Research Institute, Western University, London, ON, Canada*
[4]*Lawson Health Research Institute, Western University, London, ON, Canada*
[5]*Department of Anatomy and Cell Biology, Western University, London, ON, Canada*
[6]*King Abdullah International Medical Research Center, National Guard Health Affairs, Jeddah, Saudi Arabia*

Correspondence should be addressed to Victor K. M. Han; victor.han@lhsc.on.ca

Received 13 September 2016; Revised 22 December 2016; Accepted 18 January 2017; Published 16 February 2017

Academic Editor: Andrea Ballini

Many tissues contain adult mesenchymal stem cells (MSCs), which may be used in tissue regeneration therapies. However, the MSC availability in most tissues is limited which demands expansion in vitro following isolation. Like many developing cells, the state of MSCs is affected by the surrounding microenvironment, and mimicking this natural microenvironment that supports multipotent or differentiated state in vivo is essential to understand for the successful use of MSC in regenerative therapies. Many researchers are, therefore, optimizing cell culture conditions in vitro by altering growth factors, extracellular matrices, chemicals, oxygen tension, and surrounding pH to enhance stem cells self-renewal or differentiation. Insulin-like growth factors (IGFs) system has been demonstrated to play an important role in stem cell biology to either promote proliferation and self-renewal or enhance differentiation onset and outcome, depending on the cell culture conditions. In this review, we will describe the importance of IGFs, IGF-1 and IGF-2, in development and in the MSC niche and how they affect the pluripotency or differentiation towards multiple lineages of the three germ layers.

1. Introduction

Currently, many diseases associated with organ failure and degeneration which are untreatable by pharmaceuticals or organ replacement have seen the promise in cell-replacement and tissue regeneration therapies [1]. Such diseases include endocrine (diabetes), neurodegenerative diseases (Parkinson's, Alzheimer's, and Huntington's), and cardiovascular diseases (myocardial infarction and peripheral vascular ischemia) and injuries or chronic conditions in the cornea, skeletal muscle, skin, joints, and bones [2]. Stem cells have the potential for tissue/organ repair, replacement of dying cells, and promoting the survival of damaged tissues [3]. In addition, with the ability to generate induced pluripotent stem cells from the recipient's own somatic cells [4–6] and the availability of new gene editing technologies (e.g., CRISPR-Cas9 and TALEN) [7, 8], the use of stem cells in many genetic and acquired diseases is closer to reality in the near future.

Adult mesenchymal stem cells (MSCs) are multipotent cells with a defined capacity for self-renewal and differentiation into cell types of all three germ layers depending on their origin. Unlike embryonic stem cells, MSCs have less ethical controversies and lower tumorigenicity; however, they have restricted differentiation potential [9]. Recent research has also demonstrated a transdifferentiation ability of MSCs from cells of one germ layer to another [10]. In addition, MSCs have an immunomodulatory effect to reduce an immune response and are able to be engrafted successfully in therapy resistant graft-versus-host disease [3]. The existence of multipotent stem cells in adult tissues was first described by Till and

McCulloch in 1961 [11] and was followed by the isolation of MSCs from bone marrow by Friedenstein in 1968 [12]. Since then, MSCs have been isolated from most mature organs and tissues including skeletal muscle [13], adipose tissue [14], deciduous teeth [15], umbilical cord blood and placenta [16], peripheral blood [17], and brain [18]. Several biological markers characterize MSCs of different origins to be positive for CD73, CD105, CD29, CD44, CD71, CD90, CD106, CD120a, and CD124 and negative for CD117, CD34, CD45, and CD14 [19–21]. MSCs have been demonstrated to differentiate predominantly into mesodermal cells including osteogenic, chondrogenic, adipogenic [22], and endothelial [23] lineages. Also, MSCs can differentiate towards ectodermal lineages including corneal [24, 25] and neuronal cells [26] and also can differentiate towards insulin-producing cells of the endodermal endocrine pancreatic lineage [27].

Stem cell "niche" is a paracellular microenvironment that includes cellular and noncellular components from local and systemic sources that regulate stem cell pluripotency or multipotency, proliferation, differentiation, survival, and localization [28]. Stem cells are maintained by the surrounding microenvironment *via* several cues including physical, structural, neural, humoral, paracrine, autocrine, and metabolic interactions [29]. Therefore, a combination of different microenvironmental signals that are generated during development, healing, or disease states is capable of regulating the tissue regeneration process leading to proliferation, differentiation, or quiescence [30]. In this review, we will focus on the role of insulin-like growth factors (IGFs) in the MSC niche (Figure 1).

2. Insulin-Like Growth Factor System: Ligands, Receptors, and Binding Proteins

Insulin-like growth factors (IGFs; IGF-1 and IGF-2) are two small polypeptides (~7 kDa) that regulate survival, self-renewal, and differentiation of many types of cells, including stem cells [31]. In the systemic circulation in postnatal life, IGF-1 levels are regulated by growth hormone (GH), which induces IGF expression and is released by the liver and accounts for 70–90% of circulating IGFs [32]. Knockdown of *Igf-1* from postnatal murine liver accounted for 75% reduction in circulating IGF-1 levels accompanied by a fourfold increase in GH, which can lead to insulin resistance [33]. Even in the absence of hepatic IGF-1, postnatal growth is not affected in mice. This is likely due to extrahepatic tissue expression of IGFs in a paracrine/autocrine fashion, such as in the bone, brain, lung, uterus, ovaries, adipose tissue, and muscle [34]. Under this condition, serum IGF concentrations are regulated by several factors including gender, age, and nutrition status, leading to a variable range of IGF-1 (264–789 ng/mL) and IGF-2 (702–1042 ng/mL) in healthy individuals [35]. In prenatal (embryonic/fetal) life, the regulation of the synthesis of IGF-1 and IGF-2 by many different organs and tissues is less well understood. Most likely, the synthesis is regulated by local (paracrine) factors and cues such as nutrient status, oxygen tension, biochemistry, extracellular matrix, and other growth factors in addition to endocrine factors. Importantly, the IGFs are synthesized as required by the developmental and physiological cues within the extracellular and intracellular environment. It is likely that the fate of mesenchymal stem cells which reside in the paracellular niches in adult tissues is regulated by the tissue microenvironment.

At the molecular level, IGF-1 shares more than 60% sequence homology with IGF-2 and 50% with proinsulin [42, 43]. IGFs signal mainly *via* the IGF-1 receptor (IGF-1R), which has the highest binding affinity (Kd of 1 nM) towards IGF-1, followed by 10-fold lower affinity to IGF-2 [44]. IGF-1R is a receptor-tyrosine-kinase (RTK) which shares a structural homology domain with the insulin receptor (IR). In turn, IR is expressed in two isoforms, IR-A and IR-B, and can form hybrid receptors (HR-A and HR-B) with the IGF-1R, which binds to both IGFs with variable affinities [45]. Unlike IGF-1, IGF-2 binds to its specific receptor, IGF-2R, and, similar to insulin, it can bind to IR-A [46]. IGF-1R, IR, and HRs are mitogenic RTKs, while IGF-2R is not. Therefore, different receptor and ligand combinations can cause variable signaling outcomes, especially in stem cells. Few studies have been reported on the effects of IGF-1 on the growth, differentiation, and migratory capacity of mesenchymal stem cells [36, 38, 47]; however, the expression of different IGF receptors, insulin receptors, and hybrid receptors and their relative roles in pluripotency and differentiation have not been well studied.

Circulating IGFs are bound to six soluble (~30 kDa) IGF-binding proteins (IGFBPs, 1–6), which determine the bioavailability of free IGF ligand in the extracellular vicinity of the receptors, thus modifying the IGF actions [48]. Under normal physiological conditions, IGFs bind IGFBPs with greater affinity than they bind IGF-1R [49–51]. IGFBPs interaction with IGFs occurs *via* noncovalent binding [52] that protects them from degradation by increasing their half-life [53, 54] and facilitates delivery to specific tissues. Therefore, IGFBPs play an important role in IGF-regulated cell metabolism, development, and growth [55]. In addition, it has become apparent that the IGFBPs can be expressed and maintained within the cellular microenvironment and have additional functions independent of regulating IGFs [56]. The role of IGFBPs in MSC fate is currently being delineated and will be mentioned briefly in this review.

3. Insulin-Like Growth Factor System: Signaling Cascades

IGF-1R is a transmembrane tetramer receptor that exists as heterodimers composed of two α and β hemireceptors linked by disulfide bonds in a β–α–α–β structure [57]. Upon ligand binding, the downstream signal of IGF-1R is dependent on the differential phosphorylation pattern of its β-subunit and the resultant tyrosine residues available to initiate mitogenic signals, mainly through the phosphoinositide 3-kinase (PI3K), AKT/PKB, and the extracellular signal-regulated kinase (ERK1/2) [55, 58, 59]. In this manner, IGF-1R can induce transcriptional activity to promote survival, self-renewal, and differentiation of MSCs [60, 61].

Upon activation of the extracellular α subunits of the IGF-1R, autophosphorylation in the tyrosine residues on

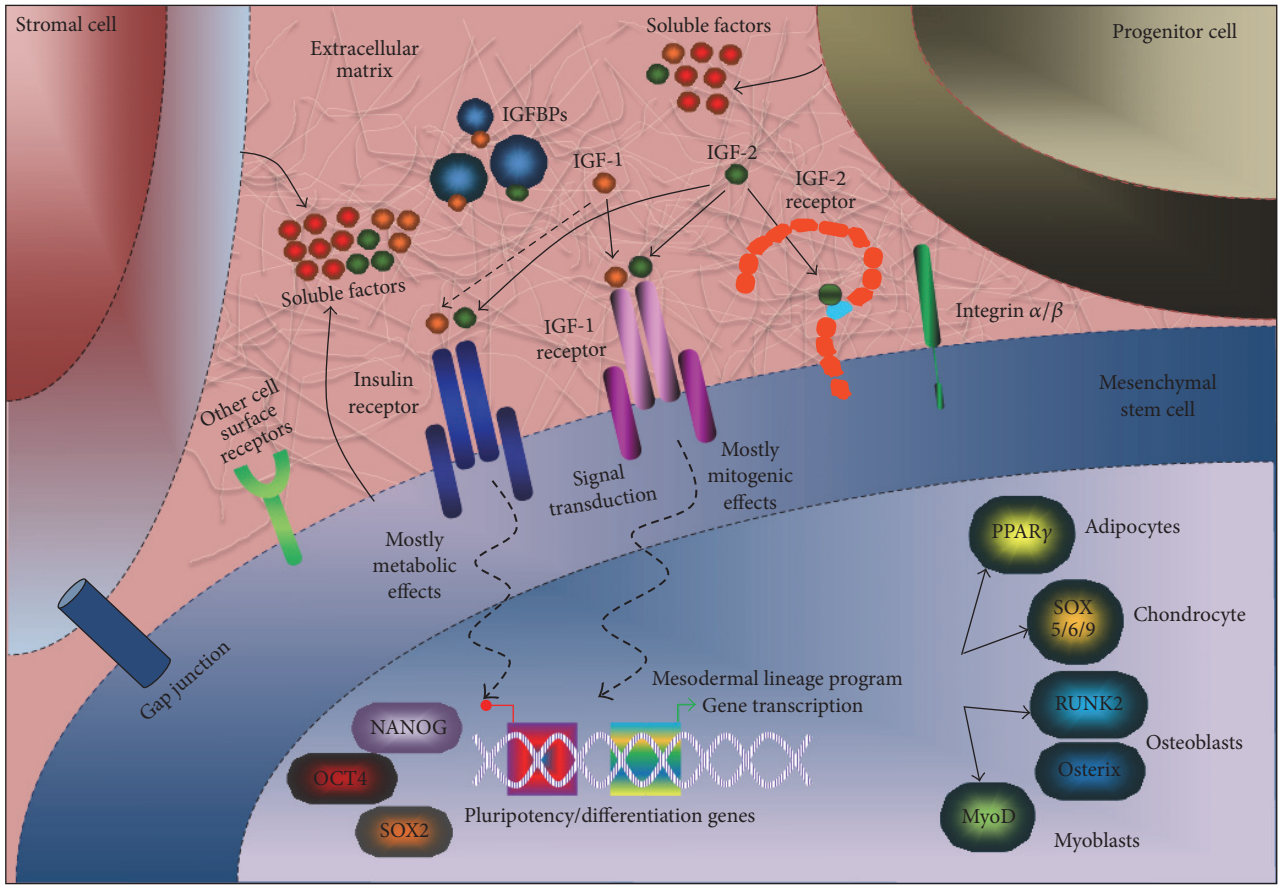

Figure 1: Stem cell niche in vivo. The stem cell niche is a complex compartment surrounding mesenchymal stem cells (MSCs) directing their identity preservation via cellular and acellular components. Various clues and signals are exchanged between MSCs, stromal cells, and progenitor cells and the extracellular matrix containing different soluble factors, oxygen tension, and pH. Therefore, MSC niche manipulates the stemness state of MSCs following growth and regeneration demand. IGFs can signal *via* paracrine/autocrine (produced locally by the tissue) or endocrine (delivered by blood supply) routes to interact with IGF-1 receptor, IGF-2 receptor, or the insulin receptor on MSCs and other cells. IGFBPs (extracellular and/or intracellular actions) can modify IGF actions and affect their stability and degradation. Other receptors and integrins are expressed in MSCs and can be affected by extracellular microenvironment. MSC differentiation occurs by signal transduction which controls the shutdown of pluripotency-associated genes, such as OCT4, SOX2, and NANOG, for the upregulation of differentiation genes. For example, MSCs can give rise to all mesodermal lineages depending on the transcription factor expressed to generate adipose, cartilage, bone, and muscle. Also, transdifferentiation of MSCs into endodermal and ectodermal lineages can occur, as reported by in vitro studies.

β-subunits creates high affinity binding sites for signaling adaptor molecules and substrates. For the ERK1/2 signaling pathway, SHC interacts directly with the IGF-1Rβ which recruits GRB2 that interacts with SOS that subsequently activates c-RAS leading to the sequential phosphorylation of RAF, MEK1/2, and then ERK1/2 [42, 62–66]. To activate the PI3K/AKT signaling, p85, the regulatory subunit of PI3K, interacts directly with IGF-1Rβ independent of SHC binding [67]. IRS-1 is a main target of the IGF-1R, implicated in the mitogenic effect of IGF-1R, inhibition of apoptosis, and transformation, whereas its downregulation has been associated with the inhibition of differentiation and the induction of apoptosis [58, 68]. The phosphorylation of IRS-1 amplifies the IGF-1R signaling by indirectly recruiting GRB2 to transduce ERK1/2 signaling [62] or p85 to transduce PI3K signaling [69]. Therefore, surrounding microenvironmental inputs would define stem cell behavior depending on receptor activation and the combination of signaling cascades.

4. The Role of IGFs in Growth and Development

During development, circulating IGF levels correlate proportionally with placental and fetal weights, and reduced levels due to poor maternal-nutrition have been suggested to lead to fetal growth restriction [70]. In human pregnancies, IGFs play an early role in promoting proliferation/differentiation and preventing cell apoptosis of various types of placental cells [61]. In mice, knockout of *Igf-1* or *Igf-1r* causes restricted growth (<60% of wild-type) and a premature death of

newborn embryos. Most pups with *Igf-1r*−/− are unable to survive due to the lack of functional muscles required for breathing, while some mouse lines with *Igf-1*−/− will survive with deficits in major organs [71–73]. On the other hand, *Igf-2* knockout mice (indistinguishable between homozygous and heterozygous) are viable at 60% birthweight of wild-type [74]. Double mutants for *Igf-1* and *Igf-2* are severely growth-deficient (30% of wild-type) and die shortly after birth of respiratory failure. Although both IGFs have an additive effect in embryonic development, IGF-1 is more important in postnatal growth, while IGF-2 is important for prenatal fetoplacental growth. Hence, IGF-1 and IGF-2 stimulate both proliferation and terminal differentiation of many organs and tissues in developing embryos and adult life. Due to the initial description of *Igf-1*, *Igf-2*, and *Igf-1r* null mice using classic knockout methodology, mice with tissue-specific knockout of these genes have been generated using Cre/loxP conditional knockout strategies with interesting and variable phenotypes [75–78]. The major differences between the models are the tissue/cell-specificity and the timing of the null mutation (prenatal or postnatal). Most of the conditional targeted models are generated with gene targeting after birth to allow examination of the role of *Igf-1* and *Igf-1r* in postnatal development without the ability to discriminate null mutation in stem or somatic cells. In classic knockout models, gene targeting occurs in the embryonic stem cells, allowing us to examine the impact of *Igf* genes in stem cells. However, only very few reports are available investigating the impact of the knockout of *Igf-1* and *Igf-1r* in stem cells. Knockout of *Igf-1r* in adult neural stem cells maintains youthful characteristics of the olfactory bulb neurogenesis within the aging brain by increasing the cumulative neuroblast production and enhancing neuronal integration into the olfactory bulb, suggesting a gain of function during aging [79].

5. The Role of IGFs in MSC Multipotency and Self-Renewal

MSCs isolated from different tissues, such as bone marrow, adipose tissue, placental chorionic villi, and fetal membranes, express and secrete IGF-1 and/or IGF-2 in vitro [80–83]. It was shown that ectopic IGF-1 expression in MSCs enhances their proliferation with lower apoptosis [84]. In this study, autocrine IGF-1 levels maintain an elevated baseline activity of ERK1/2 signaling required for enhanced self-renewal (higher OCT4), endodermal (higher CYP51) and mesodermal (higher SM22α) potential, but weakened neuronal potential (lower Nestin) [84]. Another growth factor which is basic fibroblast growth factor (bFGF) was shown to be required in maintaining stemness and proliferation in hESCs [31, 85] and in MSCs [80, 86, 87]. Further investigation showed that this bFGF effect was mediated via the IGF system that is upregulated by an autonomous expression of IGF-1R, IGF-1, and IGF-2, as shown in umbilical cord MSCs [86]. Although both IGF-1 and IGF-2 are involved in mediating stem cell fate changes, IGF-2 appears to be more prominent than IGF-1 in promoting MSC pluripotency/self-renewal. In hESCs, one study showed that IGF-2, secreted by spontaneously differentiated autologous fibroblast-like cells in response to bFGF, is required to maintain hESC pluripotency and self-renewal via the signaling of IGF-1R [31]. However, one study showed that hESCs pluripotency/self-renewal maintenance can be independent of IGF-2 secretion only when MSCs are used as a feeder layer [88]. A study, in human dental pulp MSCs (hDSCs), confirmed that IGF-1R is required for MSC multipotency and can be regarded as a selection marker for stemness, just similar to OCT4 and SOX2 [89]. In placental MSCs (PMSCs), IGF-2 is upregulated by low oxygen tension and is required to maintain MSC multipotency [80, 87]. Also, in neural stem cells (NSCs), IGF-2 was shown to play an important role in maintaining self-renewal [90]. In these NSCs, the IGF-2 self-renewal properties were mediated *via* A-isoform of IR (IR-A), independent of IGF-1R or IGF-2R [91]. For a more detailed review on insulin and IGF receptor signaling in neural stem cells, please see Ziegler et al. (2015) [92]. We verified the role of IR-A in PMSC, where we showed an elevated expression level of IR-A versus IR-B; and both IGF-1 and IGF-2 promote increased proliferation and self-renewal with a requirement that both IGF-1R and IR must be present [80]. Although IGF-1R and IR can form hybrid receptors, the role of hybrid receptor in maintaining stem cell fate (ESCs or MSCs) and pluripotency is yet to be confirmed.

6. Induction of Same-Origin MSCs towards Different Lineages

In vitro, MSC differentiation can be initiated *via* extrinsic stimulation by growth-factor-mediated differentiation [93] that requires withdrawing maintenance growth factors and adding differentiation promoting growth factors and chemicals [28, 29]. Differentiation factors can include butylated hydroxyanisole and NGF for neuronal differentiation; BMP-12 for tenocyte differentiation; dexamethasone, 3-isobutyl-1-methylxanthine, insulin, and indomethacin for adipogenic differentiation; monothioglycerol, HGF, oncostatin, dexamethasone, FGF4, insulin, transferrin, and selenium for hepatocytic differentiation; b-FGF and VEGF for endothelial differentiation; TGF-β1, insulin, transferrin, dexamethasone, and ascorbic acid for chondrogenic differentiation; insulin, transferrin, and selenium for skeletal myogenic differentiation; and dexamethasone, ascorbic acid, and β-glycerophosphate for osteogenic differentiation [94–99]. Therefore, the same MSC population in the mesoderm exposed to different extrinsic stimuli can initiate differentiation towards a specific cell type by triggering a tissue-specific transcription factor, such as SOX5/6/9 for chondrocytes, PPARγ for adipocytes, MyoD family for myoblasts, and RUNX2/Osterix for osteoblasts [100]. Moreover, MSCs are shown to transdifferentiate to lineages outside of the mesodermal lineage. In these complex differentiation processes, IGFs are shown to play a role in fine-tuning transcription factor expression levels and activity and defining commitment towards specific lineages from the three germ layers.

7. The Role of IGFs in Mesenchymal Stem Cell Fate Specification and Differentiation

7.1. Mesodermal Differentiation

7.1.1. Osteogenesis. IGF-1 and IGF-2 are secreted by skeletal bone cells for stimulation of bone formation, growth, and metabolism and prevent apoptosis in a paracrine/autocrine manner [101, 102]. Local overexpression of IGF-1 in osteoblasts can accelerate the rate of bone formation and increase the pace of matrix mineralization, which is dependent on IGF-1R [103]. Decoupling of IGF-1R signaling from IGF-1 is responsible for reduced proliferation/differentiation in primary osteoblast from osteoporosis patients, hence causing bone loss [104]. Under nondifferentiation conditions, IGF-1 transfected human MSCs were able to upregulate expression of various osteoblast genes [105]. For regeneration, bone marrow MSCs (BM-MSCs) secrete IGF-1 and the use of their conditioned media was required to restore alveolar bone regeneration prior to dental implant placement [106]. In dental pulp MSC differentiation, IGF-1 was shown to promote mTOR signaling pathway in order to trigger the expression of RUNX2, OCN, OSX, and COL1 [36]. Also, human deciduous teeth MSCs with high osteopotential express and secrete IGF-2 that is required for differentiation and mineralization [107]. Overall, IGF-1 and IGF-2 play a significant role in MSC osteogenic differentiation and bone health.

7.1.2. Myogenesis. L6E9 cells (a myoblast cell line used in late myogenesis studies), when stimulated with IGF-1, have an initial proliferative response [108]. During rapid cell division, the myogenic regulatory factors are inhibited, whereas, 30 hours later, the mitogenic effect is suppressed and Myogenin expression and activity are increased. Although the downstream factors in IGF-mediated differentiation are still under investigation, IGFs can induce myogenic transcription factors. In contrast, the overexpression of MyoD (a protein that plays a major role in regulating muscle differentiation) in C3H 10T1/2 mouse embryonic fibroblast cells induces IGF-2 expression which in turn activates IGF-1R and its downstream target AKT [109]. Specifically, IGF-2 is required for the recruitment and induction of myogenic promoters and myogenesis [110]. In particular, IGF-2 is required to allow continued recruitment of MyoD-associated proteins at the Myogenin promoter [111]. Moreover, IGF-2 specific binding protein, IGFBP-6, is expressed during embryonic development in many different tissues including the ossifying bones of the cranium, myoblasts, and the motor neurons of the spinal cord [112].

The potential use of MSCs has been investigated in treating muscular injury and myocardial infarction. Rat BM-MSCs have been used as the source of paracrine factors to treat soleus muscle injury [113]. Pretreatment of MSCs with IGF-1 improves MSC healing ability by reducing scar formation, increasing angiogenesis and faster reconstitution of muscle structure, and improving function [113]. In another study, injection of BM-MSCs into the cardiac muscle increased the proliferation and migration and inhibited apoptosis of existing cardiac muscle cells; however, IGF-1 does not induce myocardial differentiation of these MSCs [114]. In addition, transplantation of IGF-1-primed MSCs attenuates cardiac dysfunction, increases the survival of engrafted cells in the ischemic heart, decreases myocardium cell apoptosis, and inhibits the expression of inflammation cytokines such as tumor necrosis factor-alpha (TNF-α), interleukin-1β (IL-1β), and IL-6 [115]. The current research into MSCs and IGF in myogenesis is, therefore, more focused on in vivo muscle repair than on MSC-differentiated myoblast in transplantation.

7.1.3. Adipogenesis. In a comparative study between MSCs from different sources including adipose stem cells (ASCs), bone marrow stem cells (BMSCs), dermal sheath cells (DSCs), and dermal papilla cells (DPCs), IGF-1 had the highest expression and secretion in ASCs compared to the other populations [116]. Also, IGF1 could promote lineage bias and selection for adipogenic progenitor (CD31−/CD34+/CD146−) cells at the expense of the less adipogenic cells (CD31−/CD34+/CD146+) [37]. In this process, IGF-1 attenuates Wnt/β-catenin signaling by activating Axin2/PPARγ pathways to promote the selection for (CD31−/CD34+/CD146−) cells [37]. In another study, IGF-1 was shown to alter MSC fate between osteogenic and adipogenic lineages by its ability to bind and form a complex with the acid-labile subunit (ALS) [117]. The loss of this IGF-1/ALS complex shifted differentiation from osteogenesis to adipogenesis [117].

7.1.4. Chondrogenesis. In an intervertebral disc degeneration study, it was shown that IGF-1 and TGF-β3 work in synergy to enhance nucleus pulposus-derived mesenchymal stem cells viability, extracellular matrix biosynthesis, and differentiation towards nucleus pulposus cells [118]. Although TGF-β signaling is known to be important for chondroinductive differentiation from MSCs, more studies are showing that IGF-1 can regulate MSC chondrogenesis independent of TGF-β. In one study, IGF-1 can induce chondrogenic differentiation from adipose-derived MSCs with increased collagen type II, Aggrecan, and SOX9 levels [38]. Similarly, IGF-1 induced the chondrogenic potential of BM-derived MSCs stimulating proliferation, regulating apoptosis, and inducing expression of chondrogenic markers [119]. In this play of IGF-1 in chondrogenesis, IRS-1 localization was induced from being nuclear to being cytoplasmic to shift MSC proliferation to differentiation [120].

7.2. Ectodermal Differentiation

7.2.1. Corneal and Neurogenesis. IGF-1 plays an important role in ectodermal lineage differentiation. MSC differentiation towards neural progenitor cells (NPCs) is enhanced by IGF-1 with increased expression of Nestin and the rate of cell proliferation, while it inhibits apoptosis and induces higher terminal differentiation of NPC towards neurons and glial cells [40]. In another study, the administration of IGF-1 alone in addition to corneal extract stimulated differentiation of BM-MSCs into corneal-like cells more efficiently [39]. Mice with reduced IGF-1R expression in

the brain in conditional mutant *nes-Igf1r*$^{-/Wt}$ demonstrate greater neuronal damage following hypoxic-ischemic injury, suggesting the importance of IGF-1R in neuronal cells, including neuronal progenitor and stem cells [121]. IGFBP-2 promotes the keratocyte phenotype of differentiating human corneal fibroblasts from MSCs by increasing the expression of keratocan and ALDH1A1 and decreasing α-smooth muscle actin [122]. In addition, IGF-1 overexpressing UC-MSCs are able to differentiate more successfully to neural progenitor cells producing more Pax6-positive cells and Nestin-positive cells and could differentiate into astrocytes with higher efficiency [123].

7.2.2. Epidermal and Dermal Lineages. The role of MSCs and IGFs has been explored in the treatment of skin ulcers, particularly challenging clinical conditions like diabetes [124]. In the developing skin, IGF-1 is expressed in the stratum granulosum, dermal fibroblasts, and the differentiating hair follicles and sebaceous glands [125]. In particular, IGF-1 is strongly expressed in the injury area, where it plays an important role in both epidermal and dermal wound-healing [126]. Recently, BM-MSCs were used in a rodent model of diabetic foot ulceration and were demonstrated to improve wound-healing and to increase the expression of local GFs including IGF-1, EGF, and MMP2 [127].

7.3. Endodermal Differentiation

7.3.1. Endocrine Pancreas and Liver. MSC differentiation towards β-cells, derived by stepwise media formulation, has not been successful to generate fully functional and glucose-responsive insulin-secreting β-cells. However, similar to treating patients with cardiac infarction, MSC transplantation into diabetic patients is being investigated. Umbilical cord MSCs injected in vivo in an induced diabetic rat model were able to prevent hyperglycemic progression and preserve islet size and cellularity; IGF-1 secreted by MSCs was responsible for islet viability and insulin secretion in vitro [128]. Therefore, IGF-1 is a prominent trophic factor in pancreatic islet function and development, which may be required for β-cell differentiation in vitro. In hepatocyte differentiation, IGF-1 is expressed and required in the liver during development. It was shown that the addition of IGF-1 to differentiation media induced earlier hepatocyte morphology changes, albumin and AFP expression, glycogen storage, urea production, and albumin secretion [41].

8. Crosstalk between the IGF Axis and Other Signaling Pathways in MSC Proliferation and Differentiation

Adult MSCs express different genes associated with both self-renewal and differentiation, including members of the Notch, TGFB, FGF, WNT, IGF, hedgehog families, and G-protein coupled receptor-mediated and cAMP-mediated signaling [129]. Crosstalk between signaling pathways has been shown to be important for stem cells' self-renewal and differentiation; however, specific interactions with the IGF system are still being delineated in MSCs.

As shown in Figure 1, integrins can play an important role in IGF signaling. In particular, IGF-1 directly binds to $\alpha v\beta 3$ integrin and induces $\alpha v\beta 3$-IGF1-IGF1R ternary complex formation required for phosphorylation, ERK and AKT activation, and cell proliferation [130].

In primary oligodendrocyte precursors, IGF-1 signaling was shown to increase β-catenin protein abundance via the IGF-1-induced phosphorylation of AKT and GSK3 required for an increase in cyclin D1 mRNA, proliferation, and survival [131].

To enhance migration and homing after transplantation, IGF-1 upregulates the level of the CXCR4, receptor for the chemokine stromal cell-derived factor-1, and SDF-1, in MSCs and in turn can accelerate migration [132, 133]. In these MSCs, CXCR4 upregulation is mediated by the PI3K/AKT pathway downstream of the activated IGF-1R [133]. In vivo, MSC preconditioning with IGF-1, before administration, was shown to be effective in migration and homing which was required for the restoration of renal function following acute kidney injury [47].

In bone formation and osteoblast differentiation, IGF-2 was shown to potentiate the bone morphogenetic protein-9 (BMP-9), which belongs to the transforming growth factor-β (TGF-β) superfamily [134]. IGF-2, mediated via the PI3K/AKT, can potentiate BMP-9-induced activity of the early osteogenic marker alkaline phosphatase (ALP) and the expression of later markers such as osteocalcin and osteopontin in MSCs. On the other hand, IGFBP3 and IGFBP4 can inhibit the potentiation effect of IGF-2 on BMP-9-induced ALP activity and matrix mineralization in MSCs [134].

Also, in osteoblast differentiation of BM-MSCs, hedgehog (HH) via Gli2 was shown to increase IGF-2 expression that was acting via the IGF-1R/mTORC2/AKT [135]. IGF-2-mediated AKT activation served as a positive feedback loop for enhanced HH transcriptional output by stabilizing full-length Gli2 due to phosphorylation by AKT. In myogenic differentiation, sonic hedgehog (SHH), member of HH family, was also regarded as positive regulator of IGF-1 signaling in a cooperative additive effect in primary myoblast proliferation and differentiation via the MAPK/ERK and PI3K/AKT pathways [136]. In this process, Smoothened, a SHH effector, can associate with IGF-1R and is required for IGF-1 action via AKT, especially for differentiation.

Crosstalk between the IGF system and other pathways has also been explored in cancer stem cells which may not be dependent on their immediate niche but can give an insight into normal MSCs [137]. In glioma stem cells (GSC), HH via Gli1 upregulated the transcriptional activation of IRS-1 which increased GSC sensitivity to IGF-1 stimulation [138]. In lung adenocarcinoma stem-like cells, IGF-1R-mediated OCT4 expression to form a complex with β-catenin and SOX2 was crucial for the self-renewal and oncogenic potential [139]. Other signaling pathways are shown to interact with the IGF system in many cell types that are still to be elucidated in the MSC population and understand their effect in self-renewal and differentiation.

Table 1: MSC differentiation protocols with IGFs towards different lineages. Example of MSC differentiation protocols included IGFs in their differentiation media formulations.

MSC population	Differentiation	Protocol	Reference
Human dental pulp stem cells	Osteoblast-like cells	Osteogenic media supplemented with 0.1 μmol/L dexamethasone, 10 mmol/L b-glycerophosphate, 50 μg/mL ascorbic acid, and 100 ng/mL of IGF-1.	[36]
Stromal vascular fraction of adipose tissue, human adipose stem/progenitor cells	Adipocyte-like cells	StemPro® Adipogenesis Differentiation Kit supplemented with 10 ng/mL of IGF-1.	[37]
Human adipose-derived mesenchymal cells	Chondrocyte-like cells	DMEM high glucose supplemented with 1% FBS, 0.1 mM ascorbic acid-2-phosphate, 10^{-7} dexamethasone, 6.25 μg/mL transferrin, 6.25 ng/mL selenous acid, 10 ng/mL recombinant human TGF-β1, and 100 ng/mL recombinant human IGF-1.	[38]
Mouse bone marrow mesenchymal stem cells	Corneal-like cells	MSCs were cultured for 3, 7, or 10 days in complete DMEM with 20% extract from the corneas and 20 ng/mL IGF-1.	[39]
Rat bone marrow mesenchymal stem cells	Neural-like cells	Proliferation media: NeuroCult® NS-A proliferation media specific for rat supplemented with 20 ng/mL EGF, 20 ng/mL bFGF, and 100 ng/mL IGF-1. Differentiation media: NeuroCult supplemented with 10 ng/mL PDGF-BB for glial induction or 10 ng/mL rh-BDNF for neuronal differentiation.	[40]
Human bone marrow mesenchymal stem cells	Hepatocyte-like cell	Step 1: DMEM low glucose supplemented with 10% FBS, 20 ng/mL of IGF-I, 20 ng/mL of HGF, and 10^{-7} M dexamethasone for 7 days. Step 2: step 1 media with 10 ng/mL Oncostatin M for 14 days.	[41]

9. IGF-Expressing MSCs in Treating Terminal Diseases

Paracrine factors, including IGFs, secreted by MSCs are shown to play a major role in treating organ-failure-causing diseases. IGF-expressing MSCs were shown to enhance proliferation, differentiation, and repair of surrounding tissue in kidney, heart, and pancreas [81–83]. In kidney ischemic-reperfusion injury, physical interaction between MSC and kidney tissue was required to promote kidney repair and not only MSC conditioned media alone [83]. Genetically engineered IGF-1-MSCs were used to treat liver cirrhosis in mice [140]. Transplanted MSC induced higher IGF-1 and HGF expression with lowered TGF-β1 levels and less activation of hepatic satellite cells. IGF-1 effect was evident by lowered collagen expression and fibrosis with more parenchymal cell proliferation as indication of liver regeneration. Following myocardial infarction, it was shown that adult human epicardium-derived cells and cardiomyocyte progenitor cells synergistically improve cardiac function, probably instigated by complementary paracrine actions [141]. In fact, cotransplantation of unmodified MSC plus cardiovascular progenitors had elevated expression of factors promoting cardiac repair specifically IGF1 that promoted expression of prosurvival and angiogenesis genes in human cells [142].

In induced diabetes STZ mice, MSC helped to attenuate abnormal function of adipocytes, which are involved in cutaneous wound-healing, by IGF-1 secretion [143]. IGF-1 in these mice helped in activating PI3K/AKT and GLUT4 which improved glucose uptake and insulin sensitivity, therefore improving diabetic wound-healing. In hepatocellular carcinoma (HCC) treatment, fetal human MSCs conditioned media were used to inhibit cell growth [144]. It was discovered that the conditioned media contained high levels of IGFBPs which sequestered IGFs and reduced IGF-1R and AKT activation, leading to cell cycle arrest in HCC. These tumor-specific effects were not observed in matched hepatocytes or patient-derived matched normal tissue. In all these examples, MSCs expressing IGF system components are being used in enhancing tissue repair of failing organs, fighting cancer, and ameliorating diabetes.

10. Critical Use of IGF and Insulin in Cell Culture Conditions

Addition of IGFs to differentiation media leads to earlier commitment and higher onset of differentiation in several lineages including endothelial, corneal, neural, chondrocyte, adipocyte, hepatocytes, and osteoblast cells (Table 1). In this context, a typical concentration of 10–100 ng/mL of

IGF-1 is sufficient to activate only the IGF-1R and not the IR. On the other hand, not much attention is given to receptor binding affinity of IGF-1R versus IR, when insulin is used in maintenance or differentiation conditions. The inclusion in commercial biological products for stem cell research of nonphysiological concentrations of insulin (0.5, 5, and 10 μg/mL) for MSC differentiation media is 100–1,000x higher than highest insulin concentration in serum [145]. High concentrations of insulin ($\geq$1 μg/mL) not only activate IR but also activate IGF-1R [44, 145]. Therefore, using such high insulin concentrations in defined media, which can be a substitute to IGFs, cannot distinguish whether the effect is mediated via IGF-1R or IR signaling pathways and studies describing the effect of IGFs in growth and/or differentiation of stem cells in "defined medium" should recognize this potential confounding effect.

11. Summary and Conclusions

IGFs are among the earliest growth factors to be expressed in a developing embryo as early as in preimplantation embryos and putatively act as autocrine/paracrine factors on many developing cells including stem cells. They form an important component of the stem cell niche. Their expression is ubiquitous in many cell types; however, they are most abundant in the cells and tissues of mesodermal origin. Thus, MSCs are both the source and target of IGFs during development and likely play important roles in the maintenance of pluripotency as well as determining their fate to lineages of all three germ layers. Recent evidence also suggests the potential discriminating roles of IGF-1 and IGF-2 in MSCs and progenitor cells of different tissues. As MSCs are being investigated as being important for cellular replacement and regenerative therapies, delineating the roles of endogenous as well as exogenous IGFs in MSC growth and differentiation will be critical in developing these cellular therapies towards treatment of many degenerative diseases that have no viable therapeutic options at present.

Competing Interests

The authors declare that they have no competing interests.

Acknowledgments

This work was supported by CIHR Grant 111024.

References

[1] G. Q. Daley, "The promise and perils of stem cell therapeutics," *Cell Stem Cell*, vol. 10, no. 6, pp. 740–749, 2012.

[2] A. Sánchez, T. Schimmang, and J. García-Sancho, "Cell and tissue therapy in regenerative medicine," *Advances in Experimental Medicine and Biology*, vol. 741, pp. 89–102, 2012.

[3] M. B. C. Koh and G. Suck, "Cell therapy: promise fulfilled?" *Biologicals*, vol. 40, no. 3, pp. 214–217, 2012.

[4] W. E. Lowry, L. Richter, R. Yachechko et al., "Generation of human induced pluripotent stem cells from dermal fibroblasts," *Proceedings of the National Academy of Sciences of the United States of America*, vol. 105, no. 8, pp. 2883–2888, 2008.

[5] T. Aasen, A. Raya, M. J. Barrero et al., "Efficient and rapid generation of induced pluripotent stem cells from human keratinocytes," *Nature Biotechnology*, vol. 26, no. 11, pp. 1276–1284, 2008.

[6] J. Wang, Q. Gu, J. Hao et al., "Generation of Induced Pluripotent Stem Cells with High Efficiency from Human Umbilical Cord Blood Mononuclear Cells," *Genomics, Proteomics and Bioinformatics*, vol. 11, no. 5, pp. 304–311, 2013.

[7] L. Cong, F. A. Ran, D. Cox et al., "Multiplex genome engineering using CRISPR/Cas systems," *Science*, vol. 339, no. 6121, pp. 819–823, 2013.

[8] D. Reyon, S. Q. Tsai, C. Khgayter, J. A. Foden, J. D. Sander, and J. K. Joung, "FLASH assembly of TALENs for high-throughput genome editing," *Nature Biotechnology*, vol. 30, no. 5, pp. 460–465, 2012.

[9] D.-C. Ding, W.-C. Shyu, and S.-Z. Lin, "Mesenchymal stem cells," *Cell Transplantation*, vol. 20, no. 1, pp. 5–14, 2011.

[10] S. Wakao, Y. Kuroda, F. Ogura, T. Shigemoto, and M. Dezawa, "Regenerative effects of mesenchymal stem cells: contribution of muse cells, a novel pluripotent stem cell type that resides in mesenchymal cells," *Cells*, vol. 1, no. 4, pp. 1045–1060, 2012.

[11] J. E. Till and E. A. McCulloch, "A direct measurement of the radiation sensitivity of normal mouse bone marrow cells," *Radiation Research*, vol. 178, no. 2, pp. AV3–AV7, 2012.

[12] D. G. Phinney, "Building a consensus regarding the nature and origin of mesenchymal stem cells," *Journal of cellular biochemistry. Supplement*, vol. 38, pp. 7–12, 2002.

[13] R. J. Jankowski, B. M. Deasy, and J. Huard, "Muscle-derived stem cells," *Gene Therapy*, vol. 9, no. 10, pp. 642–647, 2002.

[14] D. A. De Ugarte, K. Morizono, A. Elbarbary et al., "Comparison of multi-lineage cells from human adipose tissue and bone marrow," *Cells Tissues Organs*, vol. 174, no. 3, pp. 101–109, 2003.

[15] M. Miura, S. Gronthos, M. Zhao et al., "SHED: stem cells from human exfoliated deciduous teeth," *Proceedings of the National Academy of Sciences of the United States of America*, vol. 100, no. 10, pp. 5807–5812, 2003.

[16] K. Mareschi, E. Biasin, W. Piacibello, M. Aglietta, E. Madon, and F. Fagioli, "Isolation of human mesenchymal stem cells: bone marrow versus umbilical cord blood," *Haematologica*, vol. 86, no. 10, pp. 1099–1100, 2001.

[17] N. J. Zvaifler, L. Marinova-Mutafchieva, G. Adams et al., "Mesenchymal precursor cells in the blood of normal individuals," *Arthritis Research*, vol. 2, no. 6, pp. 477–488, 2000.

[18] W. Murrell, E. Palmero, J. Bianco et al., "Expansion of multipotent stem cells from the adult human brain," *PLoS ONE*, vol. 8, no. 8, Article ID e71334, 2013.

[19] P. Bianco and P. G. Robey, "Marrow stromal stem cells," *Journal of Clinical Investigation*, vol. 105, no. 12, pp. 1663–1668, 2000.

[20] C. I. Civin, T. Trischmann, N. S. Kadan et al., "Highly purified CD34-positive cells reconstitute hematopoiesis," *Journal of Clinical Oncology*, vol. 14, no. 8, pp. 2224–2233, 1996.

[21] M. F. Pittenger, A. M. Mackay, S. C. Beck et al., "Multilineage potential of adult human mesenchymal stem cells," *Science*, vol. 284, no. 5411, pp. 143–147, 1999.

[22] B. M. Abdallah and M. Kassem, "Human mesenchymal stem cells: from basic biology to clinical applications," *Gene Therapy*, vol. 15, no. 2, pp. 109–116, 2008.

[23] Y. Jiang, B. Vaessen, T. Lenvik, M. Blackstad, M. Reyes, and C. M. Verfaillie, "Multipotent progenitor cells can be isolated from postnatal murine bone marrow, muscle, and brain," *Experimental Hematology*, vol. 30, no. 8, pp. 896–904, 2002.

[24] S. Gu, C. Xing, J. Han, M. O. M. Tso, and J. Hong, "Differentiation of rabbit bone marrow mesenchymal stem cells into corneal epithelial cells in vivo and ex vivo," *Molecular Vision*, vol. 15, pp. 99–107, 2009.

[25] Y. Ma, Y. Xu, Z. Xiao et al., "Reconstruction of chemically burned rat corneal surface by bone marrow-derived human mesenchymal stem cells," *Stem Cells*, vol. 24, no. 2, pp. 315–321, 2006.

[26] J. Sanchez-Ramos, S. Song, F. Cardozo-Pelaez et al., "Adult bone marrow stromal cells differentiate into neural cells in vitro," *Experimental Neurology*, vol. 164, no. 2, pp. 247–256, 2000.

[27] Q.-P. Xie, H. Huang, B. Xu et al., "Human bone marrow mesenchymal stem cells differentiate into insulin-producing cells upon microenvironmental manipulation in vitro," *Differentiation*, vol. 77, no. 5, pp. 483–491, 2009.

[28] D. L. Jones and A. J. Wagers, "No place like home: anatomy and function of the stem cell niche," *Nature Reviews Molecular Cell Biology*, vol. 9, no. 1, pp. 11–21, 2008.

[29] D. T. Scadden, "The stem-cell niche as an entity of action," *Nature*, vol. 441, no. 7097, pp. 1075–1079, 2006.

[30] J. A. Martinez-Agosto, H. K. A. Mikkola, V. Hartenstein, and U. Banerjee, "The hematopoietic stem cell and its niche: a comparative view," *Genes & Development*, vol. 21, no. 23, pp. 3044–3060, 2007.

[31] S. C. Bendall, M. H. Stewart, P. Menendez et al., "IGF and FGF cooperatively establish the regulatory stem cell niche of pluripotent human cells in vitro," *Nature*, vol. 448, no. 7157, pp. 1015–1021, 2007.

[32] R. I. G. Holt, "Fetal programming of the growth hormone-insulin-like growth factor axis," *Trends in Endocrinology and Metabolism*, vol. 13, no. 9, pp. 392–397, 2002.

[33] S. Yakar, J.-L. Liu, B. Stannard et al., "Normal growth and development in the absence of hepatic insulin-like growth factor," *Proceedings of the National Academy of Sciences of the United States of America*, vol. 96, no. 13, pp. 7324–7329, 1999.

[34] D. Le Roith, C. Bondy, S. Yakar, J.-L. Liu, and A. Butler, "The somatomedin hypothesis: 2001," *Endocrine Reviews*, vol. 22, no. 1, pp. 53–74, 2001.

[35] A. Akinci, K. C. Copeland, A. Garmong, and D. R. Clemmons, "Insulin-like growth factor binding proteins (IGFBPs) in serum and urine and IGFBP-2 protease activity in patients with insulin-dependent diabetes mellitus," *Metabolism: Clinical and Experimental*, vol. 49, no. 5, pp. 626–633, 2000.

[36] X. Feng, D. Huang, X. Lu et al., "Insulin-like growth factor 1 can promote proliferation and osteogenic differentiation of human dental pulp stem cells via mTOR pathway," *Development Growth and Differentiation*, vol. 56, no. 9, pp. 615–624, 2014.

[37] L. Hu, G. Yang, D. Hägg et al., "IGF1 promotes adipogenesis by a lineage bias of endogenous adipose stem/progenitor cells," *Stem Cells*, vol. 33, no. 8, pp. 2483–2495, 2015.

[38] Q. Zhou, B. Li, J. Zhao, W. Pan, J. Xu, and S. Chen, "IGF-I induces adipose derived mesenchymal cell chondrogenic differentiation in vitro and enhances chondrogenesis in vivo," *In Vitro Cellular and Developmental Biology—Animal*, vol. 52, no. 3, pp. 356–364, 2016.

[39] P. Trosan, E. Javorkova, A. Zajicova et al., "The supportive role of insulin-like growth factor-I in the differentiation of murine mesenchymal stem cells into corneal-like cells," *Stem Cells and Development*, vol. 25, no. 11, pp. 874–881, 2016.

[40] T. J. Huat, A. A. Khan, S. Pati, Z. Mustafa, J. M. Abdullah, and H. Jaafar, "IGF-1 enhances cell proliferation and survival during early differentiation of mesenchymal stem cells to neural progenitor-like cells," *BMC Neuroscience*, vol. 15, article no. 91, 2014.

[41] M. Ayatollahi, M. Soleimani, B. Geramizadeh, and M. H. Imanieh, "Insulin-like growth factor 1 (IGF-I) improves hepatic differentiation of human bone marrow-derived mesenchymal stem cells," *Cell Biology International*, vol. 35, no. 11, pp. 1169–1176, 2011.

[42] A. A. Butler, S. Yakar, I. H. Gewolb, M. Karas, Y. Okubo, and D. LeRoith, "Insulin-like growth factor-I receptor signal transduction: at the interface between physiology and cell biology," *Comparative Biochemistry and Physiology Part B: Biochemistry & Molecular Biology*, vol. 121, no. 1, pp. 19–26, 1998.

[43] E. Rinderknecht and R. E. Humbel, "The amino acid sequence of human insulin-like growth factor I and its structural homology with proinsulin," *Journal of Biological Chemistry*, vol. 253, no. 8, pp. 2769–2776, 1978.

[44] R. Rubin and R. Baserga, "Insulin-like growth factor-I receptor: its role in cell proliferation, apoptosis, and tumorigenicity," *Laboratory Investigation*, vol. 73, no. 3, pp. 311–331, 1995.

[45] T. S. Olson, M. J. Bamberger, and M. D. Lane, "Post-translational changes in tertiary and quaternary structure of the insulin proreceptor. Correlation with acquisition of function," *Journal of Biological Chemistry*, vol. 263, no. 15, pp. 7342–7351, 1988.

[46] F. Frasca, G. Pandini, P. Scalia et al., "Insulin receptor isoform A, a newly recognized, high-affinity insulin- like growth factor II receptor in fetal and cancer cells," *Molecular and Cellular Biology*, vol. 19, no. 5, pp. 3278–3288, 1999.

[47] C. Xinaris, M. Morigi, V. Benedetti et al., "A novel strategy to enhance mesenchymal stem cell migration capacity and promote tissue repair in an injury specific fashion," *Cell Transplantation*, vol. 22, no. 3, pp. 423–436, 2013.

[48] D. R. Clemmons, "IGF binding proteins: regulation of cellular actions," *Growth Regulation*, vol. 2, no. 2, pp. 80–87, 1992.

[49] J. I. Jones and D. R. Clemmons, "Insulin-like growth factors and their binding proteins: biological actions," *Endocrine Reviews*, vol. 16, no. 1, pp. 3–34, 1995.

[50] K. M. Kelley, Y. Oh, S. E. Gargosky et al., "Insulin-like growth factor-binding proteins (IGFBPs) and their regulatory dynamics," *International Journal of Biochemistry and Cell Biology*, vol. 28, no. 6, pp. 619–637, 1996.

[51] S. Shimasaki and N. Ling, "Identification and molecular characterization of insulin-like growth factor binding proteins (IGFBP-1, -2, -3, -4, -5 and -6)," *Progress in Growth Factor Research*, vol. 3, no. 4, pp. 243–266, 1991.

[52] W. S. Cohick and D. R. Clemmons, "The insulin-like growth factors," *Annual Review of Physiology*, vol. 55, pp. 131–153, 1993.

[53] A. Grimberg and P. Cohen, "Role of insulin-like growth factors and their binding proteins in growth control and carcinogenesis," *Journal of Cellular Physiology*, vol. 183, no. 1, pp. 1–9, 2000.

[54] L. A. Bach, S. J. Headey, and R. S. Norton, "IGF-binding proteins—the pieces are falling into place," *Trends in Endocrinology and Metabolism*, vol. 16, no. 5, pp. 228–234, 2005.

[55] R. Baserga, A. Hongo, M. Rubini, M. Prisco, and B. Valentinis, "The IGF-I receptor in cell growth, transformation and apoptosis," *Biochimica et Biophysica Acta*, vol. 1332, no. 3, pp. F105–F126, 1997.

[56] L. A. Bach, S. Hsieh, K.-I. Sakano, H. Fujiwara, J. F. Perdue, and M. M. Rechler, "Binding of mutants of human insulin-like growth factor II to insulin-like growth factor binding proteins 1–6," *Journal of Biological Chemistry*, vol. 268, no. 13, pp. 9246–9254, 1993.

[57] S. Benyoucef, K. H. Surinya, D. Hadaschik, and K. Siddle, "Characterization of insulin/IGF hybrid receptors: contributions of the insulin receptor L2 and Fn1 domains and the alternatively spliced exon 11 sequence to ligand binding and receptor activation," *Biochemical Journal*, vol. 403, no. 3, pp. 603–613, 2007.

[58] R. Baserga, "The insulin receptor substrate-1: a biomarker for cancer?" *Experimental Cell Research*, vol. 315, no. 5, pp. 727–732, 2009.

[59] J.-C. Chambard, R. Lefloch, J. Pouysségur, and P. Lenormand, "ERK implication in cell cycle regulation," *Biochimica et Biophysica Acta—Molecular Cell Research*, vol. 1773, no. 8, pp. 1299–1310, 2007.

[60] P. W. Zandstra and A. Nagy, "Stem cell bioengineering," *Annual Review of Biomedical Engineering*, vol. 3, pp. 275–305, 2001.

[61] K. Forbes and M. Westwood, "The IGF axis and placental function: a mini review," *Hormone Research*, vol. 69, no. 3, pp. 129–137, 2008.

[62] M. G. Myers Jr., T. C. Grammer, L.-M. Wang et al., "Insulin receptor substrate-1 mediates phosphatidylinositol 3*ı*-kinase and p70S6k signaling during insulin, insulin-like growth factor-1, and interleukin-4 stimulation," *Journal of Biological Chemistry*, vol. 269, no. 46, pp. 28783–28789, 1994.

[63] P. van der Geer, S. Wiley, G. D. Gish et al., "Identification of residues that control specific binding of the Shc phosphotyrosine-binding domain to phosphotyrosine sites," *Proceedings of the National Academy of Sciences of the United States of America*, vol. 93, no. 3, pp. 963–968, 1996.

[64] P. Van Der Geer, S. Wiley, G. D. Gish, and T. Pawson, "The Shc adaptor protein is highly phosphorylated at conserved, twin tyrosine residues (Y239/240) that mediate protein-protein interactions," *Current Biology*, vol. 6, no. 11, pp. 1435–1444, 1996.

[65] J. Blenis, "Signal transduction via the MAP kinases: proceed at your own RSK," *Proceedings of the National Academy of Sciences of the United States of America*, vol. 90, no. 13, pp. 5889–5892, 1993.

[66] B. Margolis and E. Y. Skolnik, "Activation of ras by receptor tyrosine kinases," *Journal of the American Society of Nephrology*, vol. 5, no. 6, pp. 1288–1299, 1994.

[67] B. Lamothe, D. Bucchini, J. Jami, and R. L. Joshi, "Interaction of p85 subunit of PI 3-kinase with insulin and IGF-1 receptors analysed by using the two-hybrid system," *FEBS Letters*, vol. 373, no. 1, pp. 51–55, 1995.

[68] B. Valentinis and R. Baserga, "IGF-I receptor signalling in transformation and differentiation," *Molecular Pathology*, vol. 54, no. 3, pp. 133–137, 2001.

[69] D. L. Esposito, Y. Li, A. Cama, and M. J. Quon, "Tyr^{612} and Tyr^{632} in human insulin receptor substrate-1 are important for full activation of insulin-stimulated phosphatidylinositol 3-kinase activity and translocation of GLUT4 in adipose cells," *Endocrinology*, vol. 142, no. 7, pp. 2833–2840, 2001.

[70] C. T. Roberts, J. A. Owens, A. M. Carter, J. E. Harding, R. Austgulen, and M. Wlodek, "Insulin-like growth factors and foetal programming—a workshop report," *Placenta*, vol. 24, pp. S72–S75, 2003.

[71] J.-P. Liu, J. Baker, A. S. Perkins, E. J. Robertson, and A. Efstratiadis, "Mice carrying null mutations of the genes encoding insulin-like growth factor I (Igf-1) and type 1 IGF receptor (Igf1r)," *Cell*, vol. 75, no. 1, pp. 59–72, 1993.

[72] J. Wang, J. Zhou, and C. A. Bondy, "Igf1 promotes longitudinal bone growth by insulin-like actions augmenting chondrocyte hypertrophy," *FASEB Journal*, vol. 13, no. 14, pp. 1985–1990, 1999.

[73] L. Rodriguez-de la Rosa, L. Fernandez-Sanchez, F. Germain et al., "Age-related functional and structural retinal modifications in the Igf1-/- null mouse," *Neurobiology of Disease*, vol. 46, no. 2, pp. 476–485, 2012.

[74] T. M. DeChiara, A. Efstratiadis, and E. J. Robertsen, "A growth-deficiency phenotype in heterozygous mice carrying an insulin-like growth factor II gene disrupted by targeting," *Nature*, vol. 345, no. 6270, pp. 78–80, 1990.

[75] A. A. Butler and D. LeRoith, "Tissue-specific versus generalized gene targeting of the IGF1 and IGF1R genes and their roles in insulin-like growth factor physiology," *Endocrinology*, vol. 142, no. 5, pp. 1685–1688, 2001.

[76] J.-L. Liu, S. Yakar, and D. Leroith, "Conditional knockout of mouse insulin-like growth factor-1 gene using the Cre/loxP system," *Proceedings of the Society for Experimental Biology and Medicine*, vol. 223, no. 4, pp. 344–351, 2000.

[77] M. H.-C. Sheng, X.-D. Zhou, L. F. Bonewald, D. J. Baylink, and K.-H. W. Lau, "Disruption of the insulin-like growth factor-1 gene in osteocytes impairs developmental bone growth in mice," *Bone*, vol. 52, no. 1, pp. 133–144, 2013.

[78] C. D. De Magalhaes Filho, L. Kappeler, J. Dupont et al., "Deleting IGF-1 receptor from forebrain neurons confers neuroprotection during stroke and upregulates endocrine somatotropin," *Journal of Cerebral Blood Flow & Metabolism*, vol. 37, no. 2, pp. 396–412, 2017.

[79] Z. Chaker, S. Aïd, H. Berry, and M. Holzenberger, "Suppression of IGF-I signals in neural stem cells enhances neurogenesis and olfactory function during aging," *Aging Cell*, vol. 14, no. 5, pp. 847–856, 2015.

[80] A. Youssef and V. K. M. Han, "Low oxygen tension modulates the insulin-like growth factor-1 or -2 signaling via both insulin-like growth factor-1 receptor and insulin receptor to maintain stem cell identity in placental mesenchymal stem cells," *Endocrinology*, vol. 157, no. 3, pp. 1163–1174, 2016.

[81] K. Yamahara, K. Harada, M. Ohshima et al., "Comparison of angiogenic, cytoprotective, and immunosuppressive properties of human amnion- and chorion-derived mesenchymal stem cells," *PLoS ONE*, vol. 9, no. 2, Article ID e88319, 2014.

[82] S. Sadat, S. Gehmert, Y.-H. Song et al., "The cardioprotective effect of mesenchymal stem cells is mediated by IGF-I and VEGF," *Biochemical and Biophysical Research Communications*, vol. 363, no. 3, pp. 674–679, 2007.

[83] L. Xing, R. Cui, L. Peng et al., "Mesenchymal stem cells, not conditioned medium, contribute to kidney repair after ischemia-reperfusion injury," *Stem Cell Research and Therapy*, vol. 5, no. 4, article no. 101, 2014.

[84] C. Hu, Y. Wu, Y. Wan, Q. Wang, and J. Song, "Introduction of hIGF-1 gene into bone marrow stromal cells and its effects on the cell's biological behaviors," *Cell Transplantation*, vol. 17, no. 9, pp. 1067–1081, 2008.

[85] M. H. Stewart, S. C. Bendall, and M. Bhatia, "Deconstructing human embryonic stem cell cultures: niche regulation of self-renewal and pluripotency," *Journal of Molecular Medicine*, vol. 86, no. 8, pp. 875–886, 2008.

[86] S.-B. Park, K.-R. Yu, J.-W. Jung et al., "BFGF enhances the IGFs-mediated pluripotent and differentiation potentials in multipotent stem cells," *Growth Factors*, vol. 27, no. 6, pp. 425–437, 2009.

[87] A. Youssef, C. Iosef, and V. K. M. Han, "Low-oxygen tension and IGF-I promote proliferation and multipotency of placental mesenchymal stem cells (PMSCs) from different gestations via

distinct signaling pathways," *Endocrinology*, vol. 155, no. 4, pp. 1386–1397, 2014.

[88] R. Montes, G. Ligero, L. Sanchez et al., "Feeder-free maintenance of hESCs in mesenchymal stem cell-conditioned media: distinct requirements for TGF-beta and IGF-II," *Cell Research*, vol. 19, no. 6, pp. 698–709, 2009.

[89] H. Lee, H. Chang, S. Lee et al., "Role of IGF1R$^+$ MSCs in modulating neuroplasticity via CXCR4 cross-interaction," *Scientific Reports*, vol. 6, Article ID 32595, 2016.

[90] A. N. Ziegler, J. S. Schneider, M. Qin et al., "IGF-II promotes stemness of neural restricted precursors," *Stem Cells*, vol. 30, no. 6, pp. 1265–1276, 2012.

[91] A. N. Ziegler, S. Chidambaram, B. E. Forbes, T. L. Wood, and S. W. Levison, "Insulin-like growth factor-II (IGF-II) and IGF-II Analogs with enhanced insulin receptor-a binding affinity promote neural stem cell expansion," *Journal of Biological Chemistry*, vol. 289, no. 8, pp. 4626–4633, 2014.

[92] A. N. Ziegler, S. W. Levison, and T. L. Wood, "Insulin and IGF receptor signalling in neural-stem-cell homeostasis," *Nature Reviews Endocrinology*, vol. 11, no. 3, pp. 161–170, 2015.

[93] I. Sancho-Martinez, S. H. Baek, and J. C. Izpisua Belmonte, "Lineage conversion methodologies meet the reprogramming toolbox," *Nature Cell Biology*, vol. 14, no. 9, pp. 892–899, 2012.

[94] J. Y. Lee, Z. Zhou, P. J. Taub et al., "BMP-12 treatment of adult mesenchymal stem cells in vitro augments tendon-like tissue formation and defect repair in vivo," *PLoS ONE*, vol. 6, no. 3, Article ID e17531, 2011.

[95] P. De Coppi, G. Bartsch Jr., M. M. Siddiqui et al., "Isolation of amniotic stem cell lines with potential for therapy," *Nature Biotechnology*, vol. 25, no. 1, pp. 100–106, 2007.

[96] N. Wang, R. Zhang, S.-J. Wang et al., "Vascular endothelial growth factor stimulates endothelial differentiation from mesenchymal stem cells via Rho/myocardin-related transcription factor—a signaling pathway," *International Journal of Biochemistry and Cell Biology*, vol. 45, no. 7, pp. 1447–1456, 2013.

[97] J. Oswald, S. Boxberger, B. Jørgensen et al., "Mesenchymal stem cells can be differentiated into endothelial cells in vitro," *Stem Cells*, vol. 22, no. 3, pp. 377–384, 2004.

[98] A. S. de la Garza-Rodea, I. van der Velde-van Dijke, H. Boersma et al., "Myogenic properties of human mesenchymal stem cells derived from three different sources," *Cell Transplantation*, vol. 21, no. 1, pp. 153–173, 2012.

[99] Y.-H. Zheng, W. Xiong, K. Su, S.-J. Kuang, and Z.-G. Zhang, "Multilineage differentiation of human bone marrow mesenchymal stem cells in vitro and in vivo," *Experimental and Therapeutic Medicine*, vol. 5, no. 6, pp. 1576–1580, 2013.

[100] T. Katagiri and N. Takahashi, "Regulatory mechanisms of osteoblast and osteoclast differentiation," *Oral Diseases*, vol. 8, no. 3, pp. 147–159, 2002.

[101] S. Mohan and D. J. Baylink, "Bone growth factors," *Clinical Orthopaedics and Related Research*, no. 263, pp. 30–48, 1991.

[102] T. Niu and C. J. Rosen, "The insulin-like growth factor-I gene and osteoporosis: a critical appraisal," *Gene*, vol. 361, no. 1-2, pp. 38–56, 2005.

[103] T. L. Clemens and S. D. Chernausek, "Genetic strategies for elucidating insulin-like growth factor action in bone," *Growth Hormone & IGF Research*, vol. 14, no. 3, pp. 195–199, 2004.

[104] S. Perrini, A. Natalicchio, L. Laviola et al., "Abnormalities of insulin-like growth factor-I signaling and impaired cell proliferation in osteoblasts from subjects with osteoporosis," *Endocrinology*, vol. 149, no. 3, pp. 1302–1313, 2008.

[105] H. Koch, J. A. Jadlowiec, and P. G. Campbell, "Insulin-like growth factor-I induces early osteoblast gene expression in human mesenchymal stem cells," *Stem Cells and Development*, vol. 14, no. 6, pp. 621–631, 2005.

[106] W. Katagiri, M. Osugi, T. Kawai, and H. Hibi, "First-in-human study and clinical case reports of the alveolar bone regeneration with the secretome from human mesenchymal stem cells," *Head and Face Medicine*, vol. 12, no. 1, article no. 5, 2016.

[107] R. D. Fanganiello, F. A. A. Ishiy, G. S. Kobayashi, L. Alvizi, D. Y. Sunaga, and M. R. Passos-Bueno, "Increased in vitro osteopotential in SHED associated with higher IGF2 expression when compared with hASCs," *Stem Cell Reviews and Reports*, vol. 11, no. 4, article A010, pp. 635–644, 2015.

[108] A. G. Miller, J. D. Aplin, and M. Westwood, "Adenovirally mediated expression of insulin-like growth factors enhances the function of first trimester placental fibroblasts," *The Journal of Clinical Endocrinology and Metabolism*, vol. 90, no. 1, pp. 379–385, 2005.

[109] T. E. Adams, V. C. Epa, T. P. J. Garrett, and C. W. Ward, "Structure and function of the type 1 insulin-like growth factor receptor," *Cellular and Molecular Life Sciences*, vol. 57, no. 7, pp. 1050–1093, 2000.

[110] E. M. Wilson and P. Rotwein, "Control of MyoD function during initiation of muscle differentiation by an autocrine signaling pathway activated by insulin-like growth factor-II," *Journal of Biological Chemistry*, vol. 281, no. 40, pp. 29962–29971, 2006.

[111] P. Putzer, P. Breuer, W. Götz et al., "Mouse insulin-like growth factor binding protein-6: expression, purification, characterization and histochemical localization," *Molecular and Cellular Endocrinology*, vol. 137, no. 1, pp. 69–78, 1998.

[112] M. R. Schneider, H. Lahm, M. Wu, A. Hoeflich, and E. Wolf, "Transgenic mouse models for studying the functions of insulin-like growth factor-binding proteins," *FASEB Journal*, vol. 14, no. 5, pp. 629–640, 2000.

[113] M. Pumberger, T. H. Qazi, M. C. Ehrentraut et al., "Synthetic niche to modulate regenerative potential of MSCs and enhance skeletal muscle regeneration," *Biomaterials*, vol. 99, pp. 95–108, 2016.

[114] G.-W. Zhang, T.-X. Gu, X.-Y. Guan et al., "HGF and IGF-1 promote protective effects of allogeneic BMSC transplantation in rabbit model of acute myocardial infarction," *Cell Proliferation*, vol. 48, no. 6, pp. 661–670, 2015.

[115] J. Guo, D. Zheng, W.-F. Li, H.-R. Li, A.-D. Zhang, and Z.-C. Li, "Insulin-like growth factor 1 treatment of MSCs attenuates inflammation and cardiac dysfunction following MI," *Inflammation*, vol. 37, no. 6, pp. 2156–2163, 2014.

[116] S. T.-F. Hsiao, A. Asgari, Z. Lokmic et al., "Comparative analysis of paracrine factor expression in human adult mesenchymal stem cells derived from bone marrow, adipose, and dermal tissue," *Stem Cells and Development*, vol. 21, no. 12, pp. 2189–2203, 2012.

[117] J. C. Fritton, Y. Kawashima, W. Mejia et al., "The insulin-like growth factor-1 binding protein acid-labile subunit alters mesenchymal stromal cell fate," *Journal of Biological Chemistry*, vol. 285, no. 7, pp. 4709–4714, 2010.

[118] Y. Tao, X. Zhou, C. Liang et al., "TGF- β 3 and IGF-1 synergy ameliorates nucleus pulposus mesenchymal stem cell differentiation towards the nucleus pulposus cell type through MAPK/ERK signaling," *Growth Factors*, vol. 33, no. 5-6, pp. 326–336, 2015.

[119] L. Longobardi, L. O'Rear, S. Aakula et al., "Effect of IGF-I in the chondrogenesis of bone marrow mesenchymal stem cells in the presence or absence of TGF-β signaling," *Journal of Bone and Mineral Research*, vol. 21, no. 4, pp. 626–636, 2006.

[120] L. Longobardi, F. Granero-Moltó, L. O'Rear et al., "Subcellular localization of IRS-1 in IGF-I-mediated chondrogenic proliferation, differentiation and hypertrophy of bone marrow mesenchymal stem cells," *Growth Factors*, vol. 27, no. 5, pp. 309–320, 2009.

[121] W. Liu, J. A. D'Ercole, and P. Ye, "Blunting type 1 insulin-like growth factor receptor expression exacerbates neuronal apoptosis following hypoxic/ischemic injury," *BMC Neuroscience*, vol. 12, article 64, 2011.

[122] S. H. Park, K. W. Kim, and J. C. Kim, "The role of insulin-like growth factor binding protein 2 (IGFBP2) in the regulation of corneal fibroblast differentiation," *Investigative Ophthalmology & Visual Science*, vol. 56, no. 12, pp. 7293–7302, 2015.

[123] L. Zhao, Y. Feng, X. Chen et al., "Effects of IGF-1 on neural differentiation of human umbilical cord derived mesenchymal stem cells," *Life Sciences*, vol. 151, pp. 93–101, 2016.

[124] E. Semenova, H. Koegel, S. Hasse et al., "Overexpression of mIGF-1 in keratinocytes improves wound healing and accelerates hair follicle formation and cycling in mice," *American Journal of Pathology*, vol. 173, no. 5, pp. 1295–1310, 2008.

[125] S. R. Edmondson, S. P. Thumiger, G. A. Werther, and C. J. Wraight, "Epidermal homeostasis: the role of the growth hormone and insulin-like growth factor systems," *Endocrine Reviews*, vol. 24, no. 6, pp. 737–764, 2003.

[126] V. Todorović, P. Peško, M. Micev et al., "Insulin-like growth factor-I in wound healing of rat skin," *Regulatory Peptides*, vol. 150, no. 1–3, pp. 7–13, 2008.

[127] J. Kato, H. Kamiya, T. Himeno et al., "Mesenchymal stem cells ameliorate impaired wound healing through enhancing keratinocyte functions in diabetic foot ulcerations on the plantar skin of rats," *Journal of Diabetes and Its Complications*, vol. 28, no. 5, pp. 588–595, 2014.

[128] Y. Zhou, Q. Hu, F. Chen et al., "Human umbilical cord matrix-Derived stem cells exert trophic effects on β-cell survival in diabetic rats and isolated islets," *DMM Disease Models and Mechanisms*, vol. 8, no. 12, pp. 1625–1633, 2015.

[129] T. L. B. Spitzer, A. Rojas, Z. Zelenko et al., "Perivascular human endometrial mesenchymal stem cells express pathways relevant to self-renewal, lineage specification, and functional phenotype," *Biology of Reproduction*, vol. 86, no. 2, article 58, 2012.

[130] J. Saegusa, S. Yamaji, K. Ieguchi et al., "The direct binding of insulin-like growth factor-1 (IGF-1) to integrin $\alpha v\beta 3$ is involved in IGF-1 signaling," *The Journal of Biological Chemistry*, vol. 284, no. 36, pp. 24106–24114, 2009.

[131] P. Ye, Q. Hu, H. Liu, Y. Yan, and A. J. D'Ercole, "β-catenin mediates insulin-like growth factor-I actions to promote cyclin D1 mRNA expression, cell proliferation and survival in oligodendroglial cultures," *GLIA*, vol. 58, no. 9, pp. 1031–1041, 2010.

[132] Y.-L. Huang, R.-F. Qiu, W.-Y. Mai et al., "Effects of insulin-like growth factor-1 on the properties of mesenchymal stem cells in vitro," *Journal of Zhejiang University: Science B*, vol. 13, no. 1, pp. 20–28, 2012.

[133] Y. Li, X. Yu, S. Lin, X. Li, S. Zhang, and Y.-H. Song, "Insulin-like growth factor 1 enhances the migratory capacity of mesenchymal stem cells," *Biochemical and Biophysical Research Communications*, vol. 356, no. 3, pp. 780–784, 2007.

[134] L. Chen, W. Jiang, J. Huang et al., "Insulin-like growth factor 2 (IGF-2) potentiates BMP-9-induced osteogenic differentiation and bone formation," *Journal of Bone and Mineral Research*, vol. 25, no. 11, pp. 2447–2459, 2010.

[135] Y. Shi, J. Chen, C. M. Karner, and F. Long, "Hedgehog signaling activates a positive feedback mechanism involving insulin-like growth factors to induce osteoblast differentiation," *Proceedings of the National Academy of Sciences of the United States of America*, vol. 112, no. 15, pp. 4678–4683, 2015.

[136] D. Madhala-Levy, V. C. Williams, S. M. Hughes, R. Reshef, and O. Halevy, "Cooperation between Shh and IGF-I in promoting myogenic proliferation and differentiation via the MAPK/ERK and PI3K/Akt pathways requires smo activity," *Journal of Cellular Physiology*, vol. 227, no. 4, pp. 1455–1464, 2012.

[137] L. Li and W. B. Neaves, "Normal stem cells and cancer stem cells: the niche matters," *Cancer Research*, vol. 66, no. 9, pp. 4553–4557, 2006.

[138] A. Hsieh, R. Ellsworth, and D. Hsieh, "Hedgehog/GLI1 regulates IGF dependent malignant behaviors in glioma stem cells," *Journal of Cellular Physiology*, vol. 226, no. 4, pp. 1118–1127, 2011.

[139] C. Xu, D. Xie, S.-C. Yu et al., "β-catenin/POU5F1/SOX2 transcription factor complex mediates IGF-I receptor signaling and predicts poor prognosis in lung adenocarcinoma," *Cancer Research*, vol. 73, no. 10, pp. 3181–3189, 2013.

[140] E. J. Fiore, J. M. Bayo, M. G. Garcia et al., "Mesenchymal stromal cells engineered to produce IGF-I by recombinant adenovirus ameliorate liver fibrosis in mice," *Stem Cells and Development*, vol. 24, no. 6, pp. 791–801, 2015.

[141] E. M. Winter, A. A. M. Van Oorschot, B. Hogers et al., "A new direction for cardiac regeneration therapy: application of synergistically acting epicardium-derived cells and cardiomyocyte progenitor cells," *Circulation: Heart Failure*, vol. 2, no. 6, pp. 643–653, 2009.

[142] M. Kearns-Jonker, W. Dai, M. Gunthart et al., "Genetically engineered mesenchymal stem cells influence gene expression in donor cardiomyocytes and the recipient heart," *Journal of Stem Cell Research & Therapy*, supplement 1, article 005, 2012.

[143] D. Gao, J. Xie, J. Zhang et al., "MSC attenuate diabetes-induced functional impairment in adipocytes via secretion of insulin-like growth factor-1," *Biochemical and Biophysical Research Communications*, vol. 452, no. 1, pp. 99–105, 2014.

[144] Y. Yulyana, I. A. W. Ho, K. C. Sia et al., "Paracrine factors of human fetal MSCs inhibit liver cancer growth through reduced activation of IGF-1R/PI3K/Akt signaling," *Molecular Therapy*, vol. 23, no. 4, pp. 746–756, 2015.

[145] C. Kuhn, S. A. Hurwitz, M. G. Kumar, J. Cotton, and D. F. Spandau, "Activation of the insulin-like growth factor-1 receptor promotes the survival of human keratinocytes following ultraviolet B irradiation," *International Journal of Cancer*, vol. 80, no. 3, pp. 431–438, 1999.

Hindawi
Stem Cells International
Volume 2017, Article ID 5173732, 16 pages
https://doi.org/10.1155/2017/5173732

Review Article

Mesenchymal Stem and Progenitor Cells in Regeneration: Tissue Specificity and Regenerative Potential

Rokhsareh Rohban[1,2] and Thomas Rudolf Pieber[1]

[1]*Department of Internal Medicine, Division of Endocrinology and Diabetology, Medical University of Graz, Graz, Austria*
[2]*Center for Medical Research (ZMF), Medical University of Graz, Graz, Austria*

Correspondence should be addressed to Rokhsareh Rohban; rokhsaren.rohban@medunigraz.at

Received 14 October 2016; Accepted 7 December 2016; Published 13 February 2017

Academic Editor: Andrea Ballini

It has always been an ambitious goal in medicine to repair or replace morbid tissues for regaining the organ functionality. This challenge has recently gained momentum through considerable progress in understanding the biological concept of the regenerative potential of stem cells. Routine therapeutic procedures are about to shift towards the use of biological and molecular armamentarium. The potential use of embryonic stem cells and invention of induced pluripotent stem cells raised hope for clinical regenerative purposes; however, the use of these interventions for regenerative therapy showed its dark side, as many health concerns and ethical issues arose in terms of using these cells in clinical applications. In this regard, adult stem cells climbed up to the top list of regenerative tools and mesenchymal stem cells (MSC) showed promise for regenerative cell therapy with a rather limited level of risk. MSC have been successfully isolated from various human tissues and they have been shown to offer the possibility to establish novel therapeutic interventions for a variety of hard-to-noncurable diseases. There have been many elegant studies investigating the impact of MSC in regenerative medicine. This review provides compact information on the role of stem cells, in particular, MSC in regeneration.

1. Introduction

Being first isolated in 1966 from bone marrow, mesenchymal stem cells (MSC) are adult stromal nonhematopoietic cells, well known for their potential to differentiate into osteoblasts and osteocytes [1]. They have the ability to recruit hematopoietic host cells when forming bone in vivo [2, 3]. These cells are characterized by their spindle-like shape [4] and adherence capability to polymeric surfaces, for example, plastic. Although they are most known for their osteogenic differentiation potential, MSC have the ability to commit into all three lineages (osteogenic, chondrogenic, and adipogenic). MSC express CD105, CD73, and CD90 (cell-surface markers) but lack the expression of CD14, CD19, CD34, CD45, and HLA-DR [5]. MSC have been isolated and purified not only from bone marrow where they cooperate with hematopoietic stem cells (HSC) to form the niche, but also from various tissues, such as umbilical cord [6–9] and umbilical cord blood [10–13], white adipose tissue [14–16], placenta [17], and the amniotic membrane of placenta [4, 18–20]. The capacity of MSC to differentiate into cell lineages and develop teratoma, a preserved tumor that contains normal three-germ layer tissue and organ parts, is a reason to consider them as multipotent progenitor cells suitable for regenerative therapy.

Beside their potential to differentiate into osteoblasts in the process of osteogenesis, there have been several other regenerative roles attributed to MSC. These cells can serve as pericytes [21, 22] wrapping around blood vessels to support their structure and stability [23]. MSC have also shown the potential to integrate into the outer wall of the microvessels and arteries in many organs, such as spleen, liver, kidney, lung, pancreas, and brain [24, 25]. This led to the speculation that both bone marrow- and vascular wall-derived MSC as well as white adipose tissue-, umbilical cord blood-, and amniotic membrane-derived MSC could act as cell source for regenerative therapy to treat various disorders such as osteoporosis, arthritis, and vessel regeneration after injury [26–29]. MSC may also be induced to differentiate into functional

Table 1: A selection of registered clinical trials on the basis of MSC as the relevant therapeutic tool (https://www.clinicaltrials.gov).

	Title	Recruitment	Conditions	Phases	Intervention	Sponsors
1	Mesenchymal Stem Cells in Knee Cartilage Injuries	Completed	Articular cartilage disorder of knee	Phase II	Biological: autologous mesenchymal stem cells	University of Jordan
2	"One-Step" Bone Marrow Mononuclear Cell Transplantation in Talar Osteochondral Lesions	Recruiting	Osteochondritis	Phase III	Procedure: bone marrow cells transplantation on collagen scaffold	Istituto Ortopedico Rizzoli
3	Mesenchymal Stem Cell Based Therapy for the Treatment of Osteogenesis Imperfecta	Active, not recruiting	Osteogenesis imperfecta	Phase I	Biological: mesenchymal stem cells	Hospital de Cruces; Hospital Universitario de Getafe; Hospital Infantil Universitario Niño Jesús, Madrid, Spain
4	Treatment of Patients With Newly Onset of Type 1 Diabetes With Mesenchymal Stem Cells	Completed	Type 1 diabetes mellitus	—	Biological: mesenchymal stem cells	Uppsala University Hospital
5	Mesenchymal Stem Cells for Multiple Sclerosis	Recruiting	Multiple sclerosis	Phase I Phase II	Drug: mesenchymal stem cells; drug: suspension media	University Hospital, Toulouse
6	Autologous Mesenchymal Stem Cells Transplantation in Cervical Chronic and Complete Spinal Cord Injury	Recruiting	Spinal cord injury	Phase I	Biological: autologous mesenchymal cells transplantation	Hospital Sao Rafael

neurons, corneal epithelial cells, and cardiomyocytes under specific pretreatments ex vivo and in vivo that broaden the capacity of these cells in regenerative therapeutic interventions [30–35]. In a previous study, umbilical cord matrix stem cells derived from human umbilical cord Wharton's Jelly were aimed to treat neurodegenerative disorders such as Parkinson's disease by transplantation into the brain of nonimmune-deficient, hemiparkinsonian rats [36]. Interestingly, phenotypic characterization of umbilical cord matrix-derived stem cells revealed a similar surface marker expression pattern to mesenchymal stem and progenitor cells (positive for CD10, CD13, CD29, CD44, and CD90 and negative for CD14, CD33, CD56, CD31, CD34, CD45, and HLA-DR). The transplantation resulted in a significant reduction of rotator behavior as a symptom for Parkinson's disease, thus suggesting an additional therapeutic role for umbilical cord matrix stem cells (MSC) in treating central nervous disorders [36].

These findings were enough evidences for scientists to speculate a promising role for MSC in regenerative therapy. In the past years, MSC have been used in clinical trials aiming for regeneration of tissues such as bone [37] and cartilage [38] as well as treatment of disorders such as spinal cord injury [39], multiple sclerosis (MS), Crohn's disease [2, 40], and graft-versus-host disease (GvHD) [41] due to their broad differentiation capacity and potential of hematopoietic cell recruitment [5, 42, 43].

Several clinical trials are running to identify different aspects of MSC application in terms of safety and efficacy. Table 1 indicates a number of clinical trials using MSC for various treatments and regenerative interventions. As of date (07.10.2016), a total number of 657 clinical studies were found that involve mesenchymal stem cells for different clinical phases.

2. Stem Cells as Potential Tools for Regenerative Therapy: Promise and Perils

In the recent decade, somatic stem cells have become attractive tools for cell therapy and regenerative medicine due to their proliferation and differentiation potential as well as established isolation and propagation protocols that promote a high standard of purity and functionality of the cells when applied in vivo. Adult stem cells (ASC) and progenitors, in particular mesenchymal stem cells have been derived from a variety of tissues such as umbilical cord and umbilical cord blood, placenta, bone marrow, epithelium, and white adipose tissue. These cells have been characterized, expanded, and applied for transplantation procedures in which allogeneic adult stem cells give rise to committed cells such as osteocytes, adipocytes, and chondrocytes as well as functional vessels in the process of neovasculogenesis [44–49].

The proliferation rate of adult stem cells and in particular MSC is a crucial parameter for stem cell therapeutic interventions like patient-specific tissue regeneration. There are, however, limitations with regard to the amount of tissue that can be taken from the patient, the limited propagation capacity

of the cells that are isolated from the tissue, and restrictions in terms of passage number of the cells to be utilized for regenerative therapy. Therefore, it has been of great interest to enhance the proliferation rate of (mesenchymal) stem cells, especially in terms of patient-specific regenerative therapy. In this regard, low-level laser therapy (LLLT) has been tested in vitro to stimulate and enhance proliferation capacity of the cells. According to systematic review conducted by Ginani et al., LLLT is increasingly used as a method to enhance proliferative potential of adipose tissue-, dental pulp-, periodontal tissues-, and bone marrow-derived stem cells to date [50]. Ballini et al. showed that LLLT irradiation promotes proliferation capacity of dental pulp stromal cells and enhances the expression of proteins that are involved in osteogenesis [51].

Considering the tissue-specificity property of stem cells in determining their regenerative potential, it is of interest to test and compare the impact of LLLT on proliferative potential of stem cells that are derived from different tissues to ensure a more effective regenerative strategy approach.

MSC are, however, not considered as the only cellular mediators for enhancement of regenerative therapy, as embryonic stem cells (ESC) and, later on, induced pluripotent stem cell (iPSC) technology through cellular reprogramming were introduced and aimed to push regenerative cell therapy beyond its existing limits.

Pluripotent, inner blastocyst cell mass-derived cells are defined as embryonic stem cells (ESC) that can proliferate without limitation, possess the potential of self-renewal, and are able to differentiate into different cell types derived from all the three germ layers [52]. These characteristics together with the human embryonic stem cell (hESC) capability to differentiate into human adult cells led to the speculation that hESC might be useful for allogeneic cell transplantation research as well as clinical trials for treatment of diseases such as spinal cord injury, cardiovascular disorders, and diabetes [53, 54].

Differentiating hESC to numerous cell types including osteoblasts, cardiomyocytes (CM), hepatocytes, neurons, and endothelial cells (EC) to be used in cell replacement therapy (CRT) has been increasingly taken into consideration [55]. However, the procedure of deriving tissue-specific cells from hESC is challenging and requires establishment of reproducible methods for therapeutic interventions. A number of studies focusing on hESC differentiation into tissue-specific CM that do not express stemness markers are still in progress [56]. Moreover, CM populations derived from hESC have been shown to respond to drug stimuli and thus are suitable for assessment and development of small molecule therapeutics ex vivo [55, 57].

During the past few years, several studies were carried out to investigate differentiation of ESC into dopamine-producing neural cells [58, 59] and bone tissue [60] which can shed light to the future clinical trials using hESC to treat spinal cord injuries and bone damage.

ESC research offers great promise for understanding mechanisms of cell differentiation which ultimately leads to discovery of novel treatments for diseases such as myocardial infarction [61, 62]. Pluripotent stem cells can readily be cultured in vitro and can differentiate into all types of committed cells [61, 63]. With the ongoing progress in the field of ESC and regenerative medicine, these cells could be induced to differentiate into variety of committed cells that could be used for therapeutic interventions such as regenerative transplantation. Embryonic stem cells (ESC) were therefore identified as potential playmakers for regenerative therapy.

The therapeutic potential and benefit of ESC, however, have been a matter of debate and raised ethical concerns due to the opinion that the process of deriving embryonic stem cells results in severe damage to the embryo. Moreover, the existing complications and some as-of-yet unclarities in differentiation potential and proliferation rate of ESC pose risk of undesired complications such as teratoma formation and cancer development. Therefore it is not an approved procedure in several countries. Although research has overcome many of these limitations to date, ESC are still not fully approved for being used in cell therapy procedures and regenerative application [64].

Other groups of potential playmakers in regenerative therapy, induced pluripotent stem cells (iPSC), have come to the scene by Takahashi and Yamanaka who successfully produced induced pluripotent stem cells (iPSC) using mouse embryonic and adult fibroblast cells and introducing four transcription factors SOX2, OCT 3/4, KIF4, and c-myc to cells [65]. Later, they generated iPSC also from human somatic fibroblasts and established reprogramming strategies to convert differentiated human adult cells into a pluripotent state. Park et al. were able to generate iPSC from adult, neonatal, and fetal primary cells of human including skin fibroblasts [66]. Consequently, patient- and disease-specific stem cell generation methods were developed as crucial steps towards modern regenerative medicine and cell therapy [67]. For instance, Maehr et al. generated type 1 diabetes-specific iPSC from patients by reprogramming their fibroblasts with three transcription factors (OCT4, SOX2, and KLF4) with the potential of differentiating into insulin-producing cells that could be used to treat type 1 diabetes [68]. In 2012, John B. Gurdon and Shinya Yamanaka were jointly awarded the Nobel Prize in Physiology or Medicine for discovery of the path through which differentiated cells can be reprogrammed to become pluripotent.

Several studies on the implication and capacity of iPSC technology for therapeutic approaches have been carried out through which iPSC were generated from committed and somatic cells [69, 70]. These studies investigated their cellular, molecular, and functional properties and compared them with pluripotent and multipotent stromal cells. A differentiation protocol was investigated by Moslem et al. through which human iPSC derived-MSC were generated from fibroblasts and bone marrow-derived mesenchymal stem cells (BM-MSC) [70]. The iPSC-MSC generated in this study expressed a surface marker profile similar to that of normal BM-MSC, while having a shorter population doubling period, therefore possessing a more advanced proliferation capacity. Furthermore, iPSC-MSC revealed immunomodulatory properties through eliminating the proliferation capacity of $CD4^+$ cells and reducing proinflammatory cytokines in a lymphocyte population admix [70].

Table 2: Selected genes and primers involved in human iPSC-MSC technology studies.

Gene	Implication	Primer sequence 5′-3′ Forward
Human peroxisome proliferator-activated receptor γ (PPARγ)	Proliferation capacity	CTAAAGAGCCTGCGAAAG
Human peroxisome proliferator-activated receptor α (PPARα)	Proliferation capacity	ACTCCGTCTTCTTGATGAT
Octamer-binding transcription factor 4 (OCT4)	Stemness	CCTCACTTCACTGCACTGTA
Kruppel-like factor 4 (KLF4)	Stemness	GATGAACTGACCAGGCACTA
Myc (C-MYC)	Stemness	TGCCTCAAATTGGACTTTGG
Sex determining region Y-box 2 (SOX2)	Stemness	CCCAGCAGACTTCACATGT
Lin-28 homolog A (LIN28)	Stemness	AGTAAGCTGCACATGGAAGG
Collagen 2 (COL2a)	Chondrogenesis Osteogenesis	TCTACCCCAATCCAGCAAAC
Runt-related transcription factor 2 (RUNX2)	Osteogenesis	CAGTAGATGGACCTCGGGAA
Aggrecan (ACAN)	Chondrogenesis	CTGGACAAGTGCTATGCCG
Alkaline phosphatase (ALP)	Chondrogenesis Osteogenesis	CAACAGGGTAGATTTCTCTTGG
Osteocalcin (OC)	Osteogenesis	AGTCCAGCAAAGGTGCAGCC

Kang et al. also established a method for generating iPSC-MSC with morphological characteristics and surface marker expression profile similar to that of BM-MSC [69]. The iPSC-MSC generated in this study revealed osteogenic and chondrogenic differentiation capacity comparable to those of BM-MSC, but they revealed less efficiency in terms of adipogenic differentiation capacity [69]. Table 2 indicates a selection of genes and primers that have been involved in human iPSC-MSC technology studies [69–73].

The iPSC technology has undoubtedly raised hope in regenerative biology; however its use in regenerative medicine did not appear as a facile, straight-forward procedure, as iPSC technology led to complications in cell therapy and regeneration [74]. The genetic stability in reprogrammed cells has not been proven to remain constant [75, 76] and because of genetic alterations, these cells have not been considered as reliable tools for clinical use in transplantation and regeneration to date.

In comparison with ESC and iPSC, adult somatic stem cells do not cause ethical and severe health issues and are therefore widely used in regenerative research. There have been, however, limitations concerning the in vitro expansion and pluripotency when using adult somatic stem cells for therapy [64]. Nevertheless, lower risk in terms of application, low incidence of post-therapy complications, and less ethical concerns compensate the limitations of ASC in terms of expansion rate and pluripotency to a significant extent.

Further investigations are still required for application of ESC and iPSC in regenerative medicine until these cells would be considered as effective tools for clinical regenerative therapy. For this reason, other options such as new sources of ASC, in particular, MSC as an important adult stem cell subfamily, have been considered for establishment of successful and progressive cell-based regenerative and therapeutic procedures. The need for novel cell sources is obvious because of increasing need of regenerative cell therapy for diseases that are, as of date, difficult, if not impossible to be cured.

3. Tissue Specific MSC: Diversity in Regenerative Potential

MSC are present in several adult tissues. Despite similar morphology and phenotypic properties amongst MSC that have been isolated from various tissue sources, their regenerative potential has been shown to differ. It has been previously described that activated aging mechanism in MSC has an impact on their regenerative potential, probably due to DNA damage accumulation [77] and/or impairment of metabolic system as a result of mitochondrial damage [77, 78]. Nonetheless, several studies have been carried out that show differences in regenerative capacity of MSC populations of the same passage number that have been isolated from different sites [79–81]. The variability in regenerative potential of MSC populations that are derived from various tissues might be due to the impact of stem cell niche on cell fate, known as stem cell niche theory [82], genetic variability, and/or epigenetic alterations.

3.1. Bone Marrow-Derived MSC. Bone marrow (BM) was one of the first tissues that had been used for isolation and propagation of mesenchymal stem and progenitors. Bone marrow aspirate is rich in hematopoietic and nonhematopoietic stem cells, endothelial progenitor cells (EPC) derived from embryonic hemangioblasts, and mesenchymal stem cells (MSC). MSC have been shown to participate in hematopoiesis or bone marrow regeneration [83, 84]. They also have the potential to give rise to "pericytes," the perivascular cells on the outer layer of vessels supporting the stability of capillaries and directing the blood flow [23]. Human BM-MSC have been shown to successfully participate in neovasculogenesis and collaborate with endothelial colony forming cells for establishment of perfused microvessels in vivo [85–87]. BM-MSC have been considered as gold standard tools for osteogenic and chondrogenic regeneration. There have been, however, increasing reports on the role of other source-specific MSC such as umbilical cord blood- (UCB-) MSC and adipose tissue- (AT-) MSC in promoting osteogenic and chondrogenic differentiation in vitro and in vivo [88, 89].

3.2. Adipose Tissue-Derived MSC. Adult adipose tissue is rich in fibroblast-like cells with multidifferentiation potential [90–92]. In 2001, these cells were identified as MSC [93], leading the adipose tissue (AT) to be recognized as a source of MSC isolation. Reports on the regenerative potential of AT-MSC showed that they are potent in contributing to vessel formation [94] and act as pericytes as well as being able to differentiate into bone (osteoblasts) [89, 95] and cartilage (chondrocytes) [96, 97]. These cells were isolated from the liposuction material and they expressed potential to undergo osteogenic, adipogenic, myogenic, and chondrogenic differentiation in vitro [98]. It has been shown that AT-MSC have the potential to differentiate into hepatocyte-like cells in the presence of certain growth factors such as hepatocyte growth factor (HGF) and fibroblast growth factors 1 and 4 (FGF1, FGF4) [99–101]. These hepatocyte-like cells have been shown to express phenotypes such as albumin secretion and lipoprotein absorbance that are known as liver-specific markers. Moreover, these cells have been shown to home into the liver parenchyma after being transplanted into the liver [99]. Reports show a broad range of regenerative potential attributed to the AT-MSC, from soft tissue regeneration (hepatocyte regeneration and vasculogenesis) to hard tissue formation (osteogenesis).

3.3. Umbilical Cord and Cord Blood as MSC Sources. Several studies revealed that cells isolated from Wharton's Jelly (WJ), a component of umbilical cord extracellular matrix, express stemness characteristic and multipotency [102, 103]. These cells also express biomarkers similar to those of bone marrow mesenchymal stem cells (BM-MSC). Mesenchymal stem cells derived from Wharton's Jelly within the umbilical cord have been shown to give rise to various cellular types of nerve system and connective tissue [104, 105]. Umbilical cord-derived mesenchymal stem cells (UC-MSC) express biomarkers such as Nanog and Oct3/4A [104]. These cells have been known as hypoimmunogenic cells due to their ability to modulate NK cells and promote regulatory T-cell expansion [104, 106, 107].

The potential of UC-MSC to participate in neovasculogenesis [85, 108, 109] and differentiate into hepatocyte-like cells [110] strongly suggests that UC-MSC can give rise to various cell types, which indicates the ability of UC-MSC to go beyond lineage borders. Considering their proliferation potential in vitro and their immunoregulatory properties, these cells are extremely promising for regenerative applications in various treatment settings [106].

There have been, however, contradictory reports in terms of surface markers that are expressed on UC-MSC surface [111]. According to ISCT report, CD105 is a required surface marker for verification of MSC [5]. However, several reports contradict each other, as in some studies CD105 has been shown to be present on UC-MSC surface [112–114] and its expression is constant even in different, long-term cell passages [115], whereas a number of reports have argued against the ability of UC-MSC to express CD105 as a surface marker. These studies claim that even though CD105 is expressed in UC-MSC, the expression of this surface marker is detectable up till passage 5 [116, 117].

UC-MSC have been shown to maintain a high differentiation potential in vitro as these cells have shown the ability to differentiate into adipocytes, chondrocytes, osteoblasts, muscle cells, cardiomyocytes, beta cells, endothelial cells, neurons and dopaminergic neurons, and so forth [111, 118–121].

It has been shown that regenerative potential of UC-MSC can differ if the cells are obtained from an individual with metabolic disorders such as type 1 diabetes. Kim et al. indicated that UC-MSC derived from diabetic pregnant women show lower potential of osteogenic and adipogenic differentiation, whereas their surface marker expression profile is not significantly affected. The cell population doubling has also been shown to diminish in UC-MSC from diabetic mothers when compared to UC-MSC from healthy individuals [122]. This finding leads us to conclude that metabolic disorders of the mother have an impact on biological properties of UC-MSC, which attributes to the baby. This has to be taken into consideration when choosing a cell source for clinical application and/or in case of patient-specific clinical regenerative strategies.

Umbilical cord blood (UCB) has always been considered as a source of hematopoietic stem cells (HSC) [10, 123]. Nonetheless, recent findings suggest that UCB serves as a source of MSC with a high regenerative potential [10]. It has been revealed that UCB-MSC can differentiate into osteoblasts, chondrocytes, and pericytes in course of vessel formation [85, 86, 124]. The phenotypic characterization of UCB-MSC has been shown to be consistent with that of BM-MSC [125]. There have been reports on UCB-MSC ability to differentiate into neuron-like cells [126] under certain conditions, which indicate their ability to give rise to cells of all three germ layers [124, 126].

3.4. Dental Tissue-Derived MSC. Dental tissues are specialized tissues and they do not undergo continuous remodeling as has been indicated in other bony tissues; therefore, stem cells that are obtained from dental tissue might show a

restricted differentiation capacity compared to BM-MSC [127, 128].

Dental pulp stem cells (DPSC) are amongst different human dental stem and progenitor cells that have been isolated and characterized to date [128]. DPSC possess self-renewal and differentiation capacity. Human pulp cells can differentiate into odontoblastic cells in vitro, possessing polarized cell bodies and the ability to accumulate mineralized nodules [129–131]. Although dental tissue-derived stem cells are obtained from specialized tissue and they are most potent for differentiation into odontogenic cells, DPSC also have the potential to differentiate into other cells such as adipocytes and neurons [132]. Recently, it has been revealed that DPSC have the potential to give rise to chondrocytes, osteoblasts, and myocytes in vitro [133, 134]. To date, the regenerative application of dental pulp-MSC involves regeneration of the whole tooth and partial bony substrate of the oral cavity in the process of maxillofacial surgical interventions [135–137].

The osteogenic differentiation potential of the cells isolated from dental follicle (DF) has been investigated by Mori et al. [138]. This study has revealed that stemness markers are released by dental bud stem cells. Upon differentiation, these cells have been shown to express osteoblastic biomarkers such as collagen I and alkaline phosphatase (ALP) which indicates their commitment to osteoblast-like lineage [138]. Moreover, a recent report involving the role of integrin and cadherin in differentiation of dental bud stem cells has unraveled a crucial role for integrin $\alpha V\beta 3$ during differentiation of these stem cells into osteoblasts [139]. The data elucidates the impact of extracellular matrix (ECM) proteins in directing stem cell fate towards bone formation [139].

The studies that have been carried out on dental stem cells and their regenerative potential have raised promise for using dental tissue-derived MSC in fracture healing as well as regenerative bone formation interventions due to disease or loss of the tissue [137].

3.5. Amniotic Membrane-Derived MSC. The amniotic membrane is a part of the placenta that protects the fetus during pregnancy and provides nutrient transport to fetus [140]. The amniotic membrane is known as an efficient scaffold for treatment of burns as well as during skin and corneal transplantation, since this tissue possesses anti-inflammatory property [141]. To date, the amniotic membrane is widely used as a material for clinical interventions. Decellularized amniotic membrane can serve as a scaffold and can be used for transplantation interventions.

Amniotic membrane-derived mesenchymal stem cells (AMN-MSC) have been shown to have the potential to differentiate into all three mesodermal lineage cells as well as endodermal lineage cells [142]. They have been shown to express mesenchymal surface markers such as CD105 and CD90 while lacking the hematopoietic markers such as CD29, CD34, and CD45 [143]. Moreover, it has been revealed that the amniotic membrane of placenta can express antiangiogenic and anti-inflammatory components [144]. These results further justify the potential of AMN-MSC application in regenerative medicine, since overcoming inflammation and immunogenicity issues is amongst the most important challenges for a successful outcome of regenerative transplantation. Interestingly, despite expression of pluripotent markers like Oct-4, Nanog, TRA-1-60 and TRA-1-81, AMN-MSC do not cause teratoma formation [145]. An intact amniotic membrane (AMN) promotes secretion of anti-inflammatory and antifibrosis components. It also lacks vasculature structures as well as neurons, which makes AMN a suitable scaffold for wound healing [146, 147].

4. Tissue Specific Regenerative Potential of MSC

The regenerative potential of MSC isolated from different tissues has been shown to undergo alteration according to the tissue of isolation [148, 149]. It has been shown that BM-MSC possess a higher potential in giving rise to osteoblasts and chondrocytes [79, 149], whereas adipose tissue-derived MSC (AT-MSC) have been shown to contribute more successfully to capillary-like network formation in vitro [150] as well as vasculogenesis in vivo [85, 86]. Umbilical cord blood-(UCB-) MSC also showed a high potency in giving rise to pericytes during vasculogenesis [86], whereas their potential for osteogenic differentiation has been shown to diminish compared to BM-MSC [151], which still play as the gold standard for osteogenic differentiation and regeneration.

AMN-MSC were also shown to successfully participate in neurogenesis, whereas such a regenerative potential has not been distinguished in UC-MSC [152, 153]. Amniotic membrane-derived MSC, however, have not been shown to participate in the process of vasculogenesis as successfully as UC-, UCB-, AT-, and BM-MSC did [86].

Despite the fact that DPSC and BM-MSC are regulated by similar factors and they also possess a similar protein expression profile, these populations have been shown to alter significantly in their proliferative capacity in vitro and, more importantly, in their regenerative capacity in vivo [154]. BM-MSC give rise to bone tissue in the mouse model under treatment as described in studies [155, 156]. The chondrogenic and adipogenic potential of BM-MSC has been higher compared to that of DPSC [157, 158]. Conversely, the neurogenic differentiation potential of dental mesenchymal stem cells might be more robust compared to that of BM-MSC, since these cells possess neural crest origin [127].

BM-, dental pulp- (DP-), and adipose tissue- (AT-) derived MSC have revealed a greater promise in regenerative therapy since these adult stem cells might promote patient-specific regenerative interventions.

5. MSC in Regenerative Therapy

MSC are attractive alternatives for regeneration of the injured and/or deficient cells and tissues due to their multipotent differentiation capacity as well as their immunomodulatory and anti-inflammatory properties through cellular crosstalk and production of bioactive molecules [159]. MSC have the unique potential either to directly participate in regeneration

and repair processes or to play an immune modulatory role to enhance treatment of autoimmune diseases such as type 1 diabetes (T1D).

5.1. The Role of MSC in Neovasculogenesis. The combination of multipotent endothelial progenitor cells (EPC) and mesenchymal stem cells (MSC) is an additional key tool for stem cell therapy. These cells are localized in bone marrow stroma as well as vascular inner and outer layer and perivascular niches and are capable of forming mature endothelial cells and mesenchymal cell lineages such as osteoblasts, chondrocytes, adipocytes, and myoblasts [30, 83, 160]. EPC derived from bone marrow, inner vascular wall, umbilical cord, and umbilical cord blood as well as circulating EPC are of great importance for clinical trials and cell therapy procedures. Being capable of migrating through the circulation and differentiating into committed endothelial cells, EPC are crucial mediators for promoting angiogenesis and de novo vasculogenesis as well as endothelium repair in case of vascular damage [25, 84, 161, 162]. It has been previously revealed that SDF-1 can be expressed by activated thrombocytes within blood flow, which is responsible for EPC recruitment to artery structures in vivo [163]. This shows the potential of EPC to participate in vascular repair of damaged peripheral tissues. As has been indicated in a previous study, isolation and transplantation of a human EPC subpopulation (negative for CD34 and CD14, positive for CD133 and VEGFR2) in nude mice with damaged artery resulted in a repaired endothelial layer and wound healing caused by the injected EPC subpopulation [161]. In addition, bone marrow-derived MSC within perivascular niche have been shown to form bone marrow stroma, bone, cartilage, adipose tissue, and myocytes in vivo [26, 30, 84]. Early signaling signature during stem cell mediated vessel formation has been investigated by Rohban et al. [85]. In this study, a coculture approach of mesenchymal stem cells and endothelial colony forming cells revealed that the two progenitor cells collaborate to form stable and perfused microvessels. Moreover, the study revealed that MSC and endothelial progenitor cells communicate through signaling molecules and pathways such as caspase and mitogen activated protein kinase (MAPK) to direct their fate toward vessel formation.

Mitogen activated protein kinases (MAP kinases) have been also shown to regulate MSC differentiation to osteo- or adipogenic lineage [164] with a significant expression of p38, Erk2, and JNK2 in a time-dependent manner [164] suggesting a crucial role for protein kinase signaling molecules and their phosphorylation status during differentiation. The coculture of MSC and ECFC has been shown to result in vascular structure formation in vivo. The vessels have been shown to remain stable and functional up to 6 months after transplantation [85]. This finding justifies the supportive role of MSC for maintaining the stability and functionality of neovessels. Figure 1(a) depicts the contribution of MSC and endothelial colony forming cells (ECFC) in the process of neovasculogenesis. Figure 1(b) shows the formation of neovessels in the absence of MSC resulting in the formation of unstable vasculature.

5.2. The Role of MSC in Osteogenesis and Chondrogenesis. Bone and cartilage injuries occur as a result of bone fracture, or joint diseases such as rheumatoid arthritis or osteoarthritis. These disorders have a costly economic and social impact on the quality of life amongst middle-aged patients. Despite the progress in orthopedic surgery, bone and cartilage repair have remained a major challenge because large injuries do not heal spontaneously [165–169]. The regeneration of ruptured/injured cartilage in a variety of diseases such as degenerative osteoarthritis and herniation is a major goal in cartilage regeneration studies [167, 168, 170, 171].

Studies on mesenchymal stem cells have opened a new horizon for bone and cartilage tissue engineering. Because of their multipotent capacity, MSC lineages have been successfully used in animal models to repair articular cartilage and regenerate bone [35, 165, 170, 172, 173]. Recent research studies have indicated that bone and cartilage might be repaired through percutaneous implantation of MSC [170, 172–175].

The potential of MSC and progenitor cells in prospective cell-based regenerative models has been investigated by Lohberger et al. [176]. The study investigated MSC isolated from three different intraoral bone sites, as well as dental pulp with regard to their potential of differentiating into osteogenic, adipogenic, and chondrogenic lineages. It has been shown that mesenchymal stromal cells isolated from these sites have the potential of osteogenic, but also adipogenic and chondrogenic differentiation in vitro [176].

Human mesenchymal stromal cells isolated from bone marrow (BM) and alveolar bone have been compared according to their regenerative potential by Pekovits et al. [177]. The study aimed to evaluate the potential of bone marrow (BM) and alveolar-derived MSC for regenerative applications in maxillofacial and oral tissue engineering. The results showed multilineage differentiation potential (osteogenic and chondrogenic differentiation) of alveolar bone-mesenchymal stem cells in vitro, which was comparable to that of BM-MSC in vitro [177].

Complete healing occurs when the regenerated tissue has been integrated into the neighboring host tissue and the differentiation process has been thoroughly performed [178, 179]. However, complete bone and cartilage healing is still highly demanding and complete differentiation into functional cartilage has not yet been achieved. Complete healing might be achieved by establishing novel strategies for using scaffolds in combination with pretreated and/or untreated MSC in the presence of selective differentiation factors [178, 180–182]. The long-term behavior of MSC in combination with growth factors and bioscaffolds implanted in morbid joints remains to be studied prior to any clinical application in disorders such as osteoarthritis or rheumatoid arthritis [182–184].

5.3. MSC as Tools for Cornea Regeneration. As indicated earlier, MSC can differentiate into different mesodermal cells and they also possess transdifferentiation ability to preserve phenotypes of neural ectodermal and epithelial cells [185]. It has been shown that BM-MSC can mimic limbal fibroblast cells which are crucial in maintenance of epithelial stem cells

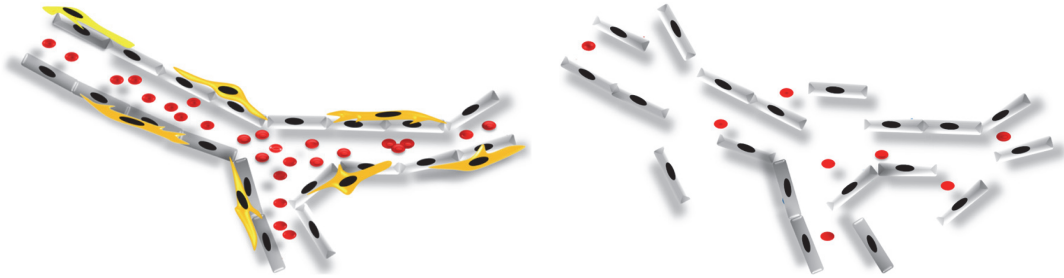

(a) (b)

Figure 1: (a) MSC and ECFC collaborate to form stable, perfused, and functional vessels in vivo. The inner layer of the vessel is established by ECFC (grey), whereas MSC (yellow) form the outer layer of neovessel to support the stability and functionality of the vasculature. (b) Unstable vessel. In the absence of mesenchymal stem cells, the inner layer of the neovessel raptures due to the lack of pericytes which play a crucial role for maintenance of vasculature stability in vivo.

in the limbal niche [186]. Both BM-MSC and limbal fibroblasts have been shown to express a similar surface marker profile, including CD106, CD54, CD166, CD90, CD29, CD71, and CD105. Moreover, both BM-MSC and keratocyte cell types express CD13, CD29, CD44, CD56, CD73, CD90, CD105, and CD133 biomarkers and lack HLA-DR, CD34, CD117, and CD45 on their surface [187]. These studies suggest that MSC can be induced to differentiate into corneal cells. However, there is no in vivo evidence which indicates differentiation of MSC to corneal epithelial cell types. Nevertheless, in vitro differentiated cells can be used in corneal tissue regeneration or treatments that involve tissue/cell replacement.

During development, surface ectoderm gives rise to the corneal epithelium [188]. It has been hypothesized that MSC might be reprogrammed to ectodermal lineage cells. A study conducted by Ma et al. indicated that the MSC population that was transplanted to cornea failed to differentiate into epithelial cells in vivo [32]. In this study, human BM-MSC were applied on amniotic membrane, serving as scaffold, and transplanted on the chemically injured rat cornea. The study revealed that BM-MSC can survive and cause cornea inflammation but did not undergo corneal epithelium differentiation [32].

In a preclinical study using rabbits, BrdU labelled BM-MSC were seeded on fibrin scaffolds and were transplanted into the alkali damaged cornea. The BrdU positive cells were shown to participate in the process of cornea healing which clearly indicated the ability of BM-MSC to differentiate into corneal epithelial cells [189].

The result of several in vitro experiments supported the idea that MSC are able to resemble cornea epithelial cell phenotype under certain conditions; however, up till now, the in vivo data has not shown supportive evidence that justifies the in vitro results.

Recently, adipose tissue-derived MSC (AT-MSC) have shown the ability to differentiate into the corneal epithelium [190]. Although several scientific groups have reported the differentiation of MSC into corneal epithelial cells, the precise mechanism remains unclear and deserves further investigation.

A number of studies have revealed the potential of umbilical cord mesenchymal stem cells (UC-MSC) and bone marrow mesenchymal stem cells (BM-MSC) to differentiate into corneal endothelial cells [191, 192]. However, the characteristics and functions of endothelial cells have not been precisely studied and need to be further investigated.

5.4. Immune Modulatory and Regenerative Potential of MSC in T1D. Immune-mediated disorders like type 1 diabetes (T1D) severely affect quality of life in several millions of patients all over the world. T1D leads to a shorter life span of the patient, has various side effects including cardiovascular and ophthalmic disorders and neuropathy. The disease puts economic pressure both on the health system and the patient. Therefore, great effort has been made to develop innovative therapeutic strategies for cell-based therapy through stem cell immune modulation, autologous/allogeneic stem cell transplantation, and small molecule mediated beta cell regeneration for treatment of T1D.

The use of MSC in cell-based therapy in T1D has been investigated by a number of scientific groups all over the world [193–203].

The potential of bone marrow-derived MSC in immunomodulation of immune-mediated disease T1D and cell-based regenerative models has been investigated by Fiorina et al., 2009 [197]. In this study, murine MSC isolated from bone marrow (BM) have been characterized with regard to their potential to modulate immunity in T1D. The results have revealed that transplantation of stromal cells from BALB/C mice but not from NOD mice into mice that were prone to diabetes delayed the onset of diabetes development. This data suggests that allogenic transplantation of MSC from a healthy donor leads to a better therapeutic outcome compared to autologous transplantation in diabetic mice. The study also showed that mouse-derived mesenchymal stromal cells isolated from BM have the potential of osteogenic, adipogenic, and chondrogenic differentiation in vitro [197].

Human mesenchymal stromal cells isolated from BM and peripheral blood (PB) have been tested in a humanized mouse model by Lee et al., 2006 [204]. In this study immune-deficient mice that have been rendered diabetic by means of streptozotocin (STZ) were used to study the impact of human MSC in treatment of diabetes. This study showed

that infusion of human MSC eliminates glucose levels and increases insulin levels in peripheral blood. Human DNA was also detected in mice kidney and pancreas which elucidates homing of human MSC in those tissues persumably for immunomodulatory/regenerative purposes.

Other studies have also focused on MSC derived from adipose tissue (AT) [201] and placenta [205]. According to the study, AT-MSC play a protective role for beta cells in diabetic animal models [201]. Talwadekar et al. have also compared immunomodulatory properties of placenta-derived MSC to those of cord-derived stromal cells [205] suggesting enhanced immunomodulatory properties for placenta-derived MSC compared to cells that are isolated from other birth-derived tissues, for instance, umbilical cord. The regeneration of insulin-producing beta cells and the use of immunomodulatory effect of stem cells in a variety of autoimmune and/or immune-mediated diseases like T1D are major goals in relevant clinical studies nowadays.

Investigations on the mesenchymal stromal cells have opened a new horizon for diabetes research. Because of their multipotent capacity, MSC lineages have been used successfully in animal models to suppress immune reactions that cause beta cell death and the onset of T1D [206]. Recent research studies have indicated that beta cells within pancreatic islets might be repaired through transplantation/infusion of MSC [194, 195, 207–209]. Other studies also showed that MSC transplantation in animals or patients with T1D can reverse the disease [195, 208]. However, most of studies showed that allogenic transplantation is more efficient in reversing diabetes rather than autologous transplantation [197, 198, 204].

6. Conclusion

Stem cells derived from a variety of sources are promising tools for regenerative cell therapy. Although stem cell therapy has opened a new horizon in regenerative medicine, there are still several obstacles that need to be overcome before this novel treatment tool can be used in large scale in clinics. However, it is obvious that regenerative stem cell therapy has been transformed from scientific fiction to a feasible medical procedure. Regenerative stem cell therapy has created a lot of hope amongst scientists and physicians for finding more effective treatment strategies; nevertheless, it is essential for this new spectrum to develop further through high quality investigations and an effective contribution of researchers and physicians to perform advanced clinical trials aiming to facilitate MSC application for clinical therapy.

Competing Interests

The authors declare that they have no competing interests.

Acknowledgments

The authors thank Beate Boulgaropoulos, Ph.D., for editorial assistance and critical review of the manuscript.

References

[1] T. J. Heino and T. A. Hentunen, "Differentiation of osteoblasts and osteocytes from mesenchymal stem cells," *Current Stem Cell Research and Therapy*, vol. 3, no. 2, pp. 131–145, 2008.

[2] A. Uccelli, L. Moretta, and V. Pistoia, "Mesenchymal stem cells in health and disease," *Nature Reviews Immunology*, vol. 8, no. 9, pp. 726–736, 2008.

[3] E. Schipani and H. M. Kronenberg, *Adult Mesenchymal Stem Cells*, StemBook, Cambridge, Mass, USA, 2008.

[4] M. G. Roubelakis, G. Tsaknakis, K. I. Pappa, N. P. Anagnou, and S. M. Watt, "Spindle shaped human mesenchymal stem/stromal cells from amniotic fluid promote neovascularization," *PLoS ONE*, vol. 8, no. 1, Article ID e54747, 2013.

[5] M. Dominici, K. Le Blanc, I. Mueller et al., "Minimal criteria for defining multipotent mesenchymal stromal cells. The International Society for Cellular Therapy position statement," *Cytotherapy*, vol. 8, no. 4, pp. 315–317, 2006.

[6] Y. A. Romanov, V. A. Svintsitskaya, and V. N. Smirnov, "Searching for alternative sources of postnatal human mesenchymal stem cells: candidate MSC-like cells from umbilical cord," *Stem Cells*, vol. 21, no. 1, pp. 105–110, 2003.

[7] R. Sarugaser, D. Lickorish, D. Baksh, M. M. Hosseini, and J. E. Davies, "Human umbilical cord perivascular (HUCPV) cells: a source of mesenchymal progenitors," *Stem Cells*, vol. 23, no. 2, pp. 220–229, 2005.

[8] M. Lübbert, "Autologous hematopoietic stem cell transplantation for myelodysplastic syndromes: which cell source is preferable?" *Haematologica*, vol. 91, no. 6, p. 723A, 2006.

[9] A. Reinisch and D. Strunk, "Isolation and animal serum free expansion of human umbilical cord derived mesenchymal stromal cells (MSCs) and endothelial colony forming progenitor cells (ECFCs)," *Journal of Visualized Experiments*, no. 23, p. e1525, 2009.

[10] A. Erices, P. Conget, and J. J. Minguell, "Mesenchymal progenitor cells in human umbilical cord blood," *British Journal of Haematology*, vol. 109, no. 1, pp. 235–242, 2000.

[11] K. Bieback, S. Kern, H. Klüter, and H. Eichler, "Critical parameters for the isolation of mesenchymal stem cells from umbilical cord blood," *Stem Cells*, vol. 22, no. 4, pp. 625–634, 2004.

[12] G. Kögler, S. Sensken, J. A. Airey et al., "A new human somatic stem cell from placental cord blood with intrinsic pluripotent differentiation potential," *The Journal of Experimental Medicine*, vol. 200, no. 2, pp. 123–135, 2004.

[13] A. Reinisch, C. Bartmann, E. Rohde et al., "Humanized system to propagate cord blood-derived multipotent mesenchymal stromal cells for clinical application," *Regenerative Medicine*, vol. 2, no. 4, pp. 371–382, 2007.

[14] S. Gronthos, D. M. Franklin, H. A. Leddy, P. G. Robey, R. W. Storms, and J. M. Gimble, "Surface protein characterization of human adipose tissue-derived stromal cells," *Journal of Cellular Physiology*, vol. 189, no. 1, pp. 54–63, 2001.

[15] P. A. Zuk, M. Zhu, P. Ashjian et al., "Human adipose tissue is a source of multipotent stem cells," *Molecular Biology of the Cell*, vol. 13, no. 12, pp. 4279–4295, 2002.

[16] S. Kern, H. Eichler, J. Stoeve, H. Klüter, and K. Bieback, "Comparative analysis of mesenchymal stem cells from bone marrow, umbilical cord blood, or adipose tissue," *Stem Cells*, vol. 24, no. 5, pp. 1294–1301, 2006.

[17] Z. Miao, J. Jin, L. Chen et al., "Isolation of mesenchymal stem cells from human placenta: comparison with human bone

marrow mesenchymal stem cells," *Cell Biology International*, vol. 30, no. 9, pp. 681–687, 2006.

[18] S.-B. Park, M.-S. Seo, J.-G. Kang, J.-S. Chae, and K.-S. Kang, "Isolation and characterization of equine amniotic fluid-derived multipotent stem cells," *Cytotherapy*, vol. 13, no. 3, pp. 341–349, 2011.

[19] T. Pirjali, N. Azarpira, M. Ayatollahi, M. H. Aghdaie, B. Geramizadeh, and T. Talai, "Isolation and characterization of human mesenchymal stem cells derived from human umbilical cord Wharton's jelly and amniotic membrane," *International Journal of Organ Transplantation Medicine*, vol. 4, no. 3, pp. 111–116, 2013.

[20] N. Sessarego, A. Parodi, M. Podestà et al., "Multipotent mesenchymal stromal cells from amniotic fluid: solid perspectives for clinical application," *Haematologica*, vol. 93, no. 3, pp. 339–346, 2008.

[21] D. J. Prockop, "Marrow stromal cells as stem cells for non-hematopoietic tissues," *Science*, vol. 276, no. 5309, pp. 71–74, 1997.

[22] M. F. Pittenger, A. M. Mackay, S. C. Beck et al., "Multilineage potential of adult human mesenchymal stem cells," *Science*, vol. 284, no. 5411, pp. 143–147, 1999.

[23] G. Bergers and S. Song, "The role of pericytes in blood-vessel formation and maintenance," *Neuro-Oncology*, vol. 7, no. 4, pp. 452–464, 2005.

[24] L. da Silva Meirelles, P. C. Chagastelles, and N. B. Nardi, "Mesenchymal stem cells reside in virtually all post-natal organs and tissues," *Journal of Cell Science*, vol. 119, no. 11, pp. 2204–2213, 2006.

[25] E. Zengin, F. Chalajour, U. M. Gehling et al., "Vascular wall resident progenitor cells: a source for postnatal vasculogenesis," *Development*, vol. 133, no. 8, pp. 1543–1551, 2006.

[26] M. E. Bernardo, J. A. M. Emons, M. Karperien et al., "Human mesenchymal stem cells derived from bone marrow display a better chondrogenic differentiation compared with other sources," *Connective Tissue Research*, vol. 48, no. 3, pp. 132–140, 2007.

[27] J. Chan, S. N. Waddington, K. O'Donoghue et al., "Widespread distribution and muscle differentiation of human fetal mesenchymal stem cells after intrauterine transplantation in dystrophic mdx mouse," *Stem Cells*, vol. 25, no. 4, pp. 875–884, 2007.

[28] Y. Yamada, S.-I. Yokoyama, X.-D. Wang, N. Fukuda, and N. Takakura, "Cardiac stem cells in brown adipose tissue express CD133 and induce bone marrow nonhematopoietic cells to differentiate into cardiomyocytes," *Stem Cells*, vol. 25, no. 5, pp. 1326–1333, 2007.

[29] S. Wolbank, A. Peterbauer, M. Fahrner et al., "Dose-dependent immunomodulatory effect of human stem cells from amniotic membrane: a comparison with human mesenchymal stem cells from adipose tissue," *Tissue Engineering*, vol. 13, no. 6, pp. 1173–1183, 2007.

[30] M. Mimeault and S. K. Batra, "Recent advances on multiple tumorigenic cascades involved in prostatic cancer progression and targeting therapies," *Carcinogenesis*, vol. 27, no. 1, pp. 1–22, 2006.

[31] M. J. D. Griffiths, D. Bonnet, and S. M. Janes, "Stem cells of the alveolar epithelium," *The Lancet*, vol. 366, no. 9481, pp. 249–260, 2005.

[32] Y. Ma, Y. Xu, Z. Xiao et al., "Reconstruction of chemically burned rat corneal surface by bone marrow-derived human mesenchymal stem cells," *Stem Cells*, vol. 24, no. 2, pp. 315–321, 2006.

[33] Y.-J. Chang, D. T.-B. Shih, C.-P. Tseng, T.-B. Hsieh, D.-C. Lee, and S.-M. Hwang, "Disparate mesenchyme-lineage tendencies in mesenchymal stem cells from human bone marrow and umbilical cord blood," *Stem Cells*, vol. 24, no. 3, pp. 679–685, 2006.

[34] S. Bobis, D. Jarocha, and M. Majka, "Mesenchymal stem cells: characteristics and clinical applications," *Folia Histochemica et Cytobiologica*, vol. 44, no. 4, pp. 215–230, 2006.

[35] M. Mimeault, R. Hauke, and S. K. Batra, "Stem cells: a revolution in therapeutics—recent advances in stem cell biology and their therapeutic applications in regenerative medicine and cancer therapies," *Clinical Pharmacology and Therapeutics*, vol. 82, no. 3, pp. 252–264, 2007.

[36] M. L. Weiss, S. Medicetty, A. R. Bledsoe et al., "Human umbilical cord matrix stem cells: preliminary characterization and effect of transplantation in a rodent model of Parkinson's disease," *Stem Cells*, vol. 24, no. 3, pp. 781–792, 2006.

[37] M. Griffin, S. A. Iqbal, and A. Bayat, "Exploring the application of mesenchymal stem cells in bone repair and regeneration," *The Journal of Bone & Joint Surgery—British Volume*, vol. 93, no. 4, pp. 427–434, 2011.

[38] C. H. Jo, Y. G. Lee, W. H. Shin et al., "Intra-articular injection of mesenchymal stem cells for the treatment of osteoarthritis of the knee: a proof-of-concept clinical trial," *Stem Cells*, vol. 32, no. 5, pp. 1254–1266, 2014.

[39] A. Uccelli, "Adult stem cells for spinal cord injury: what types and how do they work?" *Cytotherapy*, vol. 10, no. 6, pp. 541–542, 2008.

[40] A. Uccelli, G. Mancardi, and S. Chiesa, "Is there a role for mesenchymal stem cells in autoimmune diseases?" *Autoimmunity*, vol. 41, no. 8, pp. 592–595, 2008.

[41] K. Ozaki, "Novel strategy for GVHD treatment: possible use of mesenchymal stem cells and interleukin-21," *Rinsho Ketsueki*, vol. 53, pp. 483–486, 2012.

[42] B. Delorme, S. Chateauvieux, and P. Charbord, "The concept of mesenchymal stem cells," *Regenerative Medicine*, vol. 1, no. 4, pp. 497–509, 2006.

[43] E. M. Horwitz, K. Le Blanc, M. Dominici et al., "Clarification of the nomenclature for MSC: the International Society for Cellular Therapy position statement," *Cytotherapy*, vol. 7, no. 5, pp. 393–395, 2005.

[44] A. J. Friedenstein, I. I. Piatetzky-Shapiro, and K. V. Petrakova, "Osteogenesis in transplants of bone marrow cells," *Journal of Embryology and Experimental Morphology*, vol. 16, no. 3, pp. 381–390, 1966.

[45] A. J. Friedenstein, R. K. Chailakhyan, N. V. Latsinik, A. F. Panasyuk, and I. V. Keiliss-Borok, "Stromal cells responsible for transferring the microenvironment of the hemopoietic tissues: cloning in vitro and retransplantation in vivo," *Transplantation*, vol. 17, no. 4, pp. 331–340, 1974.

[46] M. S. Cairo and J. E. Wagner, "Placental and/or umbilical cord blood: an alternative source of hematopoietic stem cells for transplantation," *Blood*, vol. 90, no. 12, pp. 4665–4678, 1997.

[47] S. Rafii and D. Lyden, "Therapeutic stem and progenitor cell transplantation for organ vascularization and regeneration," *Nature Medicine*, vol. 9, no. 6, pp. 702–712, 2003.

[48] A. Reinisch, N. A. Hofmann, A. C. Obenauf et al., "Humanized large-scale expanded endothelial colony-forming cells function in vitro and in vivo," *Blood*, vol. 113, no. 26, pp. 6716–6725, 2009.

[49] N. A. Hofmann, A. Ortner, R. O. Jacamo et al., "Oxygen sensing mesenchymal progenitors promote neo-vasculogenesis

in a humanized mouse model in vivo," *PLoS ONE*, vol. 7, no. 9, Article ID e44468, 2012.

[50] F. Ginani, D. M. Soares, M. P. E. V. Barreto, and C. A. G. Barboza, "Effect of low-level laser therapy on mesenchymal stem cell proliferation: a systematic review," *Lasers in Medical Science*, vol. 30, no. 8, pp. 2189–2194, 2015.

[51] A. Ballini, F. Mastrangelo, G. Gastaldi et al., "Osteogenic differentiation and gene expression of dental pulp stem cells under low-level laser irradiation: a good promise for tissue engineering," *Journal of Biological Regulators and Homeostatic Agents*, vol. 29, pp. 813–822, 2015.

[52] M. Thomson, S. J. Liu, L.-N. Zou, Z. Smith, A. Meissner, and S. Ramanathan, "Pluripotency factors in embryonic stem cells regulate differentiation into germ layers," *Cell*, vol. 145, no. 6, pp. 875–889, 2011.

[53] R. W. Mays, W. van't Hof, A. E. Ting, R. Perry, and R. Deans, "Development of adult pluripotent stem cell therapies for ischemic injury and disease," *Expert Opinion on Biological Therapy*, vol. 7, no. 2, pp. 173–184, 2007.

[54] R. E. Newman, D. Yoo, M. A. LeRoux, and A. Danilkovitch-Miagkova, "Treatment of inflammatory diseases with mesenchymal stem cells," *Inflammation and Allergy—Drug Targets*, vol. 8, no. 2, pp. 110–123, 2009.

[55] J. C. Davila, G. G. Cezar, M. Thiede, S. Strom, T. Miki, and J. Trosko, "Use and application of stem cells in toxicology," *Toxicological Sciences*, vol. 79, no. 2, pp. 214–223, 2004.

[56] C. W. Siu, J. C. Moore, and R. A. Li, "Human embryonic stem cell-derived cardiomyocytes for heart therapies," *Cardiovascular and Hematological Disorders—Drug Targets*, vol. 7, no. 2, pp. 145–152, 2007.

[57] J. Jensen, J. Hyllner, and P. Björquist, "Human embryonic stem cell technologies and drug discovery," *Journal of Cellular Physiology*, vol. 219, no. 3, pp. 513–519, 2009.

[58] A. L. Perrier, V. Tabar, T. Barberi et al., "Derivation of midbrain dopamine neurons from human embryonic stem cells," *Proceedings of the National Academy of Sciences of the United States of America*, vol. 101, no. 34, pp. 12543–12548, 2004.

[59] C. L. Parish and E. Arenas, "Stem-cell-based strategies for the treatment of Parkinson's disease," *Neurodegenerative Diseases*, vol. 4, no. 4, pp. 339–347, 2007.

[60] E. Y. L. Waese, R. R. Kandel, and W. L. Stanford, "Application of stem cells in bone repair," *Skeletal Radiology*, vol. 37, no. 7, pp. 601–608, 2008.

[61] J.-Y. Min, Y. Yang, K. L. Converso et al., "Transplantation of embryonic stem cells improves cardiac function in postinfarcted rats," *Journal of Applied Physiology*, vol. 92, no. 1, pp. 288–296, 2002.

[62] G. Shroff, "Therapeutic potential of human embryonic stem cells in type 2 diabetes mellitus," *World Journal of Stem Cells*, vol. 8, no. 7, pp. 223–230, 2016.

[63] M. A. Laflamme, K. Y. Chen, A. V. Naumova et al., "Cardiomyocytes derived from human embryonic stem cells in prosurvival factors enhance function of infarcted rat hearts," *Nature Biotechnology*, vol. 25, no. 9, pp. 1015–1024, 2007.

[64] B. Lo and L. Parham, "Ethical issues in stem cell research," *Endocrine Reviews*, vol. 30, no. 3, pp. 204–213, 2009.

[65] K. Takahashi and S. Yamanaka, "Induction of pluripotent stem cells from mouse embryonic and adult fibroblast cultures by defined factors," *Cell*, vol. 126, no. 4, pp. 663–676, 2006.

[66] I.-H. Park, R. Zhao, J. A. West et al., "Reprogramming of human somatic cells to pluripotency with defined factors," *Nature*, vol. 451, no. 7175, pp. 141–146, 2008.

[67] K. Takahashi, K. Tanabe, M. Ohnuki et al., "Induction of pluripotent stem cells from adult human fibroblasts by defined factors," *Cell*, vol. 131, no. 5, pp. 861–872, 2007.

[68] R. Maehr, S. Chen, M. Snitow et al., "Generation of pluripotent stem cells from patients with type 1 diabetes," *Proceedings of the National Academy of Sciences of the United States of America*, vol. 106, no. 37, pp. 15768–15773, 2009.

[69] R. Kang, Y. Zhou, S. Tan et al., "Mesenchymal stem cells derived from human induced pluripotent stem cells retain adequate osteogenicity and chondrogenicity but less adipogenicity," *Stem Cell Research and Therapy*, vol. 6, no. 1, article 144, 2015.

[70] M. Moslem, I. Eberle, I. Weber, R. Henschler, and T. Cantz, "Mesenchymal stem/stromal cells derived from induced pluripotent stem cells support CD34(pos) hematopoietic stem cell propagation and suppress inflammatory reaction," *Stem Cells International*, vol. 2015, Article ID 843058, 14 pages, 2015.

[71] E. E. Golub, G. Harrison, A. G. Taylor, S. Camper, and I. M. Shapiro, "The role of alkaline phosphatase in cartilage mineralization," *Bone and Mineral*, vol. 17, no. 2, pp. 273–278, 1992.

[72] R. M. Guzzo, J. Gibson, R.-H. Xu, F. Y. Lee, and H. Drissi, "Efficient differentiation of human iPSC-derived mesenchymal stem cells to chondroprogenitor cells," *Journal of Cellular Biochemistry*, vol. 114, no. 2, pp. 480–490, 2013.

[73] W. TheinHan, J. Liu, M. Tang, W. Chen, L. Cheng, and H. H. Xu, "Induced pluripotent stem cell-derived mesenchymal stem cell seeding on biofunctionalized calcium phosphate cements," *Bone Research*, vol. 1, no. 4, pp. 371–384, 2013.

[74] J.-Y. Li, N. S. Christophersen, V. Hall, D. Soulet, and P. Brundin, "Critical issues of clinical human embryonic stem cell therapy for brain repair," *Trends in Neurosciences*, vol. 31, no. 3, pp. 146–153, 2008.

[75] M. M. Mitalipova, R. R. Rao, D. M. Hoyer et al., "Preserving the genetic integrity of human embryonic stem cells," *Nature Biotechnology*, vol. 23, no. 1, pp. 19–20, 2005.

[76] J. S. Draper, K. Smith, P. Gokhale et al., "Recurrent gain of chromosomes 17q and 12 in cultured human embryonic stem cells," *Nature Biotechnology*, vol. 22, no. 1, pp. 53–54, 2004.

[77] B. Yao, S. Huang, D. Gao, J. Xie, N. Liu, and X. Fu, "Age-associated changes in regenerative capabilities of mesenchymal stem cell: impact on chronic wounds repair," *International Wound Journal*, vol. 13, no. 6, pp. 1252–1259, 2016.

[78] G. Li, C. Luna, P. B. Liton, I. Navarro, D. L. Epstein, and P. Gonzalez, "Sustained stress response after oxidative stress in trabecular meshwork cells," *Molecular Vision*, vol. 13, pp. 2282–2288, 2007.

[79] A. Shafiee, E. Seyedjafari, M. Soleimani, N. Ahmadbeigi, P. Dinarvand, and N. Ghaemi, "A comparison between osteogenic differentiation of human unrestricted somatic stem cells and mesenchymal stem cells from bone marrow and adipose tissue," *Biotechnology Letters*, vol. 33, no. 6, pp. 1257–1264, 2011.

[80] S.-Y. Kao, J.-F. Shyu, H.-S. Wang et al., "Comparisons of differentiation potential in human mesenchymal stem cells from Wharton's jelly, bone marrow, and pancreatic tissues," *Stem Cells International*, vol. 2015, Article ID 306158, 10 pages, 2015.

[81] R. Ziadlou, M. Shahhoseini, F. Safari, F.-A. Sayahpour, S. Nemati, and M. B. Eslaminejad, "Comparative analysis of neural differentiation potential in human mesenchymal stem cells derived from chorion and adult bone marrow," *Cell and Tissue Research*, vol. 362, no. 2, pp. 367–377, 2015.

[82] H. Lin, "The stem-cell niche theory: lessons from flies," *Nature Reviews Genetics*, vol. 3, no. 12, pp. 931–940, 2002.

[83] D. Bryder, D. J. Rossi, and I. L. Weissman, "Hematopoietic stem cells: the paradigmatic tissue-specific stem cell," *American Journal of Pathology*, vol. 169, no. 2, pp. 338–346, 2006.

[84] T. Asahara and A. Kawamoto, "Endothelial progenitor cells for postnatal vasculogenesis," *American Journal of Physiology—Cell Physiology*, vol. 287, no. 3, pp. C572–C579, 2004.

[85] R. Rohban, A. Reinisch, N. Etchart et al., "Identification of an effective early signaling signature during neo-vasculogenesis in vivo by ex vivo proteomic profiling," *PLoS ONE*, vol. 8, no. 6, Article ID e66909, 2013.

[86] R. Rohban, N. Etchart, and T. Pieber, "Vasculogenesis potential of mesenchymal and endothelial stem cells isolated from various human tissues," *bioRxiv*, 2016.

[87] R. Rohban, N. Etchart, and T. Pieber, "Transplantation of endothelial progenitor cells solely leads to development of functional neo-vessels in vivo," *bioRxiv*, 2016.

[88] G. Liu, Y. Li, J. Sun et al., "In vitro and in vivo evaluation of osteogenesis of human umbilical cord blood-derived mesenchymal stem cells on partially demineralized bone matrix," *Tissue Engineering A*, vol. 16, no. 3, pp. 971–982, 2010.

[89] S. Vériter, W. André, N. Aouassar et al., "Human adipose-derived mesenchymal stem cells in cell therapy: safety and feasibility in different 'hospital exemption' clinical applications," *PLoS ONE*, vol. 10, no. 10, Article ID e0139566, 2015.

[90] C. H. Hollenberg and A. Vost, "Regulation of DNA synthesis in fat cells and stromal elements from rat adipose tissue," *Journal of Clinical Investigation*, vol. 47, no. 11, pp. 2485–2498, 1969.

[91] I. Dardick, W. J. Poznanski, I. Waheed, and G. Setterfield, "Ultrastructural observations on differentiating human preadipocytes cultured in vitro," *Tissue and Cell*, vol. 8, no. 3, pp. 561–571, 1976.

[92] W. J. Poznanski, I. Waheed, and R. Van, "Human fat cell precursors. Morphologic and metabolic differentiation in culture," *Laboratory Investigation*, vol. 29, no. 5, pp. 570–576, 1973.

[93] P. A. Zuk, M. Zhu, H. Mizuno et al., "Multilineage cells from human adipose tissue: implications for cell-based therapies," *Tissue Engineering*, vol. 7, no. 2, pp. 211–228, 2001.

[94] M. H. Moon, S. Y. Kim, Y. J. Kim et al., "Human adipose tissue-derived mesenchymal stem cells improve postnatal neovascularization in a mouse model of hindlimb ischemia," *Cellular Physiology and Biochemistry*, vol. 17, no. 5-6, pp. 279–290, 2006.

[95] E. Yoon, S. Dhar, D. E. Chun, N. A. Gharibjanian, and G. R. D. Evans, "In vivo osteogenic potential of human adipose-derived stem cells/poly lactide-co-glycolic acid constructs for bone regeneration in a rat critical-sized calvarial defect model," *Tissue Engineering*, vol. 13, no. 3, pp. 619–627, 2007.

[96] Y.-D. C. Halvorsen, D. Franklin, A. L. Bond et al., "Extracellular matrix mineralization and osteoblast gene expression by human adipose tissue-derived stromal cells," *Tissue Engineering*, vol. 7, no. 6, pp. 729–741, 2001.

[97] G. R. Erickson, J. M. Gimble, D. M. Franklin, H. E. Rice, H. Awad, and F. Guilak, "Chondrogenic potential of adipose tissue-derived stromal cells in vitro and in vivo," *Biochemical and Biophysical Research Communications*, vol. 290, no. 2, pp. 763–769, 2002.

[98] S. Arnhold and S. Wenisch, "Adipose tissue derived mesenchymal stem cells for musculoskeletal repair in veterinary medicine," *American Journal of Stem Cells*, vol. 4, pp. 1–12, 2015.

[99] A. Banas, T. Teratani, Y. Yamamoto et al., "Adipose tissue-derived mesenchymal stem cells as a source of human hepatocytes," *Hepatology*, vol. 46, no. 1, pp. 219–228, 2007.

[100] T. Ishikawa, A. Banas, K. Hagiwara, H. Iwaguro, and T. Ochiya, "Stem cells for hepatic regeneration: the role of adipose tissue derived mesenchymal stem cells," *Current Stem Cell Research and Therapy*, vol. 5, no. 2, pp. 182–189, 2010.

[101] T. Katsuda, H. Kurata, R. Tamai et al., "The in vivo evaluation of the therapeutic potential of human adipose tissue-derived mesenchymal stem cells for acute liver disease," *Methods in Molecular Biology*, vol. 1213, pp. 57–67, 2014.

[102] T. T. Sibov, L. F. Pavon, L. A. Miyaki et al., "Umbilical cord mesenchymal stem cells labeled with multimodal iron oxide nanoparticles with fluorescent and magnetic properties: application for in vivo cell tracking," *International Journal of Nanomedicine*, vol. 9, no. 1, pp. 337–350, 2014.

[103] H.-S. Wang, S.-C. Hung, S.-T. Peng et al., "Mesenchymal stem cells in the Wharton's jelly of the human umbilical cord," *Stem Cells*, vol. 22, no. 7, pp. 1330–1337, 2004.

[104] D.-W. Kim, M. Staples, K. Shinozuka, P. Pantcheva, S.-D. Kang, and C. V. Borlongan, "Wharton's jelly-derived mesenchymal stem cells: phenotypic characterization and optimizing their therapeutic potential for clinical applications," *International Journal of Molecular Sciences*, vol. 14, no. 6, pp. 11692–11712, 2013.

[105] I. Kalaszczynska and K. Ferdyn, "Wharton's jelly derived mesenchymal stem cells: future of regenerative medicine? Recent findings and clinical significance," *BioMed Research International*, vol. 2015, Article ID 430847, 11 pages, 2015.

[106] R. Anzalone, M. L. Iacono, S. Corrao et al., "New emerging potentials for human wharton's jelly mesenchymal stem cells: immunological features and hepatocyte-like differentiative capacity," *Stem Cells and Development*, vol. 19, no. 4, pp. 423–438, 2010.

[107] A. Goren, N. Dahan, E. Goren, L. Baruch, and M. Machluf, "Encapsulated human mesenchymal stem cells: a unique hypoimmunogenic platform for long-term cellular therapy," *FASEB Journal*, vol. 24, no. 1, pp. 22–31, 2010.

[108] W. Liao, J. Zhong, J. Yu et al., "Therapeutic benefit of human umbilical cord derived mesenchymal stromal cells in intracerebral hemorrhage rat: implications of anti-inflammation and angiogenesis," *Cellular Physiology and Biochemistry*, vol. 24, no. 3-4, pp. 307–316, 2009.

[109] W. Liao, J. Xie, J. Zhong et al., "Therapeutic effect of human umbilical cord multipotent mesenchymal stromal cells in a rat model of stroke," *Transplantation*, vol. 87, no. 3, pp. 350–359, 2009.

[110] Q. Zhao, H. Ren, X. Li et al., "Differentiation of human umbilical cord mesenchymal stromal cells into low immunogenic hepatocyte-like cells," *Cytotherapy*, vol. 11, no. 4, pp. 414–426, 2009.

[111] I. Arutyunyan, A. Elchaninov, A. Makarov, and T. Fatkhudinov, "Umbilical cord as prospective source for mesenchymal stem cell-based therapy," *Stem Cells International*, vol. 2016, Article ID 6901286, 17 pages, 2016.

[112] A. K. Batsali, M.-C. Kastrinaki, H. A. Papadaki, and C. Pontikoglou, "Mesenchymal stem cells derived from Wharton's jelly of the umbilical cord: biological properties and emerging clinical applications," *Current Stem Cell Research and Therapy*, vol. 8, no. 2, pp. 144–155, 2013.

[113] A. Bongso and C.-Y. Fong, "The therapeutic potential, challenges and future clinical directions of stem cells from the

Wharton's jelly of the human umbilical cord," *Stem Cell Reviews and Reports*, vol. 9, no. 2, pp. 226–240, 2013.

[114] A. Can and S. Karahuseyinoglu, "Concise review: human umbilical cord stroma with regard to the source of fetus-derived stem cells," *Stem Cells*, vol. 25, no. 11, pp. 2886–2895, 2007.

[115] Z. Shi, L. Zhao, G. Qiu, R. He, and M. S. Detamore, "The effect of extended passaging on the phenotype and osteogenic potential of human umbilical cord mesenchymal stem cells," *Molecular and Cellular Biochemistry*, vol. 401, no. 1-2, pp. 155–164, 2015.

[116] S. S. Kadam, S. Tiwari, and R. R. Bhonde, "Simultaneous isolation of vascular endothelial cells and mesenchymal stem cells from the human umbilical cord," *In Vitro Cellular & Developmental Biology—Animal*, vol. 45, no. 1-2, pp. 23–27, 2009.

[117] T. Bakhshi, R. C. Zabriskie, S. Bodie et al., "Mesenchymal stem cells from the Wharton's jelly of umbilical cord segments provide stromal support for the maintenance of cord blood hematopoietic stem cells during long-term ex vivo culture," *Transfusion*, vol. 48, no. 12, pp. 2638–2644, 2008.

[118] I. Datta, S. Mishra, L. Mohanty, S. Pulikkot, and P. G. Joshi, "Neuronal plasticity of human Wharton's jelly mesenchymal stromal cells to the dopaminergic cell type compared with human bone marrow mesenchymal stromal cells," *Cytotherapy*, vol. 13, no. 8, pp. 918–932, 2011.

[119] S. S. Kadam and R. R. Bhonde, "Islet neogenesis from the constitutively nestin expressing human umbilical cord matrix derived mesenchymal stem cells," *Islets*, vol. 2, no. 2, pp. 112–120, 2010.

[120] D.-R. Li and J.-H. Cai, "Methods of isolation, expansion, differentiating induction and preservation of human umbilical cord mesenchymal stem cells," *Chinese Medical Journal*, vol. 125, no. 24, pp. 4504–4510, 2012.

[121] Y. Chen, Y. Yu, L. Chen et al., "Human umbilical cord mesenchymal stem cells: a new therapeutic option for tooth regeneration," *Stem Cells International*, vol. 2015, Article ID 549432, 11 pages, 2015.

[122] J. Kim, Y. Piao, Y. K. Pak et al., "Umbilical cord mesenchymal stromal cells affected by gestational diabetes mellitus display premature aging and mitochondrial dysfunction," *Stem Cells and Development*, vol. 24, no. 5, pp. 575–586, 2015.

[123] H. E. Broxmeyer, G. W. Douglas, G. Hangoc et al., "Human umbilical cord blood as a potential source of transplantable hematopoietic stem/progenitor cells," *Proceedings of the National Academy of Sciences of the United States of America*, vol. 86, no. 10, pp. 3828–3832, 1989.

[124] O. K. Lee, T. K. Kuo, W.-M. Chen, K.-D. Lee, S.-L. Hsieh, and T.-H. Chen, "Isolation of multipotent mesenchymal stem cells from umbilical cord blood," *Blood*, vol. 103, no. 5, pp. 1669–1675, 2004.

[125] K. Mareschi, E. Biasin, W. Piacibello, M. Aglietta, E. Madon, and F. Fagioli, "Isolation of human mesenchymal stem cells: bone marrow versus umbilical cord blood," *Haematologica*, vol. 86, no. 10, pp. 1099–1100, 2001.

[126] H. S. Goodwin, A. R. Bicknese, S.-N. Chien et al., "Multilineage differentiation activity by cells isolated from umbilical cord blood: expression of bone, fat, and neural markers," *Biology of Blood and Marrow Transplantation*, vol. 7, no. 11, pp. 581–588, 2001.

[127] G. T.-J. Huang, S. Gronthos, and S. Shi, "Mesenchymal stem cells derived from dental tissues vs. those from other sources: their biology and role in regenerative medicine," *Journal of Dental Research*, vol. 88, no. 9, pp. 792–806, 2009.

[128] M. Tatullo, M. Marrelli, K. M. Shakesheff, and L. J. White, "Dental pulp stem cells: function, isolation and applications in regenerative medicine," *Journal of Tissue Engineering and Regenerative Medicine*, vol. 9, no. 11, pp. 1205–1216, 2015.

[129] Y. Tsukamoto, S. Fukutani, T. Shin-ike et al., "Mineralized nodule formation by cultures of human dental pulp-derived fibroblasts," *Archives of Oral Biology*, vol. 37, no. 12, pp. 1045–1055, 1992.

[130] P. E. Murray, I. About, P. J. Lumley, J.-C. Franquin, M. Remusat, and A. J. Smith, "Human odontoblast cell numbers after dental injury," *Journal of Dentistry*, vol. 28, no. 4, pp. 277–285, 2000.

[131] M.-L. Couble, J.-C. Farges, F. Bleicher, B. Perrat-Mabillon, M. Boudeulle, and H. Magloire, "Odontoblast differentiation of human dental pulp cells in explant cultures," *Calcified Tissue International*, vol. 66, no. 2, pp. 129–138, 2000.

[132] S. Gronthos, J. Brahim, W. Li et al., "Stem cell properties of human dental pulp stem cells," *Journal of Dental Research*, vol. 81, no. 8, pp. 531–535, 2002.

[133] G. Laino, R. D'Aquino, A. Graziano et al., "A new population of human adult dental pulp stem cells: a useful source of living autologous fibrous bone tissue (LAB)," *Journal of Bone and Mineral Research*, vol. 20, no. 8, pp. 1394–1402, 2005.

[134] R. d'Aquino, A. Graziano, M. Sampaolesi et al., "Human postnatal dental pulp cells co-differentiate into osteoblasts and endotheliocytes: a pivotal synergy leading to adult bone tissue formation," *Cell Death & Differentiation*, vol. 14, no. 6, pp. 1162–1171, 2007.

[135] C. Morsczeck, G. Schmalz, T. E. Reichert, F. Völlner, K. Galler, and O. Driemel, "Somatic stem cells for regenerative dentistry," *Clinical Oral Investigations*, vol. 12, no. 2, pp. 113–118, 2008.

[136] E. Matalova, J. Fleischmannova, P. T. Sharpe, and A. S. Tucker, "Tooth agenesis: from molecular genetics to molecular dentistry," *Journal of Dental Research*, vol. 87, no. 7, pp. 617–623, 2008.

[137] M. Tatullo, M. Marrelli, and F. Paduano, "The regenerative medicine in oral and maxillofacial surgery: the most important innovations in the clinical application of mesenchymal stem cells," *International Journal of Medical Sciences*, vol. 12, no. 1, pp. 72–77, 2015.

[138] G. Mori, A. Ballini, C. Carbone et al., "Osteogenic differentiation of dental follicle stem cells," *International Journal of Medical Sciences*, vol. 9, no. 6, pp. 480–487, 2012.

[139] A. Di Benedetto, G. Brunetti, F. Posa et al., "Osteogenic differentiation of mesenchymal stem cells from dental bud: role of integrins and cadherins," *Stem Cell Research*, vol. 15, no. 3, pp. 618–628, 2015.

[140] Z. Afsartala, M. A. Rezvanfar, M. Hodjat et al., "Amniotic membrane mesenchymal stem cells can differentiate into germ cells in vitro," *In Vitro Cellular & Developmental Biology—Animal*, vol. 52, no. 10, pp. 1060–1071, 2016.

[141] H. S. Dua and A. Azuara-Blanco, "Amniotic membrane transplantation," *British Journal of Ophthalmology*, vol. 83, no. 6, pp. 748–752, 1999.

[142] T. Tamagawa, S. Oi, I. Ishiwata, H. Ishikawa, and Y. Nakamura, "Differentiation of mesenchymal cells derived from human amniotic membranes into hepatocyte-like cells in vitro," *Human Cell*, vol. 20, no. 3, pp. 77–84, 2007.

[143] P. S. In't Anker, S. A. Scherjon, C. Kleijburg-van der Keur et al., "Isolation of mesenchymal stem cells of fetal or maternal origin from human placenta," *Stem Cells*, vol. 22, no. 7, pp. 1338–1345, 2004.

[144] M. Adinolfi, C. A. Akle, I. McColl et al., "Expression of HLA antigens, β2-microglobulin and enzymes by human amniotic epithelial cells," *Nature*, vol. 295, no. 5847, pp. 325–327, 1982.

[145] T. Miki, T. Lehmann, H. Cai, D. B. Stolz, and S. C. Strom, "Stem cell characteristics of amniotic epithelial cells," *Stem Cells*, vol. 23, no. 10, pp. 1549–1559, 2005.

[146] S. C. G. Tseng, D.-Q. Li, and X. Ma, "Suppression of transforming growth factor-beta isoforms, TGF-β receptor type II, and myofibroblast differentiation in cultured human corneal and limbal fibroblasts by amniotic membrane matrix," *Journal of Cellular Physiology*, vol. 179, no. 3, pp. 325–335, 1999.

[147] J. S. Kim, J. C. Kim, B. K. Na, J. M. Jeong, and C. Y. Song, "Amniotic membrane patching promotes healing and inhibits proteinase activity on wound healing following acute corneal alkali burn," *Experimental Eye Research*, vol. 70, no. 3, pp. 329–337, 2000.

[148] R. Hass, C. Kasper, S. Böhm, and R. Jacobs, "Different populations and sources of human mesenchymal stem cells (MSC): a comparison of adult and neonatal tissue-derived MSC," *Cell Communication and Signaling*, vol. 9, article no. 12, 2011.

[149] H. J. Jin, Y. K. Bae, M. Kim et al., "Comparative analysis of human mesenchymal stem cells from bone marrow, adipose tissue, and umbilical cord blood as sources of cell therapy," *International Journal of Molecular Sciences*, vol. 14, no. 9, pp. 17986–18001, 2013.

[150] A. Freiman, Y. Shandalov, D. Rozenfeld et al., "Adipose-derived endothelial and mesenchymal stem cells enhance vascular network formation on three-dimensional constructs in vitro," *Stem Cell Research and Therapy*, vol. 7, no. 1, article no. 5, 2016.

[151] A. Ardeshirylajimi, M. Mossahebi-Mohammadi, S. Vakilian et al., "Comparison of osteogenic differentiation potential of human adult stem cells loaded on bioceramic-coated electrospun poly (L-lactide) nanofibres," *Cell Proliferation*, vol. 48, no. 1, pp. 47–58, 2015.

[152] E. Y. Kim, K.-B. Lee, and M. K. Kim, "The potential of mesenchymal stem cells derived from amniotic membrane and amniotic fluid for neuronal regenerative therapy," *BMB Reports*, vol. 47, no. 3, pp. 135–140, 2014.

[153] S. Uchida, Y. Inanaga, M. Kobayashi, S. Hurukawa, M. Araie, and N. Sakuragawa, "Neurotrophic function of conditioned medium from human amniotic epithelial cells," *Journal of Neuroscience Research*, vol. 62, no. 4, pp. 585–590, 2000.

[154] S. Shi, P. G. Robey, and S. Gronthos, "Comparison of human dental pulp and bone marrow stromal stem cells by cDNA microarray analysis," *Bone*, vol. 29, no. 6, pp. 532–539, 2001.

[155] S. Gronthos, M. Mankani, J. Brahim, P. G. Robey, and S. Shi, "Postnatal human dental pulp stem cells (DPSCs) in vitro and in vivo," *Proceedings of the National Academy of Sciences of the United States of America*, vol. 97, no. 25, pp. 13625–13630, 2000.

[156] S. Batouli, M. Miura, J. Brahim et al., "Comparison of stem-cell-mediated osteogenesis and dentinogenesis," *Journal of Dental Research*, vol. 82, no. 12, pp. 976–981, 2003.

[157] W. Zhang, X. F. Walboomers, S. Shi, M. Fan, and J. A. Jansen, "Multilineage differentiation potential of stem cells derived from human dental pulp after cryopreservation," *Tissue Engineering*, vol. 12, no. 10, pp. 2813–2823, 2006.

[158] W. Sonoyama, Y. Liu, T. Yamaza et al., "Characterization of the apical papilla and its residing stem cells from human immature permanent teeth: a pilot study," *Journal of Endodontics*, vol. 34, no. 2, pp. 166–171, 2008.

[159] M. B. Murphy, K. Moncivais, and A. I. Caplan, "Mesenchymal stem cells: environmentally responsive therapeutics for regenerative medicine," *Experimental and Molecular Medicine*, vol. 45, no. 11, article no. e54, 2013.

[160] O. Ringdén, "Immunotherapy by allogeneic stem cell transplantation," *Advances in Cancer Research*, vol. 97, pp. 25–60, 2007.

[161] E. B. Friedrich, K. Walenta, J. Scharlau, G. Nickenig, and N. Werner, "$CD34^-/CD133^+/VEGFR\text{-}2^+$ endothelial progenitor cell subpopulation with potent vasoregenerative capacities," *Circulation Research*, vol. 98, no. 3, pp. e20–e25, 2006.

[162] G. C. Schatteman, M. Dunnwald, and C. Jiao, "Biology of bone marrow-derived endothelial cell precursors," *American Journal of Physiology—Heart and Circulatory Physiology*, vol. 292, no. 1, pp. H1–H18, 2007.

[163] K. Stellos and M. Gawaz, "Platelets and stromal cell-derived factor-1 in progenitor cell recruitment," *Seminars in Thrombosis and Hemostasis*, vol. 33, no. 2, pp. 159–164, 2007.

[164] R. K. Jaiswal, N. Jaiswal, S. P. Bruder, G. Mbalaviele, D. R. Marshak, and M. F. Pittenger, "Adult human mesenchymal stem cell differentiation to the osteogenic or adipogenic lineage is regulated by mitogen-activated protein kinase," *Journal of Biological Chemistry*, vol. 275, no. 13, pp. 9645–9652, 2000.

[165] A. Ventura, A. Memeo, E. Borgo, C. Terzaghi, C. Legnani, and W. Albisetti, "Repair of osteochondral lesions in the knee by chondrocyte implantation using the MACI® technique," *Knee Surgery, Sports Traumatology, Arthroscopy*, vol. 20, no. 1, pp. 121–126, 2012.

[166] H. Tsuruoka, T. Sasho, S. Yamaguchi et al., "Maturation-dependent spontaneous healing of partial thickness cartilage defects in infantile rats," *Cell and Tissue Research*, vol. 346, no. 2, pp. 263–271, 2011.

[167] M. Mathieu, S. Vigier, M.-N. Labour, C. Jorgensen, E. Belamie, and D. Noël, "Induction of mesenchymal stem cell differentiation and cartilage formation by cross-linker-free collagen microspheres," *European Cells and Materials*, vol. 28, pp. 82–97, 2014.

[168] A. Mobasheri, G. Kalamegam, G. Musumeci, and M. E. Batt, "Chondrocyte and mesenchymal stem cell-based therapies for cartilage repair in osteoarthritis and related orthopaedic conditions," *Maturitas*, vol. 78, no. 3, pp. 188–198, 2014.

[169] H. Afizah and J. H. Hui, "Mesenchymal stem cell therapy for osteoarthritis," *Journal of Clinical Orthopaedics and Trauma*, vol. 7, no. 3, pp. 177–182, 2016.

[170] M. Baghaban Eslaminejad and E. Malakooty Poor, "Mesenchymal stem cells as a potent cell source for articular cartilage regeneration," *World Journal of Stem Cells*, vol. 6, pp. 344–354, 2014.

[171] D. Correa and S. A. Lietman, "Articular cartilage repair: current needs, methods and research directions," *Seminars in Cell & Developmental Biology*, 2016.

[172] C. J. Centeno, D. Busse, J. Kisiday, C. Keohan, M. Freeman, and D. Karli, "Regeneration of meniscus cartilage in a knee treated with percutaneously implanted autologous mesenchymal stem cells," *Medical Hypotheses*, vol. 71, no. 6, pp. 900–908, 2008.

[173] J. A. Anderson, D. Little, A. P. Toth et al., "Stem cell therapies for knee cartilage repair: the current status of preclinical and clinical studies," *The American Journal of Sports Medicine*, vol. 42, no. 9, pp. 2253–2261, 2014.

[174] U. G. Longo, S. Petrillo, E. Franceschetti, A. Berton, N. Maffulli, and V. Denaro, "Stem cells and gene therapy for cartilage repair," *Stem Cells International*, vol. 2012, Article ID 168385, 9 pages, 2012.

[175] K. Gelse, K. Von der Mark, T. Aigner, J. Park, and H. Schneider, "Articular cartilage repair by gene therapy using growth factor-producing mesenchymal cells," *Arthritis and Rheumatism*, vol. 48, no. 2, pp. 430–441, 2003.

[176] B. Lohberger, M. Payer, B. Rinner et al., "Tri-lineage potential of intraoral tissue-derived mesenchymal stromal cells," *Journal of Cranio-Maxillofacial Surgery*, vol. 41, no. 2, pp. 110–118, 2013.

[177] K. Pekovits, J. M. Kröpfl, I. Stelzer, M. Payer, H. Hutter, and G. Dohr, "Human mesenchymal progenitor cells derived from alveolar bone and human bone marrow stromal cells: a comparative study," *Histochemistry and Cell Biology*, vol. 140, no. 6, pp. 611–621, 2013.

[178] A. R. Amini, C. T. Laurencin, and S. P. Nukavarapu, "Bone tissue engineering: recent advances and challenges," *Critical Reviews in Biomedical Engineering*, vol. 40, no. 5, pp. 363–408, 2012.

[179] R. Vaishya, "The journey of articular cartilage repair," *Journal of Clinical Orthopaedics and Trauma*, vol. 7, no. 3, pp. 135–136, 2016.

[180] J. M. Brunger, N. P. T. Huynh, C. M. Guenther et al., "Scaffold-mediated lentiviral transduction for functional tissue engineering of cartilage," *Proceedings of the National Academy of Sciences of the United States of America*, vol. 111, no. 9, pp. E798–E806, 2014.

[181] S. W. O'Driscoll, "The healing and regeneration of articular cartilage," *The Journal of Bone & Joint Surgery—American Volume*, vol. 80, no. 12, pp. 1795–1812, 1998.

[182] M. Ø. Olderøy, M. B. Lilledahl, M. S. Beckwith et al., "Biochemical and structural characterization of neocartilage formed by mesenchymal stem cells in alginate hydrogels," *PLoS ONE*, vol. 9, no. 3, Article ID e91662, 2014.

[183] K. Toupet, M. Maumus, J.-A. Peyrafitte et al., "Long-term detection of human adipose-derived mesenchymal stem cells after intraarticular injection in SCID mice," *Arthritis & Rheumatology*, vol. 65, no. 7, pp. 1786–1794, 2013.

[184] Y. M. Ju, K. Park, J. S. Son, J.-J. Kim, J.-W. Rhie, and D. K. Han, "Beneficial effect of hydrophilized porous polymer scaffolds in tissue-engineered cartilage formation," *Journal of Biomedical Materials Research Part B: Applied Biomaterials*, vol. 85, no. 1, pp. 252–260, 2008.

[185] D. G. Phinney and D. J. Prockop, "Concise review: mesenchymal stem/multipotent stromal cells: the state of transdifferentiation and modes of tissue repair—current views," *Stem Cells*, vol. 25, no. 11, pp. 2896–2902, 2007.

[186] N. Polisetty, A. Fatima, S. L. Madhira, V. S. Sangwan, and G. K. Vemuganti, "Mesenchymal cells from limbal stroma of human eye," *Molecular Vision*, vol. 14, pp. 431–442, 2008.

[187] P.-F. Choong, P.-L. Mok, S.-K. Cheong, and K.-Y. Then, "Mesenchymal stromal cell-like characteristics of corneal keratocytes," *Cytotherapy*, vol. 9, no. 3, pp. 252–258, 2007.

[188] J. Graw, "Eye development," *Current Topics in Developmental Biology*, vol. 90, pp. 343–386, 2010.

[189] X.-G. Sheng, J.-Z. Feng, S. Wu, L.-J. Jin, X.-Y. Yu, and B. Zhang, "Differentiation of rabbit bone marrow mesenchymal stem cells into myogenic cells in vitro and expression of vascular endothelial growth factor gene after transfection," *Academic Journal of the First Medical College of PLA*, vol. 24, no. 3, pp. 290–294, 2004.

[190] T. Nieto-Miguel, S. Galindo, R. Reinoso et al., "In vitro simulation of corneal epithelium microenvironment induces a corneal epithelial-like cell phenotype from human adipose tissue mesenchymal stem cells," *Current Eye Research*, vol. 38, no. 9, pp. 933–944, 2013.

[191] N. C. Joyce, D. L. Harris, V. Markov, Z. Zhang, and B. Saitta, "Potential of human umbilical cord blood mesenchymal stem cells to heal damaged corneal endothelium," *Molecular Vision*, vol. 18, pp. 547–564, 2012.

[192] X.-W. Lu and J.-L. Zhao, "Transplantation of autologous bone marrow mesenchymal stem cells for the treatment of corneal endothelium damages in rabbits," *Chinese Journal of Ophthalmology*, vol. 43, no. 6, pp. 540–545, 2007.

[193] A. A. Kramerov and A. V. Ljubimov, "Stem cell therapies in the treatment of diabetic retinopathy and keratopathy," *Experimental Biology and Medicine*, vol. 241, no. 6, pp. 559–568, 2016.

[194] Y. Zhao, Z. Jiang, T. Zhao et al., "Reversal of type 1 diabetes via islet β cell regeneration following immune modulation by cord blood-derived multipotent stem cells," *BMC Medicine*, vol. 10, article no. 3, 2012.

[195] R. Calafiore and G. Basta, "Stem cells for the cell and molecular therapy of type 1 diabetes mellitus (T1D): the gap between dream and reality," *American Journal of Stem Cells*, vol. 4, pp. 22–31, 2015.

[196] N. E. Rekittke, M. Ang, D. Rawat, R. Khatri, and T. Linn, "Regenerative therapy of type 1 diabetes mellitus: from pancreatic islet transplantation to mesenchymal stem cells," *Stem Cells International*, vol. 2016, Article ID 3764681, 22 pages, 2016.

[197] P. Fiorina, M. Jurewicz, A. Augello et al., "Immunomodulatory function of bone marrow-derived mesenchymal stem cells in experimental autoimmune type 1 diabetes," *The Journal of Immunology*, vol. 183, no. 2, pp. 993–1004, 2009.

[198] R. Abdi, P. Fiorina, C. N. Adra, M. Atkinson, and M. H. Sayegh, "Immunomodulation by mesenchymal stem cells: a potential therapeutic strategy for type 1 diabetes," *Diabetes*, vol. 57, no. 7, pp. 1759–1767, 2008.

[199] J. Xu, Y. Lu, F. Ding, X. Zhan, M. Zhu, and Z. Wang, "Reversal of diabetes in mice by intrahepatic injection of bone-derived GFP-murine mesenchymal stem cells infected with the recombinant retrovirus-carrying human insulin gene," *World Journal of Surgery*, vol. 31, no. 9, pp. 1872–1882, 2007.

[200] L.-X. Man, J. C. Park, M. J. Terry et al., "Lentiviral gene therapy with platelet-derived growth factor B sustains accelerated healing of diabetic wounds over time," *Annals of Plastic Surgery*, vol. 55, no. 1, pp. 81–86, 2005.

[201] H. Rahavi, S. M. Hashemi, M. Soleimani, J. Mohammadi, and N. Tajik, "Adipose tissue-derived mesenchymal stem cells exert in vitro immunomodulatory and beta cell protective functions in streptozotocin-induced diabetic mice model," *Journal of Diabetes Research*, vol. 2015, Article ID 878535, 10 pages, 2015.

[202] J. E. Tooley, F. Waldron-Lynch, and K. C. Herold, "New and future immunomodulatory therapy in type 1 diabetes," *Trends in Molecular Medicine*, vol. 18, no. 3, pp. 173–181, 2012.

[203] M. E. Castro-Manrreza and J. J. Montesinos, "Immunoregulation by mesenchymal stem cells: biological aspects and clinical applications," *Journal of Immunology Research*, vol. 2015, Article ID 394917, 20 pages, 2015.

[204] R. H. Lee, M. J. Seo, R. L. Reger et al., "Multipotent stromal cells from human marrow home to and promote repair of pancreatic islets and renal glomeruli in diabetic NOD/scid mice," *Proceedings of the National Academy of Sciences of the United States of America*, vol. 103, no. 46, pp. 17438–17443, 2006.

[205] M. D. Talwadekar, V. P. Kale, and L. S. Limaye, "Placenta-derived mesenchymal stem cells possess better immunoregulatory properties compared to their cord-derived counterparts-a

paired sample study," *Scientific Reports*, vol. 5, Article ID 15784, 2015.

[206] G. C. Davey, S. B. Patil, A. O'Loughlin, and T. O'Brien, "Mesenchymal stem cell-based treatment for microvascular and secondary complications of diabetes mellitus," *Frontiers in Endocrinology*, vol. 5, article no. 86, 2014.

[207] A. Corcione, F. Benvenuto, E. Ferretti et al., "Human mesenchymal stem cells modulate B-cell functions," *Blood*, vol. 107, no. 1, pp. 367–372, 2006.

[208] V. K. Ramiya, M. Maraist, K. E. Arfors, D. A. Schatz, A. B. Peck, and J. G. Cornelius, "Reversal of insulin-dependent diabetes using islets generated in vitro from pancreatic stem cells," *Nature Medicine*, vol. 6, no. 3, pp. 278–282, 2000.

[209] E. Kroon, L. A. Martinson, K. Kadoya et al., "Pancreatic endoderm derived from human embryonic stem cells generates glucose-responsive insulin-secreting cells in vivo," *Nature Biotechnology*, vol. 26, no. 4, pp. 443–452, 2008.

Hindawi
Stem Cells International
Volume 2017, Article ID 3537094, 27 pages
https://doi.org/10.1155/2017/3537094

Review Article

Mesenchymal Stem Cells for the Treatment of Spinal Arthrodesis: From Preclinical Research to Clinical Scenario

F. Salamanna,[1] M. Sartori,[2] G. Barbanti Brodano,[3] C. Griffoni,[3] L. Martini,[1] S. Boriani,[3] and M. Fini[1]

[1]*Laboratory of Preclinical and Surgical Studies, Rizzoli Orthopedic Institute, Bologna, Italy*
[2]*Laboratory of Biocompatibility, Technological Innovations and Advanced Therapies, Rizzoli Research Innovation Technology Department, Rizzoli Orthopedic Institute, Bologna, Italy*
[3]*Department of Oncological and Degenerative Spine Surgery, Rizzoli Orthopedic Institute, Bologna, Italy*

Correspondence should be addressed to M. Sartori; maria.sartori@ior.it

Received 23 September 2016; Accepted 5 January 2017; Published 13 February 2017

Academic Editor: Marco Tatullo

The use of spinal fusion procedures has rapidly augmented over the last decades and although autogenous bone graft is the "gold standard" for these procedures, alternatives to its use have been investigated over many years. A number of emerging strategies as well as tissue engineering with mesenchymal stem cells (MSCs) have been planned to enhance spinal fusion rate. This descriptive systematic literature review summarizes the in vivo studies, dealing with the use of MSCs in spinal arthrodesis surgery and the state of the art in clinical applications. The review has yielded promising evidence supporting the use of MSCs as a cell-based therapy in spinal fusion procedures, thus representing a suitable biological approach able to reduce the high cost of osteoinductive factors as well as the high dose needed to induce bone formation. Nevertheless, despite the fact that MSCs therapy is an interesting and important opportunity of research, in this review it was detected that there are still doubts about the optimal cell concentration and delivery method as well as the ideal implantation techniques and the type of scaffolds for cell delivery. Thus, further inquiry is necessary to carefully evaluate the clinical safety and efficacy of MSCs use in spine fusion.

1. Introduction

Spinal fusion is a common means to treat vertebral instability. Its use has quickly increased over the last decades in order to realize the stabilization of the spine in patients affected by degenerative, oncologic, and traumatic spine diseases. Autogenous bone harvested from the iliac crests is the standard procedure for spinal fusion surgery and it is used in more than 190.000 cases/year in Europe [1]. It owns all the key graft material properties, that is to say osteoconduction, osteoinduction, osteogenic potential, and also structural integrity if corticals are comprised. However, the use of autologous bone graft has been described to be linked with 5% to 35% nonunion rate, intraoperative blood loss, and residual morbidity at the donor sites in about 30% of the patients [2]. There are many factors inherent to the spine fusion failure such as tensile forces, low bone surface, and interference by surrounding musculature [3]. In addition, the time required for spinal fusion increases with advancing age and the fusion rate remains unpredictable in the ageing population [4]. Moreover, smoking, osteoporosis, and systemic illnesses have an adverse impact on bone and in particular in spinal surgery [5, 6]. The presence of these intrinsic complications has given rise to research into new materials and methods avoiding iliac crest harvesting. Thus, there are differing lines of research such as bone substitutes (allografts, demineralized bone matrix, and ceramics) and osteoinductive growth factors (bone morphogenic proteins). However, bone substitutes, which are merely osteoconductive and not osteoinductive, remain yet to be finished as substitutes for bone because the fusion achieved with them is not solid enough. In fact, for a successful spinal fusion to occur, several essential elements in addition to a biocompatible scaffold are necessary. They include the presence of the bone-forming cells or their precursors and an appropriate biological signal that direct bone synthesis. The most critical of these components are

the osteoblasts or their precursors, the mesenchymal stem cell (MSC), both of which own the ability to form bone. To overcome these limitations, researchers have focused on new treatments that will allow for safe and successful bone repair and regeneration. In this field, adult stem cells derived from mesenchymal tissue represent a promising source for bone engineering for their ability to differentiate into osteoblasts. MSCs are undifferentiated cells characterized by a high proliferation rate that were found in several adult tissues [7–9]. The multipotent nature of individual MSCs was first established in 1999 by Pittenger et al. [10], and since then they have been found to be pluripotent, giving rise to endoderm, ectoderm, and mesoderm cells [11]. Thus, MSCs are well suited to therapeutic applications also because they can be easily cultured and have high ex vivo expansive potential [12–15]. In the treatment of several musculoskeletal injuries, such as bone, articular cartilage, and other joint tissues, MSCs from bone marrow (BMSCs) are the most widely used cells, followed by MSCs from adipose tissue (ADSCs) [16–18]. Both types of cells have been demonstrated to have a significant effect on spinal fusion in a multitude of settings including a variety of culturing mechanisms, scaffolds, and added growth factors. However, MSCs represent a lesser (0.001–0.01%) fraction of the total population of the nucleated cells [19, 20]. To increase the concentration of MSCs, several techniques have been developed, especially cell ex vivo expansion, but many problems limited the clinical application, such as the sterility technique, long culture time, high cost, and the mixture of human cell culture medium with fetal bovine serum. Thus, the method of collecting MSCs, as well as the real number of MSCs to be transplanted, remains yet to be established.

To date, a great body of research on MSCs for spinal fusion procedures was performed in vitro and in vivo but a clinical customary procedure for the use of cell-based strategies for spinal fusion surgery has not been established and contrasting clinical but also preclinical results were reported in literature. More importantly, the clinical transferability of some protocols is still to be settled, to optimize time and sources when modified/stimulated cells, custom made scaffolds, and in vitro steps are required [21]. Thus, in this systematic review, we aimed to evaluate the efficacy of MSCs in spinal arthrodesis procedures considering the preclinical and clinical studies of the last 10 years to shed light on using MSCs for spinal fusion treatment.

2. Motivations

2.1. Why a Systematic Review? We have seen the necessity for performing a descriptive systematic literature review on MSCs use in spinal arthrodesis procedures in order to understand if the use of MSCs may represent a valid strategy able to facilitate and accelerate bone regeneration during spine surgery providing to researchers and clinicians a beginning point with solid foundations allowing this field to make a leap forward. Our aim is to offer answers to questions such as the following: "Since bone contains a complex environment of many cell types, are MSCs able to perform all the necessary physiological functions to achieve, facilitate, and accelerate spinal fusion?," "What happens to MSCs when they are added to a scaffold?," "Which source of MSCs is better to use and which techniques (ex vivo expansion and one-step procedure) are better to use?," "How much does the existing preclinical model reflect the data so far collected in clinical studies?," and "What do we have to do to further clarify the potential role of MSCs in spinal fusion procedures?" Specifically, we want to summarize the knowledge collected in nearly 10 years of research, learning from previous preclinical and clinical research which used MSCs for spinal fusion procedures, since there is an exigent need to have successful spinal fusion.

3. Methods

3.1. Descriptive Systematic Literature Review. Our descriptive literature review involved a systematic search that was carried out, according to the Preferred Reporting Items for Systematic Reviews and Meta-Analyses (PRISMA) statement, in three databases (https://www.ncbi.nlm.nih.gov/pubmed, https://www.webofknowledge.com, and https://www.scopus.com). In order to evaluate the ongoing clinical studies, the https://www.clinicaltrials.gov website was also checked. The keywords were mesenchymal stromal cells OR mesenchymal stem cells OR mesenchymal/progenitor stromal cells OR mesenchymal/progenitor stem cells AND spinal arthrodesis OR spinal fusion OR interbody fusion OR vertebral arthrodesis OR vertebral fusion. We sought to identify studies where MSCs were employed for spinal fusion procedures. Publications from 2006 to 2016 (original articles in English) were included. A public reference manager ("http://www.mendeley.com") was used to delete duplicate articles.

4. Results and Discussion

An initial literature search retrieved 444 references (Figure 1). Hundred and twenty-nine articles were identified using https://www.ncbi.nlm.nih.gov/pubmed, 210 articles were identified using https://www.webofknowledge.com, and 105 articles were found in https://www.scopus.com. Six additional articles were obtained from the website https://www.clinicaltrials.gov. The resulting references were selected for supplementary analysis based on the title and abstracts and 149 were considered eligible. References were submitted to a public reference manager (Mendeley 1.14, "https://www.mendeley.com") to eliminate duplicate articles. Sixty complete articles were then reviewed to establish whether the publication met the inclusion criteria and 50 articles were recognized eligible for the review considering publications from 2006 to 2016 (Figures 2(a) and 2(b)). Thirty-nine articles were in vivo studies on small, medium, and large animal models (Tables 1, 2, and 3) while the remaining 11 articles were clinical studies or clinical trials (Tables 4 and 5).

Figure 3 summarizes the main steps of spinal fusion stem cell-based therapy founded in this literature search.

We did not perform meta-analyses of the selected studies but reported the results in a descriptive fashion. By considering the studies emerging from this review, we stratified the

Table 1: Published in vivo studies in small animal models on mesenchymal stem cells for spinal arthrodesis procedures.

Animal model	MSCs source	Other biological adjuvant	Scaffold material	Experimental time (weeks)	Spinal fusion level	Experimental design	Main outcome	Reference
Ovariectomized rat	hPSCs from adipose tissue of patients with and without osteoporosis	NELL-1	DBM/β-TCP	4 weeks	L4-L5	*Group 1*: DBM/β-TCP with hPSCs (0.25×10^6 cells/mL) *Group 2*: DBM/β-TCP with hPSCs (0.75×10^6 cells/mL) *Group 3*: DBM/β-TCP with NELL-1 (33.3 μg/mL) *Group 4*: DBM/β-TCP with NELL-1 (66.6 μg/mL) *Group 5*: DBM/β-TCP with hPSCs/NELL-1 at the dosage of groups 1 and 3 *Group 6*: DBM/β-TCP with a hPSCs/NELL-1 at the dosage of groups 2 and 4	(i) Group 1 achieved a fusion rate of 20% (1/5), group 2 of 28.6% (2/7), groups 3 and 4 of 20% (1/5), and group 5 of 37.5% (3/8), and group 6 improved the fusion rates up to approximately 83.3% (5/6) (ii) Microcomputed tomography imaging and quantification further confirmed solid bony fusion in group 6	[22]
Rat	In toto rat bone marrow from femur flush (1.1×10^7 cells/mL)	bFGF	PEGDA-co-A6ACA hydrogels (poly(ethylene glycol)-diacrylate hydrogel (PEGDA) and N-acryloyl 6-aminocaproic acid (A6ACA))	2, 4, 6, and 8 weeks	L4-L5	*Group 1*: scaffold with bone marrow *Group2*: scaffold with bFGF *Group 3*: scaffold with saline solution	(i) Radiographs showed fusion masses in 4 animals out of 7 in each group at 2 weeks. At 4 weeks, all animals showed clear evidence of hard tissue formation, with progressively increase at 6 and 8 weeks (ii) μ-CT imaging at 8 weeks revealed a 51% of mineralized hard tissue for group 3, 59% for group 2, and 54% for group 1 (iii) Manual palpation provided evidence of fusion in all groups, with no significant differences in fusion indices	[23]
Rat	Fresh bone marrow (BM) cells (range, 0.60 to 2.60×10^6 BM cells)	rhBMP-2 (0.006 mg/mL)	Absorbable collagen sponge (ACS)	8 weeks	L4-L5	*Group 1*: 2ACS with fresh BM and rhBMP-2 *Group 2*: 2ACS with rhBMP-2 *Group 3*: 1ACS with rhBMP-2 *Group 4*: ACS with BM *Group 5*: ACS alone	(i) In group 1 BM plus rhBMP-2/ACS significantly increased the fusion rate to 89% (16/18) compared with a base fusion rate of 33% (4/12) in group 3 and 50% (6/12) in group 2 ($p < 0.05$) (ii) No difference in strength or stiffness was detected among group 1 and groups 2 and 3. (iii) No fusion or bone formation was observed in the rats of groups 4 and 5	[24]

Table 1: Continued.

Animal model	MSCs source	Other biological adjuvant	Scaffold material	Experimental time (weeks)	Spinal fusion level	Experimental design	Main outcome	Reference
Rat	Expanded MSCs (3×10^6) from goat BM iliac crest lentivirally transduced to express luciferase	None	HA/β-TCP	7 weeks	L1-L2 and L4-L5	*Group 1*: no cells *Group 2*: MSCs *Group 3*: MSCs gamma-irradiated (30 Gy) *Group 4*: MSCs dipped in liquid N_2	(i) The antiluciferase immunohistochemistry showed no newly formed bone or luciferase-positive cells. (ii) Histological staining with Hematoxylin/Eosin highlighted no signs of a bone formation in any groups	[25]
Rat	Expanded bone marrow from rat femur (1×10^7 cell/mL)	None	Silk fibroin (SF) and mineralized silk fibroin (mSF)	12 weeks	L4-L5	*Group 1*: SF scaffold *Group 2*: SF with MSCs *Group 3*: mSF *Group 4*: mSF with MSCs *Group 5*: autograft *Group 6*: sham group	Fusion rate, bone volume, biomechanical parameters, and histological score showed no significant differences between group 4 and group 5. Group 3 was significantly greater for most parameters than group 2	[26]
Rat	Allogenic MSCs	None		8 weeks	L4-L5	*Group 1*: trinity evolution (DBM with MSCs) *Group 2*: grafton (DBM) *Group 3*: DBM *Group 4*: decortication only	(i) Fusion rate by radiography was 8/8 for group 1, 3/8 for group 2, and 5/8 for group 3 (ii) Fusion rate by μ-CT and manual palpation was 4/8 for group 1, 3/8 for group 2, and 3/8 for group 3	[27]

Table 1: Continued.

Animal model	MSCs source	Other biological adjuvant	Scaffold material	Experimental time (weeks)	Spinal fusion level	Experimental design	Main outcome	Reference
Mouse	Bone marrow from femur and tibia (1.0×10^8 cells/mL)	PRP from donor (1.0×10^9 platelets/mL) or rhBMP-2 (31 μg/mL)	ACS	4 weeks	L4-L5 and L5-L6	*Group 1*: collagen sponge with rhBMP-2 and saline solution *Group 2*: collagen sponge with rhBMP-2 and PRP *Group 3*: collagen sponge with rhBMP-2 and BM *Group 4*: decortication only	(i) Fusion appeared radiographically and histologically similar in all three experimental groups (ii) The area, volume, and density of the fusion mass were significantly greater ($p < 0.05$) for group 3 as compared with group 1 (iii) Group 2 had intermediate fusion area and density (iv) No spinal fusion was detected in group 4	[28]
Rat	Expanded rat bone marrow from femurs (1×10^6 cells/mL)	Fibrin matrix	PCL-TCP	6 weeks	L4-L5	*Group 1*: 10 μg of rhBMP-2 with 1×10^6 undifferentiated BMSCs *Group 2*: 10 μg of rhBMP-2 with osteogenic-differentiated BMSCs *Group 3*: 2.5 μg rhBMP-2 with undifferentiated BMSCs *Group 4*: 2.5 μg rhBMP-2 with osteogenic-differentiated BMSCs *Group 5*: 0.5 μg rhBMP-2 with undifferentiated BMSCs *Group 6*: 0.5 μg rhBMP-2 with osteogenic differentiated BMSCs	(i) Predifferentiation of BMSCs before transplantation failed to promote posterolateral spinal fusion when codelivered with low-dose of rhBMP-2 in group 5 as 17% fusion rate was observed (1/6) (ii) In contrast, combined delivery of undifferentiated BMSCs with low-dose BMP-2 (2.5 μg) as in group 5 demonstrated significantly higher fusion rate (4/6 or 67%) as well as significantly increased volume of new bone formation	[29]
Rat	Human bone marrow (5×10^6 MSCs)	None	Titanium microplates with HA	8 weeks	L1–L3	*Group 1*: titanium microplates with HA *Group 2*: titanium microplates with HA/MSCs	Histology, histomorphometry, and μ-CT revealed no significant bone formation in group 2 in comparison with group 1	[30]

Table 1: Continued.

Animal model	MSCs source	Other biological adjuvant	Scaffold material	Experimental time (weeks)	Spinal fusion level	Experimental design	Main outcome	Reference
Rat	ADSCs (5×10^6 cells/scaffold)	rhBMP-2 or adenoviral vector containing BMP-2 gene	Type-I collagen sponge	4 weeks	L4-L5	*Group 1*: ADSCs transduced with an adenoviral vector containing rhBMP-2 gene *Group 2*: ADSCs with osteogenic media and 1 mg/mL of recombinant rhBMP-2 *Group 3*: rhBMP-2 (10 mg) *Group 4*: rhBMP-2 (1 mg) *Group 5*: ADSCs	(i) All animals of group 1 were characterized by fusion masses (8/8) after 4 weeks (ii) Group 1 revealed spinal fusion at the cephalad level (L3 and L4) (iii) New bone formation in groups 1 was significantly larger than those in any other treatment group ($p < 0.005$) (iv) Groups 3 and 4 showed a solid fusion in 8/8 and 4/8 animals, respectively (v) Groups 2 and 5 showed no fusion	[31]
Rat	hPSCs from adipose tissue	None	DBM	4 weeks	L4-L5	*Group 1*: DBM *Group 2*: DBM with 0.15×10^6 hPSCs *Group 3*: DBM with 0.50×10^6 hPSCs *Group 4*: DBM with 1.50×10^6 hPSCs	(i) hPSC treatment (groups 2, 3, and 4) significantly increased spinal fusion rates in comparison with group 1 (ii) Groups 2, 3, and 4 resulted in fusion rates of 100%, 80%, and 100%, respectively, compared with 20% fusion in group 1 (iii) Computerized biomechanical simulation (finite element analysis) further demonstrated bone fusion in hPSC treatment groups (iv) Histological analyses showed endochondral ossification in hPSC-treated samples	[32]
Rat	ADSCs from healthy donors (1.0×10^6) Purchased BMSCs (1.0×10^6)	Adenoviral vectors adeno-*BMP-2* and adeno-*LacZ* used to transduce ADSCs and BMSCs	ACS	8 weeks	L4-L5	*Group 1* ACS with ADSCs transfected with adeno-BMP-2 *Group 2* ACS with BMSCs transfected with adeno-BMP-2 *Group 3* ACS with rhBMP-2 *Group 4* ACS with ADSCs transfected with adeno-LacZ *Group 5* ACS with BMSCs transfected with adeno-LacZ, and *Group 6* ACS	(i) Spinal fusion was observed in groups 1, 2, and 3 rats (ii) 75% (15/20) of the animals of groups I and II had spontaneous extension of the fusion to a second level (iii) No animals in groups 4, 5, and 6 rats developed fusion (iv) New bone volume was significantly greater in groups 1 and 2 than in group 4	[33]

Table 1: Continued.

Animal model	MSCs source	Other biological adjuvant	Scaffold material	Experimental time (weeks)	Spinal fusion level	Experimental design	Main outcome	Reference
Rat	Expanded BM cells from femurs and tibias ($1 \times 10^6/60\ \mu L$)	FGF-4 ($41\ \mu g$)	HA	8 weeks	L4-L5	*Group 1*: HA *Group 2*: HA with MSCs *Group 3*: HA with MSCs and FGF-4	(i) Radiographic, high-resolution μ-CT, and manual palpation revealed spinal fusion in 5/6 (83%) in group 2 (ii) In group 1, 3/6 (60%) rats developed fusion at L4-L5 by radiography and 2/5 (40%) by manual palpation in radiographic examination (iii) In group 3, bone fusion was observed in only 50% of rats by manual palpation and radiographic examination	[34]

Table 2: Published in vivo studies in medium animal models on mesenchymal stem cells for spinal arthrodesis procedures.

Animal model	MSCs source	Other biological adjuvant	Scaffold material	Experimental time (weeks)	Spinal fusion level	Experimental design	Main outcome	Reference
Rabbit	Expanded BM from iliac crest (1.5 $\times 10^6$ cells/mL)	Osteogenic medium	HA	6 weeks	L5-L6	*Group 1*: autograft *Group 2*: HA with type I collagen gel *Group 3*: HA and type I collagen gel with MSCs *Group 4*: HA and type I collagen gel with MSCs induced toward osteogenic phenotype	The fusion rates were 4/6 in group 1; 0/6 in group 2; 2/6 in group 3; and 4/5 in group 4	[35]
Rabbit	Fresh BM from iliac crests	Fibronectin	HA	6 weeks	L4-L5	*Group 1*: autograft from iliac crest *Group 2*: autograft from transverse process bone graft *Group 3*: HA sticks and iliac bone graft *Group 4*: HA sticks with BM aspirate *Group 5*: HA sticks *Group 6*: HA sticks with FN and BM aspirate. *Group 7*: decortication only	(i) The elasticity and mechanical strength were significantly higher in group 1 than in groups 2, 4, and 5 (ii) The mechanical strength achieved in groups 3 and 6 was nearly equal to that in group 1 (iii) The mechanical strength was significantly higher in group 6 than in group 4 (iv) Histology showed intraporous osteogenesis in groups 3, 4, and 6	[36]
Rabbit	Expanded BM cells from iliac crest (1 $\times 10^6$cells/mL)	(i) rhBMP-2 (ii) bFGF (iii) Autograft	HA	6 weeks	L4–L5	*Group 1*: autograft *Group 2*: HA with MSCs *Group 3*: HA with MSCs and BMP *Group 4*: HA with MSCs and bFGF *Group 5*: HA with MSCs and BMP/bFGF	The fusion rates were 4/7 in autograft group; 0/7 in MSCs/HA group; 2/7 in MSCs/HA/BMP group; 3/7 in MSCs/HA/FGF group; and 6/7 in MSCs/HA/BMP/bFGF group	[37]

Table 2: Continued.

Animal model	MSCs source	Other biological adjuvant	Scaffold material	Experimental time (weeks)	Spinal fusion level	Experimental design	Main outcome	Reference
Rabbit	Expanded BM cells from iliac crest	None	None	8 weeks	L4-L5	*Group 1*: autograft *Group 2*: autograft with MSCs	(i) In group 1, the fusion rate was 53% (8/15) (ii) In group 2, the fusion rate was 0%	[38]
Rabbit	BM from femur, tibia, trochanter, and iliac crest	None	TCP	7 weeks	L5-L6	*Group 1*: TCP alone *Group 2*: TCP with MSCs *Group 3*: TCP with MSCs and LIPUS	(i) Significant increase in manual palpation in group 3 treated with LIPUS (86%) in comparison with groups 1 (0%) and 2 (14%) without LIPUS (ii) The bone volume of fusion mass was significantly larger in group 3 than the other two groups by quantitative computed tomographic analysis (iii) Group 3 fusion mass had a better osteointegration length between host bone and implanted composite and presented more new bone formed in the TCP implants (iv) Group 3 had osteochondral bridging, early stage of bony fusion, from histological point of view	[2]
Rabbit	Expanded BM from iliac crest	None	Poly(lactide-co-glycolide) (PLGA)/HA/ type I collagen	6 weeks or 12 weeks after grafting	L4-L5	*Group 1*: autograft *Group 2*: PLGA/HA/Type I collagen with MSCs	Radiographic, computed tomography examinations, torsional loading tests, and histologic examinations showed solid fusion in 3/5 rabbits in both experimental groups at 6 weeks and 5/5 solid fusion in both groups at 12 weeks	[39]

Table 2: Continued.

Animal model	MSCs source	Other biological adjuvant	Scaffold material	Experimental time (weeks)	Spinal fusion level	Experimental design	Main outcome	Reference
Rabbit	ADSCs from the inguinal groove	None	Nano-hydroxyapatite–collagen–polylactic acid (nHAC–PLA)	10 weeks	L5-L6	*Group 1*: autograft *Group 2*: nHAC–PLA *Group 3*: autograft with nHAC–PLA *Group 4*: ADSCs with nHAC–PLA	(i) The rate of fusion was significantly higher in group 1 and group 4 than in group 2 and group 3 (ii) Microstructural analysis of the samples showed more new bone-like tissue formation in group 1 and group 4 than in the other two groups (iii) Mechanical properties showed that the strength and stiffness of group 1 and group 4 were much higher than those of group 2 and group 3	[40]
Rabbit	BM from femur (1.0×10^8 allogeneic MSCs)	None	Bioresorbable purified fibrillar collagen and calcium phosphate ceramics containing HA and β-TCP	18 weeks	L5-L6	*Group 1*: HA/ β-TCP with MSCs *Group 2*: HA/ β-TCP	(i) In group 1 CT scanning revealed excellent fusion in 2/12 rabbits (17%), good fusion in 8/12 (66%), and fair fusion in 2/12 (17%) (ii) In group 2 a good fusion result was found in 3/12 rabbits (25%), fair fusion in 6/12 (50%), and poor fusion in 3/12 (25%)	[41]
Rabbit	Expanded human BM from iliac crest (10^7)	None	PLGA/BCP/collagen graft and MSC/PLGA/coralline HA/collagen graft	10 weeks	L4-L5	PLGA/BCP/collagen with MSCs (on the left side) PLGA/coralline HA/collagen with MSCs (on the right side)	(i) Radiographic, CT, and bone mineral content analyses showed continuous bone bridges and fusion mass incorporated with the transverse processes (ii) Bone mineral content values were higher in MSCs/PLGA/BCP/collagen group than in MSCs/PLGA/coralline HA/collagen group	[42]

Table 2: Continued.

Animal model	MSCs source	Other biological adjuvant	Scaffold material	Experimental time (weeks)	Spinal fusion level	Experimental design	Main outcome	Reference
Rabbit	Expanded BM from iliac crest (2×10^7)	Bac-BMP-7	Collagen/TCP/HA	12 weeks	L4-L5	*Group 1*: collagen/TCP/HA *Group 2*: collagen/TCP/HA with MSCs *Group 3*: collagen/TCP/HA/ Bac-BMP-7 with MSCs	(i) In the CT results, 6/12 fused segments were observed in group 1 (50%), 8/12 in group 2 (67%), and 12/12 in group 3 (100%) (ii) The fusion rate by manual palpation was 0% (0/6) in group 1, 0% (0/6) in group 2, and 83% (5/6) in group 3 (iii) Histology showed that group 3 had more new bone and matured marrow formation	[43]
Rabbit	Expanded and osteogenic induced BM from iliac crest (OMSCs)	None	ACS	8 and 12 weeks	L4-L5	*Group 1*: ACS with OMSCs *Group 2*: ACS *Group 3*: autograft *Group 4*: nothing	(i) Bony fusion was evident as early as 8 weeks in groups 1 and 3 (ii) At 8 and 12 weeks, by CT and histologic analysis, new bone formation was observed in groups 1 and 3 and fibrous tissue and absence of new bone were present in groups 2 and 4 (iii) Manual palpation showed bony fusion in 40% (4/10) of rabbits in group 1, 70% (7/10) of rabbits in group 3, and 0% (0/10) of rabbits in both groups 2 and 4	[44]
Rabbit	Expanded BM from iliac crest (10^5)	MSCs transduced with Smad1C gene	Absorbable gelatin sponge	4 weeks	L6-L7	*Group 1*: BMSCs transduced with Smad1c with Ad5 vector *Group 2*: BMSCs transduced with Smad1c with Ad5 vector retargeted to α_v integrins (RGD) *Group 3*: BMSCs transduced with BMP-2 with Ad5 vector *Group 4*: BMSCs transduced with BMP-2 with Ad5 vector retargeted to α_v integrins (RGD) *Group 5*: BMSCs transduced with an Ad5 vector expressing b-galactosidase	(i) The area of new bone formed in groups 1, 2, 3, and 4 was significantly greater than the area of new bone formed in group 5 ($p < 0.04$ for each group compared with group 5) (ii) Group 4 mediated a greater amount of new bone formation than group 3 (iii) Similarly, group 2 mediated a greater amount of new bone formation than group 1 ($p < 0.0007$) (iv) Group 2 mediated a greater amount of new bone formation than the other groups ($p < 0.02$)	[45]

Table 2: Continued.

Animal model	MSCs source	Other biological adjuvant	Scaffold material	Experimental time (weeks)	Spinal fusion level	Experimental design	Main outcome	Reference
Rabbit	Expanded and osteogenic induced BM from iliac crest (2×10^6)	rhBMP-2	Alginate scaffold	16 weeks	L4-L5	*Group 1*: autograft *Group 2*: alginate scaffold with MSCs *Group 3*: alginate scaffold with MSCs and rhBMP-2 *Group 4*: alginate scaffold with rhBMP-2	(i) Radiographic union of group 1 was 11/12, of group 2 8/11, of group 3 11/12, and of group 4 0/12 (ii) Manual palpation highlighted 6/6 solid fusion in group 1, 1/6 in group 2, 5/6 in group 3, and 0/6 in group 4 (iii) The mechanical analysis (failure torque) did not differ significantly between group 1 and group 3 that were both higher than group 2	[46]
Rabbit	Expanded and osteogenic induced BM from iliac crest (2×10^6)	None	Alginate scaffold	12 weeks	L4-L5	*Group 1*: alginate scaffold *Group 2*: alginate scaffold with MSCs *Group 3*: alginate scaffold/ hyperbaric oxygen (HBO) therapy with MSCs	Radiographic examination and manual palpation highlighted no union for group 1 (0/12), 10/22 for group 2, and 6/12 for group 3	[47]
Rabbit	Expanded BM from iliac crest	TCP	Recombinant baculovirus encoding BMP-2 (Bac-CB) and vascular endothelial growth factor (Bac-VEGF)	12 weeks	L4-L5	*Group 1*: TCP *Group 2*: TCP with MSC *Group 3*: TCP with MSCs/Bac	(i) Radiographically fusion rate was detected as being 0/12 in group 1, 4/12 in group 2, and 10/12 in group 3 (ii) Manual palpation highlighted no fusions in group 1, two solid fusions in group 2, and five solid fusions in group 3	[48]

Table 2: Continued.

Animal model	MSCs source	Other biological adjuvant	Scaffold material	Experimental time (weeks)	Spinal fusion level	Experimental design	Main outcome	Reference
Rabbit	Expanded and osteogenic induced BM from iliac crest	Bioresorbable hydrogel (pluronic F27) and coralline HA	None	6 and 12 weeks	L4-L5	*Group 1*: Pluronic 127/HA hybrid graft with MSCs *Group 2*: autograft	(i) Solid fusion was achieved in 3/5 rabbits from both group 1 and 2 at 6 weeks, and solid fusion was present in 5/5 from both group at 12 weeks (ii) No differences were detected between the two groups for biomechanical analysis and from histological point of view	[49]

Table 3: Published in vivo studies in large animal models on mesenchymal stem cells for spinal arthrodesis procedures.

Animal model	MSCs source	Other biological adjuvant	Scaffold material	Experimental time (weeks)	Spinal fusion level	Experimental design	Main outcome	Reference
Pig	ADSCs from inguinal subcutaneous tissue	None	DBM	8 and 12 weeks	L2–L6	*Group 1*: one cage was left and three filled with freeze dried irradiated cancellous pig bone graft *Group 2*: freeze dried irradiated cancellous pig bone graft *Group 3*: cancellous bone autograft *Group 4*: bone graft with 3D osteogenic differentiated ADSCs	μ-CT scan, microradiography, and histology/histomorphometry demonstrated a significant increase in bone content in group 4	[50]
Sheep	Expanded and osteogenic induced BMSCs from iliac crest ($5\text{-}6 \times 10^7$)	Fibrin	TCP/HA	12 weeks	L1–L6	*Group 1*: HA with MSCs *Group 2*: TCP/HA with MSCs *Group 3*: autograft	(i) Radiography, manual palpation, histological analysis, and SEM analyses revealed demonstrated better bone formation in group 2 compared to group 1 (ii) Histomorphometry detected 55.8% of new bone in group 3, followed by group 2 (42.7%) and group 1 (10.7%)	[51]
Sheep	Allogenic sheep mesenchymal precursor cells (MPCs) from BM from iliac crest	None	HA/TCP	16–36 weeks	L2–L5	*Group 1*: autograft *Group 2*: HA/TCP *Group 3*: HA/TCP with MPCs (25×10^6) *Group 4*: HA/TCP with MPCs (75×10^6) *Group 5*: HA/TCP with MPCs (225×10^6)	Computed tomography, high-resolution radiography, biomechanical testing, organ pathology, bone histopathology, and bone histomorphometry showed that allogeneic mesenchymal precursor cells produced fusion efficacy similar to that achieved using iliac crest autograft	[52]

Table 3: Continued.

Animal model	MSCs source	Other biological adjuvant	Scaffold material	Experimental time (weeks)	Spinal fusion level	Experimental design	Main outcome	Reference
Sheep	Allogenic MPCs from BM from sheep iliac crest	None	HA/TCP	16 weeks	L4-L5	*Group 1*: autograft *Group 2*: HA/TCP with MPCs (2.5×10^6) *Group 3*: HA/TCP with MPCs (6.5×10^6) *Group 4*: HA/TCP with MPCs (12.5×10^6)	(i) Manual palpation of the fusion site indicated solid fusion in more than 75% of MPC-treated group and 65% of group 1 (ii) Computed tomography and histomorphometry analyses showed all animals in the MPCs groups and group 1 fusion masses were present at 16 weeks	[53]
Sheep	Expanded and osteoinduced BM from iliac crest	None	HA	6 months	L4-L5	*Group 1*: autograft *Group 2*: allograft *Group 3*: HA *Group 4*: HA with MSCs.	(i) By CT scan and histology lumbar fusion were higher for groups 1 and 2 (70%) than for group 3 (22%) and group 4 (35%) (ii) New bone formation was higher for groups 1 and 2 (iii) Group 4 had a better fusion rate than group 3, but the histology showed no significant differences between them in terms of quantity of bone formation	[54]
Sheep	BM concentrate (1.5×10^6 in 0.2 mL)	None	Natural bone collagen scaffold (NBCS) from human organic bone particles	6 and 10 weeks	L3-L4 and L4-L5	*Group 1*: autograft *Group 2*: NBCS *Group 3*: BMCs *Group 4*: NBCS with BMCs	(i) Solid spinal fusion was achieved in all six segments (6/6) in group 4 at 10 weeks, compared with 4/8 segments in group 1, 2/8 segments in group 2, and 3/6 segments in group 3 (ii) The biomechanical stiffness of fusion masses and bone volume at the fusion site were higher in group 4 ($p < 0.05$) (iii) At 10 weeks, the radiographic score reached was significantly higher in group 4 than in groups 1, 2 and 3 (iv) Histological findings revealed that group 4 induced new bone formation integrated well with host bone tissue	[55]

Table 3: Continued.

Animal model	MSCs source	Other biological adjuvant	Scaffold material	Experimental time (weeks)	Spinal fusion level	Experimental design	Main outcome	Reference
Ewes	Allogenic MPCs (5×10^6) or allogenic amnion epithelial stem cells (5×10^6 AECs)	None	Fidji interbody cage made from polyetherether-ketone and HA/TCP	3 months	C3-C4	*Group 1*: cage packed with autograft *Group 2*: cage packed with HA/TCP *Group 3*: cage packed with HA/TCP and MPCs *Group 4*: cage packed with HA/TCP and AECs *Group 5*: controls	(i) Significant fusion mass was detected in group 3 compared to that in groups 1, 2, or 4 (ii) CT scan at 3 months revealed that 5/6 animals in group 3 (83%) had continuous bony bridging compared with 0/ 5 of group 4 and 1/6 of group 1 and 2/6 of group 2 ($p < 0.01$)	[56]
Ewes	Allogeneic MPCs (5×10^6 or 10×10^6)	None	Fidji interbody cage made from polyetherether-ketone and HA/TCP	3 months	C3-C4 anterior cervical discectomy and fusion with a interbody cage	*Group 1*: cage packed with autograft *Group 2*: cage packed with HA/TCP *Group 3*: cage packed with HA/TCP and 5×10^6 MPCs *Group 4*: cage packed with HA/TCP and 10×10^6 MPCs *Group 5*: controls	(i) No significant differences were found between groups 3 and 4 (ii) CT scan showed that 9/12 (75%) MPC-treated animals had continuous bony bridging compared with 1/6 of group 1 and 2/6 of group 2 ($p < 0.019$ and $p < 0.044$, resp.) (iii) By quantitative CT, density of new bone in MPC-treated animals was 121% higher than in group 2 ($p < 0.017$) and 128% higher than in group 1 ($p < 0.0001$)	[57]
Pig	BMSCs (10×10^6)	rhBMP-2 (0.6 mg)	Bioresorbable scaffolds made from medical grade poly (Σ-caprolactone)-20% tricalcium phosphate (mPCL/TCP)	9 months	L2-L3 and L4-L5	*Group 1*: mPCL/TCP with rhBMP-2 *Group 2*: mPCL/TCP with BMSCs *Group 3*: mPCL/TCP *Group 4*: autograft	(i) The mean radiographic scores were 3.0, 1.7, 1.0, and 1.8 for groups 1 to 4, respectively (ii) The bone volume fraction of group 1 was twofold higher than group 2 (iii) Histology, μ-CT, and biomechanical evaluation showed solid and comparable fusion between groups 1 and 4 (iv) Group 2 showed inferior quality of fusion when compared with groups 1 and 4 while group 3 showed no fusion even at 9 months	[58]

Table 3: Continued.

Animal model	MSCs source	Other biological adjuvant	Scaffold material	Experimental time (weeks)	Spinal fusion level	Experimental design	Main outcome	Reference
Ovine	Autogenous whole BM or BM concentrate	None	TCP	6 months	L4-L5	*Group 1*: autograft *Group 2*: TCP with BM concentrate *Group 3*: TCP with whole bone marrow/ *Group 4*: TCP .	(i) At 6 months, 33% of group 2 and 25% of the group 1 sites were fused, compared with 8% of group 3 and 0% of group 4 (ii) Histology of fused samples showed denser bone formation in group 2 than in group 1 sites	[59]

Table 4: Published clinical studies involving the use of mesenchymal stem cells for spinal arthrodesis procedures.

Arthrodesis level	MSCs source	Cell manipulation	Treatment	Patient's number (mean age)	Follow-up	Complications	Reference
Single level = 22 2 or more levels = 13	Right posterosuperior iliac crest	Fresh bone marrow	(i) Left side: autologous bone graft (ii) Right side: mixture of BCP and fresh autogenous bone marrow	35 (24 males, 11 females) Mean age = 59.2	Minimum 30 months	1 pseudoarthrosis	[60]
Single level = 14 2 levels = 23 3 levels = 4	Right and left iliac crest	Bone marrow concentrate (enriched using a cell separator)	(i) Decompression cases: locally harvested bone combined with autologous enriched MSCs/β-TCP (ii) Nondecompression cases: autologous enriched MSCs/β-TCP	41 (30 men, 11 women) Mean age = 44.0	Median 36.5 months	(i) 4 patients with transient exudation or moderate swelling in their wounds (ii) 2 pseudoarthrosis (iii) 1 patient with bursa synovialis (iv) 1 patient with progressive instability of the adjoined supra-vertebra	[20]
1 and 2 levels	Posterior iliac crest	Bone marrow concentrate	(i) Side 1: concentrated bone marrow associated with macroporous biphasic calcium phosphate ceramics graft and autologous bone (ii) Side 2: nonconcentrated bone marrow with ceramics graft and autologous bone	15 Mean age = 46.3	24 months	None	[61]
1, 2, or 3 levels	One iliac crest	Bone marrow concentrated	(i) Side 1: allograft plus autologous bone marrow concentrate (ii) Side 2: autologous iliac crest bone	25 (15 males and 10 females) Mean age = 45.6	24 months	None	[62]
Not specified	Posterior iliac crests	Bone marrow concentrate	(i) 40 patients: allograft chips alone (ii) 40 patients: spongious allograft chips mixed with bone marrow concentrate	80 (22 men, 58 females)	24 months	Two complications occurred in each of the two groups: hematoma with subsequent revision surgery and drainage during the first week postoperatively	[63]
Not specified	Single iliac crest	Bone marrow concentrate	31 patients: concentrated bone marrow aspirate with allograft and demineralized bone matrix	31 (9 men and 22 females) Mean age: 71.5	At least 12 months	(i) One seroma (ii) One pseudarthrosis (iii) Three reoperation for 3 patients for adjacent segment pathology	[64]
1 or 2 levels	Non applicable	Allograft cellular bone matrix containing native mesenchymal stem cells and osteoprogenitor cells	182 patients: allograft cellular bone matrix containing native mesenchymal stem cells and osteoprogenitor cells	182 (49% female, 51% male) Mean age: 51	24 months	(i) 1 durotomy (ii) 2 wound infections (iii) 2 incidences of new radiculopathy (iv) 1 incidence of hypotension (v) 1 incidence of hypertension (vi) 2 incidences of postoperative soft-tissue swelling	[65]

Table 5: List of clinical trials involving mesenchymal stem cells for spinal arthrodesis procedures (from clinicaltrials.gov).

ClinicalTrials.gov Identifier	Condition	Study type	Estimated enrollment/ enrolled patients	MSC data (source, manipulation, or strategy)	Number of cells	Study arms	Follow-up (months)	Activity
NCT01552707	Degenerative spondylolisthesis grades I-II	Interventional phases 1-2	62	Expanded autologous mesenchymal stem cells obtained under GMP conditions fixed in allogenic bone tissue	Not reported	(i) Group 1: instrumented spinal fusion and the tissue engineering product composed by "ex vivo" expanded autologous mesenchymal stem cells fixed in allogenic bone tissue in spinal fusion (ii) Group 2: standard treatment of instrumented spinal fusion and patient's bone iliac crest	12 months	Recruiting
NCT00549913	Posterolateral lumbar fusion	Interventional phases 1-2	42	Immunoselected, culture-expanded, nucleated, allogeneic mesenchymal progenitor cells	Not reported	(i) Experimental group 1: lowest dose of NeoFuse (ii) Experimental group 2: middle dose of NeoFuse (iii) Experimental group 3: highest dose of NeoFuse (MPCs) (iv) Control group: autologous bone graft	24 and 36 months	Completed
NCT01513694	Intervertebral disc disease	Interventional phases 1-2	15	Cell suspension of MSCs from bone marrow aspirate expanded in vitro in a specific medium enriched with platelet lysate without addition of animal products	Not reported	(i) Autologous mesenchymal stem cells arranged in a phosphate ceramic	Not reported	Unknown
NCT01603836	Spondyloarthrosis, spondylosis	Interventional	80	Spongious allograft chips mixed with bone marrow concentrate	74×10^4/L at average (range, $1.06–1.98 \times 10^4$/L)	(i) Group 1: spongious allograft chips alone (ii) Group 2: spongious allograft chips mixed with bone marrow concentrate	24 months	Completed

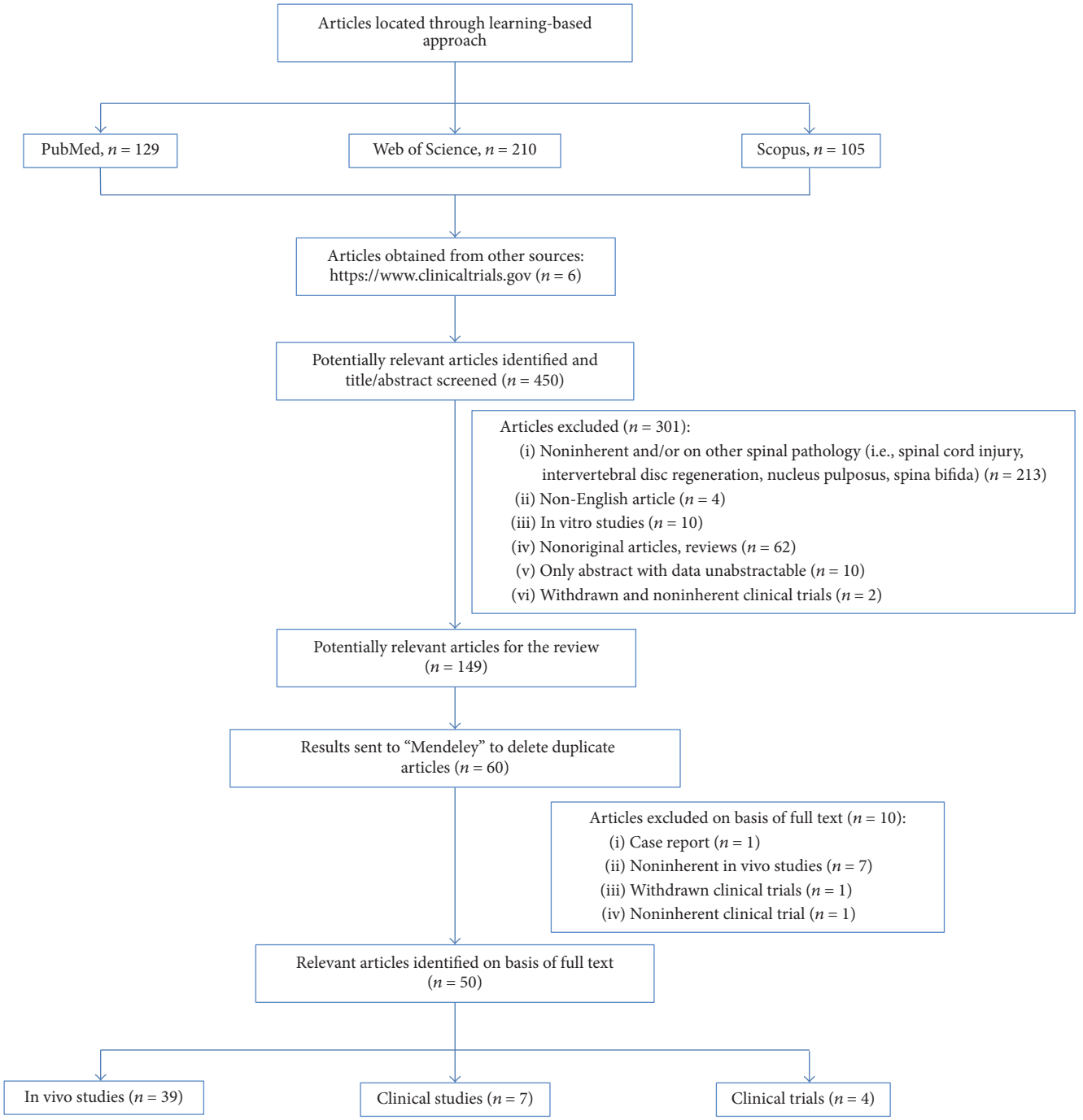

Figure 1: Systematic literature review flow diagram. Flow of information through the different phases of the systematic review.

papers according to in vivo studies (small, medium, and large animal models) and clinical trials.

4.1. In Vivo Studies

4.1.1. Small Animal Models. Thirteen studies (Table 1) employed MSCs in small animal models ($n = 1$ in mice and $n = 12$ in rats) in order to achieve or improve spinal fusion rate. In the majority of the studies the spinal fusion surgery was carried out by decortications of L4 and L5 but also L1-L2 [25] and L4–L6 [28] transverse processes. Klíma et al. [30] used titanium microplates and titanium screws to fix the spinous processes of L1–L3 vertebrae. The experimental time after surgery ranges from 4 to 8 weeks. Most of the studies used in vitro expanded MSCs [22, 25–27, 29–34] principally derived from bone marrow [25–27, 29, 30, 33, 34] but also from adipose tissue [22, 31–33]. Beyond the use of expanded MSCs, some authors, in order to take advantage not only

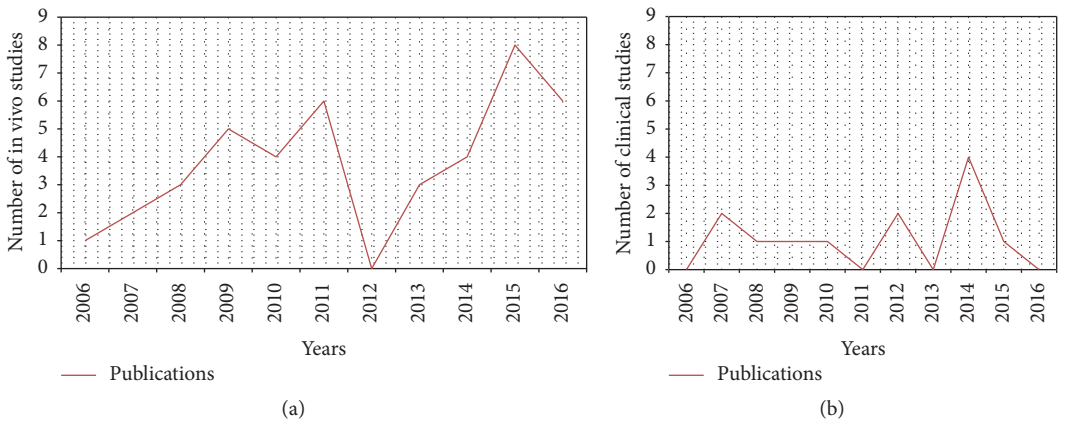

FIGURE 2: Historical distribution of (a) in vivo models and (b) clinical studies on MSCs use in spinal arthrodesis procedures according to the year of publication.

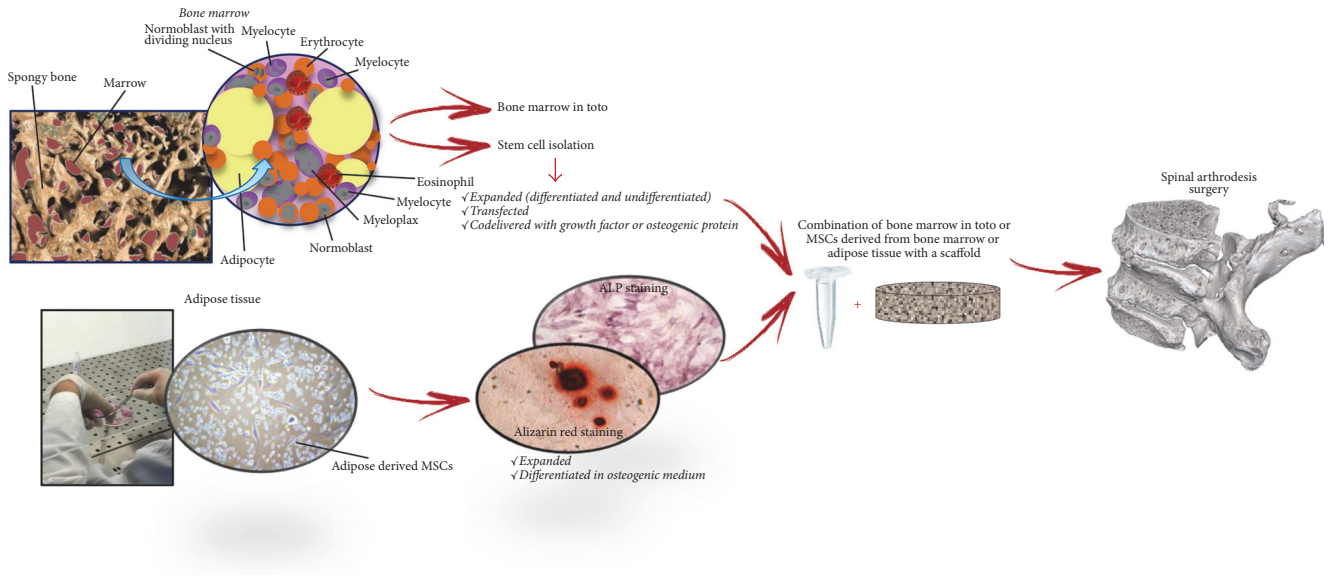

FIGURE 3: Flow chart summarizing the main steps of spinal fusion procedure when stem cell therapy is used.

by the mesenchymal component but also by the presence of trophic factors, cytokines, and extracellular matrix molecule, used bone marrow in toto [23, 24, 28]. Few studies used autologous MSCs [23, 29, 34] while the majority employed allogenic MSCs [22, 24–26, 30–33]. All the examined studies involved seeding cells into allograft [22, 27, 32] or into various scaffolds, such as ceramic [25, 30, 34], collagen sponge [24, 28, 31, 33], silk fibroin [26], and composites [23, 29]. Only one author employed autologous bone graft as control material [26] while the others used allografts or scaffolds without MSCs as control. When expanded MSCs were used the cell number, loaded on allografts or scaffolds, is $1.0–1.50 \times 10^6$ [26, 29, 32–34] but also lower concentration as in the study of Lee et al. (0.25×10^6) [22] or higher concentration was used [23, 26, 30, 31]. Differently from the studies where bone marrow in toto [23, 24, 28] and undifferentiated MSCs were cultured and loaded on a scaffold [25, 26, 30, 32–34] four studies [22, 29, 31, 34] employed cells cultured in osteogenic differentiation medium. In particular, Rao et al. examined also the role of low doses bone morphogenic protein- (BMP-) 2 codelivered with both undifferentiated and differentiated BMSCs showing that undifferentiated BMSCs with low-dose BMP-2 loaded on a composite scaffold demonstrated superior fusion rate in comparison to all the other examined groups. Low dose of BMP-2 was also evaluated in association with bone marrow in toto loaded on a collagen sponge, showing that fresh bone marrow aspirate increases the osteogenic potency and biologic efficiency of BMP-2 [24, 28] also in comparison to BMP-2 associated with other adjuvant factors such as platelet rich plasma [28]. BMP-2 was used also by Miyazaki et al. in an athymic rat model to compare the efficacy of human ADSCs and BMSCs transduced with an adenovirus containing the cDNA for BMP-2 loaded on collagen sponge. Authors showed that ADSCs transfected with adeno-BMP-2 induce abundant

bone formation in a manner similar to genetically modified BMSCs [33]. Similar results were also obtained by Hsu et al. [31] that demonstrate the potential of adipose derived stem cell as cellular vehicle for this osteoinductive factor. Contrary to the positive effect on spinal fusion derived by the association of MSCs or bone marrow with BMP-2, the association of fibroblast growth factor-4 (FGF-4) with differentiated BMSCs loaded on a HA scaffold did not stimulate fusion but appears to induce fibrotic change rather than differentiation to bone [34]. Despite these negative results, recently Shih et al. [23] suggested a good performance in promoting spinal fusion rate associating new biomineralized matrices with bone marrow or basic FGF. Differently from the abovementioned studies that used growth factors in association with BMSCs to enhance spinal fusion, other authors determined the efficacy of a β-tricalcium phosphate (TCP)/demineralized bone matrix (DBM) [22] or DBM alone [32] loaded with different doses of human perivascular stem cells (hPSCs) also in presence and absence of osteogenic protein NELL-1. Authors highlighted that both in healthy [32] and in osteoporotic condition [22] the presence of hPSCs [32] also in association with NELL-1 significantly improved spinal fusion [22]. Differently from all the other studies, Klíma et al. [30] adopted an instrumented model of interspinous fusion showing a nonsignificant new bone formation in animals treated with hydroxyapatite (HA) and BMSCs in comparison to animals treated with scaffold alone, even if in presence of BMSCs authors described minor inflammatory reaction compared to the animals treated without BMSCs. Finally, since the fate and contribution of the MSCs are not sufficiently clarified, especially at clinically relevant locations, Geuze et al. [25] using the bioluminescence imaging of luciferase-marked MSCs and adopting different experimental setup tried to elucidate and clarify the contribution made not only by MSCs itself on spinal fusion but also by the paracrine effect of MSCs when loaded on a ceramic scaffold. Results suggested that the soluble factors or the presence of extracellular matrix was not sufficient to induce bone formation; thus unfortunately they did not provide an answer to the critical question whether the principal mechanism of action of MSCs is based on their activity on the release of soluble mediators.

4.1.2. Medium Animal Model. MSCs treatment to achieve spinal fusion was employed in 16 in vivo studies that used medium sized animal models (Table 2). All the studies used a single level posterolateral transverse process arthrodesis between L4-L5 or L5-L6 or L6-L7. With the exception of one study [44] spinal fusion surgery was carried out by creating a defect between L4 and L5 (depth of 5 mm and diameter of 10 mm); in all the others studies a transverse process decortication was performed. The experimental time after surgery ranges from 4 up to 18 weeks. Unless for the study by Koga et al. [36] that use fresh bone marrow to enhance the spinal fusion rate all the other authors used expanded, autologous [2, 35, 37–40, 42–47, 49], or allogeneic [41, 48] MSCs isolated from bone marrow [2, 35, 37, 38, 41–49] or adipose tissue [40] at different dosages (from 1.0×10^6 cells to 1.0×10^8). Some authors used MSCs with osteogenic differentiation [35, 37–40, 42, 44–47, 49] to increase the fusion rate while other used undifferentiated MSCs [2, 36, 41, 43, 48]. In all the studies MSCs were loaded on a scaffold (i.e., ceramic, polymeric, collagen sponge, and gelatin sponge) with the exception of Urrutia et al. [38] that used a pellet of cultured BMSCs cografted with an autologous bone graft and showed that adding differentiated BMSCs in a pellet without a scaffold not only failed to increase fusion rate, but completely inhibited bony growth. Differently, Nakajima et al. [35], using differentiated BMSCs plus HA, obtained a high rate of lumbar fusion similar to that obtained using autograft alone. In most of the studies the experimental treatment with MSCs was compared with autologous bone but in some of them this comparison is missing [2, 41–43, 45, 47, 48]. Niu et al. [42] compared BMSCs cultured in a biphasic calcium phosphate with BMSCs cultured with coralline HA. Coralline HA was used also by Chen et al. [49] who used MSCs fluorescent labeled with PKH-67 dye in combination with a bioresorbable hydrogel and coralline HA in comparison to autograft showing similar results between groups. In addition, to the use of a ceramic graft in association with BMSCs, several authors used BMP to enhance the osteogenic potency of MSCs [37, 43, 46] showing that MSCs in combination with BMP-2 enhanced bone formation in posterolateral spine fusion exerting a more osteoinductive action than MSCs alone [46]. Favorable results were also obtained comparing the association of a composite [43] and a ceramic [48] material with baculovirus genetically modified BMSCs overexpressing BMP-7 [43] or BMP-2 associated vascular endothelial growth factor (VEGF) [48] with nongenetically modified BMSCs. Additionally, Minamide et al. [37] tested also the hypothesis that both BMP-2 and basic fibroblast growth factor (FGF) mutually acted on the proliferation and osteogenic differentiation of rabbit BMSCs. They showed that the combined treatment with BMP-2 and basic FGF produced a favorable degree of spinal fusion comparable to autograft. An increased spinal fusion rate was also obtained by Koga et al. [36] assessing the osteogenic potential of HA sticks soaked with fresh bone marrow and fibronectin (FN). Interesting were also the results obtained by Hui et al. [2] that underlined that the combination of synthetic biomaterials, autologous differentiated BMSCs, and also low-intensity pulsed ultrasound promote spinal fusion. Differently from the use of low-intensity pulsed ultrasound, the use of hyperbaric oxygen therapy administrated to the animals did not enhance the spinal fusion rate when a combination of allogenic differentiate MSCs/alginate scaffold was evaluated [47]. The effectiveness of autologous differentiated BMSCs was evaluated also by Yang et al. [44] in association with a collagen sponge showing a high fusion rate similar to autologous bone. Another approach exploited by Douglas et al. is the ex vivo transfer of a gene encoding an osteoinductive factor to BMSCs which are subsequently reimplanted into the host. In this study Smad1C gene was transferred into rabbit MSCs isolated from bone marrow. The rationale for the use of this approach is to control more efficiently bone formation mimicking the natural cascade signals and avoiding the drawbacks associated with the direct use of BMPs. Authors showed that animals BMSCs transduced ex vivo with the Smad1C-expressing tropism-modified Ad5 vector mediated a greater amount of new bone formation

than BMSCs transduced with any other vector [45]. Differently from all the other studies Urrutia et al. [38] evaluating a composite of hot compression-molded PLGA, HA, and type I collagen as an BMSCs carrier for a posterolateral spinal fusion used also a PKH fluorescence labeling system and highlighted that the transplanted BMSCs were partly responsible for the new bone formation. Positive results were also obtained using allogeneic undifferentiated rabbit BMSCs added to a type I collagen and calcium phosphate ceramics that promote spinal fusion and did not induce an adverse immune response [41]. Only one study evaluated the effectiveness of autologous ADSCs combined with a new mineralized collagen matrix (nHAC–PLA) for posterolateral spinal fusion. Results indicated that the rate of fusion was significantly higher in the autologous bone and ADSCs + nHAC-PLA groups than that in the nHAC-PLA and autologous bone + nHAC-PLA groups, demonstrating the effective impact of the scaffold also when combined with ADSCs [40].

4.1.3. Large Animal Models. Ten studies used ovine as large animal models (Table 3) [51–57, 59] while two used swine [50, 58]. These studies carried out four-level, three-level, two-level, or single level spinal fusions surgery all instrumented with screws and bars with the exception of Gupta et al. that used a single level noninstrumented lumbar fusion [59]. In these studies both autologous bone marrow or expanded MSCs [50, 51, 54, 55, 58] and allogeneic bone marrow or mesenchymal precursor cells [52, 53, 56, 57, 59] were used to enhance spinal fusion and all of them involved seeding cells into allografts [50], collagen scaffolds [55], ceramics [51–54, 56, 57, 59], and composites [58] scaffolds. Except for Schubert et al. who use MSCs derived from adipose tissue [50] and Goldschlager et al. that used amnion epithelial cells [57] all the other authors used differentiated MSCs and mesenchymal precursor cells derived from bone marrow but also bone marrow in toto loaded on the scaffolds at different dosages. Wheeler et al. also compared different dosages of MSCs [52, 53, 56]. All the researchers used autografts and grafts without cells as controls and the majority highlighted superior result of the graft associated with MSCs and bone marrow in comparison to the graft alone, while similar [50] or best [51–53, 55, 56, 59] results were seen for autografts in comparison to grafts associated with MSCs. In addition, Goldschlager et al. showed superior results of mesenchymal precursor cells loaded on *Mastergraft* material also in comparison to amnion epithelial cells [57]. Differently from the above-mentioned studies, Cuenca-López et al. observed that bone autografts performed better than MSCs loaded on hybrid constructs [54]. Inferior results were also observed for MSCs loaded on a composite scaffold in comparison to autograft but also in comparison to scaffold associated with BMP-2 [58].

4.2. Clinical Studies. The search strategy identified 10 clinical studies (Table 4) about MSCs used for spinal fusion procedures. Among these 10 articles, three were excluded: for two articles we found only the abstract and not the full-text and the other one was a case report of an 88-year-old multidiseased osteoporotic patient treated with corticocancellous bone allograft, augmented with autologous bone marrow concentrate from iliac crest aspirate enriched with platelet rich fibrin from peripheral blood. Thus, due to the treatment protocol and the lack of a control group, the real contribution of MSCs on spinal fusion procedure could not be extrapolated. Therefore, 7 articles were analyzed: by comparing the characteristics of each study, it is evident that, in all studies, with the exception of the study by Moro-Barrero et al. [60], the authors employed the concentrate autologous bone marrow in comparison to fresh one inside the operating theater [20, 61–65]. Three studies associated bone marrow with a ceramic graft [20, 60, 61] while the remaining 4 combined bone marrow with allograft [62–65]. Three studies were prospective, randomized trials [61–63], two of which with limited number of patients [61, 62], while one was a prospective, multicenter, nonrandomized study on 182 patients [65]. All the studies withdrew the bone marrow from iliac crest and performed spinal fusion surgery on 1, 2, or 3 levels with similar surgical procedures and approaches. As far as the number of transplanted cells, cell concentration was not always reported as cell number in one milliliter or was not reported at all, thus making comparison among studies extremely difficult. In addition, another variable among studies is the method used for cell concentration (cell separator based on the density gradient centrifugation, centrifugation over a gradient, or without any gradient). Obviously, the absence of procedural and methodological guidelines affected the cell yield and thus it was not possible to identify a range for the cells number to be transplanted and to correlate it with the clinical outcome. In addition to the cells number, in two studies a control group was not used [64, 65], while other two studies compared the experimental treatment with autologous bone [60, 62] and one study with allograft chips alone [63]. Another study by Gan et al. compared autologous enriched MSCs/β-TCP with locally harvested bone combined with autologous enriched MSCs/β-TCP [20], while Odri et al. in a simple blind randomized clinical, prospective, monocentric study compared a biphasic calcium phosphate ceramics graft that was associated with autologous bone and concentrated bone marrow with unconcentrated bone marrow with ceramics graft and autologous bone [61]. The follow-up of the analyzed studies ranged from 12 months to 36.5 months [20, 60–65], demonstrating, through radiographic and clinical analyses, the safety and in one case a greater efficacy [63] of MSCs use in spinal fusion; however, these studies were conducted in too small patient cohorts and there is the need to confirm these data also from preclinical animal models, where transplanted cell phenotype, fate, and contribution to healing could be monitored and quantitatively measured to exclude malignant transformation.

As of August 2016, the ongoing clinical trials on MSCs for spinal fusion applications found through https://www.clinicaltrials.gov web site are 6 (Table 5). One of them was excluded because the objective of the trial was the definition of the osteogenic potential of MSCs and their progenitors during spinal fusion complication (pseudarthrosis). Another trial has not been analyzed because it has been withdrawn prior to the patients enrollment. The remaining 4 trials were

all interventional study of phase I-II with a minimum follow-up of 12 months. Of them 2 were completed. In detail the trials assessed (1) the feasibility and safety of ex vivo expanded autologous MSCs fixed in allogenic bone tissue in comparison to autologous bone; (2) the effectiveness of autologous mesenchymal stem cells arranged in a calcium phosphate ceramic; (3) the effectiveness of allograft alone versus allograft with bone marrow concentrate; (4) the feasibility, safety, and tolerability of 3 different doses of immunoselected, culture-expanded, nucleated, allogenic mesenchymal precursor cells combined with resorbable ceramic granules in comparison to autograft alone. In all studies fusion surgery, surgical procedures, clinical approaches, and follow-up evaluations were similar. However, each trial was different from the other for patients number, MSCs manipulation or strategy, study arms, and presence and/or type of control group. In addition, the information available was not always complete. In some cases it was not clear which strategy would be employed for MSC manipulation and almost all the studies did not indicate the number of cells or the medium for cell infusion. Thus, although some studies could provide useful information, it was evident that more controlled clinical trials are necessary to understand whether MSCs can be successfully employed in spinal fusion procedures.

5. Conclusion and Future Prospective

In recent years, the basic and preclinical research literature clearly indicates the use of MSCs also in combination with various scaffolds, to repair bone defects, and many studies concern their use also for the treatment of vertebral instability. Thus, with the rapidly growing number of spine fusion surgeries performed annually, we have seen the need for performing this descriptive systematic literature review on MSCs use in spinal arthrodesis procedures in order to elucidate if the use of MSCs may really represent a valid strategy able to facilitate and accelerate spinal fusion.

In this review, several therapeutic strategies for the enhancement of spinal fusion rate based on stem cells have been developed in both preclinical and clinical studies. The application of an allograft or a scaffold, prevalently ceramics, associated with stem cells was adopted in all preclinical studies while the application of autograft, but also ceramic scaffolds, still in association with stem cell was used in the clinical setting (tissue engineering strategy). However, the use of growth factors (principally BMP-2) and other osteoinductive factors, as well as ex vivo gene therapy, was taken into consideration.

We found that numerous preliminary researches in this review were carried out in small, medium, and large animal models showing the potential for MSCs use in spinal fusion procedures. Despite the fact that in some of these studies adipose derived mesenchymal stem cells, human perivascular stem cells, and also amnion epithelial cells were used, the majority of the studies employed bone marrow cells. Based on these preclinical data it would seem that MSCs are able to perform the necessary physiological functions to achieve, facilitate, and accelerate spinal fusion. However, none of these examined studies was able to give a detailed elucidation about the fate of MSCs when they were added to a scaffold, although the success demonstrated that, in the animal models, some barriers remain prior to this therapy translation into the clinical setting. In fact, this review underlines that there are few and basic clinical trials, although some of them have shown that bone marrow cells used in humans can give a successful spine fusion. Some critical existing limitations include also the choice of the optimal cell concentration, the delivery method, the ideal manipulation procedure (ex vivo expansion and one-step procedure), and the best implantation techniques. In addition, researches that examine the optimal MSCs concentration are needed in large animal model, which are more similar to humans. These critical points also highlight the need for methods able to maximize the number of MSCs collected, as well as the presence of easy and feasible techniques in the clinical scenario. However, other matters that need further consideration comprise also the elimination of fetal calf serum, the possible reversibility of the differentiated state, the survival of the cells in vivo, the integration with the preexisting bone, and the capacity to form bone and marrow in vivo.

In conclusion, the use of MSCs as a cell-based therapy may represent a biological approach to reduce the high cost of osteoinductive factors as well as the high dose needed to induce bone formation. Thus, implementing this available potential treatment based on MSCs use and probably mitigating some adverse effects would make this kind of approach a possible therapeutic tool. Finally, although MSCs therapy remains an interesting and important opportunity of research, it is necessary that the spine surgery community carefully evaluates the safety and efficacy of MSCs use in spine fusion through randomized controlled and blinded clinical trials.

Competing Interests

The authors declare that they have no competing interests.

Acknowledgments

This work was supported by grants from Rizzoli Orthopedic Institute (Ricerca Corrente), 5 × 1000 2013 Project "Sviluppo e Validazione di Modelli Alternativi e Complementari In Vitro (Intelligent Testing Strategy) in Ortopedia e Traumatologia," Fondazione del Monte di Bologna e Ravenna 2016 Project "Cellule Mesenchimali Staminali Autologhe da Corpo Vertebrale come Prospettiva Biologica Innovativa per la Chirurgia Vertebrale," and the Operational Programme ERDF 2007–2013 in the region Emilia-Romagna: Activity 1.1 "Creation of Technology Centers for Industrial Research and Technological Transfer."

References

[1] G. F. Muschler, H. Nitto, Y. Matsukura et al., "Spine fusion using cell matrix composites enriched in bone marrow-derived cells," *Clinical Orthopaedics and Related Research*, no. 407, pp. 102–118, 2003.

[2] C. F. F. Hui, C. W. Chan, H. Y. Yeung et al., "Low-intensity pulsed ultrasound enhances posterior spinal fusion implanted with mesenchymal stem cells-calcium phosphate composite without bone grafting," *Spine*, vol. 36, no. 13, pp. 1010–1016, 2011.

[3] R. D. Rao, V. Bagaria, K. Gourab, S. T. Haworth, V. B. Shidham, and B. C. Cooley, "Autograft containment in posterolateral spine fusion," *Spine Journal*, vol. 8, no. 4, pp. 563–569, 2008.

[4] S. A. Malik, M. Murphy, P. Connolly, and J. O'Byrne, "Evaluation of morbidity, mortality and outcome following cervical spine injuries in elderly patients," *European Spine Journal*, vol. 17, no. 4, pp. 585–591, 2008.

[5] M. Fini, F. Salamanna, F. Veronesi et al., "Role of obesity, alcohol and smoking on bone health," *Frontiers in Bioscience (Elite Edition)*, vol. 4, pp. 2686–2706, 2012.

[6] M. V. Risbud, I. M. Shapiro, A. Guttapalli et al., "Osteogenic potential of adult human stem cells of the lumbar vertebral body and the iliac crest," *Spine*, vol. 31, no. 1, pp. 83–89, 2006.

[7] J. Picchi, L. Trombi, L. Spugnesi et al., "HOX and TALE signatures specify human stromal stem cell populations from different sources," *Journal of Cellular Physiology*, vol. 228, no. 4, pp. 879–889, 2013.

[8] G. B. Brodano, S. Terzi, L. Trombi et al., "Mesenchymal stem cells derived from vertebrae (vMSCs) show best biological properties," *European Spine Journal*, vol. 22, supplement 6, pp. S979–S984, 2013.

[9] M. Manfrini, G. Barbanti-Bròdano, E. Mazzoni et al., "MicroRNA regulatory networks are involved in osteogenic differentiation of human mesenchymal stem cells from bone marrow," *European Journal of Histochemistry*, vol. 57, supplement 1, p. 7, 2013.

[10] M. F. Pittenger, A. M. Mackay, S. C. Beck et al., "Multilineage potential of adult human mesenchymal stem cells," *Science*, vol. 284, no. 5411, pp. 143–147, 1999.

[11] Y. Jiang, B. Vaessen, T. Lenvik, M. Blackstad, M. Reyes, and C. M. Verfaillie, "Multipotent progenitor cells can be isolated from postnatal murine bone marrow, muscle, and brain," *Experimental Hematology*, vol. 30, no. 8, pp. 896–904, 2002.

[12] C. Morelli, G. Barbanti-Bròdano, A. Ciannilli, K. Campioni, S. Boriani, and M. Tognon, "Cell morphology, markers, spreading, and proliferation on orthopaedic biomaterials. An innovative cellular model for the 'in vitro' study," *Journal of Biomedical Materials Research Part A*, vol. 83, no. 1, pp. 178–183, 2007.

[13] M. Manfrini, M. Fiorini, G. Barbanti-Brodano, D. Pressato, and M. Tognon, "New generation of orthopaedic mimetic bioceramics assayed with human mesenchymal stem cells," *European Musculoskeletal Review*, vol. 6, no. 2, pp. 96–99, 2011.

[14] M. Manfrini, C. Di Bona, A. Canella et al., "Mesenchymal stem cells from patients to assay bone graft substitutes," *Journal of Cellular Physiology*, vol. 228, no. 6, pp. 1229–1237, 2013.

[15] G. B. Brodano, E. Mazzoni, M. Tognon, C. Griffoni, and M. Manfrini, "Human mesenchymal stem cells and biomaterials interaction: a promising synergy to improve spine fusion," *European Spine Journal*, vol. 21, supplement 1, pp. S3–S9, 2012.

[16] X. Liu, Q. Feng, A. Bachhuka, and K. Vasilev, "Surface modification by allylamine plasma polymerization promotes osteogenic differentiation of human adipose-derived stem cells," *ACS Applied Materials and Interfaces*, vol. 6, no. 12, pp. 9733–9741, 2014.

[17] A. F. Steinert, L. Rackwitz, F. Gilbert, U. Nöth, and R. S. Tuan, "Concise review: the clinical application of mesenchymal stem cells for musculoskeletal regeneration: current status and perspectives," *Stem Cells Translational Medicine*, vol. 1, no. 3, pp. 237–247, 2012.

[18] F. Veronesi, F. Salamanna, M. Tschon, M. Maglio, N. N. Aldini, and M. Fini, "Mesenchymal stem cells for tendon healing: what is on the horizon?" *Journal of Tissue Engineering and Regenerative Medicine*, 2016.

[19] D. Logeart-Avramoglou, F. Anagnostou, R. Bizios, and H. Petite, "Engineering bone: challenges and obstacles," *Journal of Cellular and Molecular Medicine*, vol. 9, no. 1, pp. 72–84, 2005.

[20] Y. Gan, K. Dai, P. Zhang, T. Tang, Z. Zhu, and J. Lu, "The clinical use of enriched bone marrow stem cells combined with porous beta-tricalcium phosphate in posterior spinal fusion," *Biomaterials*, vol. 29, no. 29, pp. 3973–3982, 2008.

[21] K. K. Hansraj, "Stem cells in spine surgery," *Surgical Technology International*, 2016.

[22] S. Lee, X. Zhang, J. Shen et al., "Brief report: human perivascular stem cells and Nel-like protein-1 synergistically enhance spinal fusion in osteoporotic rats," *Stem Cells*, vol. 33, no. 10, pp. 3158–3163, 2015.

[23] Y.-R. Shih, A. Phadke, T. Yamaguchi et al., "Synthetic bone mimetic matrix-mediated in situ bone tissue formation through host cell recruitment," *Acta Biomaterialia*, vol. 19, pp. 1–9, 2015.

[24] H. W. Bae, L. Zhao, L. E. A. Kanim, P. Wong, D. Marshall, and R. B. Delamarter, "Bone marrow enhances the performance of rhBMP-2 in spinal fusion: a rodent model," *The Journal of Bone & Joint Surgery—American Volume*, vol. 95, no. 4, pp. 338–347, 2013.

[25] R. E. Geuze, H.-J. Prins, F. C. Öner et al., "Luciferase labeling for multipotent stromal cell tracking in spinal fusion versus ectopic bone tissue engineering in mice and rats," *Tissue Engineering A*, vol. 16, no. 11, pp. 3343–3351, 2010.

[26] Y. Gu, L. Chen, H.-Y. Niu, X.-F. Shen, and H.-L. Yang, "Promoting spinal fusions by biomineralized silk fibroin films seeded with bone marrow stromal cells: an in vivo animal study," *Journal of Biomaterials Applications*, vol. 30, no. 8, pp. 1251–1260, 2016.

[27] T. Hayashi, E. L. Lord, A. Suzuki et al., "A comparison of commercially available demineralized bone matrices with and without human mesenchymal stem cells in a rodent spinal fusion model," *Journal of Neurosurgery: Spine*, vol. 25, no. 1, pp. 133–137, 2016.

[28] R. D. Rao, K. Gourab, V. B. Bagaria, V. B. Shidham, U. Metkar, and B. C. Cooley, "The effect of platelet-rich plasma and bone marrow on murine posterolateral lumbar spine arthrodesis with bone morphogenetic protein," *The Journal of Bone & Joint Surgery—American Volume*, vol. 91, no. 5, pp. 1199–1206, 2009.

[29] T. Hu, S. A. Abbah, S. Y. Toh et al., "Bone marrow-derived mesenchymal stem cells assembled with low-dose BMP-2 in a three-dimensional hybrid construct enhances posterolateral spinal fusion in syngeneic rats," *Spine Journal*, vol. 15, no. 12, pp. 2552–2563, 2015.

[30] K. Klíma, V. Vaněček, A. Kohout et al., "Stem cells regenerative properties on new rat spinal fusion model," *Physiological Research*, vol. 64, no. 1, pp. 119–128, 2015.

[31] W. K. Hsu, J. C. Wang, N. Q. Liu et al., "Stem cells from human fat as cellular delivery vehicles in an athymic rat posterolateral spine fusion model," *The Journal of Bone & Joint Surgery—American Volume*, vol. 90, no. 5, pp. 1043–1052, 2008.

[32] C. G. Chung, A. W. James, G. Asatrian et al., "Human perivascular stem cell-based bone graft substitute induces rat spinal

fusion," *Stem Cells Translational Medicine*, vol. 3, no. 10, pp. 1231–1241, 2014.

[33] M. Miyazaki, P. A. Zuk, J. Zou et al., "Comparison of human mesenchymal stem cells derived from adipose tissue and bone marrow for ex vivo gene therapy in rat spinal fusion model," *Spine*, vol. 33, no. 8, pp. 863–869, 2008.

[34] H. S. Seo, J. K. Jung, M. H. Lim, D. K. Hyun, N. S. Oh, and S. H. Yoon, "Evaluation of spinal fusion using bone marrow derived mesenchymal stem cells with or without fibroblast growth factor-4," *Journal of Korean Neurosurgical Society*, vol. 46, no. 4, pp. 397–402, 2009.

[35] T. Nakajima, H. Iizuka, S. Tsutsumi, M. Kayakabe, and K. Takagishi, "Evaluation of posterolateral spinal fusion using mesenchymal stem cells: differences with or without osteogenic differentiation," *Spine*, vol. 32, no. 22, pp. 2432–2436, 2007.

[36] A. Koga, Y. Tokuhashi, A. Ohkawa, T. Nishimura, K. Takayama, and J. Ryu, "Effects of fibronectin on osteoinductive capability of fresh iliac bone marrow aspirate in posterolateral spinal fusion in rabbits," *Spine*, vol. 33, no. 12, pp. 1318–1323, 2008.

[37] A. Minamide, M. Yoshida, M. Kawakami et al., "The effects of bone morphogenetic protein and basic fibroblast growth factor on cultured mesenchymal stem cells for spine fusion," *Spine*, vol. 32, no. 10, pp. 1067–1071, 2007.

[38] J. Urrutia, P. Mery, R. Martínez, F. Pizarro, D. Apablaza, and R. Mardones, "Cultured autologous bone marrow stem cells inhibit bony fusion in a rabbit model of posterolateral lumbar fusion with autologous bone graft," *Journal of Clinical Neuroscience*, vol. 17, no. 4, pp. 481–485, 2010.

[39] J.-W. Huang, S.-S. Lin, L.-H. Chen et al., "The use of fluorescence-labeled mesenchymal stem cells in poly(lactide-co-glycolide)/hydroxyapatite/collagen hybrid graft as a bone substitute for posterolateral spinal fusion," *Journal of Trauma—Injury, Infection and Critical Care*, vol. 70, no. 6, pp. 1495–1502, 2011.

[40] Z.-B. Tang, J.-K. Cao, N. Wen et al., "Posterolateral spinal fusion with nano-hydroxyapatite-collagen/PLA composite and autologous adipose-derived mesenchymal stem cells in a rabbit model," *Journal of Tissue Engineering and Regenerative Medicine*, vol. 6, no. 4, pp. 325–336, 2012.

[41] T.-H. Lee, Y.-H. Huang, N.-K. Chang et al., "Characterization and spinal fusion effect of rabbit mesenchymal stem cells," *BMC Research Notes*, vol. 6, article 528, 2013.

[42] C.-C. Niu, S.-S. Lin, W.-J. Chen et al., "Benefits of biphasic calcium phosphate hybrid scaffold-driven osteogenic differentiation of mesenchymal stem cells through upregulated leptin receptor expression," *Journal of Orthopaedic Surgery and Research*, vol. 10, article 111, 2015.

[43] J.-C. Liao, "Cell therapy using bone marrow-derived stem cell overexpressing BMP-7 for degenerative discs in a rat tail disc model," *International Journal of Molecular Sciences*, vol. 17, no. 2, article 147, 2016.

[44] W. Yang, Y. Dong, Y. Hong, Q. Guang, and X. Chen, "Evaluation of anterior vertebral interbody fusion using osteogenic mesenchymal stem cells transplanted in collagen sponge," *Journal of Spinal Disorders and Techniques*, 2012.

[45] J. T. Douglas, A. A. Rivera, G. R. Lyons et al., "Ex vivo transfer of the Hoxc-8-interacting domain of Smad1 by a tropism-modified adenoviral vector results in efficient bone formation in a rabbit model of spinal fusion," *Journal of Spinal Disorders & Techniques*, vol. 23, no. 1, pp. 63–73, 2010.

[46] T.-S. Fu, W.-J. Chen, L.-H. Chen, S.-S. Lin, S.-J. Liu, and S. W. N. Ueng, "Enhancement of posterolateral lumbar spine fusion using low-dose rhBMP-2 and cultured marrow stromal cells," *Journal of Orthopaedic Research*, vol. 27, no. 3, pp. 380–384, 2009.

[47] T.-S. Fu, S. W. Ueng, T.-T. Tsai, L.-H. Chen, S.-S. Lin, and W.-J. Chen, "Effect of hyperbaric oxygen on mesenchymal stem cells for lumbar fusion in vivo," *BMC Musculoskeletal Disorders*, vol. 11, article 52, 2010.

[48] T.-S. Fu, Y.-H. Chang, C.-B. Wong et al., "Mesenchymal stem cells expressing baculovirus-engineered BMP-2 and VEGF enhance posterolateral spine fusion in a rabbit model," *Spine Journal*, vol. 15, no. 9, pp. 2036–2044, 2015.

[49] W.-J. Chen, J.-W. Huang, C.-C. Niu et al., "Use of fluorescence labeled mesenchymal stem cells in pluronic F127 and porous hydroxyapatite as a bone substitute for posterolateral spinal fusion," *Journal of Orthopaedic Research*, vol. 27, no. 12, pp. 1631–1636, 2009.

[50] T. Schubert, S. Lafont, G. Beaurin et al., "Critical size bone defect reconstruction by an autologous 3D osteogenic-like tissue derived from differentiated adipose MSCs," *Biomaterials*, vol. 34, no. 18, pp. 4428–4438, 2013.

[51] B. S. Shamsul, K. K. Tan, H. C. Chen, B. S. Aminuddin, and B. H. I. Ruszymah, "Posterolateral spinal fusion with ostegenesis induced BMSC seeded TCP/HA in a sheep model," *Tissue and Cell*, vol. 46, no. 2, pp. 152–158, 2014.

[52] D. L. Wheeler, J. M. Lane, H. B. Seim III, C. M. Puttlitz, S. Itescu, and A. S. Turner, "Allogeneic mesenchymal progenitor cells for posterolateral lumbar spine fusion in sheep," *The Spine Journal*, vol. 14, no. 3, pp. 435–444, 2014.

[53] D. L. Wheeler, D. C. Fredericks, R. F. Dryer, and H. W. Bae, "Allogeneic mesenchymal precursor cells (MPCs) combined with an osteoconductive scaffold to promote lumbar interbody spine fusion in an ovine model," *Spine Journal*, vol. 16, no. 3, pp. 389–399, 2016.

[54] M. D. Cuenca-López, J. A. Andrades, S. Gómez et al., "Evaluation of posterolateral lumbar fusion in sheep using mineral scaffolds seeded with cultured bone marrow cells," *International Journal of Molecular Sciences*, vol. 15, no. 12, pp. 23359–23376, 2014.

[55] Y. Qian, Z. Lin, J. Chen et al., "Natural bone collagen scaffold combined with autologous enriched bone marrow cells for induction of osteogenesis in an ovine spinal fusion model," *Tissue Engineering—Part A*, vol. 15, no. 11, pp. 3547–3558, 2009.

[56] T. Goldschlager, P. Ghosh, A. Zannettino et al., "A comparison of mesenchymal precursor cells and amnion epithelial cells for enhancing cervical interbody fusion in an ovine model," *Neurosurgery*, vol. 68, no. 4, pp. 1025–1035, 2011.

[57] T. Goldschlager, J. V. Rosenfeld, P. Ghosh et al., "Cervical interbody fusion is enhanced by allogeneic mesenchymal precursor cells in an ovine model," *Spine*, vol. 36, no. 8, pp. 615–623, 2011.

[58] S. A. Abbah, C. X. F. Lam, A. K. Ramruttun, J. C. H. Goh, and H.-K. Wong, "Fusion performance of low-dose recombinant human bone morphogenetic protein 2 and bone marrow-derived multipotent stromal cells in biodegradable scaffolds: a comparative study in a large animal model of anterior lumbar interbody fusion," *Spine*, vol. 36, no. 21, pp. 1752–1759, 2011.

[59] M. C. Gupta, T. Theerajunyaporn, S. Maitra et al., "Efficacy of mesenchymal stem cell enriched grafts in an ovine posterolateral lumbar spine model," *Spine*, vol. 32, no. 7, pp. 720–726, 2007.

[60] L. Moro-Barrero, G. Acebal-Cortina, M. Suárez-Suárez, J. Pérez-Redondo, A. Murcia-Mazón, and A. López-Muñiz, "Radiographic analysis of fusion mass using fresh autologous

bone marrow with ceramic composites as an alternative to autologous bone graft," *Journal of Spinal Disorders and Techniques*, vol. 20, no. 6, pp. 409–415, 2007.

[61] G. A. Odri, A. Hami, V. Pomero et al., "Development of a peroperative procedure for concentrated bone marrow adjunction in postero-lateral lumbar fusion: radiological, biological and clinical assessment," *European Spine Journal*, vol. 21, no. 12, pp. 2665–2672, 2012.

[62] R. G. Johnson, "Bone marrow concentrate with allograft equivalent to autograft in lumbar fusions," *Spine*, vol. 39, no. 9, pp. 695–700, 2014.

[63] R. Hart, M. Komzák, F. Okál, D. Náhlík, P. Jajtner, and M. Puskeiler, "Allograft alone versus allograft with bone marrow concentrate for the healing of the instrumented posterolateral lumbar fusion," *Spine Journal*, vol. 14, no. 7, pp. 1318–1324, 2014.

[64] R. M. Ajiboye, J. T. Hamamoto, M. A. Eckardt, and J. C. Wang, "Clinical and radiographic outcomes of concentrated bone marrow aspirate with allograft and demineralized bone matrix for posterolateral and interbody lumbar fusion in elderly patients," *European Spine Journal*, vol. 24, no. 11, pp. 2567–2572, 2015.

[65] R. K. Eastlack, S. R. Garfin, C. R. Brown, and S. C. Meyer, "Osteocel plus cellular allograft in anterior cervical discectomy and fusion: evaluation of clinical and radiographic outcomes from a prospective multicenter study," *Spine*, vol. 39, no. 22, pp. E1331–E1337, 2014.

Hindawi
Stem Cells International
Volume 2017, Article ID 4985323, 13 pages
https://doi.org/10.1155/2017/4985323

Research Article

Overexpression of Heme Oxygenase-1 in Mesenchymal Stem Cells Augments Their Protection on Retinal Cells In Vitro and Attenuates Retinal Ischemia/Reperfusion Injury In Vivo against Oxidative Stress

Li Li,[1,2] GaiPing Du,[3] DaJiang Wang,[4] Jin Zhou,[5] Guomin Jiang,[6] and Hua Jiang[1]

[1]*Department of Ophthalmology, Jinan Military General Hospital, No. 25 Shifan Road, Tianqiao District, Jinan 250031, China*
[2]*Department of Ophthalmology, The 88th Hospital of Chinese People's Liberation Army, No. 6 Hushan East Road, Tai'an 271000, China*
[3]*Department of Ophthalmology, 401 Hospital of Chinese People's Liberation Army, No. 22 Minjiang Road, Qingdao 266071, China*
[4]*Department of Ophthalmology, Chinese People's Liberation Army General Hospital, No. 28 Fuxing Road, Haidian District, Beijing 100853, China*
[5]*Department of Cardre Ward, The 316th Hospital of Chinese People's Liberation Army, No. A2 Niangniangfu, Xiangshan Road, Haidian District, Beijing 100093, China*
[6]*Department of Ophthalmology & Visual Science, University of Louisville, 301 E. Muhammad Ali Blvd., Louisville, KY 40202, USA*

Correspondence should be addressed to Hua Jiang; Jianghua108@126.com

Received 6 September 2016; Revised 26 November 2016; Accepted 21 December 2016; Published 1 February 2017

Academic Editor: Salvatore Scacco

Retinal ischemia/reperfusion (I/R) injury, involving several ocular diseases, seriously threatens human ocular health, mainly treated by attenuating I/R-induced oxidative stress. Currently, mesenchymal stem cells (MSCs) could restore I/R-injured retina through paracrine secretion. Additionally, heme oxygenase-1 (HO-1) could ameliorate oxidative stress and thus retinal apoptosis, but the expression of HO-1 in MSC is limited. Here, we hypothesized that overexpression of HO-1 in MSC (MSC-HO-1) may significantly improve their retina-protective potentials. The overexpression of HO-1 in MSC was achieved by lentivirus transduction. Then, MSC or MSC-HO-1 was cocultured with retinal ganglion cells (RGC-5) in H_2O_2-simulated oxidative condition and their protection on RGC-5 was systemically valuated in vitro. Compared with MSC, MSC-HO-1 significantly attenuated H_2O_2-induced injury of RGC-5, including decrease in cellular ROS level and apoptosis, activation of antiapoptotic proteins p-Akt and Bcl-2, and blockage of proapoptotic proteins cleaved caspase 3 and Bax. In retinal I/R rats model, compared with control MSC, MSC-HO-1-treated retina significantly retrieved its structural thickness, reduced cell apoptosis, markedly attenuated retinal oxidative stress level, and largely regained the activities of typical antioxidant enzymes, SOD and CAT. Therefore, it could be concluded that overexpression of HO-1 provides a promising strategy to enhance the MSC-based therapy for I/R-related retinal injury.

1. Introduction

Retinal ischemia/reperfusion (I/R) injury plays a pivotal role in the pathogenesis of a series of ocular diseases, including diabetic retinopathy, acute glaucoma, and retinopathy of prematurity. Usually, I/R injury may result in vision-loss and even blindness due to permanent damage to the retina, especially retinal neurons [1–3]. Retinal I/R generally consisted of two courses, the ischemia and the successive reperfusion. During the ischemia status, blood flow to retina was blocked, causing the deficiency of oxygen and other nutrients and thus the depletion of adenosine triphosphate [4], while, in the course of the reperfusion, the tissue damage was aggravated due to the generation of reactive oxygen species (ROS) and proinflammatory mediators that subsequently led to oxidative stress and inflammation [5, 6]. Retinal neuronal injury is mainly ascribed to oxidative stress [7, 8] and thus antioxidative treatments were regarded as one of the main therapies for retinal I/R injury [9].

Currently, cell transplantation attracted a widespread interest in medical applications due to the production of various trophic factors in vivo via the immature cells, such as stem cells [10, 11]. Mesenchymal stem cells (MSC) are the archetype of multipotent stem cells for their abundant autologous source and delivery via an allogeneic fashion [12]. In addition, MSC were also able to secrete several cytokines and nutrients [13, 14], which can significantly reduce surrounding cellular oxidative stress and the resulting apoptosis [15, 16]. Furthermore, the developing technologies of cell culture and genetic engineering [17, 18] further promote the therapeutic application of MSC through integrating other positive treatments [19, 20], which also can overcome the possible side effects from monotherapy in clinical practice [21]. Previous study confirmed that MSC transplantation can treat retinal I/R injury by expressing neurotropic factors [22]. However, key therapeutic factors, such as HO-1, were naturally low expressed in MSC.

Heme oxygenase-1 (HO-1), an antioxidant and cytoprotective enzyme [23], is one of members of the heme oxygenase family [24, 25], which equimolarly decompose heme to biliverdin, free iron, and carbon monoxide (CO). A series of studies, including HO-1 promoter polymorphisms, HO-1 antisense, and knockout, have clarified the central role of HO-1 in intracellular antioxidant defenses [26, 27]. Its product of decomposition, biliverdin, can further be metabolically degraded into bilirubin. Both of them display a potent antioxidative capacity against intracellular oxidative stress. Moreover, bilirubin also possesses cytoprotective and anti-inflammatory capability [28, 29]. It has been evidenced that CO, another product of the HO-1 induced degradation of heme, has antiapoptotic and cytoprotective role in the process of anti-inflammatory [30]. Additionally, recent study has applied HO-1 to treat retina related diseases against oxidative stress, harvesting plausible protective effects on retinal endothelial cells [20].

Based on the capacity of HO-1 to protect retina against oxidative stress, we herein incorporated HO-1 gene into MSC through lentivirus transduction, aiming to promote the therapeutic efficiency of MSC. The feasibility was first confirmed by employing in vitro transwell indirect culture in H_2O_2-simulated oxidative stress medium. Subsequently, we transplanted HO-overexpressing MSC into rats with retinal post-I/R injury for practical attempts. In addition, we preliminarily studied the underlying mechanism of enhanced restoration of retina with HO-1 overexpression MSC by investigating the level of antioxidant enzyme and the expression of apoptosis-related proteins.

2. Materials and Methods

2.1. Isolation and Culture of Cells. Rat retinal ganglion cells (RGC-5, American Type Culture Collection) were cultivated with DMEM (Gibco) supplemented with 10% FCS (PAA Laboratories), 100 IU/mL penicillin, and 100 μg/mL streptomycin (Sigma). RGC-5 were grown to confluency and then enzymatically dissociated with 0.2% trypsin (Invitrogen) and 0.05% EDTA (PAA Laboratories). The medium was refreshed every 3 days.

Two-week-old Sprague-Dawley rats were used for the isolation of MSC from the inguinal adipose tissue according to the previously described protocol [12]. In brief, the inguinal hair of rats was carefully shaved and the exposed inguinal skin successively underwent 5 min sterilization with 75% ethanol. Subsequently, the tissue isolation surgery was carried out under sterile condition. The obtained adipose tissue was washed thoroughly with PBS and cut into small mass. Then, the tissues were digested for 30 min with 0.1% collagenase I (Sigma) and 0.05% trypsin in serum-free αMEM (Gibco). The digestion was ceased by supplementing equal volume of αMEM containing 10% FBS (Hyclone). The mixed solution was filtered through 80 μm mesh. The cell remains were further placed onto culture dishes and incubated in αMEM containing 10% FBS at 37°C and 5% CO_2. The adherent cells were used as the first passage of MSC and these MSC were expanded to the 5th passage. Cells were passaged when they reached about 90% confluence and passage 3 cells were used in the in vitro and in vivo experiments. Subsequently, fluorescence-activated cell sorting (FACS) with CD29, CD90, CD45, and CD34 markers was used to verify the cellular identity of cells.

2.2. Multipotent Differentiation

Osteogenic Induction. MSC at the density of 5,000 cells/cm^2 were induced towards osteogenic differentiation for 21 days (alpha MEM medium supplemented with 100 nM dexamethasone, 10 mM β-glycerophosphate, and 50 mM ascorbic acid-2-phosphate (Wako Chemicals, Richmond, VA) with 10% FBS and 1% penicillin and streptomycin). Afterwards, the osteoblasts were bathed in 95% ice-cold ethanol for 5 minutes and stained with 2% Alizarin Red Solution (pH = 4.0). Calcium deposits recognized as orange-red stained areas in cells were identified under light microscopy.

Adipogenic Induction. MSC at the density of 20,000 cells/cm^2 were induced towards adipogenic differentiation for 21 days (alpha MEM medium supplemented with 10% FBS, 1% penicillin and streptomycin, 1 mM dexamethasone, 500 mM 3-isobutyl-1-methylxanthine, 10 mg/mL insulin, and 100 mM indomethacin). The induced cells were fixed with 4% paraformaldehyde for 30 min at room temperature and stained with fresh Oil Red O solution for another 50 min. The formed fat droplets were observed under bright field microscope.

2.3. Modification of HO-1 Gene in MSC via Lentiviral Transduction. Lentiviral vectors with or without HO-1 were labeled by GFP. First, total RNA was harvested via the usage of the PrimeScript RT reagent kit, according to the manufacturer's instructions (TAKARA-BIO, Shiga, Japan). The obtained RNA was then converted into complementary DNA (cDNA) using a Reverse Transcription System Kit (Applied Biosystems, Foster City, CA, USA). The primers of HO-1 gene were synthesized using Primer Premier 5.0 software, based on its cDNA sequences from the GenBank database (GenBank, Accession: NM_012580.2). The PCR-amplified gene was inserted into the LV5 vector (GenePharma Co., Ltd.,

Shanghai, China), according to the manufacturer's protocols. The EF-1α promoter was used to trigger gene expression. After transfecting into 293 T cells for 3 days, the viruses were collected and concentrated by ultracentrifugation.

Lentivirus transductions without (MSC) or with HO-1 gene (MSC-HO-1) were conducted according to the previously established method with small modifications. Briefly, MSC were incubated with lentivirus at the MOI of 20 for 24 h at 37°C. Subsequently, cells were washed with PBS for several times to remove redundant lentivirus. Then, the cells were incubated with fresh culture medium. Two days later, the transfection activities of MSC were investigated by the expression of GFP through a fluorescent microscope. Those uninfected cells were removed by adding puromycin (1 μg/mL).

2.4. MSC and RGC-5 Transwell Coculture. The coculture of MSC and RGC-5 was conducted according to previously reported method [31]. In brief, MSC were seeded at 1×10^5 cells/well onto 24-well transwell permeable support (pore size: 0.4 μm, Corning, NY, USA), followed with overnight incubation at 37°C, 5% CO_2. RGC at a density of 5×10^4 cells/well were then seeded into the bottom of 24-well plates. After cocultivation for 24 h, 100 μM of H_2O_2 was added in the coculture medium and cells were incubated for another 24 h.

2.5. Determination of Intracellular Reactive Oxygen Species Levels. For determining the level of intracellular ROS, RGC-5 were incubated with 10 μM oxidation-sensitive fluorescent probe: 2′,7′-dichlorodihydrofluorescein diacetate (S carboxy-H2DCFDA) at 37°C in the darkness for 20 min. Subsequently, the cells were rinsed with 1x PBS (pH 7.4) to remove the unloaded dye. The cells were trypsinized, collected with polystyrene tubes with cell-strainer caps (Falcon), and examined with flow cytometry. Geometric distributions of side-angle light scatter height (SSC-H) and carboxyl-DCF fluorescence were obtained and analyzed using FACS (FACScan, Becton Dickinson) and Cell Quest 3.2 (Becton Dickinson) software.

2.6. Retinal Ischemia/Reperfusion Injury. Sprague-Dawley rats with similar body weights were first anesthetized using sodium pentobarbital and underwent surgery according to previous description [32]. Briefly, a 27-gauge infusion needle linked to normal saline reservoir was cannulated into the anterior chamber of the right eye. The intraocular pressure was modulated up to 110 mmHg for 60 min through augmenting the amount of normal saline. The fundus whitening and the retinal blood flow restoration were used to confirm retinal ischemia and reperfusion. The control group was treated with Sham-procedure, maintaining normal ocular tension.

2.7. Cell Transplantation. Transplantation of MSC was performed according to the previous method [32]. The right eye of rat was chosen to receive injection treatment. After anesthetization, pupils of rats were dilated and the eyes were then slowly protruded with a rubber sleeve. A 90° peritomy was conducted in the temporal quadrant followed by a sclerotomy at ~1 mm behind the limbus with a 27-gauge needle. Afterwards, a 33-gauge blunt-tip needle was tangentially inserted towards the posterior pole of the eye. 5 μL MSC suspension (1×10^5 cells/mL) or 5 μL PBS was gently injected into the subretinal space. Rats were euthanatized and the eyes were enucleated after 7, 14, and 21 days, respectively.

2.8. Western Blotting Assay. Cells grown in 6-well plates were washed with PBS twice and lysed harnessing Laemmli Sample Buffer (Bio-Rad). After centrifugation at 4°C, the protein part was collected and was analyzed using BCA™ Protein Assay Kit (Pierce). Protein sample (60 μg) was loaded in sodium dodecyl sulfate PAGE gel. The obtained discrete gel proteins were then electrophoretically transferred to nitrocellulose membranes, followed by incubating with primary antibodies against HO-1, p-Akt, cleaved caspase 3, Bax, or Bcl-2 overnight at 4°C. The corresponding secondary antibodies marked with HRP were incubated for 1 h at room temperature. Akt was used as the internal reference for p-Akt, while GAPDH served as internal reference for other three factors. The antibodies used in this study were all purchased from Cell Signal Technology.

2.9. Measurement of Retinal Thickness. The retinal thicknesses of rats were measured according to the previously described method. Briefly, the rats received surgeries under anaesthetization at day 21 and their eyes were then enucleated. After the careful removal of cornea, lens, and vitreous, the eye-cups were fixed in 4% paraformaldehyde for 2 h, immersed in 30% sucrose solution overnight at 4°C, and then embedded in OCT media (Sakura Finetek). Retinal sections of 0.5 mm, attained by cutting along the vertical meridian of eye and crossing the optic nerve head, were stained with hematoxylin and eosin (H&E) and tested using light microscope. Measurements were taken at every 250 μm in a range of 800–1200 μm centralized at the optic nerve head.

2.10. Terminal Deoxynucleotidyl Transferase dUTP Nick End Labeling (TUNEL) Assay for Cell Apoptosis. TUNEL was performed using the "one step cell death detection kit-fluorescein" (Beyotime Biotechnology) with fluorescein isothiocyanate (FITC) for the in vitro assay or streptavidin-tetramethylrhodamine (TRITC) for the in vivo assay, according to the manufacturer's protocols. Typically, the air-dried cells were fixed in 4% paraformaldehyde for 1 h at 20°C and permeabilized for 2 min on ice with 0.1% Triton X-100 containing 0.1% sodium citrate. The TUNEL reagent was incubated with the cells for 1 h at 37°C in the darkness. After removing unreacted compounds with 10 mM PBS, the cells were placed onto glass slides and cultured with a DAPI-containing antifade mounting medium. As for the in vivo TUNEL assay, rats were first euthanized and retinal sections were harvested as described above. TUNEL staining (green in vitro and red in vivo) was imaged and recorded via an Olympus (Tokyo, Japan) FluoView-FV300 Laser Scanning Confocal System. The cellular apoptosis was expressed as

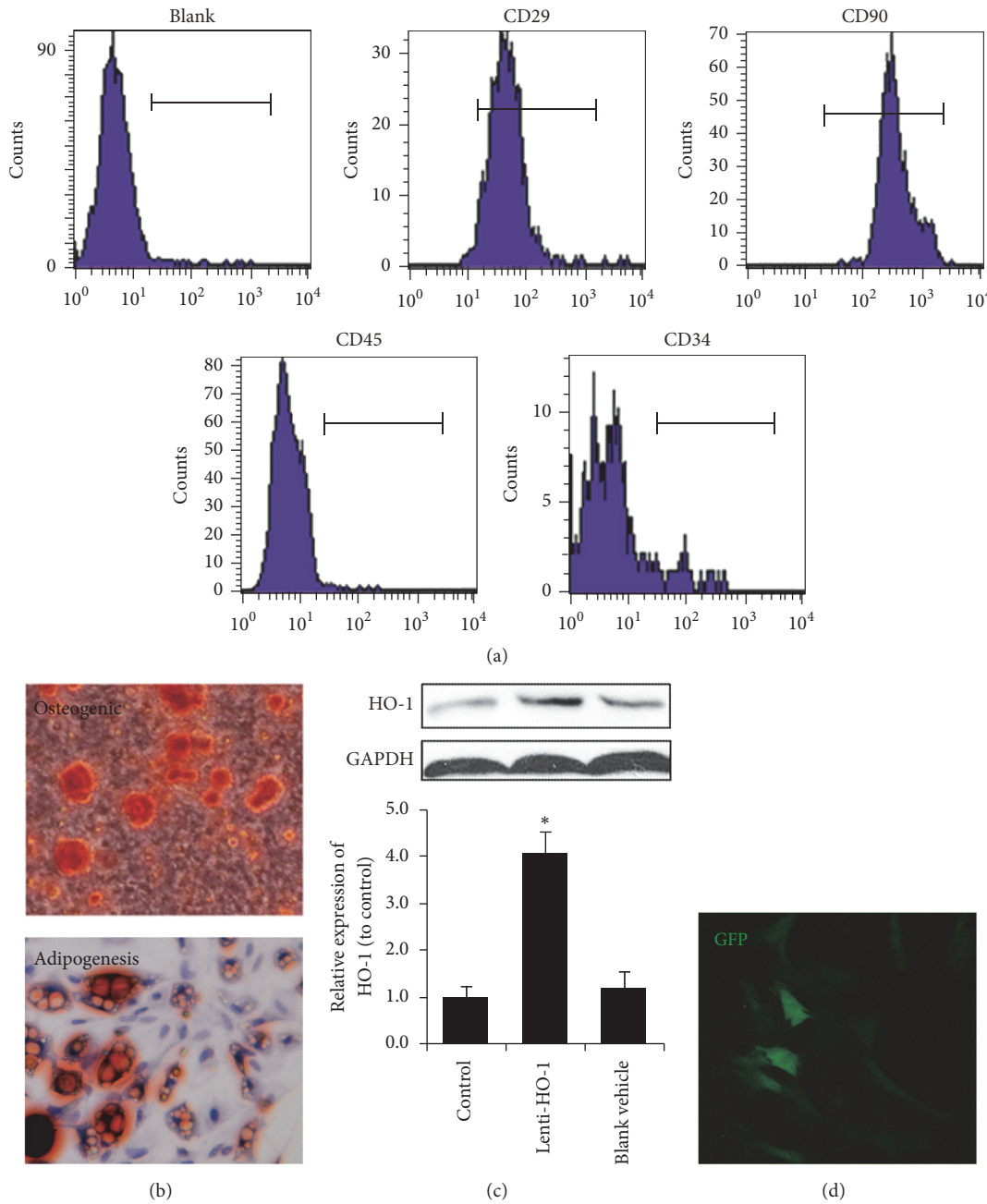

Figure 1: Characteristics of MSC and HO-1 transduction by lentiviral vectors. (a) Flow cytometry demonstrated that most MSC expressed CD29 and CD90 but less CD45 and CD34. (b) Multipotency of MSC, differentiating into adipocytes stained by Oil Red O and osteocytes stained by Alizarin Red S. (c) HO-1 expressions in control and MSC transduced with lenti-HO-1 and blank vehicle, $n = 5$. (d) GFP image of MSC after transduction by lentiviral vectors. $^{*}P < 0.01$ compared with control.

the proportion of TUNEL-positive with DAPI-positive (blue) nuclei.

2.11. Measurement of Reactive Oxygen Species in the Retina. The ROS levels in the rat retina were analyzed using luminol (5-amino-2,3-dihydro-1,4-phthalazinedione, Sigma) and lucigenin (bis-N-methylacridiniumnitrate, Sigma). Briefly, retinas were isolated at weeks 1, 2, and 3 after surgery and then homogenized with 10 mM PBS. Tissue samples were transferred into vials in the presence of PBS-HEPES buffer (0.5 M PBS containing 20 mM HEPES, pH 7.2). The levels of ROS were assessed by adding the chemilumigenic probes lucigenin and luminol (final concentration of 0.2 mM). The luminescent counts were recorded at 1 min intervals at room temperature via luminescence reader (BioTek). Results were given as counts per min (counts/min) for a counting period of 5 min (rlu/mg tissue).

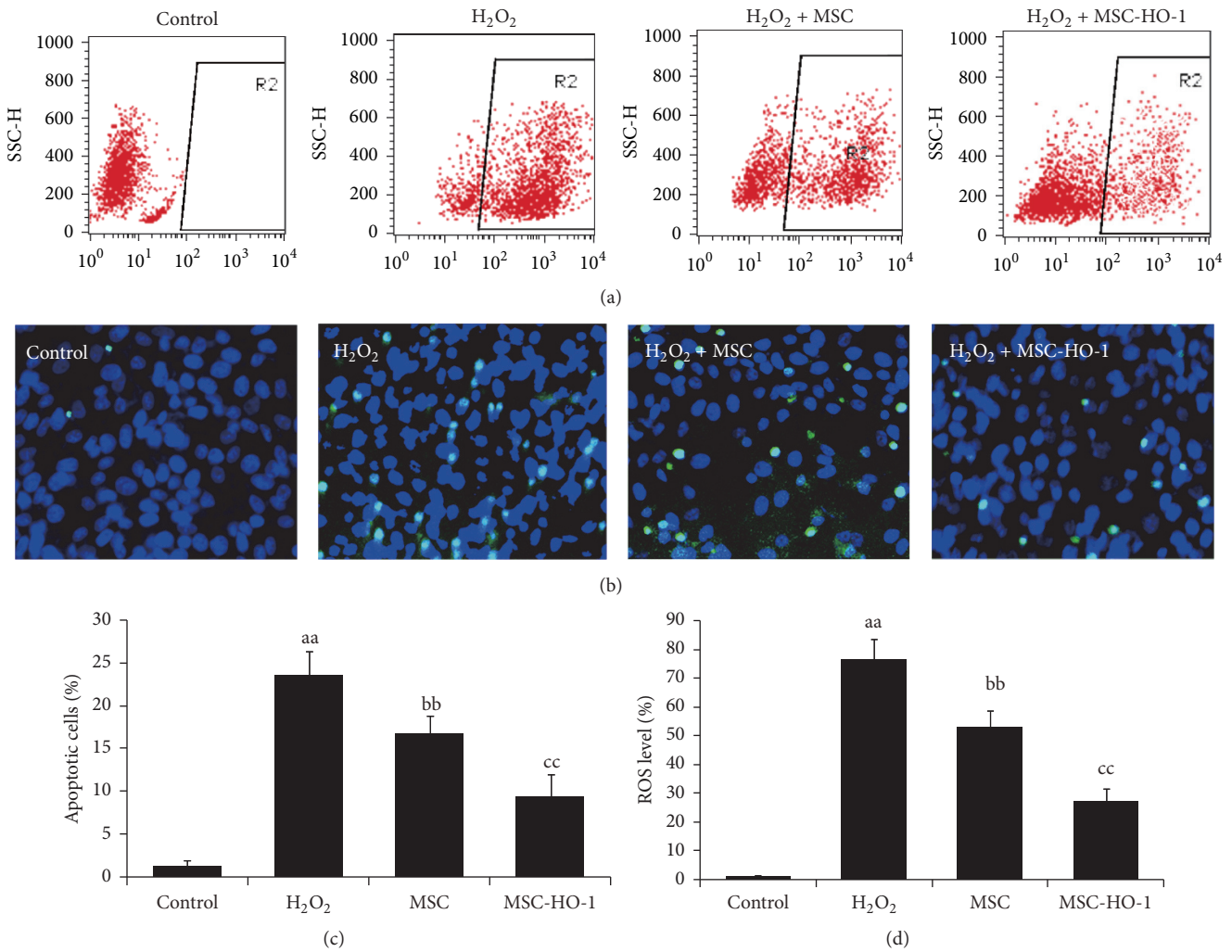

FIGURE 2: The effects of HO-1 overexpression in MSC on intracellular ROS levels and apoptosis. MSC or MSC-HO-1 were indirectly cocultivated with RGC-5 after adding H_2O_2. (a) Intracellular ROS levels in RGC-5 were analyzed by flow cytometry. (b) Representative TUNEL images of RGC-5. (c) and (d) The quantitative detection of ROS levels and apoptosis of RGC-5 ($n = 5$). $^{aa}P < 0.01$ compared with control; $^{bb}P < 0.01$ compared with H_2O_2 group; $^{cc}P < 0.01$ compared with MSC group.

2.12. Measurements of the Activities of Antioxidant Enzymes in the Retina. Superoxide dismutase (SOD) and catalase (CAT) activities in the retina were measured by colorimetric assays at weeks 1, 2, and 3. Both SOD and CAT assay kits were from Cayman Chemical (Ann Arbor, MI, USA). Assay procedures and tissue homogenate preparations were conducted according to the manufacturer's protocols.

2.13. Statistical Analysis. Data were expressed as mean ± standard deviation (SD). Statistical significance was set at P values < 0.05. The analysis among groups exploited one-way ANOVAs followed by Tukey's post hoc test for multiple pairwise examinations.

3. Results

3.1. Characteristics of MSC and HO-1 Transduction by Lentiviral Vectors. We first systematically characterized the immune phenotype and differentiation potential of isolated cells to verify their identities. As showed in Figure 1(a), the majority of the isolated cells were positive CD29 and CD90, while they were negative for CD31 and CD45. The multipotency of MSC was analyzed by osteogenic and adipogenic differentiation. As shown in Figure 1(b) the oil droplets stained with Oil Red O and osteoblasts producing calcium stained with Alizarin Red Sin clearly demonstrated their multidifferentiation capabilities.

After lentiviral transduction, we examine the expression of HO-1. As showed in Figure 1(c), a significantly higher expression was observed only in the HO-1 gene transduction group, while there were no differences between control and blank vehicle group. GFP was used to identify grafted cells and the fluorescence of GFP was observed in MSC after lentiviral transduction (Figure 1(d)).

3.2. HO-1 Overexpression in MSC Protects RGC-5 against Oxidative Stress. To assess whether HO-1 overexpression in

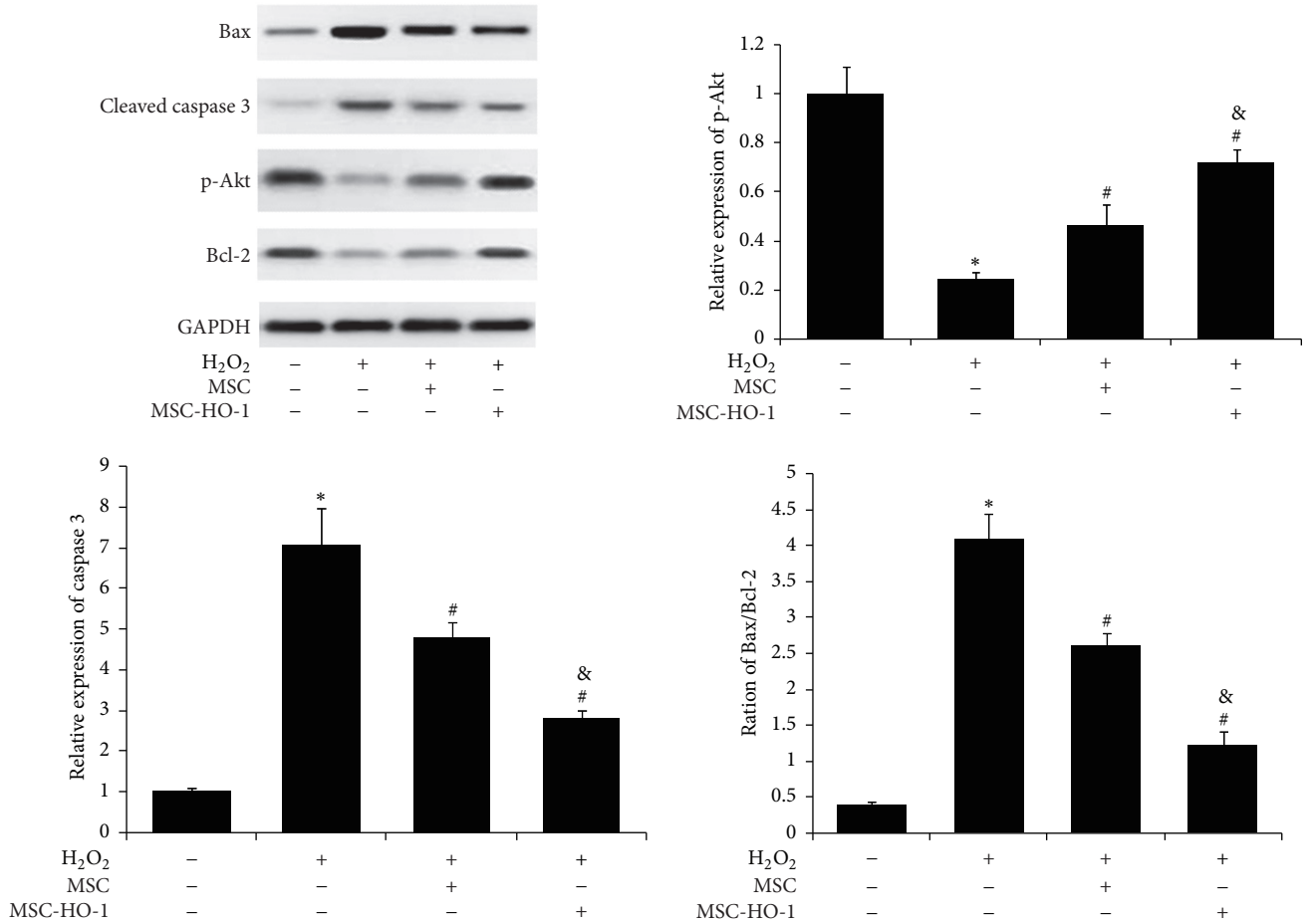

Figure 3: Assessment of apoptosis-related proteins in RGC-5. The levels of apoptotic proteins in H_2O_2 treated RGC-5 without or with MSC or MSC-HO-1, respectively, were analyzed by western blotting ($n = 5$). $^{*}P < 0.01$ compared with control; $^{\#}P < 0.01$ compared with H_2O_2 group; $^{\#}P < 0.01$ compared with H_2O_2 + MSC group.

MSC was able to reduce apoptosis of RGC-5 against oxidative stress, H_2O_2 were supplemented in RGC-5 culture medium to induce intracellular oxidative stress and ROS levels were first investigated. As showed in Figure 2(a), normal cells contain a relatively lower ROS level and weak carboxyl-DCF fluorescence was detected, while the majority of cells in H_2O_2 treated group were detected with high-ROS level. After introducing MSC, the augment of high-ROS cells produced by H_2O_2 could be offset and this effect could be further enhanced by the overexpression of HO-1 in MSC. The typical TUNEL staining imaging (Figure 2(b)) also complied with the flow cytometry results, showing that TUNEL-positive cells were much less presented in the MSC-HO-1 treated group than that in the MSC-treated one. The following quantification results (Figures 2(c) and 2(d)) showed that apoptosis in MSC-HO-1 treated group was significantly lower than MSC-treated group, as well as the intracellular ROS level.

3.3. Assessment of Apoptosis-Related Proteins. To further understand the underlying mechanism, we investigated the expression of apoptotic proteins in RGC-5. As shown in Figure 3, H_2O_2 treatment significantly upregulated proapoptotic proteins, Bax and cleaved caspase 3, and downregulated antiapoptotic proteins, p-Akt and Bcl-2. These changes in RGC-5 were significantly reversed when MSC were introduced. We also found that the MSC-based restoration could be further promoted by the overexpression of HO-1. Together, these findings demonstrated the potent protection of MSC overexpressing HO-1 on RGC-5 against oxidative stress.

3.4. Effects of MSC Overexpressing HO-1 on Retinal Histology after I/R Injury. As showed in Figure 4, retinal I/R injury obviously slimed the whole retina compared with control group at day 21. There was marked restoration of the structure in the MSC group, especially in the MSC-HO-1 group, compared with the I/R group. The data of bar plotting clearly demonstrated that the significant decrease in the total retinal thickness, inner plexiform layer (IPL), inner nuclear layer (INL), and outer nuclear layer (ONL) in the eyes of I/R group was significantly attenuated by introducing MSC. Moreover, the beneficial effect of MSC could be further amplified by the overexpression of HO-1 (Figure 4).

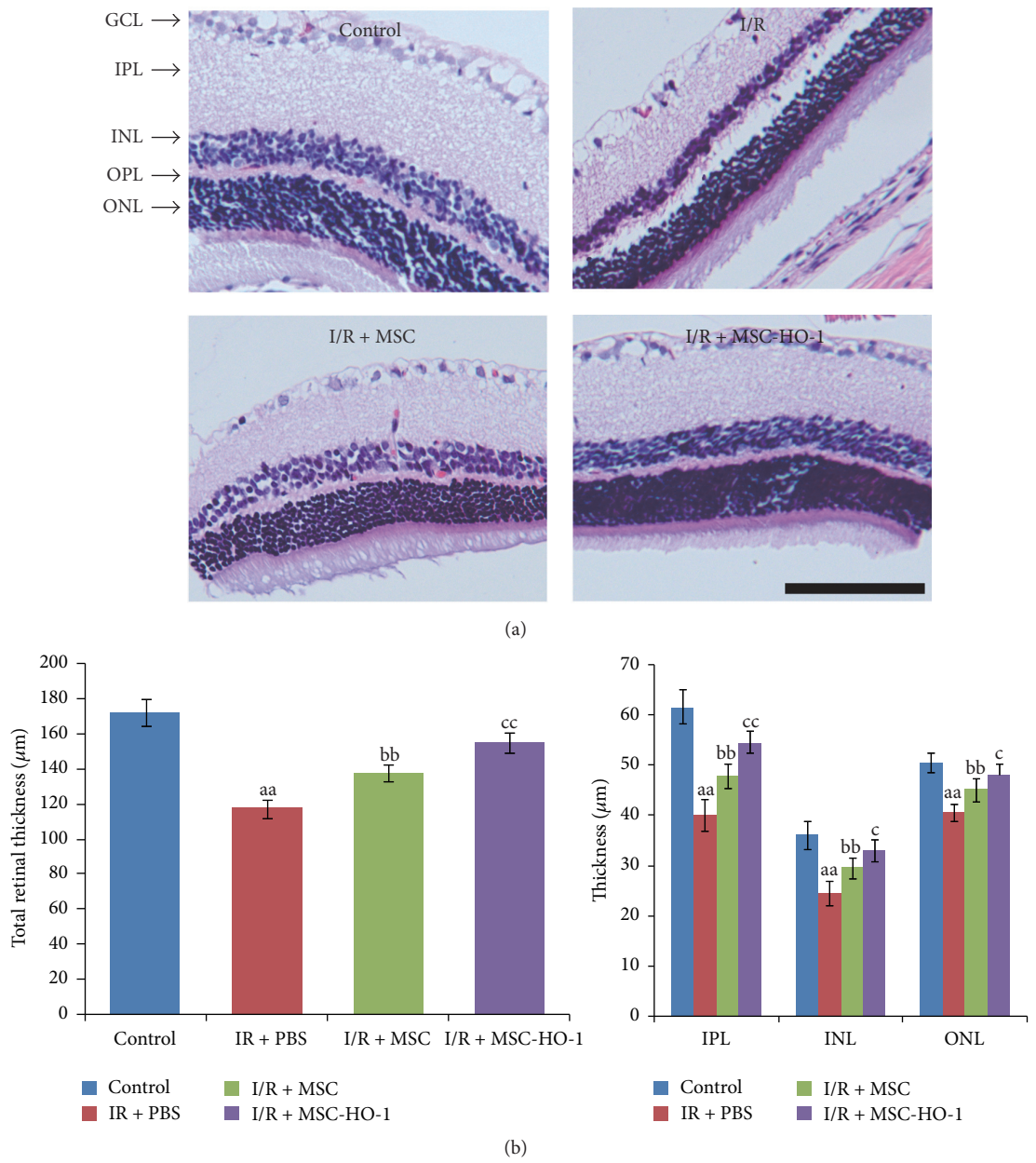

Figure 4: Effects of MSC-HO-1 on retinal histology at 21 days after I/R injury. (a) Representative retinal section images of control, I/R + PBS, I/R + MSC, or I/R + MSC-HO-1 group were achieved by H&E-staining. (b) The thickness of total retina (from the inner limiting membrane to the pigment epithelium), the inner plexiform layer (IPL), the inner nuclear layer (INL), and the outer nuclear layers (ONL) was investigated in the eyes of control, I/R + PBS, I/R + MSC, or I/R + MSC-HO-1 group, respectively ($n = 5$). $^{aa}P < 0.01$ compared with control group; $^{bb}P < 0.01$ compared with IR + PBS group; $^{cc}P < 0.01$ compared with IR + MSC group; $^{c}P < 0.05$ compared with IR + MSC group.

3.5. Effects of MSC-HO-1 Transplantation on Retinal Apoptosis. As showed in Figure 5, the fluorescent image of tissues clearly displayed that there were much more TUNEL-positive cells in the retinas of the I/R only group than the control group, whereas the amount of TUNEL-positive cells of retinas in animals receiving MSC transplantation was markedly reduced. Meanwhile, MSC-HO-1 further reduced TUNEL-positive cells in retina, indicating potent preservation against I/R-induced apoptosis.

3.6. Effects of MSC-HO-1 on the Expression of Retinal Apoptosis-Related Protein. 21 days after I/R injury, the expression of antiapoptosis factor p-Akt was significantly downregulated compared with the control (Figure 6). When introducing MSC, the expression of p-Akt was significantly promoted. This promotion of p-Akt expression in I/R injury retinas was further strengthen by the overexpression of HO-1 in MSC. On the contrary, I/R injury amplified the expression of proapoptosis factors, cleaved caspase 3 and Bax/Bcl-2 ratio,

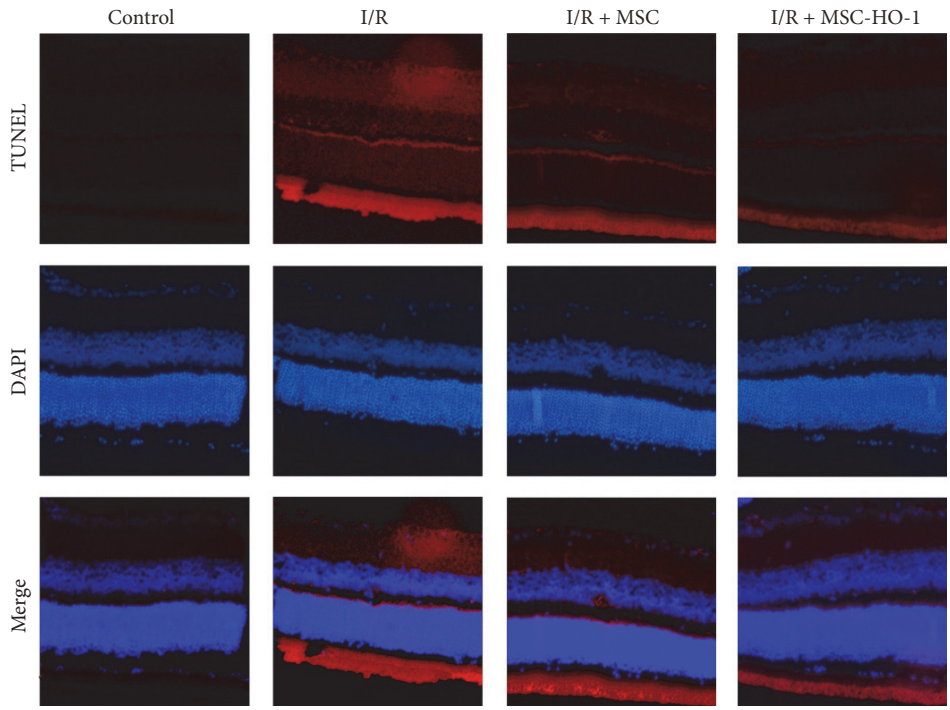

Figure 5: Effects of MSC-HO-1 on retinal cell apoptosis after I/R injury. At day 21, the retinas of control, I/R + PBS, I/R + MSC, or I/R + MSC-HO-1 group were stained utilizing TUNEL and DAPI. TUNEL staining is denoted in red and DAPI staining of nuclei in blue.

which could be significantly offset by MSC, especially MSC-HO-1.

3.7. Effects of MSC-HO-1 on the Level of ROS and the Activity of Antioxidases. We finally examined the changes of oxidative states in retinas by assessing the level of ROS and the activity of antioxidant enzymes. First, we employed lucigenin- and luminol-enhanced chemiluminescence (CL) methods to investigate the ROS level at weeks 1, 2, and 3, respectively. The counts of luminol- and lucigenin-enhanced CL could be dose-dependently quenched by ROS and superoxide. Administration with MSC significantly decreased mean luminol- and lucigenin-enhanced CL signal over 3 weeks compared with untreated group (Figures 7(a) and 7(b)). Similarly, HO-1 overexpression in MSC further reinforced the restoring effects. SOD and CAT played key roles in the antioxidant defense system. As shown in Figures 7(c) and 7(d), the significant decrease in the activity of SOD and CAT enzymes caused by retinal I/R injury was markedly suppressed by treatment with MSC, particularly MSC overexpressing HO-1 at weeks 1, 2, and 3.

3.8. Survival of MSC in Retina. After transplantation for 21 days, we checked the viability of transplanted MSC in rat retina. As showed in Figure 8, in the control MSC, a few MSC was observed based on the expression of GFP. Meanwhile, much more MSC were identified in MSC-HO-1 group, indicating that HO-1 overexpression was also able to promote the survival of MSC, which may also strengthen the therapeutic effect of cell-based transplantation.

4. Discussion

The generation of ROS and thus oxidative stress has been regarded as one of main retinal damage induced by I/R injury [33, 34]. Thus, drugs or methods that are capable of attenuating ROS level in retina are the mainstream for retinal I/R injury treatments [33]. H_2O_2 belonged to one of the most important members in ROS, due to its relatively more stable and central role of ROS metabolism [35, 36]. These characteristics enable H_2O_2 gradually to become a model molecule for the in vitro study of ROS or oxidative stress [19, 37]. Here, we first employed H_2O_2 to simulate the in vitro oxidative stress microenvironment to investigate whether MSC have a protective effect on retinal cells, particularly retinal ganglion cells (RGC), which play a pivotal role to fulfil the physiological function of retina [38].

Conventionally, stem cells based transplantation therapies were considered as their capacity to differentiate into multiple cells after engrafting. However, this point of view has been challenged [39] because the therapeutic benefit could still sustain in vivo, even though the transplanted cells were vanished [40]. Thus, paracrine secretion roles of stem cells, reinforcing and improving function and structure of host cells and tissues, were gradually valued and studied broadly [16]. Utilizing an indirect coculture manner by transwell system, we found that MSC could significantly reduce intracellular ROS level and thus apoptosis in RGC-5. The next measurement of the apoptosis-related factors gave us more details about the MSC-based protection on RGC in molecular level. The augment of intracellular ROS blocked the Akt pathway [41], causing cell death by the inhibition of survival signals,

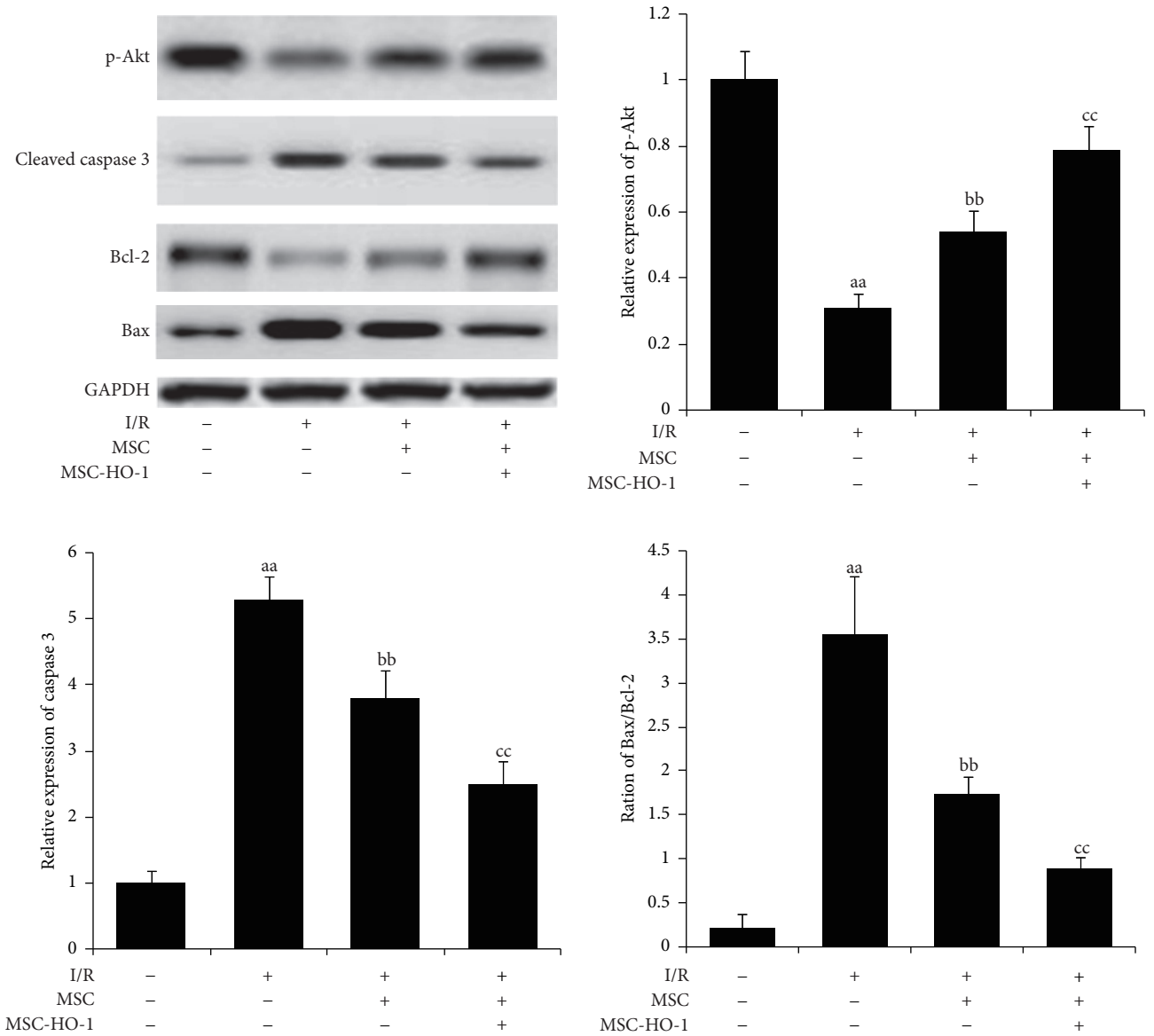

Figure 6: Effects of MSC-HO-1 on the expression of apoptosis-related proteins in retinal cells after I/R injury. At day 21, the expression of apoptosis-related proteins in retinas of control, I/R + PBS, I/R + MSC, or I/R + MSC-HO-1 group was investigated via western blotting ($n = 5$). $^{aa}P < 0.01$ compared with control group; $^{bb}P < 0.01$ compared with IR + PBS group; $^{cc}P < 0.01$ compared with IR + MSC group.

such as Bcl-2 and the activation of proapoptotic signals, including Bax and cleaved caspase [42]. Meanwhile, the high level of ROS could also open the permeability transition gates of mitochondria, resulting in releasing apoptosis-activating proteins [43]. On the membrane outer layer of mitochondria, the expression of proapoptotic protein, Bax, was initiated, while the expression of antiapoptotic protein, Bcl-2, was inhibited. Further apoptotic response also stimulated the release of CytoC, ultimately activating the late-stage apoptotic protein, cleaved caspase 3 [44, 45]. Despite the plausible restoration of RGC, the therapeutic efficiency of MSC was far more from enough, especially compared with the normal RGC, which encouraged us to seek for an alternative strategy to improve MSC-based therapy of RGC.

In comparison with traditional drugs or nutrient based treatment, one of the most important benefits using cells therapy is that individual cell can serve as a "factory," in situ producing certain factors. Owing to the development of gene engineering, cells could be modified by exogenous gene, specifically overexpressing certain factors or proteins [46, 47]. HO-1 has been evidenced to possess the antioxidative and protective properties, preventing toxic effect of oxidative stress on retinal endothelial cells. We thus incorporated MSC with HO-1 gene to obtain MSC overexpressing HO-1. The protection of H_2O_2-treated RGC by MSC-HO-1 indicated that the overexpression of HO-1 in MSC could greatly promote the therapeutic efficiency of MSC, increasing up to 2 times as that of MSC alone. Likewise, the oxidative stress

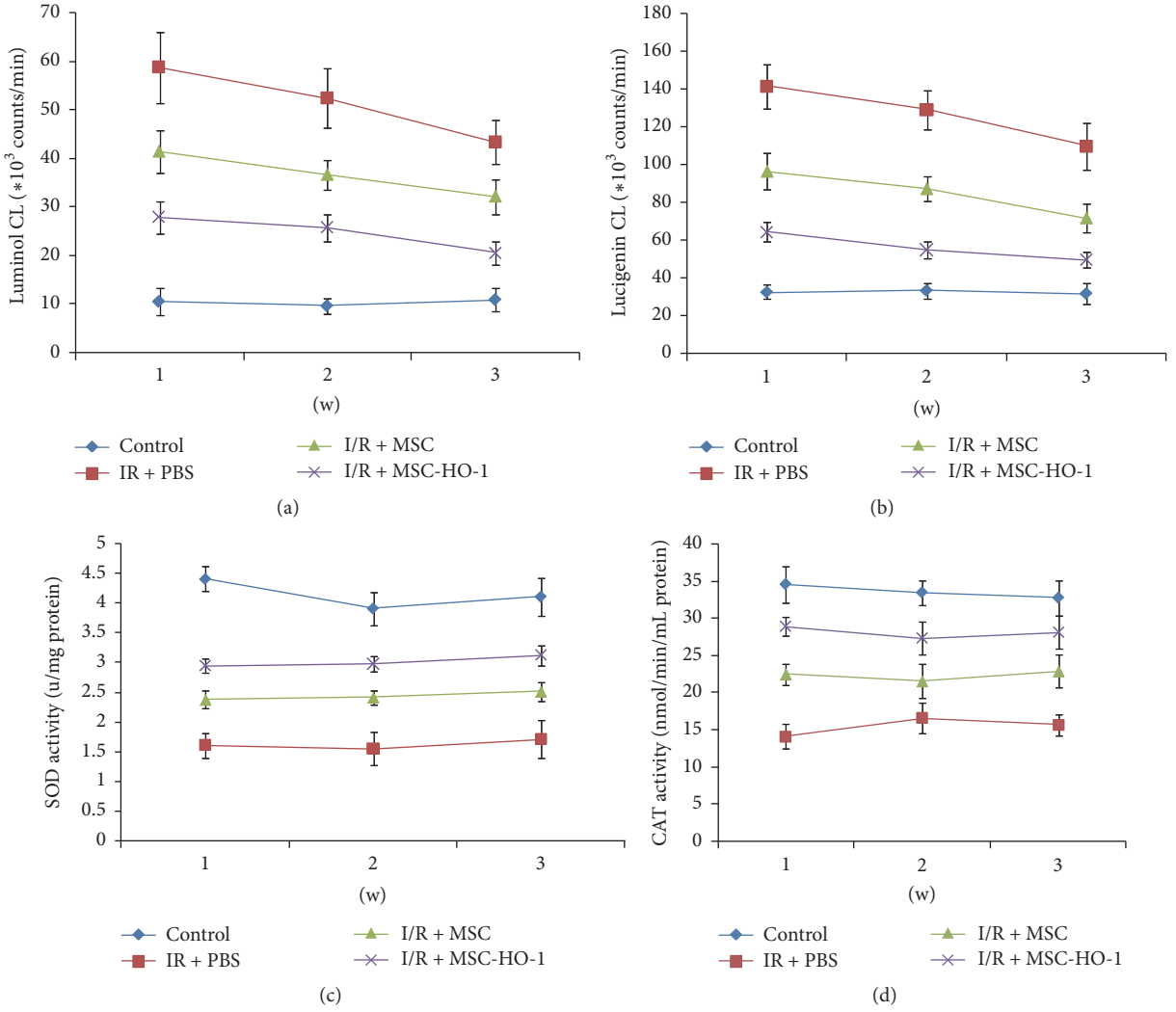

Figure 7: Effects of MSC-HO-1 transplantation on retinal ROS and antioxidase activity after I/R injury. (a) Luminol- and (b) lucigenin-enhanced chemiluminescence and the activity of (c) SOD and (d) CAT enzymes in retinas of the control, I/R + PBS, I/R + MSC, or I/R + MSC-HO-1 group were investigated at weeks 1, 2, and 3, respectively ($n = 5$).

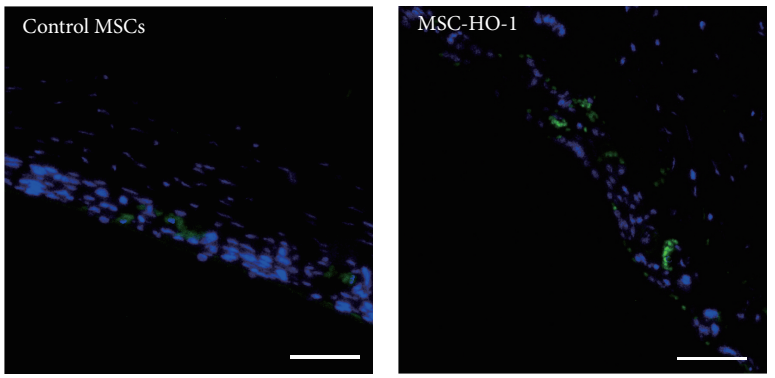

Figure 8: Survival of transplanted MSC in rat retina. After transplantation for 21 days, the survival of transplanted MSC was examined based on the expression of GFP. Bar = 50 μm.

induced expression of apoptosis-related proteins was largely offset. Together, these findings suggested that overexpression of HO-1 strengthened the therapeutic potential of MSC for retinal I/R injury.

Afterwards, we performed I/R injury in rat retina and observed that I/R injury caused the structural loss of retina, reaping flimsy tissues. The following apoptosis examination revealed that a myriad of cells suffered apoptosis, expressing more proapoptotic proteins and less antiapoptotic factors after I/R injury. Many studies have suggested that I/R injury would generate a large amount of ROS, resulting in cellular damage in varied animal models [1, 33]. We thus assessed the in vivo ROS level in a comprehensive way with luminol and lucigenin. The former one responded to a variety of radicals, including H_2O_2, OH^-, hypochlorite, and peroxynitrite, while lucigenin served as the detector to superoxide radicals. Our data of in vivo ROS analysis were in accordance with previous studies [32], indicating that I/R injury induced apoptosis in retina was accompanied by the significant augments of ROS level. Additionally, the high level of ROS suggested the decrease of oxidant scavenges, typically SOD and CAT [32]. After I/R injury, the activities of antioxidant enzymes, SOD and CAT, in retina were dramatically hampered, further weakening the capacity of degrading intracellular ROS.

MSC were then implanted into rat retina and their therapeutic effects were evaluated. MSC were reported to be able to secrete a variety of tropic or antioxidative factors, which were conducive to restore adjacent microenvironment and cells. HO-1, as a potent antioxidant enzyme [37], further attenuated the increase of ROS level. After transplantation of MSC overexpressing HO-1, the abnormalities of both ROS level and representative antioxidant enzyme activities were dramatically corrected. The decrease of oxidative stress facilitated lowering the expression of apoptosis-related proteins in damaged retina. The proapoptotic proteins, cleaved caspase 3 and Bax, were strongly downregulated, while the antiapoptotic proteins, p-Akt and Bcl-2, were significantly upregulated. The decrease of retinal cells suffering apoptosis contributed to the recovery of retina, ultimately leading to the marked augment of retinal thickness. Albeit plausible results in retinal treatment after I/R injury, how the proteins or factors secreted from MSC affected surrounding cells was still obscure. We hence need more detailed investigations to verify related signal pathways in the future.

In conclusion, we here utilized the in vitro system of H_2O_2-simulated oxidative stress to imitate retinal cells suffering I/R injury, revealing that overexpression of HO-1 could enhance the protection of MSC on retinal cells. The next in vivo study demonstrated that I/R injury induced oxidative stress could be potently attenuated by transplanting MSC-HO-1. The reduction of apoptotic retinal cells and thus the raise of retinal thickness fully evidenced that the therapeutic effects of MSC on I/R injury were improved by HO-1 overexpression.

Competing Interests

The authors declare that there is no conflict of interests regarding the publication of this paper.

Acknowledgments

This work was supported by the *China Postdoctoral Science Foundation* (Grant no. 20100471803).

References

[1] N. N. Osborne, R. J. Casson, J. P. M. Wood, G. Chidlow, M. Graham, and J. Melena, "Retinal ischemia: mechanisms of damage and potential therapeutic strategies," *Progress in Retinal and Eye Research*, vol. 23, no. 1, pp. 91–147, 2004.

[2] M. E. Szabo, D. Haines, E. Garay et al., "Antioxidant properties of calcium dobesilate in ischemic/reperfused diabetic rat retina," *European Journal of Pharmacology*, vol. 428, no. 2, pp. 277–286, 2001.

[3] J. Kusari, E. Padillo, S. X. Zhou et al., "Effect of brimonidine on retinal and choroidal neovascularization in a mouse model of retinopathy of prematurity and laser-treated rats," *Investigative Ophthalmology and Visual Science*, vol. 52, no. 8, pp. 5424–5431, 2011.

[4] H. Yokota, S. P. Narayanan, W. Zhang et al., "Neuroprotection from retinal ischemia/reperfusion injury by NOX2 NADPH oxidase deletion," *Investigative Ophthalmology and Visual Science*, vol. 52, no. 11, pp. 8123–8131, 2011.

[5] Y. Wei, J. Gong, T. Yoshida et al., "Nrf2 has a protective role against neuronal and capillary degeneration in retinal ischemia-reperfusion injury," *Free Radical Biology and Medicine*, vol. 51, no. 1, pp. 216–224, 2011.

[6] I. Laskowski, J. Pratschke, M. J. Wilhelm, M. Gasser, and N. L. Tilney, "Molecular and cellular events associated with ischemia/reperfusion injury," *Annals of Transplantation*, vol. 5, no. 4, pp. 29–35, 2000.

[7] S. M. Hong and Y. S. Yang, "A potential role of crystallin in the vitreous bodies of rats after ischemia-reperfusion injury," *Korean Journal of Ophthalmology*, vol. 26, no. 4, pp. 248–254, 2012.

[8] Z. Zhang, X. Qin, X. Zhao et al., "Valproic acid regulates antioxidant enzymes and prevents ischemia/reperfusion injury in the rat retina," *Current Eye Research*, vol. 37, no. 5, pp. 429–437, 2012.

[9] H. Pan, M. He, R. Liu, N. C. Brecha, A. C. H. Yu, and M. Pu, "Sulforaphane protects rodent retinas against ischemia-reperfusion injury through the activation of the Nrf2/HO-1 antioxidant pathway," *PLoS ONE*, vol. 9, no. 12, Article ID e114186, 2014.

[10] H. Kamihata, H. Matsubara, T. Nishiue et al., "Implantation of bone marrow mononuclear cells into ischemic myocardium enhances collateral perfusion and regional function via side supply of angioblasts, angiogenic ligands, and cytokines," *Circulation*, vol. 104, no. 9, pp. 1046–1052, 2001.

[11] T. Kinnaird, E. Stabile, M. S. Burnett, and S. E. Epstein, "Bone marrow–derived cells for enhancing collateral development: mechanisms, animal data, and initial clinical experiences," *Circulation Research*, vol. 95, no. 4, pp. 354–363, 2004.

[12] X. Wang, C. Liu, S. Li et al., "Hypoxia precondition promotes adipose-derived mesenchymal stem cells based repair of diabetic erectile dysfunction via augmenting angiogenesis and neuroprotection," *PLoS ONE*, vol. 10, no. 3, Article ID e0118951, 2015.

[13] M. F. Pittenger, A. M. Mackay, S. C. Beck et al., "Multilineage potential of adult human mesenchymal stem cells," *Science*, vol. 284, no. 5411, pp. 143–147, 1999.

[14] M. Dominici, K. Le Blanc, I. Mueller et al., "Minimal criteria for defining multipotent mesenchymal stromal cells. The International Society for Cellular Therapy position statement," *Cytotherapy*, vol. 8, no. 4, pp. 315–317, 2006.

[15] F. Arslan, R. C. Lai, M. B. Smeets et al., "Mesenchymal stem cell-derived exosomes increase ATP levels, decrease oxidative stress and activate PI3K/Akt pathway to enhance myocardial viability and prevent adverse remodeling after myocardial ischemia/reperfusion injury," *Stem Cell Research*, vol. 10, no. 3, pp. 301–312, 2013.

[16] Y. Zhou, H. Xu, W. Xu et al., "Exosomes released by human umbilical cord mesenchymal stem cells protect against cisplatin-induced renal oxidative stress and apoptosis in vivo and in vitro," *Stem Cell Research and Therapy*, vol. 4, no. 2, article 34, 2013.

[17] Y. Jiang, B. N. Jahagirdar, R. L. Reinhardt et al., "Pluripotency of mesenchymal stem cells derived from adult marrow," *Nature*, vol. 418, no. 6893, pp. 41–49, 2002.

[18] E. Kroon, L. A. Martinson, K. Kadoya et al., "Pancreatic endoderm derived from human embryonic stem cells generates glucose-responsive insulin-secreting cells in vivo," *Nature Biotechnology*, vol. 26, no. 4, pp. 443–452, 2008.

[19] D. Cia, J. Vergnaud-Gauduchon, N. Jacquemot, and M. Doly, "Epigallocatechin gallate (EGCG) prevents H_2O_2-induced oxidative stress in primary rat retinal pigment epithelial cells," *Current Eye Research*, vol. 39, no. 9, pp. 944–952, 2014.

[20] Á. F. Castilho, C. A. Aveleira, E. C. Leal et al., "Heme oxygenase-1 protects retinal endothelial cells against high glucose- and oxidative/nitrosative stress-induced toxicity," *PLOS ONE*, vol. 7, no. 8, Article ID e42428, 2012.

[21] G. Pittenger and A. Vinik, "Nerve growth factor and diabetic neuropathy," *Experimental Diabesity Research*, vol. 4, no. 4, pp. 271–285, 2003.

[22] N. Li, X. R. Li, and J. Q. Yuan, "Effects of bone-marrow mesenchymal stem cells transplanted into vitreous cavity of rat injured by ischemia/reperfusion," *Graefe's Archive for Clinical and Experimental Ophthalmology*, vol. 247, no. 4, pp. 503–514, 2009.

[23] M. P. Soares, S. Brouard, R. N. Smith, and F. H. Bach, "Heme oxygenase-1, a protective gene that prevents the rejection of transplanted organs," *Immunological Reviews*, vol. 184, pp. 275–285, 2001.

[24] I. Cruse and M. D. Maines, "Evidence suggesting that the two forms of heme oxygenase are products of different genes," *Journal of Biological Chemistry*, vol. 263, no. 7, pp. 3348–3353, 1988.

[25] W. K. Mccoubrey Jr., T. J. Huang, and M. D. Maines, "Isolation and characterization of a cDNA from the rat brain that encodes hemoprotein heme oxygenase-3," *European Journal of Biochemistry*, vol. 247, no. 2, pp. 725–732, 1997.

[26] K. D. Poss and S. Tonegawa, "Reduced stress defense in heme oxygenase 1-deficient cells," *Proceedings of the National Academy of Sciences of the United States of America*, vol. 94, no. 20, pp. 10925–10930, 1997.

[27] M. Exner, E. Minar, O. Wagner, and M. Schillinger, "The role of heme oxygenase-1 promoter polymorphisms in human disease," *Free Radical Biology and Medicine*, vol. 37, no. 8, pp. 1097–1104, 2004.

[28] R. Foresti, H. Goatly, C. J. Green, and R. Motterlini, "Role of heme oxygenase-1 in hypoxia-reoxygenation: requirement of substrate heme to promote cardioprotection," *American Journal of Physiology—Heart and Circulatory Physiology*, vol. 281, no. 5, pp. H1976–H1984, 2001.

[29] S. Hayashi, R. Takamiya, T. Yamaguchi et al., "Induction of heme oxygenase-1 suppresses venular leukocyte adhesion elicited by oxidative stress: role of bilirubin generated by the enzyme," *Circulation Research*, vol. 85, no. 8, pp. 663–671, 1999.

[30] L. E. Otterbein, F. H. Bach, J. Alam et al., "Carbon monoxide has anti-inflammatory effects involving the mitogen-activated protein kinase pathway," *Nature Medicine*, vol. 6, no. 4, pp. 422–428, 2000.

[31] S.-J. Mo, Q. Zhong, Y.-F. Zhou, D. B. Deng, and X.-Q. Zhang, "Bone marrow-derived mesenchymal stem cells prevent the apoptosis of neuron-like PC12 cells via erythropoietin expression," *Neuroscience Letters*, vol. 522, no. 2, pp. 92–97, 2012.

[32] I.-M. Fang, C.-M. Yang, C.-H. Yang, S.-H. Chiou, and M.-S. Chen, "Transplantation of induced pluripotent stem cells without C-Myc attenuates retinal ischemia and reperfusion injury in rats," *Experimental Eye Research*, vol. 113, pp. 49–59, 2013.

[33] I.-M. Fang, C.-M. Yang, and C.-H. Yang, "Chitosan oligosaccharides prevented retinal ischemia and reperfusion injury via reduced oxidative stress and inflammation in rats," *Experimental Eye Research*, vol. 130, pp. 38–50, 2015.

[34] M. E. Szabo, M. T. Droy-Lefaix, M. Doly, C. Carre, and P. Braquet, "Ischemia and reperfusion-induced histologic changes in the rat retina. Demonstration of a free radical-mediated mechanism," *Investigative Ophthalmology and Visual Science*, vol. 32, no. 5, pp. 1471–1478, 1991.

[35] D. Xu, D. Liu, B. Wang et al., "In Situ OH Generation from O_2^- and H_2O_2 plays a critical role in plasma-induced cell death," *PLOS ONE*, vol. 10, no. 6, Article ID e0128205, 2015.

[36] H. Sies, "Role of metabolic H_2O_2 generation: redox signaling and oxidative stress," *Journal of Biological Chemistry*, vol. 289, no. 13, pp. 8735–8741, 2014.

[37] T. Ma, T. Chen, P. Li et al., "Heme oxygenase-1 (HO-1) protects human lens epithelial cells (SRA01/04) against hydrogen peroxide (H_2O_2)-induced oxidative stress and apoptosis," *Experimental Eye Research*, vol. 146, pp. 318–329, 2016.

[38] I. Tochitsky, A. Polosukhina, V. E. Degtyar et al., "Restoring visual function to blind mice with a photoswitch that exploits electrophysiological remodeling of retinal ganglion cells," *Neuron*, vol. 81, no. 4, pp. 800–813, 2014.

[39] A. J. Hill, I. Zwart, H. H. Tam et al., "Human umbilical cord blood-derived mesenchymal stem cells do not differentiate into neural cell types or integrate into the retina after intravitreal grafting in neonatal rats," *Stem Cells and Development*, vol. 18, no. 3, pp. 399–409, 2009.

[40] A.-J. Carr, A. A. Vugler, S. T. Hikita et al., "Protective effects of human iPS-derived retinal pigment epithelium cell transplantation in the retinal dystrophic rat," *PLOS ONE*, vol. 4, no. 12, Article ID e8152, 2009.

[41] E. Panieri, V. Gogvadze, E. Norberg, R. Venkatesh, S. Orrenius, and B. Zhivotovsky, "Reactive oxygen species generated in different compartments induce cell death, survival, or senescence," *Free Radical Biology and Medicine*, vol. 57, pp. 176–187, 2013.

[42] B. M. Marte and J. Downward, "PKB/Akt: connecting phosphoinositide 3-kinase to cell survival and beyond," *Trends in Biochemical Sciences*, vol. 22, no. 9, pp. 355–358, 1997.

[43] L. Sun, Y. Jin, L. Dong, R. Sumi, R. Jahan, and Z. Li, "The neuroprotective effects of coccomyxa gloeobotrydiformis on the ischemic stroke in a rat model," *International Journal of Biological Sciences*, vol. 9, no. 8, pp. 811–817, 2013.

[44] Q. Zhang, W.-D. Huang, X.-Y. Lv, and Y.-M. Yang, "Ghrelin protects H9c2 cells from hydrogen peroxide-induced apoptosis through NF-κB and mitochondria-mediated signaling," *European Journal of Pharmacology*, vol. 654, no. 2, pp. 142–149, 2011.

[45] J. Han, P. Tan, Z. Li et al., "Fuzi attenuates diabetic neuropathy in rats and protects schwann cells from apoptosis induced by high glucose," *PLOS ONE*, vol. 9, no. 1, Article ID e86539, 2014.

[46] S. M. Pereira, D. Moss, S. R. Williams, P. Murray, and A. Taylor, "Overexpression of the MRI reporter genes ferritin and transferrin receptor affect iron homeostasis and produce limited contrast in mesenchymal stem cells," *International Journal of Molecular Sciences*, vol. 16, no. 7, pp. 15481–15496, 2015.

[47] V. Ionta, W. Liang, E. H. Kim et al., "SHOX2 overexpression favors differentiation of embryonic stem cells into cardiac pacemaker cells, improving biological pacing ability," *Stem Cell Reports*, vol. 4, no. 1, pp. 129–142, 2015.

Hindawi
Stem Cells International
Volume 2017, Article ID 7316354, 13 pages
https://doi.org/10.1155/2017/7316354

Research Article

Kindlin-2 Modulates the Survival, Differentiation, and Migration of Induced Pluripotent Cell-Derived Mesenchymal Stromal Cells

Mohsen Moslem,[1,2] Reto Eggenschwiler,[2] Christian Wichmann,[1] Raymund Buhmann,[1] Tobias Cantz,[2,3] and Reinhard Henschler[1,4,5]

[1]*Department of Transfusion Medicine, Cell Therapeutics and Hemostaseology, Ludwig-Maximilians University Hospital, Munich, Germany*
[2]*Translational Hepatology and Stem Cell Biology, REBIRTH Cluster of Excellence and Department of Gastroenterology, Hepatology, and Endocrinology, Hannover Medical School, Hannover, Germany*
[3]*Cell and Developmental Biology, Max Planck Institute for Molecular Biomedicine, Münster, Germany*
[4]*Blood Transfusion Service, SRC, Zürich, Switzerland*
[5]*Blood Transfusion Service, SRC, Chur, Switzerland*

Correspondence should be addressed to Reinhard Henschler; rhenschler@gmx.de

Received 23 September 2016; Revised 24 November 2016; Accepted 12 December 2016; Published 9 January 2017

Academic Editor: Andrea Ballini

Kindlin-2 is a multidomain intracellular protein that can be recruited to β-integrin domains to activate signaling, initiate transcriptional programs, and bind to E-cadherin. To explore its involvement in cell fate decisions in mesenchymal cells, we studied the effects of Kindlin-2 modification (overexpression/knockdown) in induced pluripotent cell-derived mesenchymal stromal cells (iPSC-MSCs). Kindlin-2 overexpression resulted in increased proliferation and reduced apoptosis of iPSC-MSCs, as well as inhibition of their differentiation towards osteocytes, adipocytes, and chondrocytes. In contrast, siRNA-mediated Kindlin-2 knockdown induced increased apoptosis and increased differentiation response in iPSC-MSCs. The ability of iPSC-MSCs to adhere to VCAM-1/SDF-1α under shear stress and to migrate in a wound scratch assay was significantly increased after Kindlin-2 overexpression. In contrast, inhibition of mixed lymphocyte reaction (MLR) was generally independent of Kindlin-2 modulation in iPSC-MSCs, except for decreased production of interleukin-2 (IL-2) after Kindlin-2 overexpression in iPS-MSCs. Thus, Kindlin-2 upregulates survival, proliferation, stemness, and migration potential in iPSC-MSCs and may therefore be beneficial in optimizing performance of iPSC-MSC in therapies.

1. Introduction

Kindlins are intracellular multidomain proteins with binding motifs that mediate their interaction with integrins, the cytoskeleton, or, in the case of Kindlin-2, E-cadherin [1]. Kindlins can activate integrins by adhering to their β cytoplasmic chain using the FERM domain to engage a-actinin, migfilin, or integrin-linked kinase (ILK), which leads to actin remodeling, cell migration, and lamellipodia formation [2]. Kindlin-2 was found to play a role during embryogenesis by altering the proliferation potential and migration behaviour of different cell types, and the deregulation of Kindlin-2 can halt embryonic development and induce embryonic lethality [3]. Kindlin-2 was found to trigger epithelial mesenchymal transition (EMT) by activating Wnt signaling in vitro [4], resulting in increased adhesion, migration, and proliferation [5]. Kindlin-2 may also inhibit the growth and migration of colorectal cancer cells [6]. Because EMT occurs during induced pluripotent stem cells (iPSCs) differentiation towards mesenchymal-like cells [7], we aimed to investigate the role of Kindlin-2 in the functions of iPSC-derived MSC. We hypothesized that Kindlin-2 may increase proliferation,

enhance migration and adhesion, and increase functional activation of iPSC-MSCs and thus might provide a basis for engineering iPSC-MSCs in a therapeutically desirable manner.

Obtaining sufficient amounts of MSCs has been a limiting factor for their use in transplantation. Furthermore, the robust functional activation of MSCs, such as migration towards injured tissues, adhesion for homing in areas in need of tissue repair, and resistance to apoptosis after transfusion, was thought to be crucial for therapeutic efficiency in recipients [8, 9]. So far, it is not clear to what extent alterations in the proliferation, migration, and adhesion of therapeutically applied MSCs might influence the capability of the cells to mediate tissue repair or immune regulation. Altogether, "superfunctional" MSCs should display high expandability and survival and boosted adhesion and migration with preserved immunoregulatory properties that are likely to promote the therapeutic potential of MSCs in cellular therapies.

In a previous study, we characterized the differentiation of iPSCs towards MSCs to obtain a functional substitute for ex vivo MSCs [7, 10]. We have shown that iPSCs can be differentiated into MSCs, including development from "epithelial-like" iPSCs towards spindle-shaped MSCs that are capable of proliferation in an undifferentiated stage and of induction into multilineage differentiation. Moreover, iPSC-MSCs showed similar hematopoietic support and immunomodulatory effects to BM-MSCs [10]. In this study, we aimed to modify Kindlin-2 expression in iPSC-MSCs to modulate their proliferative and functional properties. We demonstrate that Kindlin-2 expression levels modulate the adhesion and migration properties of iPSC-MSCs as well as their proliferation, apoptosis, differentiation, and immunesuppression properties.

2. Materials and Methods

2.1. iPS Cell Culture and Mesenchymal Differentiation. Human iPSCs were provided from in-house supplies as described [11]. Briefly, human fetal liver fibroblasts (FLF) were transduced via lentiviral expression of reprogramming factors Oct4, Sox2, Klf4, and c-Myc (OSKM) and cultured on irradiated mouse embryonic fibroblasts (MEF) in medium containing DMEM/F-12, 20% knockout serum replacement (Thermo Fisher, Waltham, MA, USA), 20 ng/mL human recombinant basic fibroblast growth factor (bFGF, provided from Leibniz University Hannover), 0.1 mM β-mercaptoethanol (Thermo Fisher), 1 mM L-glutamine, 1% nonessential amino acids, and 1% penicillin/streptomycin (all from Sigma-Aldrich). Cells were split weekly using collagenase IV (Thermo Fisher), and cells were plated on Matrigel-coated (Corning) plates. Differentiation/enrichment of iPSCs to MSCs was conducted as described [10]. In brief, human iPSC colonies grown on Matrigel were maintained with MSC induction media consisting of DMEM (low-glucose, Sigma-Aldrich, Darmstadt, Germany), 10% defined fetal bovine serum (FBS, Stem Cell Technologies, Vancouver, BC, Canada), 1% nonessential amino acids, 1% penicillin-streptomycin, and 2 ng/mL human recombinant bFGF for 7 days. Next, cells were treated with collagenase IV for 3 min at 37°C, dissociated by glass beads and gentle pipetting, and then passed through 40 mm cell strainers (Fisher Scientific, Schwerte, Germany). Single cells were seeded onto gelatin-coated plates at 1×10^4 cells/cm^2 in MSC media.

2.2. Transfection and Establishment of a Stable Cell Line. The iPSC-MSCs were transfected with four different constructs, including Flag-Kindlin-2 or Flag vector, control short hairpin RNA (shRNA), or Kindlin-2 shRNA. The vectors were received as a gift from Hongquan Zhang, Peking University Health Science Center, Beijing, China. Plasmid structures were described by An et al. [12]. The cells were plated in 6-well plates at a density of 1×10^4 cells/cm^2 24 h before transfection. The plasmids were expanded in *Escherichia coli* (*E. coli* strain DH5a) for 16 h and purified by QIAfilter Maxi Kit (Qiagen, Hilden, Germany) following the manufacturer's protocol. The purified plasmid DNA (3 mg/mL) was resuspended in 97.5 μL of low-glucose DMEM, and then 2.5 μL of 0.1 mM polyethylenimine (PEI) was added (Sigma-Aldrich). The PEI/plasmid DNA solution was vortexed immediately to make the PEI/plasmid complexes. The complexes were allowed to interact for 15 min before they were used at room temperature. Then, 600 μL of low-glucose DMEM with 10% FBS was added to the complexes to make a transfection mixture; finally, the mixture was added to the cells. After 3 hours, the medium was removed and replaced with normal MSCs media for 2 days. After two days, cells were cultured under 500 μg/mL G418 (Sigma-Aldrich) selection until all nontransfected cells disappeared.

2.3. Proliferation Assays. Cell proliferation assays were performed with WST-1 and BrdU colorimetric assays (both from Roche) according to the manufacturer's protocols. For the WST-1 assay, cells were plated in 96-well plates at an initial density of 2000 cells/well. The growth graphs were made five days after transfection by measuring Formazan dye in the conditioned media. For the quantitative colorimetric BrdU proliferation assay (Roche), BrdU was added 12 hours before fixation. Then, anti-BrdU-POD was added, and the reaction was detected by adding the subsequent substrate. Colorimetric assays were detected with a scanning multiwell spectrophotometer (Bio-Rad). BrdU-incorporated cells were counted five days after transfection. Cells were fixed with 4% paraformaldehyde (PFA) and then subjected to immunofluorescence staining for 5-bromo-2′-deoxyuridine (BrdU) (Abcam). The cells were counted under a fluorescent microscope, and the ratio of BrdU positive nuclei to the total number of nuclei stained with DAPI (Sigma-Aldrich) was determined.

2.4. Flow Cytometry. To assess the expression of CXCR-4 after modulation of Kindlin-2 expression, flow cytometric analysis was performed 3 days after transfection as follows: single cell suspensions were prepared by trypsin digestion (Life Technologies) and washed with cold PBS containing 1% bovine serum albumin BSA (Merck Millipore). Next, 2×10^5 cells were incubated for 30 minutes with the respective APC-conjugated monoclonal antibody of CXCR-4 (all from BD Biosciences) and the suspensions were resuspended at a

density of 2×10^5 cells per 200 μL in cold PBS containing 1% BSA. Nonspecific fluorescence was determined by incubation of cell aliquots with isotype-matched monoclonal antibody. Samples were run on a FACSCalibur (BD Biosciences, CA, USA) cytometer using FACS Diva software. For each analysis, a minimum of 10,000 cells were assayed. Data were further processed using FlowJo software (Tree Star, Ashland, Oregon, USA).

2.5. Flow Chamber Adhesion Assay. For adhesion assays, 10^5 iPSC-MSCs were allowed to rest for 3 min on a laminar flow chamber slide (μ-slide, ibiTreat; IBIDI Systems, Munich, Germany) mounted on an inverted microscope as previously described [13]. Briefly, flow chambers were precoated with 2 μg/mL VCAM-1 fusion protein and cocoated with SDF-1, both from R&D Systems (1 μg/mL). Subsequently, HBSS/0.1% BSA (prewarmed to 37°C) was flushed through the chambers at the indicated calculated shear stresses with increases in steps between 0.35 and 15 dyn/cm^2 every 30 s. Images were taken, and the adherent cells were counted in four fields for every condition.

2.6. Migration Assay. Cells were seeded at a density of 3×10^4 cells on each side of an Ibidi culture insert for live cell analysis (Ibidi, Munich, Germany) with 500 μM separation between each side of the well and were allowed to grow for 24 h. Cells were pretreated with 30 μM mitomycin C for 30 min before removal of the insert, and cells in the insert were incubated in DMEM with or without 30 μM mitomycin C. The cells were photographed using the 10x objective (Zeiss) after insert removal (0 h) and following 24 and 36 h of incubation. Transmigration assays were performed in transwells (Corning, New York, USA) 6.5 mm in diameter with 8 μm pore filters. The upper side of the transwell filter was coated for 1 hour at 37°C with 0.1% bovine gelatin (Sigma-Aldrich) in phosphate-buffered saline (PBS). Then, 5×10^5 transfected iPSC-MSCs suspended in 200 μL of migration medium containing RPMI with 0.25% bovine serum albumin (Sigma-Aldrich) were added to the upper chambers, and 600 μL of migration medium supplemented with 10% FBS was added to the bottom chamber. After 24 h and 48 h incubation of the transwells at 37°C/5% CO_2, the upper side of the filters was carefully washed with cold PBS, and cells remaining on the upper face of the filters were removed with a cotton wool swab. Transwell filters were stained using a Giemsa solution (Sigma-Aldrich), cut out with a scalpel, and mounted onto glass slides with the lower face turned upwards. The total number of cells that had migrated was counted using light microscopy at 200x magnification. Each experiment was performed in triplicate.

2.7. Real-Time PCR. Total cellular RNA was isolated using TRIzol reagent (Life Technologies). Resultant RNA was subjected to DNase treatment and cDNA Synthesis Kit (Life Technologies) with random hexamers. Power SYBR Green Master Mix qRT PCR assays were performed with the StepOne Plus Cycler (Applied Biosystems) using the standard settings. Samples were collected from at least three independent experiments. Kindlin-2 primers used in the real-time PCR were forward sequence 5′-TGTCTCCCCGCT-ATCTAAAAAAGT-3 and reverse sequence 5′-TGATGG-GCCTCCAAGATTCT-3. GAPDH was used as an internal control with the forward sequence 5′-CTGAGAACGGGA-AGCTTGT-3 and reverse sequence 5′-GGGTGCTAAGCA-GTTGGT-3. Expression of genes was determined using the comparative CT method ($2^{-\Delta\Delta CT}$).

2.8. Immune-Suppression Assays. Twenty-four hours after transfection of iPSC-MSCs, mixed lymphocyte reaction (MLR) cultures were inoculated with 5×10^4 mitomycin C-treated (Sigma-Aldrich) human peripheral blood mononuclear cells (PBMCs) as stimulators and 2×10^5 human CD8$^+$ T-cells isolated from normal blood donors after informed consent in 96-well round-bottom plates in 200 μL of complete medium containing RPMI 1640 (Life Technologies) supplemented with 0.1 mM β-mercaptoethanol, 10% FBS, GlutaMAX I (Life Technologies), 100 U/mL penicillin, and 100 μg/mL streptomycin in the presence or absence of iPSC-MSCs and BM-MSCs as previously described [10]. Cultures were incubated for 5 days in 37°C/5% CO_2. BrdU was added to the mixed lymphocyte reaction 12 hours before fixation. Then, anti-BrdU-POD was added, and the reaction was detected by adding the subsequent substrate. Colorimetric assays were detected with a scanning multiwell spectrophotometer (Bio-Rad). IL-2 and IFN-γ concentrations were determined in MSC/MLR coculture supernatants using commercially available ELISA (BD Biosciences) according to the manufacturer's instructions. Briefly, 50 μL of ELISA diluent was added to the IL-2 or IFN-γ coated 96-well plates. Then, 100 μL of sample supernatant or standard controls was added to the wells for 2 hours at room temperature. After washing the samples five times, 100 μL of the prepared working detector was incubated in each well for 1 hour in RT. After washing the samples seven times, 100 μL of TMB substrate was added and incubated for 30 minutes in RT, followed by adding 50 μL of stop solution. Colorimetric assays were detected at 450 nm using a multiwell spectrophotometer (Bio-Rad).

2.9. Annexin V Assay. Viability of iPSC-MSCs after transfection was monitored by FACS analysis using annexin V-propidium iodide staining. Cultured iPSC-MSCs were detached, centrifuged, suspended in PBS, and stained with annexin V-FITC and propidium iodide (BD Pharmingen, San Diego, CA, USA). Apoptotic cells were identified as an annexin V-positive/propidium iodide-negative population using the FACSCalibur cytometer (BD) and FlowJo software (Tree Star).

2.10. Differentiation of iPSC-MSCs after Kindlin-2 Modification. Differentiation induction of iPSC-MSCs was carried out for 21 days in different differentiation media, 24 hours after transfection. In total, 10^4 cells were seeded per well in six-well plates (TPP). To induce osteogenic differentiation, cells were cultured with MSC medium containing 1 μM dexamethasone, 0.5 μM ascorbic acid, and 10 mM b-glycerol phosphate (all from Sigma-Aldrich). For adipogenic induction, cells were cultured in MSC medium supplemented with

50 μg/mL indomethacin (Sigma-Aldrich), 50 μg/mL ascorbic acid, and 100 nM dexamethasone. For chondrogenic differentiation, iPSC-MSCs were centrifuged in 0.2 mL of medium at 500 g for 10 min in 15 mL Falcon tubes to form a pellet. The pellets were cultured in MSC medium supplemented with 0.01 μM dexamethasone, 397 μg/mL ascorbic acid-2-phosphate (Sigma-Aldrich), 1 mM sodium pyruvate (Sigma-Aldrich), 10 ng/mL transforming growth factor-β1 (TGF-β1, Life Technologies), and 1% insulin-transferrin-selenium (Life Technologies). Osteogenesis was assessed by Alizarin Red staining, adipogenesis was assessed by Oil Red-O staining, and chondrogenesis was assessed by Alcian Blue staining (all from Sigma-Aldrich).

2.11. Statistical Analysis. The results were expressed as the mean ± standard error of the mean (SEM). Analyses of iPSC-MSCs in vitro were performed using one-way repeated measures analysis of variance (ANOVA) followed by Tukey's post hoc test multiple group comparison to analyze the group differences of the in vivo data. The mean difference was significant at the $p < 0.05$ level. For quantification with ImageJ software, a total of 30 fields of each group were assayed.

3. Results

3.1. Kindlin-2 Expression Pattern and Targets in iPSC-MSCs. As a first approach to assess the role of Kindlin-2 in MSCs, we analyzed its mRNA levels of Kindlin-2 in iPS, BM-MSC, and iPS-MSCs. We found that BM-MSCs express higher levels of Kindlin-2 RNA compared with iPSCs ($p \leq 0.05$, Figure 1(a)). Different passages of iPSC-MSCs showed a slight increase in mRNA and protein expression levels of Kindlin-2 compared to iPS cells, but still lower than BM-MSCs (Figure 1(b)). For overexpression/knockdown experiments, we used iPSC-MSCs passages 4–6. Quantitative RT-PCR results demonstrated the successful transfection of iPSC-MSCs with Kindlin-2 constructs compared to control plasmids (Figure 1(c)). The corresponding expression of Kindlin-2 protein is shown in Figures 1(d) and 1(e).

3.2. Kindlin-2 Promotes Proliferation/Survival and Suppresses Apoptosis of iPSC-MSCs. Previously, we showed that iPSC-MSCs displayed a shorter doubling time than BM-MSCs and reached senescence at later passages than BM-MSCs [10]. To investigate the effects of Kindlin-2 on proliferation and survival in iPS-MSCs, we performed a BrdU incorporation assay (Figure 2(a)) that showed a significant increase after Kindlin-2 Flag transfection compared to the vector control. In contrast, a small but insignificant decrease in BrdU incorporation was observed after Kindlin-2 shRNA transfection. The same pattern was observed in a WST-1 assay (Figure 2(b)). We confirmed these data by counting the BrdU-incorporated iPSC-MSCs after transfection. The number of $BrdU^+$ cells was also significantly higher in Kindlin-2 Flag transfected cells, and there was a minor decrease after Kindlin-2 shRNA transfection compared to control vectors (Figures 2(c) and 2(d)). We next looked for apoptosis via annexin V expression after transfection (Figures 3(a) and 3(b)). The percentage of apoptotic cells was significantly decreased to 3–6% in Kindlin-2 Flag transfected cells when compared to the corresponding control group (7–12%). Moreover, Kindlin-2 knockdown significantly increased the apoptotic cell population in Kindlin-2 shRNA transfected cells to 17–21% (Figures 3(a) and 3(b)). In parallel, expression of the MSC undifferentiated cell markers, CD73 and CD105, was increased in Kindlin-2 overexpressing cells and decreased after Kindlin-2 knockdown (Figures 3(c) and 3(d)).

3.3. Differentiation Potential after Kindlin-2 Overexpression in iPSC-MSCs. To investigate whether the cells may have various differentiation capabilities after transfection, we performed gene expression analysis and morphological analysis on iPSC-MSCs cultured for 21 days under various conditions. During osteogenic differentiation, we detected less calcium accumulation in Kindlin-2 Flag transfected iPSC-MSCs with significantly lower expression of osteocalcin and alkaline phosphatase, whereas expression of alkaline phosphatase was significantly ($p \leq 0.05$) higher in Kindlin-2 shRNA transfected cells compared to control vector (Figure 4(a)). In chondrogenic differentiation, Kindlin-2 Flag transfected cells produced a small and undifferentiated cartilage pellet; however, the other groups created a larger and fully differentiated cell pellet observed in histological analysis (Figure 4(b)). Furthermore, Kindlin-2 overexpression significantly ($p \leq 0.05$) decreased aggrecan mRNA levels while cells transfected with Kindlin-2 shRNA had significantly ($p \leq 0.05$) higher expression of aggrecan and collagen type II (Figure 4(b)). We observed increased numbers of lipid droplets in Kindlin-2 shRNA transfected iPSC-MSCs and a significantly higher expression ($p \leq 0.05$) of PPAR-γ and LPL, while the number of lipid droplets was decreased in iPSC-MSCs transfected with Kindlin-2 Flag vector with significantly lower expression ($p \leq 0.05$) of PPAR-γ and LPL (Figure 4(c)).

3.4. Adhesion of iPSC-MSCs under Shear Stress. To investigate how iPSC-MSCs interact with a relevant homing receptor that activates integrins under shear flow, a parallel plate flow chamber system was used with VCAM-1 + SDF-1α coating. We assessed adhesion of iPSC-MSCs and determined the percentage of their capability to remain adherent in different shear stresses from low (0.35 dynes/cm^2) to high (15 dynes/cm^2) levels. Determination of numbers of adherent cells at each shear stress indicated that Kindlin-2 Flag transfected cells had a higher affinity to adhere to VCAM-1 + SDF-1α coated surface than control vector transfected cells. As shown in Figure 5, after increasing the shear stress to 2 dynes/cm^2, 59 ± 5% of the Kindlin-2 Flag transfected cells remained attached to the surface compared to 42 ± 6% of the control vector and 36 ± 6% of Kindlin-2 shRNA transfected cells. A more prominent difference was observed after increasing the shear stress to 5 dynes/cm^2 in which on average 51 ± 4% of Kindlin-2 Flag transfected cells remained attached, whereas control cells declined to 25 ± 5%, and the cells in the Kindlin-2 shRNA group declined to 19 ± 4%. In parallel, 25.5 ± 4.2% of Kindlin-2 Flag cells were also found positive for CXCR4 by flow cytometry, compared to 0.052±0.05% in control vector, 0.02±0.01% in control shRNA, and 0 ± 0% in Kindlin-2 shRNA iPS-MSCs, respectively

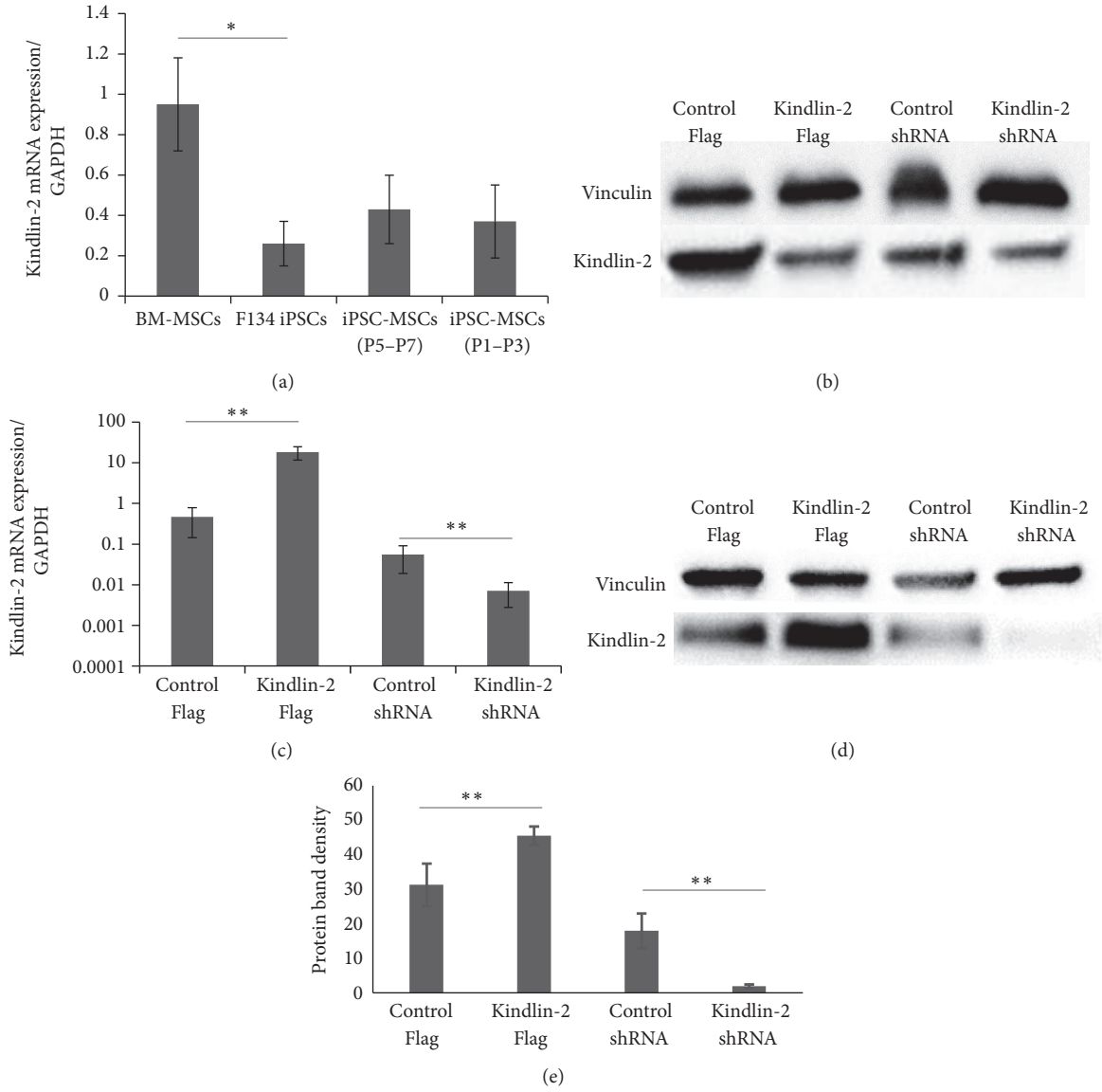

Figure 1: Kindlin-2 expression pattern, overexpression/knockdown, and targets. (a) mRNA expression levels of Kindlin-2 in F134 iPSCs and different passages of iPSC-MSCs indicated significant differences with BM-MSCs; total proteins were extracted from all cell types. (b) Western blotting was performed using an anti-Kindlin-2 monoclonal antibody. (c) Real-time qPCR was performed to quantify mRNA levels of Kindlin-2 in iPSC-MSCs (passages 1–3) with Kindlin-2 overexpression or knockdown. (d, e) Western blot analysis (d) and densitometry (e) performed with ImageJ software were performed and indicate efficient overexpression and knockdown. Data represents the mean expression values normalized to the housekeeping gene GAPDH. *Significance difference $p \leq 0.05$. **Significance difference $p \leq 0.01$.

(means + SD; $n = 3$; not shown in figure). Thus, Kindlin-2 overexpression significantly ($p \leq 0.05$) increased the adhesion to VCAM-1 + SDF1α coated flow chamber slides at shear stresses between 2 and 15 dynes/cm^2, along with an increased expression of CXCR4.

3.5. Migration Potential of iPSC-MSCs after Kindlin-2 Overexpression. We next investigated the migration potential of iPSC-MSCs after transfection with the Kindlin-2 constructs using transwell culture inserts. We found a significant difference in the number of transmigrated cells both at 24 h and at 36 h between Kindlin-2 Flag transfected cells (52 ± 13% versus 20 ± 11% after 24 h and 86 ± 11% versus 37 ± 7% after 36 h). However, these differences were not significant between Kindlin-2 shRNA and control groups (Figure 6(a)). We observed that, at 24 h after transfection, 429 ± 31 cells migrated to the lower surface of the culture insert in Kindlin-2 Flag transfected iPSC-MSCs, but only 285 ± 66 cells were counted in the control group ($p \leq 0.05$). Moreover, the numbers of cells that migrated decreased to 212 ± 37 in Kindlin-2 shRNA transfected cells, which was significantly lower ($p \leq 0.05$) than the control group. Kindlin-2 Flag transfected cells also migrated significantly better ($p \leq 0.05$) than cells in the control group after 48 h of incubation (969 ± 140 cells for

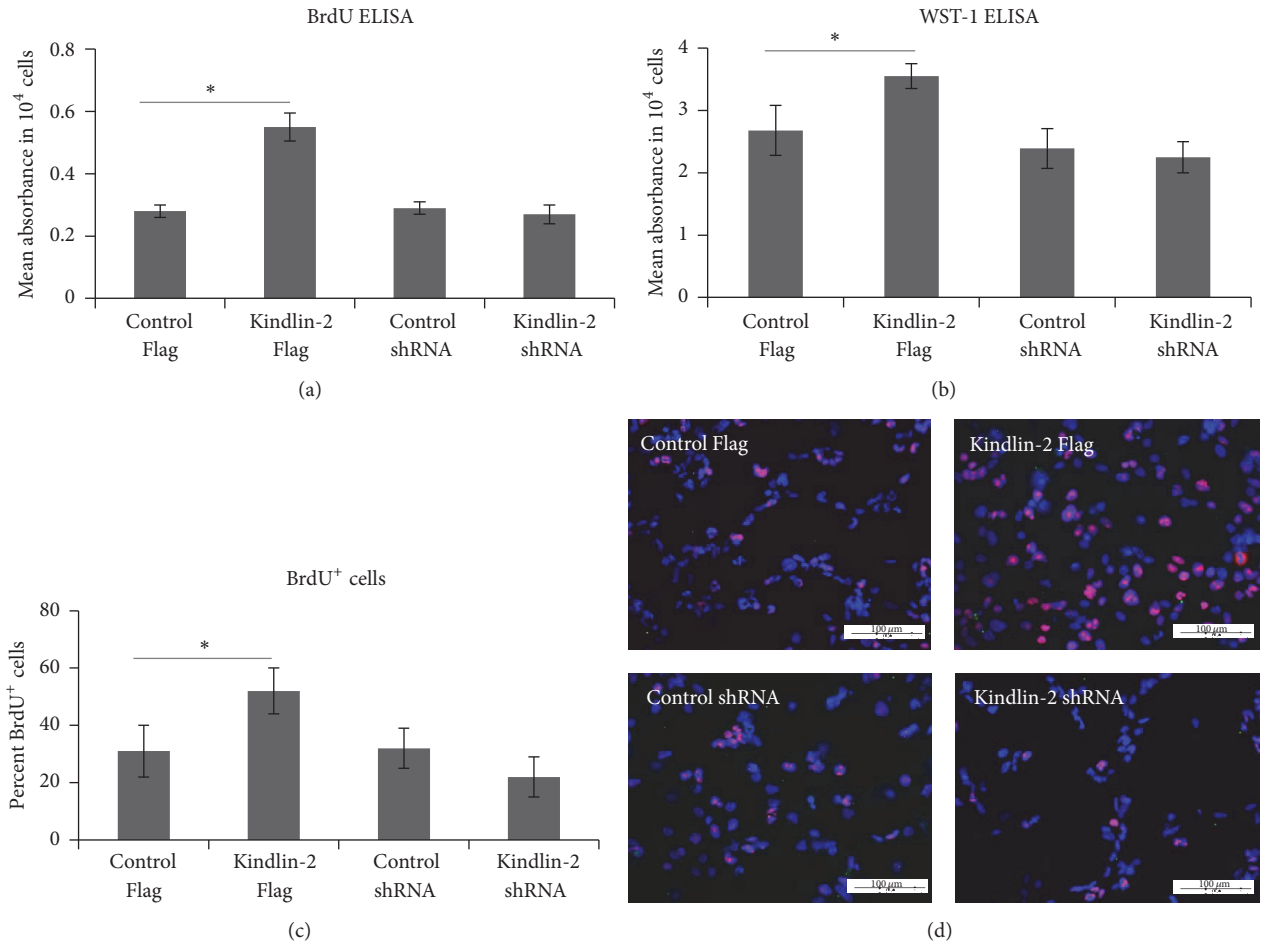

Figure 2: Kindlin-2 regulates iPSC-MSCs cell growth. Cell growth was measured with BrdU (a) and WST-1 (b) ELISA assays and indicated a significantly higher proliferation potential of Kindlin-2 overexpressing cells. BrdU$^+$ cells were counted 5 days after transfection and showed a significantly higher percentage of BrdU$^+$ cells in Kindlin-2 overexpressing cells compared to control Flag (c and d). DAPI was used as a counterstain. *Significance difference between the indicated groups $p \leq 0.05$.

Kindlin-2 Flag versus 633 ± 157 cells for control). Although we observed a reduced number of migrating cells in the Kindlin-2 shRNA group compared to the control group, this difference was not statistically significant (Figure 6(b)). In conclusion, Kindlin-2 levels resulted in modulated migration of iPS-MSCs.

3.6. Kindlin-2 and Anti-Inflammatory Effects of iPSC-MSCs. Previously, we have shown that iPSC-MSCs exhibit potent immunomodulatory function in a mixed lymphocyte culture (MLR) assay by decreasing CD4$^+$ T-lymphocyte proliferation and decreasing IFN-γ secretion. In this study, we used Kindlin-2 Flag/shRNA transfected iPSC-MSCs and BM-MSCs to determine whether Kindlin-2 expression levels may differentially affect the immunomodulatory properties of these cells in an MLR assay. Overall, our results indicate that there was no significant difference in Kindlin-2 Flag/shRNA expressing iPS-MSCs compared to corresponding controls. However, all groups of iPSC-MSCs as well as BM-MSCs could significantly reduce numbers of CD4$^+$ T-cells or release of IFN-γ compared to MLR without the feeder layer (Figures 7(a) and 7(b)). However, there were no significant differences in released IFN-γ in all MLR assays between iPSC-MSCs or BM-MSCs used as feeder cells (Figure 7(b)). Only Kindlin-2 expressing iPSC-MSCs or BM-MSCs were able to significantly decrease in IL-2 secretion, while the other 3 groups did not show statistically significant differences with the control group (Figure 7(c)).

4. Discussion

4.1. Kindlin-2 Expression during Derivation of iPSC-MSCs. This study shows that Kindlin-2 is an integrin-associated protein that can alter the phenotype of iPSC-MSCs in terms of proliferation as well as adhesive and migratory properties towards a more primitive phenotype and in a way that is desirable for MSCs to be used as cellular therapeutics [14, 15]. It has been previously reported that Kindlin-2 can regulate cell-cell and cell-ECM adhesion as well as cell migration via integrin and integrin-linked kinase (ILK) activation [16–18]. Kindlin-2 has been shown to play a crucial role in modulation of integrin signaling and activation, which assists the cell in sensing and interacting with the surrounding environment [19]. Kindlin-2 not only modulates inside-out signaling by

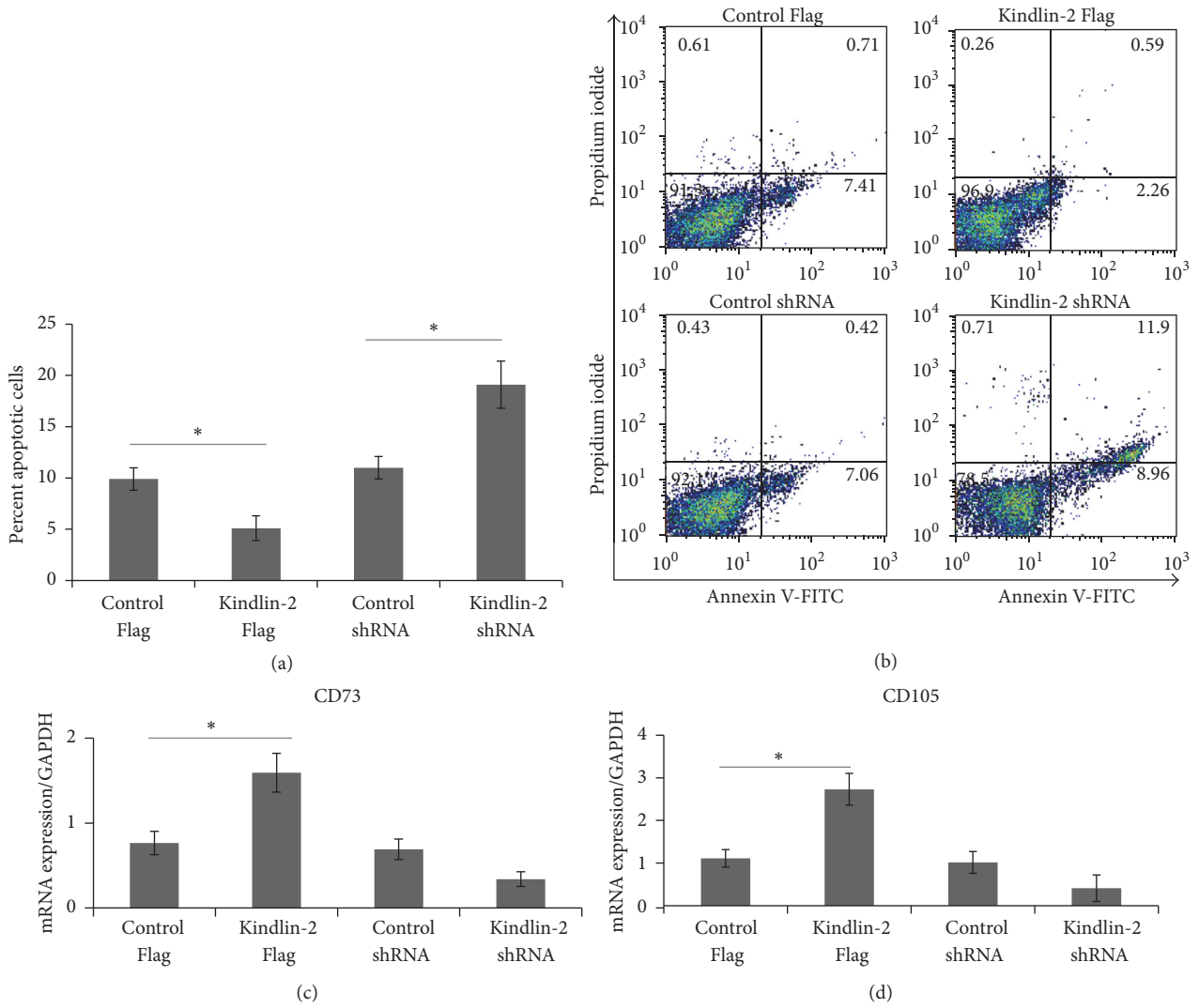

Figure 3: Kindlin-2 regulates apoptosis and stem cell markers in iPSC-MSCs. The iPSC-MSCs were stained using annexin V and propidium iodide for analyzing cell apoptosis after transfection with Kindlin-2 constructs and quantified for early and late apoptotic cells. Kindlin-2 knockdown significantly increased apoptotic cells while Kindlin-2 overexpression significantly decreased apoptotic cells compared to control Flag (a). Data were presented as the mean ± SEM from three independent experiments. Dot plots showing single experiments for annexin V/propidium iodide double positive cells for late apoptotic cells (b). (c) and (d) show quantitative RNA expression of the MSC stemness markers CD73 and CD105 in Kindlin-2 overexpressing and knockdown cells and their controls, respectively. Numbers in (b) indicate % cells in quadrant gate. *Significance difference $p \leq 0.05$.

interacting with integrin β chains [20], but also contributes to outside-in signaling by binding to integrin-linked kinase [21]. More recently, it has been shown that Kindlin-2 can regulate integrin β1 protein expression in adult cardiomyocytes [22]. Kindlin-2 is also involved in regulating cancer cell invasions with varying functions in different cancer types [23].

Generally, affinity regulation but not regulation of integrin expression levels influences integrin activation. Although a variety of targets of Kindlin-2 such as the MIR-200 family and migfilin have been already described [24, 25] as mediators for enhanced adhesion, migration, and invasion, these effects remained controversial because Kindlin-2 overexpression/knockdown is not always the same in different cell types. For instance, Kindlin-2 overexpression promotes prostate cancer stem cell proliferation [26], whereas it reduces both cell division in colorectal cancer cells [6] and mesenchymal cancer invasion [27]. The use of a Kindlin-2 mutant with a defect in binding to integrin could further clarify the involvement of integrin binding in the observed functions of Kindlin-2 in our study.

We hypothesized that if Kindlin-2 increased proliferation, adhesion, and migration in iPS-MSCs, studying this protein might provide highly proliferative MSCs that can retain or outperform the therapeutically desired functional characteristics of normal MSCs and might address their deficiencies [28, 29]. Our data indicated that Kindlin-2 was expressed in BM-MSCs at significantly higher levels than the iPSCs that we used to differentiate iPSC-MSCs

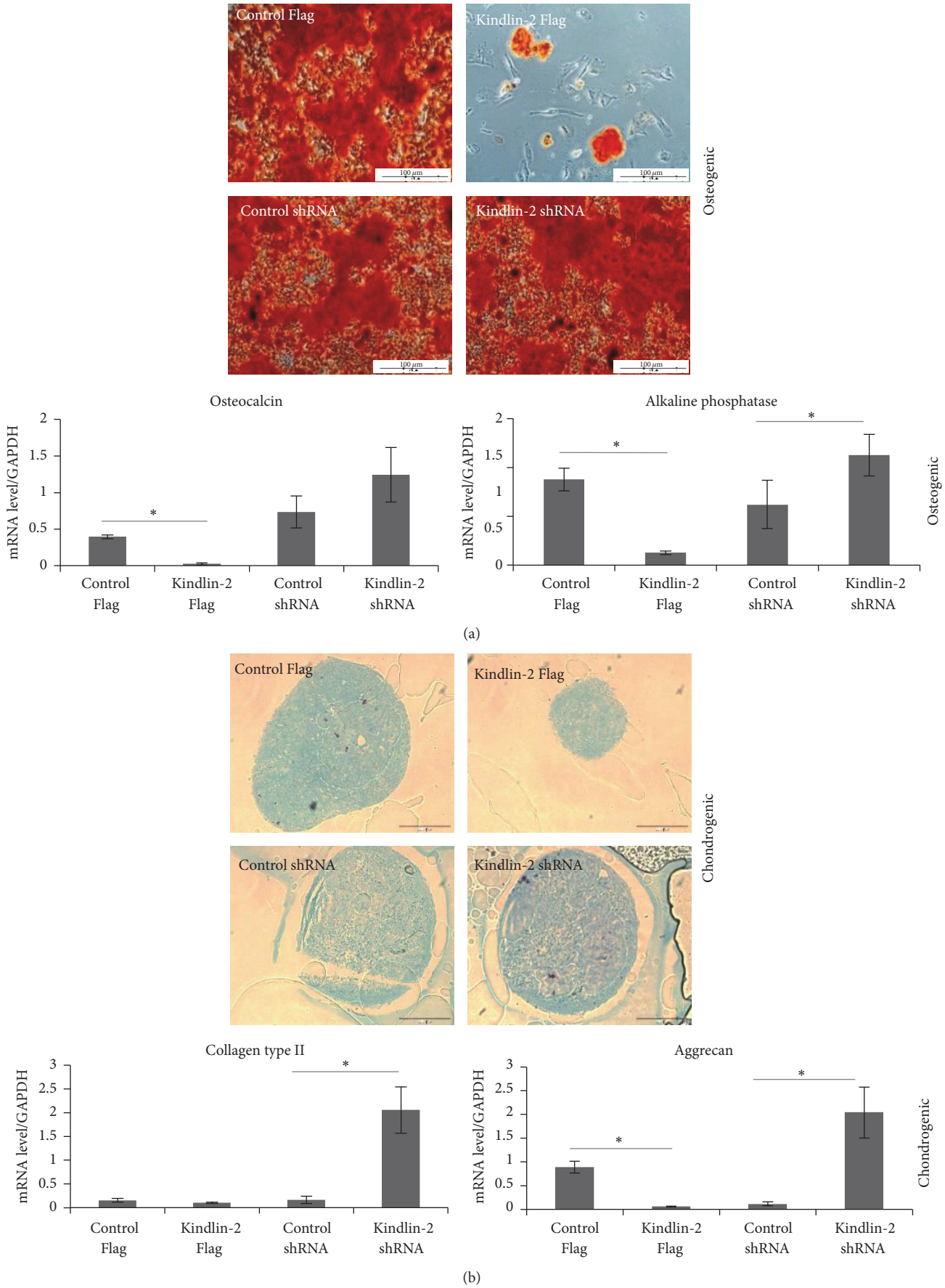

Figure 4: Continued.

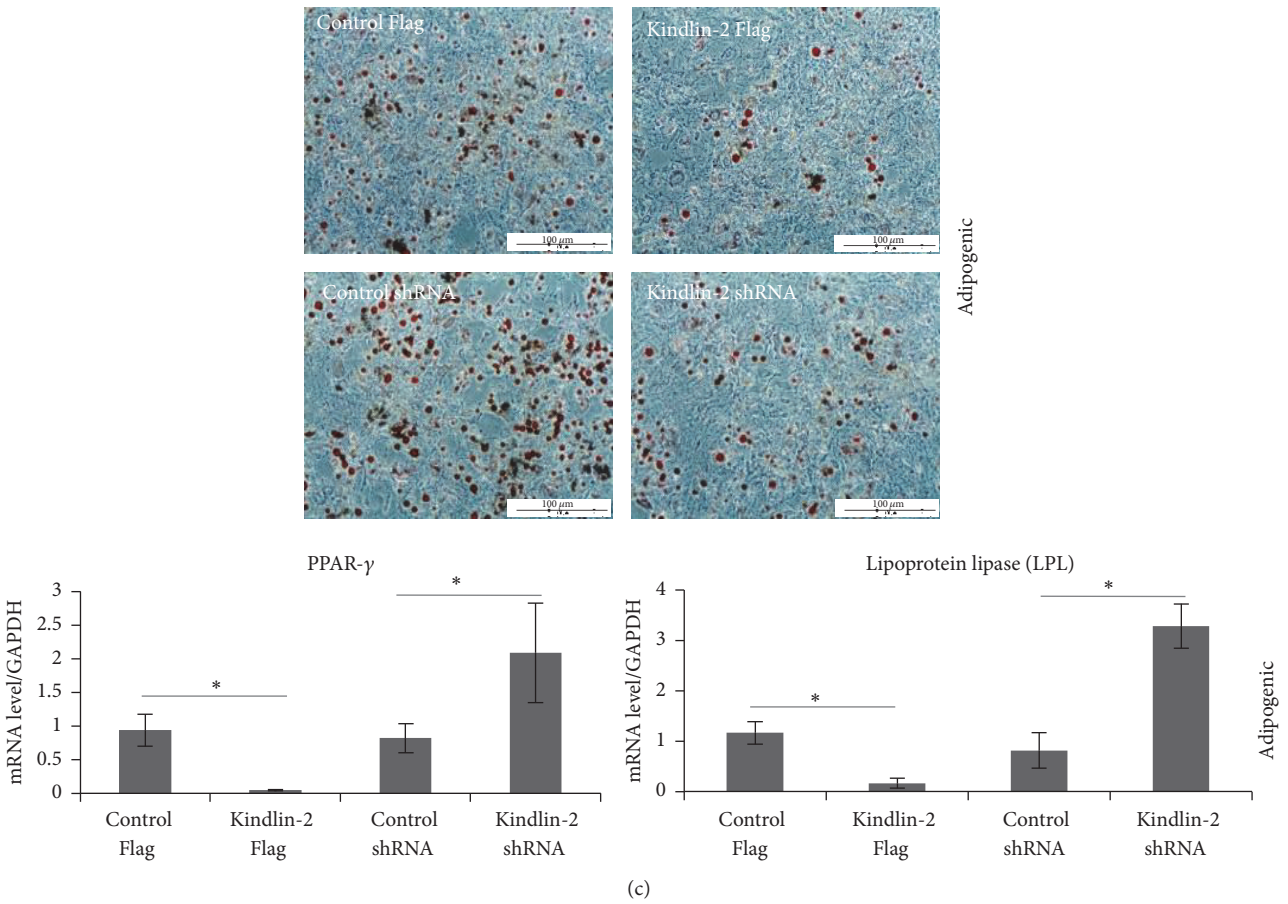

Figure 4: Differentiation capacity of iPSC-MSCs after Kindlin-2 transfection. Osteogenic, chondrogenic, and adipogenic differentiation potential of hiPSC-MSCs after transfection with constructs modulating Kindlin-2. Alizarin Red staining for mineralized deposits (a), Alcian Blue staining for chondrocyte pellets (b), and Oil Red-O staining for lipid formation (c) formed by the three iPSC-MSC cell lines. The mRNA expression level of the relative expression of genes associated with osteogenesis (osteocalcin and alkaline phosphatase), chondrogenesis (collagen type II and aggrecan), and adipogenesis (PPAR-γ and LPL). The data represent the mean expression values normalized to the housekeeping gene GAPDH. Magnification is 10x. *Significance difference $p \leq 0.05$.

(Figure 1(a)). During embryonic development, Kindlin-2, which is weakly expressed in embryonic stem cells, begins to accumulate at increased levels in mesodermal-derived tissues [3, 30, 31]. Furthermore, the expression of Kindlin-2 increases as epithelial-shape embryonic stem cells proceed through epithelial-mesenchymal transition (EMT) towards mesodermal-differentiated cells [32]. As shown in Figure 1(a), newly differentiated iPSC-MSCs expressed relatively low amounts of Kindlin-2 mRNA and protein. However, this expression increased in later passages.

4.2. Kindlin-2 Targets the CXCR-4/SDF-1α Axis. We also showed that alteration of Kindlin-2 expression in iPS-MSCs (Figure 1(b)) positively influenced expression of the newly identified Kindlin-2 target, CXCR-4. This indicates that Kindlin-2 may increase cell adhesion and migration through increasing expression of CXCR4 or its availability at the cell surface [33]. Engineered MSCs with high expression of CXCR-4 were shown to have an enhanced migration capacity and also homing ability in irradiated mice, which is related to SDF-1α levels inside the bone marrow [34]. Moreover, the CXCR-4/SDF-1α axis had a major influence on MSCs recruitment to tissues, chemotaxis, and homing [35].

Increased levels of CXCR-4 in iPSC-MSCs due to Kindlin-2 overexpression may be the key factor in the boosted adhesive capability of the cells to VCAM-1/SDF-1α coated flow chamber slides under high levels of shear stress and also better migratory potential. We performed an adhesion assay with VCAM-1 and fibronectin, which were not affected by Kindlin-2 overexpression/knockdown (Supplementary Figure 1 in Supplementary Material available online at https://doi.org/10.1155/2017/7316354). Our findings support previous studies that indicated that enhanced CXCR-4 expression could lead to improved migration potential and MSCs adhesion in the affected sites [36–38].

4.3. Kindlin-2 Overexpression Upregulates Proliferation in iPSC-MSCs. Yet, there is still controversy about the influence of Kindlin-2 on cell proliferation. Previously, Kindlin-2 was known as a mitogen-activating protein that led to enhanced proliferation [for a review, see [39]]. However, recently, it has been demonstrated that Kindlin-2 overexpression does not

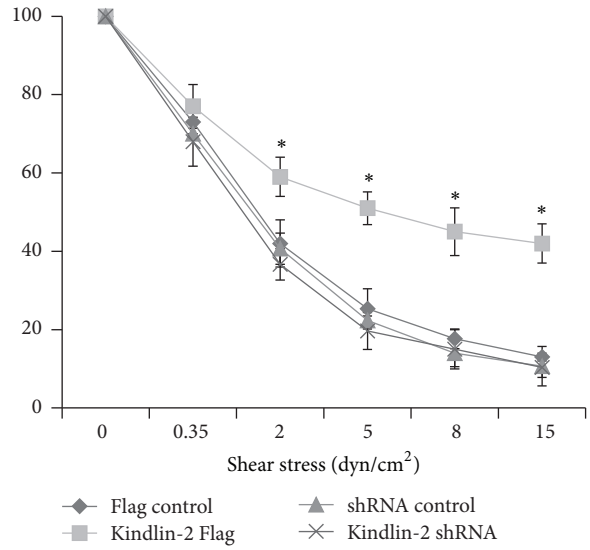

Figure 5: Kindlin-2 boosts iPSC-MSCs adhesion to slides coated with VCAM-1 + SDF1α. The iPSC-MSCs transfected with Kindlin-2 Flag and shRNA adhered to the flow chamber slide coated with VCAM-1/SDF-1α under shear stress. Kindlin-2 Flag transfected iPSC-MSCs had significantly higher attachment to the slides cocoated with VCAM-1 + SDF-1α under shear flow velocities of 0, 2, and 5 dynes/cm^2 with 10x magnification compared to control Flag. The values shown are mean ± SEM of three independent experiments. *Significance difference against Flag control $p \leq 0.05$.

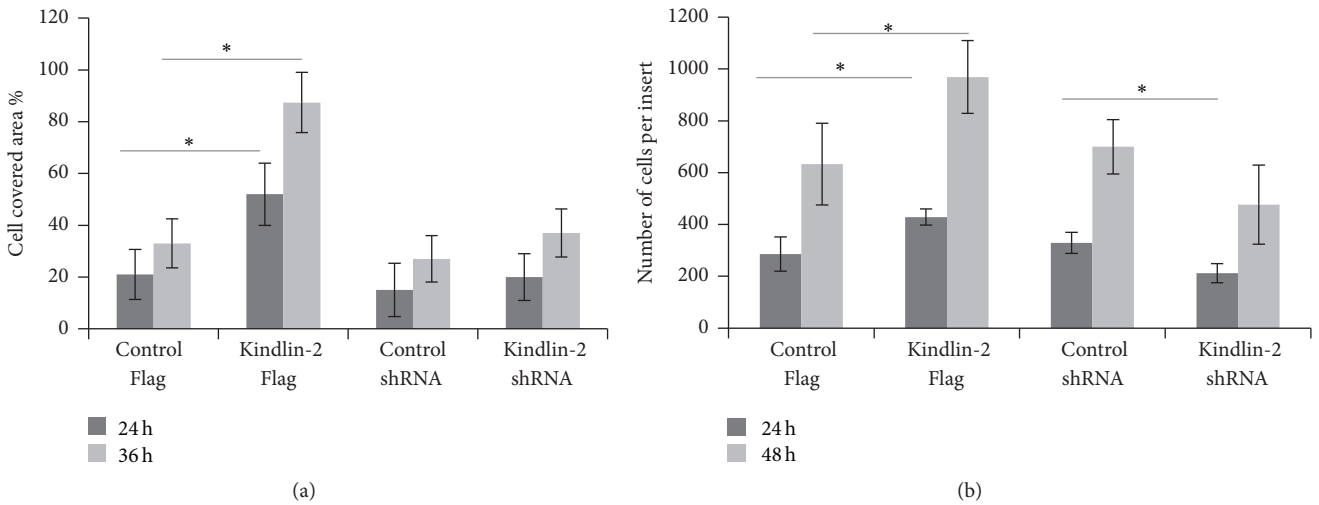

Figure 6: Kindlin-2 affects migration potential of iPSC-MSCs. An in vitro migration assay was performed with an IBIDI culture insert containing two reservoirs separated by a 500 μm thick wall. Kindlin-2 Flag transfected iPS-MSCs had significantly increased migration potential after 24 h and 36 h compared to control groups (a). Moreover, the migration assay with a transwell system showed significantly increased migrating iPSC-MSCs on the lower face of the filters after 48 h of incubation in Kindlin-2 Flag transfected iPSC-MSCs compared to control Flag (b). The covered area between the two reservoirs was analyzed with ImageJ software. *Significance difference $p \leq 0.05$. $n = 3$.

always amplify proliferation but decreases cell division [6, 27]. To this end, we showed here that Kindlin-2 overexpression led to higher proliferation in iPSC-MSCs, whereas its knockdown increased apoptosis. Regarding MSCs infusion therapies, MSCs with enhanced proliferation, migration, and homing ability (adhesion) are favorable and have long-term beneficial effects on the healing of injured areas [40]. So far, our Kindlin-2 Flag transfected iPSC-MSCs are approaching the characteristics of "superfunctional" MSCs as a suitable substitute for normal MSCs in cell infusion therapies. However, it is still necessary to transplant them and investigate their tumorigenic potential.

4.4. Kindlin-2 Overexpression Downregulates Multilineage Differentiation of iPSC-MSCs. We have described the intact differentiation potential and the immune suppressive abilities of iPSC-MSCs in a previous study [10]. Here, we found that Kindlin-2 knockdown rendered iPSC-MSCs more

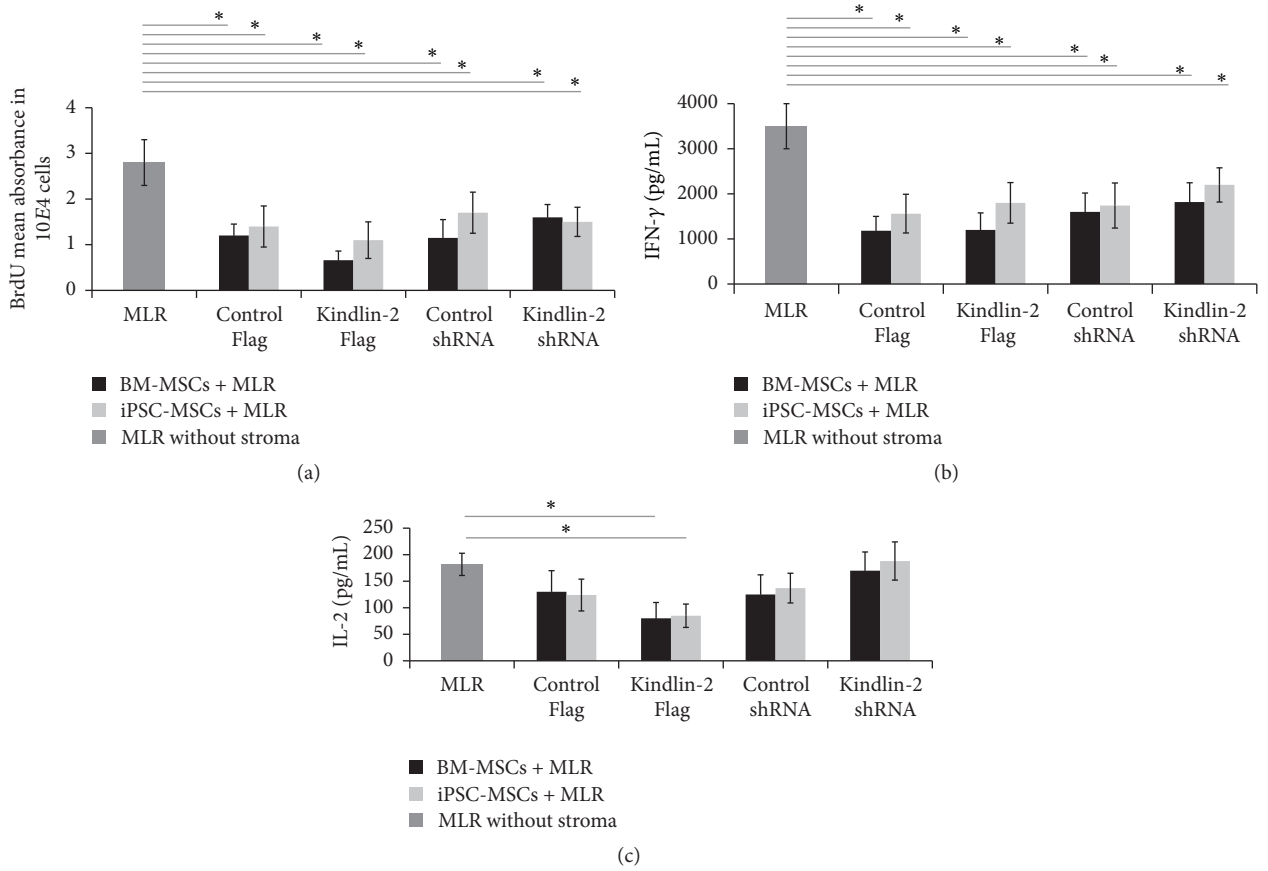

Figure 7: iPSC-MSCs suppress inflammatory reaction after transfection with Kindlin-2. To investigate the immunomodulatory properties of iPSC-MSCs after Kindlin-2 overexpression/knockdown, mixed lymphocyte reaction (MLR) was used to mimic an inflammatory reaction by mixing $CD4^+$ lymphocytes with healthy donor peripheral blood mononuclear cells (PMNCs) on iPSC-MSCs or BM-MSCs feeder layers. (a) $CD4^+$ lymphocyte proliferation in an MLR assay using BrdU incorporation. The iPSC-MSCs/BM-MSCs could significantly ($p \leq 0.05$) decrease lymphocyte proliferation in all four groups compared to MLR without a feeder layer. No significant differences were found between the different MSC groups (not indicated). (b and c) Production of cytokines IFN-γ and IL-2 in the supernatant of MLR assays from the iPSC-MSC/BM-MSCs coculture experiments. A significant decrease of IFN-γ levels was observed between controls without MSCs and iPSC-MSC or BM-MSCs coculture experiments in all four groups, but no significant differences were noted between MSC groups (b). Compared to MLC without MSCs, IL-2 significantly decreased only in the Kindlin-2 overexpression group and not in other groups compared to MLR without a feeder (c). *Significance difference $p \leq 0.05$.

prone to differentiation into three mesodermal lineages, whereas Kindlin-2 overexpression dampened these processes. Recently, Wu et al. showed that Kindlin-2 knockdown in differentiated cells, such as chondrocytes, reduced their density by inhibiting TGF-β1-induced Smad-2 phosphorylation, which led to lower cell doubling rates and increased apoptosis. Those results are in line with our findings [41]. However, Kindlin-2 knockdown mice in this previous study lacked primary ossification centers and differentiated chondrocytes due to increased apoptosis in primary mesenchymal progenitors in vivo [41]. Our data indicates that, after Kindlin-2 Flag transfection, the differentiation affinity of iPSC-MSCs is significantly diminished using both morphology and differentiation markers, whereas Kindlin-2 knockdown increased the differentiation potential of iPSC-MSCs in vitro.

4.5. Kindlin-2 Overexpression Did Not Change Immunomodulatory Effects of iPSC-MSCs. The immune suppressive capacity of iPSC-MSCs and BM-MSCs remained intact after Kindlin-2 overexpression/knockdown in our study. The capability to induce immune tolerance of pluripotent stem cell-derived MSCs and BM-MSCs is one of the fundamental criteria that makes them a promising source for cell transplantation therapies in graft versus host disease (GVHD) [42, 43]. Recently, Cheng et al. have shown reduced proliferation of $CD4^+$ and $CD8^+$ T-cell populations along with a reduction in the proinflammatory cytokines IFN-γ and IL-2 and an increased number of regulatory T-cells after transplantation of pancreatic islets with iPSC-MSCs [44]. We previously showed that iPSC-MSCs could suppress immune reactions the same as BM-MSCs [10]. In the current study, after Kindlin-2 overexpression and knockdown, iPSC-MSCs could

still significantly reduce the number of $CD4^+$ T-cells (Figure 7(a)) and proinflammatory cytokines (IL-2 and IFN-γ) secretion (Figures 7(b) and 7(c)). This indicates that Kindlin-2 overexpression and knockdown did not eliminate the beneficial role of iPSC-MSCs and BM-MSCs in suppressing the immune reaction.

5. Conclusion

Based on our hypothesis, we found that Kindlin-2 overexpression increased the proliferative potential of iPSC-MSCs with less apoptosis and enhanced their migration potential and adhesion to VCAM-1/SDF-1α under shear stress by increasing the expression of CXCR-4. We also showed that Kindlin-2 overexpression decreased the ability of iPSC-MSCs to differentiate into the adipogenic, osteogenic, or chondrogenic lineages, while maintaining stemness markers. Our findings indicated that the functional ability of iPSC-MSCs to reduce the proliferation of $CD\text{-}4^+$ T-cells and decrease proinflammatory cytokines (IFN-γ and IL-2) in an MLR assay is still intact and generally not affected by Kindlin-2 modification. Together, our data suggest that targeting Kindlin-2 in iPSC-MSCs opens a new way towards cell-therapeutic approaches employing functionally enhanced MSCs.

Disclosure

Tobias Cantz and Reinhard Henschler are shared last authors.

Competing Interests

The authors declare no competing interests.

Acknowledgments

The authors would like to thank Hongquan Zhang (Peking University Health Science Center) for his support with Kindlin-2 constructs and Axel Schambach (Hannover Medical School) for his support with lentiviral vectors. The authors are grateful to Matthias Ballmaier and the flow cytometry unit of Hannover Medical School for their technical assistance. They also thank Irina Eberle (University of Frankfurt) for her help in designing the project as well as Verena Platt and Angelika Helmbrecht (Ludwig Maximilians University, Munich) for their technical assistance. Parts of the study were funded through the REBIRTH Cluster of Excellence DFG (EXC 62/2), Research Funds by Ludwig Maximilans University, Munich, and the Max Planck Institute for Molecular Biomedicine, Münster, Germany.

References

[1] J. E. Lai-Cheong, M. Parsons, and J. A. McGrath, "The role of kindlins in cell biology and relevance to human disease," *The International Journal of Biochemistry & Cell Biology*, vol. 42, no. 5, pp. 595–603, 2010.

[2] E. Rognoni, R. Ruppert, and R. Fässler, "The kindlin family: functions, signaling properties and implications for human disease," *Journal of Cell Science*, vol. 129, no. 1, pp. 17–27, 2016.

[3] E. Montanez, S. Ussar, M. Schifferer et al., "Kindlin-2 controls bidirectional signaling of integrins," *Genes and Development*, vol. 22, no. 10, pp. 1325–1330, 2008.

[4] Y. Yu, J. Wu, Y. Wang et al., "Kindlin 2 forms a transcriptional complex with β-catenin and TCF4 to enhance Wnt signalling," *EMBO Reports*, vol. 13, no. 8, pp. 750–758, 2012.

[5] Y. Yu, J. Wu, L. Guan et al., "Kindlin 2 promotes breast cancer invasion via epigenetic silencing of the microRNA200 gene family," *International Journal of Cancer*, vol. 133, no. 6, pp. 1368–1379, 2013.

[6] Y. Ren, H. Jin, Z. Xue et al., "Kindlin-2 inhibited the growth and migration of colorectal cancer cells," *Tumor Biology*, vol. 36, no. 6, pp. 4107–4114, 2015.

[7] M. Moslem, M. R. Valojerdi, B. Pournasr, A. Muhammadnejad, and H. Baharvand, "Therapeutic potential of human induced pluripotent stem cell-derived mesenchymal stem cells in mice with lethal fulminant hepatic failure," *Cell Transplantation*, vol. 22, no. 10, pp. 1785–1799, 2013.

[8] Q. Lian, Y. Zhang, J. Zhang et al., "Functional mesenchymal stem cells derived from human induced pluripotent stem cells attenuate limb ischemia in mice," *Circulation*, vol. 121, no. 9, pp. 1113–1123, 2010.

[9] M. E. Bernardo and W. E. Fibbe, "Mesenchymal stromal cells and hematopoietic stem cell transplantation," *Immunology Letters*, vol. 168, no. 2, pp. 215–221, 2015.

[10] M. Moslem, I. Eberle, I. Weber, R. Henschler, and T. Cantz, "Mesenchymal stem/stromal cells derived from induced pluripotent stem cells support $CD34^{pos}$ hematopoietic stem cell propagation and suppress inflammatory reaction," *Stem Cells International*, vol. 2015, Article ID 843058, 14 pages, 2015.

[11] E. Warlich, J. Kuehle, T. Cantz et al., "Lentiviral vector design and imaging approaches to visualize the early stages of cellular reprogramming," *Molecular Therapy*, vol. 19, no. 4, pp. 782–789, 2011.

[12] Z. An, K. Dobra, J. G. Lock, S. Strömblad, A. Hjerpe, and H. Zhang, "Kindlin-2 is expressed in malignant mesothelioma and is required for tumor cell adhesion and migration," *International Journal of Cancer*, vol. 127, no. 9, pp. 1999–2008, 2010.

[13] F. Ciuculescu, M. Giesen, E. Deak, V. Lang, E. Seifried, and R. Henschler, "Variability in chemokine-induced adhesion of human mesenchymal stromal cells," *Cytotherapy*, vol. 13, no. 10, pp. 1172–1179, 2011.

[14] Y. Zhuang, D. Li, J. Fu, Q. Shi, Y. Lu, and X. Ju, "Comparison of biological properties of umbilical cord-derived mesenchymal stem cells from early and late passages: immunomodulatory ability is enhanced in aged cells," *Molecular Medicine Reports*, vol. 11, no. 1, pp. 166–174, 2015.

[15] M. F. Uranio, M. E. Dell'Aquila, M. Caira et al., "Characterization and in vitro differentiation potency of early-passage canine amnion- and umbilical cord-derived mesenchymal stem cells as related to gestational age," *Molecular Reproduction and Development*, vol. 81, no. 6, pp. 539–551, 2014.

[16] M. Theodosiou, M. Widmaier, R. T. Böttcher et al., "Kindlin-2 cooperates with talin to activate integrins and induces cell spreading by directly binding paxillin," *eLife*, vol. 5, no. 2016, Article ID e10130, 2016.

[17] J. Zhan, J. Song, P. Wang et al., "Kindlin-2 induced by TGF-β signaling promotes pancreatic ductal adenocarcinoma progression through downregulation of transcriptional factor HOXB9," *Cancer Letters*, vol. 361, no. 1, pp. 75–85, 2015.

[18] C. Huet-Calderwood, N. N. Brahme, N. Kumar et al., "Differences in binding to the ILK complex determines kindlin isoform

adhesion localization and integrin activation," *Journal of Cell Science*, vol. 127, no. 19, pp. 4308–4321, 2014.

[19] D. A. Calderwood, I. D. Campbell, and D. R. Critchley, "Talins and kindlins: partners in integrin-mediated adhesion," *Nature Reviews Molecular Cell Biology*, vol. 14, no. 8, pp. 503–517, 2013.

[20] K. Bledzka, K. Bialkowska, H. Nie et al., "Tyrosine phosphorylation of integrin β3 regulates kindlin-2 binding and integrin activation," *Journal of Biological Chemistry*, vol. 285, no. 40, pp. 30370–30374, 2010.

[21] K. Fukuda, K. Bledzka, J. Yang, H. D. Perera, E. F. Plow, and J. Qin, "Molecular basis of kindlin-2 binding to integrin-linked kinase pseudokinase for regulating cell adhesion," *Journal of Biological Chemistry*, vol. 289, pp. 28363–28375, 2014.

[22] Z. Zhang, Y. Mu, J. Veevers et al., "Postnatal loss of kindlin-2 leads to progressive heart failure," *Circulation: Heart Failure*, vol. 9, no. 8, Article ID e003129, 2016.

[23] M. Yan, L. Zhang, Y. Wu et al., "Increased expression of kindlin-2 is correlated with hematogenous metastasis and poor prognosis in patients with clear cell renal cell carcinoma," *FEBS Open Bio*, vol. 6, no. 7, pp. 660–665, 2016.

[24] H.-F. Zhang, K. Zhang, L.-D. Liao et al., "miR-200b suppresses invasiveness and modulates the cytoskeletal and adhesive machinery in esophageal squamous cell carcinoma cells via targeting Kindlin-2," *Carcinogenesis*, vol. 35, no. 2, Article ID bgt320, pp. 292–301, 2014.

[25] H.-F. Zhang, A. Alshareef, C. Wu et al., "Loss of miR-200b promotes invasion via activating the Kindlin-2/integrin β1/AKT pathway in esophageal squamous cell carcinoma: an E-cadherin-independent mechanism," *Oncotarget*, vol. 6, no. 30, pp. 28949–28960, 2015.

[26] J.-R. Yang, T.-J. Pan, H. Yang et al., "Kindlin-2 promotes invasiveness of prostate cancer cells via NF-κB-dependent upregulation of matrix metalloproteinases," *Gene*, vol. 576, no. 1, pp. 571–576, 2016.

[27] X. Shi and C. Wu, "A suppressive role of mitogen inducible gene-2 in mesenchymal cancer cell invasion," *Molecular Cancer Research*, vol. 6, no. 5, pp. 715–724, 2008.

[28] M. Giuliani, N. Oudrhiri, Z. M. Noman et al., "Human mesenchymal stem cells derived from induced pluripotent stem cells down-regulate NK-cell cytolytic machinery," *Blood*, vol. 118, no. 12, pp. 3254–3262, 2011.

[29] Y. Jung, G. Bauer, and J. A. Nolta, "Concise review: induced pluripotent stem cell-derived mesenchymal stem cells: progress toward safe clinical products," *Stem Cells*, vol. 30, no. 1, pp. 42–47, 2012.

[30] J. Zhan, M. Yang, X. Chi et al., "Kindlin-2 expression in adult tissues correlates with their embryonic origins," *Science China Life Sciences*, vol. 57, no. 7, pp. 690–697, 2014.

[31] S. Ussar, H.-V. Wang, S. Linder, R. Fässler, and M. Moser, "The Kindlins: subcellular localization and expression during murine development," *Experimental Cell Research*, vol. 312, no. 16, pp. 3142–3151, 2006.

[32] X. Wei, X. Wang, Y. Xia et al., "Kindlin-2 regulates renal tubular cell plasticity by activation of Ras and its downstream signaling," *American Journal of Physiology - Renal Physiology*, vol. 306, no. 2, pp. F271–F278, 2014.

[33] H. Liu, W. Xue, G. Ge et al., "Hypoxic preconditioning advances CXCR4 and CXCR7 expression by activating HIF-1α in MSCs," *Biochemical and Biophysical Research Communications*, vol. 401, no. 4, pp. 509–515, 2010.

[34] W. Chen, M. Li, H. Cheng et al., "Overexpression of the mesenchymal stem cell Cxcr4 gene in irradiated mice increases the homing capacity of these cells," *Cell Biochemistry and Biophysics*, vol. 67, no. 3, pp. 1181–1191, 2013.

[35] H. D. Theiss, M. Vallaster, C. Rischpler et al., "Dual stem cell therapy after myocardial infarction acts specifically by enhanced homing via the SDF-1/CXCR4 axis," *Stem Cell Research*, vol. 7, no. 3, pp. 244–255, 2011.

[36] C. H. Ryu, S. A. Park, S. M. Kim et al., "Migration of human umbilical cord blood mesenchymal stem cells mediated by stromal cell-derived factor-1/CXCR4 axis via Akt, ERK, and p38 signal transduction pathways," *Biochemical and Biophysical Research Communications*, vol. 398, no. 1, pp. 105–110, 2010.

[37] W.-G. Zhang, L. He, X.-M. Shi et al., "Regulation of transplanted mesenchymal stem cells by the lung progenitor niche in rats with chronic obstructive pulmonary disease," *Respiratory Research*, vol. 15, no. 1, article no. 33, 2014.

[38] N. Li, X. Lu, X. Zhao et al., "Endothelial nitric oxide synthase promotes bone marrow stromal cell migration to the ischemic myocardium via upregulation of stromal cell-derived factor-1alpha," *Stem Cells*, vol. 27, no. 4, pp. 961–970, 2009.

[39] M. Moser, K. R. Legate, R. Zent, and R. Fässler, "The tail of integrins, talin, and kindlins," *Science*, vol. 324, no. 5929, pp. 895–899, 2009.

[40] A. Keating, "Mesenchymal stromal cells: new directions," *Cell Stem Cell*, vol. 10, no. 6, pp. 709–716, 2012.

[41] C. Wu, H. Jiao, Y. Lai et al., "Kindlin-2 controls TGF-β signalling and Sox9 expression to regulate chondrogenesis," *Nature Communications*, vol. 6, article 7531, 2015.

[42] A. Thiel, G. Yavanian, M.-D. Nastke et al., "Human embryonic stem cell-derived mesenchymal cells preserve kidney function and extend lifespan in NZB/W F1 mouse model of lupus nephritis," *Scientific Reports*, vol. 5, Article ID 17685, 2015.

[43] L. Sánchez, I. Gutierrez-Aranda, G. Ligero et al., "Enrichment of human ESC-derived multipotent mesenchymal stem cells with immunosuppressive and anti-inflammatory properties capable to protect against experimental inflammatory bowel disease," *Stem Cells*, vol. 29, no. 2, pp. 251–262, 2011.

[44] P.-P. Cheng, X.-C. Liu, P.-F. Ma et al., "IPSC-MSCs combined with low-dose rapamycin induced islet allograft tolerance through suppressing Th1 and enhancing regulatory T-cell differentiation," *Stem Cells and Development*, vol. 24, no. 15, pp. 1793–1804, 2015.

Hindawi Publishing Corporation
Stem Cells International
Volume 2016, Article ID 1929536, 11 pages
http://dx.doi.org/10.1155/2016/1929536

Research Article

Exosomes from Human Umbilical Cord Mesenchymal Stem Cells: Identification, Purification, and Biological Characteristics

Bin Zhang,[1] Li Shen,[1] Hui Shi,[1] Zhaoji Pan,[1] Lijun Wu,[1] Yongmin Yan,[1] Xu Zhang,[1] Fei Mao,[1] Hui Qian,[1] and Wenrong Xu[1,2]

[1]*Key Laboratory of Laboratory Medicine of Jiangsu Province, School of Medicine, Jiangsu University, Zhenjiang, Jiangsu, China*
[2]*The Affiliated Hospital, Jiangsu University, Zhenjiang, Jiangsu 212000, China*

Correspondence should be addressed to Hui Qian; lstmmmlst@163.com and Wenrong Xu; icls@ujs.edu.cn

Received 18 June 2016; Revised 19 July 2016; Accepted 20 July 2016

Academic Editor: Andrea Ballini

Our and other groups have discovered that mesenchymal stem cells (MSCs) derived exosomes are a novel therapeutical modality for many diseases. In this study, we summarized a method to extract and purify hucMSCs-exosomes using ultrafiltration and gradient centrifugation in our laboratory and proved that hucMSCs-exosomes prepared according to our procedure were stable and bioactive. Results showed that exosomes derived from hucMSC were 40~100 nm and CD9 and CD81 positive. Functionally, hucMSCs-exosomes promoted cell proliferation and protected against oxidative stress-induced cell apoptosis *in vitro* by activation of ERK1/2 and p38. Interestingly, UV exposure abrogated the regulatory roles of exosomes under oxidative stress, indicating that hucMSCs-exosomes may regulate cell growth and apoptosis by exosomal shuttle of RNA. Furthermore, cytokine profile analysis revealed that hucMSCs-exosomes contained high dose of IL-6, IL-8, and other cytokines. The established method is practical and efficient, which provides a basis for further evaluating the potential of hucMSCs-exosomes as therapeutic agents.

1. Introduction

Exosomes are 40–100 nm extracellular membrane vesicles of endocytic origin, which were firstly discovered in the early 1980s [1–3]. Exosomes are released into the extracellular environment upon fusion of multivesicular bodies with the plasma membrane [2, 4–6]. Exosomes are secreted by most cells that have been examined so far, including mast cells, dendritic cells [7, 8], B cells [6], T cells [9], tumor cells [10, 11], and epithelial cells. In addition, exosomes have been found in many biological fluids [1, 11–16] including plasma [12], urine [13], saliva [14], and breast milk [15].

It has been shown that the exosomal protein composition depends on the cellular source of the studied exosomes. Regardless of origin, several common proteins are found in exosomes, including chaperones, cytoskeletal proteins, and tetraspanins such as CD9, CD63, and CD81 [17–20]. Furthermore, more studies have indicated that exosomes also contain a substantial amount of small molecules that can be transferred from one cell to another. Exosomes could easily communicate with target cells through specific receptor-ligand interactions and shuttle defined patterns of components such as proteins, bioactive lipids, and RNA to induce biological effects [19, 21–24]. Therefore, many investigations have been performed to demonstrate the role of exosomes in paracrine/endocrine process and genetic information exchange between different cells due to their important bioactivity in tissue microenvironment [21, 22].

Increasing studies have pointed out the potential contribution of human mesenchymal stem cells in the recovery of different types of tissue injury [25–28]. Although it has been demonstrated that MSCs mediate tissue repair through paracrine and transdifferentiation mechanisms, the details responsible for their roles are not well understood. Our recent studies showed that exosomes derived from human umbilical cord MSCs (hucMSCs) alleviate CCl4-induced liver fibrosis, enhance cutaneous wound healing, and repair cisplatin-induced acute kidney injury (AKI) [29–33]. In these studies,

we established a method to extract and purify exosomes from hucMSCs with ultrafiltration and gradient centrifugation. Herein, we uncovered more detailed information about this method and other functions of hucMSC-exosome *in vitro*.

2. Materials and Methods

2.1. Isolation and Purification of Exosomes. HucMSCs were isolated as previously described in our work [34]. All experiment protocols were approved by the Ethics Committee of Jiangsu University. The 70%–80% of the confluent hucMSCs cultures were washed twice with phosphate-buffered saline (PBS) and then incubated in serum-free low glucose Dulbecco's modified Eagle's medium (LG-DMEM) for 48 hours. The conditioned medium was collected and centrifuged at 1,000 ×g for 20 minutes to remove cell debris, followed by centrifugation at 2,000 ×g for 20 minutes and 10,000 ×g for 20 minutes. The supernatant was collected and concentrated using 100 KDa MWCO (Millipore, USA) at 1,000 ×g for 30 minutes. The concentrated supernatant was loaded upon 5 mL of 30% sucrose/D_2O cushions and then ultracentrifuged at 100,000 ×g for 60 minutes (optimal-90K, Beckman Coulter). The microvesicles-enriched fraction was harvested and diluted with PBS and then centrifuged thrice at 1,000 ×g for 30 minutes using 100 KDa MWCO. Finally, the purified exosomes were collected and subjected to filtration on 0.22 μm pore filter (Millipore, USA) and stored at −70°C.

2.2. Transmission Electron Microscopy. 20 μL drops of purified exosomes were adsorbed onto copper grids, placed for 1 minute at room temperature, adsorbed onto the superfluous exosomes, and stained with 30 g/L phosphotungstic acid (pH 6.8) for 5 minutes at room temperature; the sample dried under half-watt lamp. Samples were imaged using a transmission electron microscopy (FEI Tecnai 12, Philips).

2.3. SDS-PAGE Analysis and Western Blotting. For SDS-PAGE analysis, total proteins in hucMSCs and exosomes were separated on 12% SDS-polyacrylamide gels and stained with Coomassie Blue. For Western blot assay, the proteins were electroblotted onto a nitrocellulose membrane after separating on 12% SDS-PAGE. The membrane was blocked and incubated with the primary antibodies followed by incubation with the horseradish peroxidase-coupled secondary antibody. The bands were visualized with ECL plus system from Amersham Pharmacia Biotech (Buckinghamshire, UK). The sources of primary antibodies were as follows: CD9 (Bioworld Technology, USA), CD81 (Epitomics, USA), β-actin (Bioworld Technology, USA), p-ERK1/2, T-ERK1/2, p-P38, P38 (Santa Cruz Biotechnology, USA), PCNA (Bioworld Technology, USA), and GAPDH (Shanghai KangChen Biotechnology, China).

2.4. Cell Culture and Oxidative Stress Treatment. H9C2(2-1) cells were cultured in HG-DMEM with 10% fetal bovine serum (FBS, Gibco, USA). HL-7702 cells were cultured in RPMI-1640 with 20% NBS. NRK-52E cells were cultured in HG-DMEM with 10% NBS. To induce oxidative stress, H9C2(2-1), HL-7702, and NRK-52E cells were exposed to 300, 300, and 500 μM H_2O_2 for 24, 6, and 6 hours, respectively. H9C2(2-1), HL-7702, and NRK-52E cell lines were all bought from the Cell Bank of the Chinese Academy of Sciences, Shanghai.

2.5. Cell Viability. Cell viability was assessed by MTT assay ($n = 5$). 1×10^3 cells were seeded per well under normal condition and 5×10^3 cells were seeded per well under oxidative condition in 96-well plate, respectively. Then, cells were treated with different doses of hucMSCs-exosomes (100 and 800 μg/mL) for 24 and 48 hours under normal condition or pretreated with hucMSCs-exosomes (800 μg/mL) for 24 hours under oxidative condition. After incubation, the absorbance was measured at 570 nm using a microplate reader.

2.6. Cell Apoptosis. Cell apoptosis was evaluated using a terminal deoxynucleotidyl transferase mediated dUTP nick end labeling (TUNEL) assay and mitochondria membrane electric potential assay. The TUNEL assay was performed using an *in situ* cell death detection kit (Boster Bioengineering, Wuhan, China) according to the manufacturer's instructions. TUNEL-positive apoptotic cells were counted in 10 consecutive fields in the slides. The mitochondria membrane electric potential was performed using a JC-1 detection kit (Beyotime Institute of Biotechnology, Shanghai, China) according to the manufacturer's instructions. The fluorescent signal was observed under a fluorescence microscopy.

2.7. Immunohistochemistry. Immunohistochemical staining of proliferative cell nuclear antigen (PCNA) was performed using an SABC immunohistochemistry detection kit (Boster Bioengineering, Wuhan, China) according to the manufacturer's instructions. The cells were fixed, blocked, and incubated with the primary antibody (1 : 200) for 2 hours followed by the secondary antibody for 1 hour. PCNA-positive cells were counted in 10 consecutive fields in the slides.

2.8. UV Exposure. HucMSCs-exosomes were subjected to UV exposure (254 nm) for 1 hour at 4°C [35, 36]. The control was kept at 4°C for 1 hour without UV exposure. These two exosomes were then added to the cells at the concentration of 800 μg/mL and the cells were cultured under H_2O_2-induced oxidative stress.

2.9. Cytokine Array. The profile and concentration of cytokines in hucMSCs-exosomes and the conditioned medium of hucMSCs were quantified using Luminex assay.

2.10. Statistical Analysis. Data was presented as mean ± SD. Statistical variance was analyzed by ANOVA using Prism software (Graph Pad, San Diego, USA). Statistical p values less than 0.05 were considered significant.

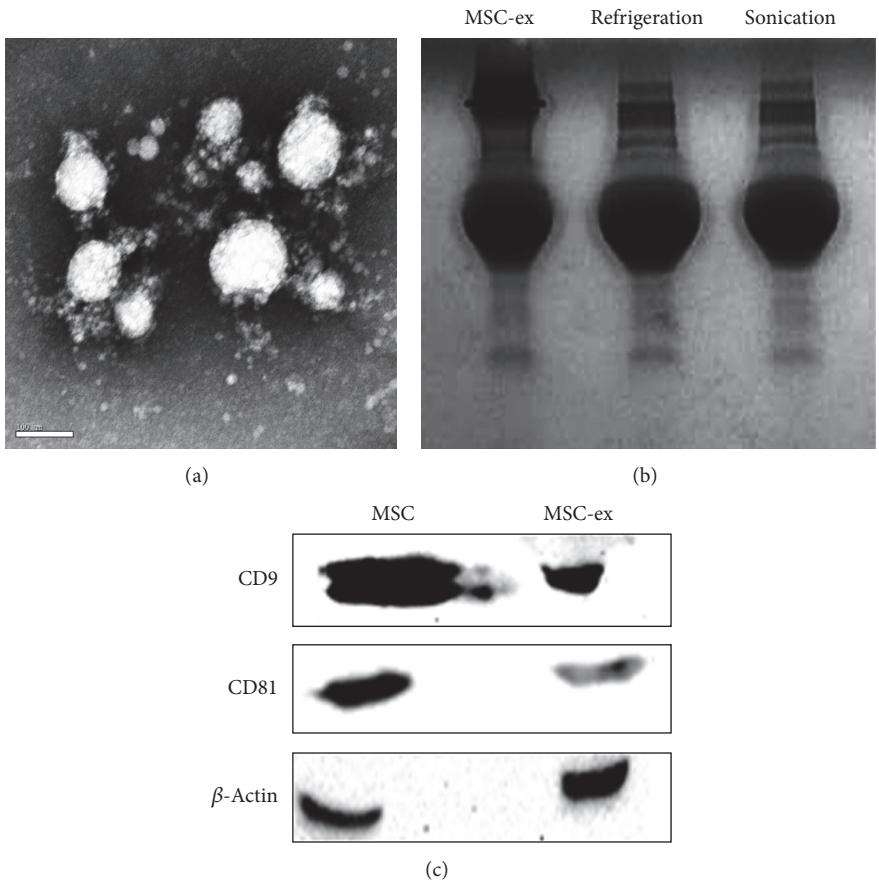

Figure 1: Characterization of exosomes from hucMSCs. (a) Transmission electron microscopy analysis of extracellular vesicles secreted by hucMSCs. Scale bar: 100 nm. (b) Coomassie Blue staining. The protein extracts of hucMSCs-exosomes were separated by SDS-PAGE. (c) Western blotting analyses of exosomal markers using antibodies against CD9 and CD81.

3. Results

3.1. Characterization of HucMSCs-Exosomes. Transmission electron microscopy analysis showed a spheroid morphology of the purified exosomes, with a mean diameter of 40–100 nm (Figure 1(a)). The protein extract of exosomes was separated on 12% SDS-PAGE gel and stained with Coomassie Blue. As shown in Figure 1(b), the extract of exosomes enriched proteins with molecular weight ranging from 55 to 72 KDa and this enrichment was not affected by refrigeration or sonication. Equal amounts of protein extracts from hucMSCs and hucMSCs-exosomes were analyzed by Western blotting using antibodies specific to CD9 and CD81, which were exosomal markers. The results showed that CD9 and CD81 were constitutively expressed in hucMSCs-exosomes (Figure 1(c)). Together, these results indicate that we have successfully isolated and identified exosomes from the extracellular medium of hucMSCs.

3.2. HucMSCs-Exosomes Stimulate Cell Proliferation In Vitro. Incubation of H9C2(2-1), HL-7702, and NRK-52E cells with hucMSCs-exosomes promoted cell proliferation in a dose- and time-dependent manner compared to the control cells which were incubated with vehicle alone (conditioned medium) (Figure 2(a)). To further demonstrate the signaling pathway regulated by exosomes, we detected the levels of total and phosphorylated ERK1/2 as this pathway is tightly linked with cell growth. The results showed that exosomes treatment resulted in an increase in the phosphorylation of ERK1/2 (Figure 2(b)), suggesting that hucMSCs-exosomes may promote cell growth through upregulation of ERK1/2 phosphorylation.

3.3. HucMSCs-Exosomes Protect Cell Viability In Vitro. Oxidative stress induced by H_2O_2 leads to loss of cell viability *in vitro*. We further test if hucMSCs-exosomes promoted cell survival under H_2O_2-induced oxidative stress. Exosomes that derived from different sources were added to the cells for 24 hours, and then the cells were exposed to oxidative stress for different periods of time and the cell viability was examined by MTT assay. As shown in Figure 3(a), H_2O_2 decreased the viability of cells, but hucMSCs-exosomes increased the percentage of cell viability compared to H_2O_2 group, suggesting that exosomes' pretreatment antagonizes H_2O_2-induced cell death. And we also found that exosome-free conditioned medium did not show the repair role as

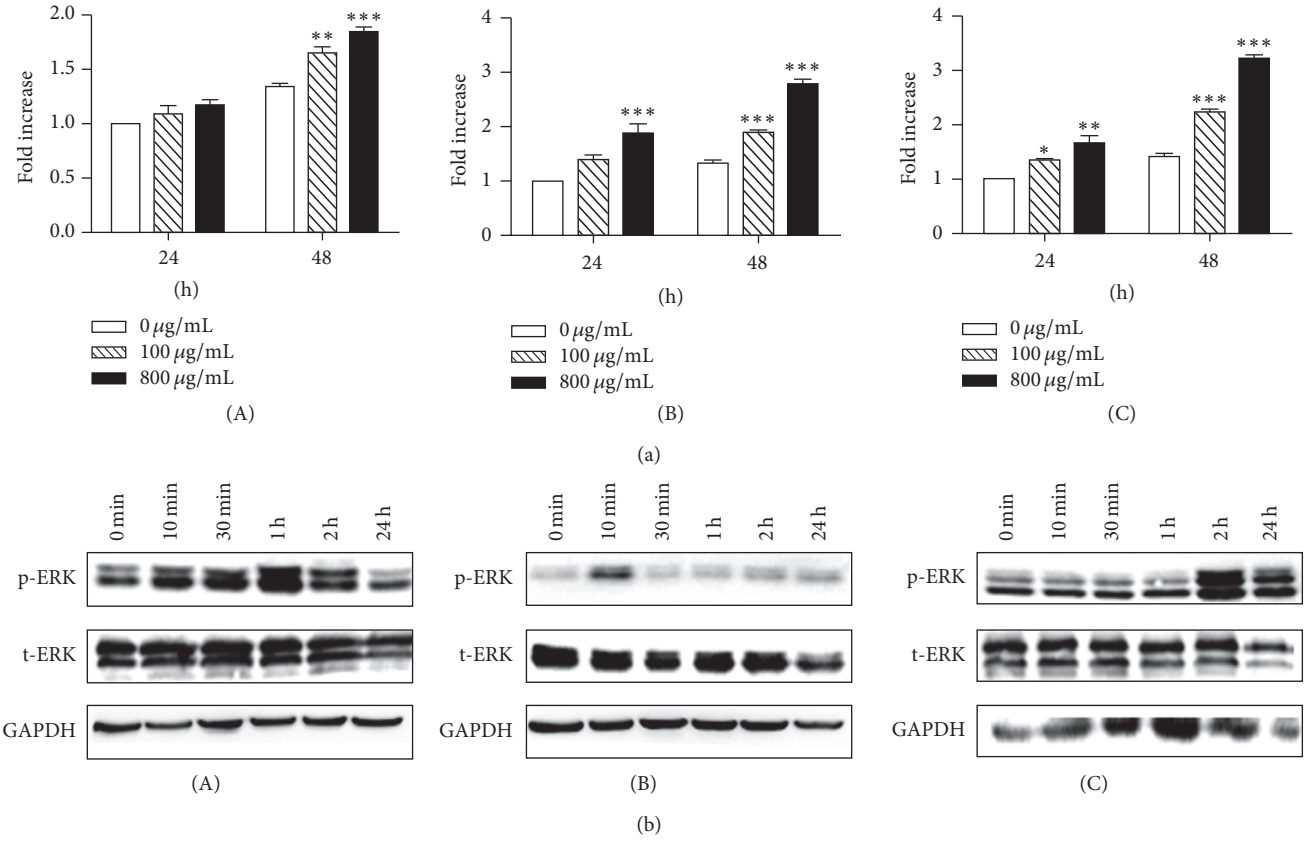

Figure 2: HucMSCs-exosomes promote cell proliferation *in vitro*. (a) HucMSCs-exosomes promote cell proliferation in a dose- and time-dependent manner. Results were shown as mean ± SD ($n = 5$). $^{*}P < 0.05$, $^{**}P < 0.01$, and $^{***}P < 0.001$ compared to control group. (b) Western blotting analysis of phosphorylated ERK1/2 in cells treated with 800 μg/mL hucMSCs-exosomes as indicated. (A) H9C2(2-1); (B) HL-7702; and (C) NRK-52E.

hucMSC-exosome and could not reverse the H_2O_2-induced inhibition of proliferation (Figure 3(b)). We confirmed that this protective role was specific to hucMSCs-exosomes as the exosomes from human fibroblast-like cells (the Cell Bank of the Chinese Academy of Sciences, Shanghai) (HFL-exosomes) did not have the protective role. Exosomal shuttle of RNA is critical for the function of exosomes. To test if the exosomes-mediated cell protection was due to the transfer of RNA to injured cells, we exposed exosomes to UV (254 nm) for 1 hour as UV exposure inactivates RNA functions. The results showed that the exosomes that exposed to UV lost their protective effects on the cell viability (Figure 3(a)). We further demonstrated that H_2O_2 treatment inhibited the phosphorylation of p38 in the cells, but pretreatment with exosomes restored the level of phosphorylated p38 (Figure 3(b)).

3.4. HucMSCs-Exosomes Promote Cell Proliferation under Oxidative Stress. We further confirmed the protective role of hucMSCs-exosomes on cell viability by immunohistochemical staining of proliferative cell nuclear antigen (PCNA). HucMSCs-exosomes were added to the cells for 24 hours, and then the cells were exposed to oxidative stress for different periods of time. The results showed that H_2O_2 treatment inhibited the percentage of proliferative cells, while exosomes' treatment abrogated this effect (Figures 4(a) and 4(b)).

3.5. HucMSCs-Exosomes Inhibit H_2O_2-Induced Apoptosis In Vitro. TUNEL staining showed that H_2O_2 treatment resulted in an increase in the percentage of apoptotic cells, but pretreatment with hucMSCs-exosomes decreased the percentage of apoptotic cells to a less extent (Figures 5(a) and 5(b)), indicating that hucMSCs-exosomes inhibited H_2O_2-induced apoptosis *in vitro*. To further demonstrate if exosomes regulated cell apoptosis pathways, we performed mitochondria membrane electric potential analysis and the results showed that H_2O_2 treatment increased the mitochondria membrane electric potential of H9C2(2-1), HL-7702, and NRK-52E cells (results not shown), while hucMSCs-exosomes treatment decreased the mitochondria membrane electric potential compared to that of H_2O_2 group (Figure 6). Collectively, hucMSCs-exosomes inhibit H_2O_2-induced apoptosis through regulating mitochondria-mediated cell apoptosis pathway.

3.6. Cytokine Profile of HucMSCs-Exosomes. Exosomes contain certain types of cytokines which may mediate its function. We then determined the concentration of cytokines

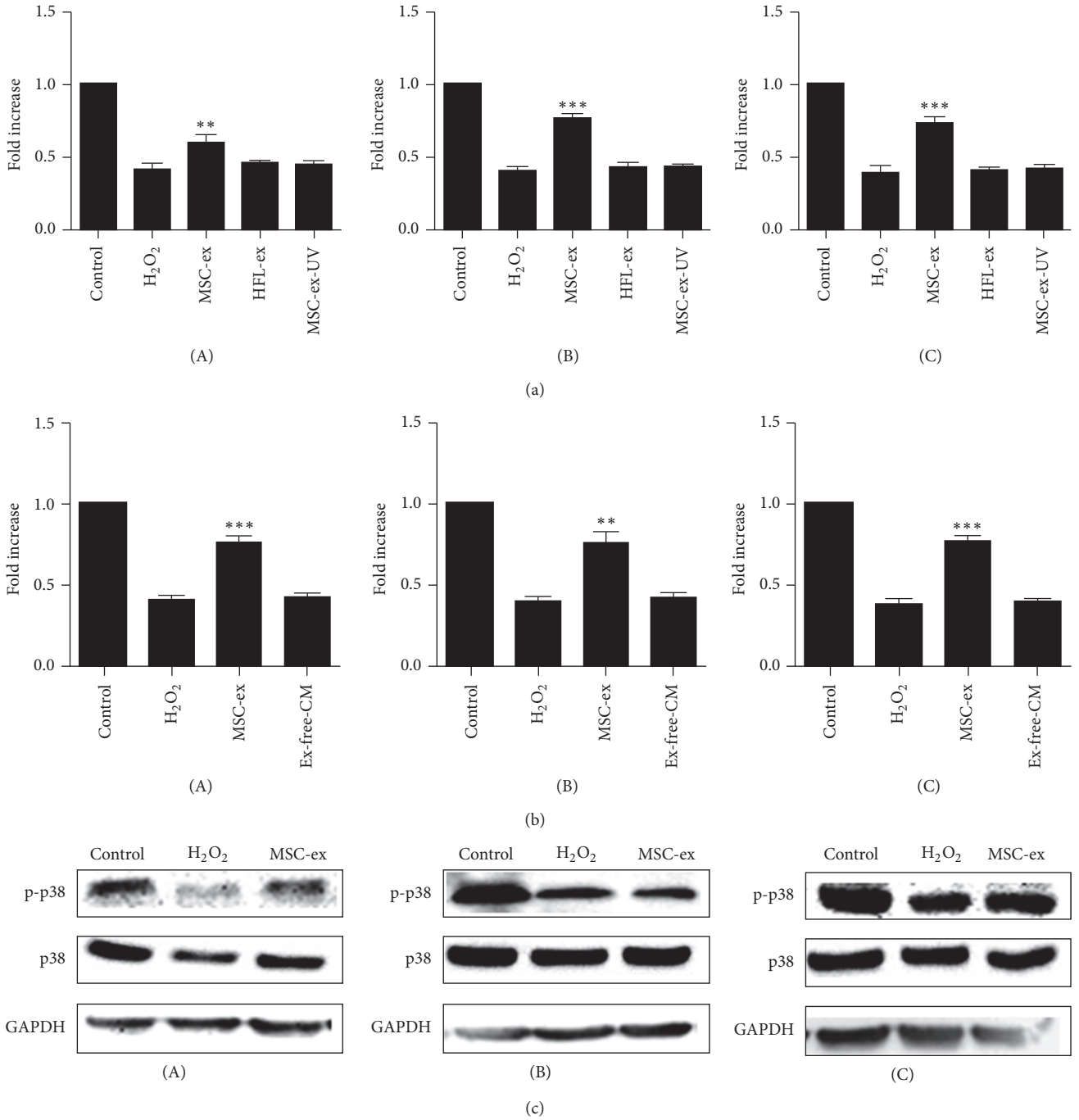

Figure 3: HucMSCs-exosomes protect cell viability *in vitro*. (a) MTT assay. H9C2(2-1), HL-7702, and NRK-52E cells were pretreated with different sources of hucMSCs-exosomes (800 μg/mL) for 24 hours, followed by exposure to H_2O_2(300 μM) for 24 hours. Results were shown as mean ± SD ($n = 5$). $^{**}p < 0.01$ and $^{***}p < 0.001$ compared to H_2O_2 group. (b) MTT assay. H9C2(2-1), HL-7702, and NRK-52E cells were pretreated with different sources of hucMSCs-exosomes (800 μg/mL) or exosomes-free conditioned medium collected from hucMSCs (EX-free-CM) for 24 hours, followed by exposure to H_2O_2 (300 μM) for 24 hours. Results were shown as mean ± SD ($n = 5$). $^{**}p < 0.01$ and $^{***}p < 0.001$ compared to H_2O_2 group. (c) Western blotting analysis of phosphorylated p38. H9C2(2-1), HL-7702, and NRK-52E cells were pretreated with hucMSCs-exosomes (800 μg/mL) followed by exposure to H_2O_2as described above.

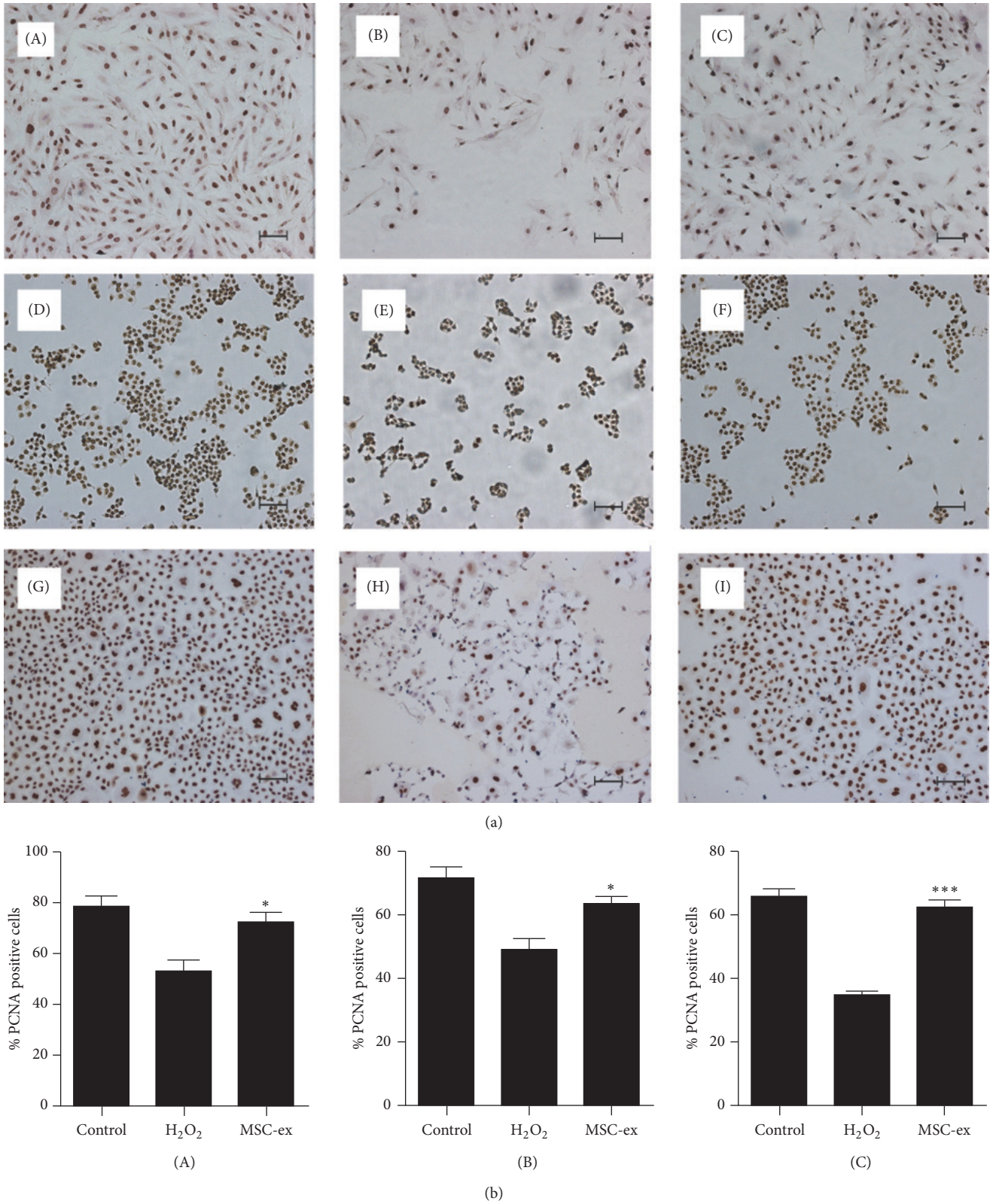

Figure 4: HucMSCs-exosomes promote cell proliferation under oxidative stress. (a) Immunohistochemical staining of proliferative cell nuclear antigen. H9C2(2-1), HL-7702, and NRK-52E cells were pretreated with hucMSCs-exosomes (800 μg/mL) for 24 hours, followed by exposure to H_2O_2(300, 300, and 500 μM) for different time points (24, 6, and 6 hours). (A–C) H9C2(2-1); (D–F) HL-7702; and (G–I) NRK-52E. Control (A, D, and G); H_2O_2 (B, E, and H); and hucMSCs-exosomes (C, F, and I). Scale bar: 100 μm. (b) Quantitative analysis of the percentage of PCNA-positive cells. $^{*}p < 0.05$ and $^{***}p < 0.001$ compared to H_2O_2 group.

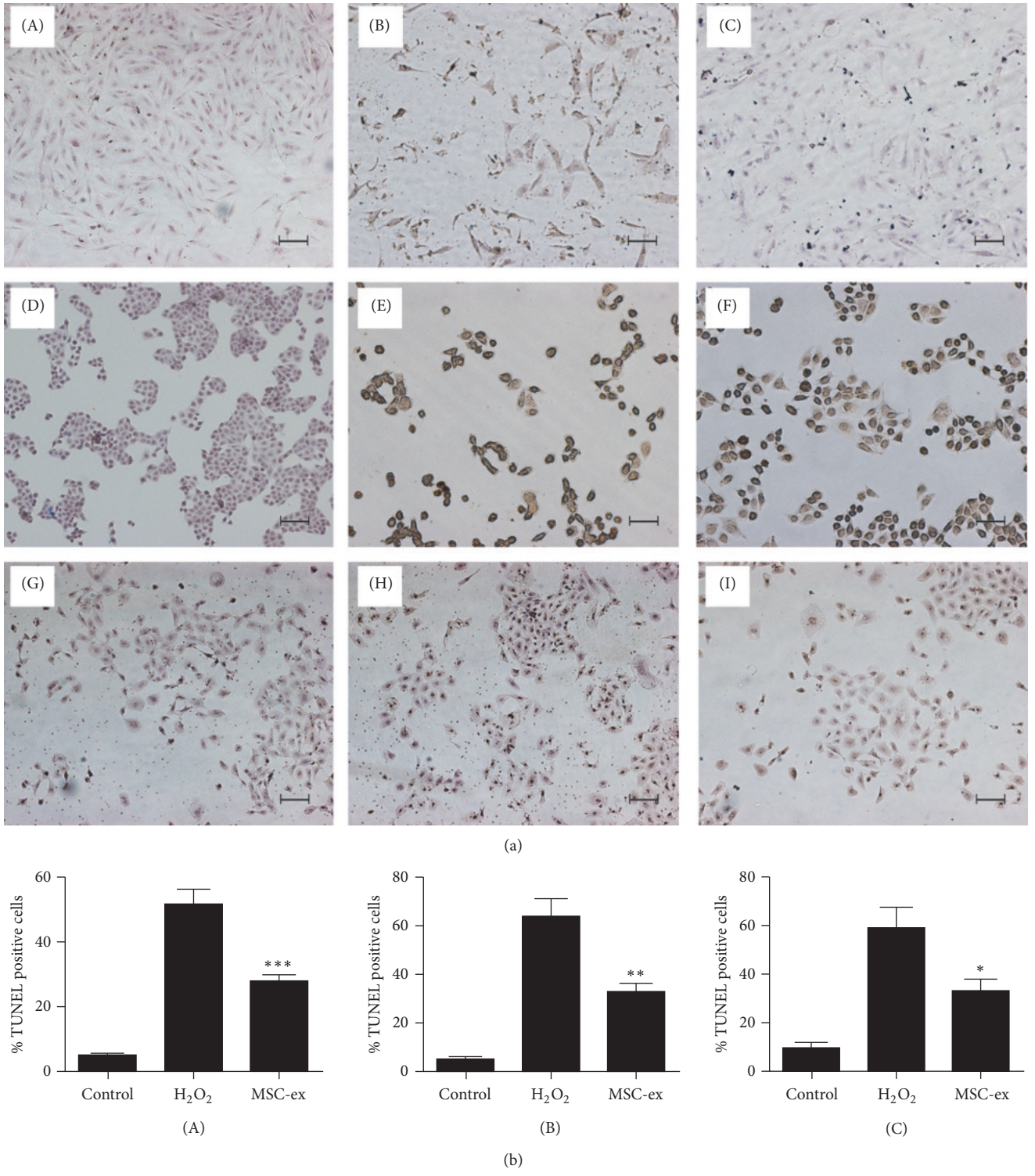

FIGURE 5: HucMSCs-exosomes inhibit H_2O_2-induced apoptosis. (a) TUNEL staining. H9C2(2-1), HL-7702, and NRK-52E cells were pretreated with hucMSCs-exosomes (800 μg/mL) for 24 hours, followed by exposure to H_2O_2(300, 300, and 500 μM) for different time points (24, 6, and 6 hours). (A–C) H9C2(2-1); (D–F) HL-7702; and (G–I) NRK-52E. Control (A, D, and G); H_2O_2 (B, E, and H); hucMSCs-exosomes (C, F, and I). Scale bar: 100 μm. (b) Quantitative analysis of the percentage of TUNEL-positive cells. $^*P < 0.05$ compared to H_2O_2 group.

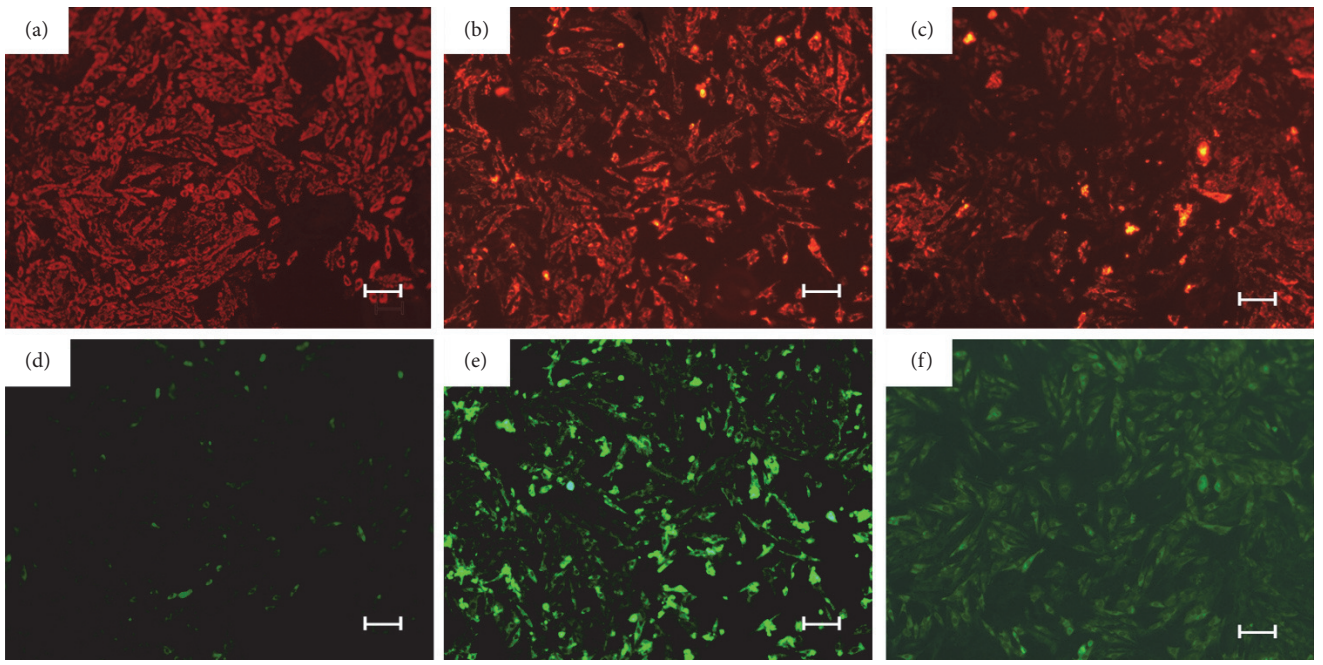

Figure 6: HucMSCs-exosomes inhibit H_2O_2-induced mitochondria activation. H9C2(2-1) were pretreated with hucMSCs-exosomes (800 μg/mL) for 24 hours, followed by exposure to H_2O_2(300 μM) for 24 hours. The cells were subjected to JC-1 staining for 15 min. The signals were observed under fluorescence microscope. Control (a, d); H_2O_2(b, e); and hucMSCs-exosomes (c, f).

Table 1: Identification of cytokine from hucMSCs-exosomes and hucMSCs using Luminex.

Cytokine name	HucMSCs-exosomes (pg/mL)	HucMSCs (pg/mL)
GM-CSF	1.75	8.94
IL-15	4.02	0.51
IL-17	<0	<0
IL-6	123.57	649.96
IL-8	285.26	5024.88
TNF-α	0.02	0.11
IL-β	0.05	0.31
IL-2	0.06	0.21
EGF	<0	3.54
IL-10	0.74	0.73
VEGF	<0	13.65

in hucMSCs-exosomes and the conditioned medium of hucMSCs by Luminex assay ($n = 3$). The results showed that hucMSCs-exosomes expressed a lot of cytokines including GM-CSF, IL-15, IL-6, IL-8, TNF-α, IL-1β, IL-2, and IL-10 (Table 1), in which IL-6 and IL-8 were present in high dose (>100 pg/mL).

4. Discussion

In this study, we have isolated and identified exosomes from human umbilical cord MSCs in terms of their biophysical and biological properties: (1) floating at a cushion of 30% sucrose that is a specific attribute of exosomes; (2) nanometer-sized distribution of exosomes (40–100 nm); and (3) exosomal protein expression (CD9 and CD81) [17–20]. Our results confirmed that the microvesicles we isolated from the extracellular medium of hucMSCs were exosomes. The method we established is a practical and efficient procedure to isolate and purify exosomes from hucMSCs.

The exact functions of exosomes are not yet fully understood, although exosomes harvested from different cells have been shown to mediate a multitude of biological effects, including antigen presentation, induction of apoptosis, and promotion of cancer cell growth [6, 37–42]. It seems that the exosomes from different cells have various functions. In the current study, we demonstrated that exosomes derived from hucMSCs had stimulatory effect on cell proliferation and protective role against H_2O_2-induced cell death [43], suggesting that the exosomes from hucMSCs prepared using our procedure are bioactive and have supportive role in the growth of cells such as cardiomyocytes, hepatocytes, and renal cells.

The work from different laboratories has indicated that the release of exosomes is a mechanism by which cells transfer material and signals to other cells. Exosomes are round membrane vesicles. The nucleic acid and proteins in the exosomes are protected by the membrane structure. Exosomes have a particular composition reflecting their origin and can transfer not only membrane components but also nucleic acid between different cells. UV exposure of exosomes abrogated their effects on preventing oxidative stress-induced cell death, suggesting that the RNA shuttled by exosomes is one of the critical effectors of their biological effects. We also verify that the exosomes contain several types

of cytokines, in which IL-6 and IL-8 are the major ones. Further studies are required to define the physiological role of these cytokines in hucMSCs-exosomes.

The advantage of using exosomes in regenerative medicine rather than the stem cells themselves is avoidance of possible long-term pathologic differentiation of engrafted cells. Compared to cell-based therapies, non-cell-based therapies are generally easier to manufacture and safer as they are nonviable and do not elicit immune rejection. Therefore, the isolation and identification of exosomes from hucMSCs provide a novel approach to treat diseases such as myocardial ischemia/reperfusion injury.

In addition to their tissue regenerative capacity, MSCs and their exosome also display immune-modulatory properties [44, 45]. MSCs constitutively express low levels of major histocompatibility complex-I molecules and do not express costimulatory molecules such as CD80, CD86, or CD40, thus lacking immunogenicity [46]. Based on these properties, MSCs are being used in the treatment of autoimmune diseases and graft-versus-host disease. The earliest indications of the immunosuppressive nature of MSC were derived from studies with human, baboon, and murine MSC demonstrating that MSCs were able to suppress T-lymphocyte activation and proliferation *in vitro* [46–49]. MSCs inhibit immunoglobulin production and arrest B-lymphocytes in the G0/G1 phase of the cell cycle [50]. In conclusion, MSCs possess a remarkably diverse array of immunosuppressive characteristics [51]. MSCs-exosomes might play a different role in immune-modulating activities and mechanisms. Rahman et al. reported that abnormal or excess exosomes released by these MSC-like precursor cells in islets may trigger tissue-specific autoimmunity in the NOD mouse strain [52]. MSC-derived extracellular vesicles also prevent postischemic immunosuppression [45]. These two studies hold the review that MSC-exosome can enhance the activation of immunity. However, other groups believed that MSC-exosome inhibited the inflammatory response to induce tissue regeneration. MSCs-derived exosome suppressed the secretion of proinflammatory factors TNF-α and IL-1β but increased the concentration of anti-inflammatory factor TGF-β [53]. Zhang et al. considered that MSC-secreted exosome has the potential to attenuate an activated immune system through the induction of anti-inflammatory cytokines and Tregs [54]. The aforementioned studies show that immune regulation may also be an important mechanism of exosome in tissue regeneration.

In conclusion, in this study, we have established a practical and efficient method to isolate and identify exosomes from human umbilical cord stem cells and demonstrated the role of hucMSCs-exosomes in stimulating cell proliferation and protecting against oxidative stress-induced apoptosis. Our work provides a basis for further evaluating the potential of hucMSCs-exosomes as therapeutic agents.

Competing Interests

The authors declare that they have no competing interests.

Authors' Contributions

Bin Zhang, Li Shen, and Hui Shi contributed equally to this work.

Acknowledgments

This work was supported by the National Natural Science Foundation of China (Grants nos. 31340040, 81272481, 81270214, 81572075, 81670549, and 81670502), Jiangsu Province for Outstanding Sci-Tech Innovation Team in Colleges and Universities (Grant SJK2013-10), Jiangsu Province's Outstanding Medical Academic Leader and Sci-Tech Innovation Team Program (Grant no. LJ201117), and the Priority Academic Program Development of Jiangsu Higher Education Institutions.

References

[1] R. M. Johnstone, M. Adam, J. R. Hammond, L. Orr, and C. Turbide, "Vesicle formation during reticulocyte maturation. Association of plasma membrane activities with released vesicles (exosomes)," *The Journal of Biological Chemistry*, vol. 262, no. 19, pp. 9412–9420, 1987.

[2] B.-T. Pan, K. Teng, C. Wu, M. Adam, and R. M. Johnstone, "Electron microscopic evidence for externalization of the transferrin receptor in vesicular form in sheep reticulocytes," *Journal of Cell Biology*, vol. 101, no. 3, pp. 942–948, 1985.

[3] B.-T. Pan and R. M. Johnstone, "Fate of the transferrin receptor during maturation of sheep reticulocytes in vitro: selective externalization of the receptor," *Cell*, vol. 33, no. 3, pp. 967–978, 1983.

[4] N. Chaput, J. Taïeb, N. E. C. Schartz, F. André, E. Angevin, and L. Zitvogel, "Exosome-based immunotherapy," *Cancer Immunology, Immunotherapy*, vol. 53, no. 3, pp. 234–239, 2004.

[5] C. Théry, L. Zitvogel, and S. Amigorena, "Exosomes: composition, biogenesis and function," *Nature Reviews Immunology*, vol. 2, no. 8, pp. 569–579, 2002.

[6] G. Raposo, H. W. Nijman, W. Stoorvogel et al., "B lymphocytes secrete antigen-presenting vesicles," *The Journal of Experimental Medicine*, vol. 183, no. 3, pp. 1161–1172, 1996.

[7] L. Zitvogel, A. Regnault, A. Lozier et al., "Eradication of established murine tumors using a novel cell-free vaccine: dendritic cell-derived exosomes," *Nature Medicine*, vol. 4, no. 5, pp. 594–600, 1998.

[8] C. Théry, A. Regnault, J. Garin et al., "Molecular characterization of dendritic cell-derived exosomes. Selective accumulation of the heat shock protein hsc73," *The Journal of Cell Biology*, vol. 147, no. 3, pp. 599–610, 1999.

[9] N. Blanchard, D. Lankar, F. Faure et al., "TCR activation of human T cells induces the production of exosomes bearing the TCR/CD3/ζ complex," *Journal of Immunology*, vol. 168, no. 7, pp. 3235–3241, 2002.

[10] J. Wolfers, A. Lozier, G. Raposo et al., "Tumor-derived exosomes are a source of shared tumor rejection antigens for CTL cross-priming," *Nature Medicine*, vol. 7, no. 3, pp. 297–303, 2001.

[11] F. Andre, N. E. C. Schartz, M. Movassagh et al., "Malignant effusions and immunogenic tumour-derived exosomes," *The Lancet*, vol. 360, no. 9329, pp. 295–305, 2002.

[12] M.-P. Caby, D. Lankar, C. Vincendeau-Scherrer, G. Raposo, and C. Bonnerot, "Exosomal-like vesicles are present in human

blood plasma," *International Immunology*, vol. 17, no. 7, pp. 879–887, 2005.

[13] T. Pisitkun, R.-F. Shen, and M. A. Knepper, "Identification and proteomic profiling of exosomes in human urine," *Proceedings of the National Academy of Sciences of the United States of America*, vol. 101, no. 36, pp. 13368–13373, 2004.

[14] V. Palanisamy, S. Sharma, A. Deshpande, H. Zhou, J. Gimzewski, and D. T. Wong, "Nanostructural and transcriptomic analyses of human saliva derived exosomes," *PLoS ONE*, vol. 5, no. 1, article e8577, 2010.

[15] C. Admyre, S. M. Johansson, K. R. Qazi et al., "Exosomes with immune modulatory features are present in human breast milk," *The Journal of Immunology*, vol. 179, no. 3, pp. 1969–1978, 2007.

[16] C. Admyre, J. Grunewald, J. Thyberg et al., "Exosomes with major histocompatibility complex class II and co-stimulatory molecules are present in human BAL fluid," *The European Respiratory Journal*, vol. 22, no. 4, pp. 578–583, 2003.

[17] C. Olver and M. Vidal, "Proteomic analysis of secreted exosomes," *Sub-Cellular Biochemistry*, vol. 43, pp. 99–131, 2007.

[18] S. Keller, M. P. Sanderson, A. Stoeck, and P. Altevogt, "Exosomes: from biogenesis and secretion to biological function," *Immunology Letters*, vol. 107, no. 2, pp. 102–108, 2006.

[19] H. Valadi, K. Ekström, A. Bossios, M. Sjöstrand, J. J. Lee, and J. O. Lötvall, "Exosome-mediated transfer of mRNAs and microRNAs is a novel mechanism of genetic exchange between cells," *Nature Cell Biology*, vol. 9, no. 6, pp. 654–659, 2007.

[20] W. Stoorvogel, M. J. Kleijmeer, H. J. Geuze, and G. Raposo, "The biogenesis and functions of exosomes," *Traffic*, vol. 3, no. 5, pp. 321–330, 2002.

[21] M. Simons and G. Raposo, "Exosomes—vesicular carriers for intercellular communication," *Current Opinion in Cell Biology*, vol. 21, no. 4, pp. 575–581, 2009.

[22] E. Pap, É. Pállinger, M. Pásztói, and A. Falus, "Highlights of a new type of intercellular communication: microvesicle-based information transfer," *Inflammation Research*, vol. 58, no. 1, pp. 1–8, 2009.

[23] T. S. Chen, R. C. Lai, M. M. Lee, A. B. H. Choo, C. N. Lee, and S. K. Lim, "Mesenchymal stem cell secretes microparticles enriched in pre-microRNAs," *Nucleic Acids Research*, vol. 38, no. 1, pp. 215–224, 2009.

[24] W. Koh, C. T. Sheng, B. Tan et al., "Analysis of deep sequencing microRNA expression profile from human embryonic stem cells derived mesenchymal stem cells reveals possible role of let-7 microRNA family in downstream targeting of hepatic nuclear factor 4 alpha," *BMC Genomics*, vol. 11, supplement 1, article S6, 2010.

[25] L. Sun, D. Wang, J. Liang et al., "Umbilical cord mesenchymal stem cell transplantation in severe and refractory systemic lupus erythematosus," *Arthritis & Rheumatism*, vol. 62, no. 8, pp. 2467–2475, 2010.

[26] Y. Chen, H. Qian, W. Zhu et al., "Hepatocyte growth factor modification promotes the amelioration effects of human umbilical cord mesenchymal stem cells on rat acute kidney injury," *Stem Cells and Development*, vol. 20, no. 1, pp. 103–113, 2011.

[27] H. Cao, H. Qian, W. Xu et al., "Mesenchymal stem cells derived from human umbilical cord ameliorate ischemia/reperfusion-induced acute renal failure in rats," *Biotechnology Letters*, vol. 32, no. 5, pp. 725–732, 2010.

[28] Y. Yan, W. Xu, H. Qian et al., "Mesenchymal stem cells from human umbilical cords ameliorate mouse hepatic injury in vivo," *Liver International*, vol. 29, no. 3, pp. 356–365, 2009.

[29] T. Li, Y. Yan, B. Wang et al., "Exosomes derived from human umbilical cord mesenchymal stem cells alleviate liver fibrosis," *Stem Cells and Development*, vol. 22, no. 6, pp. 845–854, 2013.

[30] B. Zhang, M. Wang, A. Gong et al., "HucMSc-exosome mediated-Wnt4 signaling is required for cutaneous wound healing," *Stem Cells*, vol. 33, no. 7, pp. 2158–2168, 2015.

[31] B. Zhang, X. Wu, X. Zhang et al., "Human umbilical cord mesenchymal stem cell exosomes enhance angiogenesis through the Wnt4/β-catenin pathway," *Stem Cells Translational Medicine*, vol. 4, no. 5, pp. 513–522, 2015.

[32] Y. Zhou, H. Xu, W. Xu et al., "Exosomes released by human umbilical cord mesenchymal stem cells protect against cisplatin-induced renal oxidative stress and apoptosis *in vivo* and *in vitro*," *Stem Cell Research & Therapy*, vol. 4, no. 2, article 34, 2013.

[33] Y. Zhao, X. Sun, W. Cao et al., "Exosomes derived from human umbilical cord mesenchymal stem cells relieve acute myocardial ischemic injury," *Stem Cells International*, vol. 2015, Article ID 761643, 12 pages, 2015.

[34] C. Qiao, W. Xu, W. Zhu et al., "Human mesenchymal stem cells isolated from the umbilical cord," *Cell Biology International*, vol. 32, no. 1, pp. 8–15, 2008.

[35] H. Ponta, M.-L. Pfennig-Yeh, E. F. Wagner, M. Schweiger, and P. Herrlich, "Radiation sensitivity of messenger RNA," *Molecular & General Genetics*, vol. 175, no. 1, pp. 13–17, 1979.

[36] E. J. Wurtmann and S. L. Wolin, "RNA under attack: cellular handling of RNA damage," *Critical Reviews in Biochemistry and Molecular Biology*, vol. 44, no. 1, pp. 34–49, 2009.

[37] G. Camussi, M. C. Deregibus, and C. Tetta, "Paracrine/endocrine mechanism of stem cells on kidney repair: role of microvesicle-mediated transfer of genetic information," *Current Opinion in Nephrology and Hypertension*, vol. 19, no. 1, pp. 7–12, 2010.

[38] M. Eldh, K. Ekström, H. Valadi et al., "Exosomes communicate protective messages during oxidative stress; possible role of exosomal shuttle RNA," *PLoS ONE*, vol. 5, no. 12, Article ID e15353, 2010.

[39] W. Zhu, L. Huang, Y. Li et al., "Exosomes derived from human bone marrow mesenchymal stem cells promote tumor growth in vivo," *Cancer Letters*, vol. 315, no. 1, pp. 28–37, 2012.

[40] C. Admyre, S. M. Johansson, S. Paulie, and S. Gabrielsson, "Direct exosome stimulation of peripheral human T cells detected by ELISPOT," *European Journal of Immunology*, vol. 36, no. 7, pp. 1772–1781, 2006.

[41] M. Karlsson, S. Lundin, U. Dahlgren, H. Kahu, I. Pettersson, and E. Telemo, "'Tolerosomes' are produced by intestinal epithelial cells," *European Journal of Immunology*, vol. 31, no. 10, pp. 2892–2900, 2001.

[42] A. Clayton and Z. Tabi, "Exosomes and the MICA-NKG2D system in cancer," *Blood Cells, Molecules, & Diseases*, vol. 34, no. 3, pp. 206–213, 2005.

[43] M. Takeda, I. Shirato, M. Kobayashi, and H. Endou, "Hydrogen peroxide induces necrosis, apoptosis, oncosis and apoptotic oncosis of mouse terminal proximal straight tubule cells," *Nephron*, vol. 81, no. 2, pp. 234–238, 1999.

[44] G. Maria Spaggiari and L. Moretta, "Cellular and molecular interactions of mesenchymal stem cells in innate immunity," *Immunology and Cell Biology*, vol. 91, no. 1, pp. 27–31, 2013.

[45] T. R. Doeppner, J. Herz, A. Görgens et al., "Extracellular vesicles improve post-stroke neuroregeneration and prevent postischemic immunosuppression," *Stem Cells Translational Medicine*, vol. 4, no. 10, pp. 1131–1143, 2015.

[46] C. Herrero and J. A. Perez-Simon, "Immunomodulatory effect of mesenchymal stem cells," *Brazilian Journal of Medical and Biological Research*, vol. 43, no. 5, pp. 425–430, 2010.

[47] A. Bartholomew, C. Sturgeon, M. Siatskas et al., "Mesenchymal stem cells suppress lymphocyte proliferation in vitro and prolong skin graft survival in vivo," *Experimental Hematology*, vol. 30, no. 1, pp. 42–48, 2002.

[48] M. Di Nicola, C. Carlo-Stella, M. Magni et al., "Human bone marrow stromal cells suppress T-lymphocyte proliferation induced by cellular or nonspecific mitogenic stimuli," *Blood*, vol. 99, no. 10, pp. 3838–3843, 2002.

[49] S. Glennie, I. Soeiro, P. J. Dyson, E. W.-F. Lam, and F. Dazzi, "Bone marrow mesenchymal stem cells induce division arrest anergy of activated T cells," *Blood*, vol. 105, no. 7, pp. 2821–2827, 2005.

[50] A. Corcione, F. Benvenuto, E. Ferretti et al., "Human mesenchymal stem cells modulate B-cell functions," *Blood*, vol. 107, no. 1, pp. 367–372, 2006.

[51] K. English and B. P. Mahon, "Allogeneic mesenchymal stem cells: agents of immune modulation," *Journal of Cellular Biochemistry*, vol. 112, no. 8, pp. 1963–1968, 2011.

[52] M. J. Rahman, D. Regn, R. Bashratyan, and Y. D. Dai, "Exosomes released by islet-derived mesenchymal stem cells trigger autoimmune responses in NOD mice," *Diabetes*, vol. 63, no. 3, pp. 1008–1020, 2014.

[53] W. Chen, Y. Huang, J. Han et al., "Immunomodulatory effects of mesenchymal stromal cells-derived exosome," *Immunologic Research*, vol. 64, no. 4, pp. 831–840, 2016.

[54] B. Zhang, Y. Yin, R. C. Lai, S. S. Tan, A. B. H. Choo, and S. K. Lim, "Mesenchymal stem cells secrete immunologically active exosomes," *Stem Cells and Development*, vol. 23, no. 11, pp. 1233–1244, 2014.

Hindawi Publishing Corporation
Stem Cells International
Volume 2016, Article ID 3865315, 14 pages
http://dx.doi.org/10.1155/2016/3865315

Research Article

PS1/γ-Secretase-Mediated Cadherin Cleavage Induces β-Catenin Nuclear Translocation and Osteogenic Differentiation of Human Bone Marrow Stromal Cells

Danielle C. Bonfim,[1,2] Rhayra B. Dias,[1,2] Anneliese Fortuna-Costa,[2,3] Leonardo Chicaybam,[4,5] Daiana V. Lopes,[1,2] Hélio S. Dutra,[1,2] Radovan Borojevic,[1,2] Martin Bonamino,[4] Claudia Mermelstein,[1] and Maria Isabel D. Rossi[1,2]

[1] *Institute of Biomedical Sciences, Federal University of Rio de Janeiro, Rio de Janeiro, RJ, Brazil*
[2] *Clementino Fraga Filho University Hospital, Federal University of Rio de Janeiro, Rio de Janeiro, RJ, Brazil*
[3] *Institute of Medical Biochemistry, National Institute of Cancer, Rio de Janeiro, RJ, Brazil*
[4] *Molecular Carcinogenesis Program, National Institute of Cancer, Rio de Janeiro, RJ, Brazil*
[5] *Evandro Chagas Clinical Research Institute, Oswaldo Cruz Institute (FIOCRUZ), Rio de Janeiro, RJ, Brazil*

Correspondence should be addressed to Maria Isabel D. Rossi; idrossi@hucff.ufrj.br

Received 12 September 2016; Accepted 1 November 2016

Academic Editor: Andrea Ballini

Bone marrow stromal cells (BMSCs) are considered a promising tool for bone bioengineering. However, the mechanisms controlling osteoblastic commitment are still unclear. Osteogenic differentiation of BMSCs requires the activation of β-catenin signaling, classically known to be regulated by the canonical Wnt pathway. However, BMSCs treatment with canonical Wnts *in vitro* does not always result in osteogenic differentiation and evidence indicates that a more complex signaling pathway, involving cadherins, would be required to induce β-catenin signaling in these cells. Here we showed that Wnt3a alone did not induce TCF activation in BMSCs, maintaining the cells at a proliferative state. On the other hand, we verified that, upon BMSCs osteoinduction with dexamethasone, cadherins were cleaved by the PS1/γ-secretase complex at the plasma membrane, and this event was associated with an enhanced β-catenin translocation to the nucleus and signaling. When PS1/γ-secretase activity was inhibited, the osteogenic process was impaired. Altogether, we provide evidence that PS1/γ-secretase-mediated cadherin cleavage has as an important role in controlling β-catenin signaling during the onset of BMSCs osteogenic differentiation, as part of a complex signaling pathway responsible for cell fate decision. A comprehensive map of these pathways might contribute to the development of strategies to improve bone repair.

1. Introduction

Human bone marrow stromal cells (BMSCs) constitute a heterogeneous population of clonogenic progenitors [1], characterized *in vitro* by the expression of CD90, CD73, CD105, CD146, and the ability to differentiate into osteoblasts, chondrocytes, and adipocytes [2–4]. Due to their proliferative capacity and differentiation potential, BMSCs are envisioned as a tool for bone bioengineering [5, 6]. However, the mechanisms that direct differentiation towards osteoblasts are still not fully understood.

Developmental studies using mice models showed that the differentiation of mesenchymal progenitors into the osteoblastic lineage requires the upregulation of Runx-2 [7, 8] downstream of β-catenin signaling [9, 10]. This pathway is classically known to be activated by receptor-mediated canonical Wnt signaling, which turns off the β-catenin destruction complex composed by GSK3β (Glycogen synthase kinase), Axin, and APC (Adenomatous Polyposis Coli) [11, 12]. Under these circumstances, β-catenin translocates to the nucleus, where it forms a complex with TCF/LEF (T Cell Factor/Lymphoid Enhancer

Factor) transcription factors to activate gene transcription [11–14].

Nevertheless, attempts to osteoinduce BMSCs with canonical Wnt proteins have shown contradictory results. While some studies showed enhanced osteogenic differentiation [15, 16], others reported increased cell proliferation and impaired differentiation [17, 18]. A possible explanation to these findings came from the observation that the Wnt coreceptor LRP5/6 (low-density lipoprotein receptor-related protein) is frequently associated with the adhesion protein N-cadherin in osteoprogenitor cells, which prevents its activation and the transduction of Wnt signaling [19]. In this way, a more complex transduction signaling pathway, involving the regulation of cadherins, would be required to induce β-catenin signaling in these cells [20]. Indeed, sustained N-cadherin expression in osteoprogenitors has been associated to maintenance of the "undifferentiated" state [21–25], and its downmodulation was observed during the progression of osteogenic differentiation *in vitro* and *in vivo* [21, 23, 26–28]. However, how cadherin modulation allows progression towards the osteogenic differentiation pathway is still under scrutiny.

One of the mechanisms that control cadherin stability in the plasma membrane is the proteolytic cleavage mediated by matrix metalloproteases (MMP) and Presenilin-1 (PS1)/γ-secretase, an enzymatic complex involved in the proteolysis of several transmembrane proteins, such as Notch [29–34]. Following the cleavage of the amino-terminal domain by a MMP, the membrane-associated, C-terminal fragment (CTF-1) of the cadherin molecule is subsequently cleaved by PS1/γ-secretase, generating a second fragment (CTF-2) that is released in the cytosol [30, 34–37]. In vascular smooth cells and embryonic fibroblasts, cadherin cleavage resulted in the release of β-catenin from cadherin complexes, followed by its nuclear translocation, which altered cellular functions such as proliferation [38] and migration [39].

Here we evaluated whether cadherin cleavage would occur during BMSCs osteoinduction, as a mechanism regulating β-catenin signaling function. We also evaluated the effects of isolated Wnt3a treatment in β-catenin-mediated signaling and BMSCs behavior. A comprehensive map of the net of signaling pathways controlling BMSCs osteogenic differentiation will be a fundamental step for the development of strategies for bone repair.

2. Materials and Methods

2.1. Samples and Cells. Iliac crest bone marrow aspirates were obtained from healthy donors at the Bone Marrow Transplant Unit, Hematology Service of the Clementino Fraga Filho University Hospital (HUCFF), at the Federal University of Rio de Janeiro, Rio de Janeiro, RJ, Brazil. All protocols and experimental procedures were approved by the Investigational Review Board at HUCFF. Mouse Wnt3a transfected L cells (L-Wnt3a) were obtained from the American Type Culture Collection (ATCC, Manassas, VA). Human breast cancer cell line MDA-MB-231 was obtained from the Rio de Janeiro Cell Bank (BCRJ, Rio de Janeiro, RJ, Brazil).

2.2. Antibodies and Reagents. The following primary antibodies were used: rabbit anti-Pan-cadherin (C3678, Sigma-Aldrich, St. Louis, MO) that recognizes the conserved C-terminal domain of classic cadherins, mouse anti-N-cadherin (clone 32) and anti-E-cadherin (clone 36), both from BD Biosciences (Franklin Lakes, New Jersey, USA), rabbit anti-β-catenin (Invitrogen-Molecular Probes, Carlsbad, CA), mouse anti-active-β-catenin (clone 8E7, Millipore, Billerica, MA, USA), mouse anti-lamin A\C (BD Biosciences), and mouse anti-α-tubulin (clone DM1a, Sigma-Aldrich). Secondary antibodies were Alexa Fluor™ 488 goat anti-rabbit IgG, Alexa Fluor™ 546 rabbit anti-mouse IgG (Invitrogen, Life Technologies, Brazil, São Paulo, SP, Brazil), and peroxidase-conjugated goat anti-rabbit and rabbit anti-mouse (Promega, Madison, WI). DAPI dihydrochloride (Invitrogen) was used for nuclear staining. The γ-secretase activity inhibitor Dapt (N-N[-(3,5-Difluorophenacetyl-l-alanyl)]-S-phenylglycine-t-butyl-ester) was from Merck Biosciences (Darmstadt, Germany). Nuclear and cytoplasmic fractions were extracted using NE-PER® Nuclear and Cytoplasmic Extraction Reagents (Pierce Biotechnology, Rockford, IL).

2.3. Isolation and Culture of Human Bone Marrow Stromal Cells (BMSCs). BMSCs were isolated as previously described [40]. Bone marrow collection kits were washed with phosphate buffered saline (PBS) after bone marrow aspirates were transferred to infusion bags. Cell suspensions were diluted 6 : 1 in Hespan® (hydroxyethyl starch saline, American Hospital Supply Corp., McGaw Park, IL) and incubated for 30 min at room temperature (RT) for hemosedimentation. Supernatants were collected, washed with PBS, plated at 1.0×10^6 cells/mL in Dulbecco's medium (DMEM low-glucose, LGC, São Paulo, SP, Brazil) supplemented with 10% fetal bovine serum (FBS, Cultilab, Campinas, SP, Brazil) and antibiotics (100 U/mL of penicillin and 100 mg/mL of streptomycin, both from Sigma-Aldrich, St. Louis, USA), and incubated at 37°C in a humidified atmosphere containing 5% CO_2. After 3 days, nonadherent cells were removed, and adherent cells were washed with PBS and maintained until 70% confluence. Cells were harvested by enzymatic digestion with 0.125% trypsin and 0.78 mM EDTA (both from Sigma-Aldrich) and expanded in DMEM with 10% FBS and antibiotics (expansion medium, EM).

2.4. Mouse L-Cell Culture and Wnt3a-Conditioned Medium Preparation. L cells were cultured in DMEM supplemented with 10% FBS and 0.4 mg/mL neomycin (Invitrogen) to maintain transgene expression during cell culture expansion. Conditioned medium from L-Wnt3a was collected according to the manufacturer's instructions and as described [41]. Briefly, 1.3×10^6 cells were plated in 75 cm^2 culture flasks with 14 mL of medium without antibiotics and left to grow for four days. The first batch of medium was collected and replaced with 14 mL of fresh medium for another three days. The second batch of medium was then collected and the cells discarded. Both batches were mixed, sterile-filtered (0.22 μm), and stored at −20°C. The presence of Wnt3a

protein in medium obtained with the same cell lineage used in this study has been shown previously in [42]. Activity of the conditioned medium was tested by the TCF/LEF luciferase reporter assay using MDA-MB-231 cells as described below and in previous studies of our group, using both HEK 293T cells and myoblasts [41, 42].

2.5. Osteogenic and Adipogenic Differentiation. BMSCs were plated at 2.5×10^4 cells/cm^2 and cultured in EM until confluence. Osteogenic differentiation was induced after the cells reached confluence. Cells were maintained for up to 21 days in osteogenic medium (OM), that is, DMEM containing 10% FBS and antibiotics, 5 μg/mL ascorbic acid 2-phosphate, 10 mM β-glycerophosphate, and 10^{-6} M dexamethasone (all from Sigma-Aldrich). Dexamethasone at 10^{-6} M was shown to efficiently induce osteogenic differentiation of BMSC (Supplementary Figure 1 in Supplementary Material available online at http://dx.doi.org/10.1155/2016/3865315) and osteoblast cell lines [43] when the treatment is initiated after cells reach confluence. Medium was changed in every 2-3 days. Differentiation was evaluated by alkaline phosphatase activity and quantification of mineralized foci after Von Kossa staining. Adipogenic potential was evaluated by maintaining the cells in DMEM supplemented with 10% FBS, 0.5 mM isobutyl-methylxanthine (IBMX), 10^{-6} M dexamethasone, 200 μM indomethacin (all from Sigma-Aldrich), 10 μM insulin (Humulin®, Lilly, São Paulo, SP, Brazil), and antibiotics for up to 21 days. Accumulation of cytoplasmic lipids was identified by Oil Red O staining.

2.6. PSI/γ-Secretase Activity Assay. To investigate the role of PS-1/γ-secretase in osteogenic differentiation of BMSCs, 20 μM of Dapt [44] was added to the cultures 24 h prior to osteoinduction or 24 h, 48 h, and 4 days after addition of OM. Once added, Dapt was maintained throughout the differentiation protocol.

2.7. Wnt3a Treatment. Different concentrations (1%, 5%, or 10% v/v) of Wnt3a-conditioned medium (Wnt3a-CM) were added to EM or incomplete OM (iOM), which did not contain dexamethasone. During osteogenic induction, Wnt3a-CM was added to the cultures at the onset of osteoinduction (0 h) or 48 h and 4 days after control osteoinduction with OM. In all assays, medium was exchanged at every 3 days.

2.8. Alkaline Phosphatase Activity Assay. Alkaline phosphatase (ALP) activity was determined by colorimetric assay using an ALP kit (Labtest Diagnóstica, Lagoa Santa, MG, Brazil), following manufacturer instructions. BMSCs were osteoinduced under the different conditions stated above for 7 and 14 days and total protein extracts were obtained by scrapping the monolayers in 300 μL of 125 mM Tris-HCl (pH 6.8) 0.5% Triton X-100 buffer. Equal volumes of substrate (22 mmol/L thymolphthalein monophosphate) and protein extracts were mixed and incubated in a water bath at 37°C for 10 min. Reaction was stopped by adding a 250 mmol/L NaOH 94 mmol/L Na_3CO_2 colorimetric solution. The optical density (OD) of the product was measured at 590 nm. Protein concentration of cell extracts was measured with Bradford Reagent (Sigma-Aldrich), and ALP activity was shown as (OD of test sample/OD of standard control sample) × 45/mg of total protein.

2.9. Von Kossa and Oil Red O Staining. BMSCs monolayers were fixed with 4% paraformaldehyde in PBS for 1 h at RT and stained with either Von Kossa or Oil red O as described [45]. Von Kossa staining was performed by incubating monolayers with 2% silver nitrate solution for 1 h in the absence of light. Monolayers were washed five times with water to remove excess stain and plates were then exposed to UV light for 10 minutes. For Oil Red O staining, monolayers were incubated for 2 minutes with propylene glycol and then with 0.5% Oil Red O in propylene glycol for 20 minutes. Monolayers were washed with 85% propylene glycol solution for 1 minute and finally twice with water. To quantify the extent of mineralization and the number of fat accumulating cells, wells were photographed using an inverted microscope (Nikon Eclipse TS100, Nikon, Tokyo, Japan) equipped with a EC3 digital camera (Leica, Wetzlar, Germany). The mineralized area in 15 random fields was quantified using NIH Image J software and is represented as the percentage of the total area. Number of fat accumulating cells is expressed as number of cells per field.

2.10. Proliferation Assay and Doubling Population. A total of 1.0×10^4 BMSCs were plated per well in 24-well dishes in control expansion medium (EM) and left to adhere overnight. On the next day, cells from three sample wells were recovered with 0.125% trypsin 0.78 mM EDTA solution and counted in a Neubauer chamber. Viability was evaluated by the Trypan Blue exclusion method. The mean value obtained from these wells was considered as the initial number of adherent cells per well. The culture medium of the remaining wells was replaced by either EM or incomplete osteogenic medium (iOM) containing 2% FBS alone or supplemented with 1% or 10% Wnt3a conditioned medium. Cells in each well were harvested after 2, 6, 8, and 10 days of culture and quantified as described above. The number of population doublings was calculated using the following equation: PD = $({}_fN - {}_iN)/\log_{10}(2)$, where ${}_fN$ is the final cell harvest number and ${}_iN$ is the initial cell number.

2.11. Clonogenic Assay (CFU-F, Colony-Forming Unit-Fibroblast). CFU-F was performed by plating 100 cells/cm^2 in quadruplicate with DMEM with 10% FBS [3]. Cultures were maintained for 14 days. After this period, cells were fixed with 4% paraformaldehyde and stained with 1% crystal violet. Colonies with more than 50 cells were counted.

2.12. Immunofluorescence and Confocal Microscopy. Immunofluorescence labeling for confocal microscopy (TCS SP5, Leica) was performed as described [46]. BMSCs were fixed with 4% paraformaldehyde in PBS for 10 min at RT, permeabilized with 0.5% Triton X-100 in PBS (PBS-T), and incubated with the primary antibodies rabbit anti-Pan-cadherin, mouse anti-N-cadherin, mouse anti-E-cadherin, or

rabbit anti-β-catenin diluted 1 : 50 in PBS-T for 1 h at 37°C in a humid chamber. Subsequently, cells were incubated with the secondary antibodies for 1 h at 37°C in a humid chamber. Nuclei were stained with 0.1 μg/mL DAPI in 0.9% NaCl. Control experiments with no primary antibodies showed only a faint background staining.

2.13. Protein Sample Preparations and Western Blotting. For total cell extract collection, BMSCs cultures were scrapped in Ripa buffer (0.05 M Tris-HCl pH 7.4; 0.15 M NaCl; 1% NP-40; 0.25% sodium deoxycholate, 2 mM EDTA) containing protease inhibitors (1 mg/mL aprotinin, 1 mg/mL leupeptin, 1 mg/mL pepstatin, 1 mM phenylmethylsulfonyl fluoride (PMSF), 10 mM N-ethylmaleimide, 1 mM sodium fluoride, and 1 mM sodium orthovanadate, all from Sigma-Aldrich). Nuclear and cytoplasmic fractions were extracted according to the manufacturer's instructions. All cell extracts were diluted 1 : 2 in SDS-PAGE buffer (125 mM Tris-HCl pH 6.8, 4% sodium dodecyl sulfate, 20% glycerol, 10% β-mercaptoethanol, and 0.002% bromophenol blue) and boiled for 5 min. The amount of protein in each sample was determined with Bradford Reagent (Sigma-Aldrich), using bovine serum albumin as a standard. Protein electrophoresis and blotting were performed as described in [46]. Samples were loaded in 12% SDS-PAGE and transferred to polyvinylidenfluoride membranes (GE Healthcare Lifesciences, New Jersey, USA). Proteins immobilized on the membranes were blocked for 1 h at RT with 5% nonfat dry milk and incubated with the primary antibodies rabbit anti-Pan-cadherin, rabbit anti-β-catenin, mouse anti-active-β-catenin, mouse anti-lamin A\C, or mouse anti-α-tubulin. Membranes were incubated with goat anti-rabbit or rabbit anti-mouse peroxidase-conjugated antibodies and the bands visualized using the Super Signal WestPico ECL Pierce kit (Pierce). Molecular weight of detected bands was estimated using the protein molecular weight standards Kaleidoscope (Bio-Rad, Hercules, CA, USA) and Rainbow (GE Healthcare Lifesciences). Densitometric analysis was performed in scanned images (Scanjet G2710, HP, CA, USA) using Image J software.

2.14. Cell Electroporation, Lentivirus Transduction, and Luciferase Assay. Electroporation was performed as described [47]. A total of 5.0×10^5 BMSCs were resuspended in 100 μL electroporation buffer (5 mM KCl; 15 mM MgCl2; 120 mM Na_2HPO_4 pH7.2; 25 mM Sodium Succinate; 25 mM Manitol) containing 4 μg of the reporter system 7xTcf-FFluc//SV40-PuroR (7TFP, Addgene plasmid 24308) to evaluate the activation of Wnt signaling [48] and 0.4 μg of TK-Renilla (Promega). The cells were immediately transferred to a sterile 0.2 cm cuvette (Mirus Biotech®, Madison, WI, USA) and electroporated using the program U23 of the Lonza® Nucleofactor® II electroporation system. After transfection, 1.0×10^5 cells were plated per well in 48-well plates and left to adhere overnight at 37°C and 5% CO_2. On the following day, cultures were rinsed with PBS and incubated in triplicate with EM, OM, OM supplemented with 20 μm Dapt, iOM, or iOM supplemented with 10% and 50% Wnt3a-CM for 48 h or 5 days. As internal controls, MDA-MB-231-7TFP reporter lineages were also obtained by either electroporation, using the same conditions described above, or by lentivirus transduction [49]. Cells were incubated overnight with lentiviral particles containing the 7TFP sequence in the presence of 8 μg/mL polybrene in Iscove's Modified Medium (IMDM) containing 10% FBS. After incubation, the medium was replaced and 2 μg/mL puromycin (Invitrogen, A1113802) was added to select the transduced cells. After the specific treatments, cells were lysed with lysis buffer (Promega) and luciferase activity was detected by adding the enzyme substrate according to the manufacturer's protocol. Samples were read in a microplate reader (Modulus II, Turner Biosystems, CA, USA). To normalize the data, the luciferase activity index was calculated by dividing the luciferase values by the Renilla luciferase values.

2.15. Real-Time Polymerase Chain Reaction (RT-PCR). mRNA from undifferentiated, 48 h and 5 days osteoinduced cells were isolated using Trizol (Invitrogen) reagent, according to the manufacturer's instructions, and quantified using a Nanodrop spectrophotometer. Two micrograms of total RNA was used as a template for cDNA synthesis, using the High Capacity cDNA Reverse Transcription kit (Life Technologies). SYBR Green PCR master mix (Life Technologies) was used to quantify human Axin-2 and Hes-1 expression levels, with GAPDH as an endogenous control. Real-time reactions were performed in triplicate using a Line Gene 9600 Real-Time thermocycler (Bioer). Relative quantification was performed using the Delta-Delta Ct method. Primer sequences were as follows: Axin-2, forward: 5′-GTCTCTACCTCATTTCCCGAGAAC-3′, reverse: 5′-CGAGATCAGCTCAGCTGCAA-3′; Hes-1: forward: 5′-AGAAAGATAGCTCGCGGCATT-3′, reverse: 5′-GGTGCTTCACTGTCATTTCCA-3; GAPDH, forward: 5′-ACTGTGTTGGCGTACAGGTC-3′, reverse: 5′-CATGAGTCCTTCCACGATACCA-3′.

2.16. Statistical Analysis. Statistical analysis was carried out using the GraphPad Prism software version 5. Results of at least three independent experiments (always performed with cells isolated from different donors) were compared by One-Way ANOVA. Differences between groups were evaluated with the posttest of Tukey. Data are shown as mean ± standard deviation (SD). p values < 0.05 were considered significant.

3. Results

3.1. β-Catenin/TCF Signaling Is Activated during Osteogenic Differentiation of BMSCs But Is Not Induced by Wnt3a-CM. To confirm the activation of β-catenin/TCF signaling during BMSCs osteoinduction, we first evaluated the expression of Axin-2, a known β-catenin/TCF target [50]. After 48 h of BMSCs incubation with osteogenic medium containing dexamethasone (OM), Axin-2 mRNA levels were upregulated; and this increased expression was maintained even after 5 days of osteoinduction (Figure 1(a)). To confirm this observation, we transfected BMSCs with a plasmid containing a luciferase reporter gene, downstream of seven β-catenin/TCF

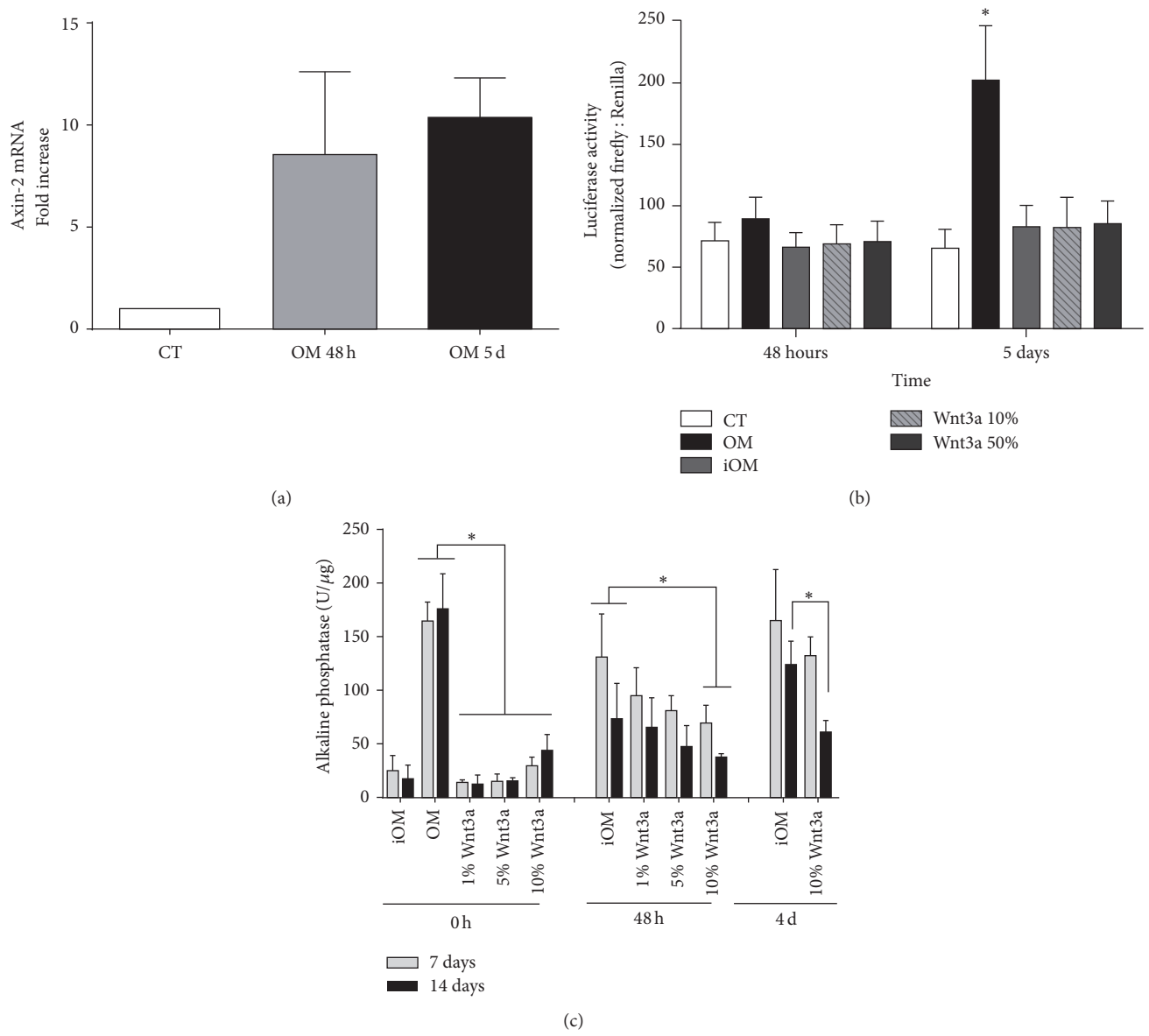

Figure 1: Osteogenic medium, but not Wnt3a-CM, induces β-catenin signaling and BMSCs osteogenic differentiation. (a) BMSCs were cultured in osteogenic medium (OM) for 48 h and 5 days and Axin-2 mRNA fold increase was evaluated. Bars represent mean ± SD of 3 independent experiments performed in triplicate. (b) Luciferase activity in BMSCs containing a SuperTop TCF reporter, osteoinduced for 48 h and 5 days with incomplete osteogenic medium (iOM, without dexamethasone), osteogenic medium (OM), or iOM containing 10% or 50% Wnt3a-CM. CT = undifferentiated cells. Bars represent mean ± SD of 4 experiments performed in triplicate. (c) Alkaline phosphatase activity in BMSC cultures after 7 and 14 days of osteoinduction with OM or iOM containing 1%, 5%, and 10% Wnt3a-CM. iOM supplemented with Wnt3a-CM was added at the onset of induction (0 h) or after 48 h and 4 days of osteoinduction with OM. Mean ± SD of 5 independent experiments with triplicates is shown. $^{*}p < 0.05$.

binding sites. A significant luciferase activity was observed in cells treated for 5 days with OM (Figure 1(b)), thus confirming β-catenin signaling activation upon osteoinduction. Next, we asked whether canonical Wnt3a would mimic this effect and induce β-catenin signaling in BMSCs. We observed that the replacement of dexamethasone by 10% or 50% Wnt3a-conditioned medium (Wnt3a-CM) did not increase luciferase activity in BMSCs over basal levels (Figure 1(b)). As parallel experiments performed with MDA-MB-231 cells, as internal controls, showed a significant luciferase induction upon Wnt3a-CM treatment (Supplementary Figure 2), we thereby concluded that Wnt3a was unable to induce β-catenin signaling in BMSCs.

To further investigate the effects of Wnt3a treatment in BMSCs osteoinduction, we then evaluated alkaline phosphatase (ALP) activity, an enzyme upregulated in the first week of the *in vitro* osteogenic program [51]. After 7 and 14 days of BMSCs treatment with 1%, 5%, or 10% Wnt3a-CM,

no increases in ALP were observed in any concentrations of Wnt3a-CM tested, as opposed to cells induced with OM (Figure 1(c)). Considering this finding, we next asked whether Wnt3a was only insufficient to trigger the osteogenic program or was actually inhibiting differentiation. To test this hypothesis, we preosteoinduced BMSCs with OM for 48 hours or 4 days and then replaced dexamethasone by 1%, 5%, or 10% Wnt3a-CM. In the 48 h preosteoinduced cells, we observed a dose-dependent decrease in OM-induced ALP activity, which became significant ($p < 0.05$) at the concentration of 10% Wnt3a-CM (Figure 1(c)). Similar results were observed in the cells preosteoinduced for 4 days (Figure 1(c)), supporting the notion that Wnt3a can inhibit an ongoing osteogenic process.

In fact, we noticed that Wnt3a treatment seemed to stimulate and maintain a proliferative cellular state. To confirm this observation, we cultured BMSCs with either expansion medium (EM) or incomplete OM (iOM, without dexamethasone), each containing 1% or 10% Wnt3a-CM. After 10 days, cells expanded in the presence of 10% Wnt3a-CM had an increased number of population doublings, indicative of a higher proliferative rate (Figures 2(a)-2(b)). Moreover, when replated in clonal density, a higher number of colonies originated from Wnt3a-CM expanded cells (Figures 2(c)-2(d)), pointing to an enhancement in clonogenic potential (1 colony/33.23 cells compared to 1 colony/42.43 in control cells). Lastly, when subjected to standard *in vitro* differentiation, Wnt3a-expanded cells had a decreased capacity for both matrix mineralization and lipid accumulation (Figures 2(e)-2(f)). Therefore, we concluded that Wnt3a-mediated signaling induces a proliferative status in BMSCs, impairing differentiation programs.

3.2. Cadherins Are Cleaved by a PS1/γ-Secretase-Mediated Mechanism during BMSCs Osteoinduction. Next we investigated the occurrence of cadherin cleavage in BMSCs. We first verified that both undifferentiated and 48 h-osteoinduced BMSCs expressed E-cadherin (Figure 3(a)) and N-cadherin (Figure 3(b)), in a linear/punctate pattern at the plasma membrane, and punctate in the cytosol. A similar membrane staining pattern was observed for β-catenin (Figure 3(c)). However, when 20 μM of Dapt—a PS1 specific inhibitor—was added to OM, a stronger and more defined membrane staining of both N-cadherin (Figure 3(b)) and β-catenin (Figure 3(c)) was observed, suggesting a reduced turnover of these proteins at the plasma membrane.

Because both E-cadherin and N-cadherin are targets of the PS1/γ-secretase complex [29, 30, 35, 52, 53], we investigated the occurrence of cadherin cleavage in BMSCs with a Pan-cadherin antibody that specifically recognizes the conserved C-terminal region of classic cadherins [54]. With this approach, a similar staining pattern of cadherins as of the specific previous antibodies was observed (Figure 3(d)). However, we also observed a staining in the nucleus (Figure 3(d)), which strengthened the hypothesis that cadherins were cleaved and its CTF-2 were translocated to the nucleus. To confirm this finding, we analyzed whole protein extracts of undifferentiated and 48 h-osteoinduced BMSCs by western blot, using the Pan-cadherin antibody. We observed a 135 kDa band, accompanied by a 35 kDa fragment (Figure 4(a)), which, respectively, agrees with the molecular weights of N-cadherin and its CTF-2 [29, 30]. However, the 135 KDa band was significantly decreased in osteoinduced cells (Figures 4(a)-4(b)). In Dapt-treated cells, an additional 40 kDa band was detected (Figure 4(a)), in agreement with the expected molecular weight of CTF-1, which is only detected when PS1/γ-secretase activity is inhibited [29, 30]. We also observed a decrease in the 35 kDa band (Figure 4(a)), corroborating the notion that the latter is originated from the former, after PS1/γ-secretase cleavage. We then evaluated the presence of the 35 kDa band (CTF-2) in isolated cytosolic and nuclear fractions, since solubilized CTF-2 might translocate to the nucleus [37]. As expected, CTF-2 was detected in both cellular compartments (Figure 4(c)), but its nuclear expression was diminished in Dapt-treated cells (Figure 4(d)). Taken collectively, these results indicate that cadherins are cleaved during osteogenic differentiation of BMSCs by a PS1/γ-secretase-dependent mechanism, generating soluble fragments that are translocated to the nucleus.

3.3. Pharmacological Inhibition of PS1/γ-Secretase during Osteoinduction Reduces β-Catenin Nuclear Translocation and Signaling. We then sought to investigate the dynamics of β-catenin expression and signaling under PS1/γ-secretase inhibition. Analysis of the total amount of β-catenin showed no significant differences in expression after 48 hours of induction (Figures 5(a) and 5(b)). However, using an antibody that specifically recognizes the active (unphosphorylated) signaling form of β-catenin (ABC) [55, 56], we detected an increase in its nuclear localization at 48 h of osteoinduction (Figures 5(c) and 5(d)). On the other hand, Dapt-treated cells showed a reduced accumulation of ABC in the nucleus (Figures 5(c) and 5(d)). This effect was observed in cells isolated from different donors, though in different intensities of response. To confirm this observation, we evaluated the levels of luciferase activity in BMSCs transfected with the TCF reporter system and observed a significant impairment of β-catenin/TCF signaling after 5 days of osteoinduction in the presence of Dapt (Figure 5(e)). Taken altogether, the data indicate that β-catenin nuclear translocation and signaling during BMSCs osteoinduction depend on PS1/γ-secretase activity.

3.4. Osteogenic Differentiation Is Impaired under PS1/γ-Secretase Inhibition. To verify whether PS1/γ-secretase inhibition would indeed impact the acquisition of the osteoblastic phenotype, Dapt was added to BMSCs at different time points, starting 24 h before osteoinduction, or later at 24 h, 48 h, or 4 days after induction with OM. We verified that Dapt inhibited the induction of ALP activity, but only when treatment commenced before osteoinduction or during its first 48 h (Figure 6(a)). In these conditions, the mineralized area fraction was significantly reduced at day 21 (Figures 6(b)–6(f)), and fat accumulating cells appeared (Figures 6(c)–6(e)), indicating a shift from the osteogenic to the adipogenic program.

Although Notch signaling is known to be a negative regulator of osteogenic differentiation and shown to be inhibited

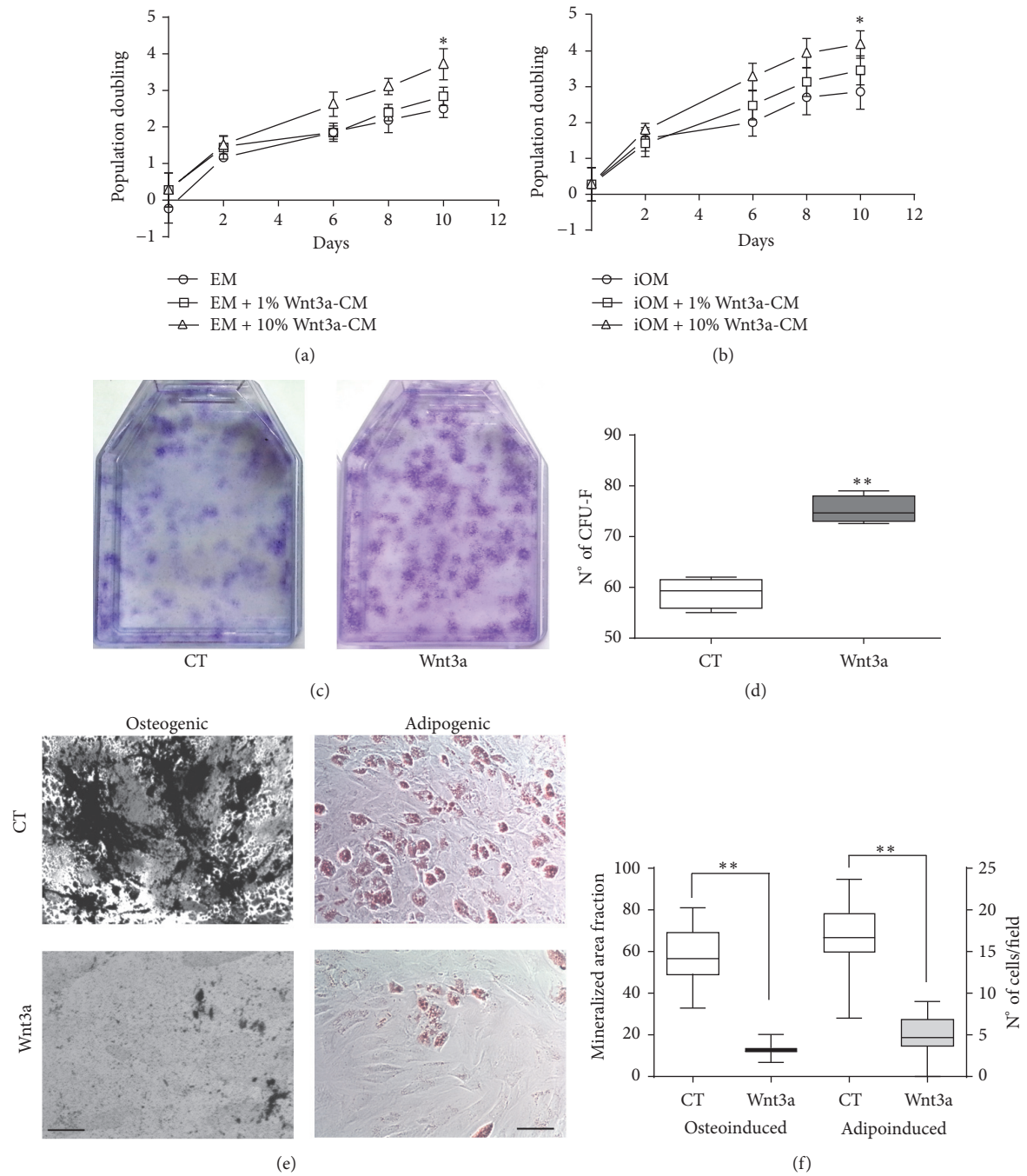

Figure 2: Wnt3a-CM stimulates proliferation and impairs BMSCs differentiation. (a-b) Cumulative population doublings of BMSCs cultured with either expansion medium (EM (a)) or incomplete osteogenic medium (iOM, without dexamethasone (b)) supplemented with 1% or 10% Wnt3a-CM. Data represent mean ± SD of 3 independent experiments with triplicates. (c-d) BMSCs expanded in the presence of 10% Wnt3a-CM for 10 days were plated at clonal density and maintained in control expansion medium for another 14 days. Morphology (c) and quantification (d) of CFU-F formed by control (CT) and Wnt3a-expanded BMSCs are shown. Data represent mean ± SD of 4 experiments with quadruplicates. (e) Representative micrographs of control and Wnt3a-expanded BMSCs induced towards the osteogenic (left panel) and adipogenic lineages (right panel) stained with Von Kossa and Oil Red O, respectively. Bars = 100 μm. (f) Quantification of total mineralized area and fat accumulating cells per field of view. Data represent mean ± SD of 4 experiments with triplicates. $^{*}P < 0.05$; $^{**}P < 0.001$.

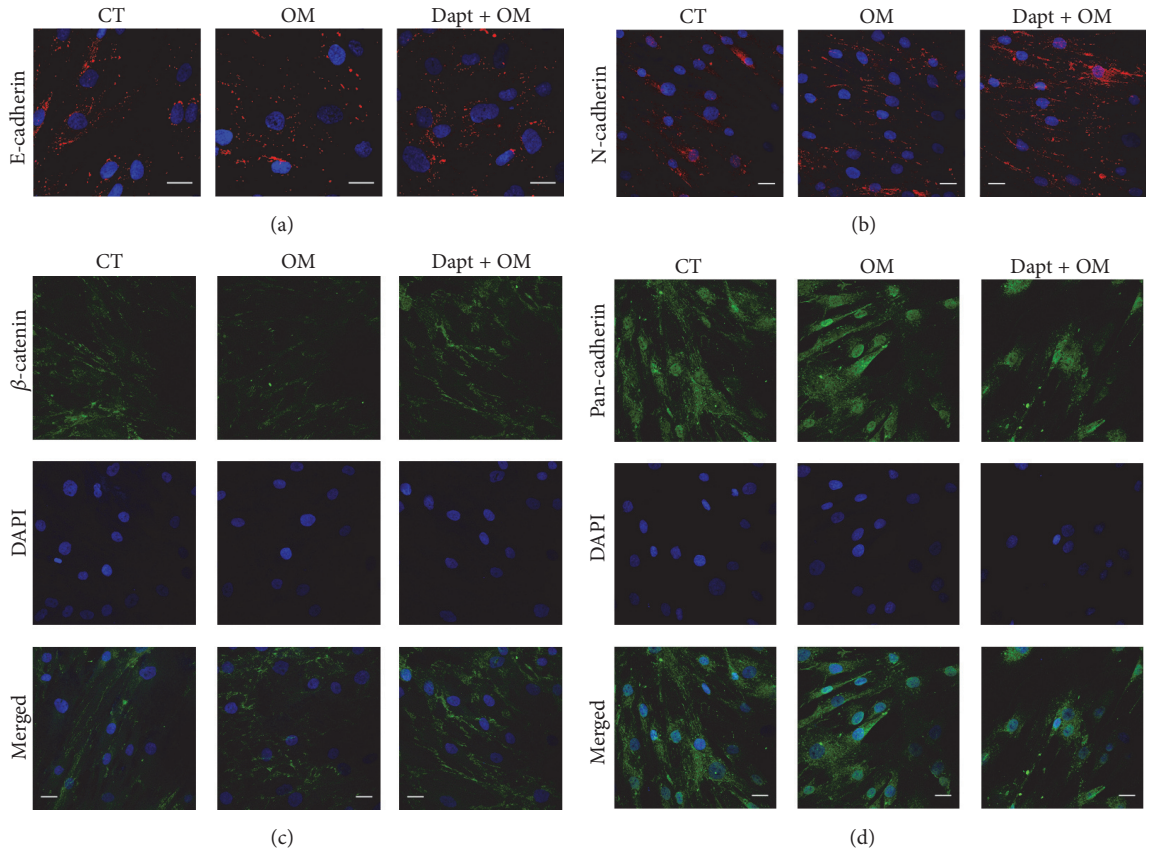

Figure 3: Expression of E-cadherin, N-cadherin, and β-catenin in osteoinduced and Dapt-treated BMSCs. Confocal microscopy images showing the expression of E-cadherin ((a) red), N-cadherin ((b) red), β-catenin ((c) green), and Pan-cadherin ((d) green) by BMSCs cultured for 48 h with expansion medium (CT, control undifferentiated), osteogenic medium (OM), or osteogenic medium containing 20 μM of the PS1/γ-secretase inhibitor Dapt (Dapt + OM). Dapt was added 24 h before the addition of OM. Nuclei were stained with DAPI (blue). Scale bars = 25 μm.

upon osteogenic commitment [57–60], we lastly evaluated Notch regulation in order to verify its possible interplay in our observations. Analysis of Hes-1, the intracellular mediator of Notch [59], confirmed that this gene is significantly downmodulated in both 48 h- and 5 day-osteoinduced cells (Figure 6(g)). Considering that Dapt treatment would further inhibit Notch and therefore enhance osteogenic differentiation, we concluded that this signaling pathway does not take part in the results observed hereby.

4. Discussion

Bone marrow stromal cells (BMSCs) have a high potential for bone bioengineering and clinical application [5, 6]. However, the molecular mechanisms that drive commitment and differentiation along the osteoblastic lineage are not completely understood. Because evidence showed that receptor-mediated canonical Wnt signaling would be just one of the players of a major and intricate signaling complex responsible for cell fate decision, in which cadherin molecules also participate [19, 20, 24], we focused on understanding how these signaling pathways influence downstream β-catenin signaling and osteogenic differentiation. We observed that Wnt3 was not able to stimulate β-catenin signaling, maintaining BMSCs in a proliferative state. On the other hand, PS1/γ-secretase activity occurs upon osteoinduction, cleaving N-cadherin and enhancing β-catenin signaling. The inhibition of PS1/γ-secretase activity was associated to the impairment of osteogenic differentiation.

The specific effects of Wnt signaling activation in BMSCs were explored in several studies with conflicting results, either stimulating or inhibiting osteogenic differentiation [16–18, 61, 62]. More recently, Caverzasio and colleagues further explored the issue and strengthened the notion that Wnt3a stimulates BMSC proliferation by a β-catenin-independent pathway [61]. This kind of signaling transactivation mediated by canonical Wnts has been previously observed in other systems, such as during morphogenetic movements in vertebrate gastrulation [63], and is thought to be evolutionarily ancient [14]. Since we did not observe β-catenin/TCF activation in Wnt3a-treated cells, we hypothesize that the enhanced proliferation observed is probably related to the activation of an alternative, β-catenin-independent pathway.

However, we did observe that cells osteoinduced under standard conditions (with the osteogenic cocktail) showed

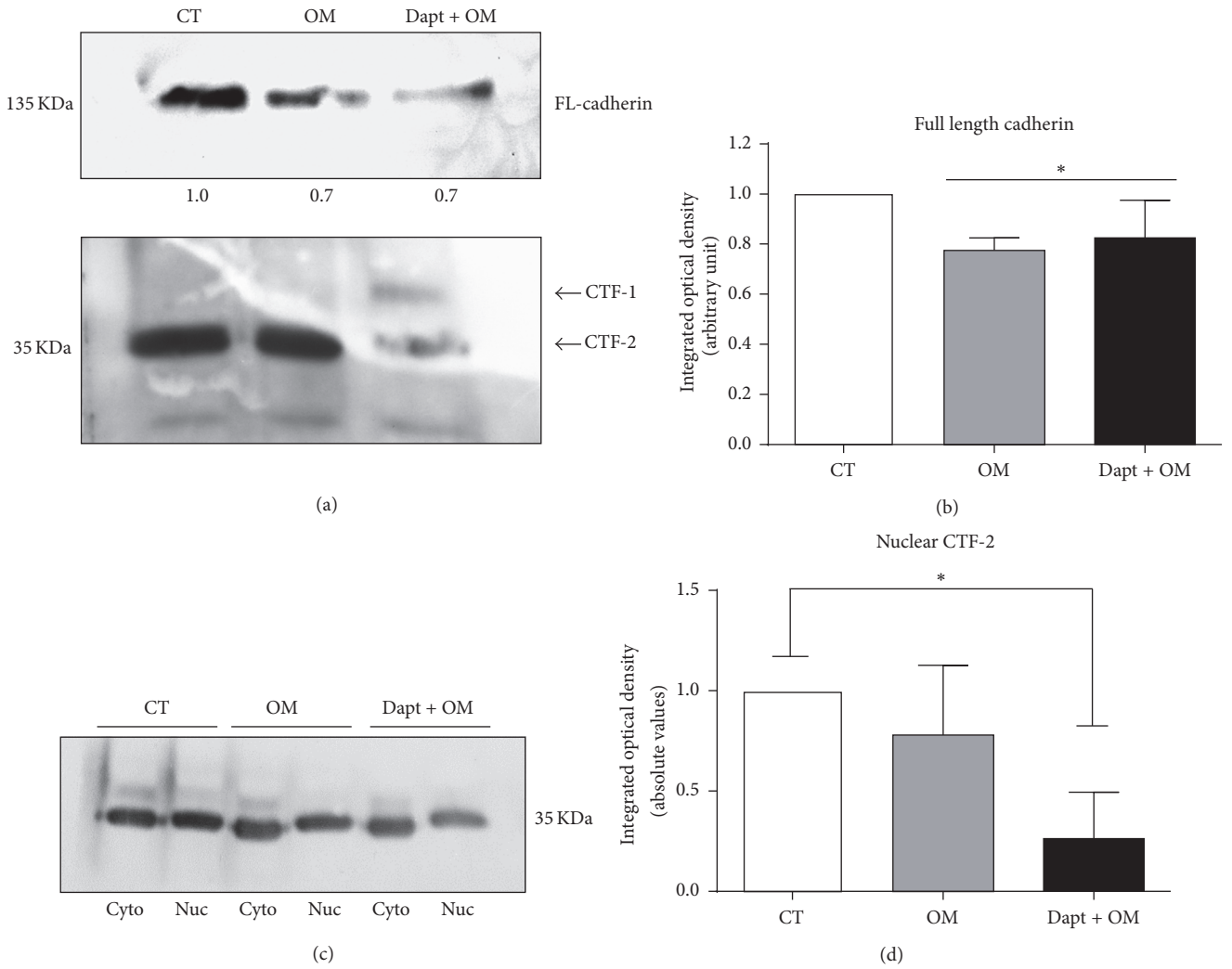

Figure 4: PS1/γ-secretase-mediated cadherin cleavage occurs during osteogenic differentiation of BMSCs, generating a C-terminal intracellular fragment (CTF-2) that translocates to nucleus. BMSCs were osteoinduced for 48 h in the presence of Dapt. (a) Representative immunoblotting showing a full-length cadherin band (135 kDa) and its cleavage products (CTF-1 and CTF-2) in total protein extracts. (b) Densitometric quantification of the 135 kDa cadherin band. Bars show mean ± SD of 4 independent experiments. (c) Representative immunoblotting showing CTF-2 fragments (35 kDa) in cytoplasmic and nuclear fractions. (d) Quantification of nuclear CTF-2 in 3 experiments. CT = control undifferentiated cells; OM = osteogenic medium; Dapt + OM = osteogenic medium with Dapt. $^{*}P < 0.05$ relative to CT.

an increased expression of the β-catenin responsive gene Axin-2, as well as an approximately 4-fold increase in TCF activation, confirming that β-catenin signaling is activated during the osteogenic program. Therefore, considering that (i) β-catenin is a component of cadherin adhesion complexes [64, 65]; (ii) stable expression of N-cadherin in cells of the osteoblastic lineage inhibits differentiation and impairs bone formation [66]; (iii) N-cadherin expression is downmodulated upon osteogenic commitment and differentiation [21, 23, 26–28]; and (iv) cadherin cleavage can influence β-catenin availability for signaling [31, 33, 36–38, 52, 53], we investigated whether this mechanism would influence β-catenin/TCF signaling activation during BMSCs osteoinduction. To date, this mechanism had not been shown during osteogenic differentiation of human BMSCs.

Consistent with our hypothesis, western blotting analysis showed a significant expression of a 135 kDa cadherin molecule, which was decreased after osteoinduction, even in the presence of Dapt. This observation was not surprising, once the first step of cleavage is MMP-dependent [31, 38]. Most importantly, as seen in previous reports [29, 30, 34], a 35 kDa cadherin fragment was observed in both undifferentiated and osteoinduced cells; and when Dapt was added, its expression was diminished and an additional 40 kDa fragment was observed, indicating that these fragments were, respectively, the cleavage product and the substrate of PS1/γ-secretase. The molecular weight of the full-length protein and its fragments suggests that N-cadherin [29, 30, 34] is the major target of PS1/γ-secretase in BMSCs. However, it must be considered that the amount of unprocessed E-cadherin

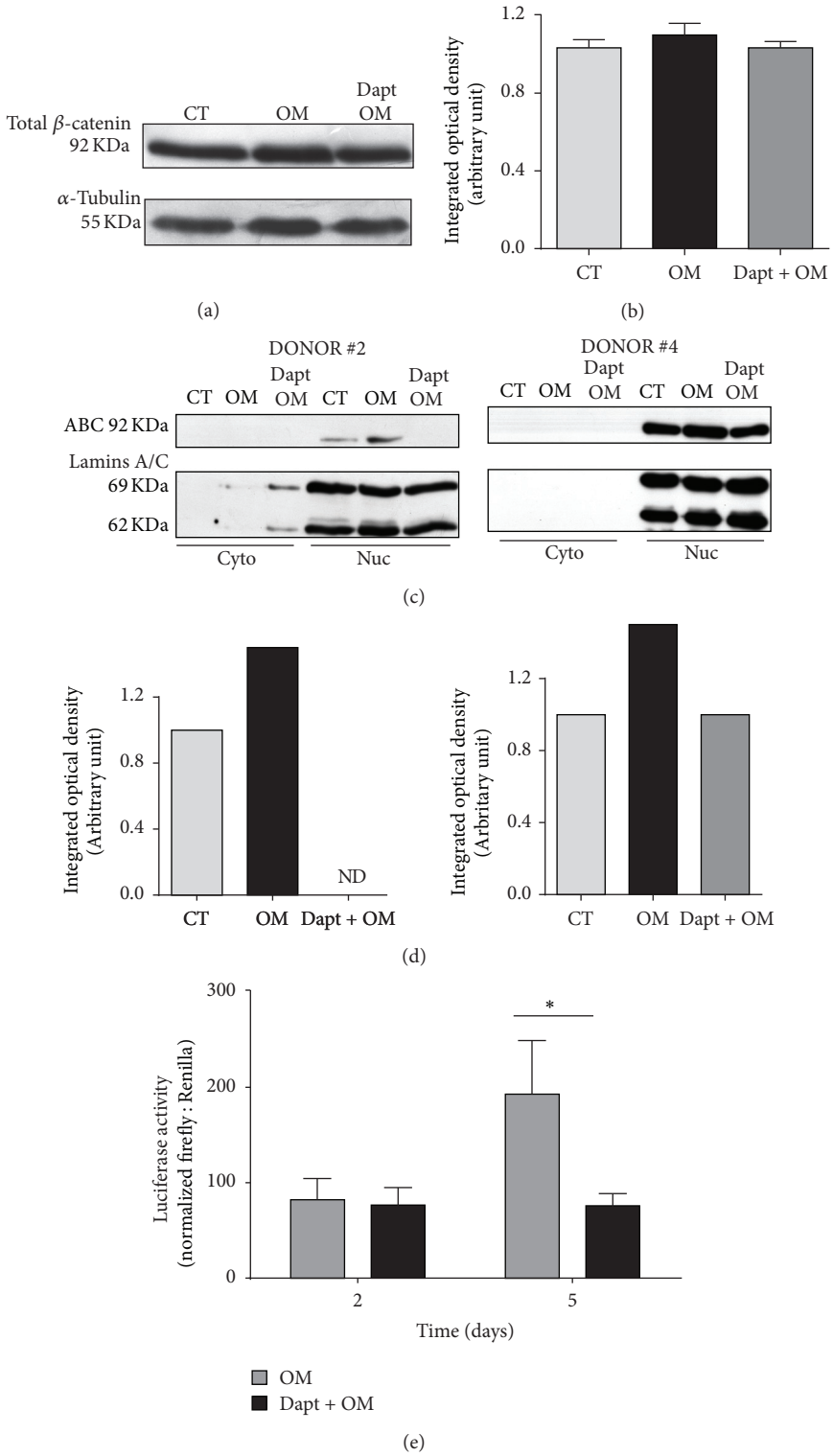

Figure 5: PS1/γ-secretase inhibition impairs β-catenin nuclear translocation and signaling. (a) Representative immunoblotting of total β-catenin in whole protein extracts. (b) Densitometry of total β-catenin bands obtained in 5 independent experiments. Data represent mean ± SD. (c) Representative immnunoblotting of the active form of β-catenin (ABC) in cytoplasmic and nuclear cell fractions from two different donors. (d) Densitometry of ABC nuclear bands normalized by lamin A. (e) Luciferase activity in BMSCs containing a SuperTop TCF reporter, osteoinduced for 2 and 5 days in the presence of Dapt. Bars represent mean ± SD of 5 different donors performed in triplicate. CT = control undifferentiated cells; OM = osteogenic medium; Dapt + OM = osteogenic medium with Dapt. $^{*}p < 0.05$.

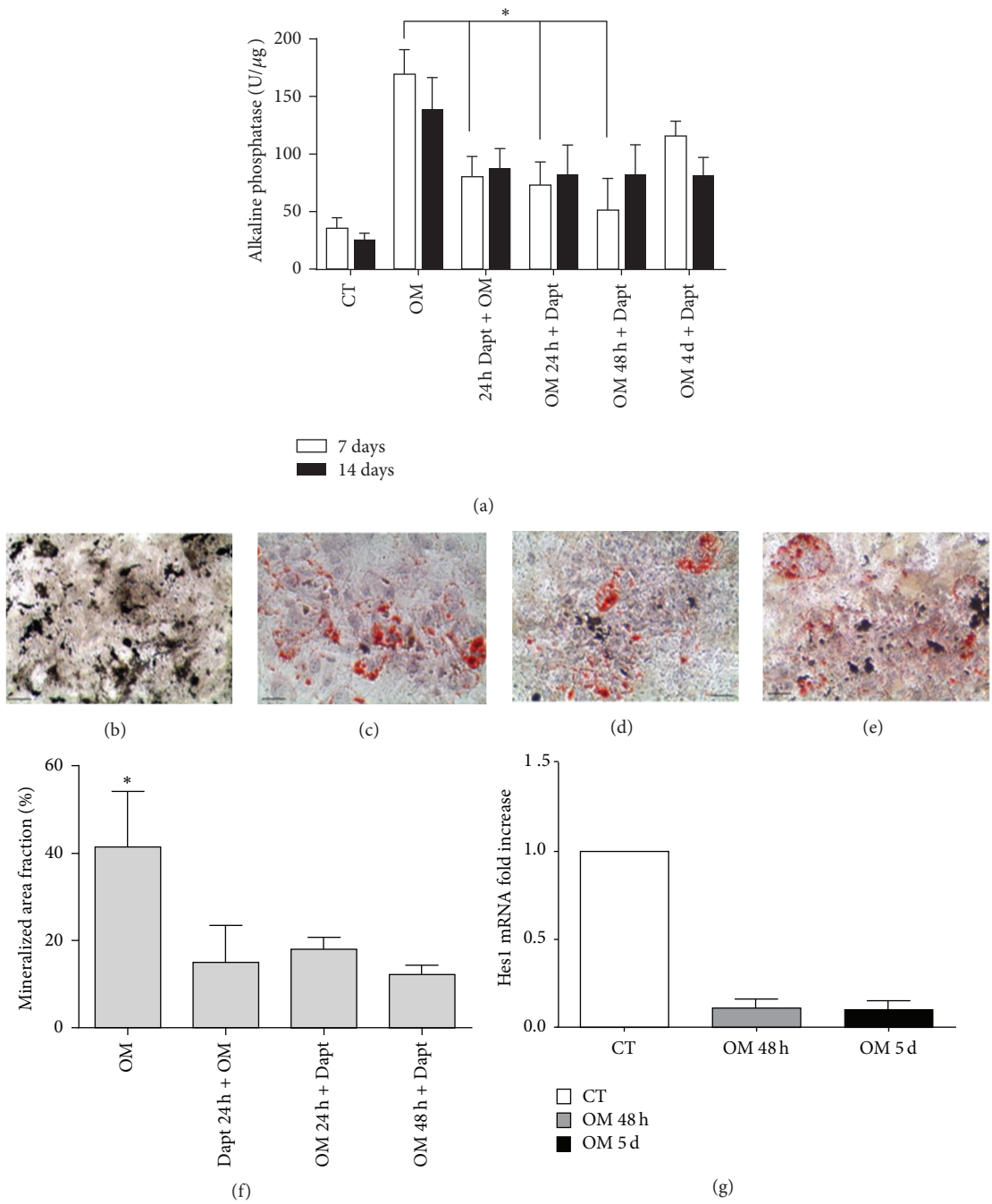

Figure 6: PS1/γ-secretase inhibition impairs BMSCs osteogenic differentiation. BMSCs were osteoinduced in the presence of Dapt, added either 24 hours before OM (24 h Dapt + OM) or at 24 h (OM 24 h + Dapt), 48 h (OM 48 h + Dapt), or 4 days after OM (OM 4 days + Dapt). (a) Alkaline phosphatase activity measured after 7 and 14 days. Graph represents the mean ± SD of 6 independent experiments. (b–e) Von Kossa and Oil Red O double staining. (b) Control osteoinduced, (c) 24 h Dapt + OM, (d) OM 24 h + Dapt, and (e) OM 48 h + Dapt. Scale bars = 100 μm. Data are representative of 4 independent experiments. (f) Quantification of total mineralized area revealed by Von Kossa staining. Data represent mean ± SD of 3 independent experiments. $^*p < 0.05$. (g) Analysis of Hes-1 mRNA in BMSCs osteoinduced for 48 h and 5 days. Bars represent the mean ± SD of 3 independent experiments performed in triplicate.

might be under the limit of detection of the assay, and therefore, we cannot rule out that E-cadherin is also cleaved.

In several cell lineages, cadherin cleavage by PS1/γ-secretase released β-catenin from cell-adhesion complexes, favoring its translocation to the nucleus [30, 31, 33, 36–38, 52, 53]. Here we observed that, following osteoinduction, the amount of active, nonphosphorylated β-catenin (ABC) increased in the nucleus and resulted in TCF activation.

However, this effect was impaired in all Dapt-treated cells, isolated from different donors. It is important to note that BMSCs are a highly heterogeneous population, containing progenitors in different levels of commitment [1, 67–69]. Therefore, the differences seen in the intensity of β-catenin translocation impairment among the different samples are not unexpected but are rather an intrinsic characteristic of the population. Furthermore, the pharmacological inhibition of PS1/γ-secretase significantly reduced TCF activation in the luciferase assays—which also varied among donors (23.6% to 69.8% in range)—confirming that β-catenin-mediated gene transcription in BMSCs is dependent on PS1/γ-secretase activity.

In agreement with the observed impairment of β-catenin signaling by PS1/γ-secretase inhibition, we found that the differentiation of BMSCs down to the osteoblastic lineage was arrested and redirected towards the alternative adipogenic program. This adipogenic enhancement following BMSCs treatment with Dapt was also described previously by Vujovic and colleagues [44], in a dose-dependent manner.

Although we were not able to confirm our observations with cells expressing cleavage-resistant cadherin molecules, which was a limitation of this study, our data demonstrate for the first time that BMSCs osteogenic differentiation is dependent on PS1/γ-secretase activity, which positively regulates both cadherin cleavage and β-catenin/TCF signaling, suggesting that this might indeed constitute a signaling axis leading to osteogenic commitment. This hypothesis is also strengthened by the observation that the expression of Hes-1 is inhibited upon BMSCs osteoinduction, which weakens the possibility of Notch signaling involvement in our findings. In this way, our study adds to the current literature as it provides evidence that both canonical Wnt and cadherin cleavage are central mechanisms of a complex and integrated net of signaling pathways responsible for BMSCs fate decisions, but with distinct outcomes. A better understanding of the specific roles of each mechanism in BMSCs, as well as when and how to modulate their function, will be a fundamental step for the development of effective strategies to improve BMSCs-based bone bioengineering and repair.

5. Conclusions

Osteogenic differentiation of BMSCs depends on the activity of PS1/γ-secretase, which cleaves cadherins and stimulates β-catenin signaling. In contrast, Wnt3a signaling is related to the maintenance of a proliferative state. Altogether, we provide evidence that corroborate the notion that cadherins and receptor-mediated Wnt signaling are central players in a major signaling pathway that can be differentially balanced leading to either BMSCs proliferation or differentiation.

Disclosure

The funders had no role in study design, data collection and analysis, decision to publish, or preparation of the manuscript. The current affiliation for Danielle C. Bonfim is Craniofacial and Skeletal Diseases Branch, National Institute of Dental and Craniofacial Research, National Institutes of Health, Bethesda, MD, USA. Rhayra B. Dias is at the National Institute of Traumatology and Orthopedics, Rio de Janeiro, RJ, Brazil, and Daiana V. Lopes is at the Federal University of Rio de Janeiro (Macae campus), Macae, RJ, Brazil.

Competing Interests

All authors state that they have no competing interests.

Acknowledgments

The authors wish to thank Dr. Débora Portilho who helped us set up the western blotting assay, Dr. José Garcia Abreu who kindly provided us with the Renilla plasmids, Bárbara Fonseca and Fábio Mendes for help with the luciferase assay, and Grasiella Matioszek for confocal assistance. The authors are also grateful to Dr. Roel Nusse for sharing the lentivirus plasmid used in this study with the scientific community at Addgene. This work was supported by grants from the Brazilian agencies Fundação de Amparo à Pesquisa do Estado do Rio de Janeiro, Conselho Nacional de Pesquisa, Coordenação de Aperfeiçoamento de Pessoal de Nível Superior, and Associação e Programa de Biologia Celular Aplicada à Medicina.

References

[1] A. J. Friedenstein, R. K. Chailakhjan, and K. S. Lalykina, "The development of fibroblast colonies in monolayer cultures of guinea-pig bone marrow and spleen cells," *Cell and Tissue Kinetics*, vol. 3, no. 4, pp. 393–403, 1970.

[2] M. F. Pittenger, A. M. Mackay, S. C. Beck et al., "Multilineage potential of adult human mesenchymal stem cells," *Science*, vol. 284, no. 5411, pp. 143–147, 1999.

[3] B. Sacchetti, A. Funari, S. Michienzi et al., "Self-renewing osteoprogenitors in bone marrow sinusoids can organize a hematopoietic microenvironment," *Cell*, vol. 131, no. 2, pp. 324–336, 2007.

[4] P. Bianco, P. G. Robey, and P. J. Simmons, "Mesenchymal stem cells: revisiting history, concepts, and assays," *Cell Stem Cell*, vol. 2, no. 4, pp. 313–319, 2008.

[5] P. Bianco, X. Cao, P. S. Frenette et al., "The meaning, the sense and the significance: translating the science of mesenchymal stem cells into medicine," *Nature Medicine*, vol. 19, no. 1, pp. 35–42, 2013.

[6] P. Bianco and P. G. Robey, "Skeletal stem cells," *Development*, vol. 142, no. 6, pp. 1023–1027, 2015.

[7] P. Ducy, R. Zhang, V. Geoffroy, A. L. Ridall, and G. Karsenty, "Osf2/Cbfa1: a transcriptional activator of osteoblast differentiation," *Cell*, vol. 89, no. 5, pp. 747–754, 1997.

[8] F. Otto, A. P. Thornell, T. Crompton et al., "Cbfa1, a candidate gene for cleidocranial dysplasia syndrome, is essential for osteoblast differentiation and bone development," *Cell*, vol. 89, no. 5, pp. 765–771, 1997.

[9] T. F. Day, X. Guo, L. Garrett-Beal, and Y. Yang, "Wnt/β-catenin signaling in mesenchymal progenitors controls osteoblast and chondrocyte differentiation during vertebrate skeletogenesis," *Developmental Cell*, vol. 8, no. 5, pp. 739–750, 2005.

[10] T. Gaur, C. J. Lengner, H. Hovhannisyan et al., "Canonical WNT signaling promotes osteogenesis by directly stimulating *Runx2* gene expression," *Journal of Biological Chemistry*, vol. 280, no. 39, pp. 33132–33140, 2005.

[11] C. Y. Logan and R. Nusse, "The Wnt signaling pathway in development and disease," *Annual Review of Cell and Developmental Biology*, vol. 20, pp. 781–810, 2004.

[12] M. D. Gordon and R. Nusse, "Wnt signaling: multiple pathways, multiple receptors, and multiple transcription factors," *The Journal of Biological Chemistry*, vol. 281, no. 32, pp. 22429–22433, 2006.

[13] V. S. W. Li, S. S. Ng, P. J. Boersema et al., "Wnt signaling through inhibition of β-catenin degradation in an intact Axin1 complex," *Cell*, vol. 149, no. 6, pp. 1245–1256, 2012.

[14] H. Clevers, K. M. Loh, and R. Nusse, "An integral program for tissue renewal and regeneration: Wnt signaling and stem cell control," *Science*, vol. 346, no. 6205, Article ID 1248012, 2014.

[15] S. L. Etheridge, G. J. Spencer, D. J. Heath, and P. G. Genever, "Expression profiling and functional analysis of Wnt signaling mechanisms in mesenchymal stem cells," *Stem Cells*, vol. 22, no. 5, pp. 849–860, 2004.

[16] J. De Boer, H. J. Wang, and C. Van Blitterswijk, "Effects of Wnt signaling on proliferation and differentiation of human mesenchymal stem cells," *Tissue Engineering*, vol. 10, no. 3-4, pp. 393–401, 2004.

[17] G. M. Boland, G. Perkins, D. J. Hall, and R. S. Tuan, "Wnt 3a promotes proliferation and suppresses osteogenic differentiation of adult human mesenchymal stem cells," *Journal of Cellular Biochemistry*, vol. 93, no. 6, pp. 1210–1230, 2004.

[18] J. De Boer, R. Siddappa, C. Gaspar, A. Van Apeldoorn, R. Fodde, and C. Van Blitterswijk, "Wnt signaling inhibits osteogenic differentiation of human mesenchymal stem cells," *Bone*, vol. 34, no. 5, pp. 818–826, 2004.

[19] E. Haÿ, E. Laplantine, V. Geoffroy et al., "N-cadherin interacts with axin and LRP5 to negatively regulate Wnt/β-catenin signaling, osteoblast function, and bone formation," *Molecular and Cellular Biology*, vol. 29, no. 4, pp. 953–964, 2009.

[20] E. Haÿ, T. Buczkowski, C. Marty, S. Da Nascimento, P. Sonnet, and P. J. Marie, "Peptide-based mediated disruption of N-cadherin-LRP5/6 interaction promotes Wnt signaling and bone formation," *Journal of Bone and Mineral Research*, vol. 27, no. 9, pp. 1852–1863, 2012.

[21] F. Lecanda, S.-L. Cheng, C. S. Shin et al., "Differential regulation of cadherins by dexamethasone in human osteoblastic cells," *Journal of Cellular Biochemistry*, vol. 77, no. 3, pp. 499–506, 2000.

[22] A. Di Benedetto, M. Watkins, S. Grimston et al., "N-cadherin and cadherin 11 modulate postnatal bone growth and osteoblast differentiation by distinct mechanisms," *Journal of Cell Science*, vol. 123, no. 15, pp. 2640–2648, 2010.

[23] A. Di Benedetto, G. Brunetti, F. Posa et al., "Osteogenic differentiation of mesenchymal stem cells from dental bud: role of integrins and cadherins," *Stem Cell Research*, vol. 15, no. 3, pp. 618–628, 2015.

[24] E. Hay, F.-X. Dieudonne, Z. Saidak et al., "N-cadherin/Wnt interaction controls bone marrow mesenchymal cell fate and bone mass during aging," *Journal of Cellular Physiology*, vol. 229, no. 11, pp. 1765–1775, 2014.

[25] L. Xu, F. Meng, M. Ni, Y. Lee, and G. Li, "N-cadherin regulates osteogenesis and migration of bone marrow-derived mesenchymal stem cells," *Molecular Biology Reports*, vol. 40, no. 3, pp. 2533–2539, 2013.

[26] P. Liu, J.-H. Lin, and B. Zhang, "Differential regulation of cadherin expression by osteotropic hormones and growth factors in vitro in human osteoprogenitor cells," *Acta Pharmacologica Sinica*, vol. 26, no. 6, pp. 705–713, 2005.

[27] F. L. Chung, S.-L. Cheng, G. Mbalaviele et al., "Accentuated ovariectomy-induced bone loss and altered osteogenesis in heterozygous N-cadherin null mice," *Journal of Bone and Mineral Research*, vol. 21, no. 12, pp. 1897–1906, 2006.

[28] M. Eijken, M. Koedam, M. Van Driel, C. J. Buurman, H. A. P. Pols, and J. P. T. M. Van Leeuwen, "The essential role of glucocorticoids for proper human osteoblast differentiation and matrix mineralization," *Molecular and Cellular Endocrinology*, vol. 248, no. 1-2, pp. 87–93, 2006.

[29] K. Reiss, T. Maretzky, A. Ludwig et al., "ADAM10 cleavage of N-cadherin and regulation of cell-cell adhesion and β-catenin nuclear signalling," *The EMBO Journal*, vol. 24, no. 4, pp. 742–752, 2005.

[30] K. Uemura, T. Kihara, A. Kuzuya et al., "Characterization of sequential N-cadherin cleavage by ADAM10 and PS1," *Neuroscience Letters*, vol. 402, no. 3, pp. 278–283, 2006.

[31] B. Schulz, J. Pruessmeyer, T. Maretzky et al., "ADAM10 regulates endothelial permeability and T-Cell transmigration by proteolysis of vascular endothelial cadherin," *Circulation Research*, vol. 102, no. 10, pp. 1192–1201, 2008.

[32] I. Raurell, M. Codina, D. Casagolda et al., "Gamma-secretase-dependent and -independent effects of presenilin1 on β-catenin·Tcf-4 transcriptional activity," *PLoS ONE*, vol. 3, no. 12, Article ID e4080, 2008.

[33] C. McCusker, H. Cousin, R. Neuner, and D. Alfandari, "Extracellular cleavage of cadherin-11 by ADAM metalloproteases is essential for Xenopus cranial neural crest cell migration," *Molecular Biology of the Cell*, vol. 20, no. 1, pp. 78–89, 2009.

[34] C. Jang, J.-K. Choi, Y.-J. Na et al., "Calsenilin regulates presenilin 1/γ-secretase-mediated N-cadherin ε-cleavage and β-catenin signaling," *The FASEB Journal*, vol. 25, no. 12, pp. 4174–4183, 2011.

[35] P. Marambaud, J. Shioi, G. Serban et al., "A presenilin-1/γ-secretase cleavage releases the E-cadherin intracellular domain and regulates disassembly of adherens junctions," *EMBO Journal*, vol. 21, no. 8, pp. 1948–1956, 2002.

[36] K. Uemura, T. Kihara, A. Kuzuya et al., "Activity-dependent regulation of β-catenin via ε-cleavage of N-cadherin," *Biochemical and Biophysical Research Communications*, vol. 345, no. 3, pp. 951–958, 2006.

[37] E. C. Ferber, M. Kajita, A. Wadlow et al., "A role for the cleaved cytoplasmic domain of E-cadherin in the nucleus," *Journal of Biological Chemistry*, vol. 283, no. 19, pp. 12691–12700, 2008.

[38] A. Dwivedi, S. C. Slater, and S. J. George, "MMP-9 and -12 cause N-cadherin shedding and thereby β-catenin signalling and vascular smooth muscle cell proliferation," *Cardiovascular Research*, vol. 81, no. 1, pp. 178–186, 2009.

[39] T. Maretzky, K. Reiss, A. Ludwig et al., "ADAM10 mediates E-cadherin shedding and regulates epithelial cell-cell adhesion, migration, and β-catenin translocation," *Proceedings of the National Academy of Sciences of the United States of America*, vol. 102, no. 26, pp. 9182–9187, 2005.

[40] A. P. D. N. De Barros, C. M. Takiya, L. R. Garzoni et al., "Osteoblasts and bone marrow mesenchymal stromal cells control hematopoietic stem cell migration and proliferation in 3D *in vitro* model," *PLoS ONE*, vol. 5, no. 2, Article ID e9093, 2010.

[41] L. S. Thiago, E. S. Costa, D. V. Lopes et al., "The Wnt signaling pathway regulates Nalm-16 b-cell precursor acute lymphoblastic leukemic cell line survival and etoposide resistance," *Biomedicine & Pharmacotherapy*, vol. 64, no. 1, pp. 63–72, 2010.

[42] D. M. Portilho, E. R. Martins, M. L. Costa, and C. S. Mermelstein, "A soluble and active form of Wnt-3a protein is involved in myogenic differentiation after cholesterol depletion," *FEBS Letters*, vol. 581, no. 30, pp. 5787–5795, 2007.

[43] N. Leclerc, C. A. Luppen, V. V. Ho et al., "Gene expression profiling of glucocorticoid-inhibited osteoblasts," *Journal of Molecular Endocrinology*, vol. 33, no. 1, pp. 175–193, 2004.

[44] S. Vujovic, S. R. Henderson, A. M. Flanagan, and M. O. Clements, "Inhibition of γ-secretases alters both proliferation and differentiation of mesenchymal stem cells," *Cell Proliferation*, vol. 40, no. 2, pp. 185–195, 2007.

[45] P. A. Zuk, M. Zhu, H. Mizuno et al., "Multilineage cells from human adipose tissue: implications for cell-based therapies," *Tissue Engineering*, vol. 7, no. 2, pp. 211–228, 2001.

[46] C. S. Mermelstein, D. M. Portilho, F. A. Mendes, M. L. Costa, and J. G. Abreu, "Wnt/β-catenin pathway activation and myogenic differentiation are induced by cholesterol depletion," *Differentiation*, vol. 75, no. 3, pp. 184–192, 2007.

[47] L. Chicaybam, A. L. Sodre, B. A. Curzio, and M. H. Bonamino, "An efficient low cost method for gene transfer to T lymphocytes," *PLoS ONE*, vol. 8, no. 3, Article ID e60298, 2013.

[48] C. Fuerer and R. Nusse, "Lentiviral vectors to probe and manipulate the Wnt signaling pathway," *PLoS ONE*, vol. 5, no. 2, Article ID e9370, 2010.

[49] L. G. Lima, A. S. Oliveira, L. C. Campos et al., "Malignant transformation in melanocytes is associated with increased production of procoagulant microvesicles," *Thrombosis and Haemostasis*, vol. 106, no. 4, pp. 712–723, 2011.

[50] B. Lustig, B. Jerchow, M. Sachs et al., "Negative feedback loop of Wnt signaling through upregulation of conductin/axin2 in colorectal and liver tumors," *Molecular and Cellular Biology*, vol. 22, no. 4, pp. 1184–1193, 2002.

[51] C. G. Bellows, J. E. Aubin, and J. N. M. Heersche, "Initiation and progression of mineralization of bone nodules formed in vitro: the role of alkaline phosphatase and organic phosphate," *Bone and Mineral*, vol. 14, no. 1, pp. 27–40, 1991.

[52] P. Marambaud, P. H. Wen, A. Dutt et al., "A CBP binding transcriptional repressor produced by the PS1/ε-cleavage of N-cadherin is inhibited by PS1 FAD mutations," *Cell*, vol. 114, no. 5, pp. 635–645, 2003.

[53] M. S. Elston, A. J. Gill, J. V. Conaglen et al., "Nuclear accumulation of E-Cadherin correlates with loss of cytoplasmic membrane staining and invasion in pituitary adenomas," *Journal of Clinical Endocrinology and Metabolism*, vol. 94, no. 4, pp. 1436–1442, 2009.

[54] B. Geiger, T. Volberg, D. Ginsberg, S. Bitzur, I. Sabanay, and R. O. Hynes, "Broad spectrum pan-cadherin antibodies, reactive with the C-terminal 24 amino acid residues of N-cadherin," *Journal of Cell Science*, vol. 97, part 4, pp. 607–614, 1990.

[55] M. T. Maher, A. S. Flozak, A. M. Hartsell et al., "Issues associated with assessing nuclear localization of N-terminally unphosphorylated β-catenin with monoclonal antibody 8E7," *Biology Direct*, vol. 4, article 5, 2009.

[56] M. T. Maher, R. Mo, A. S. Flozak, O. N. Peled, and C. J. Gottardi, "β-Catenin phosphorylated at serine 45 is spatially uncoupled from β-catenin phosphorylated in the GSK3 domain: implications for signaling," *PLoS ONE*, vol. 5, no. 4, Article ID e10184, 2010.

[57] V. Deregowski, E. Gazzerro, L. Priest, S. Rydziel, and E. Canalis, "Notch 1 overexpression inhibits osteoblastogenesis by suppressing Wnt/β-catenin but not bone morphogenetic protein signaling," *Journal of Biological Chemistry*, vol. 281, no. 10, pp. 6203–6210, 2006.

[58] S. Zanotti, A. Smerdel-Ramoya, L. Stadmeyer, D. Durant, F. Radtke, and E. Canalis, "Notch inhibits osteoblast differentiation and causes osteopenia," *Endocrinology*, vol. 149, no. 8, pp. 3890–3899, 2008.

[59] Y. Zhang, J. B. Lian, J. L. Stein, A. J. Van Wijnen, and G. S. Stein, "The Notch-responsive transcription factor Hes-1 attenuates osteocalcin promoter activity in osteoblastic cells," *Journal of Cellular Biochemistry*, vol. 108, no. 3, pp. 651–659, 2009.

[60] R. Salie, M. Kneissel, M. Vukevic et al., "Ubiquitous overexpression of Hey1 transcription factor leads to osteopenia and chondrocyte hypertrophy in bone," *Bone*, vol. 46, no. 3, pp. 680–694, 2010.

[61] J. Caverzasio, E. Biver, and C. Thouverey, "Predominant role of PDGF receptor transactivation in Wnt3a-Induced osteoblastic cell proliferation," *Journal of Bone and Mineral Research*, vol. 28, no. 2, pp. 260–270, 2013.

[62] W. Qiu, T. E. Andersen, J. Bollerslev, S. Mandrup, B. M. Abdallah, and M. Kassem, "Patients with high bone mass phenotype exhibit enhanced osteoblast differentiation and inhibition of adipogenesis of human mesenchymal stem cells," *Journal of Bone and Mineral Research*, vol. 22, no. 11, pp. 1720–1731, 2007.

[63] R. van Amerongen and R. Nusse, "Towards an integrated view of Wnt signaling in development," *Development*, vol. 136, no. 19, pp. 3205–3214, 2009.

[64] M. Ozawa, H. Barbault, and R. Kemler, "The cytoplasmic domain of the cell adhesion molecule uvomorulin assoicates with three independent proteins structurally related in different species," *EMBO Journal*, vol. 8, no. 6, pp. 1711–1717, 1989.

[65] P. D. McCrea and B. M. Gumbiner, "Purification of a 92-kDa cytoplasmic protein tightly associated with the cell-cell adhesion molecule E-cadherin (uvomorulin). Characterization and extractability of the protein complex from the cell cytostructure," *The Journal of Biological Chemistry*, vol. 266, no. 7, pp. 4514–4520, 1991.

[66] P. J. Marie, E. Haÿ, D. Modrowski, L. Revollo, G. Mbalaviele, and R. Civitelli, "Cadherin-mediated cell-cell adhesion and signaling in the skeleton," *Calcified Tissue International*, vol. 94, no. 1, pp. 46–54, 2014.

[67] S. A. Kuznetsov, P. H. Krebsbach, K. Satomura et al., "Single-colony derived strains of human marrow stromal fibroblasts form bone after transplantation in vivo," *Journal of Bone and Mineral Research*, vol. 12, no. 9, pp. 1335–1347, 1997.

[68] B. J. Sworder, S. Yoshizawa, P. J. Mishra et al., "Molecular profile of clonal strains of human skeletal stem/progenitor cells with different potencies," *Stem Cell Research*, vol. 14, no. 3, pp. 297–306, 2015.

[69] M. Owen and A. J. Friedenstein, "Stromal stem cells: marrow-derived osteogenic precursors," *Ciba Foundation symposium*, vol. 136, pp. 42–60, 1988.

Hindawi Publishing Corporation
Stem Cells International
Volume 2016, Article ID 9783408, 14 pages
http://dx.doi.org/10.1155/2016/9783408

Review Article

Mesenchymal Stem Cells as Therapeutics Agents: Quality and Environmental Regulatory Aspects

Patricia Galvez-Martin,[1,2] Roger Sabata,[1] Josep Verges,[1] José L. Zugaza,[3,4,5] Adolfina Ruiz,[2] and Beatriz Clares[2]

[1] *Advanced Therapies Area, Bioibérica S.A., 08029 Barcelona, Spain*
[2] *Department of Pharmacy and Pharmaceutical Technology, School of Pharmacy, University of Granada, 180171 Granada, Spain*
[3] *Department of Genetics, Physical Anthropology and Animal Physiology, University of the Basque Country, 48940 Leioa, Spain*
[4] *Achucarro Basque Center for Neuroscience, Bizkaia Science and Technology Park, Building No. 205, 48170 Zamudio, Spain*
[5] *IKERBASQUE, Basque Foundation for Science, María Díaz de Haro 3, 48013 Bilbao, Spain*

Correspondence should be addressed to Patricia Galvez-Martin; galmafarma@gmail.com

Received 22 September 2016; Accepted 18 October 2016

Academic Editor: Marco Tatullo

Mesenchymal stem cells (MSCs) are one of the main stem cells that have been used for advanced therapies and regenerative medicine. To carry out the translational clinical application of MSCs, their manufacturing and administration in human must be controlled; therefore they should be considered as medicine: stem cell-based medicinal products (SCMPs). The development of MSCs as SCMPs represents complicated therapeutics due to their extreme complex nature and rigorous regulatory oversights. The manufacturing process of MSCs needs to be addressed in clean environments in compliance with requirements of Good Manufacturing Practice (GMP). Facilities should maintain these GMP conditions according to international and national medicinal regulatory frameworks that introduce a number of specifications in order to produce MSCs as safe SCMPs. One of these important and complex requirements is the environmental monitoring. Although a number of environmental requirements are clearly defined, some others are provided as recommendations. In this review we aim to outline the current issues with regard to international guidelines which impact environmental monitoring in cleanrooms and clean areas for the manufacturing of MSCs.

1. Introduction

Mesenchymal stem cells (MSCs) hold considerable promise as a source of cells for novel therapies treating many serious diseases and injuries, including metabolic, degenerative, and inflammatory diseases, repair and regeneration of damaged tissues, and cancer. MSCs can be isolated from different tissues of the human body, expanded and/or differentiated *in vitro*, and subsequently processed and administered to patients as medicine or stem cell-based medicinal products (SCMPs). The scope of potential MSCs-based therapies has expanded in recent years due to advances in stem cell research focused in regenerative medicine. Currently several SCMPs with MSCs have been approved by the regulatory authorities in different countries.

The manufacturing of MSCs for translational clinical research should be performed with appropriate controls that ensure their safety and quality. In this context, new regulatory regimes for advanced and complex treatments such as cell therapies, tissue engineering, and gene therapies have grown substantially in importance in developing countries because they offer ground-breaking new opportunities for the treatment of disease and injury [1, 2]. These measures require laboratories to gain new knowledge of cell manufacturing and regulatory strategies because there are a number of factors that contribute to the product quality, such as starting materials, packaging materials, validated processes, personnel, procedures, equipment, and premises and environment [3, 4]. Any procedure related to clinical application of MSCs requires a strict control in the production facilities. This includes the

manufacturing space, the storage warehouse for raw and finished product, and support laboratory areas [5]. All these organized according to Good Manufacturing Practice (GMP) for pharmaceutical manufacturers. Among all these requirements, environmental contamination assessment for the manufacturing of MSCs plays an important role in minimizing the risk of contamination by particles or microorganisms. Contamination of MSCs can cause adverse reactions in patients (e.g., fever, chills, infections, and irreversible septic shock) and even death. Therefore it will be necessary to standardize and validate all procedures and analytical techniques involved in its manufacture by the implementation of quality control programs [6]. An environmental monitoring program must be established in the therapy laboratory. This formal program should clearly stipulate and evaluate all circumstances involving the microbiological quality of the process and the MSCs [7]. The amount and type of evidence required for microbiological quality control should be defined according to different regulatory bodies, such as national Pharmacopeias, regulatory authorities, and the International Standards Organization (ISO). Each analytical technique must be validated to assure that the adopted procedure does not alter the method and consequently the result [4].

This review provides all the necessary requirements to manufacture MSCs as medicine in order to present themselves as a new therapeutic alternative.

The current state of legislation and methodology for the environmental control monitorization are described.

2. Environmental Monitoring

The processing of MSCs for use in cell therapy protocols requires a specific environment in which air quality is controlled, in order to minimize the risk of contamination of cells. To control air quality monitorization of viable and nonviable particles must be carried out throughout the whole process. In this field, a viable particle is a particle that contains one or more living microorganisms. A nonviable particle is a particle that does not contain a living microorganism.

The environmental monitoring should include a series of physical controls (concentration of particles in the air, flow of air, integrity of high efficiency particulate air (HEPA) filters, differential pressure, temperature, and relative humidity) and microbiological tests [7]. Other aspects should be also determined: places and the frequency of the sampling, a map of the installations on which sampling points can be recorded, the actions required when the alert and action levels are observed, and the personnel control. In short, the main objective is to develop and preserve a controlled environment that minimizes the risk contamination of MSCs, with special care to critical processes with higher level risk.

Regular monitoring of the environment, process, and finished product with MSCs must occur according to a written procedure and in line with the published written standards and guidelines [8]. This written procedure is known as the environmental monitoring program which is designed to routinely monitor particulates and microorganisms in critical areas and provides meaningful information on the quality of the aseptic processing environment as well as environmental trends of ancillary clean areas [9].

3. Regulatory Sources

For a descriptive overview of the regulatory authorities and documents the following classification is presented below. However, this is a difficult task by the range of different regulatory documents and standards [10]. To date regulatory and other concerned authorities have not been able to unify and standardize the criteria for manufacturing of MSCs as SCMPs worldwide. There are still some differences over specific issues.

3.1. US Food Drug Administration (FDA). The Food and Drug Administration (FDA) publishes guidance documents (not mandatory) to provide general requirements for investigators from the US Code of Federal Regulations (CFR). CFR is a compilation of all published federal laws in USA. All food and drug related laws are contained in its Title 21. Within this, part 211 is as follows: "Current Good Manufacturing Practice for finished Pharmaceuticals" [11]. One of the most important FDA guidances related to environmental monitoring is the "Guidance for industry: Sterile Drug Products Produced by Aseptic Processing—Current Good Manufacturing Practice" (FDA-cGMP) [9].

3.2. European Good Manufacturing Practices (EU-GMP). The body of European Union legislation in the pharmaceutical sector is compiled in the publication "The Rules Governing Medicinal Products in the European Union" published by the European Commission [12]. This consists of 10 volumes. Volume 4 contains guidance for the interpretation of the principles and guidelines of GMP for medicinal products for human and veterinary use.

The European Medicines Agency (EMA) is the responsible public body for the scientific evaluation of medicines. Important documents of this regulation are Volume 4, annex 1: "Manufacture of Sterile Medicinal Products" [13] and annex 2: "Manufacture of Biological Active Substances and Medicinal Products for Human Use" [14]. On the other hand, EMA issued the "Guideline on Scientific Requirements for the Environmental Risk Assessment of Gene Therapy Medicinal Products" [15].

3.3. World Health Organization (WHO). The WHO was the first international organization who established detailed guidelines for GMP. GMP guidelines for biological products were approved in 1992 by both the WHO Expert Committee on Biological Standardization and the WHO Expert Committee on Specifications for Pharmaceutical Preparations [16]. This guidance contains different annexes which have been revised over the course of the years. One of the most important annexes is annex 6 "WHO-GMP for Sterile Pharmaceutical Products" [17]. Specific keys for the manufacture of sterile products are also described in order to minimize the risk of microbiological contamination, including viable and nonviable particles and pyrogens. Based on scientific

developments and GMP, some technical requirements may be modified [18].

3.4. Pharmaceutical Inspection Convention and the Pharmaceutical Inspection Cooperation Scheme (PIC/S). The Pharmaceutical Inspection Convention and Pharmaceutical Inspection Cooperation Scheme are two international bodies, made up of 46 representatives participating authorities from different countries with competencies in the field of GMP. The PIC/S aim to harmonize inspection procedures by developing common standards of GMP. They also aim to facilitate cooperation and contacts between the competent authorities, regional and international organizations, thereby increasing mutual trust. As GMP guide of interest for this article was that issued by PIC/S is the "Guide to GMP for Medicinal Products" PE 009 and revisions [19].

Originally, the PIC/S GMP guide ("PIC Basic Standards" of 1972) derived from the WHO-GMP guide. However, it was further adapted and expanded to satisfy the requirements of states taking part in PIC/S. In 1989, the EU adopted its own GMP guide. Since then the EU and PIC/S GMP guidelines have been developed in parallel but differ on small points such as expressions or references to Pharmacopeias.

3.5. International Standard Organization (ISO). ISO is an independent, nongovernmental membership organization developer of voluntary international standards. Its main aim is to promote the development of worldwide harmonization of standards. ISO publishes numerous standards of relevance to pharmaceutical manufacturing, but not all of these standards are associated with GMP conditions. The most important GMP guide related to the topic at hand is the standard ISO 14644: "Cleanrooms and Associated Controlled Environments" and its series [20]. These standards are referenced both in EU-GMP and FDA-cGMP.

3.6. International Conference on Harmonization of Technical Requirements for Registration of Pharmaceuticals for Human Use (ICH). Harmonization of regulatory requirements was pioneered by the European Union (formerly European Community) in the 1980s moved towards the development of a single market for pharmaceuticals. At the same time, bilateral meetings between Europe, Japan, and the USA took place. Finally, at the WHO Conference of Drug Regulatory Authorities, in Paris (1989), clear statements began to materialize.

It publishes quality and GMP documentation. Launched in 1990, ICH is a unique undertaking that brings together the drug regulatory authorities and the pharmaceutical industry of Europe, Japan, and the USA. Among others, an important document regarding environment monitoring is "Good Manufacturing Practice Guide for Active Pharmaceutical Ingredients Q7" [21]. Some guidelines have been assumed by EU-GMP and FDA-cGMP.

3.7. Pharmacopeias. The main international Pharmacopeias regarding this field are European Pharmacopeia (EP), Japanese Pharmacopeia (JP), and the United States Pharmacopeia (USP). Pharmacopeias issue some aspects with direct relevance mainly to sterility testing and other laboratory test methods. An example is the *Mycoplasma* testing [22–24].

3.8. Other Guidance Sources. Some countries possess national regulatory agencies that publish additional documents of guidance such as Australia, Canada, Japan, and Singapore. These agencies include Parenteral Drug Association (PDA), American Society for Testing and Materials (ASTM), Pharmaceutical Microbiology Interest Group (Pharmig), Pharmaceutical and Healthcare Sciences and Society (PHSS), IPSE (International Society for Pharmaceutical Engineering) [10].

4. Facilities to Translational Clinical Application

A MSCs production laboratory for clinical use must meet the minimum requirements for the product sterility manufacture. These facilities are called cleanrooms or clean areas. Environmental parameters such as size and number of airborne particulates, temperature, humidity, air pressure, airflow patterns (speed and direction), air motion, vibration, noise, viable (living) organisms, radiation, and lighting must be strictly controlled [25].

According to the degree of purity of air three different international standards have been proposed and only particle contamination is used for classification purposes.

4.1. Federal Standard 209. This standard was first published in 1963 in the USA entitled "Cleanroom and Work Station Controlled Environments" and posteriorly revised five times until 1992. Finally, it was canceled in 2001. The Federal Standard categorized cleanrooms in six general classes, depending on the particle count (particles per cubic foot) and size in μm. When expressed in SI units, the numerical designation of the class is derived from the logarithm (base 10, with the mantissa truncated to a single decimal place) of the maximum allowable number of particles, 0.5 m and larger, per cubic meter of air. When expressed in English (US customary) units, the numerical designation of the class is derived from the maximum allowable number of particles, 0.5 m and larger, per cubic foot of air (Table 1). For alternative classes less clean than class M4.5, verification shall be performed by measurement in different particle size ranges. This standard was superseded by ISO standard. However, many organizations refused to change due to expensive costs and currently; it is commonly accepted in some facilities in the USA and Asia.

4.2. ISO. Cleanrooms are classified according to the air cleanliness. In the international domain, the ISO Technical Committee 209 decided to draft an international standard on these cleanrooms, whose mission was to establish the criteria that should govern the cleanrooms without making specific reference to a particular through the ISO 14644 series [20]. The first international standard was the ISO 14644-1 [26], which was slowly replacing the Federal Standard 209E ratings. It is based on metric measurements. ISO 14644-1 covers the classification of air cleanliness in cleanrooms and

Table 1: Federal Standard 209E. Class limits are given for each class name.

Class name		Class limits									
		≥0.1 μm		≥0.2 μm		≥0.3 μm		≥0.5 μm		≥5 μm	
SI	English	m^3	ft^3	m^3	ft^3	m^3	ft^3	m^3	ft^3	m^3	ft^3
M1		350	9.91	75.7	2.14	30.9	0.875	10.0	0.283		
M1.5	1	1,240	35	265	7.50	106	3.00	35.3	1.00		
M2		3,500	99.1	757	21.4	309	8.75	100	2.83		
M2.5	10	12,400	350	2,650	75.0	1,060	30.0	353	10.0		
M3		35,000	991	7,570	214	3,090	87.5	1,000	28.3		
M3.5	100			26,500	750	10,600	300	3,530	100		
M4				75,700	2,140	30,900	875	10,000	283		
M4.5	1,000							35,300	1,000	247	7.00
M5								100,000	2,830	618	17.5
M5.5	10,000							353,000	10,000	2,470	70.0
M6								1,000,000	28,300	6,180	175
M6.5	100,000							3,350,000	100,000	24,700	700
M7								10,000,000	283,000	61,800	1,750

Table 2: ISO-14664, cleanrooms, and associated controlled environments (particles/m^3).

ISO classification number (N)	Class limits					
	≥0.1 μm	≥0.2 μm	≥0.3 μm	≥0.5 μm	≥1.0 μm	≥5.0 μm
1	10	2				
2	100	24	10	4		
3	1,000	237	102	35	8	
4	10,000	2,370	1,020	352	83	
5	100,000	23,700	10,200	3,520	832	29
6	1,000,000	237,000	102,000	352,000	8,320	293
7				3,520,000	83,200	2,930
8				35,200,000	832,000	29,300
9					8,320,000	293,000

other controlled environments. ISO 14644-1 has been revised as a new, second-edition Draft International Standard (DIS), the ISO/DIS 14644-1.2 [27]. However, it is not yet adopted as an American National Standard until published as such. The classification of this standard is based solely on the concentration of suspended particles (Table 2). Moreover, the only particle populations that are considered for classification are the cumulative distribution based on thresholds (lower limit) from 0.1 to 5 μm.

4.3. EU-GMP. Each manufacturing operation requires an appropriate level of environmental cleaning to minimize the risk of microbial contamination or particles in the product or materials being handled. EU-GMP, annex 1: "Manufacture of Sterile Medicinal Products of GMP" [13], details the new considerations to make in the production of advanced drug therapies products making control of the number of particles in the working environment of the cleanroom. For the manufacture of sterile medicinal products four grades can be distinguished: grade A in the local zone for high risk operations, grade B for aseptic preparation and filling operations (background environment of the grade A zone), and grades C and D for clean areas in which less critical stages are carried out in the manufacture of sterile products.

Two conditions are defined depending on the manufacturing activity: "*in operation*" and "*at rest*." And thus different air-cleanliness levels must be specified. As the EU-GM itself defines, the "*at rest*" state is one in which the cleanroom is operational, with all the equipment and HVAC systems without staff present. On the other hand, in the "*in operation*" state the installation is in the operating mode with all staff, which will be previously defined [13]. Table 3 reports the airborne particulate classification for these grades, according to the PIC/S GMP and EU-GMP. There is a correspondence between these guidance conditions and that specified in the ISO 14644-1 at a particle size of 0.5 μm.

To achieve the degree of air A, B, C, and D, the number of air changes should be related to the size of the room and the equipment and personnel present in it; the air system must have appropriate filters such as HEPA grades A, B, and C. The HEPA filter is not mentioned for grade D.

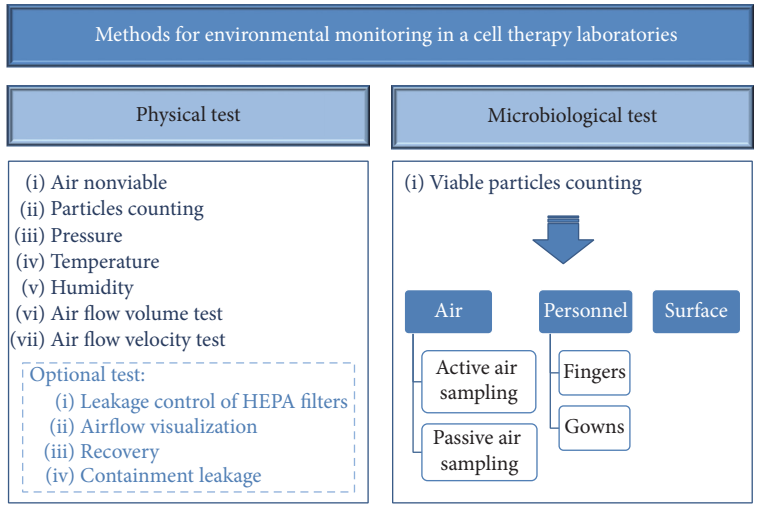

Figure 1: Scheme of environmental control requirements for the manufacture of SCMPs in cell therapy laboratories for the monitorization of viable and nonviable particles.

Table 3: Airborne particulate classification for these grades, according to the PIC/S GMP and EU-GMP.

Grade	Maximum number of particles permitted/m^3			
	At rest		In operation	
	≥0.5 μm	≥5.0 μm	≥0.5 μm	≥5.0 μm
A[a]	3,520	20	3,520	20
B	3,520	29	352,000	2,900
C	352,000	2,900	3,520,000	29,000
D	3,520,000	29,000	Not defined	Not defined

[a]All areas must be free particles of size greater than 5 μm. Limits are set to 1 particle/m^3 because it is impossible to ensure the absence of particles with any statistical significance. The periodic classification of facilities (cleanroom) must show that all areas meet the defined limits.

5. Methods for Environmental Monitoring of Cleanrooms

Airborne particles can be shaped and composed of different materials. They can also act as "carriers" for bacteria and other microorganisms. Hence, to distinguish between viable particles and inert particles (nonviable), analysis methods in a cleanroom can be classified as microbiological and physical tests. Microbiological tests consist of viable particles counting in both air and surfaces. Physical tests consist of air nonviable particles counting, pressure, and temperature analysis. Monitoring of both physical and microbiological contamination remains essential in aseptic operations to provide ongoing information on the maintenance of a stable and suitable environment for the aseptic preparation of products for administration to patients. It is vital that test methodologies exist as part of the environmental monitoring programme. Each test method selected for routine monitoring should be validated [8]. Techniques used for monitoring should be easy to perform, produce meaningful results, and must not contribute to contamination. Figure 1 schematizes environmental control requirements for viable and nonviable particles.

ISO 14644 specifies basic requirements for cleanroom operations. This standard considers all classes of cleanrooms used to produce all types of products and does not address specific requirements for the pharmaceutical industry. A total of thirteen tests are described in this standard. However, only specific tests for cleanrooms intended for the production of SCMPs are commented on in the following sections. Some of them are mandatory but others are voluntary. The key controlling factors in the quality level of any cleanroom are the owner's requirements and what measurements are necessary to achieve that level of performance.

5.1. Frequency and Collection Sites. The frequency of environmental testing should have a direct relationship to the operations performed and be sufficient to allow for meaningful statistical calculations. FDA-cGMP, EU-GMP, USP, or ISO do not provide specific references for that issue but rather general recommendations as shown in Table 4. On the other hand, the WHO paper for manufacturers of human vaccines also provides indications in this respect [28].

The minimum number of sampling point locations (NL, rounded up to a whole number) is defined by ISO 14644-1, annex B, through the following equation:

$$\mathrm{NL} = \sqrt{A}, \tag{1}$$

where A is the area of the cleanroom or clean zone in m^2. In the case of unidirectional horizontal airflow, the area may be considered as the cross section of the moving air perpendicular to the direction of the airflow. Samples should be taken at approximately by dividing the clean area into a grid (one sample from each location) at 1 m above the floor approximately or at height of the work area. In the case of only one location, three samples are required. The required volume per sample depends on the cleanliness and the functional

Table 4: Recommended frequency of environmental monitoring testing.

Clean area type			Frequency sampling			
FS209E	ISO	EU-GMP	FDA-cGMP	EU-GMP		USP
				At rest	In operation	
M3.5 (100)	5	A	Should cover all production shifts	Frequent to detect system deterioration	For the duration of critical operations	Each operating shift
M4.5 (1,000)	6	—[a]	Should cover all production shifts	—	—	Each operating shift
M5.5 (10,000)	7	B	Should cover all production shifts	Frequent to detect system deterioration	For the duration of critical operations	Each operating shift
M6.5 (100,000)	8	C	Should cover all production shifts	Frequent to detect system deterioration	In line with quality risk management	Twice a week
		D	—	In line with quality risk management	In line with quality risk management	Once a week[b] —

[a]There is no correspondence between FS209 M3.5 (100) and ISO 6 classes with EU-GMP cleanroom classification.

[b]Other support areas to aseptic processing areas but nonproduct contact.

Figure 2: Diagram of cleanrooms and sampling points of environmental monitoring for stem cell units. Sampling N should be carried out whenever an activity is performed (in operation). The sampling rate for the points A, P, S, and W must be previously validated according to the requirements of the operations.

state of the environment. The minimal sample volume (V_s, L) for qualification is established by annex B of the ISO 14644-1 guideline through the equation

$$V_s = \frac{20}{C_{n,m}} \times 1{,}000, \quad (2)$$

where $C_{n,m}$ is the class limit (number of particles per m^3) for the largest considered particle size specified for the relevant class and 20 is the number of samples that could be counted if the particle concentration was at the class limit. The volume sampled at each location shall be at least 2 L, with the minimum sampling time at each location being 1 min. When V_s is very large, the time required for sampling can be substantial. In these cases the sequential sampling procedure described in annex F is followed, and both the required sample volume and time required to obtain samples may be reduced. Figure 2 schematizes sampling points according to the clean area type. This type and the conditions will determine the frequency (Table 4).

6. Physical Tests

Measurement and determination of different physical operation aspects of the cleanroom are essential to ensure that a suitable environment is maintained for the preparation of aseptically prepared products.

6.1. Nonviable Particle Counts. For the measurement of particle concentration in grade A and B areas a continuous system should be used, with the establishment of the required

frequency and alert limits. The volume of the air sample should not be less than 1 m^3 in both areas and also in grade C areas. Table 3 shows the maximum airborne particle concentration allowed in each area with light variations according to EU-GMP [12].

The locations of the monitoring systems of particles (according to risk analysis and classification results) should be next point to the product on display and working height, point of greater transfer of personnel and/or material, point on the remote environment of the area of influence of flow, and points with less effectively treated air flow (measured by the smoke test). Risk analysis is the quantitative or qualitative estimation of the likelihood associated with the previously identified hazards. A documented risk analysis to try to identify, evaluate, measure, and prevent possible failures that can initiate and trigger undesired events should be conducted by the manufacturer for ascertaining the appropriate GMP. Each cleanroom is different and therefore each of them should analyze all aspects related to the required environment. The risk analysis should consider all foreseeable hazards that may cause the input of pollutants. The location chosen for monitoring should be checked to ensure that the positions reflect the worst case. For room monitoring, the counts should be performed in locations where there is most operator activity. For the filling environment the counts should be performed adjacent to the filling zone and where components are exposed in such way as to detect operator activity within these areas.

Monitoring systems airborne particle counters may consist of independent particles, a network of sampling points for sequential access by a collector connected to a single particle counter, or a combination of both. The selected system must be appropriate to the particle size considered. It should be noted that sampling cannot compromise the laminar airflow in the critical zone and that the counting device is oriented in the direction of air flow input. It is standard practice to utilize modern technology and use an optical particle counter where the air sample is drawn into the instrument and passed through a light scattering device.

The terminology of ISO 14644-7 "Cleanrooms and Associate Controlled Environments" is "*separative devices*," which includes laminar flow cabinets, minienvironments glove boxes, and isolators. These devices normally operate at EU-GMP Grade A/ISO Class 5. In Europe "*cabinet*" is the most common term to refer to "*hood*," which is more typical in USA [29].

6.2. Pressure. Temperature and pressure devices are used to monitor the process. Automatic systems should be previously validated. The air pressure values will depend on the laboratory design, but a differential pressure from the most critical room to the outside of at least 30 Pa and 10–15 Pa between rooms is recommended [9, 30]. According to the ISO 14644-3, annex B5 pressure differential readings should be logged in all classes of cleanrooms in a maximal time interval of 12 months [31]. However, the interval between tests should be defined depending on the product and the process. Equally, recommendations regarding air supplies and pressure differentials may need to be modified depending on requirements [19]. A warning system and indicators of pressure with regular recording should be installed between areas.

6.3. Airflow Volume and Velocity. In grade A cleanrooms should be provided with laminar air flow with air speed of 0.36–0.54 m/s with regular validation [19]. Airflow volume test is intended to verify the air change rates by means of air flow readings and air change rates. It may be determined by either velocity or volume measurement techniques according to ISO 14644-3, annex B13 [32].

Verification laminar flow protection systems and the suitability of the containment conditions are performed to control the airflow velocity to be measured according to ISO 14644-3, annex B4 [33]. The acceptance criterion, according to EU-GMP and FDA-cGMP guidelines, is 0.45 m/s ± 20%.

Both tests should be performed in all cleanrooms at maximal period of twelve months as a reference in the operational and the at rest state. These tests could be performed by the installation of anemometers (direct air velocity measurement), manometers (indirect air velocity measurement), and pitot tube (single-point probe).

6.4. Optional Tests. Other optional tests such as installed filter leakage, airflow visualization, recovery, and containment leakage are defined in the ISO 14644-3 and suggest a retesting interval of 24 months.

6.4.1. Installed Filter Leakage. Any air admitted should be passed through a HEPA filter [19]. HEPA filters are of paramount importance in obtaining viable and nonviable cleanliness levels, which retain particles greater than 0.3 μm. Two filter integrity test methods for HEPA filters are reported in the ISO 14644-3, annex B6 [34]. Both methods require an evenly distributed aerosol challenge and the scanning of the filter gasket, filter frame, and filter media downstream of the filter.

The first *in situ* HEPA filter test method is DOP (dioctyl phthalate) test. This test utilizes the aerosol photometer as the measuring device and an aerosol generator to produce an aerosol challenge (scan testing). This method has been used since the 1950s and appears in many different standards such as MIL-STD-282 [35], IES RP-CC-001-83 [36], and European standard EN 1822-1 [37]. Now PAO (poly-alpha-olefin), diethylhexyl sebacate (DEHS), and paraffin are often used as aerosols. Sometimes the term DOP test is used to describe a HEPA filter leak test without intending to specify the use of DOP as the aerosol.

The second method offered in the standard is the particle counting method. This method also requires that the filter be evenly challenged with a known recorded concentration of aerosol, an aerosol diluter, and a discrete particle counter (volumetric testing). This procedure is implemented by using dissolution chambers and other devices that minimize the exposure of the delicate optical part of the device [38]. Results from both methods are not directly comparable. An unacceptable leak is defined as a penetration of 0.03% or more of particles 0.3 μm and larger than the reference calibration curve for 99.97% efficient filters or as penetration of 0.01%

or greater of particles 0.3 μm and larger than reference calibration curve for 99.99% efficient filters [38].

6.4.2. Airflow Visualization. This gives some idea as to how quickly contamination may be removed from the cleanroom provided that there is acceptable mixing of air in the room. An assessment of air flows (from clean to dirty areas) is a specification for the manufacture of sterile products, to evaluate ISO class 5 (Grade A zone) and the surrounding ISO class 7 (Grade B) room and uniformly from unidirectional air flow units. This is undertaken by visualizing actual or videotaped the air flow with the use of smoke in accordance with ISO 14644-3, annex B7 [39].

6.4.3. Recovery. Also known as the clean-up time, recovery is the time elapsed in a cleanroom to return to the static condition (in terms of particulates), according to its classification, after an incident. In accordance with ISO 14644-3, annex B13 [32], it should not take more than 15 min. This standard contains two test methods known as cleanliness recovery performance and cleanliness recovery rate.

6.4.4. Containment Leakage. It is designed to ensure that no airborne contamination can occur via leaks from higher pressure work areas to others adjacent to it. Airborne contamination can come into a cleanroom from less clean adjacent areas and pass through doors and hatches, as well as through holes and cracks in the walls, ceilings, and other parts of the cleanroom. In this way the absence of cross-contamination can be verified by the airflow direction smoke tests and room air pressures measurement in accordance to ISO 14644-3, annex B4 [33].

6.5. Less Critical Tests. A correct air quantity is necessary to displace particles, pressurize required spaces, and control temperature and humidity. This parameter is calculated as air changes per hour. According to ISO specifications it should be >120 air changes/h, >40 air changes/h, and >20 air changes/h for 100, 10,000, and 100,000 class cleanroom or clean area class, respectively. Airflow can also be used to determine the number of air changes that occur in a space over a period of one hour. This is accomplished by determining the supply (cm^3/h) and dividing it by the total volume of a space (length × width × height) to come up with the number of air exchanges per hour.

Cleanrooms should have other requirements as temperature and humidity. These measurements will also assure the correct performance of the heating, ventilation, and air-conditioning (HVAC) system. However, some process steps require appropriate temperature. Moreover, the personnel commodity wearing special clothing should be taken into consideration. Relative humidity also affects occupant comfort, productivity, and operating costs. In general acceptance criteria are 22 ± 3°C (72 ± 5°F) temperature and 30–50% relative humidity.

On the other hand, the illuminance should be in accordance with the task to be performed. A range of 400 to 750 lux is recommended [10].

Finally, other physical tests for parameters as noise, vibration, or radiation have little or no applicability in cleanrooms for the processing of SCMPs.

7. Microbiological Tests

A major consideration in the operation of cleanroom technology for aseptic dispensing is the monitoring of viable contamination within clean environments [24]. Environmental monitoring is aimed to detect changing trends of microbial counts and microflora growth within the cleanroom [6, 40]. The results of the environmental monitoring provide information about the physical construction of the room, the performance of HVAC system [41], personnel cleanliness, gowning practices, and equipment and cleaning operations [42]. The microorganisms present in an environment will depend on the facilities, people, materials, equipment, processes, and environmental conditions of the area (temperature, humidity, presence of biocides, etc.). The most common potential forms of contamination in cell cultures are bacteria (including *Mycoplasma*), yeasts, and fungi, and these can be readily assessed on a routine basis [40].

The alert and action limits, expressed in cfu, should be established on the basis of levels of detection of microbial contamination. Action levels for nonviable particles are defined in the various regulatory and compendial documents for each room or area classification. Action levels are those that, when exceeded, indicate the appropriate corrective measure to return to the appropriate environmental safety. USA and European regulations, as well as, in the USP, chapter 1116, "Microbiological Control and Monitoring Environments Used for the Manufacture of Healthcare Products," established the acceptable number of viable particles per m^3 that can be found in determined cleanroom or clean area. WHO adopted the European standards. However, each company should set its own microbiological levels based on the aseptic requirements of it production. ISO does not refer to microbiological levels.

The methods used for microbiological monitoring include active air sampling (air sampler), passive air sampling (settle plates), surface sampling (contact plates and swabs), and personnel sampling (finger plates/plates of gowns). In order to carry out these operations the licensed manufacturer must be certified as a GMP manufacturer accredited by a recognized certification body in accordance with ISO 17025 or equivalent. However, it is not possible in Europe, where the GMP manufacturing is authorized by the national competent authority and recognized across the border on the basis of an international treaty. Currently, the US GMP authorization by FDA is not recognized in Europe and vice versa. The use of outside laboratories to carry out microbiological analysis can be accepted for particular reasons, as many companies are outsourcing technical testing activities and reducing in-house capabilities in an effort to control costs, but this should be stated in the quality control records. Manufacturers should use a risk-based approach to determine whether a preapproval audit is required before approving a contract laboratory. Various Agency guidance documents indicate how quality management principles relate to contract these operations.

The ICH guidance for industry Q7 [21] recommends that manufacturers evaluate contractors for GMP compliance both by establishing a formal agreement that delineates GMP responsibilities, including quality measures, and by auditing the contractor's facilities [43].

7.1. Collection Sites and Frequency. The sampling plan for viable particles should define the number of points sampled in each of the areas of a cleanroom and determine how often to perform the sampling. According to the FDA-cGMP monitoring locations that present the highest potential contamination risk to the product and trending performance should be selected by assessing the critical activities taking place, the flow of personnel in the processing area, and the position of filters to determine the most potential high risk contamination locations. This approach is also stated in EU-GMP and ICH Q9 recommendations [12, 44]. Hazard Analysis Critical Control Points (HACCP) and Failure Mode Effect Analysis (FMEA) techniques are designed for this task. Sample locations for settle plates in cleanrooms should include those areas with the lowest air movement.

As discussed, the ISO 14644-1 guideline [26] provides a formula for the calculation of the minimum sampling locations for qualification of nonviable by dividing the area into a grid. Currently a randomly selection method using the grid is not recommended. Using a risk-based approach drives a continual review of trends and a periodic reassessment of the environmental programme.

Regarding the sampling frequency, it depends on the classification: the lower the maximum permitted particulate the higher the frequency of monitoring. GMP guidelines do not go into details. Table 4 shows recommendations of FDA-cGMP, EU-GMP, and USP. The reason why all these documents described only recommendation is because sample timing, frequency, and location should be carefully selected by the manufacturer based on the requirements of the operations performed and should be sufficient for allowing meaningful statistical calculations. Certain especial situations make necessary new microbiological testing such as corrective actions, after specifications changes, due to a change of activity or changes of environmental control equipment. Finally, when the specified microbial level of the cleanroom environment is exceeded, a documentation review and investigation should be carried out.

7.2. Microbial Growth Media. The selection of the growth media should assure the growth of microbes existing in the controlled environment. Thus, according to ISO 14698-1 [26], it is preferable to use a growth medium with low selectivity that is capable of supporting a broad spectrum of microorganisms including aerobes, anaerobes, fungi, and yeast, containing additive to overcome the residual effect of biocides and cleaning agents. The growth media should be validated thoroughly prior to using. Table 5 lists EP recommendations for growth promotion test and the validation test. Specifications are similar to USP. The recommended size of solid media is 90 mm in diameter (approximate internal area 64 cm^2) for settle plates and 55 mm (surface area 25 cm^2) for contact plates. However, since 2012, FDA has permitted the use of alternative rapid microbiological methods.

Both USP and EP describe several adequate culture media for the sampling and quantification of microorganisms. As per USP Soybean Casein Digest Agar (SCDA) is the standard medium for sampling or quantitation of microorganisms in controlled environments. Yeasts and moulds may also be specifically sought out. Sabouraud Dextrose Agar is used especially for yeasts and moulds. As per EP fluid thioglycollate medium is primarily intended for the culture of anaerobic bacteria; however, it will also detect aerobic bacteria and SCDA for the culture of both fungi and aerobic bacteria.

For "settle plate" methods, Trypticase Soy Agar (TSA) is the most recommended medium for bacteria. It contains a mixture of peptones that promote the growth of most microorganisms. Agar Sabouraud Dextrose Chloramphenicol (SDC) is the recommended medium for fungi and yeast. Its high concentration of glucose optimizes the growth of fungi and its pH and chloramphenicol content improve the selectivity.

In order to choose the most efficient parameters for the test methodology, microbiologically, the best media and incubation conditions should be previously assayed, and parameters that yield the highest microbial recovery with the shortest incubation period are chosen for routine testing. Whether surfaces of testing were treated with detergents or disinfectant products, a neutralizing agent must be included in the recovery media. In this line, an antibiotic inactivating product must be incorporated in the recovery media if the testing surfaces have been treated with antibiotics.

7.3. Incubation Conditions. Total aerobic microbial count (TAMC) is determined by incubation in those media. The incubation conditions should be previously selected and validated. Culture conditions differ between microorganisms, 48 h at 32.5 ± 2.5°C for bacteria versus 72 h at 22.5 ± 2.5°C for fungi and moulds. Posteriorly, USP considered the possibility of longer incubation times. Equally, in case of absence of confirmatory evidence, one single plate may be incubated at both a low and a higher temperature. EP for its part recommends incubating the plates not more than 3 days in the case of bacteria at 30–35°C and not more than 5 days in the case of fungi at 20–25°C [45].

USP lists other permitted alternative media, liquid or solid. Furthermore, other alternative media to those listed can be used whether they are validated for the purpose intended.

7.4. Active Air Sampling Collection. Critical areas' monitoring should be carried out under "worst case" conditions for contamination with process equipment running and personnel performing normal operations ("*in operation*") state [12]. Monitoring control should not interfere with critical work zone protection or compromise the quality of any products prepared that may be administered to patients. Measurements are performed as cfu per cubic meter of air (cfu/m^3). All active air samplers work on the principle of sucking or blowing a stream of air at a sufficiently high velocity to cause any microorganisms in the sample to be impacted against

Table 5: Strains of the test microorganisms suitable for use in the growth promotion test and the validation test.

Microorganism		Strains
Aerobic	*Staphylococcus aureus*	ATCC 6538, CIP 4.83, NCTC 10788, NCIMB 9518
	Bacillus subtilis	ATCC 6633, CIP 52.62, NCIMB 8054
	Pseudomonas aeruginosa	ATCC 9027, NCIMB 8626, CIP 82.118
Anaerobic	*Clostridium sporogenes*	ATCC 19404, CIP 79.3, NCTC 532 or ATCC 11437
Fungi	*Candida albicans*	ATCC 10231, IP 48.72, NCPF 3179
	Aspergillus niger	ATCC 16404, IP 1431.83, IMI 149007

Table 6: Recommended limits for viable airborne particles in the environment according to FDA-cGMP, EU-GMP, and USP.

Clean area type			Maximal number of cfu in the environment				
			FDA-cGMP		EU-GMP		USP
FS209E	ISO	EU-GMP	Air sample (cfu/m^3)	Settle plates[a] (diam. 90 mm; cfu/4 h)	Air sample (cfu/m^3)	Settle plates (diam. 90 mm; cfu/4 h)[b]	Air sample (cfu/m^3)
M3.5 (100)	5	A	1[c]	1[c]	<1	<1	<3
M4.5 (1,000)	6		7	3	—	—	
M5.5 (10,000)	7	B	10	5	10	5	<20
M6.5 (100,000)	8	C	100	50	100	50	<100
		D	—	—	200	100	—

[a]The additional use of settling plates is optional.
[b]Individual settle plates may be exposed for less than 4 hours.
[c]Samples from class 100 (ISO 5) environments should normally yield no microbiological contaminants.

a chosen medium. The two main types of equipment are the centrifugal and impaction devices. In all cases after the specified sampling time, the agar strip, plate, or filter in the sampler is removed, incubated under appropriate conditions, and then examined for microbiological growth. Preservation of the biological integrity and growth capacity of the microorganisms following impact are critical [46]. The sample size of air to be sampled is one of the main limitations of mechanical air samplers. The choice of an air sampler can be determined by the validation of the instrument, either by the manufacturer or a third party, in agreement with annex B of the ISO 14698-1 [26]. Recommended action limits for microbiological active monitoring of cleanrooms and clean areas are depicted in Table 6.

7.5. Passive Air Sampling Collection. Passive air or sedimentation sampling is based on the fact that, in absence of any kind of influence, airborne microorganisms which typically are attached to large particles will deposit onto open culture plates (settle plates) [47]. Thus, Petri dishes containing agar medium are opened and exposed in the cleanroom at working height for a specific time period (4 h to prevent media desiccation). Positive and negative controls should be also exposed. This method allows continuous sampling throughout a given work period, although they cannot indicate variation of contamination levels throughout the sampling period.

The cleanroom should be "*at rest*" to monitor baseline contamination levels. However, if the test conducted when operational, it will be affected by movements of the personnel and air flow. But it is considered a qualitative method and does not represent concentration of airborne microorganism. After incubation, results are reported as number of cfu per 4 h according to EU-GMP and FDA-cGMP. Recommended action limits for microbiological passive monitoring of cleanrooms and clean areas are depicted in Table 6.

7.6. Surfaces Sampling. EU-GMP [12] and USP [48] require surface monitoring of facilities (wall, floor, work surfaces, ceiling, etc.) furniture, equipment, and garment at the end of processing and after sanitation. Surfaces may become contaminated in a number of ways, for example, microorganisms settling out from the environment or from the direct touch by an operator [49]. One of the objectives of surface sampling is to determine the efficiency of routine cleaning procedures in removing contamination. The most frequent method is using contact plates. These are Petri dishes filled with appropriate growth medium and effective area of 25 cm^2 according to EU-GMP or from 24 to 30 cm^2 according to USP. Specially designed plates for this task are the RODAC (replicate organism detection and counting) plates commercially available with TSA or SDC with Lecithin and Polysorbate 80 added to inactivate residual disinfectants. Contact plates have a raised agar surface which is placed lightly onto the surface for 15 s and then incubated. After sampling collection with an agar-containing device, it should be cleaned with 70% alcohol to avoid the promotion of microbes.

Another contact method for surfaces where contact plates could not be utilized is to undertake a swabbing with sterile swabs. When swabbing is used in sampling, the area covered should be greater than or equal to 24 cm^2 but no larger than 30 cm^2 as stated by USP. After swabbing, the swab should be

Table 7: Recommended limits for viable airborne particles on surfaces according to EU-GMP and USP.

Clean area type			Maximal number of cfu on surfaces		
			EU GMP	USP	
FS209E	ISO	EU GMP	Contact plates (diam. 55 mm; cfu/plate)	Contact plates (area 24–30 cm^2; cfu/plate)[a]	
				Surfaces	Floor
M3.5 (100)	5	A	<1	3	3
M4.5 (1,000)	6		—	—	—
M5.5 (10,000)	7	B	5	5	10
M6.5 (100,000)	8	C	25	—	—
		D	50	—	—

[a]Contact plate areas vary from 24 to 30 cm^2. When swabbing is used in sampling, the area covered should be greater than or equal to 24 cm^2 but no larger than 30 cm^2.

Table 8: Recommended limits for viable airborne particles on personnel according to FDA-cGMP, EU-GMP, and USP.

Clean area type			Maximal number of cfu		
			EU-cGMP	USP	
FS209E	ISO	EU GMP	Glove print (5 fingers) (cfu/glove)	cfu per contact plate	
				Gloves	Personnel clothing and garb
M3.5 (100)	5	A	<1	3	5
M5.5 (10,000)	7	B	5	10	20

placed into a suitable culture medium or a diluent, vortexed for about 30 s, and then tested by pour-plate or membrane filtration method [50]. This method sampling should be used in areas with probability of contamination.

Finally, flexible films are reported by the PDA [8]. The media are deposited on a flexible substrate which can be used in an identical manner to that employed for contact plates. After incubation, results are reported as number of cfu per plate according to EU-GMP and USP. Recommended action limits for surface sampling monitoring of cleanrooms and clean areas are depicted in Table 7.

7.7. Personnel Sampling Monitoring. Only personnel who are qualified and appropriately gowned should be permitted access to the aseptic manufacturing area. Personnel can significantly affect the quality of the environment in which the product is processed; for this reason only the minimum number of personnel required should be present in cleanroom. Methods for personnel microbiological testing should include gloves and protection clothes at the end of each working session prior to the operator carrying out any cleaning or tidying operations. For this the desired area of the protection clothing is placed lightly onto the surface of the agar medium of the settle plate. On the other hand, the glove finger count checking is done randomly among individuals by finger dab plates in each of the five fingers of both hands. Finger dabs can be performed using either standard 90 mm diameter settle plates or 55 mm diameter contact plates. After incubation, results are reported as number of cfu per glove according to EU-GMP or cfu/plate according to FDA-cGMP. Recommended action limits for personnel sampling monitoring of cleanrooms and clean areas are depicted in Table 8.

8. Microorganism Identification

FDA-cGMP has clearly recommended the establishment of a listing of common microorganisms found in the aseptic manufacturing environment [9]. The identification of microorganisms to the species (or, where appropriate, genus) provides vital information for the environmental monitoring and for investigation. Some species are more prone to be promoted for human activity (*Staphylococcus*, *Micrococcus*). Contrary, other species are supposed to be related to environment (*Bacillus*, *Penicillium*, or *Pseudomonas*).

It is so important to have knowledge of the "normal" background flora of a cleanroom facility. Any unusual organisms or deviation from "normal" flora may require corrective actions.

9. Test Report

ISO 14644-1 includes the elaboration of a test report after testing in this way. The results from testing each cleanroom or clean zone shall be recorded and submitted as a comprehensive report, along with a statement of compliance or noncompliance with the specified designation of airborne particulate cleanliness classification. This standard provides for the inclusion, among other information, physical description of facilities, designation criteria for the cleanroom or clean zone, test methods, and test results.

10. Conclusions

The field of MSCs manufacture includes the task of interpreting and harmonizing international guidelines to ensure their acceptable quality for translational clinical use in regenerative medicine. One of the great challenges for the future is to set

a single regulatory framework for the SCMPs manufacture, through harmonization of all the requirements for their production whatever their use or intended final purpose: gene therapy, cell therapy, or tissue engineering or whenever their production: USA, Europe, Japan, and so forth.

Competing Interests

The authors declare no conflict of interests.

References

[1] S. C. Sethe, "The implications of 'advanced therapies' regulation," *Rejuvenation Research*, vol. 13, no. 2-3, pp. 327–328, 2010.

[2] F. Belardelli, P. Rizza, F. Moretti, C. Carella, M. C. Galli, and G. Migliaccio, "Translational research on advanced therapies," *Annali dell'Istituto Superiore di Sanita*, vol. 47, no. 1, pp. 72–78, 2011.

[3] C. Mason and E. Manzotti, "Regen: the industry responsible for cell-based therapies," *Regenerative Medicine*, vol. 4, no. 6, pp. 783–785, 2009.

[4] P. Gálvez, B. Clares, M. Bermejo, A. Hmadcha, and B. Soria, "Standard requirement of a microbiological quality control program for the manufacture of human mesenchymal stem cells for clinical use," *Stem Cells and Development*, vol. 23, no. 10, pp. 1074–1083, 2014.

[5] A. B. Dietz, D. J. Padley, and D. A. Gastineau, "Infrastructure development for human cell therapy translation," *Clinical Pharmacology and Therapeutics*, vol. 82, no. 3, pp. 320–324, 2007.

[6] P. G. Martín, M. B. González, A. R. Martínez, V. G. Lara, and B. C. Naveros, "Isolation and characterization of the environmental bacterial and fungi contamination in a pharmaceutical unit of mesenchymal stem cell for clinical use," *Biologicals*, vol. 40, no. 5, pp. 330–337, 2012.

[7] G. Ottria, M. Dallera, O. Aresu et al., "Environmental monitoring programme in the cell therapy facility of a research centre: preliminary investigation," *Journal of Preventive Medicine and Hygiene*, vol. 51, no. 4, pp. 133–138, 2010.

[8] Parenteral Drug Association (PDA), "Fundamentals of an environmental monitoring program," *PDA Journal of Pharmaceutical Science and Technology*, vol. 55, pp. 19–20, 2001.

[9] Food and Drug Administration (FDA), *Guidance for Industry: Sterile Drug Products Produced by Aseptic Processing—Current Good Manufacturing Practice*, FDA, Rockville, Md, USA, 2004.

[10] T. Sandle, *Sterility, Sterilisation and Sterility Assurance for Pharmaceuticals: Technology, Validation and Current Regulations*, Woodhead, Cambridge, UK, 2013.

[11] Code of Federal Regulations (21CFR211), *Current Good Manufacturing Practice for Finished Pharmaceuticals*, US Government Printing Office, Washington, DC, USA, 2007.

[12] European Commission (Euradlex), *The Rules Governing Medicinal Products in the European Community*, European Commission, Brussels, Belgium, 2009.

[13] European Commission (Euradlex), *The Rules Governing Medicinal Products in the European Community. Vol. 4, EU Guidelines to Good Manufacturing Practice. Medicinal Products for Human and Veterinary Use. Annex 1, Manufacture of Sterile Medicinal Products*, European Commission, Brussels, Belgium, 2009.

[14] European Commission (Euradlex), *The rules governing medicinal products in the European Community. Vol. 4, EU Guidelines to Good Manufacturing Practice. Medicinal Products for Human and Veterinary Use. Annex 2, Manufacture of Biological Active Substances and Medicinal Products for Human Use*, European Commission, Brussels, Belgium, 2009.

[15] European Medicines Agency (EMA), *Guideline on Scientific Requirements for the Environmental Risk Assessment of Gene Therapy Medicinal Products (EMEA/CHMP/GTWP/125491/2006)*, EMA, London, UK, 2008.

[16] World Health Organization (WHO), "WHO expert committee on biological standardization," Technical Report Series No. 822, WHO Technical Report Series, Geneva, Switzerland, 1992.

[17] World Health Organization (WHO), *Technical Report Series No. 961. Annex 6, WHO Good Manufacturing Practices for Sterile Pharmaceutical Products*, WHO Technical Report Series, Geneva, Switzerland, 2011.

[18] World Health Organization (WHO), "Quality assurance of pharmaceuticals: a compendium of guidelines and related materials," in *Good Manufacturing Practices and Inspection*, vol. 2, WHO Press, Geneva, Switzerland, 2nd edition, 2007.

[19] The Pharmaceutical Inspection Convention and Pharmaceutical Inspection Co-operation Scheme (PIC/S), *Guide to Good Manufacturing Practice for Medicinal Products (PE 009-11)*, PIC/S Secretariat, Geneva, Switzerland, 2014.

[20] International Standards Organization (ISO), "Cleanrooms and associated controlled environments," ISO 14644, ISO, Geneva, Switzerland, 1999.

[21] International Conference on Harmonisation of Technical Requirements for Registration of Pharmaceuticals for Human Use (ICH), *Harmonised Tripartite Guideline Q7: Good Manufacturing Practice Guide for Active Pharmaceutical Ingredients*, ICH, Geneva, Switzerland, 2000.

[22] Japanese Pharmacopoeia, *Mycoplasma Testing for Cell Substrates Used for the Production of Biotechnological/biological Products*, Ministry of Health, Labour and Welfare, Tokyo, Japan, 2006.

[23] European Pharmacopoeia, *Section 2.6.7 (Mycoplasma)*, Maisonneuve SA, Sainte-Ruffine, France, 7th edition, 2008.

[24] United States Pharmacopeia, *Mycoplasma Tests*, chapter 63, The United States Pharmacopeial Convention, Rockville, Md, USA, 2010.

[25] W. Whyte, *Cleanroom Technology: Fundamentals of Design, Testing, and Operation*, John Wiley & Sons, Chichester, UK, 2001.

[26] International Standards Organization (ISO), "Cleanrooms and associated controlled environments. Part 1: classification of air cleanliness," ISO 14644-1, ISO, Geneva, Switzerland, 1999.

[27] International Standards Organization (ISO), *Cleanrooms and Associated Controlled Environments. Part 1: Classification of Air Cleanliness by Particle Concentration (ISO/DIS 14644-1.2)*, ISO, Geneva, Switzerland, 2014.

[28] World Health Organization (WHO), *Environmental Monitoring of Clean Rooms in Vaccine Manufacturing Facilities*, WHO Press, Geneva, Switzerland, 2012.

[29] T. Sandle, "General considerations for the risk assessment of isolators used for aseptic processes," *PMPS*, vol. 15, pp. 43–47, 2004.

[30] The Pharmaceutical Inspection Convention and Pharmaceutical Inspection Co-operation Scheme (PIC/S), *Recommendation on Sterility Testing (PI 012-1)*, PIC/S Secretariat, Geneva, Switzerland, 2007.

[31] International Standards Organization (ISO), *Cleanrooms and Associated Controlled Environments. Part 3: Test Methods (ISO 14644-3)*, Annex B5: Pressure Difference Test, ISO, Geneva, Switzerland, 2005.

[32] International Standards Organization (ISO), *Cleanrooms and Associated Controlled Environments. Part 3: Test Methods (ISO 14644-3)*, Annex B13: Containment Leak Test, ISO, Geneva, Switzerland, 2005.

[33] International Standards Organization (ISO), "Cleanrooms and associated controlled environments. Part 3: test methods (ISO). Annex B4: airflow test," ISO 14644-3, ISO, Geneva, Switzerland, 2005.

[34] International Standards Organization (ISO), *Cleanrooms and Associated Controlled Environments. Part 3: Test Methods (ISO 14644-3)*, Annex B6: Installed Filter System Leakage Test, ISO, Geneva, Switzerland, 2005.

[35] Military Standard, "Filter units, protective clothing, gas-mask components and related products: performance test methods," Tech. Rep. MIL-STD-282, US Government Printing Office, Washington, DC, USA, 1956.

[36] Institute of Environmental Sciences and Technology (IES), *Standards and Recommended Practices, Recommended Practice for Hepa Filters (IES RP-CC-001-83)*, Institute-Environ Sciences, Arlington Heights, Ill, USA, 1983.

[37] European Committee for Standardization (CEN), *High Efficiency Air Filters (EPA, HEPA and ULPA) (EN 1822)*, CEN, Brussels, Belgium, 1998.

[38] F. Vecchi, "Validation of environmental control systems used in parenteral facilities," in *Validation of Pharmaceutical Processes*, J. P. Agalloco and F. J. Carleton, Eds., pp. 27–50, CRC Press, New York, NY, USA, 2007.

[39] International Standards Organization (ISO), *Cleanrooms and Associated Controlled Environments. Part 3: Test Methods (ISO 14644-3)*, Annex B7: Airflow Direction Test and Visualization, ISO, Geneva, Switzerland, 2005.

[40] F. Cobo, G. N. Stacey, C. Hunt et al., "Microbiological control in stem cell banks: approaches to standardisation," *Applied Microbiology and Biotechnology*, vol. 68, no. 4, pp. 456–466, 2005.

[41] World Health Organization (WHO), *Technical Report Series no. 961. Annex 5, WHO Good Manufacturing Practices for Sterile Pharmaceutical Products*, WHO Technical Report Series, Geneva, Switzerland, 2011.

[42] R. M. Baird, "Monitoring microbiological quality: conventional testing methods," in *Guide to Microbiological Control in Pharmaceuticals and Medical Devices*, S. P. Denyer and R. M. Baird, Eds., pp. 155–182, CRC Press, New York, NY, USA, 2007.

[43] Food and Drug Administration (FDA), *Guidance for Industry: Contract Manufacturing Arrangements for Drugs: Quality Agreements*, FDA, Rockville, Md, USA, 2013.

[44] *International Conference on Harmonisation of Technical Requirements for Registration of Pharmaceuticals for Human Use (ICH). Harmonised Tripartite Guideline Q9: Quality Risk Management*, ICH, Geneva, Switzerland, 2005.

[45] C. L. Moser and B. K. Meyer, "Comparison of compendial antimicrobial effectiveness tests: a review," *AAPS PharmSciTech*, vol. 12, no. 1, pp. 222–226, 2011.

[46] J. Guns, R. Janssens, and M. Vercammen, "Air quality management," in *Practical Manual of In Vitro Fertilization: Advanced Methods and Novel Devices*, Z. P. Nagy, A. C. Varghese, and A. Agarwal, Eds., pp. 17–25, Springer, New York, NY, USA, 2012.

[47] P. A. Solomon and C. Sioutas, "Continuous and semicontinuous monitoring techniques for particulate matter mass and chemical components: a synthesis of findings from EPA's particulate matter supersites program and related studies," *Journal of the Air and Waste Management Association*, vol. 58, no. 2, pp. 164–195, 2008.

[48] United States Pharmacopeia, *Microbiological Control and Monitoring of Aseptic Processing Environments*, chapter 1116, The United States Pharmacopeial Convention, Rockville, Md, USA, 2010.

[49] F. Cobo, D. Crela, and A. Concha, "Airborne particle monitoring in clean room environments for stem cell cultures," *Biotechnology Journal*, vol. 3, no. 1, pp. 43–52, 2008.

[50] L. Clontz, *Microbial Limit and Bioburden Tests: Validation Approaches and Global Requirements*, CRC Press, New York, NY, USA, 2009.

Hindawi Publishing Corporation
Stem Cells International
Volume 2016, Article ID 9150819, 9 pages
http://dx.doi.org/10.1155/2016/9150819

Research Article

Vitamin D Effects on Osteoblastic Differentiation of Mesenchymal Stem Cells from Dental Tissues

Francesca Posa,[1] Adriana Di Benedetto,[1] Graziana Colaianni,[2] Elisabetta A. Cavalcanti-Adam,[3,4] Giacomina Brunetti,[2] Chiara Porro,[1] Teresa Trotta,[1] Maria Grano,[2] and Giorgio Mori[1]

[1]*Department of Clinical and Experimental Medicine, Medical School, University of Foggia, Foggia, Italy*
[2]*Section of Human Anatomy and Histology, Department of Basic and Medical Sciences, Neurosciences and Sense Organs, University of Bari, Bari, Italy*
[3]*Institute of Physical Chemistry, Department of Biophysical Chemistry, University of Heidelberg, Heidelberg, Germany*
[4]*Max Planck Institute for Intelligent Systems, Stuttgart, Germany*

Correspondence should be addressed to Francesca Posa; francesca.posa@unifg.it

Received 12 July 2016; Revised 24 August 2016; Accepted 25 September 2016

Academic Editor: Dario Coletti

1α,25-Dihydroxyvitamin D_3 (1,25$(OH)_2D_3$), the active metabolite of vitamin D (Vit D), increases intestinal absorption of calcium and phosphate, maintaining a correct balance of bone remodeling. Vit D has an anabolic effect on the skeletal system and is key in promoting osteoblastic differentiation of human Mesenchymal Stem Cells (hMSCs) from bone marrow. MSCs can be also isolated from the immature form of the tooth, the dental bud: Dental Bud Stem Cells (DBSCs) are adult stem cells that can effectively undergo osteoblastic differentiation. In this work we investigated the effect of Vit D on DBSCs differentiation into osteoblasts. Our data demonstrate that DBSCs, cultured in an opportune osteogenic medium, differentiate into osteoblast-like cells; Vit D treatment stimulates their osteoblastic features, increasing the expression of typical markers of osteoblastogenesis like RUNX2 and Collagen I (Coll I) and, in a more important way, determining a higher production of mineralized matrix nodules.

1. Introduction

Vitamin D (Vit D) is crucial for many biological processes, that is, the bone mineralization of vertebrates, the maintenance of calcium homeostasis, cell proliferation, and differentiation.

The actions of Vit D are carried out by its active metabolite, 1,25-dihydroxycholecalciferol [1,25$(OH)_2D_3$ or calcitriol], that is produced through a series of enzymatic steps starting from cholecalciferol or vitamin D_3.

The main portion of vitamin D_3 is derived from the conversion of 7-dehydrocholesterol (Provitamin D) after the exposure of the skin to ultraviolet radiation. Age, skin surface exposed to the sun, thickness, and irradiation time are all factors that control Vit D synthesis [1].

Foods provide only few units of Vit D compared to the amount produced by the skin in response to sunlight.

Vit D is fat-soluble and is absorbed in the duodenum and jejunum and subsequently distributed through the lymphatic circulation [1].

1,25$(OH)_2D_3$ exerts its action by binding to a specific nuclear receptor, that is, the vitamin D receptor (VDR). It is a member of the class II steroid hormones [2].

Mice with targeted ablation of the nuclear VDR (conventional-VDR knockout mice) represent an important model to study the actions of the system 1,25$(OH)_2D_3$/VDR. The KO mice showed, after weaning, alopecia, an early development of hypocalcemia, which in turn induces a state of secondary hyperparathyroidism, infertility, and severely impaired bone formation: these are typical features recurrent in humans with vitamin D-dependent rickets type II [3–6].

Osteoblasts are among the cells expressing VDR; therefore they represent a functional target of 1,25$(OH)_2D_3$ action.

$1,25(OH)_2D_3$ can affect human osteoblast growth and differentiation stimulating bone formation and mineralization [7]. Moreover $1,25(OH)_2D_3$ modulates bone deposition process preventing excessive and pathological mineralization [8].

The effects of $1,25(OH)_2D_3$ on bone matrix protein expression have been also studied in cultures of calvaria cells, comparing young cells with more differentiated ones for different time periods. Following treatment with $1,25(OH)_2D_3$, mature osteoblasts were more inhibited, favoring those which were in an earlier state of differentiation [9].

Vit D effects on osteoblast differentiation may be dissimilar according to the animal species considered; a discrepant responsiveness has been shown between two categories: human/rat osteoblasts and murine osteoblasts. Thus, in contrast to the stimulatory effect of Vit D on human and rat osteoblasts, Vit D has been demonstrated to determine an inhibitory effect on murine osteoblasts [10].

Vit D has been reported to induce alkaline phosphatase activity and to increase Collagen Type I expression in the course of proliferation and differentiation of human osteoblasts; this effect is less evident when lower concentrations are used [11].

Kveiborg et al. have shown that $1,25(OH)_2D_3$ is able to offset, in aging osteoblasts *in vitro*, the reduction of gene expression which is normally required for osteoblast functionality [12].

Osteoblasts precursors are present on periosteal surface and in bone marrow; moreover they can differentiate from Mesenchymal Stem Cells (MSCs).

Adult stem cells are pluripotent cells capable of regenerating different tissues. Bone marrow contains cells with a high clonogenic capacity, the Colony-Forming Units Fibroblasts (CFU-Fs), which give rise to the cells of bone tissue, cartilage tissue, adipose, and fibrous tissues [13]. These CFU-Fs cells are called MSCs.

MSCs can be induced to differentiate into osteocytes, adipocytes, or chondrocytes [14] and also neuronal cells [15] or hepatocytes [16].

It is estimated that about 15% have a "stem" power, and among them there are those who can give origin to osteoblasts [13]. The commitment of MSCs towards differentiated cell lines is regulated by transcriptional mechanisms called master switches.

RUNX2 is a transcription factor with a key role in the control of osteoblast differentiation and function.

$1,25(OH)_2D_3$ is an important regulator of the RUNX2, with which it cooperates in inducing the expression of osteocalcin, that is, the key protein regulating bone matrix mineralization [17].

There are a lot of data in literature about the effect of Vit D on MSCs isolated from bone marrow, in particular concerning their osteogenic differentiation.

$1,25(OH)_2D_3$ influences human MSCs (hMSCs) inhibiting cell proliferation and stimulating their differentiation into osteoblasts [18, 19]. It has also been demonstrated, in hMSCs preimplantation cultures, that Vit D is able to determine the formation of mature osteoblasts, resulting in an increase of mineralized matrix formation, but after implantation of these cells the same Vit D is not sufficient in enhancing bone formation [20]. That leads to assuming a different *in vivo* effect of Vit D.

In order to overcome some negative aspects connected with the use of MSCs from bone marrow, that is, morbidity, pain, and low yield of cells, other sources of MSCs have been examined.

MSCs can be isolated from tissues different from the bone marrow such as adipose tissue, brain, skin, liver, and several fetal tissues; little is known about Vit D influence in osteogenic differentiation of MSCs from these alternative sources. Anyway, with MSCs from adipose tissue, the capacity of Vit D in osteoblast formation has been confirmed [21].

According to the evidence based research dental tissues represent an alternative and promising source of postnatal MSCs [22–26].

Deciduous teeth, or the wisdom tooth, that is a tooth with a limited chewing function and that often creates problems of overcrowding, can be used to isolate MSCs. In the case of immature teeth, a productive source of MSC is the dental bud (DB) that consists in noncalcified tissues; in the case of the mature tooth the sources are the periodontal ligament [27], the Dental Pulp (DP) [27–30], and the apical papilla [31].

Dental Pulp Stem Cells (DPSCs) are obtained from wisdom teeth pulp of adult donors, while Dental Bud Stem Cells (DBSCs) come from the DB. The DB, which is the immature form and therefore not yet fully calcified of the tooth, is an excellent source of stem cells; since it is considerably larger, it is comprised of cells more undifferentiated than the ones composing the pulp and can be removed in children of age between 8 and 12 in case of expected overcrowding with a safe technique called piezosurgery.

The advantage of the tooth bud, compared to the pulp, is first of all dimensional, it contains a greater number of cells, and moreover almost all the tissue is made from stem cells that have a high proliferative capacity and an excellent degree of stemness [24, 32, 33].

The tissues constituting the mature tooth, cement and periodontal ligament, enamel, dentin, pulp, and the central part of the bud, corresponding to the dental papilla, are all derived from DBSCs, obtained from the DB, thus containing MSCs which can successfully differentiate into osteoblast-like cells.

DBSCs are more undifferentiated MSCs, if compared to the ones isolated from the bone marrow; for this reason they can be considered an ideal model for studying the early stages of the osteoblastic differentiation process.

The differentiation into osteogenic lineage has already been demonstrated in DPSCs [27–29, 34] and a considerable mineral matrix deposition has been observed using innovative scaffolds for their culturing [35, 36]; moreover these cells, if cultured on β-tricalcium phosphate/poly (l-lactic acid/caprolactone) three-dimensional scaffolds, showed an increased osteogenesis in the presence of Vit D compared to dexamethasone [37].

The aim of this study is to analyze the effect of the active metabolite of Vit D, $1,25(OH)_2D_3$, on DBSCs which represent a useful model to understand the anabolic activity of the bone cells, starting from very undifferentiated osteoblasts precursors.

2. Patients, Materials, and Methods

2.1. Materials. 1α,25-Dihydroxyvitamin D_3, ascorbic acid, β-glycerophosphate, dexamethasone, Alizarin Red powder, and alkaline phosphatase kit were from Sigma Aldrich, Milan, Italy.

Anti-RUNX2 antibody was from Abnova, anti-Coll I, anti-OPN, and anti-BSP II were from Abcam, Cambridge, UK.

2.2. Patients and Cell Cultures. Normal human third molar buds were collected from tooth buds of 10 healthy pediatric patients, 8–12 years of age, that underwent extractions for orthodontic reasons, mainly overcrowding, after informed consent from both patient parents.

The central part of DBs, corresponding to the dental papilla, was cut in small pieces and digested with agitation for 1 hour at 37°C in a solution of 3 mg/mL type I collagenase plus 4 mg/mL dispase (Gibco Ltd., Uxbridge, UK). Single-cell suspension was obtained by passing the cells through a 70 μm BD Falcon strainer (Falcon) (Becton & Dickinson, Sunnyvale, CA).

After filtration, single-cell suspension was centrifuged at 1300 rpm for 5 min; the pellet was resuspended and cultured in Mesenchymal Stem Cell Culture medium supplemented with 5% fetal bovine serum (FBS), 100 U/mL penicillin-G, and 100 μg/mL streptomycin (Gibco Limited, Uxbridge, UK). Cells were seeded at a density of 5×10^3 cells/cm^2.

Flasks were incubated at 37°C and 5% CO_2 and the medium was changed every 3 days.

In order to induce osteoblastic differentiation, 1500 cells/cm^2 were seeded and cultured in osteogenic medium consisting of α-MEM supplemented with 5% FBS, 10^{-8} M dexamethasone, and 50 μg/mL ascorbic acid (Sigma Aldrich, Milan, Italy).

For the evaluation of DBSCs ability to form mineralized matrix nodules *in vitro*, cells were cultured in the osteogenic medium supplemented with 10 mM β-glycerophosphate (Sigma Aldrich, Milan, Italy).

1,25$(OH)_2D_3$ (Sigma Aldrich, Milan, Italy) was reconstituted at 10^{-4} M in 95% ethanol and stored at −20°C.

For all cell cultures, a 95% ethanol (vehicle) control was included at a concentration equivalent to that of Vit D. Thus cells were cultured in replicates with 1,25$(OH)_2D_3$ and an equivalent dilution of 95% ethanol.

2.3. Alizarin Red Staining (ARS). The ability of DBSCs to generate mineralized matrix nodules *in vitro*, a feature normally attributed to osteoblasts, was assessed by performing Alizarin Red Staining on cells cultured for 21 days in osteogenic medium.

Thus, cells were gently rinsed with PBS and fixed with 10% formaldehyde at room temperature for 10 min.

Then they were washed twice with deionized water and incubated with 1% ARS solution for 10 min at room temperature. Cells were afterwards washed twice with deionized water, to remove excess staining, and air dried. The monolayer appeared to be red stained.

To quantify the ARS, cells were incubated with 10% acetic acid at room temperature for 30 min with shaking. The cell layer was scraped and vortexed and then the solution was incubated for 10 min at 85°C. After 5 min on wet ice, the suspension was centrifuged at 20,000 ×g for 15 min and 500 μL of the supernatant was treated with 10% ammonium hydroxide to neutralize the acid. The Optical Density (OD) was read in triplicate at 405 nm.

2.4. Alkaline Phosphatase (ALP). The expression of alkaline phosphatase, which is a marker of osteoblast differentiation, was assessed with the Leukocyte Alkaline Phosphatase kit (Sigma Aldrich).

Briefly, cell media were removed and cells were fixed in 0.5 mL of a fixative solution for 5 min at room temperature, according to manufacturer's instructions.

Subsequently, the wells were washed with deionized water and cells were stained with 0.3 mL ALP solution (a mixture of FRV-Alkaline Solution, Naphthol AS-BI Alkaline Solution, Sodium Nitrite Solution) in each well. Following a 15 min incubation in the dark, the wells were washed again with deionized water and air dried and cells were then inspected under the microscope.

2.5. Western Blot. Detection of osteoblastic markers as protein levels was performed by SDS-PAGE gel electrophoresis and western blot analysis. DBSCs were lysed after 7, 14, and 21 days of osteogenic differentiation; the cell lysates were cleared with a centrifugation at 13000 rpm for 15 min at 4°C. The total protein concentration of the supernatant was determined using a protein assay (BIORAD).

Equal amounts of protein for each sample were separated by SDS-PAGE and transferred to nitrocellulose membranes (Amersham, UK) with a Trans-Blot (Biorad, USA). The membranes were probed with primary antibodies overnight at 4°C and then samples were incubated for 90 min with secondary antibodies conjugated to horseradish peroxidase at room temperature. The reaction was analyzed with the Odyssey Infrared Imaging System of LI-COR (LI-COR Biotechnology Lincoln, Nebraska, USA).

2.6. Statistical Analyses. Statistical analyses were performed by Student's *t*-test with the Statistical Package for the Social Sciences (spssx/pc) software (SPSS, Chicago, IL, USA). The results were considered statistically significant for $P < 0.05$.

3. Results

3.1. ALP Positivity and Calcium-Rich Deposits in DBSCs. In order to investigate Vit D ability to induce the differentiation of DBSCs into osteoblasts, cells were cultured in osteogenic medium and stimulated with 1,25$(OH)_2D_3$ 10^{-8} M. This concentration has been observed as the most efficacious among Vit D physiological concentrations analyzed in previous experiments.

DBSCs cultures were stopped at 7, 14, and 21 days after continuous Vit D treatment in differentiating conditions.

We used histochemical assay to evaluate the expression of alkaline phosphatase, a marker of osteoblastic differentiation, a key enzyme in the process of osteodeposition.

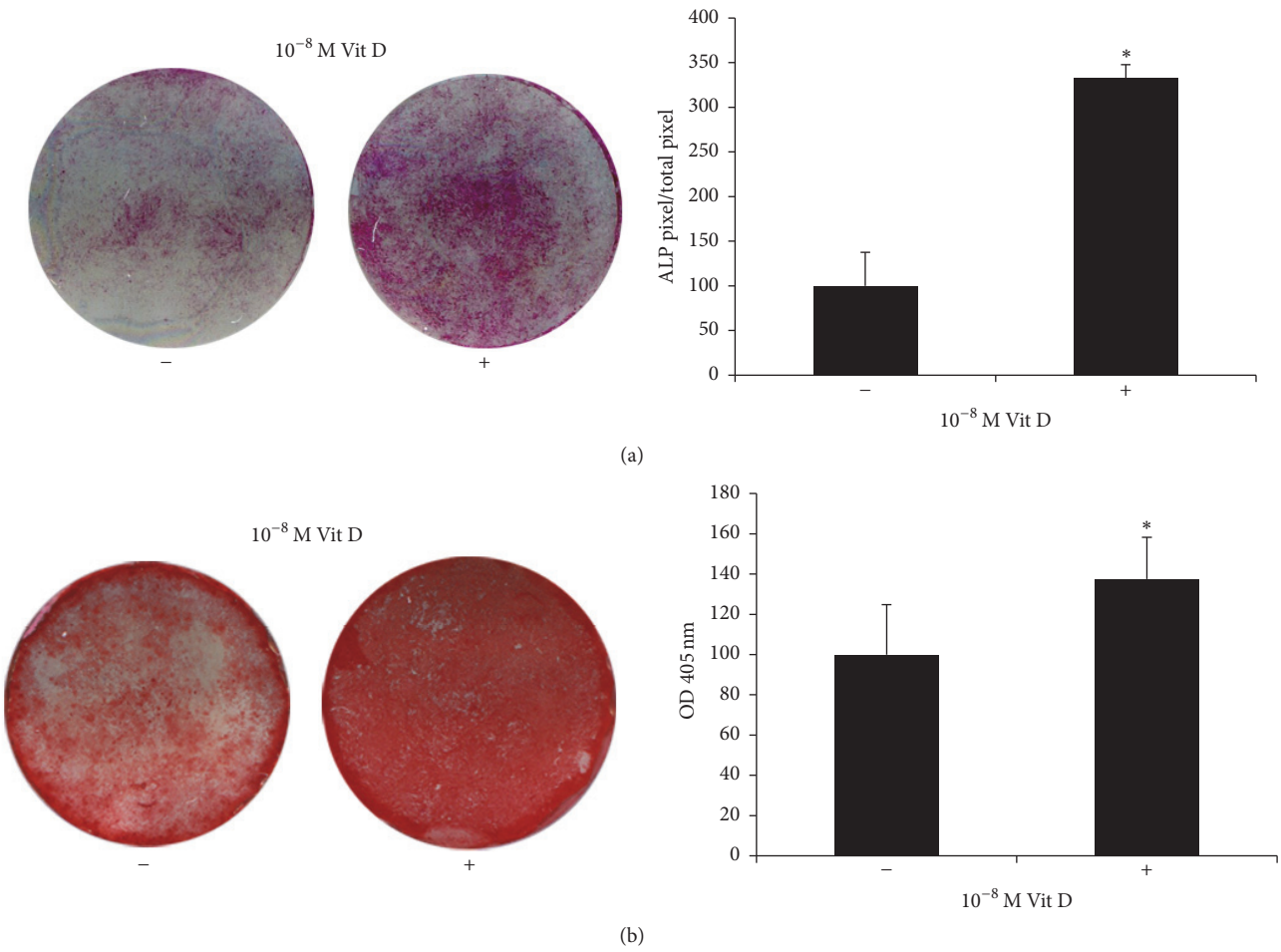

Figure 1: ALP positivity and mineralized nodules formation. (a) ALP histochemical assay (purple staining) performed on DBSCs seeded and differentiated for 7 days with vehicle (−) and 1,25$(OH)_2D_3$ (+). The graph shows quantification of positive staining as percentage compared to untreated cells (−) ($^*P < 0.05$) and is representative for 3 independent donors. Data are presented as mean ± SEM. Student's t-test was used for single comparisons. (b) Alizarin Red (red staining) shows mineralized nodules formation by DBSCs incubated for 21 days in osteogenic medium with vehicle (−) and 1,25$(OH)_2D_3$ (+). The graph shows quantification of ARS with the Optical Density (OD) at 405 nm (b); *indicates statistical significance ($P < 0.001$). Data are representative for 3 independent donors and are presented as mean ± SEM. Student's t-test was used for single comparisons.

We found that DBSCs cultured in an osteogenic medium and treated with 1,25$(OH)_2D_3$ expressed higher levels of ALP after 7 days, compared to those of the control (Figure 1(a)). There was a considerable increase of ALP levels after 14 days, with slight differences between vehicle and treatment (data not shown).

Moreover, long-term cultures of DBSCs demonstrated the capacity to form calcium-rich deposits; this activity, representing the osteoblast final step matrix secretion, was assessed with ARS quantification.

Interestingly DBSCs deposition of mineral matrix nodules was significantly higher in cells cultured with Vit D, compared to the control (Figure 1(b)).

3.2. Osteoblast Markers Expression in DBSCs. The main osteoblastic markers, such as Collagen I (Coll I), its precursor Pro-Collagen I (Pro-Coll I), RUNX2, Bone Sialoprotein (BSP), and Osteopontin (OPN), were analyzed in DBSCs during the different steps of their osteogenic differentiation.

RUNX2 is the master gene of osteogenic differentiation; it directs MSCs to an osteoblastic lineage and inhibits their differentiation into other lineages such as adipocytes and chondrocytes [38].

As shown in Figure 2(a), RUNX2 expression raised in a quite constant way during DBSCs osteogenic differentiation; however the addiction of Vit D greatly increased its expression level after 7 and 14 days of treatment. At 21 days of culture, no difference between vehicle and Vit D was observed.

A trend similar to the one already described for RUNX2 was observed for Coll I (Figure 2(b)): Vit D upregulated its expression in the first 7 days of differentiation; the effect was still present, although attenuated, after 14 and 21 days of treatment.

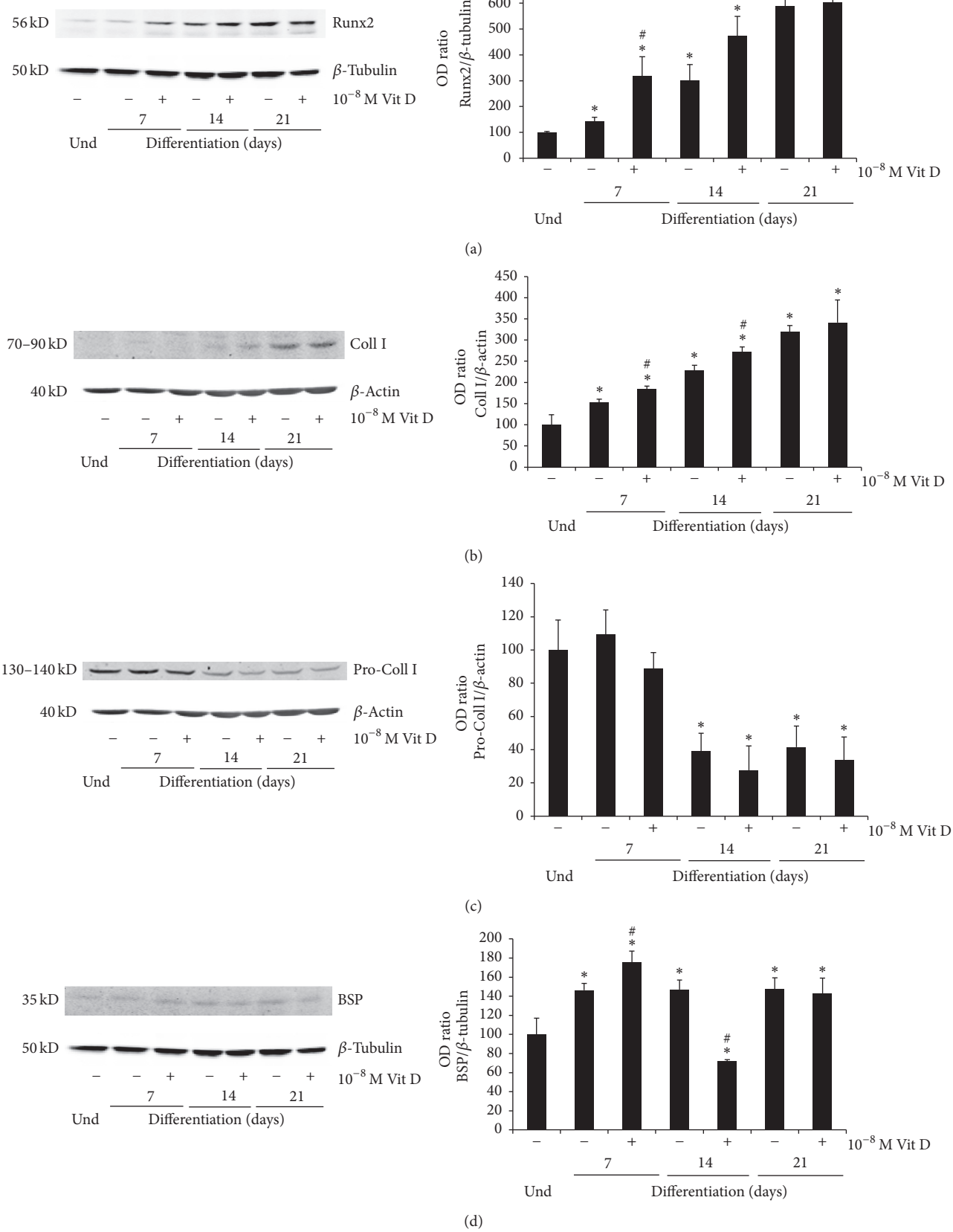

Figure 2: Continued.

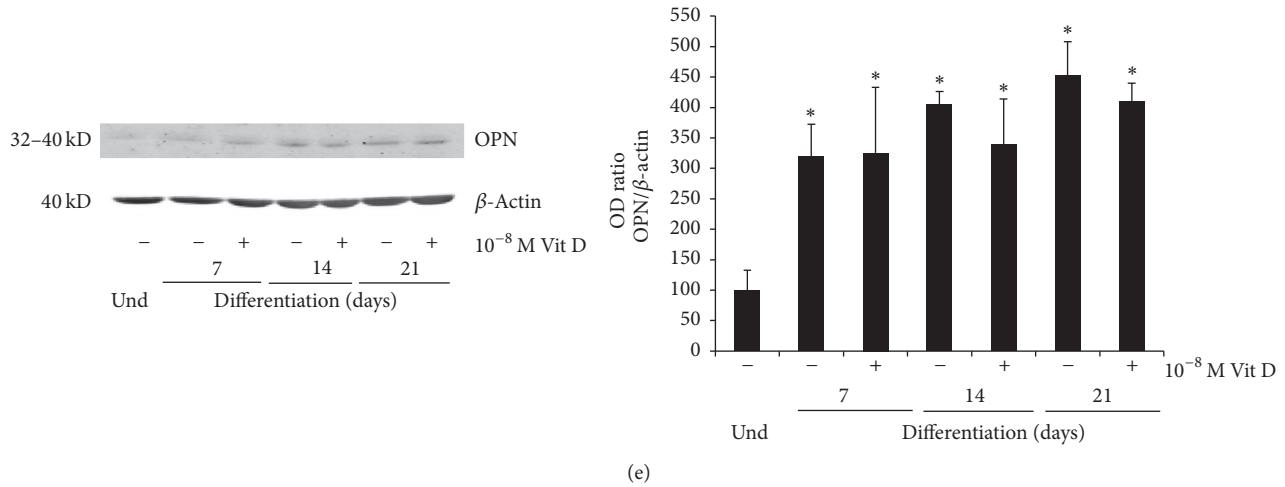

Figure 2: Protein expression. Immunoblots showing the trend expression of RUNX2 (a), Coll I (b), Pro-Coll I (c), BSP (d), and OPN (e) during the osteogenic differentiation process (0–21 days) of DBSCs cultured in osteogenic medium with vehicle (−) and 1,25$(OH)_2D_3$ (+). Each graph represents means ± SEM of 3 independent experiments. $^*P < 0.01$ compared to undifferentiated samples (und) and $^\#P < 0.05$ compared to untreated samples (−). Student's t-test was used for single comparison.

Interestingly Pro-Coll I**,** the immature precursor form of Coll I, showed a reverse trend (Figure 2(c)): Vit D reduced its expression at 7, 14, and 21 days of culture suggesting that this treatment promotes the conversion of Pro-Coll I in the mature Coll I.

It is remarkable how these data confirmed the typical trends of Coll I and its precursor during osteoblastogenesis, indicating that DBSCs are a reliable model of osteoblastic differentiation: moreover Vit D can sustain and increase this process.

Then we evaluated the expression of OPN and BSP which are considered the most important noncollagenous proteins produced by bone cells during the formation of bone matrix *in vitro* [39–41].

The expression of BSP was slightly upregulated after 7 days of Vit D treatment, while at 14 days there was a remarkable reduction; at 21 days BSP did not exhibit significant expression changes (Figure 2(d)).

No significant effect was attributed to the Vit D treatment on the expression of OPN (Figure 2(e)).

4. Discussion

The main actions of Vit D are those concerning mineral and skeletal homeostasis. The protracted deficiency of Vit D has different skeletal consequences in humans determining decreased bone mass and mineralization, with the manifestation of diseases known as Rickets in children and osteomalacia in adults [42, 43]. Low levels of Vit D also result in osteopenia or osteoporosis mainly attributed to an increased osteoclast bone resorption. These effects depend mostly on the indirect actions of 1,25$(OH)_2D_3$. Vit D may affect the bone indirectly, stimulating the intestinal calcium absorption, or directly, that is, by acting on bone cells; which of the two actions is prevailing is still debated [44] and the mechanisms whereby Vit D affects osteoblasts are mostly unknown [45].

Some studies have described 1,25$(OH)_2D_3$ as being able to increase human osteoblasts mineralization, leading to earlier and higher rate of mineral deposition [46], and able to accelerate hMSCs commitment with the subsequent osteoblast maturation [47, 48].

The bone marrow has been considered the major source of MSCs; however these cells can be obtained from other tissues and organs, which in some cases could represent an easier harvesting site being perceived as less invasive for donors. This is the case of stem cells isolated from the dental tissues.

Contrary to other sources used in adults to obtain MSCs, the dental tissues are formed at an older age, this is due to the late completion of odontogenesis and tooth eruption; consequently these tissues contain a higher amount of stem cells that have been discovered to be multipotent cells [22, 49]. DPSCs and DBSCs can be isolated from the third molar, in adult donors or in children, respectively. The dental bud is an immature organ, which originates several years after birth and is composed of undifferentiated cells with a higher proliferation rate than that observed for MSCs from bone marrow.

DBSCs fully satisfy the requirements to be considered MSCs; in fact it has been shown that they express more than 95% of mesenchymal stem markers (CD44, CD73, CD90, CD105, CD146, and HLA-I) and express the typical mesenchymal adhesion molecules [33]. Therefore all these mesenchymal features of DBSCs, together with their easy accessibility, make MSCs from dental tissues an excellent substitute to the bone marrow cells.

We have already demonstrated that osteoblastogenesis can successfully, and in a very productive way, take place from dental follicle, which is the peripheral part of the dental

bud [32] and from dental bud [33]. These cells differentiate toward an osteoblastic phenotype; they express RUNX2, Coll I, and ALP, characteristic osteoblast markers, and produce mineralized matrix nodules.

In this work we analyzed how Vit D could influence the osteogenic differentiation of DBSCs. To this purpose we studied the expression of typical osteoblastic markers and mineral matrix deposition during DBSCs osteogenic differentiation in the presence, or not, of $1,25(OH)_2D_3$. Our results confirmed the functional osteogenic differentiation of DBSCs [33]; in addition in this work we demonstrated that Vit D treatment enhances the commitment of DBSCs toward osteoblastic lineage. Indeed we observed that DBSCs treated with $1,25(OH)_2D_3$ expressed increased levels of the main osteoblastic markers, RUNX2, Coll I, and ALP. Furthermore our results showed that enhanced commitment of DBSCs in presence of Vit D was also accompanied with an augmented production of mineralized matrix.

The enhanced expression of RUNX2, which is an early marker of osteoblastic differentiation, indicated that Vit D acts on uncommitted cells, prompting them to differentiate toward osteogenic lineage and then to express the typical osteoblastic markers ALP and Coll I. These proosteogenic effects exerted by $1,25(OH)_2D_3$ on undifferentiated mesenchymal progenitor cells result subsequently in an accelerated formation of mineralized matrix nodules *in vitro* after 21 days of differentiation.

Our results also showed that the expression of RUNX2 and Coll I was accentuated in cells treated with Vit D during the early phases of osteogenic differentiation (7–14 days), while their expression turned to the control levels around 21 days of culture, indicating that the effects of Vit D are predominant at the beginning of the culture.

These results suggest that Vit D probably acts on the first steps of MSCs differentiation toward the osteoblastic phenotype, becoming less efficacious on differentiated cells. Our data are in line with previous data on human osteoblasts that the effect of Vit D depends on the time and the cells differentiation phase seeming to vanish in ongoing mineralization [46].

Our observations demonstrated that also stem cells from dental tissues respond to Vit D signal and are consistent with the data in literature which attribute to Vit D a key role in inducing osteogenic differentiation of MSCs [18, 47, 50] from human bone marrow. These results confirm that MSCs from dental tissues share similar features with MSCs from bone marrow and suggest that cultures of DBSCs in presence of Vit D could be taken in consideration for bone regenerative therapies.

Thus these data reflect the mesenchymal origin of DBSCs and their osteogenic capacity; moreover this study shows that osteoblastic differentiation of DBSCs was stimulated by $1,25(OH)_2D_3$; our observations suggest that Vit D acts directly on these cells that can be considered osteoblast precursors, directing them to an increased bone matrix deposition.

The point of force of this work is that DBSCs are postnatal stem cells more undifferentiated than those isolated from bone marrow, that is, adult stem cells comparable to embryonic stem cells. The limit of our data is that all these conclusions have been already reported for MSCs from bone marrow; they are anyway a confirmation.

5. Conclusion

It is known that the efficacy of calcium intake on osteoporosis and fracture prevention is conditioned by the concomitant assumption of Vit D. Without adequate Vit D assumption only the 10–15% of the calcium can be utilized for building new bone [51].

Our finding that Vit D stimulates osteoblastic differentiation of DBSCs with the subsequent increase of bone mineral matrix deposition suggests in addition a possible use of Vit D as food aid in reconstructive therapies of bone with MSCs.

Widening the $1,25(OH)_2D_3$ intake in the population could be recommend for both preventive and therapeutic purposes in bone diseases and trauma.

Abbreviations

MSCs:	Mesenchymal Stem Cells
DB:	Dental bud
DBSCs:	Dental Bud Stem Cells
Vit D, $1,25(OH)_2D_3$:	Vitamin D
VDR:	Vitamin D receptor
Coll I:	Collagen I
Pro-Coll I:	Pro-Collagen I
BSP:	Bone Sialoprotein
OPN:	Osteopontin
DP:	Dental Pulp
DPSCs:	Dental Pulp Stem Cells
DFSCs:	Dental Follicle Stem Cells
ALP:	Alkaline phosphatase
ARS:	Alizarin Red Staining.

Competing Interests

The authors have declared that no competing interests exist.

Acknowledgments

Funding for this work was awarded from Ministero dell'Istruzione, dell'Università e della Ricerca—PRIN 20098KM9RN Mori (Progetto di Ricerca d'Interesse Nazionale—Grant 2009); EACA is grateful for the support from the DFG (SFB TRR 79 TPB5); the author A. Di Benedetto is funded by Fondo di Sviluppo e Coesione 2007-2013, APQ Ricerca Regione Puglia "Programma regionale a sostegno della specializzazione intelligente e della sostenibilità sociale ed ambientale-FutureInResearch".

References

[1] M. F. Holick, "Resurrection of vitamin D deficiency and rickets," *Journal of Clinical Investigation*, vol. 116, no. 8, pp. 2062–2072, 2006.

[2] H. F. DeLuca, "Overview of general physiologic features and functions of vitamin D," *The American Journal of Clinical Nutrition*, vol. 80, no. 6, pp. 1689S–1696S, 2004.

[3] Y. C. Li, A. E. Pirro, M. Amling et al., "Targeted ablution of the vitamin D receptor: an animal model of vitamin D-dependent rickets type II with alopecia," *Proceedings of the National Academy of Sciences of the United States of America*, vol. 94, no. 18, pp. 9831–9835, 1997.

[4] K.-I. Takeyama, Y. Yamamoto, and S. Kato, "VDR knockout mice and bone mineralization disorders," *Clinical Calcium*, vol. 17, no. 10, pp. 1560–1566, 2007.

[5] T. Yoshizawa, Y. Handa, Y. Uematsu et al., "Mice lacking the vitamin D receptor exhibit impaired bone formation, uterine hypoplasia and growth retardation after weaning," *Nature Genetics*, vol. 16, no. 4, pp. 391–396, 1997.

[6] R. G. Erben, D. W. Soegiarto, K. Weber et al., "Deletion of deoxyribonucleic acid binding domain of the vitamin D receptor abrogates genomic and nongenomic functions of vitamin D," *Molecular Endocrinology*, vol. 16, no. 7, pp. 1524–1537, 2002.

[7] J. van de Peppel and J. P. T. M. van Leeuwen, "Vitamin D and gene networks in human osteoblasts," *Frontiers in Physiology*, vol. 5, article 137, 2014.

[8] V. J. Woeckel, B. C. J. Van der Eerden, M. Schreuders-Koedam, M. Eijken, and J. P. T. M. Van Leeuwen, "1α,25-dihydroxyvitamin D3 stimulates activin A production to fine-tune osteoblast-induced mineralization," *Journal of Cellular Physiology*, vol. 228, no. 11, pp. 2167–2174, 2013.

[9] C. G. Bellows, S. M. Reimers, and J. N. M. Heersche, "Expression of mRNAs for type-I collagen, bone sialoprotein, osteocalcin, and osteopontin at different stages of osteoblastic differentiation and their regulation by 1,25 dihydroxyvitamin D_3," *Cell and Tissue Research*, vol. 297, no. 2, pp. 249–259, 1999.

[10] M. van Driel and J. P. T. M. van Leeuwen, "Vitamin D endocrine system and osteoblasts," *BoneKEy Reports*, vol. 3, article 493, 2014.

[11] M. van Driel, H. A. P. Pols, and J. P. T. M. van Leeuwen, "Osteoblast differentiation and control by vitamin D and vitamin D metabolites," *Current Pharmaceutical Design*, vol. 10, no. 21, pp. 2535–2555, 2004.

[12] M. Kveiborg, S. I. S. Rattan, B. F. C. Clark, E. F. Eriksen, and M. Kassem, "Treatment with 1,25-dihydroxyvitamin D3 reduces impairment of human osteoblast functions during cellular aging in culture," *Journal of Cellular Physiology*, vol. 186, no. 2, pp. 298–306, 2001.

[13] A. Friedenstein, "Osteogenic stem cells in bone marrow," in *Bone and Mineral Research*, J. N. M. Heersche and J. A. Kanis, Eds., pp. 243–272, Elsevier Science, Amsterdam, The Netherlands, 1990.

[14] M. F. Pittenger, A. M. Mackay, S. C. Beck et al., "Multilineage potential of adult human mesenchymal stem cells," *Science*, vol. 284, no. 5411, pp. 143–147, 1999.

[15] M. Dezawa, H. Kanno, M. Hoshino et al., "Specific induction of neuronal cells from bone marrow stromal cells and application for autologous transplantation," *The Journal of Clinical Investigation*, vol. 113, no. 12, pp. 1701–1710, 2004.

[16] J. M. Luk, P. P. Wang, C. K. Lee, J. H. Wang, and S. T. Fan, "Hepatic potential of bone marrow stromal cells: development of in vitro co-culture and intra-portal transplantation models," *Journal of Immunological Methods*, vol. 305, no. 1, pp. 39–47, 2005.

[17] Y.-L. Li and Z.-S. Xiao, "Advances in Runx2 regulation and its isoforms," *Medical Hypotheses*, vol. 68, no. 1, pp. 169–175, 2007.

[18] P. Lui, B. O. Oyajobi, R. G. G. Russell, and A. Scutt, "Regulation of osteogenic differentiation of human bone marrow stromal cells: interaction between transforming growth factor-β and 1,25$(OH)_2$ Vitamin D_3 in vitro," *Calcified Tissue International*, vol. 65, no. 2, pp. 173–180, 1999.

[19] S. Geng, S. Zhou, and J. Glowacki, "Effects of 25-hydroxyvitamin D3 on proliferation and osteoblast differentiation of human marrow stromal cells require CYP27B1/1α- hydroxylase," *Journal of Bone and Mineral Research*, vol. 26, no. 5, pp. 1145–1153, 2011.

[20] I. J. De Kok, K. C. Hicok, R. J. Padilla, R. G. Young, and L. F. Cooper, "Effect of vitamin D pretreatment of human mesenchymal stem cells on ectopic bone formation," *The Journal of Oral Implantology*, vol. 32, no. 3, pp. 103–109, 2006.

[21] L. V. Logovskaya, T. B. Bukharova, A. V. Volkov, E. B. Vikhrova, O. V. Makhnach, and D. V. Goldshtein, "Induction of osteogenic differentiation of multipotent mesenchymal stromal cells from human adipose tissue," *Bulletin of Experimental Biology and Medicine*, vol. 155, no. 1, pp. 145–150, 2013.

[22] S. Gronthos, M. Mankani, J. Brahim, P. G. Robey, and S. Shi, "Postnatal human dental pulp stem cells (DPSCs) *in vitro* and *in vivo*," *Proceedings of the National Academy of Sciences of the United States of America*, vol. 97, no. 25, pp. 13625–13630, 2000.

[23] G. Mori, G. Brunetti, A. Ballini et al., "Biological characteristics of dental stem cells for tissue engineering," *Key Engineering Materials*, vol. 541, pp. 51–59, 2013.

[24] A. Di Benedetto, C. Carbone, and G. Mori, "Dental pulp stem cells isolation and osteogenic differentiation: a good promise for tissue engineering," *Methods in Molecular Biology*, vol. 1210, pp. 117–130, 2014.

[25] M. Miura, S. Gronthos, M. Zhao et al., "SHED: stem cells from human exfoliated deciduous teeth," *Proceedings of the National Academy of Sciences of the United States of America*, vol. 100, no. 10, pp. 5807–5812, 2003.

[26] A. Ballini, S. Capodiferro, M. Toia et al., "Evidence-based dentistry: what's new?" *International Journal of Medical Sciences*, vol. 4, no. 3, pp. 174–178, 2007.

[27] A. Ballini, G. De Frenza, S. Cantore et al., "In vitro stem cell cultures from human dental pulp and periodontal ligament: new prospects in dentistry," *International Journal of Immunopathology and Pharmacology*, vol. 20, no. 1, pp. 9–16, 2007.

[28] G. Mori, G. Brunetti, A. Oranger et al., "Dental pulp stem cells: osteogenic differentiation and gene expression," *Annals of the New York Academy of Sciences*, vol. 1237, no. 1, pp. 47–52, 2011.

[29] G. Mori, M. Centonze, G. Brunetti et al., "Osteogenic properties of human dental pulp stem cells," *Journal of Biological Regulators and Homeostatic Agents*, vol. 24, no. 2, pp. 167–175, 2010.

[30] E. Giorgini, C. Conti, P. Ferraris et al., "FT-IR microscopic analysis on human dental pulp stem cells," *Vibrational Spectroscopy*, vol. 57, no. 1, pp. 30–34, 2011.

[31] W. Sonoyama, Y. Liu, T. Yamaza et al., "Characterization of the apical papilla and its residing stem cells from human immature permanent teeth: A Pilot Study," *Journal of Endodontics*, vol. 34, no. 2, pp. 166–171, 2008.

[32] G. Mori, A. Ballini, C. Carbone et al., "Osteogenic differentiation of dental follicle stem cells," *International Journal of Medical Sciences*, vol. 9, no. 6, pp. 480–487, 2012.

[33] A. Di Benedetto, G. Brunetti, F. Posa et al., "Osteogenic differentiation of mesenchymal stem cells from dental bud: role of integrins and cadherins," *Stem Cell Research*, vol. 15, no. 3, pp. 618–628, 2015.

[34] A. Ballini, F. Mastrangelo, G. Gastaldi et al., "Osteogenic differentiation and gene expression of dental pulp stem cells

under low-level laser irradiation: a good promise for tissue engineering," *Journal of Biological Regulators and Homeostatic Agents*, vol. 29, no. 4, pp. 813–822, 2015.

[35] F. Paduano, M. Marrelli, L. J. White, K. M. Shakesheff, M. Tatullo, and X. Liu, "Odontogenic differentiation of human dental pulp stem cells on hydrogel scaffolds derived from decellularized bone extracellular matrix and collagen type i," *PLoS ONE*, vol. 11, no. 2, Article ID e0148225, 2016.

[36] M. Marrelli, G. Falisi, A. Apicella et al., "Behaviour of dental pulp stem cells on different types of innovative mesoporous and nanoporous silicon scaffolds with different functionalizations of the surfaces," *Journal of Biological Regulators and Homeostatic Agents*, vol. 29, no. 4, pp. 991–997, 2015.

[37] R. Khanna-Jain, B. Mannerström, A. Vuorinen, G. K. B. Sándor, R. Suuronen, and S. Miettinen, "Osteogenic differentiation of human dental pulp stem cells on β-tricalcium phosphate/poly (l-lactic acid/caprolactone) three-dimensional scaffolds," *Journal of Tissue Engineering*, vol. 3, no. 1, pp. 1–11, 2012.

[38] T. Komori, "Regulation of osteoblast differentiation by transcription factors," *Journal of Cellular Biochemistry*, vol. 99, no. 5, pp. 1233–1239, 2006.

[39] T. Nagata, C. G. Bellows, S. Kasugai, W. T. Butler, and J. Sodek, "Biosynthesis of bone proteins [SPP-1 (secreted phosphoprotein-1, osteopontin), BSP (bone sialoprotein) and SPARC (osteonectin)] in association with mineralized-tissue formation by fetal-rat calvarial cells in culture," *Biochemical Journal*, vol. 274, no. 2, pp. 513–520, 1991.

[40] T. Nagata, H. A. Goldberg, Q. Zhang, C. Domenicucci, and J. Sodek, "Biosynthesis of bone proteins by fetal porcine calvariae in vitro. Rapid association of sulfated sialoproteins (secreted phosphoprotein-1 and bone sialoprotein) and chondroitin sulfate proteoglycan (CS-PGIII) with bone mineral," *Matrix*, vol. 11, no. 2, pp. 86–100, 1991.

[41] S. Kasugai, R. Todescan Jr., T. Nagata, K.-L. Yao, W. T. Butler, and J. Sodek, "Expression of bone matrix proteins associated with mineralized tissue formation by adult rat bone marrow cells in vitro: inductive effects of dexamethasone on the osteoblastic phenotype," *Journal of Cellular Physiology*, vol. 147, no. 1, pp. 111–120, 1991.

[42] M. F. Holick, "High prevalence of vitamin D inadequacy and implications for health," *Mayo Clinic Proceedings*, vol. 81, no. 3, pp. 353–373, 2006.

[43] M. F. Holick, "Vitamin D deficiency: what a pain it is," *Mayo Clinic Proceedings*, vol. 78, no. 12, pp. 1457–1459, 2003.

[44] D. D. Bikle, "Vitamin D and bone," *Current Osteoporosis Reports*, vol. 10, no. 2, pp. 151–159, 2012.

[45] R. St-Arnaud, "The direct role of vitamin D on bone homeostasis," *Archives of Biochemistry and Biophysics*, vol. 473, no. 2, pp. 225–230, 2008.

[46] V. J. Woeckel, R. D. A. M. Alves, S. M. A. Swagemakers et al., "1α,25-$(OH)_2D_3$ acts in the early phase of osteoblast differentiation to enhance mineralization via accelerated production of mature matrix vesicles," *Journal of Cellular Physiology*, vol. 225, no. 2, pp. 593–600, 2010.

[47] E. Piek, L. S. Sleumer, E. P. van Someren et al., "Osteo-transcriptomics of human mesenchymal stem cells: accelerated gene expression and osteoblast differentiation induced by vitamin D reveals c-MYC as an enhancer of BMP2-induced osteogenesis," *Bone*, vol. 46, no. 3, pp. 613–627, 2010.

[48] S. Zhou, J. Glowacki, S. W. Kim et al., "Clinical characteristics influence in vitro action of 1,25-dihydroxyvitamin D_3 in human marrow stromal cells," *Journal of Bone and Mineral Research*, vol. 27, no. 9, pp. 1992–2000, 2012.

[49] G. T.-J. Huang, S. Gronthos, and S. Shi, "Mesenchymal stem cells derived from dental tissues *vs*. those from other sources: their biology and role in regenerative medicine," *Journal of Dental Research*, vol. 88, no. 9, pp. 792–806, 2009.

[50] S. Zhou, M. S. LeBoff, and J. Glowacki, "Vitamin D metabolism and action in human bone marrow stromal cells," *Endocrinology*, vol. 151, no. 1, pp. 14–22, 2010.

[51] M. F. Holick and M. Garabedian, "Vitamin D: photobiology, metabolism, mechanism of action, and clinical applications," in *Primer on the Metabolic Bone Diseases and Disorders of Mineral Metabolism*, pp. 106–114, American Society for Bone and Mineral Research, Washington, DC, USA, 6th edition, 2006.

Hindawi Publishing Corporation
Stem Cells International
Volume 2016, Article ID 2685147, 9 pages
http://dx.doi.org/10.1155/2016/2685147

Research Article

Expression of BMP and Actin Membrane Bound Inhibitor Is Increased during Terminal Differentiation of MSCs

Christian G. Pfeifer, Alexandra Karl, Arne Berner, Johannes Zellner, Paul Schmitz, Markus Loibl, Matthias Koch, Peter Angele, Michael Nerlich, and Michael B. Mueller

Department of Trauma and Orthopaedic Surgery, University Clinic Regensburg, Regensburg, Germany

Correspondence should be addressed to Christian G. Pfeifer; christian.pfeifer@ukr.de

Received 2 September 2016; Accepted 27 September 2016

Academic Editor: Andrea Ballini

Chondrogenic differentiating mesenchymal stem cells (MSCs) are mimicking embryonal endochondral ossification and become hypertrophic. BMP (bone morphogenetic protein) and Activin Membrane Bound Inhibitor (BAMBI) is a pseudoreceptor that regulates the activity of transforming growth factor-β (TGF-β) and BMP signalling during chondrogenesis. Both TGF-β and BMP signalling are regulators of chondrogenic cell differentiation. Human bone marrow derived MSCs were chondrogenically predifferentiated in aggregate culture for 14 days. Thereafter, one group was subjected to hypertrophy enhancing media conditions while controls were kept in chondrogenic medium until day 28. Histological evaluation, gene expression by PCR, and Western blot analysis were carried out at days 1, 3, 7, 14, 17, 21, and 28. A subset of cultures was treated with the BMP inhibitor Noggin to test for BMP dependent expression of BAMBI. Hypertrophic differentiated pellets showed larger cells with increased collagen 10 and alkaline phosphatase staining. There was significantly increased expression of BAMBI on gene expression and protein level in hypertrophic cultures compared to the chondrogenic control and increased BMP4 gene expression. Immunohistochemistry showed intense staining of BAMBI in hypertrophic cells. BAMBI expression was dose-dependently downregulated by Noggin. The pseudoreceptor BAMBI is upregulated upon enhancement of hypertrophy in MSC chondrogenic differentiation by a BMP dependent mechanism.

1. Introduction

The healing capacity of cartilage is very limited and therefore various tissue engineering approaches have been investigated to create pheno- and genotypically stable articular cartilage. Mesenchymal stem cells (MSCs) are promising candidates for the use of cell based tissue engineering applications. The chondrogenic potential of MSCs has been shown in different matrix-free and matrix based cell culture systems [1–5]. However, chondrogenic differentiating MSCs express markers like collagen type X, alkaline phosphatase (ALP), and MMP-13 [6–11], indicating hypertrophic conversion. This behaviour of chondrogenic differentiating MSCs mirrors the developmental pathway of growth plate chondrocytes during endochondral ossification. Additional characteristics of terminal differentiation like vascular invasion and matrix calcification have also been observed after in vivo transplantation of human chondrogenic MSC pellet cultures into mice [12, 13]. This hypertrophic conversion of chondrogenic differentiating MSCs raises concerns for a tissue engineering application of MSCs in articular cartilage repair. It is important to better understand the mechanisms that regulate late differentiation steps in chondrogenic differentiating MSCs to find ways to inhibit hypertrophy. The similarity of MSC chondrogenesis and embryonic endochondral ossification indicates that similar mechanisms are involved in both biological processes [14]. The different steps of endochondral bone development are regulated by a number of signalling molecules including bone morphogenetic proteins (BMPs), transforming growth factor-β (TGF-β), fibroblast growth factors (FGFs), parathyroid hormone-related peptide (PTHrP), Indian hedgehog (Ihh), and Wnts (Wingless-related integration sites) [15, 16].

The TGF-β superfamily consists of signalling molecules including TGF-β, BMPs, activins, inhibins, and growth and

differentiation factors (GDFs). These growth factors have been implicated in the regulation of various processes during embryonic development including cell growth and differentiation, pattern formation, and tissue specification [17, 18].

BMPs form a subgroup within the TGF-β superfamily. BMPs are dimeric proteins and more than 20 BMP related proteins have been characterized. In the main signalling pathway, BMPs bind to a heterodimeric receptor complex composed of type I and type II serine/threonine kinase receptors [19, 20]. Upon ligand binding, type II receptor phosphorylates type I receptor.

The pseudoreceptor BAMBI (BMP and activin membrane bound inhibitor) is a transmembrane protein with structural similarity to type I receptors of the TGF-β superfamily but has a shorter intracellular domain. Lack of this intracellular serine/threonine kinase domain precludes enzymatic activity [21, 22]. BAMBI inhibits TGF-β and BMP signalling by blocking the interaction between type I and type II receptors [21]. Further on BAMBI is tightly coexpressed with BMP4 during embryonic development and may act as a negative feedback regulator of BMP signalling [21, 22]. BMP4 induction has been shown to be an important factor in the enhancement of hypertrophy in MSC chondrogenesis [23]. Finally, BAMBI mediates a considerable degree of crosstalk between the BMP signalling pathway and TGF-β signalling pathways.

Interestingly Chen et al. [24] found no developmental defects in mice lacking alleles for BAMBI. These transgenic mice were viable and fertile and did not show discernible developmental defects [24]. In contrast Guillot et al. [25] found swollen cells in myocardial and glomerular capillaries in BAMBI deficient mice. Most importantly in respect of limb development and the role of BAMBI in terminal differentiation of growth plate chondrocytes, Montero et al. [26] described the role of BAMBI during limb morphogenesis. Upon repression of BAMBI expression by activin, an increase in SMAD 1, 5, and 8 could be observed, which was followed by formation of ectopic cartilage.

Therefore this study was set up in order to investigate the expression pattern and possible downstream effects of BAMBI in late stage chondrogenesis. We therefore used an established hypertrophy model [14] in human MSCs using triiodothyronine as well as a refined hypertrophy model using BMP4 [23] for hypertrophic conversion of chondrogenically differentiated MSCs.

2. Material and Methods

2.1. Isolation of MSCs. Upon approval by the local ethics committee and written consent by the donors human MSCs were isolated from iliac crest bone marrow aspirates of seven male patients, aged 21 to 42 years, undergoing surgery that required autologous bone grafting from the iliac crest. MSCs were isolated by Ficoll (Biochrom) gradient centrifugation followed by polystyrene adhesion. Cells were expanded in Dulbecco's Modified Eagle's Medium (DMEM) low glucose (Invitrogen) with 10% fetal calf serum (PAN Biotech GmbH) and 1% penicillin/streptomycin (Invitrogen) at 37°C with 5% CO_2. Growth medium was changed twice a week and cells were trypsinized at 80% confluence and frozen for later use in liquid nitrogen. After thawing and monolayer expansion, cells were used for the experiments at passage 1.

2.2. Chondrogenic Differentiation and Enhancement of Hypertrophy. For differentiation experiments MSCs were trypsinized and seeded in V-bottomed 96-well polypropylene plates at 200,000 cells per well in order to form 3D aggregates. Aggregates were assembled by centrifugation at 250 ×g for 5 min and chondrogenically differentiated in standard chondrogenic medium (chon) containing DMEM with high glucose (Invitrogen), 1% ITS (Sigma Aldrich), 50 μg/mL ascorbate-2-phosphate (Sigma Aldrich), 40 μg/mL L-proline (Sigma Aldrich), 100 nM dexamethasone (Sigma Aldrich), 1 mM sodium pyruvate (Invitrogen), and 10 ng/mL TGF-β1 (R&D Systems).

Aggregates were predifferentiated for 14 days. Medium conditions were then changed and aggregates were distributed in five different groups: (1) standard chondrogenic medium (chon); (2) chondrogenic medium with BMP4 (chon + BMP); (3) standard hypertrophy enhancing medium (chon without TGF-β and without dexamethasone, including 1 nM triiodothyronine (T3) (Sigma Aldrich) (hyp)); (4) hypertrophy enhancing medium without T3 (hyp − T3); (5) hypertrophy enhancing medium with BMP4 instead of T3 (hyp − T3 + BMP; BMP4 was used at 100 ng/mL) (Figure 1).

In order to test for BMP4 dependent regulation of BAMBI, the BMP inhibitor Noggin was employed at 10 ng/mL and 100 ng/mL from day 1 in aggregates treated by hyp − T3 + BMP protocol (Figure 1).

Aggregates were harvested at d1, d3, d7, d14, d17, d21, and d28 for gene expression analysis.

2.3. Histology. Aggregates for histological analysis were harvested on d14 and d28, fixed in 4% paraformaldehyde. 10 μm thick frozen sections were cut on a cryomicrotome (HM 500 OM Cryostat; Microm, Berlin, Germany). Sections were stained with 1,9-dimethylmethylene blue (DMMB) (Sigma Aldrich) for sulphated glycosaminoglycans (GAGs).

2.4. Histochemistry and Immunohistochemistry. For histochemical investigations 10 μm thick sections were prepared as well. Histochemical ALP staining was performed with an alkaline phosphatase kit (Sigma Aldrich) with neutral red as counterstain.

For immunohistochemistry mouse anti-BAMBI (1 : 10, eBioscience), rabbit anti-BMP4 (1 : 250, Abcam), mouse anti-collagen type X (1 : 20, Quartett Immunodiagnostika und Biotechnologie GmbH), and mouse anti-collagen type II (1 : 100, Calbiochem) antibodies were used and immunohistochemistry was carried out as follows: after rinsing samples in washing buffer for 5 minutes blocking of endogenous peptidases (3% H_2O_2/10% methanol in PBS) was performed for 30 minutes. Then sections were incubated in blocking buffer (10% fetal bovine serum/10% goat serum in PBS) for 60 minutes at RT followed by incubation anti-BAMBI primary antibody in blocking buffer overnight at 4°C. Immunolabeling was detected by a biotinylated secondary antibody (1 : 100;

Table 1

Gene	Sequence (forward)	Sequence (reverse)	Concentration
HPRT	CGAGATGTGATGAAGGAGATGG	GCAGGTCAGCAAAGAATTTATAGC	150 nM
BAMBI	CGATGTTCTCTCTCCTCCCAG	AATCAGCCCTCCAGCAATGG	150 nM

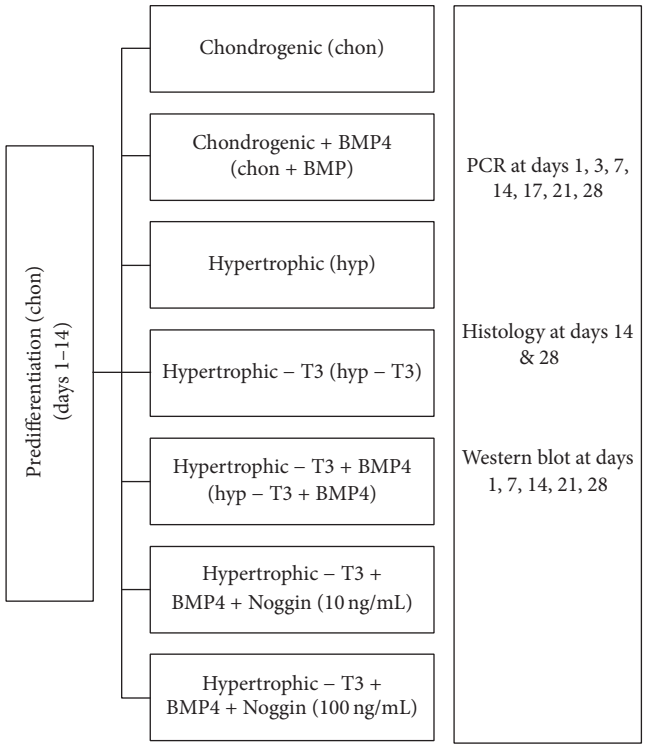

Figure 1: Schematic of groups and treatments: left bar shows chondrogenic predifferentiation in TGF-β containing medium from days 1–14. Midline bars show treatment of groups after chondrogenic predifferentiation from day 14 to day 28. Right column shows outcome measurements in regard of time points. Overall culture duration after expansion was 28 days.

Dianova), horse reddish peroxidase conjugated streptavidin (Vector Laboratories, Burlingame), and metal enhanced diaminobenzidine as a substrate (Sigma Aldrich).

2.5. RNA Isolation, cDNA Synthesis, and Gene Expression Analysis. For each of the 7 different independent donors 8 to 10 aggregates per condition and time point were pooled for the experiments, homogenized in 1 mL TRI Reagent (Sigma Aldrich) using the Power Gen 1000 homogenizer (Fischer Scientific), and RNA was isolated by the Trizol method. Reverse transcription was performed with Transcriptor First Strand cDNA Synthesis kit (Roche). Semiquantitative real-time PCR was performed with Brilliant SYBR Green QPCR mix (Stratagene) and the Mx3000P QPCR System (Stratagene). Gene expression was normalized to hypoxanthine guanine phosphoribosyltransferase (HPRT).

For real-time PCR the primers in Table 1 were used.

2.6. Western Blot Analysis. For Western blot analysis, the following antibodies were used: mouse anti-BAMBI (1 : 1000, eBioscience) and rabbit anti-β actin (1 : 10000, Abcam).

5 to 8 MSC pellets per time point and per condition for each patient were pooled, washed in ice cold PBS, and homogenized in 500 μL 6 M urea/2% SDS solution containing a protease inhibitor cocktail (Sigma) and a phosphatase inhibitor (Sigma) using the Power Gen 1000 homogenizer (Fischer Scientific). The lysate was centrifuged for 5 minutes at 1000 ×g (4°C) and the supernatant was transferred to a new tube. The protein concentration of the supernatant was determined using the BCA Protein Assay kit (Biorad, DC Protein Assay) according to the manufacturer's instructions.

Lysates were supplemented with 4x LDS sample buffer (Invitrogen) and 10 mM dithiothreitol (DTT) and proteins were denatured for 5 minutes at 95°C. For gel electrophoresis, equal amounts of protein (10 μg) were loaded and separated on a 4–12% Bis-Tris Gel (Novex by Life Technologies) at 120 V. After gel electrophoresis proteins were transferred from the gel to polyvinylidenfluoride (PVDF) membrane (Millipore). Blotting was performed for 2 hours at 100 V. After transfer, the membrane was blocked for 1 hour in 5% skim milk powder in Tris buffered saline with Tween 20 (TBST). The membrane was then incubated in primary antibody in 5% skim milk powder in TBST over night at 4°C. The next day, the membrane was washed three times for 10 minutes in TBST and afterwards incubated in HPR-coupled secondary antibody (1 : 1000, Pierce) in 5% skim milk powder in TBST at room temperature for 1 hour. The membrane was washed three times in TBST for 10 minutes. Chemoluminescence was detected with the ECL western kit (Pierce) and by using X-ray sensitive films (ECL Hyperfilm, Amersham). The films were developed in a photo developer (Curix 60, AGFA).

Western blot membranes were stripped using ReBlot Plus (Millipore) according to manufactures instructions.

2.7. Statistical Analysis. Gene expression was analysed by calculating the means of every relative expression normalized to the housekeeping gene HPRT. After check for normal distribution by Kolmogorov-Smirnov testing two-tailed Student's t-test was used. To maintain an overall p-level of $p < 0.05$, post hoc Bonferroni testing was carried out.

3. Results

3.1. Induction of Hypertrophy. Induction of hypertrophy was achieved by addition of T3 and withdrawal of dexamethasone after chondrogenic predifferentiation. The enhancement of hypertrophy was shown by an increased cell size, stronger collagen type X staining, and higher ALP activity under

prohypertrophic conditions compared to standard chondrogenic conditions. Extracellular matrix analysis revealed poorer glycosaminoglycan content (Figures 2(a) and 2(b)). Immunohistochemically we observed equal to less collagen type 2 staining (Figures 2(c) and 2(d)) and analysis for hypertrophic markers showed increased collagen type 10 staining (Figures 2(e) and 2(f)) as well as strongly increased staining for the preapoptotic marker alkaline phosphatase (Figures 2(g) and 2(h)) for samples after hypertrophic conversion compared to nonconverted samples. These findings are in line with previously described characteristics of hypertrophic chondrocytes found in the growth plate [5, 14, 27], allowing using this hypertrophy model for further analysis. Both collagen type 2 and type 10 expression increases over time in both groups without significant difference between the groups (Supplementary Figure 1 in Supplementary Material available online at http://dx.doi.org/10.1155/2016/2685147). This is not concordant with the immunohistochemical results, which show higher collagen type 10 deposition in the hypertrophic group. This is a known phenomenon in this model and has also been discussed in previous papers [14]. The reason for this discrepancy is that we are dealing with mixed cell populations and not all cells respond to the switch to hypertrophy enhancing medium to the same extent. While some cells undergo hypertrophic differentiation, the TGF-β withdrawal may lead to dedifferentiation in other cells. This heterogeneous response can explain the missing significant difference in gene expression levels.

3.2. Gene Expression of BAMBI Is Increased upon Hypertrophic Conversion. Real-time PCR analysis of BAMBI revealed a pronounced increase in BAMBI gene expression under hypertrophic (hyp) conditions compared to chondrogenic (chon) conditions. BAMBI gene expression is significantly upregulated at day 17, day 21, and day 28 in hypertrophic stimulated MSC pellets compared to chondrogenic pellets (Figure 3(a)). Similarly gene expression of BMP4 is also upregulated in hypertrophic conditions and reaches significant difference compared to chondrogenic conditions (Figure 3(b)). All gene expressions were normalized to the housekeeping gene HPRT.

To confirm this result on protein level we performed Western blot analysis for BAMBI on days 21 and 28. Again, in hypertrophic stimulated MSC pellets strong signals for BAMBI protein could be detected, while under chondrogenic conditions no signal was found. Remarkably, neither BAMBI gene expression nor BAMBI protein levels changed significantly under chondrogenic conditions throughout the whole time course of our experiment.

3.3. Immunohistochemical Staining of BAMBI Is Increased upon Hypertrophic Conversion. To further prove the increase of BAMBI expression, immunohistochemistry for BAMBI protein was performed. Thereby we also looked for the intracellular distribution of BAMBI protein. Immunohistochemistry revealed increased staining for BAMBI in hypertrophic aggregates compared to chondrogenic aggregates on day 28 (Figure 4). In terms of intracellular distribution of BAMBI, we observed pronounced staining of the cell membranes (black arrows, Figure 4). As BAMBI is a membrane bound protein this finding was expected and confirms the presence of BAMBI protein within the cells' membranes.

3.4. Gene Expression of BAMBI Is Induced by BMP4. To further investigate the role of BAMBI in the induction of hypertrophy, we analysed the expression of BAMBI after BMP4 and Noggin treatment. It was previously shown that induction of hypertrophy by T3 and withdrawal of dexamethasone and TGF-β is mediated by BMP4 [23]. This is also revealed by increased BMP4 protein staining in hypertrophically converted groups compared to chondrogenic controls (Figure 5). Therefore we suggested that similar expression patterns for BAMBI are achieved upon hypertrophic conversion by BMP4 (Hyp − T3 + BMP).

BMP4 treatment significantly increases BAMBI expression on day 28 under chondrogenic conditions (nonsignificant increase on day 21). Under hypertrophic conditions BAMBI expression is significantly increased in MSC pellets that were treated with BMP4 compared to hypertrophic medium without T3 (hyp − T3) (Figure 6). In comparison to hypertrophic medium with T3 (hyp), we only could detect nonsignificantly increased gene expression levels upon BMP4 treatment (hyp − T3 + BMP) on day 21 but not day 28 (Figure 6). Both conditions, hyp and hyp − T3 + BMP, showed higher levels of BAMBI gene expression compared to BMP4 treatment under chondrogenic conditions.

3.5. Gene Expression of BAMBI Is Downregulated by BMP Inhibition. According to these findings we further investigated whether these BAMBI expression patterns can be avoided by addition of the BMP inhibitor Noggin to hypertrophic (hyp) conditions. In order to estimate whether this inhibition was dose dependent we used two different doses of Noggin (10 and 100 ng/mL). For controls we added the same doses to chondrogenic controls.

Treatment with the BMP inhibitor Noggin does not alter BAMBI expression under chondrogenic conditions on day 21 and day 28. Under hypertrophic conditions, addition of 100 ng/mL Noggin significantly decreases BAMBI expression on day 21 and day 28 compared to hyp-conditions (Figure 7). However, decrease of BAMBI expression upon addition of 10 ng/mL Noggin is only significant on day 21, when compared to hyp-conditions. Besides the fact that BAMBI expression is downregulated under hypertrophic conditions and concurrent addition of the BMP inhibitor Noggin we could also show that this downregulation is dose dependent.

4. Discussion

4.1. Induction of Hypertrophy. Human MSCs are able to differentiate into a chondrogenic lineage. However some hypertrophic markers are expressed nevertheless, whether in short term culture or long term culture [28]. According to these findings it has been shown that cultured chondrogenic MSCs follow the intrinsic pathway of growth plate chondrocytes [12] and therefore inevitably become hypertrophic.

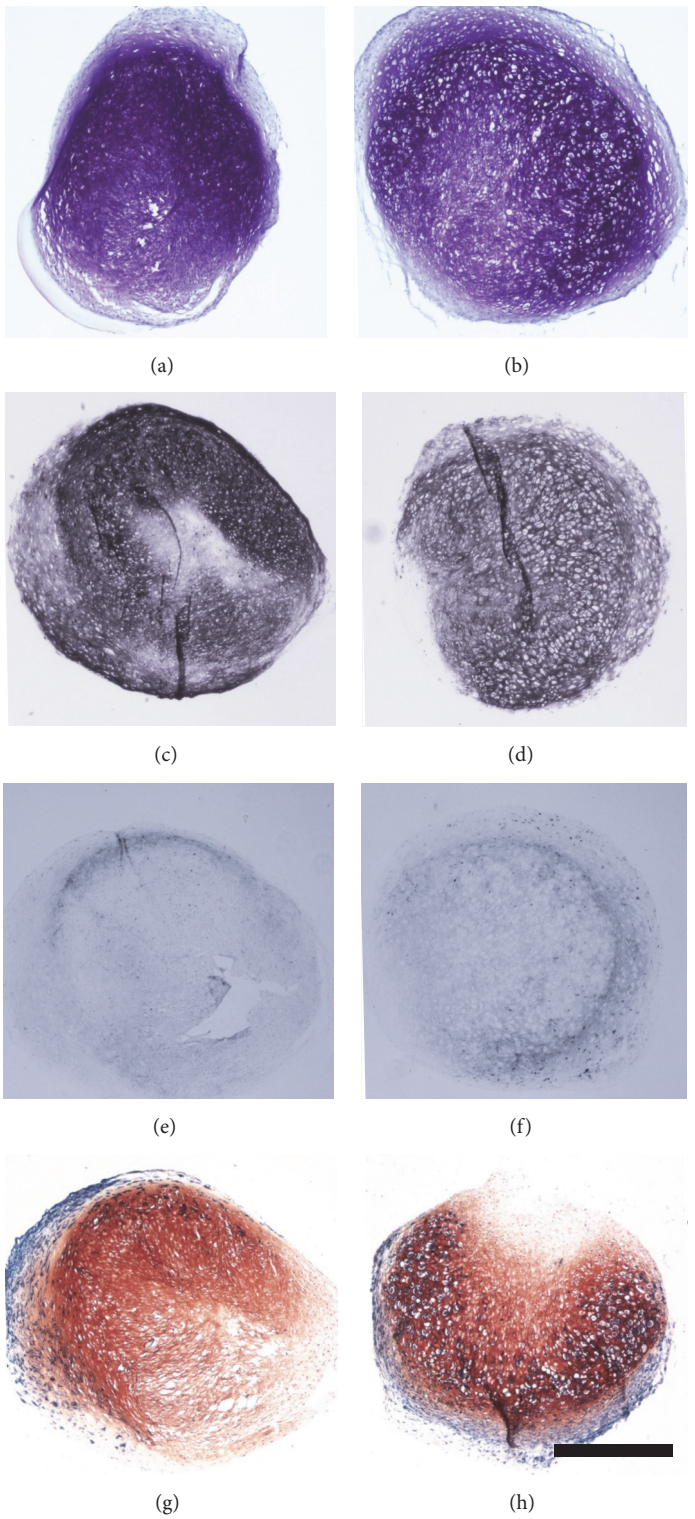

Figure 2: Differences in glycosaminoglycan content shown by DMMB staining of cell pellets after chondrogenic (chon) (a) and hypertrophic (hyp) conditions (b), as well as different collagen 2 production as revealed by immunohistochemistry against collagen 2 of cell pellets after chondrogenic (c) and hypertrophic conditions (d). Enhancement of hypertrophy shown by immunohistochemistry against collagen 10 between chondrogenic (e) and hypertrophic (f) conditioned cell pellets as well as by ALP staining of chondrogenic (g) and hypertrophic (h) conditioned cell pellets. Scale bar = 500 μm.

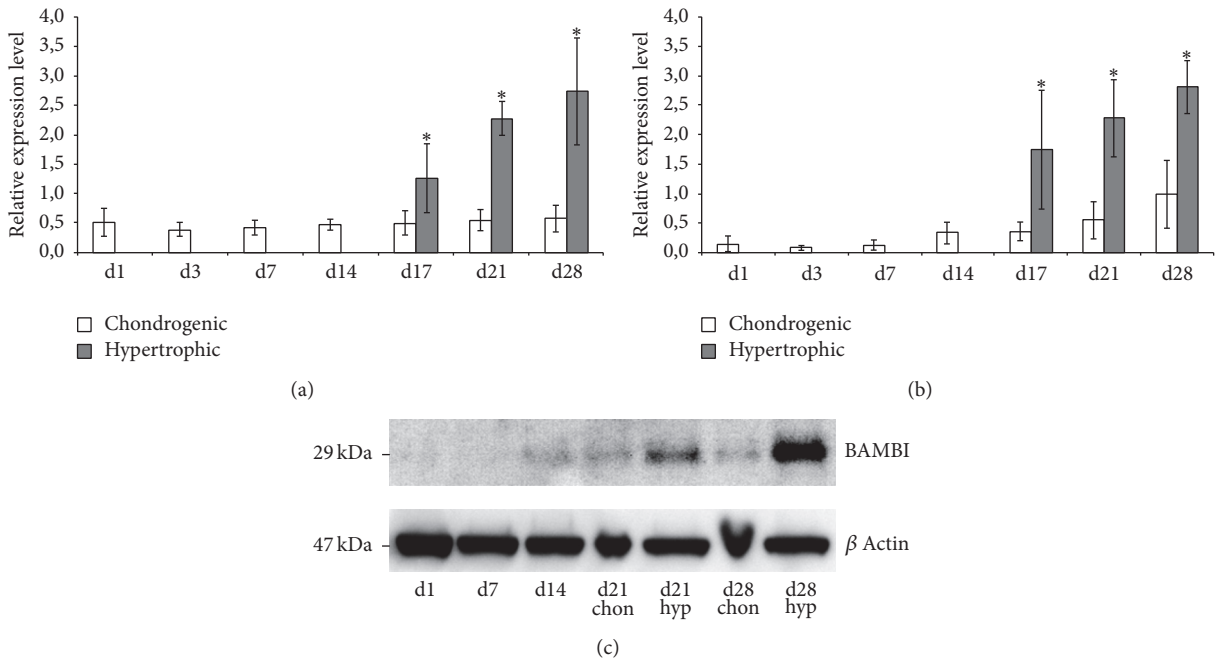

Figure 3: (a) Gene expression analysis of BAMBI and (b) BMP4 normalized to HPRT in MSC pellet cultures under chondrogenic and hypertrophy enhancing conditions analysed by real-time PCR. BAMBI and BMP4 are significantly upregulated under hypertrophic conditions compared to chondrogenic controls on days 17, 21, and 28. $n = 7$ different donors, $^{*}p < 0.001$. (c) Western blot analysis of BAMBI: increased amount of BAMBI protein can be detected under hypertrophic conditions on days 21 and 28 compared to chondrogenic conditions.

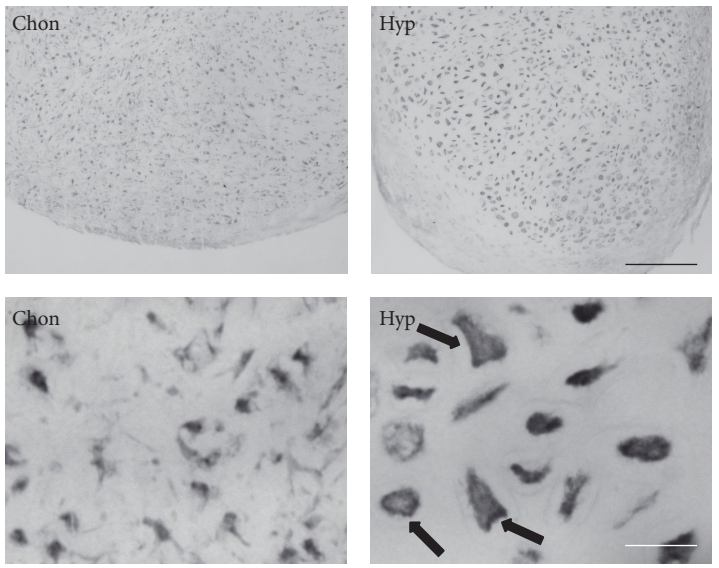

Figure 4: Immunohistochemistry for BAMBI. BAMBI staining is increased under hypertrophic conditions compared to chondrogenic conditions. Pronounced staining at cell membranes is detected especially under hypertrophic conditions (black arrows). Black scale bar = 200 μm; white scale bar = 50 μm.

This hypertrophic phenotype of chondrogenic differentiated MSCs can be experimentally enhanced by changing medium conditions from chondrogenic to hypertrophy enhancing medium as described previously [12, 14]. This change in medium conditions includes withdrawal of TGF-β and dexamethasone and the addition of the thyroid hormone T3. Using this in vitro hypertrophy model for MSCs we could significantly increase the hypertrophic phenotype of chondrogenic differentiated human MSCs. The enhancement of hypertrophy was clearly shown by an increased cell size, stronger collagen type X staining, and stronger ALP staining in hypertrophic MSC pellets. Hypertrophic markers are not exclusively expressed under prohypertrophic conditions but also under standard chondrogenic conditions even though to

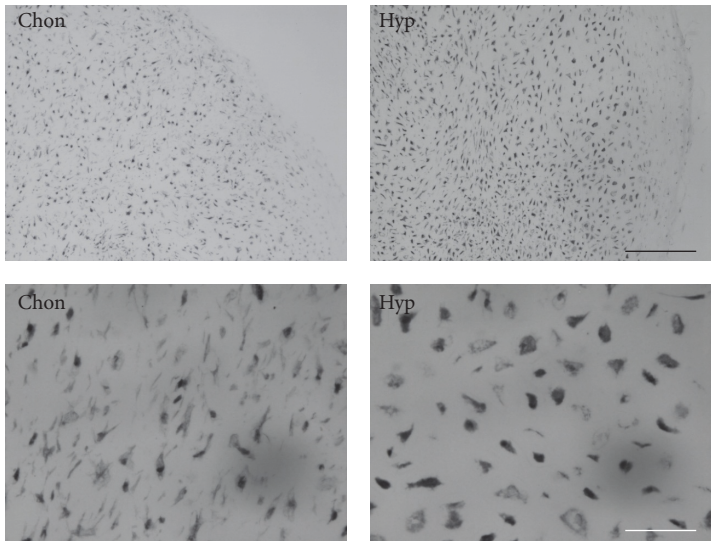

Figure 5: Immunohistochemical staining of BMP4 of day 28 MSC pellets. BMP4 protein staining is increased under hypertrophy (hyp) enhancing conditions as compared to chondrogenic (chon) conditions. Black scale bar = 200 μm; white scale bar = 50 μm.

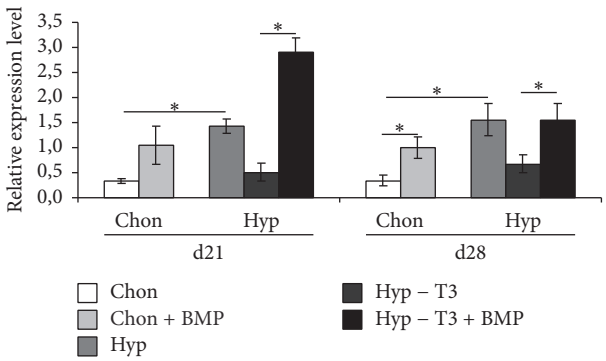

Figure 6: Gene expression analysis of BAMBI normalized to HPRT in MSC pellet cultures after BMP4 treatment under chondrogenic (chon) and hypertrophy (hyp) enhancing conditions analysed by real-time PCR. BAMBI expression is increased under chondrogenic and hypertrophic conditions after BMP4 treatment. $n = 4$ different donors, $^{*}p < 0.05$.

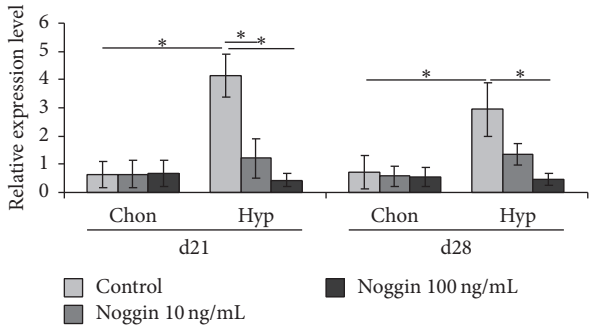

Figure 7: Gene expression analysis of BAMBI normalized to HPRT in MSC pellet cultures after Noggin treatment under chondrogenic (chon) and hypertrophy (hyp) enhancing conditions analysed by real-time PCR. Noggin treatment significantly decreases BAMBI expression under hypertrophic conditions. $n = 4$ different donors, $^{*}p < 0.05$.

a lower degree. There are some ALP positive cells in the center of chondrogenic MSC pellets but ALP activity is mainly restricted to the periphery of the pellet. It was described previously that fibroblast-like cells surround MSC pellets [7]. Based on this finding, we suggest that the ALP positive ring around the pellet consists mainly of fibroblast-like cells rather than hypertrophic chondrocytes. After hypertrophic induction, areas of cellular hypertrophy as well as dedifferentiated areas were detected.

4.2. Gene Expression of BAMBI Is Increased upon Hypertrophic Conversion. BAMBI is a transmembrane protein with structural similarity to TGF-β and BMP receptor type I but lacks the intracellular kinase domain [21]. Thus, BAMBI is able to inhibit both TGF-β and BMP signalling. BAMBI has been shown to be coexpressed with BMP4 during xenopus and mouse embryogenesis [21, 22]. Further on BMP4 induces BAMBI expression through an evolutionary preserved promoter BMP responsive enhancer 7 (Bre7) [29]. Additionally also TGF-β is able to enhance BAMBI expression through SMAD 3/4 signalling [30].

We detected a significant upregulation of BAMBI under hypertrophic conditions using T3 and withdrawal of dexamethasone and TGF-β for hypertrophic conversion (Figure 3). The upregulation was proven for gene expression as well as on protein level by Western blotting. The final function of this strong upregulation of BAMBI however is still unclear. Preferential inhibition of TGF-β signalling diminishes the antihypertrophic effect of TGF-β, resulting in further enhancement of the hypertrophic phenotype. On the other hand, predominant interaction with BMP receptor could ameliorate the BMP induced terminal differentiation

[23] in our prohypertrophic culture conditions. BAMBI may act as a negative feedback loop to inhibit BMP signalling in response to increased BMP4 expression.

4.3. Immunohistochemical Staining of BAMBI Is Increased upon Hypertrophic Conversion. The same observation of upregulation of BAMBI expression was conducted using immunohistochemistry (IHC) with primary antibodies against the BAMBI pseudoreceptor. Particularly the membrane binding nature of the pseudoreceptor, which is also known as a transmembrane receptor, was shown in higher magnifications of IHC. The membrane binding character was described earlier by several working groups [21, 31].

4.4. Gene Expression of BAMBI Is Induced by BMP4. To further clarify the induction of BAMBI expression we conducted an experiment in which hypertrophic conversion by T3 (hyp) was compared to hypertrophic conversion by BMP4 (hyp − T3 + BMP4). As evidenced by PCR BAMBI was increased, upregulated upon stimulation by BMP4. The induction of BAMBI expression by T3 is most probably also mediated by BMP. It was shown in previous works that Noggin and dorsomorphin as BMP inhibitors are capable of inhibiting T3 induced hypertrophy [23]. Therefore the effects of T3 on BAMBI expression will be most likely achieved by enhanced BMP expression and as a consequence increased BAMBI expression.

4.5. Gene Expression of BAMBI Is Downregulated by BMP Inhibition. This hypothesis is further supported by the finding that BAMBI expression in T3 induced hypertrophy is dose-dependently downregulated upon addition of the BMP inhibitor Noggin. This crosstalk between T3 triggered cell differentiation and BMP4 was shown in human MSCs [23] and chicken embryos [32], while other working groups suggested BMP2 as main mediator of hypertrophic conversion in chick limb buds [33].

It is still under discussion which exact temporospatial distribution BAMBI has during limb development and whether its role is pivotal or not. It seems that BAMBI, which is a negative regulator of chondrogenesis, might be a target in order to stabilize the chondrogenic phenotype of chondrogenically differentiated MSCs.

5. Conclusion

These experiments showed that the expression of the pseudoreceptor BAMBI is strongly upregulated under hypertrophy enhancing conditions in human MSCs. T3, BMP4, and Noggin treatment are able to modulate BAMBI expression. The function of BAMBI is not clear and needs to be investigated by functional experiments with knockdown and overexpression of BAMBI in the future.

Competing Interests

The authors declare that they have no competing interests.

Acknowledgments

The authors thank Ms. D. Drenkard and Mr. R. Kujat for technical support. This work was funded by DFG grant MU2318/3-1.

References

[1] S. Ichinose, M. Tagami, T. Muneta, and I. Sekiya, "Morphological examination during in vitro cartilage formation by human mesenchymal stem cells," *Cell and Tissue Research*, vol. 322, no. 2, pp. 217–226, 2005.

[2] U. Nöth, R. Tuli, A. M. Osyczka, K. G. Danielson, and R. S. Tuan, "In vitro engineered cartilage constructs produced by press-coating biodegradable polymer with human mesenchymal stem cells," *Tissue Engineering*, vol. 8, no. 1, pp. 131–144, 2002.

[3] I. Sekiya, J. T. Vuoristo, B. L. Larson, and D. J. Prockop, "In vitro cartilage formation by human adult stem cells from bone marrow stroma defines the sequence of cellular and molecular events during chondrogenesis," *Proceedings of the National Academy of Sciences of the United States of America*, vol. 99, no. 7, pp. 4397–4402, 2002.

[4] L. Song, D. Baksh, and R. S. Tuan, "Mesenchymal stem cell-based cartilage tissue engineering: cells, scaffold and biology," *Cytotherapy*, vol. 6, no. 6, pp. 596–601, 2004.

[5] A. M. Mackay, S. C. Beck, J. M. Murphy, F. P. Barry, C. O. Chichester, and M. F. Pittenger, "Chondrogenic differentiation of cultured human mesenchymal stem cells from marrow," *Tissue Engineering*, vol. 4, no. 4, pp. 415–428, 1998.

[6] B. Johnstone, T. M. Hering, A. I. Caplan, V. M. Goldberg, and J. U. Yoo, "In vitro chondrogenesis of bone marrow-derived mesenchymal progenitor cells," *Experimental Cell Research*, vol. 238, no. 1, pp. 265–272, 1998.

[7] J. U. Yoo, T. S. Barthel, K. Nishimura et al., "The chondrogenic potential of human bone-marrow-derived mesenchymal progenitor cells," *Journal of Bone and Joint Surgery—Series A*, vol. 80, no. 12, pp. 1745–1757, 1998.

[8] F. Barry, R. E. Boynton, B. Liu, and J. M. Murphy, "Chondrogenic differentiation of mesenchymal stem cells from bone marrow: differentiation-dependent gene expression of matrix components," *Experimental Cell Research*, vol. 268, no. 2, pp. 189–200, 2001.

[9] A. Winter, S. Breit, D. Parsch et al., "Cartilage-like gene expression in differentiated human stem cell spheroids: a comparison of bone marrow-derived and adipose tissue-derived stromal cells," *Arthritis & Rheumatism*, vol. 48, no. 2, pp. 418–429, 2003.

[10] F. Mwale, D. Stachura, P. Roughley, and J. Antoniou, "Limitations of using aggrecan and type X collagen as markers of chondrogenesis in mesenchymal stem cell differentiation," *Journal of Orthopaedic Research*, vol. 24, no. 8, pp. 1791–1798, 2006.

[11] M. B. Mueller, M. Fischer, J. Zellner et al., "Hypertrophy in mesenchymal stem cell chondrogenesis: effect of TGF-β isoforms and chondrogenic conditioning," *Cells Tissues Organs*, vol. 192, no. 3, pp. 158–166, 2010.

[12] K. Pelttari, A. Winter, E. Steck et al., "Premature induction of hypertrophy during in vitro chondrogenesis of human mesenchymal stem cells correlates with calcification and vascular invasion after ectopic transplantation in SCID mice," *Arthritis & Rheumatism*, vol. 54, no. 10, pp. 3254–3266, 2006.

[13] C. Scotti, B. Tonnarelli, A. Papadimitropoulos et al., "Recapitulation of endochondral bone formation using human adult

mesenchymal stem cells as a paradigm for developmental engineering," *Proceedings of the National Academy of Sciences of the United States of America*, vol. 107, no. 16, pp. 7251–7256, 2010.

[14] M. B. Mueller and R. S. Tuan, "Functional characterization of hypertrophy in chondrogenesis of human mesenchymal stem cells," *Arthritis & Rheumatism*, vol. 58, no. 5, pp. 1377–1388, 2008.

[15] E. Minina, C. Kreschel, M. C. Naski, D. M. Ornitz, and A. Vortkamp, "Interaction of FGF, Ihh/Pthlh, and BMP signaling integrates chondrocyte proliferation and hypertrophic differentiation," *Developmental Cell*, vol. 3, no. 3, pp. 439–449, 2002.

[16] E. Minina, H. M. Wenzel, C. Kreschel et al., "BMP and lhh/PTHrP signaling interact to coordinate chondrocyte proliferation and differentiation," *Development*, vol. 128, no. 22, pp. 4523–4534, 2001.

[17] D. M. Kingsley, "The TGF-β superfamily: new members, new receptors, and new genetic tests of function in different organisms," *Genes & Development*, vol. 8, no. 2, pp. 133–146, 1994.

[18] B. L. M. Hogan, "Bone morphogenetic proteins in development," *Current Opinion in Genetics and Development*, vol. 6, no. 4, pp. 432–438, 1996.

[19] R. Derynck and X.-H. Feng, "TGF-β receptor signaling," *Biochimica et Biophysica Acta*, vol. 1333, no. 2, pp. F105–F150, 1997.

[20] X.-H. Feng and R. Derynck, "A kinase subdomain of transforming growth factor-β (TGF-β) type I receptor determines the TGF-β intracellular signaling specificity," *The EMBO Journal*, vol. 16, no. 13, pp. 3912–3923, 1997.

[21] D. Onichtchouk, Y.-G. Chen, R. Dosch et al., "Silencing of TGF-β signalling by the pseudoreceptor BAMBI," *Nature*, vol. 401, no. 6752, pp. 480–485, 1999.

[22] L. Grotewold, M. Plum, R. Dildrop, T. Peters, and U. Rüther, "Bambi is coexpressed with Bmp-4 during mouse embryogenesis," *Mechanisms of Development*, vol. 100, no. 2, pp. 327–330, 2001.

[23] A. Karl, N. Olbrich, C. Pfeifer et al., "Thyroid hormone-induced hypertrophy in mesenchymal stem cell chondrogenesis is mediated by bone morphogenetic protein-4," *Tissue Engineering Part A*, vol. 20, no. 1-2, pp. 178–188, 2014.

[24] J. Chen, J. O. Bush, C. E. Ovitt, Y. Lan, and R. Jiang, "The TGF-β pseudoreceptor gene Bambi is dispensable for mouse embryonic development and postnatal survival," *Genesis*, vol. 45, no. 8, pp. 482–486, 2007.

[25] N. Guillot, D. Kollins, V. Gilbert et al., "BAMBI regulates angiogenesis and endothelial homeostasis through modulation of alternative TGFβ signaling," *PLoS ONE*, vol. 7, no. 6, Article ID e39406, 2012.

[26] J. A. Montero, C. I. Lorda-Diez, Y. Gañan, D. Macias, and J. M. Hurle, "Activin/TGFβ and BMP crosstalk determines digit chondrogenesis," *Developmental Biology*, vol. 321, no. 2, pp. 343–356, 2008.

[27] R. T. Ballock and A. H. Reddi, "Thyroxine is the serum factor that regulates morphogenesis of columnar cartilage from isolated chondrocytes in chemically defined medium," *Journal of Cell Biology*, vol. 126, no. 5, pp. 1311–1318, 1994.

[28] M. J. Farrell, M. B. Fisher, A. H. Huang, J. I. Shin, K. M. Farrell, and R. L. Mauck, "Functional properties of bone marrow-derived MSC-based engineered cartilage are unstable with very long-term in vitro culture," *Journal of Biomechanics*, vol. 47, no. 9, pp. 2173–2182, 2014.

[29] E. Karaulanov, W. Knöchel, and C. Niehrs, "Transcriptional regulation of BMP4 synexpression in transgenic *Xenopus*," *The EMBO Journal*, vol. 23, no. 4, pp. 844–856, 2004.

[30] T. Sekiya, T. Oda, K. Matsuura, and T. Akiyama, "Transcriptional regulation of the TGF-β pseudoreceptor BAMBI by TGF-β signaling," *Biochemical and Biophysical Research Communications*, vol. 320, no. 3, pp. 680–684, 2004.

[31] K. L. Loveland, M. Bakker, T. Meehan et al., "Expression of Bambi is widespread in juvenile and adult rat tissues and is regulated in male germ cells," *Endocrinology*, vol. 144, no. 9, pp. 4180–4186, 2003.

[32] L. Lassová, Z. Niu, E. B. Golden, A. J. Cohen, and S. L. Adams, "Thyroid hormone treatment of cultured chondrocytes mimics in vivo stimulation of collagen X mRNA by increasing BMP 4 expression," *Journal of Cellular Physiology*, vol. 219, no. 3, pp. 595–605, 2009.

[33] R. T. Ballock and R. J. O'Keefe, "The biology of the growth plate," *The Journal of Bone & Joint Surgery—American Volume*, vol. 85, no. 4, pp. 715–726, 2003.

Hindawi Publishing Corporation
Stem Cells International
Volume 2016, Article ID 6104780, 11 pages
http://dx.doi.org/10.1155/2016/6104780

Research Article

Feasibility and Efficiency of Human Bone Marrow Stromal Cell Culture with Allogeneic Platelet Lysate-Supplementation for Cell Therapy against Stroke

Chengbo Tan,[1] Hideo Shichinohe,[1] Zifeng Wang,[1] Shuji Hamauchi,[1] Takeo Abumiya,[1] Naoki Nakayama,[1] Ken Kazumata,[1] Tsuneo Ito,[2] Kohsuke Kudo,[3] Shigeru Takamoto,[4] and Kiyohiro Houkin[1]

[1]*Department of Neurosurgery, Hokkaido University Graduate School of Medicine, Sapporo, Japan*
[2]*Hokkaido University Hospital Clinical Research and Medical Innovation Center, Sapporo, Japan*
[3]*Department of Radiology, Hokkaido University Graduate School of Medicine, Sapporo, Japan*
[4]*Japanese Red Cross, Hokkaido Block Blood Center, Sapporo, Japan*

Correspondence should be addressed to Hideo Shichinohe; hshichi@med.hokudai.ac.jp

Received 5 August 2016; Revised 16 September 2016; Accepted 29 September 2016

Academic Editor: Andrea Ballini

Currently, there is increasing interest in human bone marrow stromal cells (hBMSCs) as regeneration therapy against cerebral stroke. The aim of the present study was to evaluate the feasibility and validity of hBMSC cultures with allogeneic platelet lysates (PLs). Platelet concentrates (PC) were harvested from healthy volunteers and made into single donor-derived PL (sPL). The PL mixtures (mPL) were made from three different sPL. Some growth factors and platelet cell surface antigens were detected by enzyme-linked immunosorbent assay (ELISA). The hBMSCs cultured with 10% PL were analyzed for their proliferative potential, surface markers, and karyotypes. The cells were incubated with superparamagnetic iron oxide (SPIO) agents and injected into a pig brain. MRI and histological analysis were performed. Consequently, nine lots of sPL and three mPL were prepared. ELISA analysis showed that PL contained adequate growth factors and a particle of platelet surface antigens. Cell proliferation capacity of PLs was equivalent to or higher than that of fetal calf serum (FCS). No contradiction in cell surface markers and no chromosomal aberrations were found. The MRI detected the distribution of SPIO-labeled hBMSCs in the pig brain. In summary, the hBMSCs cultured with allogeneic PL are suitable for cell therapy against stroke.

1. Introduction

Although studies have provided a few treatment options, ischemic stroke remains a leading cause of death and disability because of the limited regenerative capacity of the central nervous system (CNS) [1]. In recent years, the therapeutic potential of cell transplantation has been investigated in various pathological conditions of CNS [2].

Human bone marrow stromal cells (hBMSCs) are regarded as a potential cell source for ischemic stroke therapy, owing to their potential to differentiate into multiple cell lineages, their neuroprotective effects, and their ability to promote functional neural recovery of patients [3–8]. A number of experimental studies have demonstrated that transplanted BMSCs can extensively migrate towards lesions, express the phenotypes of neural cells, and improve neurological function [7, 9, 10]. Although these results are encouraging, several problems still remain unresolved, thus impeding their clinical applications. Notably, the establishment of a feasible protocol to safely expand hBMSC is a critical need. Quality, safety, and expansion are the main elements in hBMSC culture and clinical-grade expansion protocols. Particularly for clinical application, cell products must be generated in accordance with good manufacturing practice (GMP) conditions to maintain cellular quality while also minimizing the risk of adverse events.

Expansion of hBMSCs in *in vitro* culture requires the addition of supplements to the basal culture medium [11].

Fetal calf serum (FCS), an expansion supplement isolated from the clotted blood of unborn bovine fetuses, has been commonly added to cell culture mediums because of its high levels of growth stimulatory factors and low levels of growth inhibitory factors [9, 12–14]. However, there are increasing safety concerns regarding the use of FCS in clinical-scale cellular preparations because the administration of animal products to humans may theoretically cause transmittable spongiform encephalopathy (TSE) and zoonoses contamination [15–18]. Moreover, hBMSCs can internalize protein components of FCS and elicit immune reactions in the host when these foreign proteins act as antigenic substrates once transplanted [19, 20].

Human platelet lysate (PL) is a concentration of various growth factors in human platelets, obtained by lysing platelet bodies through freeze/thaw cycles or by addition of calcium chloride or thrombin activation [21]. Numerous studies have demonstrated that human PL is very effective in promoting cell expansion as well as FCS [18, 21–23]. It is known that PL includes platelet-derived growth factors (PDGFs), transforming growth factor-β (TGF-β), brain-derived neurotrophic factor (BDNF), basic fibroblast growth factor (b-FGF), vascular endothelial growth factor (VEGF), insulin-like growth factor-1 (IGF-1), and other important elements [24–26]. These factors are thought to exert important roles in promoting hBMSC expansion [21].

Now we are preparing a new clinical trial called the Research on Advanced Intervention using Novel Bone Marrow Stem Cell (RAINBOW) study, which is a phase 1 study for acute ischemic stroke patients [2]. Autologous BMSCs are cultured with allogeneic PL in the cell processing center (CPC) up to 2 cell doses: 20 million cells in the low dose group and 50 million cells in the high dose one. And BMSCs are labeled with superparamagnetic iron oxide (SPIO) for cell tracking using magnetic resonance imaging (MRI) the day before cell transplantation. They are then stereotactically transplanted around the infarct. The MRI is performed to track the donor cells until one year after the transplantation sequentially. In the present study, we aimed to evaluate the feasibility and the efficacy of hBMSC culture with allogeneic PL as GMP level and to translate the results into the RAINBOW study.

2. Materials and Methods

2.1. Isolation and Preparation of PL from Human Peripheral Blood. All experiments were performed after informed consent was obtained from healthy volunteers according to Hokkaido University's guidelines approved by the Hokkaido University Hospital's Institutional Review Board. Nine lots of platelet concentrates (PC; lots numbers 1, 2, 3, 4, 6, 7, 8, 9, and 10) were collected from nine healthy volunteers with an apheresis system for clinical use. The amount of each PC was 10 units in lots numbers 4 and 6, 20 units in numbers 8 and 10, and 15 units in others. The "unit" indicates the standard of PC preparation in Japan; that is, 10 units include $2.0–3.0 \times 10^{11}$ cells in approximately 200 mL, 15 units include $3.0–4.0 \times 10^{11}$ cells in approximately 250 mL, and 20 units include more than 4.0×10^{11} cells in approximately 250 mL. In CPC, each PC was transferred into the bags for cryopreservation (F100, Nipro, Osaka, Japan), and they were stocked in the freezer at −150°C. The PC was thawed at 37°C and transferred into the polypropylene tubes (225 mL, Ina-optika, Osaka, Japan), and then 2.5% heparin sodium (Novo-Heparin® 5000 units/5 mL, Mochida Pharmaceutical Co., Ltd., Tokyo, Japan) was added. Centrifugation with 2000 ×g for 20 min was performed twice as well incubation at 56°C for 30 min because of inactivation. Moreover, centrifugation with 500 ×g for 5 min was performed twice as well as aliquoting into polypropylene tubes (50 mL, Corning, NY) [27]. Nine lots of single donor-derived PLs (sPL; lots numbers 1, 2, 3, 4, 6, 7, 8, 9, and 10) which were derived from each PC and 3 lots of mixtures of PL (mPL) which were made from three different sPL (lots numbers 1 + 2 + 3, 4 + 6 + 7, and 8 + 9 + 10) were frozen at −80°C until being thawed just before use. We did not employ any filtration in PL preparation; filter (0.45 μm, Nalgene Rapid-Flow®, Thermo Fisher Scientific, Rochester, NY) was used to reduce the impurity when 10% PL was added to the medium.

2.2. Measurement of Platelet Surface Antigens and Growth Factors by Enzyme-Linked Immunosorbent Assay (ELISA). In order to clarify the residual particles of cell membranes indirectly, specific platelet cell surface antigens, CD41 (human integrin alpha-IIb ELISA kit, CUSABIO, College Park, MD) and CD61 (human integrin beta-3 ELISA kit, CUSABIO), were measured using commercially available ELISA kits in 12 PL production samples (9 sPL and 3 mPL) according to the manufacturer's instructions. Optical densities were measured by using a spectrophotometer (model 550 reader; Bio-Rad, Hercules, CA). All samples and standards were run in triplicate. The growth factor level was extrapolated from a standard curve. If any obtained data were under the mean minimum detectable dose, they were considered as nondetectable (ND) in the analysis.

Concentrations of PDGF-BB (DBB00, R&D Systems, Minneapolis, MN), TGF-β1 (DB100B, R&D Systems), and BDNF (DBD00, R&D Systems) in 12 PL production samples (9 sPL and 3 mPL) were also measured using commercially available ELISA kits according to the manufacturer's instructions. When the concentrations were measured, PL samples were diluted to 1 : 20 in PDGF-BB or 1 : 100 in TGF-β1 and BDNF.

2.3. Culture of hBMSCs for Cell Proliferation Assay. Two sources of hBMSCs were adopted in our present study. One was derived from a young donor by purchasing from Cell Applications Inc. (San Diego, CA). According to the manufacturer's manual, the ampoule including the frozen cells was quickly thawed in a 37°C water bath. Aseptically, the hBMSC suspension was transferred to a 15 mL tube with 10 mL of respective medium (described below) and was centrifuged at 200 ×g for 5 min. Pellets were resuspended and plated in 175 cm^2 noncoated flasks (Easy Flask 159910; Nunc, Sigma-Aldrich, St. Louis, MO) with 25 mL of Dulbecco's modified Eagle medium (DMEM)/low glucose (D6046; Sigma-Aldrich) containing 10% preselected FCS (lot number 1355888, Gibco, Thermo Fisher Scientific, Waltham, MA) and 1% penicillin/streptomycin (P/S, Sigma-Aldrich). Cells were

incubated at 5% CO_2 at 37°C. After 2 or 3 days, nonadherent cells were washed off. The culture medium was replaced 2 or 3 times a week. After the third passage, cells were detached with a 5 min application of 0.05% Trypsin-EDTA (Gibco) at 37°C, counted, and seeded on 6-well plates (6000 cells/well) with FCS-containing DMEM ($n = 6$) or 12 lots of 10% PL-supplemented minimum essential medium alpha (αMEM, M0894; Sigma-Aldrich) containing gentamicin sulfate (GS, 40 μg/mL; MSD, Tokyo, Japan), respectively ($n = 3$ in each PL). After 2 weeks, the cells were counted by an automated cell counter (Invitrogen, Thermo Fisher Scientific).

2.4. Isolation and Culture of hBMSCs in CPC. The second cell source of hBMSCs was obtained by extracting approximately 50 mL of bone marrow from a healthy volunteer. The bone marrow was brought to CPC of Hokkaido University Hospital, and the following processes were performed in the closed operation system (CPWS System Cell Processing Work Station, Panasonic Healthcare Co., Tokyo, Japan). Bone marrow mononuclear cells were isolated via density-gradient centrifugation with Ficoll-Hypaque (Pharmacia, Uppsala, Sweden), and 1.1×10^7 cells were plated in a 75 cm^2 noncoated flasks (Easy Flask 156499; Nunc) with 15 mL of αMEM with 10% mPL and 40 μg/mL GS. After 48 h, nonadherent cells were removed by changing the medium. The culture medium was replaced 2 or 3 times a week. The hBMSCs were passed three times for the subsequent transplantation. In order to label the cells for MRI tracking, 1 μL/mL Ferucarbotran (27.9 μg Fe/mL, Resovist®, Fujifilm RI Pharma Co., Ltd., Tokyo, Japan), a SPIO agent, was added into the culture medium to be incubated with hBMSCs 24 h before cell injection. SPIO-labeled hBMSCs in flasks were lifted using 4 mL TrypLe Select® (a recombinant trypsin substitute, Gibco) and incubated for 5 min. After fully agitating, cell suspensions were transferred into test tubes and centrifuged at 800 ×g, 5 min at 15°C. The supernatant was decanted and the cells were gently resuspended by Artcereb® (the irrigation and perfusion solution for cerebrospinal surgery; Otsuka Pharmaceutical Factory, Inc., Naruto, Japan) to 5×10^7 cells/mL. In order to analyze SPIO-positive hBMSCs, 600 μL/well cell suspensions were seeded on a fibronectin-coated four-well (1.7 cm^2 per well) chamber slide. After 24 h, the medium was discarded and the cells on the culture slide were rinsed twice with phosphate buffered saline (PBS). The cells were fixed with 4% acetone for 3 min and then immersed in PBS for 10 min. Subsequently, the slide was stained by Turnbull's Blue method and counted to analyze the concentration of SPIO-labeled hBMSCs.

2.5. Flow Cytometric Analysis. Flow cytometric analysis was performed to evaluate the surface markers of hBMSCs. The hBMSCs cultured with PL in CPC were suspended with PBS containing 3% FCS. They were incubated with either a mouse monoclonal antibody against human CD19 (R&D Systems; dilution, 1 : 100), CD44 (R&D Systems; 1 : 100), CD45 (R&D Systems; 1 : 100), CD90 (R&D Systems; 1 : 100), CD105 (R&D Systems; 1 : 100), CD106 (R&D Systems; 1 : 100), CD146 (R&D Systems; 1 : 100), CD166 (R&D Systems; 1 : 100), or each mouse isotypic control for 30 min on ice. Cell suspensions were then incubated with Alexa Fluor 488-conjugated secondary antibodies (Molecular Probes, Thermo Fisher Scientific; 1 : 200) for 30 min on ice. Flow cytometric analysis was performed after two washes using a cytometer (Attune® Acoustic Focusing Cytometer, Applied Biosystems, Thermo Fisher Scientific). Live events (10,000) were acquired for analysis.

2.6. Karyotype Analysis. Karyotype analysis was performed by Q-banding using conventional methods (Nihon Gene Research Laboratories Inc., Sendai, Japan). The hBMSCs obtained by purchasing from Cell Applications Inc. (San Diego, CA) were prepared as mentioned above. The cells were cultured with autologous PL supplementation and passed twice before the analysis. The cells were divided into two groups about pretreatment; thus, one was treated with the synchronous culture using thymidine, while the other was not treated with it. The cells in both groups were incubated in quinacrine mustard dihydrochloride for 10 min and then immersed in PBS. They were stained with Hoechst 33258 for 10 min and immersed in distilled water. They were mounted on the slides with an antifade reagent.

2.7. Cell Injection into Decapitated Pig Brain Parenchyma and MR Imaging. The SPIO-labeled hBMSCs were injected into the striatum of a decapitated pig brain. A burr hole was made 3 cm left of the bregma using a small dental drill. A cell injection needle (Mizuho Co., Tokyo, Japan) attached to a syringe was inserted 4 cm into the brain parenchyma. Then, 300 μL of the cell suspension (5×10^4 cells/μL) was injected over 5 min. After injection, the needle was left *in situ* for 5 min to avoid leakage of the injected fluid through the needle tract [28].

All MRI data were acquired using a clinical MR scanner (TRILLIUM OVAL, Hitachi, Tokyo, Japan). Quantitative susceptibility mapping (QSM) images were acquired by the use of an RSSG EPI sequence. The sequence parameters were repetition time (TR) = 30 msec, echo time (TE) = 15 msec, flip angle = 15°, number of acquisition (AC) = 0, matrix = 512 × 512, and slice thickness = 1.2 mm.

2.8. Histological Analysis. The decapitated pig brain in which SPIO-hBMSCs were injected for MR imaging was used for histological analysis. The day after cell injection, the brain was removed from the skull and stored in 4% paraformaldehyde for one week. It was then sliced and embedded in Tissue Freezing Medium OCT Compound (Sakura Finetek Japan Co., Ltd., Tokyo, Japan) and quickly frozen in liquid nitrogen. Frozen sections of 12 μm thickness were mounted on silane-coated glass slides. During immunohistochemical analysis, sections were treated with peroxidase blocking reagent (Dako Japan, Tokyo, Japan) and then incubated with 1% block ace solution (DS Pharma Biomedical, Osaka, Japan) for 30 min. Sections were treated with a primary mouse anti-human nuclei monoclonal antibody (MAB1281; 1 : 100, Chemicon, Temecula, California, USA) at 4°C overnight. Dako EnVision+ Kit (Dako Japan) was then applied for 1 h. The DAB Substitute Kit (Dako Japan) was also employed according to the manufacturer's instructions. After staining, sections

were dipped into 10% ammonium sulfide solution (Sigma-Aldrich) overnight, followed by incubation with compound solution mixed in 20% potassium ferricyanide (Wako, Osaka, Japan) and 1% HCL solution for 20 min. Nuclear fast red solution was used for counterstaining. Another section was treated with MAB1281 (1 : 100) alone and then colored with Dako EnVision+ kit and DAB Substitute Kit. Hematoxylin was applied for counterstaining.

For fluorescent immunohistochemistry, after blocking nonspecific reactions, sections were treated with MAB1281 (1 : 100 dilution) as the primary antibody at 4°C overnight followed by incubation with Alexa Fluor 594 Goat Anti-mouse IgG (H + L) Antibody (1 : 200, Life Technologies, Thermo Fisher Scientific) as the secondary antibody at room temperature for 1 h. The fluorescence emitted was observed through each appropriate filter on a fluorescence microscope (BX51, Olympus, Tokyo, Japan) and was digitally photographed using a cooled CCD camera (model VB-6000/6010, Keyence, Osaka, Japan).

3. Results

3.1. Residues of Cell Membrane in PL. ELISA analysis demonstrated that the platelet cell surface antigen CD41 of all PL samples was not detected (the lower limitation of detect range: 156 pg/mL). CD61 was detected in the all samples; however, the mean amount was extremely small (210 ± 63 pg/mL; mean ± SD, Figure 1(a)).

3.2. Growth Factors Contained in PL. The mean concentrations of human PDGF-BB, TGF-β1, and BDNF were 3.36 ± 2.20 ng/mL, 44.9 ± 23.0 ng/mL, and 14.3 ± 8.9 ng/mL in all PL samples, respectively (Figure 1(b)). The concentration in each PL seemed to be correlated among the growth factors and there was a big difference between each sample, especially sPL, for every growth factor. When the data were analyzed for the platelet units in original PC, we found that the amount of these growth factors correlated with platelet units in original PC (Figure 3(a)). Among mPL, there was a relatively small difference in concentrations because they were balanced by mixtures of 3 different sPL (Figure 1(b)).

3.3. Cell Proliferative Potential of PL. Cell proliferation assays demonstrated the expansive capacity of hBMSCs with 12 lots of PL-supplemented αMEM (9 sPL and 3 mPL) or FCS-supplemented DMEM. Two weeks after cell seeding, a distinct difference existed between each quantity of cell proliferation (Figure 2(a)). Compared with the cell proliferation in FCS medium, most of the PL medium had the equivalent or much higher expansive ability. However, the sPL derived from 10 unit-PC, which includes $2.0–3.0 \times 10^{11}$ cells in approximately 200 mL, were lower than FCS (number 4 and number 6). Moreover, one of the mPL, number 4 + 6 + 7, also had a lower proliferative potential because it was made of number 4 and number 6 in sPL (Figure 2(a)). Thus, when the data were analyzed regarding the platelet units in original PC, we found a correlation between the unit number and proliferative potential (Figure 2(b)). Moreover, the proliferative potential was positively correlated with the concentrations of PDGF-BB ($r = 0.74$), TGF-β1 ($r = 0.80$), and BDNF ($r = 0.73$, Figure 3(b)).

The hBMSCs derived from 4 healthy volunteers (lots numbers 1, 2, 3, and 4) were cultured in CPC as a simulation of the RAINBOW study (Figure 2(c)). The cells in each lot were passed first on day 7 or 8 after the culture. The cells in 3 lots were passed second on day 15, and the cell numbers in each lot reached over 5×10^7 cells which is the target in the high dose group. On the other hand, the cells in lot number 3 were passed second on day 13 and the cell numbers reached 3.5×10^7 cells. The cell numbers were over 20 million which is the target in the low dose group (Figure 2(c)). Thus, the cell numbers could almost reach the target in our clinical trials (low dose: 4/4, high dose: 3/4) with 2 passages for 2 weeks.

3.4. Surface Marker of hBMSC. Flow cytometric analysis was performed to assay the surface markers of hBMSCs cultured with PL-supplemented αMEM. These cells expressed CD44 (96.5±2.5%), CD90 (97.3±3.5%), CD105 (98.5±0.6%), CD106 (51.5±14.8%), CD146 (36.8±18.1%), and CD166 (97.8±1.5%), while there was absence of CD19 (2.8 ± 1.7%) and CD45 (1.8 ± 0.5%) ($n = 4$ in each, Figure 4).

3.5. Karyotype of hBMSC. The hBMSCs were cultured with 10% PL-supplemented αMEM, and the karyotype was analyzed after second passage. Karyotype analysis showed that hBMSCs had normal chromosome number and karyotype when they did not have synchronous culture as pretreatment (Figure 5(a)). But the pretreatment with the synchronous culture using thymidine influenced the analysis to produce artifact (Figure 5(b)). Thus the synchronous culture caused abnormal chromosome number (45; [2/50]) and karyotype (46, XY, chtb(3)(q21); [2/20], 45, XY, −18; [1/20], 46, XY, chtb(1)(q23), chtb(3)(q21); [1/20], 46, XY, chtb (11)(p11); [1/20]) as artifact (Figure 5(c)).

Moreover, these cells were checked for soft agar colony forming test and *in vivo* tumorigenicity test with nude rats as preclinical test, and no tumorigenicity was shown (data was not shown).

3.6. SPIO-Labeled hBMSC and QSM MRI. Turnbull's Blue staining demonstrated that approximately 34% of the PL-cultured hBMSCs were labeled with SPIO 24 h after incubation with SPIO nanoparticles (Figure 6(a)). The MRI for clinical use could visualize the bolus of SPIO-hBMSCs engrafted in the decapitated pig brain. The cell bolus showed a strong signal loss when imaged with QSM methods (Figure 6(b)). Histological analysis clearly revealed that some SPIO-positive cells (Figure 6(c)) or human cells (Figure 6(d)) were found around the injection region. These findings were consistent with the results of MRI.

4. Discussion

In the present study, we harvested 12 lots of human PLs as growth supplements instead of FCS. ELISA analysis showed that PL contained sufficient growth factors to nourish hBMSCs and very small amount of platelet surface antigens. Although the PL had equivalent or higher cell proliferation

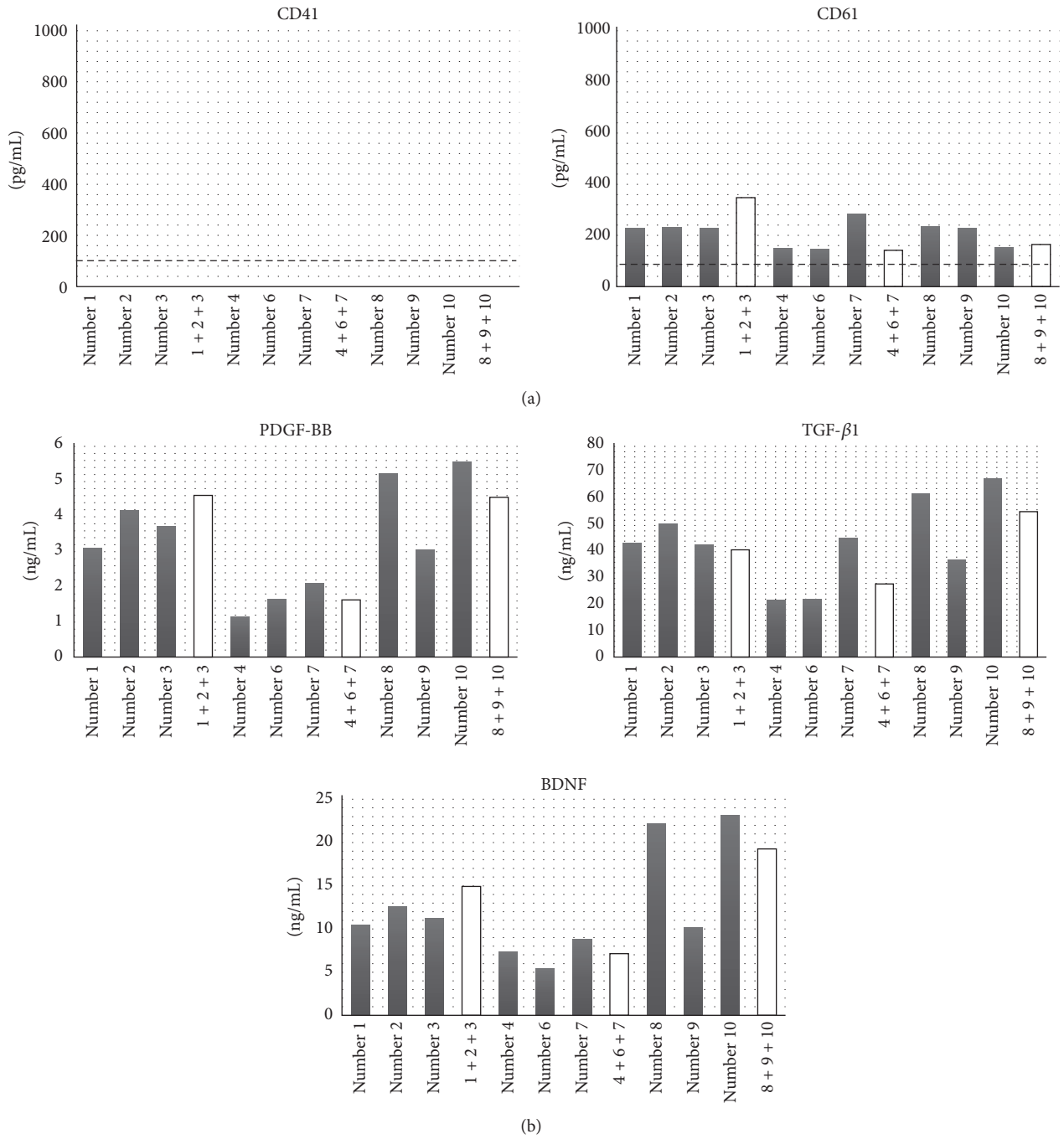

Figure 1: (a) shows ELISA analysis for cell surface antigens of platelets (left: CD41, right: CD61). The broken lines indicate each mean minimum detectable dose. (b) shows the measurement of growth factors in PL samples. Each graph indicates the concentration of human PDGF-BB, TGF-β1, and BDNF in the 12 lots of fresh PL samples, respectively. Gray bars: single donor-derived PL (sPL); white bars: mixtures type of PL (mPL).

capacity compared with FCS, there was no contradiction to BMSC for cell surface markers and no abnormal karyotype in hBMSC-PL. About 2 weeks, the cell numbers could reach up to 2×10^7 cells which is the target in our clinical trials in every lot. When SPIO-labeled hBMSCs were injected into the pig brain, MRI could detect their distribution the same as histological analysis.

When PL products are made from human PC in accordance with GMP, we noticed the existence of fragments of platelet membranes as residue materials. Instead of fragments of platelet membranes, we analyzed the platelet surface antigens in PL products because it is difficult to detect the residual fragments themselves. In the present study, we detected a very small amount of CD61, but not CD41. The findings suggested

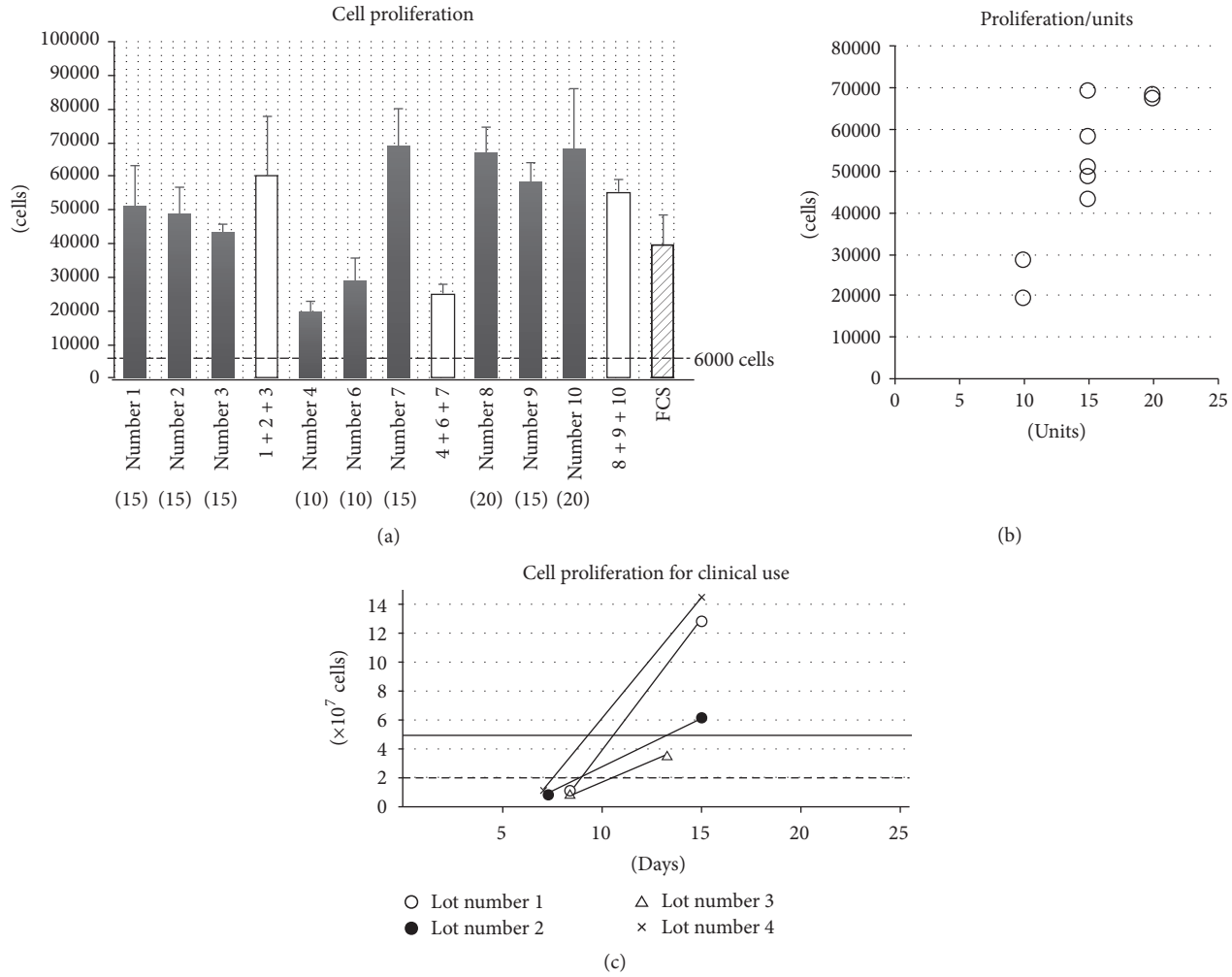

Figure 2: Cell proliferative potential for PL or FCS medium. (a) shows the quantity of cultured cells in PL- or FCS-supplemented culture medium. Gray bars: cells cultured with sPL; white bars: cells cultured with mPL; striped bar: the cells cultured with FCS. Error bars: SD. Broken line: the quantity of seeded cells on a well (6000 cells). (b) shows the quantity of cultured cells in PL-supplemented culture medium. x-axis: numbers of the platelet units in original PC. (c) showed the cell proliferation when cultured in CPC as a simulation of the clinical trials, the RAINBOW study. Broken line: 20 million cells as the target in the low dose group. Solid line: 50 million cells as the target in the high dose group.

that the amount of CD61 in PL was useful for quality control of residue materials when produced on GMP level. In fact, the mean content of CD61 in PL was 210 ± 63 pg/mL (the lower limitation of detect range: 125 pg/mL) in our present data., so the presence of CD61 is unable to be detected in culture medium because only 10% PL was added to the medium and filtering was employed to reduce the impurity. This finding demonstrated that our PL products held adequate safety and quality for clinical application.

Various studies have indicated that growth factors such as PDGF-BB, TGF-β1, and BDNF play a prominent role in BMSC culture. PDGF-BB can elicit a mitogenic response from BMSCs and stimulates these cells to proliferate [29–31]. It has also been demonstrated that TGF-β1 could stimulate the proliferation of undifferentiated MSC [31, 32]. In contrast, our previous report showed that the concentration of human BDNF, which was derived from PL, markedly decreased in the medium after hBMSC culture. These results strongly suggested that the cultured hBMSCs may consume human BDNF for their survival and proliferation [17]. In the present study, we found that the content of these growth factors in each PL was relevant to the amount of platelets in original PC. Furthermore, the ability of cell expansion correlated with the contents of the growth factors in each PL. When the contents of platelets in original PC reached more than 15 units, the cell proliferating potential of PL was equivalent or much higher compared with the FCS. This indicated that the PL supplement contains adequate essential growth factors and nutrition as well as FCS for the expansion of hBMSC. When made in accordance with GMP, however, the findings suggested that we could check the contents of a growth factor, PDGF-BB, TGF-β1, or BDNF as a quality control of PL products instead of the potential for cell expansion. Moreover, because there was a smaller difference among mPL

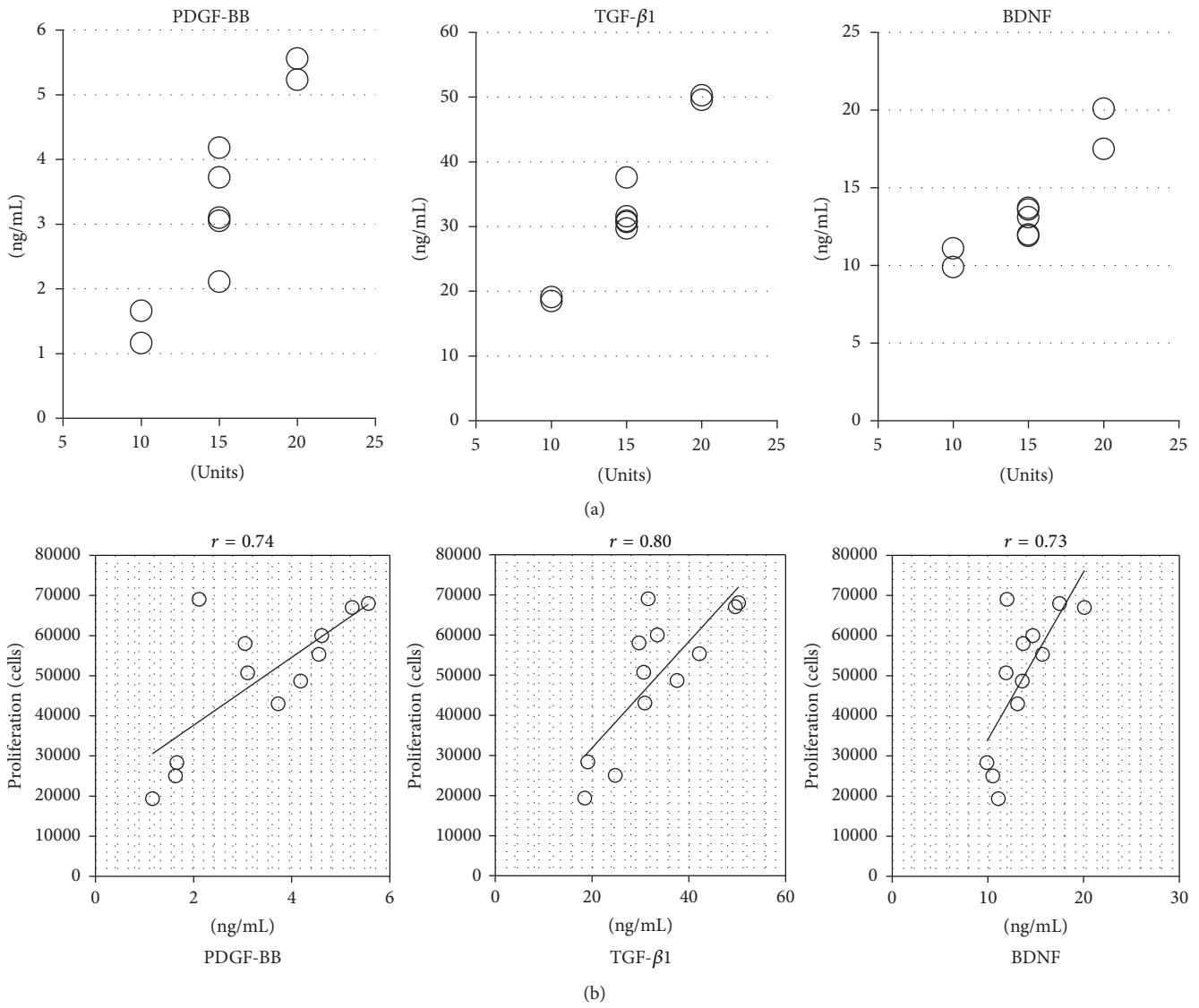

Figure 3: Cell proliferative potential and growth factors. (a) shows the concentration of each growth factor (left: PDGF-BB; center: TGF-β1; right: BDNF). x-axis: numbers of the platelet units in original PC. (b) shows the correlation between cell proliferative potential and the concentration of each growth factor (left: PDGF-BB; center: TGF-β1; right: BDNF).

compared with sPL regarding the contents of growth factors, pooled PL should be useful in mass production.

It is well known that hBMSCs express CD44, CD90, CD105, CD106, CD146, and CD166 but not CD14, CD19, CD34, and CD45 [33–35]. In our previous study, no significant differences were observed between hBMSCs cultured using 5% PL and using 10% FCS [17]. In the present study, although the concentration of PL was changed to 10%, we confirmed that the hBMSCs were identical for surface markers. Thus, our findings demonstrate that 10% PL-cultured hBMSCs are reliable for clinical application as well as 5% PL-cultured cells. In the productions of hBMSC products, moreover, the present results suggested that CD44, CD90, CD105, and CD166, but not CD106 or CD146, should be suitable positive makers for the specific test, because of their high percentage and low SD.

In our present study, karyotype analysis showed that 10% PL-cultured hBMSCs had normal chromosome number and karyotype after 2 passages. Because the commercial cells had 3 passages before usage, in fact the karyotype analysis was done after 5 passages. We have to urge caution about the artifact as abnormal karyotype due to the synchronous culture using thymidine. Although the mechanism is unclear, it suggested that the pretreatment might be unsuitable for karyotype analysis with hBMSC.

In our new clinical trials, RAINBOW study, the subjects are acute ischemic stroke patients. Autologous bone marrow is obtained 2 weeks after the stroke onset. And then BMSCs are cultured with allogeneic PL in CPC up to 2 cell doses: 20 million cells in the low dose group and 50 million cells in the high dose one. In the present study, the cell numbers could reach up to 5×10^7 cells in only 3 lots, though the numbers

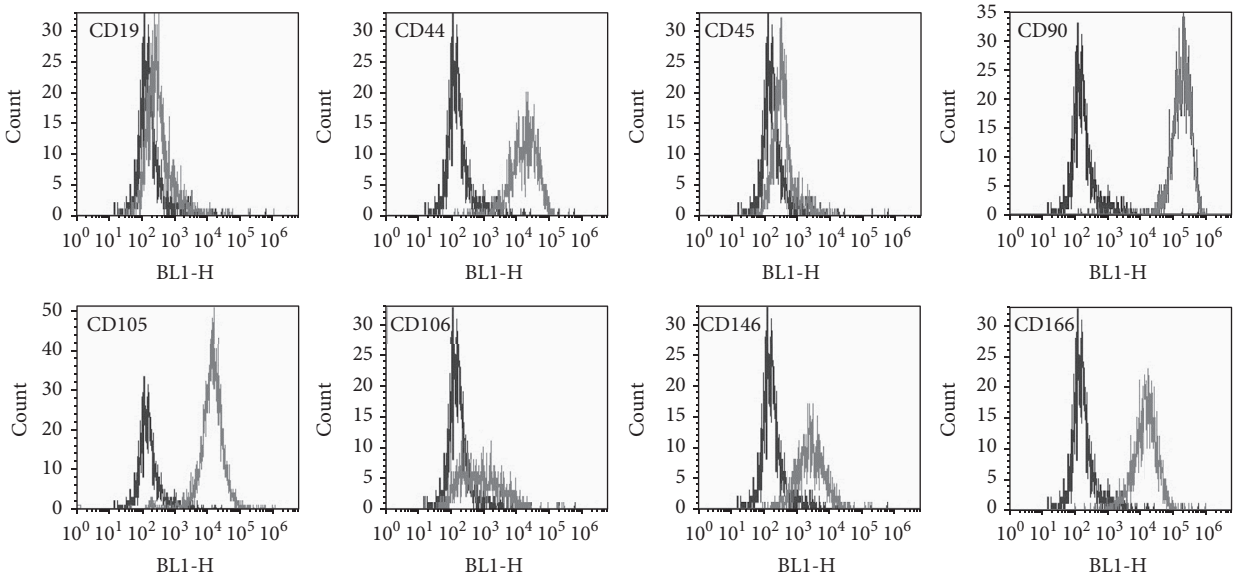

Figure 4: Flow cytometric analysis of the surface markers. Gray lines: each specific antibody (CD44, CD90, CD105, CD106, CD146, CD166, CD19, and CD45); black lines: each isotopic antibody.

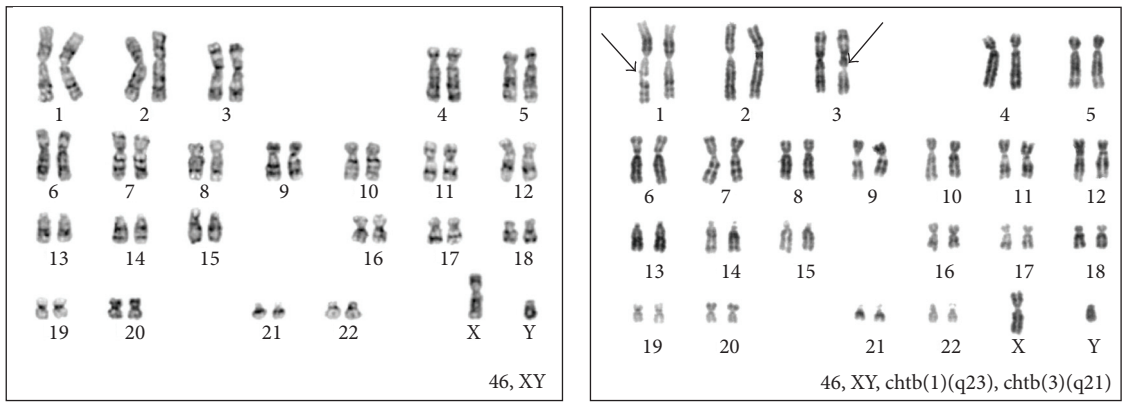

(a) (b)

	Synchronous culture (−)	Synchronous culture (+)
Chromosome number	46; [50]	46; [48]
		45; [2]
Karyotype	46, XY; [20/20]	46, XY; [15/20]
		46, XY, chtb(3)(q21); [2/20]
		45, XY, −18; [1/20]
		46, XY, chtb(1)(q23), chtb(3)(q21); [1/20]
		46, XY, chtb(11)(p11); [1/20]

(c)

Figure 5: Karyotype analysis. (a) and (b) show the representative photomicrographs of karyotype ((a) no pretreatment and (b) the pretreatment with the synchronous culture). Arrows on (b): the location of the chromatid breaks (chtb). Table (c) shows the summary of karyotype analysis.

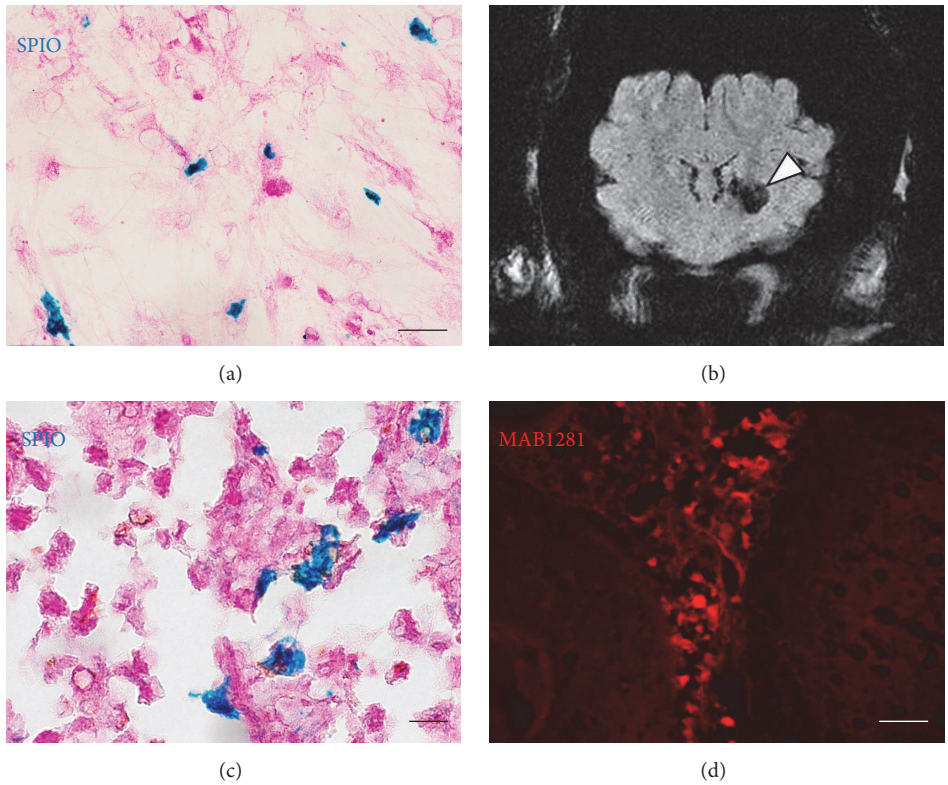

Figure 6: MRI and histological analysis of pig's brain with SPIO-labeled hBMSC injection. (a) shows the photomicrographs of the cultured SPIO-hBMSCs after Turnbull's Blue staining (blue: SPIO). Scale bars: 50 μm. (b) represents QSM MR images. Arrowheads indicate the signal extinctions caused by the bolus of SPIO-labeled hBMSCs in the left striatum. (c) and (d) display representative photomicrographs of the region around the SPIO-hBMSC injection after Turnbull's Blue staining (blue: SPIO, (c)) and fluorescence immunostaining (red: MAB1281, (d)). Scale bars: 20 μm (c) and 50 μm (d).

could increase over 2×10^7 cells in every 4 lots 2 weeks after the start of culture. So we decided to translate the results to the protocol of RAINBOW study. Thus, in the patient allocated to the high dose group, the patient would be shifted to the low dose group if the cell numbers could not reach up to 5×10^7 cells in a period.

In addition, hBMSCs were visualized in a decapitated pig brain. Cell labeling with SPIO was employed to track donor cells in the host brain by means of MRI. Cultured hBMSCs can uptake SPIO nanoparticles into their cytoplasm when the particles are added to the culture medium [7]. In the present study, Turnbull's Blue staining analysis showed that 34% hBMSCs in a chamber slide contained SPIO nanoparticles. Because SPIO nanoparticles have clearly detectable signal extinctions, SPIO-labeled cells were easily tracked anatomically with QSM MR images [7]. Histological analysis gained the same hBMSC distribution compared with MRI. Our previous study identified the long term safety of SPIO-labeled BMSCs [7]. Thus, we believe that MRI cell tracking with SPIO based labeling agents is a good resource to monitor cell distribution after hBMSC transplantation. We hope this technology can be used for cell therapy in clinical applications.

In conclusion, our present findings demonstrate that hBMSCs cultured with allogeneic PL may be valuable, feasible, and safe for cell therapy against ischemic stroke.

Competing Interests

The authors have no conflict of interests to anyone or any organization.

Acknowledgments

The study was supported by Initiative for Accelerating Regulatory Science in Innovative Drug, Medical Device, and Regenerative Medicine (funds from Ministry of Health, Labour and Welfare in Japan), Research Project for Practical Applications of Regenerative Medicine (funds from Japan Agency for Medical Research and Development), and Otsuka Toshimi scholarship foundation, no. 15-S17.

References

[1] H. Shichinohe, C. Tan, T. Abumiya et al., "Neuroprotective effects of cilostazol are mediated by multiple mechanisms in a mouse model of permanent focal ischemia," *Brain Research*, vol. 1602, pp. 53–61, 2015.

[2] H. Shichinohe and K. Houkin, "Cell therapy for stroke: review of previous clinical trials and introduction of our new trials," *Neurologia Medico-Chirurgica*, vol. 56, no. 10, pp. 592–596, 2016.

[3] S. A. Azizi, D. Stokes, B. J. Augelli, C. DiGirolamo, and D. J. Prockop, "Engraftment and migration of human bone marrow stromal cells implanted in the brains of albino rats—similarities to astrocyte grafts," *Proceedings of the National Academy of Sciences of the United States of America*, vol. 95, no. 7, pp. 3908–3913, 1998.

[4] M. Chopp and Y. Li, "Treatment of neural injury with marrow stromal cells," *The Lancet Neurology*, vol. 1, no. 2, pp. 92–100, 2002.

[5] O. Y. Bang, J. S. Lee, P. H. Lee, and G. Lee, "Autologous mesenchymal stem cell transplantation in stroke patients," *Annals of Neurology*, vol. 57, no. 6, pp. 874–882, 2005.

[6] S. Kuroda, H. Shichinohe, K. Houkin, and Y. Iwasaki, "Autologous bone marrow stromal cell transplantation for central nervous system disorders—recent progress and perspective for clinical application," *Journal of Stem Cells and Regenerative Medicine*, vol. 7, no. 1, pp. 2–13, 2011.

[7] C. Tan, H. Shichinohe, T. Abumiya et al., "Short-, middle- and long-term safety of superparamagnetic iron oxide-labeled allogeneic bone marrow stromal cell transplantation in rat model of lacunar infarction," *Neuropathology*, vol. 35, no. 3, pp. 197–208, 2015.

[8] H. Shichinohe, T. Ishihara, K. Takahashi et al., "Bone marrow stromal cells rescue ischemic brain by trophic effects and phenotypic change toward neural cells," *Neurorehabilitation and Neural Repair*, vol. 29, no. 1, pp. 80–89, 2015.

[9] T. Sugiyama, S. Kuroda, T. Osanai et al., "Near-infrared fluorescence labeling allows non-invasive tracking of bone marrow stromal cells transplanted into rat infarct brain," *Neurosurgery*, vol. 68, pp. 1036–1047, 2011.

[10] M. Ito, H. Shichinohe, K. Houkin, and S. Kuroda, "Application of cell sheet technology to bone marrow stromal cell transplantation for rat brain infarct," *Journal of Tissue Engineering and Regenerative Medicine*, 2014.

[11] N. Fekete, M. Gadelorge, D. Fürst et al., "Platelet lysate from whole blood-derived pooled platelet concentrates and apheresis-derived platelet concentrates for the isolation and expansion of human bone marrow mesenchymal stromal cells: production process, content and identification of active components," *Cytotherapy*, vol. 14, no. 5, pp. 540–554, 2012.

[12] P. A. Sotiropoulou, S. A. Perez, M. Salagianni, C. N. Baxevanis, and M. Papamichail, "Characterization of the optimal culture conditions for clinical scale production of human mesenchymal stem cells," *STEM CELLS*, vol. 24, no. 2, pp. 462–471, 2006.

[13] H. Shichinohe, S. Kuroda, K. Kudo et al., "Visualization of the Superparamagnetic Iron Oxide (SPIO)-labeled bone marrow stromal cells using a 3.0-T MRI-a pilot study for clinical testing of neurotransplantation," *Translational Stroke Research*, vol. 3, no. 1, pp. 99–106, 2012.

[14] F. Mannello and G. A. Tonti, "Concise review: no breakthroughs for human mesenchymal and embryonic stem cell culture: conditioned medium, feeder layer, or feeder-free; medium with fetal calf serum, human serum, or enriched plasma; serum-free, serum replacement nonconditioned medium, or ad hoc formula? All that glitters is not gold!," *Stem Cells*, vol. 25, no. 7, pp. 1603–1609, 2007.

[15] J. Reinhardt, A. Stühler, and J. Blümel, "Safety of bovine sera for production of mesenchymal stem cells for therapeutic use," *Human Gene Therapy*, vol. 22, no. 6, pp. 775–776, 2011.

[16] L. Sensebé, P. Bourin, and K. Tarte, "Good manufacturing practices production of mesenchymal stem/stromal cells," *Human Gene Therapy*, vol. 22, no. 1, pp. 19–26, 2011.

[17] H. Shichinohe, S. Kuroda, T. Sugiyama et al., "Biological features of human bone marrow stromal cells (hBMSC) cultured with animal protein-free medium-safety and efficacy of clinical use for neurotransplantation," *Translational Stroke Research*, vol. 2, no. 3, pp. 307–315, 2011.

[18] P. Horn, G. Bokermann, D. Cholewa et al., "Impact of individual platelet lysates on isolation and growth of human mesenchymal stromal cells," *Cytotherapy*, vol. 12, no. 7, pp. 888–898, 2010.

[19] A. Heiskanen, T. Satomaa, S. Tiitinen et al., "*N*-glycolylneuraminic acid xenoantigen contamination of human embryonic and mesenchymal stem cells is substantially reversible," *STEM CELLS*, vol. 25, no. 1, pp. 197–202, 2007.

[20] M. Sundin, O. Ringdén, B. Sundberg, S. Nava, C. Götherström, and K. Le Blanc, "No alloantibodies against mesenchymal stromal cells, but presence of anti-fetal calf serum antibodies, after transplantation in allogeneic hematopoietic stem cell recipients," *Haematologica*, vol. 92, no. 9, pp. 1208–1215, 2007.

[21] T. Burnouf, D. Strunk, M. B. Koh, and K. Schallmoser, "Human platelet lysate: replacing fetal bovine serum as a gold standard for human cell propagation?" *Biomaterials*, vol. 76, pp. 371–387, 2016.

[22] K. Plöderl, C. Strasser, S. Hennerbichler, A. Peterbauer-Scherb, and C. Gabriel, "Development and validation of a production process of platelet lysate for autologous use," *Platelets*, vol. 22, no. 3, pp. 204–209, 2011.

[23] T. Yamauchi, H. Saito, M. Ito, H. Shichinohe, K. Houkin, and S. Kuroda, "Platelet lysate and granulocyte-colony stimulating factor serve safe and accelerated expansion of human bone marrow stromal cells for stroke therapy," *Translational Stroke Research*, vol. 5, no. 6, pp. 701–710, 2014.

[24] M. E. Bernardo, M. A. Avanzini, C. Perotti et al., "Optimization of in vitro expansion of human multipotent mesenchymal stromal cells for cell-therapy approaches: further insights in the search for a fetal calf serum substitute," *Journal of Cellular Physiology*, vol. 211, no. 1, pp. 121–130, 2007.

[25] B. L. Eppley, J. E. Woodell, and J. Higgins, "Platelet quantification and growth factor analysis from platelet-rich plasma: implications for wound healing," *Plastic and Reconstructive Surgery*, vol. 114, no. 6, pp. 1502–1508, 2004.

[26] C. Doucet, I. Ernou, Y. Zhang et al., "Platelet lysates promote mesenchymal stem cell expansion: a safety substitute for animal serum in cell-based therapy applications," *Journal of Cellular Physiology*, vol. 205, no. 2, pp. 228–236, 2005.

[27] T. Sugiyama, S. Kuroda, Y. Takeda et al., "Therapeutic impact of human bone marrow stromal cells expanded by animal serum–free medium for cerebral infarct in rats," *Neurosurgery*, vol. 68, no. 6, pp. 1733–1742, 2011.

[28] H. Shichinohe, T. Yamauchi, H. Saito, K. Houkin, and S. Kuroda, "Bone marrow stromal cell transplantation enhances recovery of motor function after lacunar stroke in rats," *Acta Neurobiologiae Experimentalis*, vol. 73, no. 3, pp. 354–363, 2013.

[29] J. Donovan, D. Abraham, and J. Norman, "Platelet-derived growth factor signaling in mesenchymal cells," *Frontiers in Bioscience*, vol. 18, no. 1, pp. 106–119, 2013.

[30] K. Kikuchi, Y. Soma, M. Fujimoto et al., "Dermatofibrosarcoma protuberans: increased growth response to platelet-derived growth factor BB in cell culture," *Biochemical and Biophysical Research Communications*, vol. 196, no. 1, pp. 409–415, 1993.

[31] H. S. Cho, I. H. Song, S.-Y. Park, M. C. Sung, M.-W. Ahn, and K. E. Song, "Individual variation in growth factor concentrations

in platelet-rich plasma and its influence on human mesenchymal stem cells," *The Korean Journal of Laboratory Medicine*, vol. 31, no. 3, pp. 212–218, 2011.

[32] V. Devescovi, E. Leonardi, G. Ciapetti, and E. Cenni, "Growth factors in bone repair," *La Chirurgia degli Organi di Movimento*, vol. 92, no. 3, pp. 161–168, 2008.

[33] K. Fukiage, T. Aoyama, K. R. Shibata et al., "Expression of vascular cell adhesion molecule-1 indicates the differentiation potential of human bone marrow stromal cells," *Biochemical and Biophysical Research Communications*, vol. 365, no. 3, pp. 406–412, 2008.

[34] A. B. Adesida, A. Mulet-Sierra, and N. M. Jomha, "Hypoxia mediated isolation and expansion enhances the chondrogenic capacity of bone marrow mesenchymal stromal cells," *Stem Cell Research & Therapy*, vol. 3, no. 2, article 9, 2012.

[35] M. Dominici, K. Le Blanc, I. Mueller et al., "Minimal criteria for defining multipotent mesenchymal stromal cells. The International Society for Cellular Therapy position statement," *Cytotherapy*, vol. 8, no. 4, pp. 315–317, 2006.

Hindawi Publishing Corporation
Stem Cells International
Volume 2016, Article ID 8768162, 16 pages
http://dx.doi.org/10.1155/2016/8768162

Review Article

Medication-Related Osteonecrosis of the Jaw: New Insights into Molecular Mechanisms and Cellular Therapeutic Approaches

Thomas Lombard,[1,2] Virginie Neirinckx,[1] Bernard Rogister,[1,3] Yves Gilon,[2] and Sabine Wislet[1]

[1]*Laboratory of Nervous System Diseases and Therapy, GIGA-Neuroscience, University of Liège, Liège, Belgium*
[2]*Department of Maxillofacial Surgery, CHU, University of Liège, Liège, Belgium*
[3]*Department of Neurology, CHU, University of Liège, Liège, Belgium*

Correspondence should be addressed to Sabine Wislet; s.wislet@ulg.ac.be

Received 7 July 2016; Accepted 9 August 2016

Academic Editor: Marco Tatullo

In recent years, medication-related osteonecrosis of the jaw (MRONJ) became an arising disease due to the important antiresorptive drug prescriptions to treat oncologic and osteoporotic patients, as well as the use of new antiangiogenic drugs such as VEGF antagonist. So far, MRONJ physiopathogenesis still remains unclear. Aiming to better understand MRONJ physiopathology, the first objective of this review would be to highlight major molecular mechanisms that are known to be involved in bone formation and remodeling. Recent development in MRONJ pharmacological treatments showed good results; however, those treatments are not curative and could have major side effects. In parallel to pharmacological treatments, MSC grafts appeared to be beneficial in the treatment of MRONJ, in multiple aspects: (1) recruitment and stimulation of local or regional endogenous cells to differentiate into osteoblasts and thus bone formation, (2) beneficial impact on bone remodeling, and (3) immune-modulatory properties that decrease inflammation. In this context, the second objective of this manuscript would be to summarize the molecular regulatory events controlling osteogenic differentiation, bone remodeling, and osteoimmunology and potential beneficial effects of MSC related to those aspects, in order to apprehend MRONJ and to develop new therapeutic approaches.

1. Introduction

In 2014, the American Association of Oral and Maxillofacial Surgeons (AAOMS) has updated the definition of bisphosphonate-related osteonecrosis of the jaw (BRONJ) [1], given the increasing number of osteonecrosis of the jaw cases reported in patients treated with bisphosphonates (BPs). However, since this clinical condition is also encountered in patients treated with denosumab or other antiangiogenic drugs [2–4], the term "medication-related osteonecrosis of the jaw" (MRONJ) should be favored. MRONJ is defined by three features: (1) current or previous treatment with antibone resorptive or antiangiogenic agents, (2) exposed bone or bone that can be probed through an intraoral or extraoral fistula in the maxillofacial region that stays for longer than 8 weeks, and (3) no previous history of radiation therapy or obvious metastatic disease towards the jaws [1].

In osteoporotic patients, the incidence of MRONJ is 1.04 to 69 per 100,000 patient-years if treated by oral BPs, 0 to 90 per 100,000 patient-years if treated by i.v. BPs, and 0 to 30,2 per 100,000 patient-years if treated by denosumab [5–7]. In oncologic patients, the incidence of MRONJ is 0 to 12,222 per 100,000 patient-years if treated by i.v. BPs and 0 to 2,316 per 100,000 patient-years if treated by denosumab [5–7]. Risk factors for MRONJ are multiples; the major ones are i.v. BPs (depending on dose and duration), Zoledronate, dental extraction, dental or periodontal disease, glucocorticoid, chemotherapy, smoking, and obesity [8, 9].

MRONJ is two times more frequent in the mandible than in the maxilla [10]. The most accepted clinical staging system for MRONJ has been developed by Ruggiero and colleagues and has been adopted by the AAOMS [1]. This clinical scale describes five stages: at risk, 0, 1, 2, and 3. Stage "at risk" includes patients undergoing treatment with oral

Table 1: Drugs demonstrated to be implied in the triggering of the jaw osteonecrosis: name, mode of action or molecular target, and therapeutic indications.

Drugs	Mode of action	Indications
Biphosphonate: SBPs N-BPs	Nonhydrolysable cytotoxic analogs of ATP Farnesyl-diphosphate (FPP) synthase inhibition	Osteoporosis Paget's disease Hypercalcemia of malignancy Tumor-associated osteolysis
Denosumab	Monoclonal antibody that inactivates RANKL	Osteoporosis Tumor-associated osteolysis
Bevacizumab	Monoclonal antibody that inactivates VEGF	Glioblastoma Metastatic cancers: breast, renal, lung, colorectal
Sunitinib, Sorafenib, Cabozantinib	Tyrosine kinase inhibitors that block VEGF receptor	Metastatic cancers: breast, renal, lung, colorectal
Everolimus, Temsirolimus®	mTor inhibitors	Metastatic renal cell carcinoma

or intravenous nitrogen-containing BPs, with no evidence of necrotic bone. Stage 0 includes patients presenting nonspecific clinical findings, radiographic changes, and symptoms with no clinical evidence of bone necrosis. Stage 1 includes asymptomatic patients presenting an exposed and necrotic bone or fistulae. Stage 2 includes symptomatic patients (pain, erythema, and signs of infection) presenting an exposed and necrotic bone or fistulae. Stage 3 includes stage 2 patients with one of the following: (1) bone lesions extending beyond the region of the alveolar bone resulting in pathologic fracture, extraoral fistula, or oroantral/oronasal communication or (2) osteolysis extending to the inferior border of the mandible or sinus floor.

In this review, after considering drugs that have been shown to be responsible of MRONJ, we will briefly comment on current physiopathological hypotheses that could explain this particular clinical situation. We will then review several putative treatments, with a deeper focus on cellular therapy protocols, including (1) drug-based manipulation of bone marrow stem cells and (2) mesenchymal stem cell (MSC) grafts, which are both experimental therapeutic approaches currently used to treat this incapacitating clinical situation. Aiming to better understand MRONJ physiopathology, we will also summarize molecular mechanisms that are known to be involved in bone formation and remodeling, as well as MSC involvement in these processes. Finally, we will discuss the link between bone homeostasis and the immune system, referred to as "osteoimmunology." Indeed, the MSC effect could also include a modulation of this osteoimmunological homeostasis, explaining their therapeutic effects.

2. Drugs-Related Osteonecrosis of the Jaw

Antiresorptive and antiangiogenic drugs were previously shown as implied in the development of MRONJ [2–4] (Table 1). Antiresorptive drugs (bisphosphonate and denosumab) are monoclonal antibodies directed against Receptor Activator of Nuclear Factor Kappa-B Ligand (RANKL). Antiangiogenic drugs (Sunitinib® and Bevacizumab®) are humanized monoclonal antibodies directed against several activated receptors tyrosine kinase (i.e., VEGFR (vascular endothelial growth factor receptor)).

(A) *Bisphosphonates (BPs)* are used to treat a wide variety of diseases characterized by excessive osteoclast-mediated bone resorption, such as tumor-associated osteolysis, Paget's disease, hypercalcemia of malignancy, and osteoporosis [7]. BPs are stable and nonhydrolysable analogs of pyrophosphates that are composed of a carbon atom linked to two phosphonate groups (P–C–P) to mimic the pyrophosphate molecular structure (P–O–P). Simple BPs (SBPs) (etidronate and clodronate) should be distinguished from nitrogen-BPs (N-BPs) (pamidronate, alendronate risedronate, ibandronate, and Zoledronate) because of the presence of nitrogen on the side chains of the latter. This structural difference has an impact on the mechanism of action. Indeed, in addition to their analog effect, only SBPs are metabolized into intracellular and nonhydrolysable cytotoxic analogs of ATP, which accumulate in the osteoclasts and trigger their apoptosis [17]. In contrast, N-BPs inhibit osteoclast function only by acting as potent inhibitors of the enzyme farnesyl-diphosphate (FPP) synthase in the cholesterol (or mevalonate) biosynthetic pathway. This inhibition is responsible of a decrease of GTPase activity in cytoskeletal rearrangement and vesicular trafficking in osteoclasts [18]. N-BPs might also have an effect on the immune system, especially on macrophages and monocytes, but this effect remains controversial [19]. It has also to be noted that N-BPs are 100 to 10,000 times more potent than SBPs [20]. More recently, it has been demonstrated that BPs (alendronate and Zoledronate®) induce osteogenic gene expression, such as bone morphogenic protein-2 (BMP-2), osteocalcin, and alkaline phosphatase in endothelial and mesenchymal stem cell [21].

(B) *Denosumab* is a recent antiresorptive drug that showed better results than alendronate in improving bone mineral density in different skeletal sites [22].

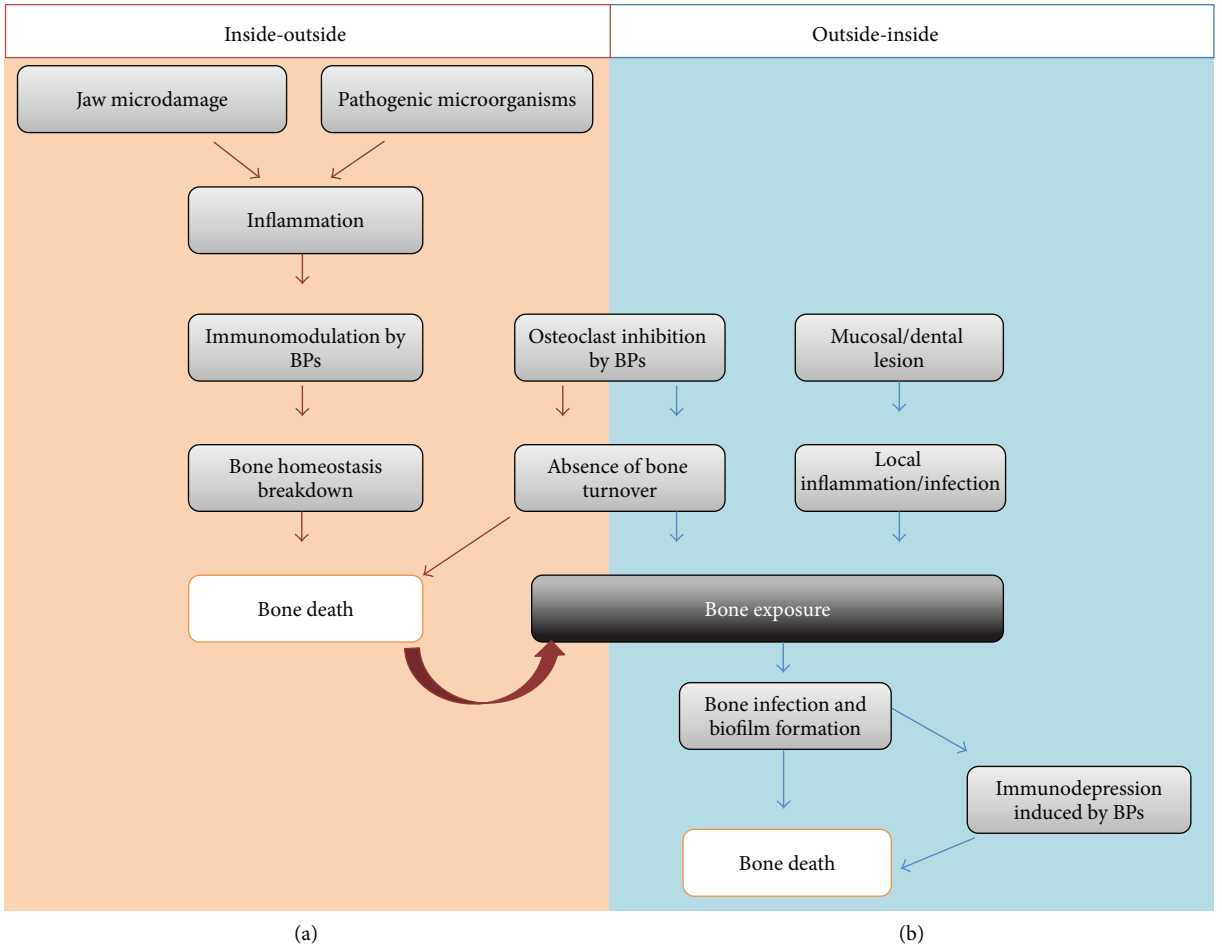

Figure 1: Two MRONJ pathogenesis theories: inside-outside and outside-inside theory.

This human monoclonal antibody targets the Receptor Activator of Nuclear Factor Kappa-B Ligand (RANKL) [23]. In humans, bone remodeling depends on a balance between osteoprotegerin (OPG) and RANKL that are both produced by osteoblasts (see molecular signaling controlling bone remodeling section below). RANKL binds to its receptor (RANK) expressed by preosteoclasts and osteoclasts and induces, respectively, their full differentiation and activation. OPG and denosumab have the same mechanism of action: they bind to RANKL, then blocking its interaction with RANK, inhibiting the osteoclast maturation, function, and survival, and reducing bone resorption [23].

(C) An increasing number of MRONJ cases are now reported in patients treated with antiangiogenic drugs [20]. These drugs are VEGF antagonists and might be divided into two categories: (1) monoclonal antibodies that bind VEGF and, thereby, neutralize its biological activity (Bevacizumab) and (2) small molecule tyrosine kinase inhibitors (TKIs) that block the VEGF receptor and its downstream signaling pathways (Sunitinib, Sorafenib®, Cabozantinib®). VEGF antagonists are used to treat metastatic cancer such as renal, colorectal, lung, and breast carcinomas [20]. Inhibitors of mammalian target of rapamycin (mTOR) (Everolimus® and Temsirolimus®) are recent therapeutic agents used in the treatment of metastatic renal carcinoma. These drugs have also been reported as MRONJ inducers in two case reports [24, 25].

3. Pathogenesis of MRONJ

The pathogenesis of MRONJ has been studied for multiple years but still remains unresolved. However, two theories are emerging (Figure 1). The first one, called "inside-outside," is based on an inhibition of the osteoclastic activity and a bone turnover decrease, both conditions induced by previously mentioned drugs. This decrease in bone remodeling despite the jaw microdamage induced by chewing and local inflammation results in a constant exposition of bone to high concentrations of various pathogenic microorganisms (Figure 1(a)). These conditions would lead to bone tissue death and then to bone exposure [26]. In various ONJ (Osteonecrosis of the Jaws) animal models, it has been reported several times that most of the specimens present

a histological osteonecrosis, but only a minority of them show an exposed bone (not covered by epithelium) [27, 28]. Another histological study of ONJ lesions in humans also concluded that bone necrosis precedes the clinical onset and is then responsible of an inflammation-associated process [29]. All of these findings suggest thus that bone exposure could not be a prerequisite for bone necrosis. Moreover, the fact that two different antiresorptive drugs (BPs and denosumab) with different mechanisms of action are implied into MRONJ underlines the central role played by bone resorption inhibition in mechanically stressed jaws. This possible central role of bone resorption inhibition in the physiopathology of MRONJ is also strengthened by encouraging results reported for Teriparatide® drug, a recombinant human parathyroid hormone that stimulates osteoclast activity [30]. All these observations corroborate the bone resorption inhibition theory as the etiology of MRONJ. However, there is so far no reported case of ONJ in patients with a reduced bone turnover condition, such as hypoparathyroidism.

The second theory, named "outside-inside," is based on a local immune-depression, probably caused by BPs or denosumab associated with mucosal/dental lesions that would lead to a local infection and/or inflammation spreading to the bone and, there, inducing the osteonecrosis (Figure 1(b)). It has been established that dental diseases are an important risk factor in MRONJ: the efficient prevention of MRONJ in patients with cancer is observed by improvements in their dental hygiene [31]. It is also important to highlight that most of the tooth extractions were done because of an existing periodontal or periapical disease [32]. Recent studies also demonstrated that periodontal or periapical diseases associated with i.v. BPs could cause MRONJ in animal models [27, 28]. Finally, it has been reported that exposed bone areas in MRONJ are recovered by a complex biofilm with multiple microorganisms which could explain therapy failures [33].

The reason why medication-related osteonecrosis specifically affects the jaw is still unknown, but some clues can be pointed out. The jaw is one of the least-protected bones from infection in the human skeleton. Indeed, the mandibular and maxilla bones are just separated from the pathogens of the oral mucosal lesion by a thin mucoperiosteal cover, whereas deep soft tissues and skin protect other bones. Moreover, jaw is subjected to repeated microtraumas due to the presence of teeth and the force of mastication. Indeed, the alveolar bone turnover is 10-fold greater than in the long bones which could justify the fact that alveolar bone could incorporate much more BPs than other skeleton sites [34]. Finally, the jaw has a specific embryologic development. It arises from neural-crest cells which form at the border of the neural tube during neurulation, and not from the mesoderm like other bone cells of the body [35]. Furthermore, in a recent study [36], it has been demonstrated that jaw bone defects could be healed through neural-crest cell recruitment.

For an unknown reason, it appears that tissue homeostasis in the mandibular and maxilla bones is disrupted in MRONJ patients, by the combination of (1) drugs acting more or less on bone turnover, (2) the proximity of a highly septic environment, and (3) the mechanical stress induced by chewing several times a day. This misbalance in tissue homeostasis leads to necrosis, which itself increases and/or maintains this misbalance, triggering a vicious circle. Treatments should therefore address this misbalance by acting on regenerative processes, in attempt to reequilibrate this compromised situation.

A clear understanding of MRONJ pathogenesis is mandatory before considering any therapeutic perspective. We suggest three potential etiologies: (1) the lack of bone formation caused by the absence of osteogenic differentiation from MSC, (2) the imbalance in bone remodeling caused by BPs or denosumab, and (3) the homeostasis disruption between the immune system and bone which refers to the new concept of osteoimmunology. In the next few paragraphs, we will therefore focus on the molecular patterns that underlie these potential etiologies.

3.1. Molecular Signaling Pathways Controlling Osteogenic Differentiation. During development, bone formation begins with MSCs aggregation and, then, cells differentiate sequentially into chondrocytes and osteoblasts during endochondral ossification [14]. After condensation, MSCs could also directly differentiate into osteoblasts in a process called "membranous bone ossification." Sox9 and Run-related transcription factor 2 (Runx2) are two essential transcription factors expressed in MSCs during osteoblast differentiation. Sox9 induces cell condensation which is precluding their conversion and differentiation into chondrocytes [37]. Runx2 stimulates chondrocyte proliferation and growth into larger cells and then into osteoblasts [38]. Besides this intracellular signalization, there are five extracellular pathways that are identified in osteoblastogenesis as summarized in Figure 2: (1) Ihh, (2) PTH and PTHrp, (3) BMP, (4) Wnt-β catenin canonical, and (5) MAPK pathways.

During fetal bone formation, MSCs are recruited. Runx2 expression is then activated, which induces MSCs differentiation into osteochondroblast progenitors [38] (Figure 3(a)). In this early stage, mostly Ihh pathway activates Runx2. At later stage, BMPs and MAPK pathways stimulate Runx2 but also Dlx5 expression. Dlx5 is an osteogenic homeobox protein involved in osteoblasts maturation [39]. Depending on Dlx5 levels, Msx2, another osteogenic homeobox protein, induces immature cell proliferation.

Osteochondroblast progenitors ($Runx2^+$, $Dlx5^+$, and $Msx2^+$ cells) mature into committed preosteoblast cells, which express osterix (Osx), collagen 1α1 (Col1α1), alkaline phosphatase (ALP), and PTH-R1. Osterix is a transcriptional factor acting as an essential regulator of late osteogenesis through the inhibition of chondrogenesis [40]. This process of maturation for osteochondroblast is induced by BMP and Wnt canonical pathways. Preosteoblast cells (Osx^+, $Col1\alpha1^+$, ALP^+, and $PTH\text{-}R1^+$ cells) are then maturing in osteoblasts. On the one hand, this maturation is due to Wnt canonical pathway. On the other hand, osteochondroblast progenitors ($Runx2^+$, $Dlx5^+$, and $Msx2^+$ cells) are able to secrete Ihh, which induces PTHrp production. Both molecules participate in preosteoblastic cell maturation. Mature osteoblast expresses specific bone proteins such as osteocalcin (OSC), bone sialoprotein (BSP), PTH-R1, and osteonectin [14].

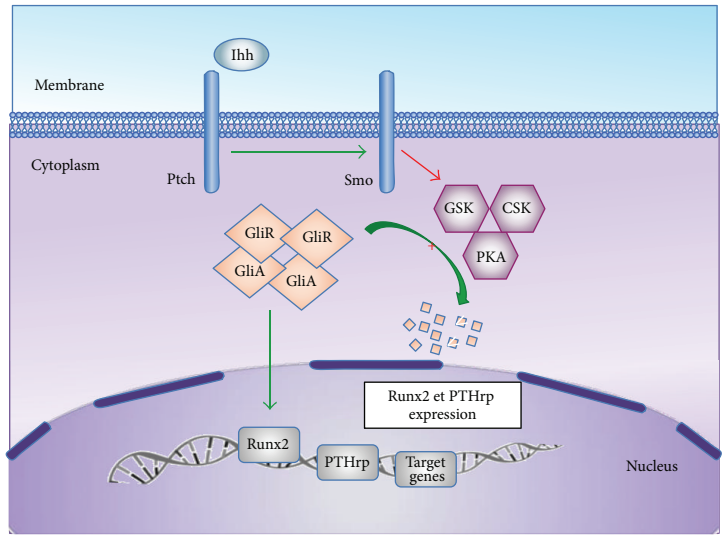

(a)

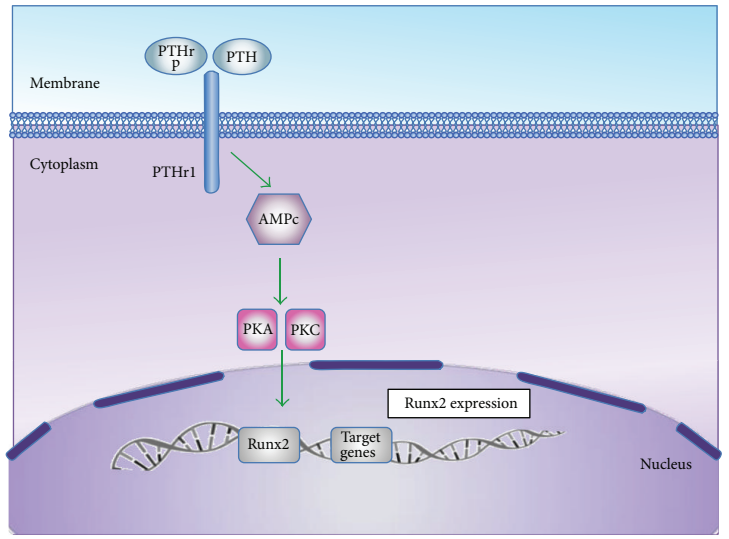

(b)

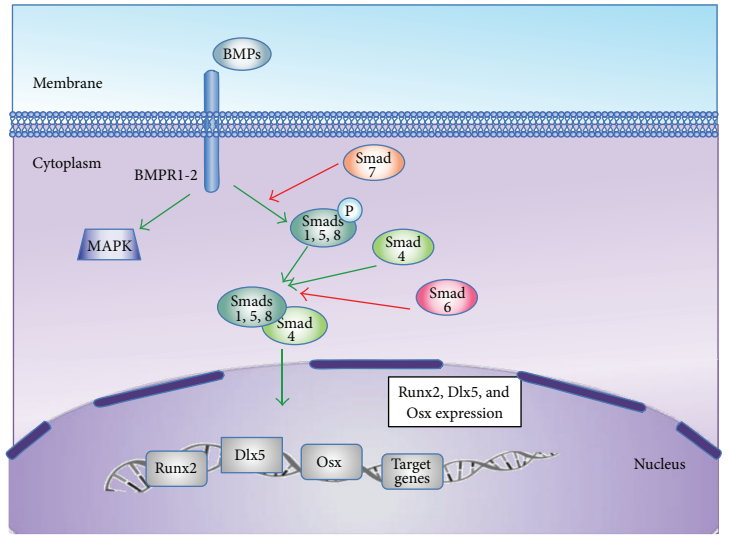

(c)

Figure 2: Continued.

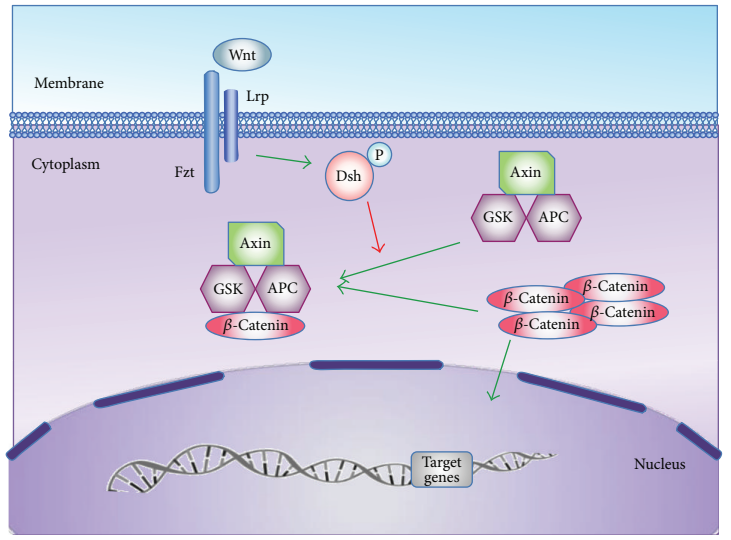

(d)

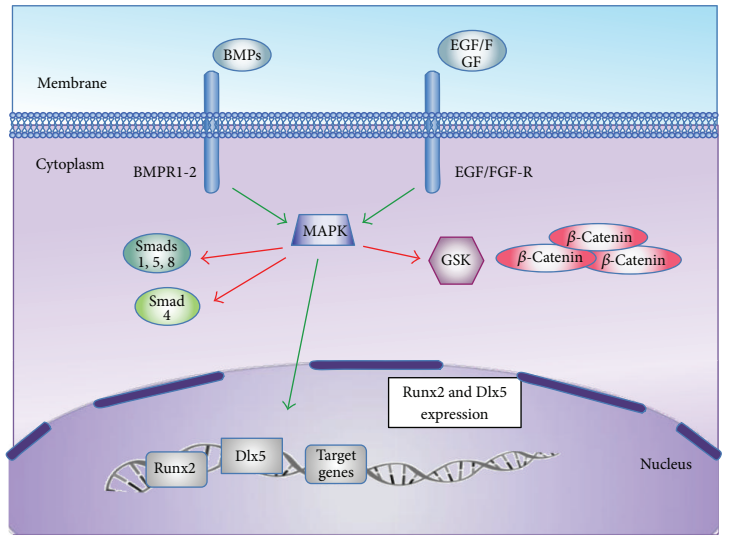

(e)

Figure 2: Molecular regulation of MSCs during bone formation. (a) *Ihh pathway*: Indian hedgehog (Ihh) stimulates, directly or indirectly (through the parathyroid hormone-related peptide (PTHrp) synthesis), chondrocytes proliferation and their differentiation into hypertrophic or larger cells. Ihh binds to its receptor Patched (Ptch), which inhibits Smoothened (Smo). The resulting activation of Smo leads to an increase of intracellular concentration of Gli proteins (Gli activator (GliA) and Gli repressor (GliR)) subsequent of the inhibition of their degradation regulated by glycogen synthase kinase (GSK3β), protein kinase A (PKA), and casein kinase (CSK). After translocation into the nucleus, Gli activator could bind to its promoter and stimulate various genes' expression, especially Runx2 [11, 12]. (b) *PTH and PTHrp pathway*: parathyroid hormone (PTH) and parathyroid hormone-related (PTHrp) bind to PTH-receptor1 (PTHr1), which is a G protein-coupled receptor that activates adenylate cyclase. This leads to cAMP production, PKA and PKC stimulation, and Runx2 expression. The exact mechanism leading to Runx2 is still unknown. (c) *BMP pathway*: bone morphogenetic proteins (BMPs) binds to a tetrameric receptor encompassing type I (BMPR1) and type II (BMPR2) receptors that are serine-threonine kinases. The receptor activation induces signal transduction through Smads or mitogen-activated protein kinase (MAPK). Smads are cytoplasmic molecules that are classified into 3 subsets: (1) receptor-regulated Smads (Smads 1, 2, 3, 5, and 8); (2) common-partner Smads (Smad 4); (3) inhibitory Smads (Smads 6, 7). Smads 1, 5, and 8 are activated by phosphorylation induced by BMPs interacting with their receptors. Receptor-regulated phosphorylated Smads are then able to form a dimeric complex with Smad 4 allowing its nuclear translocation. When phosphorylated, Smads 6 and 7 both inhibit Smads 1, 5, and 8 phosphorylation and Smad 4 linking [13]. In the nucleus, the dimeric Smad complex will induce the target genes expression such as Runx2, distal-less homeobox 5 (Dlx5), and osterix (Osx) which are osteoblastic genes [14, 15]. (d) *Wnt-β catenin canonical pathway*: Wnt molecules are involved in multiple cell functions, including osteogenesis. Wnt-1, Wnt-3a, Wnt-4, Wnt-5, Wnt-10b, and Wnt-13, are essential in bone formation [16]. Wnt binds to its receptor Frizzled (Fzd) and coreceptor, low-density lipoprotein receptor-related protein (Lrp). In absence of binding, dishevelled (Dsh) remains inactivated in the cytoplasm and β catenin can form a complex with GSK3β, adenomatous polyposis coli (APC), and axin that leads to their degradation by ubiquitination. When Wnt binds to its receptor, phosphorylated Dsh induces axin and GSK3β inhibition and thus leads to β-catenin accumulation. β-Catenin is then able to translocate into the nucleus where it drives the target genes expression. (e) *MAPK pathway*: mitogen-activated protein kinases (MAPKs) are able to phosphorylate and inhibit GSK3β and Smads 1, 5, and 8 activities. They are also able to induce Runx2 and Dlx5 expression. MAPK can be triggered by epithelial growth factor (EGF), fibroblast growth factor (FGF), and BMPs.

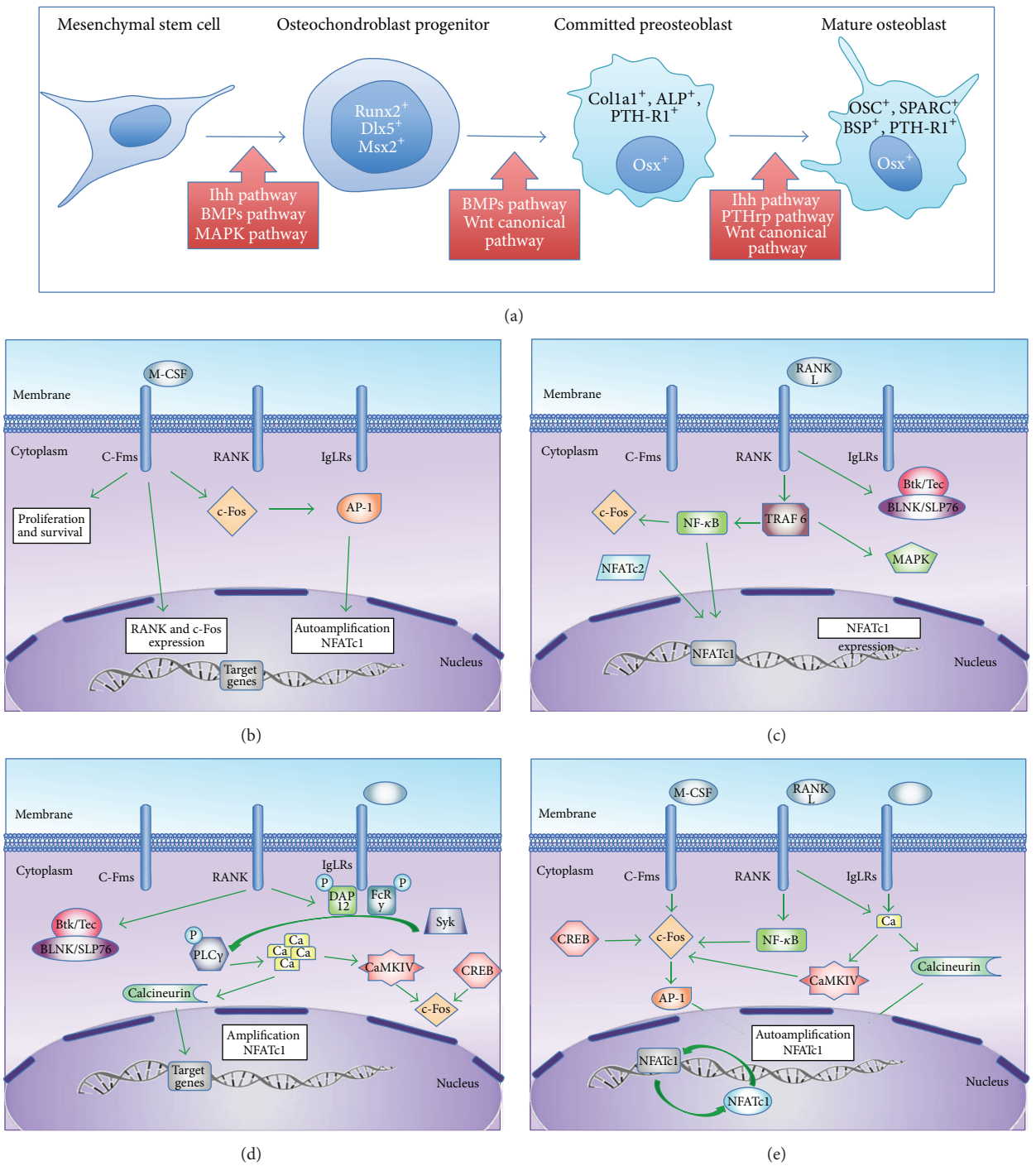

Figure 3: Bone remodeling: (a) in precursor cell stage, the macrophage-colony stimulating factor (M-CSF) binds to its receptor (c-Fms). It promotes survival and proliferation of osteoclast precursors, as well as RANK and c-Fos expression. (b) *c-Fms pathway*: M-CSF binds to c-Fms and promotes cell proliferation and survival. It also promotes RANK and c-Fos expression as well as NFATc1 autoamplification through AP1. (c) *RANK pathway*: the binding of RANKL to RANK promotes the recruitment of tumor necrosis factor receptor-associated factor 6 (TRAF6), which can activate the nuclear factor-κB (NF-κB) and mitogen-activated protein kinases (MAPKs), such as p38 and Jun N terminal kinase (JNK). TRAF6-activated NF-κB induces the expression of NFATc1, an important transcription factor for osteoclastogenesis. This NFATc1 expression is also stimulated by the nuclear factor of activated T cells cytoplasmic 2 (NFATc2). Finally, RANK also activates the tyrosine kinases Btk and Tec that are involved in the phosphorylation of phospholipase Cγ (PLC γ). NF-κB can also stimulate the c-Fos induction. (d) *IgLRs pathway and calcium signaling*: RANK activation leads to phosphorylation of DAP12 and FcRγ. These molecules are both associated with IgLRs and stimulate Syk. Activated Btk/Tec/BLNK/SLP76 complex and Syk will phosphorylate PLC-γ which will mediate the calcium release from intracellular stores. Calcium will activate calcineurin phosphatase which is involved in NFATC1 autoamplification. It also stimulates C-Fos through CaMKIV activation. (e) *NFATc1 autoamplification*: by these three pathways, AP-1, calcineurin and NFATc1 participate in NFATc1 autoamplification. Indeed, AP-1 and the continuous calcium signaling are essential for NFATc1 amplification. The NFATc1 promoter is epigenetically activated through histone acetylation and contains NFAT binding sites. Thus, NFATc1 specifically autoregulates its own promoter and is responsible for its robust induction. NFATc1 is negatively regulated by other transcription factors, such as IRF8, MafB, and Bcl6 that are, in turn, inhibited by Blimp1, a transcriptional target of NFATc1.

Based on all these molecular pathways, various therapeutic approaches were investigated:

(i) *Teriparatide and BMPs*, as described below, were used to stimulate the bone formation and to treat MRONJ [41, 42].

(ii) *Dickkopfs 1 (DKK1)* is a natural Wnt-antagonist that binds Lrp5/6. $DKK1^{+/-}$ mice show an increase in all bone formation parameters [43]. By inhibiting DKK1, another study has observed an increase of bone density in a multiple myeloma mouse model [44].

(iii) Another study reported that MSCs graft coupled with lithium chloride treatment, a *GSK3β inhibitor*, stimulates their differentiation into osteoblast *in vivo* and *in vitro* [45].

(iv) *Sclerostin* is another Wnt-antagonist that binds Lrp5/6, but in a different region from DKK1. Li et al. (2009) reported that antisclerostin antibody treatment increases bone formation and bone mass in a rat model of osteoporosis [46].

3.2. Molecular Signaling Controlling Bone Remodeling. Even in adulthood, bone remains a highly dynamic organ in constant remodeling. Two principal actors take part in bone remodeling processes: (1) MSC-derived osteoblasts, which promote bone formation and osteoclast, and (2) CD34+ hematopoietic progenitor-derived osteoblasts, which promote bone resorption. The bone remodeling balance between osteoformation and osteoresorption is regulated by several cytokines. The most characterized mechanism is the balance between osteoprotegerin (OPG) and the Receptor Activator of Nuclear Factor Kappa-B Ligand (RANKL), which are both expressed and secreted by osteoblasts. As an autocrine factor, RANKL binds to its transmembrane receptor (RANK) present on preosteoclasts and osteoclasts and induces their differentiation and activation, respectively. The balance is due to OPG that binds to RANKL, blocking its interaction with RANK and, thus, inhibiting the osteoclast maturation, function, and survival. The balance consequently tips towards reducing bone resorption in presence of OPG [23]. Globally, RANK activation leads to the expression and activation of nuclear factor of activated T cells cytoplasmic 1 (NFATc1). The primordial and sufficient role of this transcription factor in osteoclastogenesis has been demonstrated *in vitro* and *in vivo* [47].

The signaling pathway during osteoclastogenesis is based on three receptors: c-Fms, RANK, and Immunoglobin-Like Receptors (IgLRs) (OSCAR, PIR-A, SIRPβ1, and TREM 2), as described in Figures 3(b)–3(e).

3.3. Molecular Signaling Controlling Osteoimmunology. During the last decade, the involvement of immunological cells and cytokines in bone remodeling took a greater place. For example, OPG is expressed by B cells and dendritic cells [48]. RANKL is expressed by B cells, T cells, and $\gamma\delta$-T cells, while RANK is expressed by macrophages and monocytes [49]. Besides these examples of bone cytokines playing a role in immune system, it was also demonstrated that several immune cytokines could modulate the bone biology: (1) important inflammatory cytokines such as IL-1, IL-6, and TNF-α stimulate RANKL expression and accelerate bone destruction and (2) a variety of cytokines such as IFN-γ, granulocyte/macrophage-colony stimulating factor (GM-CSF), IL-4, and IL-10 were shown to stimulate bone formation [50].

Unraveling bone homeostasis regulation allows for highlighting connections between bone remodeling and immune cells. The role of T cells in osteoclastogenesis was more specifically analyzed and summarized in Figure 4. Looking at that figure, we could conclude that Th17 cells are the link between bone destruction and the immune system. On the other hand, if Th17 are the immune cells responsible for the stimulation of osteoclastogenesis, regulatory T cells or Treg should be regarded as immune cells that stimulate bone formation by downregulation of osteoresorption. Treg are $CD4^+CD25^+FOXP3^+$ cells that are specialized in tolerance, immunity inhibition, autoimmune pathology prevention, and regulation of inflammation [51]. Treg also express specific surface molecules including GITR and CTLA-4 [52]. Noteworthily, FoxP3 has been described as specific and mandatory for the development and activity of Treg cells [53]. These cells are also known to secrete IL-10 and TGF-β, which both trigger reduction of inflammation and bone destruction and have an inhibitory effect on osteoclastogenesis [54]. However, controversial studies reported that IL-10, IL-4, and TGF-β have the higher antiosteoclastic effects. Globally, TGF-β, IL-4, and IL-10 are potent antiosteoclastic cytokines, but further studies are mandatory to understand their mechanisms of action [55]. Treg cells are also known to inhibit osteoclastic formation by a cell-to-cell contact via cytotoxic T lymphocyte antigen 4 (CTLA4) [54].

Bisphosphonates are able to modify immune cell activities. This was particularly demonstrated with $\gamma\delta$-T cells. These cells represent 5% of $CD3^+$ T cells in human peripheral blood and most of them belong to the Vγ9Vδ2 subset. Their name is based on the fact that they express a heterodimeric T cell receptor (TCR) composed of γ and δ chains, in contrast with the classic TCR, composed of α and β chains [56]. These cells were detected in rheumatoid arthritis patients and were shown to be capable of secreting IL-17 and IFN-γ according to environmental cues [57]. It has also been demonstrated that N-BPs such as Zoledronate could induce IFN-γ production by $\gamma\delta$ T cells *in vitro* and *in vivo* [19]. This activation is likely to be due to the inhibition of farnesyl-diphosphate synthase by N-BPs that would lead to the accumulation of isopentenyl diphosphate and dimethylallyl diphosphate, which are two agonists of Vγ9Vδ2-TCR [19]. Therefore, $\gamma\delta$ T cell stimulation may potentiate the antiresorptive effects of N-BPs.

In a recent study, Komatsu et al. (2014) [58] have unraveled the link between Th17 cells and Treg cells. They showed that, in arthritic conditions, $CD25^+CD4^+Foxp3^+$ T cells lost FoxP3 expression and went through a "transdifferentiation" process into Th17 cells, induced by the synovial fibroblasts-derived IL-6. These ex-FoxP3 Th17 cells had more pronounced osteoclastic effects than naïve $CD4^+$T cell-derived Th17 cells. They were also characterized by the expression of

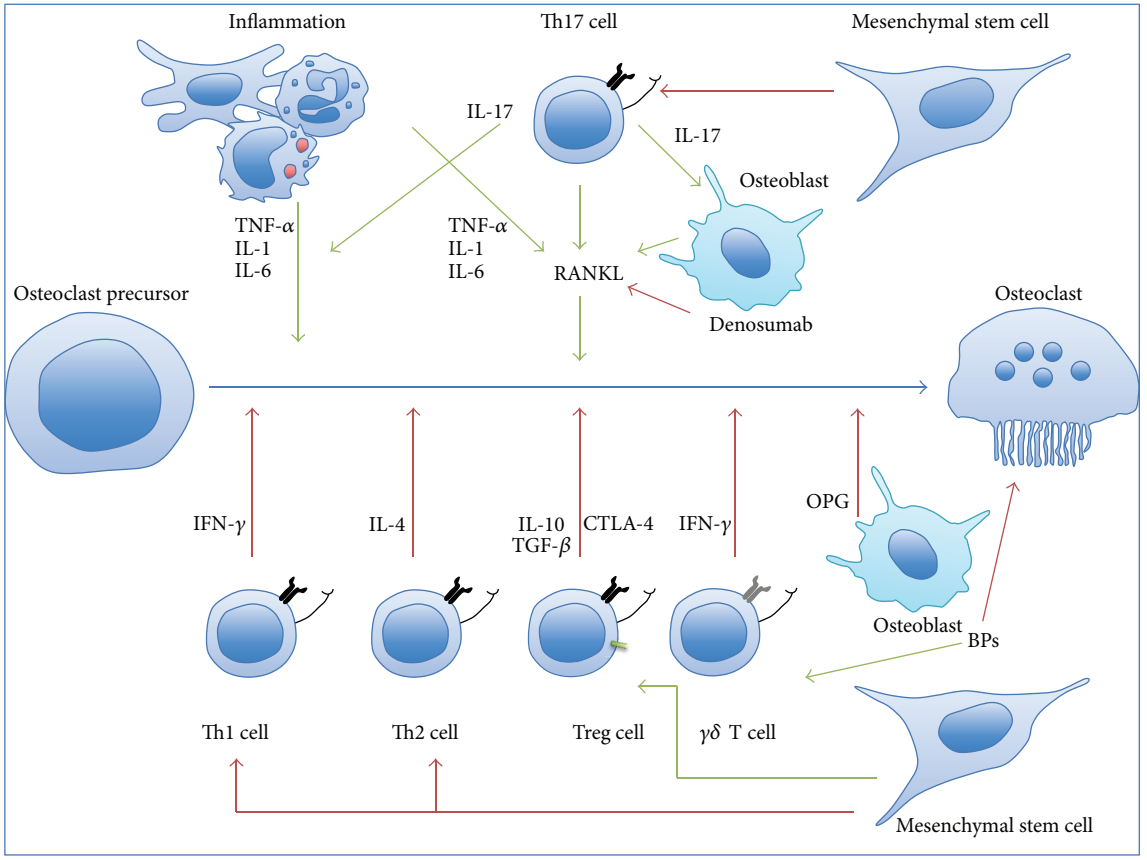

Figure 4: Osteoimmunology: differentiation of osteoclast precursor into mature osteoclast. Synthesis of osteoblast, immune, and mesenchymal cell action in osteoclastogenesis: (1) *T helper cells type 1 (Th1)* that are playing a role in cellular immunity, are induced by IL-12, and secrete IL-2 and INF-γ (which has antiosteoclastogenic properties). (2) *T helper cells type 2 (Th2)* are involved in humoral immunity. They are induced by IL-4 and secrete IL-4 and IL-13. IL-4 has also antiosteoclastogenic properties. (3) *The T helper cell type 17 (Th17)* differentiates from naïve T CD4+ cells, has a proinflammatory role, and is implicated into autoimmune disease. Th17 is induced by TGF-β, IL-6, IL-21, and especially IL-23. Th17 cells secrete IL-17, IL-21, and IL-22. IL-17 is a major inflammatory cytokine and IL-21 stimulates Th17 differentiation and inhibits Th1 and Treg cells actions. In osteoclastogenesis, IL-17 can produce and induce RANKL expression by osteoblast, a situation that favors osteoresorption. This is not the only stimulatory activity of Th17 on osteoresorption as these cells express also higher levels of RANKL compared to Th1 and Th2. Finally, they also have higher levels of IL-1, IL-6, and TNF-α.

Sox4, CCR6, CCL20, IL-23 receptor (IL-23R), and RANKL [58].

A new therapy for rheumatoid arthritis based on CTLA-4 immunoglobulin underlined also the connection between bone and immune system. On the one hand, CTLA-4 immunoglobulin was used to suppress immune responses by targeting T lymphocyte activation antigens CD80/86 on antigen-presenting cells and thus blocking the costimulation [59]. On the other hand, Bozec and collaborators have shown that CTLA-4 immunoglobulin induced the activation of indoleamine 2,3-dioxygenase (IDO) in osteoclast precursors. IDO is known to metabolize tryptophan, promote apoptosis, and, therefore, decrease bone destruction [60].

Bone remodeling is also modulated in inflammation and during early responses of immune system. Toll-like receptors 2 (TLR2) and 4 (TLR4) activation by pathogen-associated molecular patterns (PAMPs) or damage-associated molecular patterns (DAMPs) in macrophages could stimulate TNF-α production and, thus, bone resorption [61].

Cathepsin K is a cysteine protease that is highly expressed by osteoclasts. It degrades type I collagen, which is required to adsorb calcium hydroxyapatite and leads to bone resorption [62]. The cathepsin K-specific inhibitor NC-2300 was initially developed to suppress bone destruction, but it has also shown anti-inflammatory properties when tested in animal model of rheumatoid arthritis. Indeed, cathepsin K participates in TLR9 activation in dendritic cells and stimulated IL-6 and IL-23 production [63]. A recent study used NC-2300 to treat periapical lesion in a rat model and they observed a reduction of inflammation and bone destruction [64]. Odanacatib, another cathepsin K inhibitor, has been developed for the treatment of postmenopausal osteoporosis with encouraging results [65].

4. Recent Advances in MRONJ Treatments

Treatments of MRONJ depend on multiple variables such as age, sex, disease status, ONJ stage, comorbidities, and

symptoms. Globally, two approaches are currently considered in clinical practice: (1) conservative nonsurgical and (2) surgical procedures. Conservative management focuses on maintaining optimal oral hygiene (home self-care and professional dental care), elimination of active dental and periodontal disease, topical antimicrobial mouth rinses (chlorhexidine 0.12%), and systemic antibiotic therapy. When required, surgical therapy consists of a surgical debridement and/or resection covered by a full-thickness mucoperiosteal flap. Indeed, surgery provides pain control and infection control, relieves soft tissue irritations, and decreases osteolysis [7, 66]. Beside these approaches, several treatments have been developed and used to treat MRONJ:

(A) *Teriparatide*: as we previously mentioned, Teriparatide is a recombinant human parathyroid hormone, which has stimulatory effects on osteoblasts and osteoclasts and leads to an increase in bone turnover and bone formation, as an osteoanabolic agent [67]. This treatment has shown encouraging results in MRONJ patients [30] and might be recommended in future years in osteoporotic patients without cancer or radiation therapy, for a short-time therapy. Indeed, preclinical studies demonstrated an increased risk of osteosarcoma with long-term therapy [67].

(B) *Bone morphogenetic proteins (BMPs)*: another potential treatment concerns the use of bone morphogenetic proteins (BMPs), a subgroup of the transforming growth factor-β (TGF-β) family. BMPs are implied in bone and cartilage formation during development and growth [68]. Among them, BMP-2 and BMP-7 are recognized as effective bone formation inducers and have been approved by the Food and Drug Administration (FDA) in 2001-2002 for this therapeutic indication [69]. They have been used in orthopedics and oral/maxillofacial surgery, including MRONJ [43]. In this clinical situation, BMP-2 was delivered during surgery in the cleaned bone cavity, inducing a successful healing of the necrotic area and new bone formation. Unfortunately, BMPs could exhibit important side effects such as inflammation, bone resorption, swelling, seroma, and carcinogenic effects but these side effects could be dose-dependent [69]. Nevertheless, future well-designed randomized clinical trials are needed to ascertain the safety and efficacy of BMPs.

(C) *Platelet concentrates*: the use of autologous platelet concentrate as a topical agent during bone resection could also constitute a promising therapeutic strategy. These concentrates are composed of human platelets and are thus enriched in growth factors such as platelet-derived growth factor (PDGF), transforming growth factor-β (TGF-β), vascular endothelial growth factor (VEGF), and epidermal grow factor (EGF) [70]. Dohan Ehrenfest et al. [71] defined four groups of platelet concentrates based on their fibrin and leucocyte content: leucocyte and platelet-rich fibrin (L-PRF); leucocyte and platelet-rich plasma (L-PRP); pure platelet-rich plasma (PRP); and pure platelet-rich fibrin (P-PRF). PRP is the most used agent in the prevention and treatment of MRONJ [72]. Nevertheless, L-PRF showed also promising benefits [73] as leucocytes present in L-PRF can address infection and regulate the immune system [74] while physiological fibrin matrix is easier to manipulate during surgery and concentrate the growth factors [75]. Autologous platelet concentrates appear more and more to constitute a valuable implementation for surgical procedures, although no specific guidelines are available so far. The setup of those guidelines is still restrained by the lack of standardized parameters and biological properties of these platelets concentrates, according to various preparation techniques [76]. Another problem is to keep theses factors at grafted site and, thus, the treatment might be variable between patients.

(D) *Platelet-derived growth factor-BB (PDGF-BB)*: platelet-derived growth factor-BB (PDGF-BB) is a new key factor involved in angiogenesis and osteoformation. It is secreted by preosteoclasts and promotes CD31+ and Emcn+ (Endomucin) vessel subtype formation, as well as MSC and endothelial progenitor cell migration [77]. Treatment with PDGF-BB has been shown to increase vasculogenesis and bone formation in ovariectomy-induced osteoporotic mouse model [78]. This new molecule may constitute a new target in bone resorptive pathology.

(E) *Low-level laser therapy (LLLT)* with Nd: YAG laser or GaAlAs diode laser has been reported to be useful in the treatment and prevention of MRONJ in association with conservative and surgical management [79–81]. LLLT mechanism of action seems to be photochemical: the photon energy absorbed is converted into metabolic energy that will be used to produce proteins and mitoses [82, 83]. LLLT provides an improvement in vascularisation of mucous membrane, bone regeneration, and pain reduction. It may constitute a safe and effective adjunct therapy but it is not recommended yet as a monotherapy.

(F) *Hyperbaric oxygen (HBO)* is an effective technique mainly used in difficult healing situation. This healing effect is attributed to the increasing oxygen concentration, immunologic regulation, and reactive oxygen species (ROS) and reactive nitrogen species (RNS) production [84–86]. HBO gives a fast wound healing and pain and swelling reduction in the treatment of MORNJ [86–88]. A randomized controlled trial of HBO therapy in MRONJ, by Freiberger et al. 2012, came to the conclusion that HBO seems to be a useful adjunct to ONJ treatment, especially in severe cases [89].

(G) *Medical ozone therapy (MOT)* has been demonstrated as antimicrobial, wound healing, vasculogenic, and immunostimulating therapy [90, 91]. MOT acts by preserving the endogenous antioxidant system and

by blocking xanthine/xanthine oxidase system [91]. It has been used as an adjuvant treatment in MRONJ cases with a reduction of 90% of the symptoms and the authors indicate that MOT is not a substitute of recommended treatment [92, 93].

For the moment, all these new therapies are adjunctive therapies. Likewise, due to the lack of data or the limited number of studies, it is not possible to evaluate the real effectiveness of those treatments. MRONJ remains a complex and a noneffectively treatable disease. This situation could be a direct consequence of the lack of molecular understanding that is mandatory in order to elaborate an efficient pharmacological agent. This could be the reason why MSCs were investigated in multiple studies with a dual objective: (1) cellular therapy and (2) a tool to identify new molecular targets favoring the bone reconstruction in such a disease.

5. Mesenchymal Stem Cell Therapy in MRONJ

MSCs are multipotent stem cells that are increasingly used in regenerative medicine. MSCs contribute actively to organogenesis during embryogenesis and, thereafter, to the maintenance of adult tissues. To be considered as MSCs, cells must present three characteristics: (1) adherence to plastic culture dishes; (2) expression of CD105, CD73, and CD90 but absence of expression of CD34, CD45, CD14 or CD11b, CD79a or CD19, and HLA-DR markers; and (3) capacity to differentiate into osteoblasts, chondrocytes, and adipocytes [94]. In adulthood, MSCs are usually isolated from bone marrow or adipose tissue but are also present in various other tissues [95]. Due to their ability to differentiate into osteocytes but most importantly due to the recent characterization of their immunomodulatory properties, MSCs should strongly be regarded as grafting material in osteonecrosis foci [96].

5.1. Immunomodulatory Effects of MSCs. Three different cells together constitute the innate immune system: natural killer (NK) cells, dendritic cells (DCs), and macrophages. NK cells are involved in antiviral or antitumoral defense and are known to kill infected or tumor cells without MHC1 restriction [97]. MSCs are able to inhibit NK cells proliferation by secreting indolamine 2,3-dioxygenase (IDO) and prostaglandin E2 (PGE2) [98]. DC are antigen-presenting cells that link the innate and adaptive immune system [99]. MSCs exert an inhibitory effect on dendritic cells (DCs) differentiation through soluble factors (IL-6, PGE2) and cell-to-cell contact [100, 101]. Macrophages are monocyte-derived phagocytic cells that are basically divided into two categories: M1 macrophages promote proinflammatory reaction, and M2 macrophages are rather involved in wound healing [102]. There is a temporal relation between M1 and M2 macrophages: inflammatory M1 macrophages are predominant at early stages of tissue lesion and, later, wound healing M2 macrophages become predominant. M1 macrophage stage is necessary to clear dead tissue or infectious agents, and M2 macrophage stage allows the resolution of the injury [103]. This balance between these two phenotypes constitutes an important target in future therapies and can be influenced by MSCs. Interestingly, MSCs support M2 macrophages proliferation over M1 macrophages by increasing IL-4 and IL-13 levels and by decreasing TNF-α and IL-6 levels [104].

T cells and B cells are the actors of the adaptive immune system. Although the effect of MSCs on B cells is still unclear, some studies support that MSCs are able to inhibit B cell differentiation and to decrease immunoglobulin production [105]. However, those results are still questioned [106]. The role of MSCs in modulating T cells depends on T cell subtypes. MSCs are indeed able to inhibit cytotoxic T lymphocyte proliferation and generate regulatory $CD8^+$ cells in coculture conditions [107]. It has also been demonstrated that MSCs support regulatory T (Treg) cell proliferation by secreting Il-10, PGE2, and TGF-β and by promoting the expression of Foxp3 [108]. Globally, MSCs inhibit Th1, Th2, and Th17 proliferation. However, it has also been demonstrated that grafting MSC could increase Th2 activity in non-Th2-dominated autoimmunity and in allotransplant models [109]. The exact mechanism by which MSCs suppress T helper cell proliferation is poorly understood, but interesting theories are rising up. Indeed, Sato et al. suggested that MSCs secrete nitric oxide (NO), which would suppress STAT5 phosphorylation and T helper cell proliferation [110]. Meisel et al. showed that IDO, which catalyzes the conversion from tryptophan to kynurenine, was produced by MSCs and could be a T cell inhibitory effector pathway [111]. Finally, it is important to underline that, in those conditions, MSCs needed to be previously activated by IFN-γ to exert their immunomodulatory effects which could also be linked to their effects on inflammation [106, 112].

5.2. Therapeutic Effects of MSC in MRONJ. Several studies exploited these interesting MSC-related immunomodulatory effects in the treatment of MRONJ. MSC grafts have been performed in mice, pigs, and humans with encouraging results [113–115]. Of note, the key of the success obtained with MSCs seems to be more linked to their immunomodulatory properties rather than their possible osteoblast differentiation. Indeed, the efficacy of MSC grafts is dependent on their capacity to decrease levels of IL-17, IL-6, c-reactive protein, and Th17 cells and to increase levels of IL-10, TGF-β1, and Treg cells [113, 114]. So, although MSCs are able to differentiate into osteoblast precursors [100], there is no evidence that grafted MSCs directly participate in bone regeneration by osteoblast differentiation. Indeed, median survival of grafted MSCs is about one or two weeks: this timeframe is not consistent with a direct bone regeneration but is more related to an indirect effect [116]. Moreover, the absence of direct participation of grafted MSCs in tissue regeneration by differentiation has also been reported in various neurological diseases models where grafted MSCs did not last at the transplantation site, despite their beneficial effects on neuronal regeneration [117]. All these observations led to the hypothesis that MSCs beneficial effects are due to their capacity to secrete cytokines and/or growth factors, gathered under the term "*secretome.*" Furthermore, from this point of view, this MSC secretome should promote endogenous tissue regeneration, apoptosis inhibition, and angiogenesis. Therefore, MSC-conditioned

culture medium has been injected into rat MRONJ-like model, and full recovery was indeed observed in 63% cases. Histological analyses showed that MSC secretome exhibits anti-inflammatory, osteogenic, angiogenic, and antiapoptotic properties [118].

On the other hand, it has been demonstrated that the jaw bone cells arise from cranial neural-crest stem cells (NCSCs) [35]. Furthermore, using cell tracing or mapping strategies [36], it has been recently demonstrated that jaw bone defects are healed through neural-crest cell recruitment. Based on these observations, grafting NCSCs or NCSC secretome in MRONJ cases might be a new and relevant therapeutic strategy to investigate. Interestingly, it was recently demonstrated that adult bone marrow MSCs, but also adult adipose tissue derived MSCs, are heterogeneous populations containing NCSCs as well. The use of pure populations of MSCs or NCSCs (or their respective secretomes) therefore deserves to be considered in MRONJ animal models.

Altogether, although grafted MSCs/NCSCs are not directly responsible for bone regeneration observed in MRONJ animal models, they are suspected to recruit and stimulate local or regional endogenous cells to differentiate into osteoblasts and thus bone formation (1). Knowing the beneficial effect of grafted MSC in MRONJ, we can suggest that MSC would have an impact on bone remodeling (2) which is targeted by BPs and denosumab. As described before, MSCs exhibit immunomodulatory properties (3) and seem to decrease the inflammation in MRONJ. In this context, it would therefore be useful to recapitulate the molecular regulatory events controlling osteogenic differentiation, bone remodeling, and osteoimmunology.

6. Conclusions

Despite the recent advances in MRONJ pharmacological treatments, we are still looking forward to a curative treatment without dangerous side effects and an understanding of MRONJ physiopathogenesis. During last decade, cell therapy was considered to be efficient for treating different medical conditions and, in this view, MSC grafting in MRONJ is a recent therapeutic strategy that shows good results. However, after first clinical trials, cell therapy of MRONJ using MSC has to get back to the laboratory in order to understand their effects, at the molecular and the cellular levels as little information is available concerning the MSC mechanisms of action. Research studies should therefore now focus on the molecular mechanisms underlying the beneficial effects of MSC grafts. Likewise, it is unclear if the major impact of this cellular therapy is immunological or bone related. This unclear situation is possibly related to the fact that MRONJ is not a simple bone disease but could represent a model of osteoimmunology pathology similar to what we observed in rheumatoid arthritis. This could explain the absence of a strictly defined treatment and a proper characterization of MRONJ physiopathology. We strongly believe that a molecular dissection of grafted MSC effects in MRONJ would allow us to get a better understanding of the physiopathological sequences in this clinical situation but also to design new pharmacological approaches to help patients.

Competing Interests

The authors declare that they have no competing interests.

Acknowledgments

This work was supported by a grant from the Télévie, Fonds National de la Recherche Scientifique (FNRS) of Belgium, by a grant of the Fonds Spéciaux of the University of Liège, Belgium, and by a grant of Leon Fredericq Foundation/Lejeune-Lechien Foundation.

References

[1] S. L. Ruggiero, T. B. Dodson, J. Fantasia et al., "American association of oral and maxillofacial surgeons position paper on medication-related osteonecrosis of the jaw—2014 update," *Journal of Oral and Maxillofacial Surgery*, vol. 72, no. 10, pp. 1938–1956, 2014.

[2] T. L. Aghaloo, A. L. Felsenfeld, and S. Tetradis, "Osteonecrosis of the jaw in a patient on denosumab," *Journal of Oral and Maxillofacial Surgery*, vol. 68, no. 5, pp. 959–963, 2010.

[3] K. H. Taylor, L. S. Middlefell, and K. D. Mizen, "Osteonecrosis of the jaws induced by anti-RANK ligand therapy," *British Journal of Oral and Maxillofacial Surgery*, vol. 48, no. 3, pp. 221–223, 2010.

[4] P. Diz, J. L. López-Cedrún, J. Arenaz, and C. Scully, "Denosumab-related osteonecrosis of the jaw," *Journal of the American Dental Association*, vol. 143, no. 9, pp. 981–984, 2012.

[5] A. A. Khan, L. P. Rios, G. K. B. Sándor et al., "Bisphosphonate-associated osteonecrosis of the jaw in Ontario: a survey of oral and maxillofacial surgeons," *Journal of Rheumatology*, vol. 38, no. 7, pp. 1396–1402, 2011.

[6] M. Ulmner, F. Jarnbring, and O. Törring, "Osteonecrosis of the jaw in sweden associated with the oral use of bisphosphonate," *Journal of Oral and Maxillofacial Surgery*, vol. 72, no. 1, pp. 76–82, 2014.

[7] A. A. Khan, A. Morrison, D. A. Hanley et al., "Diagnosis and management of osteonecrosis of the jaw: a systematic review and international consensus," *Journal of Bone and Mineral Research*, vol. 30, no. 1, pp. 3–23, 2015.

[8] A. Barasch, J. Cunha-Cruz, F. A. Curro et al., "Risk factors for osteonecrosis of the jaws: a case-control study from the CONDOR dental PBRN," *Journal of Dental Research*, vol. 90, no. 4, pp. 439–444, 2011.

[9] A. O. Hoff, B. B. Toth, K. Altundag et al., "Frequency and risk factors associated with osteonecrosis of the jaw in cancer patients treated with intravenous bisphosphonates," *Journal of Bone and Mineral Research*, vol. 23, no. 6, pp. 826–836, 2008.

[10] R. Fliefel, M. Tröltzsch, J. Kühnisch, M. Ehrenfeld, and S. Otto, "Treatment strategies and outcomes of bisphosphonate-related osteonecrosis of the jaw (BRONJ) with characterization of patients: a systematic review," *International Journal of Oral and Maxillofacial Surgery*, vol. 44, no. 5, pp. 568–585, 2015.

[11] L. Lum and P. A. Beachy, "The Hedgehog response network: sensors, switches, and routers," *Science*, vol. 304, no. 5678, pp. 1755–1759, 2004.

[12] F. Long, U.-I. Chung, S. Ohba, J. McMahon, H. M. Kronenberg, and A. P. McMahon, "Ihh signaling is directly required for the

osteoblast lineage in the endochondral skeleton," *Development*, vol. 131, no. 6, pp. 1309–1318, 2004.

[13] D. Chen, M. Zhao, and G. R. Mundy, "Bone morphogenetic proteins," *Growth Factors*, vol. 22, no. 4, pp. 233–241, 2004.

[14] F. Deschaseaux, L. Sensébé, and D. Heymann, "Mechanisms of bone repair and regeneration," *Trends in Molecular Medicine*, vol. 15, no. 9, pp. 417–429, 2009.

[15] N. Holleville, S. Matéos, M. Bontoux, K. Bollerot, and A.-H. Monsoro-Burq, "Dlx5 drives Runx2 expression and osteogenic differentiation in developing cranial suture mesenchyme," *Developmental Biology*, vol. 304, no. 2, pp. 860–874, 2007.

[16] F. Liu, S. Kohlmeier, and C.-Y. Wang, "Wnt signaling and skeletal development," *Cellular Signalling*, vol. 20, no. 6, pp. 999–1009, 2008.

[17] J. C. Frith, J. Mönkkönen, S. Auriola, H. Mönkkönen, and M. J. Rogers, "The molecular mechanism of action of the antiresorptive and antiinflammatory drug clodronate: evidence for the formation in vivo of a metabolite that inhibits bone resorption and causes osteoclast and macrophage apoptosis," *Arthritis and Rheumatism*, vol. 44, no. 9, pp. 2201–2210, 2001.

[18] J. E. Dunford, K. Thompson, F. P. Coxon et al., "Structure-activity relationships for inhibition of farnesyl diphosphate synthase in vitro and inhibition of bone resorption in vivo by nitrogen-containing bisphosphonates," *Journal of Pharmacology and Experimental Therapeutics*, vol. 296, no. 2, pp. 235–242, 2001.

[19] K. Thompson, A. J. Roelofs, M. Jauhiainen, H. Mönkkönen, J. Mönkkönen, and M. J. Rogers, "Activation of $\gamma\delta$ T cells by bisphosphonates," in *Osteoimmunology*, vol. 658 of *Advances in Experimental Medicine and Biology*, pp. 11–20, Springer, Boston, Mass, USA, 2010.

[20] I. S. Hamadeh, B. A. Ngwa, and Y. Gong, "Drug induced osteonecrosis of the jaw," *Cancer Treatment Reviews*, vol. 41, no. 5, pp. 455–464, 2015.

[21] V. Ribeiro, M. Garcia, R. Oliveira, P. S. Gomes, B. Colaço, and M. H. Fernandes, "Bisphosphonates induce the osteogenic gene expression in co-cultured human endothelial and mesenchymal stem cells," *Journal of Cellular and Molecular Medicine*, vol. 18, no. 1, pp. 27–37, 2014.

[22] D. L. Kendler, C. Roux, C. L. Benhamou et al., "Effects of denosumab on bone mineral density and bone turnover in postmenopausal women transitioning from alendronate therapy," *Journal of Bone and Mineral Research*, vol. 25, no. 1, pp. 72–81, 2010.

[23] D. A. Hanley, J. D. Adachi, A. Bell, and V. Brown, "Denosumab: mechanism of action and clinical outcomes," *International Journal of Clinical Practice*, vol. 66, no. 12, pp. 1139–1146, 2012.

[24] F. Giancola, G. Campisi, L. Lo Russo, L. L. Muzio, and O. Di Fede, "Osteonecrosis of the jaw related to everolimus and bisphosphonate: a unique case report?" *Annali di Stomatologia*, vol. 4, supplement 2, pp. 20–21, 2013.

[25] D. W. Kim, Y.-S. Jung, H.-S. Park, and H.-D. Jung, "Osteonecrosis of the jaw related to everolimus: a case report," *British Journal of Oral and Maxillofacial Surgery*, vol. 51, no. 8, pp. e302–e304, 2013.

[26] S. Hoefert, I. Schmitz, A. Tannapfel, and H. Eufinger, "Importance of microcracks in etiology of bisphosphonate-related osteonecrosis of the jaw: a possible pathogenetic model of symptomatic and non-symptomatic osteonecrosis of the jaw based on scanning electron microscopy findings," *Clinical Oral Investigations*, vol. 14, no. 3, pp. 271–284, 2010.

[27] B. Kang, S. Cheong, T. Chaichanasakul et al., "Periapical disease and bisphosphonates induce osteonecrosis of the jaws in mice," *Journal of Bone and Mineral Research*, vol. 28, no. 7, pp. 1631–1640, 2013.

[28] T. L. Aghaloo, B. Kang, E. C. Sung et al., "Periodontal disease and bisphosphonates induce osteonecrosis of the jaws in the rat," *Journal of Bone and Mineral Research*, vol. 26, no. 8, pp. 1871–1882, 2011.

[29] P. Lesclous, S. Abi Najm, J.-P. Carrel et al., "Bisphosphonate-associated osteonecrosis of the jaw: a key role of inflammation?" *Bone*, vol. 45, no. 5, pp. 843–852, 2009.

[30] A. Cheung and E. Seeman, "Teriparatide therapy for alendronate-associated osteonecrosis of the jaw," *The New England Journal of Medicine*, vol. 363, no. 25, pp. 2473–2474, 2010.

[31] A. Bramati, S. Girelli, G. Farina et al., "Prospective, mono-institutional study of the impact of a systematic prevention program on incidence and outcome of osteonecrosis of the jaw in patients treated with bisphosphonates for bone metastases," *Journal of Bone and Mineral Metabolism*, vol. 33, no. 1, pp. 119–124, 2015.

[32] R. E. Marx, Y. Sawatari, M. Fortin, and V. Broumand, "Bisphosphonate-induced exposed bone (osteonecrosis/osteopetrosis) of the jaws: risk factors, recognition, prevention, and treatment," *Journal of Oral and Maxillofacial Surgery*, vol. 63, no. 11, pp. 1567–1575, 2005.

[33] P. P. Sedghizadeh, S. K. S. Kumar, A. Gorur, C. Schaudinn, C. F. Shuler, and J. W. Costerton, "Identification of microbial biofilms in osteonecrosis of the jaws secondary to bisphosphonate therapy," *Journal of Oral and Maxillofacial Surgery*, vol. 66, no. 4, pp. 767–775, 2008.

[34] S. L. Ruggiero, E. R. Carlson, and L. A. Assael, "Comprehensive review of bisphosphonate therapy: implications for the oral and maxillofacial surgery patient," *Journal of Oral and Maxillofacial Surgery*, vol. 67, no. 5, supplement, p. 1, 2009.

[35] Y. Chai and R. E. Maxson Jr., "Recent advances in craniofacial morphogenesis," *Developmental Dynamics*, vol. 235, no. 9, pp. 2353–2375, 2006.

[36] P. Leucht, J.-B. Kim, R. Amasha, A. W. James, S. Girod, and J. A. Helms, "Embryonic origin and Hox status determine progenitor cell fate during adult bone regeneration," *Development*, vol. 135, no. 17, pp. 2845–2854, 2008.

[37] H. Akiyama, M.-C. Chaboissier, J. F. Martin, A. Schedl, and B. De Crombrugghe, "The transcription factor Sox9 has essential roles in successive steps of the chondrocyte differentiation pathway and is required for expression of Sox5 and Sox6," *Genes and Development*, vol. 16, no. 21, pp. 2813–2828, 2002.

[38] E. Hinoi, P. Bialek, Y.-T. Chen et al., "Runx2 inhibits chondrocyte proliferation and hypertrophy through its expression in the perichondrium," *Genes and Development*, vol. 20, no. 21, pp. 2937–2942, 2006.

[39] R. F. Robledo, L. Rajan, X. Li, and T. Lufkin, "The D1x5 and D1x6 homeobox genes are essential for craniofacial, axial, and appendicular skeletal development," *Genes and Development*, vol. 16, no. 9, pp. 1089–1101, 2002.

[40] W.-Y. Baek, M.-A. Lee, W. J. Ji et al., "Positive regulation of adult bone formation by osteoblast-specific transcription factor osterix," *Journal of Bone and Mineral Research*, vol. 24, no. 6, pp. 1055–1065, 2009.

[41] R. P. Harper and E. Fung, "Resolution of bisphosphonate-associated osteonecrosis of the mandible: possible application

for intermittent low-dose parathyroid hormone [rhPTH(1-34)]," *Journal of Oral and Maxillofacial Surgery*, vol. 65, no. 3, pp. 573–580, 2007.

[42] M. Cicciù, A. S. Herford, G. Juodžbalys, and E. Stoffella, "Recombinant human bone morphogenetic protein type 2 application for a possible treatment of bisphosphonates-related osteonecrosis of the jaw," *Journal of Craniofacial Surgery*, vol. 23, no. 3, pp. 784–788, 2012.

[43] F. Morvan, K. Boulukos, P. Clément-Lacroix et al., "Deletion of a single allele of the Dkk1 gene leads to an increase in bone formation and bone mass," *Journal of Bone and Mineral Research*, vol. 21, no. 6, pp. 934–945, 2006.

[44] D. J. Heath, A. D. Chantry, C. H. Buckle et al., "Inhibiting Dickkopf-1 (Dkk1) removes suppression of bone formation and prevents the development of osteolytic bone disease in multiple myeloma," *Journal of Bone and Mineral Research*, vol. 24, no. 3, pp. 425–436, 2009.

[45] S. J. Rodda and A. P. McMahon, "Distinct roles for Hedgehog and caronical Wnt signaling in specification, differentiation and maintenance of osteoblast progenitors," *Development*, vol. 133, no. 16, pp. 3231–3244, 2006.

[46] X. Li, M. S. Ominsky, K. S. Warmington et al., "Sclerostin antibody treatment increases bone formation, bone mass, and bone strength in a rat model of postmenopausal osteoporosis," *Journal of Bone and Mineral Research*, vol. 24, no. 4, pp. 578–588, 2009.

[47] M. Asagiri, K. Sato, T. Usami et al., "Autoamplification of NFATc1 expression determines its essential role in bone homeostasis," *The Journal of Experimental Medicine*, vol. 202, no. 9, pp. 1261–1269, 2005.

[48] T. J. Yun, P. M. Chaudhary, G. L. Shu et al., "OPG/FDCR-1, a TNF receptor family member, is expressed in lymphoid cells and is up-regulated by ligating CD40," *The Journal of Immunology*, vol. 161, no. 11, pp. 6113–6121, 1998.

[49] M. M. Guerrini and H. Takayanagi, "The immune system, bone and RANKL," *Archives of Biochemistry and Biophysics*, vol. 561, pp. 118–123, 2014.

[50] T. Nakashima and H. Takayanagi, "Osteoimmunology: crosstalk between the immune and bone systems," *Journal of Clinical Immunology*, vol. 29, no. 5, pp. 555–567, 2009.

[51] L. C. de Rezende, I. V. Silva, L. B. Rangel, and M. C. Guimarães, "Regulatory T cell as a target for cancer therapy," *Archivum Immunologiae et Therapiae Experimentalis*, vol. 58, no. 3, pp. 179–190, 2010.

[52] K. Nakamura, A. Kitani, and W. Strober, "Cell contact–dependent immunosuppression by $CD4^+CD25^+$ regulatory T cells is mediated by cell surface–bound transforming growth factor β," *Journal of Experimental Medicine*, vol. 194, no. 5, pp. 629–644, 2001.

[53] J. D. Fontenot, M. A. Gavin, and A. Y. Rudensky, "Foxp3 programs the development and function of $CD4^+CD25^+$ regulatory T cells," *Nature Immunology*, vol. 4, no. 4, pp. 330–336, 2003.

[54] M. M. Zaiss, R. Axmann, J. Zwerina et al., "Treg cells suppress osteoclast formation: a new link between the immune system and bone," *Arthritis and Rheumatism*, vol. 56, no. 12, pp. 4104–4112, 2007.

[55] Y. G. Kim, C.-K. Lee, S.-S. Nah, S. H. Mun, B. Yoo, and H.-B. Moon, "Human CD4+CD25+ regulatory T cells inhibit the differentiation of osteoclasts from peripheral blood mononuclear cells," *Biochemical and Biophysical Research Communications*, vol. 357, no. 4, pp. 1046–1052, 2007.

[56] A. C. Hayday, "$\gamma\delta$ Cells: a right time and a right place for a conserved third way of protection," *Annual Review of Immunology*, vol. 18, pp. 975–1026, 2000.

[57] A. Pappalardo and K. Thompson, "Activated $\gamma\delta$ T cells inhibit osteoclast differentiation and resorptive activity *in vitro*," *Clinical & Experimental Immunology*, vol. 174, no. 2, pp. 281–291, 2013.

[58] N. Komatsu, K. Okamoto, S. Sawa et al., "Pathogenic conversion of $Foxp3^+$ T cells into T_H17 cells in autoimmune arthritis," *Nature Medicine*, vol. 20, no. 1, pp. 62–68, 2014.

[59] A. Picchianti Diamanti, M. M. Rosado, M. Scarsella et al., "Abatacept (cytotoxic T lymphocyte antigen 4-immunoglobulin) improves B cell function and regulatory T cell inhibitory capacity in rheumatoid arthritis patients non-responding to anti-tumour necrosis factor-α agents," *Clinical and Experimental Immunology*, vol. 177, no. 3, pp. 630–640, 2014.

[60] A. Bozec, M. M. Zaiss, R. Kagwiria et al., "T cell costimulation molecules CD80/86 inhibit osteoclast differentiation by inducing the IDO/tryptophan pathway," *Science Translational Medicine*, vol. 6, Article ID 235ra60, 2014.

[61] T. Yoshitaka, T. Mukai, M. Kittaka et al., "Enhanced TLR-MYD88 signaling stimulates autoinflammation in SH3BP2 cherubism mice and defines the etiology of cherubism," *Cell Reports*, vol. 8, no. 6, pp. 1752–1766, 2014.

[62] P. Saftig, E. Hunziker, O. Wehmeyer et al., "Impaired osteoclastic bone resorption leads to osteopetrosis in cathepsin-K-deficient mice," *Proceedings of the National Academy of Sciences of the United States of America*, vol. 95, no. 23, pp. 13453–13458, 1998.

[63] M. Asagiri, T. Hirai, T. Kunigami et al., "Cathepsin K-dependent toll-like receptor 9 signaling revealed in experimental arthritis," *Science*, vol. 319, no. 5863, pp. 624–627, 2008.

[64] N. Suzuki, K. Takimoto, and N. Kawashima, "Cathepsin K inhibitor regulates inflammation and bone destruction in experimentally induced rat periapical lesions," *Journal of Endodontics*, vol. 41, no. 9, pp. 1474–1479, 2015.

[65] R. D. Chapurlat, "Odanacatib: a review of its potential in the management of osteoporosis in postmenopausal women," *Therapeutic Advances in Musculoskeletal Disease*, vol. 7, no. 3, pp. 103–109, 2015.

[66] P. Lesclous, S. Grabar, S. Abi Najm et al., "Relevance of surgical management of patients affected by bisphosphonate-associated osteonecrosis of the jaws. A Prospective Clinical and Radiological Study," *Clinical Oral Investigations*, vol. 18, no. 2, pp. 391–399, 2014.

[67] E. Quattrocchi and H. Kourlas, "Teriparatide: a review," *Clinical Therapeutics*, vol. 26, no. 6, pp. 841–854, 2004.

[68] P. C. Bessa, M. Casal, and R. L. Reis, "Bone morphogenetic proteins in tissue engineering: the road from the laboratory to the clinic, part I (basic concepts)," *Journal of Tissue Engineering and Regenerative Medicine*, vol. 2, no. 1, pp. 1–13, 2008.

[69] A. C. Carreira, F. H. Lojudice, E. Halcsik, R. D. Navarro, M. C. Sogayar, and J. M. Granjeiro, "Bone morphogenetic proteins: facts, challenges, and future perspectives," *Journal of Dental Research*, vol. 93, no. 4, pp. 335–345, 2014.

[70] N. S. Arora, T. Ramanayake, Y.-F. Ren, and G. E. Romanos, "Platelet-rich plasma: a literature review," *Implant Dentistry*, vol. 18, no. 4, pp. 303–310, 2009.

[71] D. M. Dohan Ehrenfest, L. Rasmusson, and T. Albrektsson, "Classification of platelet concentrates: from pure platelet-rich plasma (P-PRP) to leucocyte- and platelet-rich fibrin (L-PRF)," *Trends in Biotechnology*, vol. 27, no. 3, pp. 158–167, 2009.

[72] F. Longo, A. Guida, C. Aversa et al., "Platelet rich plasma in the treatment of bisphosphonate-related osteonecrosis of the jaw: personal experience and review of the literature," *International Journal of Dentistry*, vol. 2014, Article ID 298945, 7 pages, 2014.

[73] J.-W. Kim, S.-J. Kim, and M.-R. Kim, "Leucocyte-rich and platelet-rich fibrin for the treatment of bisphosphonate-related osteonecrosis of the jaw: A Prospective Feasibility Study," *British Journal of Oral and Maxillofacial Surgery*, vol. 52, no. 9, pp. 854–859, 2014.

[74] P. A. M. Everts, A. van Zundert, J. P. A. M. Schönberger, R. J. J. Devilee, and J. T. A. Knape, "What do we use: platelet-rich plasma or platelet-leukocyte gel?" *Journal of Biomedical Materials Research A*, vol. 85, no. 4, pp. 1135–1136, 2008.

[75] D. M. Dohan, J. Choukroun, A. Diss et al., "Platelet-rich fibrin (PRF): a second-generation platelet concentrate. Part III: leucocyte activation: a new feature for platelet concentrates?" *Oral Surgery, Oral Medicine, Oral Pathology, Oral Radiology and Endodontology*, vol. 101, no. 3, pp. e51–e55, 2006.

[76] M. Del Fabbro, G. Gallesio, and M. Mozzati, "Autologous platelet concentrates for bisphosphonate-related osteonecrosis of the jaw treatment and prevention. A systematic review of the literature," *European Journal of Cancer*, vol. 51, no. 1, pp. 62–74, 2015.

[77] R. Gianni-Barrera, M. Bartolomeo, B. Vollmar, V. Djonov, and A. Banfi, "Split for the cure: VEGF, PDGF-BB and intussusception in therapeutic angiogenesis," *Biochemical Society Transactions*, vol. 42, no. 6, pp. 1637–1642, 2014.

[78] H. Xie, Z. Cui, L. Wang et al., "PDGF-BB secreted by preosteoclasts induces angiogenesis during coupling with osteogenesis," *Nature Medicine*, vol. 20, no. 11, pp. 1270–1278, 2014.

[79] P. Vescovi, I. Giovannacci, S. Otto et al., "Medication-related osteonecrosis of the jaw: an autofluorescence-guided surgical approach performed with Er:YAG laser," *Photomedicine and Laser Surgery*, vol. 33, no. 8, pp. 437–442, 2015.

[80] P. Vescovi, M. Meleti, E. Merigo et al., "Case series of 589 tooth extractions in patients under bisphosphonates therapy. Proposal of a clinical protocol supported by Nd: YAG low-level laser therapy," *Medicina Oral, Patologia Oral y Cirugia Bucal*, vol. 18, no. 4, pp. e680–e685, 2013.

[81] M. A. Altay, F. Tasar, E. Tosun, and B. Kan, "Low-level laser therapy supported surgical treatment of bisphosphonate related osteonecrosis of jaws: a retrospective analysis of 11 cases," *Photomedicine and Laser Surgery*, vol. 32, no. 8, pp. 468–475, 2014.

[82] G. A. Guzzardella, M. Fini, P. Torricelli, G. Giavaresi, and R. Giardino, "Laser stimulation on bone defect healing: an in vitro study," *Lasers in Medical Science*, vol. 17, no. 3, pp. 216–220, 2002.

[83] Y. Ueda and N. Shimizu, "Effects of Pulse Frequency of Low-Level Laser Therapy (LLLT) on Bone nodule formation in rat calvarial cells," *Journal of Clinical Laser Medicine and Surgery*, vol. 21, no. 5, pp. 271–277, 2003.

[84] R. E. Marx, "A new concept in the treatment of osteoradionecrosis," *Journal of Oral and Maxillofacial Surgery*, vol. 41, no. 6, pp. 351–357, 1983.

[85] D. R. Knighton, V. D. Fiegel, T. Halverson, S. Schneider, T. Brown, and C. L. Wells, "Oxygen as an antibiotic. The effect of inspired oxygen on bacterial clearance," *Archives of Surgery*, vol. 125, no. 1, pp. 97–100, 1990.

[86] J. J. Freiberger, "Utility of hyperbaric oxygen in treatment of bisphosphonate-related osteonecrosis of the jaws," *Journal of Oral and Maxillofacial Surgery*, vol. 67, no. 5, pp. 96–106, 2009.

[87] J. V. Boykin Jr. and C. Baylis, "Hyperbaric oxygen therapy mediates increased nitric oxide production associated with wound healing: a preliminary study," *Advances in Skin & Wound Care*, vol. 20, no. 7, pp. 382–388, 2007.

[88] J. J. Freiberger, R. Padilla-Burgos, A. H. Chhoeu et al., "Hyperbaric oxygen treatment and bisphosphonate-induced osteonecrosis of the jaw: a case series," *Journal of Oral and Maxillofacial Surgery*, vol. 65, no. 7, pp. 1321–1327, 2007.

[89] J. J. Freiberger, R. Padilla-Burgos, T. McGraw et al., "What is the role of hyperbaric oxygen in the management of bisphosphonate-related osteonecrosis of the jaw: a randomized controlled trial of hyperbaric oxygen as an adjunct to surgery and antibiotics," *Journal of Oral and Maxillofacial Surgery*, vol. 70, no. 7, pp. 1573–1583, 2012.

[90] A. Dyas, B. J. Boughton, and B. C. Das, "Ozone killing action against bacterial and fungal species; microbiological testing of a domestic ozone generator," *Journal of Clinical Pathology*, vol. 36, no. 10, pp. 1102–1104, 1983.

[91] V. Bocci, "Ozone as Janus: this controversial gas can be either toxic or medically useful," *Mediators of Inflammation*, vol. 13, no. 1, pp. 3–11, 2004.

[92] A. Agrillo, F. Filiaci, V. Ramieri et al., "Bisphosphonate-related osteonecrosis of the jaw (BRONJ): 5 year experience in the treatment of 131 cases with ozone therapy," *European Review for Medical and Pharmacological Sciences*, vol. 16, no. 12, pp. 1741–1747, 2012.

[93] A. Agrillo, P. Sassano, C. Rinna, P. Priore, and G. Iannetti, "Ozone therapy in extractive surgery on patients treated with bisphosphonates," *Journal of Craniofacial Surgery*, vol. 18, no. 5, pp. 1068–1070, 2007.

[94] M. Dominici, K. Le Blanc, I. Mueller et al., "Minimal criteria for defining multipotent mesenchymal stromal cells. The International Society for Cellular Therapy position statement," *Cytotherapy*, vol. 8, no. 4, pp. 315–317, 2006.

[95] M. Crisan, S. Yap, L. Casteilla et al., "A perivascular origin for mesenchymal stem cells in multiple human organs," *Cell Stem Cell*, vol. 3, no. 3, pp. 301–313, 2008.

[96] M. Di Ianni, B. Del Papa, M. De Ioanni et al., "Mesenchymal cells recruit and regulate T regulatory cells," *Experimental Hematology*, vol. 36, no. 3, pp. 309–318, 2008.

[97] M. J. Robertson and J. Ritz, "Biology and clinical relevance of human natural killer cells," *Blood*, vol. 76, no. 12, pp. 2421–2438, 1990.

[98] G. M. Spaggiari, A. Capobianco, H. Abdelrazik, F. Becchetti, M. C. Mingari, and L. Moretta, "Mesenchymal stem cells inhibit natural killer-cell proliferation, cytotoxicity, and cytokine production: role of indoleamine 2,3-dioxygenase and prostaglandin E2," *Blood*, vol. 111, no. 3, pp. 1327–1333, 2008.

[99] M. Rossi and J. W. Young, "Human dendritic cells: potent antigen-presenting cells at the crossroads of innate and adaptive immunity," *Journal of Immunology*, vol. 175, no. 3, pp. 1373–1381, 2005.

[100] G. M. Spaggiari, H. Abdelrazik, F. Becchetti, and L. Moretta, "MSCs inhibit monocyte-derived DC maturation and function by selectively interfering with the generation of immature DCs: central role of MSC-derived prostaglandin E2," *Blood*, vol. 113, no. 26, pp. 6576–6583, 2009.

[101] Y.-P. Li, S. Paczesny, E. Lauret et al., "Human mesenchymal stem cells license adult CD34+ hemopoietic progenitor cells to differentiate into regulatory dendritic cells through activation of the notch pathway," *Journal of Immunology*, vol. 180, no. 3, pp. 1598–1608, 2008.

[102] A. Mantovani, A. Sica, and M. Locati, "Macrophage polarization comes of age," *Immunity*, vol. 23, no. 4, pp. 344–346, 2005.

[103] N. Mokarram and R. V. Bellamkonda, "A perspective on immunomodulation and tissue repair," *Annals of Biomedical Engineering*, vol. 42, no. 2, pp. 338–351, 2014.

[104] H. Nakajima, K. Uchida, A. R. Guerrero et al., "Transplantation of mesenchymal stem cells promotes an alternative pathway of macrophage activation and functional recovery after spinal cord injury," *Journal of Neurotrauma*, vol. 29, no. 8, pp. 1614–1625, 2012.

[105] S. Tabera, J. A. Pérez-Simón, M. Díez-Campelo et al., "The effect of mesenchymal stem cells on the viability, proliferation and differentiation of B-lymphocytes," *Haematologica*, vol. 93, no. 9, pp. 1301–1309, 2008.

[106] M. Krampera, L. Cosmi, R. Angeli et al., "Role for interferon-γ in the immunomodulatory activity of human bone marrow mesenchymal stem cells," *Stem Cells*, vol. 24, no. 2, pp. 386–398, 2006.

[107] C. Prevosto, M. Zancolli, P. Canevali, M. R. Zocchi, and A. Poggi, "Generation of CD4+ or CD8+ regulatory T cells upon mesenchymal stem cell-lymphocyte interaction," *Haematologica*, vol. 92, no. 7, pp. 881–888, 2007.

[108] S. Ghannam, C. Bouffi, F. Djouad, C. Jorgensen, and D. Noël, "Immunosuppression by mesenchymal stem cells: mechanisms and clinical applications," *Stem Cell Research and Therapy*, vol. 1, article 2, 2010.

[109] L. Bai, D. P. Lennon, V. Eaton et al., "Human bone marrow-derived mesenchymal stem cells induce Th2-polarized immune response and promote endogenous repair in animal models of multiple sclerosis," *Glia*, vol. 57, no. 11, pp. 1192–1203, 2009.

[110] K. Sato, K. Ozaki, I. Oh et al., "Nitric oxide plays a critical role in suppression of T-cell proliferation by mesenchymal stem cells," *Blood*, vol. 109, no. 1, pp. 228–234, 2007.

[111] R. Meisel, A. Zibert, M. Laryea, U. Göbel, W. Däubener, and D. Dilloo, "Human bone marrow stromal cells inhibit allogeneic T-cell responses by indoleamine 2,3-dioxygenase-mediated tryptophan degradation," *Blood*, vol. 103, no. 12, pp. 4619–4621, 2004.

[112] Y. Wang, X. Chen, W. Cao, and Y. Shi, "Plasticity of mesenchymal stem cells in immunomodulation: pathological and therapeutic implications," *Nature Immunology*, vol. 15, no. 11, pp. 1009–1016, 2014.

[113] T. Kikuiri, I. Kim, T. Yamaza et al., "Cell-based immunotherapy with mesenchymal stem cells cures bisphosphonate-related osteonecrosis of the jaw-like disease in mice," *Journal of Bone and Mineral Research*, vol. 25, no. 7, pp. 1668–1679, 2010.

[114] Y. Li, J. Xu, L. Mao et al., "Allogeneic mesenchymal stem cell therapy for bisphosphonate-related jaw osteonecrosis in swine," *Stem Cells and Development*, vol. 22, no. 14, pp. 2047–2056, 2013.

[115] L. Cella, A. Oppici, M. Arbasi et al., "Autologous bone marrow stem cell intralesional transplantation repairing bisphosphonate related osteonecrosis of the jaw," *Head and Face Medicine*, vol. 7, article 16, 2011.

[116] C. E. Zimmermann, M. Gierloff, J. Hedderich, Y. Açil, J. Wiltfang, and H. Terheyden, "Survival of transplanted rat bone marrow-derived osteogenic stem cells in vivo," *Tissue Engineering—Part A*, vol. 17, no. 7-8, pp. 1147–1156, 2011.

[117] V. Neirinckx, D. Cantinieaux, C. Coste, B. Rogister, R. Franzen, and S. Wislet-Gendebien, "Concise review: spinal cord injuries: how could adult mesenchymal and neural crest stem cells take up the challenge," *STEM CELLS*, vol. 32, no. 4, pp. 829–843, 2014.

[118] K. Ogata, W. Katagiri, M. Osugi et al., "Evaluation of the therapeutic effects of conditioned media from mesenchymal stem cells in a rat bisphosphonate-related osteonecrosis of the jaw-like model," *Bone*, vol. 74, pp. 95–105, 2015.

Hindawi Publishing Corporation
Stem Cells International
Volume 2016, Article ID 6901286, 17 pages
http://dx.doi.org/10.1155/2016/6901286

Review Article

Umbilical Cord as Prospective Source for Mesenchymal Stem Cell-Based Therapy

Irina Arutyunyan,[1] Andrey Elchaninov,[2] Andrey Makarov,[1] and Timur Fatkhudinov[1,2]

[1] *Research Center for Obstetrics, Gynecology and Perinatology, Ministry of Healthcare of the Russian Federation, No. 4, Oparin Street, Moscow 117997, Russia*
[2] *Pirogov Russian National Research Medical University, Ministry of Healthcare of the Russian Federation, No. 1, Ostrovitianov Street, Moscow 117997, Russia*

Correspondence should be addressed to Timur Fatkhudinov; tfat@yandex.ru

Received 27 April 2016; Accepted 14 July 2016

Academic Editor: Salvatore Scacco

The paper presents current evidence on the properties of human umbilical cord-derived mesenchymal stem cells, including origin, proliferative potential, plasticity, stability of karyotype and phenotype, transcriptome, secretome, and immunomodulatory activity. A review of preclinical studies and clinical trials using this cell type is performed. Prospects for the use of mesenchymal stem cells, derived from the umbilical cord, in cell transplantation are associated with the need for specialized biobanking and transplant standardization criteria.

1. Introduction

Many researchers consider the transplantation of mesenchymal stem cells (MSCs) to be the most effective tool for cell therapy, due to the simultaneous activation of multiple mechanisms (paracrine, trophic, immunomodulatory, and differentiation), affecting all stages of the regeneration of damaged tissues. Bone marrow-derived MSCs (BM-MSCs) are the most extensively characterized as they are the historically accepted "gold standard" of MSCs. Nevertheless, currently there is active research work regarding MSCs from other sources—adipose tissue, peripheral and umbilical cord blood, amniotic fluid, skin, dental pulp, synovium, umbilical cord tissue, placental complex, endometrium, and others. In fact, evidence has suggested that MSCs may be present virtually in any vascularized tissue throughout the whole body [1]. All these cell types meet the minimum criteria for MSCs but have significant differences in their features. Our review focuses on umbilical cord-derived MSCs (UC-MSCs), cells that have a unique combination of prenatal and postnatal stem cell properties.

2. The Origin and Morphology of the Human Umbilical Cord

The umbilical cord develops from the yolk sac and allantois and becomes a conduit between the developing embryo or fetus and the placenta. The umbilical cord stroma contains gelatinous substance called Wharton's jelly after Thomas Wharton (1614–1673), an English physician and anatomist. Wharton's jelly protects the blood vessels (two umbilical arteries and one umbilical vein) from clumping and provides cord flexibility. This substance is made largely from glycosaminoglycans, especially hyaluronic acid and chondroitin sulfate. Collagen fibers are the main fibrillary component, while elastic fibers are absent. The cell component is presented by mesenchyme-derived cells (fibroblasts, myofibroblasts, smooth muscle cells, and mesenchymal stem cells) [2]. In contrast to most tissues of the body, there are no capillaries in Wharton's jelly: there is an active process of hematopoiesis and capillaries formation in umbilical cord stroma at week 6 of development; however, at 7–9 weeks, hematopoiesis stops and capillaries regress [3]. Cross-section of the human umbilical cord is shown in Figure 1.

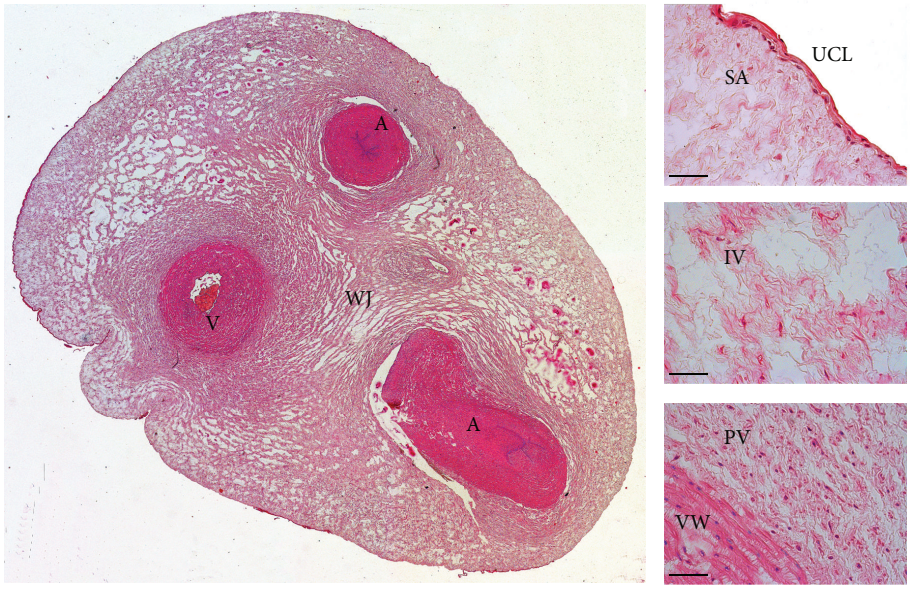

Figure 1: Cross-section of the human umbilical cord. A: artery; V: vein; WJ: Wharton's jelly; UCL: umbilical cord lining; SA, IV, and PV: subamnion, intervascular, and perivascular zones of Wharton's jelly; VW: blood vessel wall. Hematoxylin and eosin staining, scale bar = 200 μm.

3. The Umbilical Cord as a Source of Mesenchymal Stem Cells

In 1974, umbilical cord blood was declared to be the source of hematopoietic stem and progenitor cells [4], and the remaining umbilical cord tissue was considered medical waste with no scientific value. This point of view was completely revised in 1991, when McElreavey et al. isolated fibroblast-like cells from Wharton's jelly and characterized them [5]. In 2004, these fibroblast-like cells were proved to be MSCs as they expressed CD29, CD44, CD51, CD73, and CD105, lacked expression of CD34 and CD45, and were able to differentiate into cells of the adipogenic and osteogenic lineages [6]. Currently, the umbilical cord MSCs include cells derived from the total umbilical cord or its different sections (perivascular, intervascular, and subamnion zones of Wharton's jelly and subendothelial layer but not from umbilical cord lining or inner blood vessel walls) [2].

Figure 2 shows the characteristics of cultured cells derived from Wharton's jelly according to the minimal criteria to define human MSCs as proposed by the Mesenchymal and Tissue Stem Cell Committee of the International Society for Cellular Therapy (ISCT): (1) MSCs must be plastic-adherent when maintained in standard culture conditions; (2) MSCs must express CD105, CD73, and CD90 and lack expression of CD45, CD34, CD14 or CD11b, CD79a or CD19, and HLA-DR surface molecules; (3) MSCs must differentiate into osteoblasts, adipocytes, and chondroblasts *in vitro* [40].

4. The Origin of Wharton's Jelly MSCs

In 2008, Wang et al. presumed that early in embryogenesis, hematopoietic cells and MSCs migrate from the yolk sac and aorta-gonad-mesonephros to the placenta and then back to the fetal liver and bone marrow through the umbilical cord. During these two migration waves, some cells are trapped in Wharton's jelly and are retained therein throughout the whole period of gestation. The new microenvironment changes the properties of migrating cells, which probably explains their differences from BM-MSCs [41].

5. Isolation of Primary Cell Culture from Wharton's Jelly

Most protocols for primary cell culture isolation from Wharton's jelly consist of three steps:

(1) Removal of the epithelial, vascular, and perivascular tissues.

(2) Mechanical grinding and enzymatic digestion using trypsin, collagenases I, II, or IV, dispase, protease, and hyaluronidase.

(3) Transfer into the culture medium (standard culture media with human or fetal calf serum which may be supplemented with growth factors FGFb, EGF, PDGF, and VEGF) [2, 7, 42].

In addition, an explant culture method can be applied; it avoids the damaging effects of enzymes on cells and reduces the processing time of the biomaterial ("plate and wait" procedure) [43]. The common explant method of isolating UC-MSCs involves mincing the umbilical cords into small fragments, which are then attached to a culture dish bottom from which the cells migrate. One of the disadvantages of this method is that the fragments frequently float up from the bottom of the dish, thereby reducing the cell recovery rate. In some protocols, a stainless steel mesh is used to protect the tissue from floating [44].

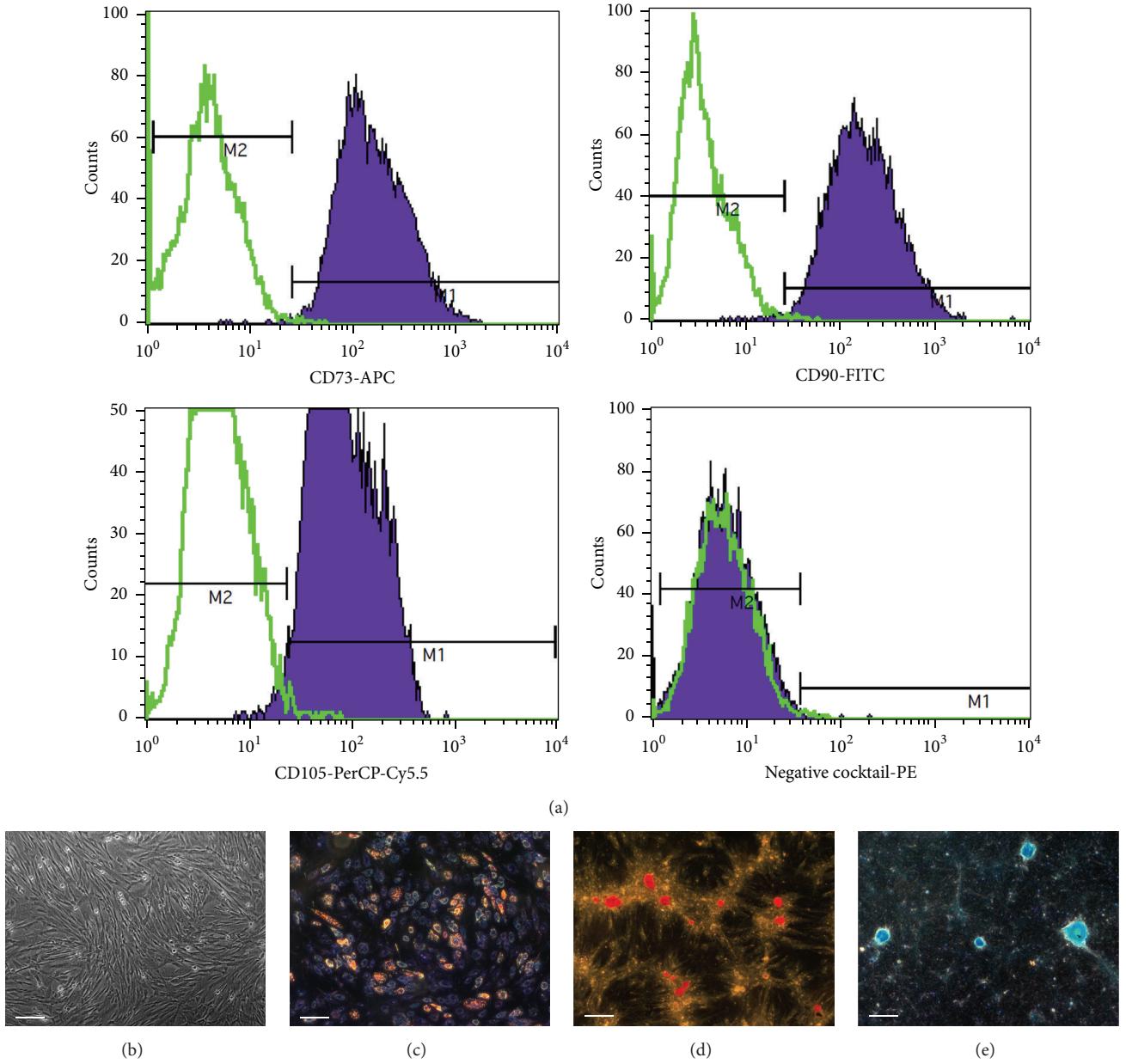

Figure 2: The characteristics of cultured cells derived from Wharton's jelly according to minimal criteria to define human MSCs proposed by ISCT. (a) Analysis of immunophenotype with BD Stemflow™ hMSC Analysis Kit (BD Biosciences). Negative MSC cocktail includes PE CD45, PE CD34, PE CD11b, PE CD19, and PE HLA-DR antibody conjugates. (b) Phase contrast capture of UC-MSCs at the fourth passage. Scale bar: 200 μm. (c) Adipogenic differentiation with StemPro® Adipogenesis Differentiation Kit (Gibco). Lipid droplets are stained with Sudan III. Scale bar: 200 μm. (d) Osteogenic differentiation with StemPro Osteogenesis Differentiation Kit (Gibco). Calcificated nodules are stained with Alizarin red S (pH = 4.1). Scale bar: 200 μm. (e) Chondrogenic differentiation with StemPro Chondrogenesis Differentiation Kit (Gibco). Mucopolysaccharides are stained with Alcian blue (pH = 2.5). Scale bar: 200 μm.

According to some reports, the explant method allows the selection of a cell fraction with higher proliferative potential [45, 46], but a remarkable variation of cell phenotype expressions was distinguished compared to enzymatic digestion [47, 48]. In a recent study, three explant culture methods and three enzymatic methods were compared. MSC isolation using the 10 mm size tissue explant method led to shorter primary culture time, higher numbers of isolated cells, and higher proliferation rates compared with other isolation methods. Immune phenotype and multilineage differentiation capacity did not differ significantly among six groups [49]. It was also found that UC-MSCs isolated by explant technique always reached proliferation arrest earlier, irrespective of initial population doubling times, but the mechanism explaining this effect is still unclear [50]. On the contrary, later studies showed that cells obtained from explants presented similar

characteristics (morphology, population doubling time, post-thaw survival, differentiation capacity, and phenotype) to those from enzymatic protocols [51].

According to published data [52, 53] and our own laboratory data, the efficacy of isolation of primary cell culture from Wharton's jelly amounts to 100%. In comparison, the efficacy of MSC isolation from umbilical cord blood does not exceed 60%; amniotic fluid is 90%; placenta varies from 62.5% to 100% [52, 53]. Wharton's jelly tissue yields the highest concentration of allogeneic mesenchymal stem cells: yields for bone marrow ranged from 1 to 317,400 cells/mL; yields for adipose tissue ranged from 4,737 to 1,550,000 cells/mL of tissue; and yields for umbilical cord tissue ranged from 10,000 to 4,700,000 cells/cm of umbilical cord [54].

It should be particularly noted that almost all culture laboratories use umbilical cords obtained after Caesarean sections, because vaginal delivery significantly increases the risk of contamination of primary biological material. Some researchers suppose that viable MSCs can only be isolated from fresh umbilical cord tissue, not from frozen tissue fragments [55]. According to another report, MSCs derived from frozen cord tissue exhibited decreased plating efficiency and increased doubling times but near equivalent maximum cell expansion compared with fresh cord tissue [56].

6. The Proliferative Potential and the Karyotype Stability of UC-MSCs

UC-MSCs have higher proliferative potential than BM-MSCs (the "gold standard" for MSCs comparison) or MSCs from other postnatal (adipose tissue) and neonatal sources (placenta and amniotic membrane) [13, 16, 17, 57, 58]. The mean of CFU-F (colony-forming unit-fibroblast) colonies per 1×10^6 nucleated cells was significantly higher in UC-MSCs (800, range 300–2000) than in BM-MSCs (36, range 16–64) as determined by the CFU-F assay based on Castro-Malaspina's method [57]. CFU-F frequency determined by limiting dilution assay also confirmed a higher frequency of CFU-F in UC-MSCs ($1 : 1609 \pm 0.18$) than in BM-MSCs ($1 : 35700 \pm 0.01$) [57]. According to another report, typical CFU-F efficiency (the ratio of number of cells forming colonies under clonal conditions and number of cells seeded directly after isolation) for BM-MSCs ranged from 0.001% to 0.01%, while for UC-MSCs it reached 0.2–1.8% [59].

It has been reported that cell doubling time for UC-MSCs approximates 21 h [58], 24 h [57], 40 h [13, 46], and 45 h [56]. Importantly, according to recent data, each individual UC-MSCs sample exhibited different population doubling rates and reached senescence at different passages due to unique genetic and epigenetic profiles, irrespective of isolation protocol [50]. A sufficient amount of the starting biomaterial (umbilical cord weight is nearly 40 g) and high telomerase activity of UC-MSCs permit obtaining 10^9 cells from one cord while maintaining their normal karyotype for 6 passages [60, 61]. Since passage 7, the telomerase activity of UC-MSCs is significantly reduced; but cell karyotype is stable for at least 25 passages [22, 62].

Table 1: The expression of cell surface markers on UC-MSCs (according to [2, 7–9]).

Positive markers		Contradictory data	Negative markers	
CD10	CD58	CD54	CD3	CD49a
CD13	CD59	CD105	CD11b	CD50
CD29	CD61	CD106	CD14	CD53
CD44	CD73	CD117	CD19	CD56
CD49b	CD90	CD144	CD31	CD71
CD49c	CD106	CD146	CD33	CD80
CD49d	CD166		CD34	CD86
CD49e	CD325		CD38	CD133
CD51	HLA-I		CD40	CD140α
CD56			CD45	HLA-II

Table 2: The expression of pluripotency markers on UC-MSCs (according to [2, 7–11]).

Positive markers	Contradictory data
REX2	STRO-1
GD2	OCT4
SOX2	SSEA-4
NANOG	
Tra-1-60	
Tra-1-81	
SSEA-1	
DNMT3B	
GABRB3	

7. UC-MSCs Phenotype

To date, the expression profile of surface markers and pluripotency markers of UC-MSCs has been investigated extensively (Tables 1 and 2).

Particular attention is drawn to CD105 (endoglin, a part of the TGF beta receptor complex). According to ISCT decision, CD105 is a required marker for MSCs verification [40]; however, different data contradict each other. In most studies, it has been shown that CD105 presents on UC-MSCs surface [2, 7–9], and its expression is maintained during long-term cultivation (at least 16 passages) [63]. However, a few studies have demonstrated that UC-MSCs do not express CD105 at all [64] or until passage 5 [65]. Reduction in mesenchymal-marker (CD73, CD90, and CD105) expression on UC-MSCs may occur under ischemic conditions influenced mainly by hypoxia [66]. In accordance with our laboratory data, more than 98% of the UC-MSCs express CD105 on passages 2–5 as measured by flow cytometry (Figure 2).

Data about the expression of pluripotent specific markers on UC-MSCs are contradictory. In different reports, the expression of these markers was shown only under certain conditions: solely on early passages [67], or when grown in the presence of human embryonic stem cells medium on mouse feeder cells [10], or after lowering O_2 concentration from 21% to 5% level [68], or after the selection of CD105+ cells and their subsequent cultivation under suspension culture condition [69]. Flow cytometric analysis revealed

Table 3: The genes expressed at higher levels in UC-MSCs compared to MSCs derived from adipose tissue, bone marrow, and skin (according to [12]).

Genes	Functions	Expression levels in UC-MSCs compared to		
		BM-MSC	AT-MSC	Skin-MSC
HAND1 Heart and neural crest derivatives expressed 1	Plays a critical role in heart development	Higher*	Higher	Higher
AFP Alpha-fetoprotein	The major plasma protein produced in the liver during fetal life	Higher	Higher	Higher
DKK1 Dickkopf homolog 1	An inhibitor of the WNT-signaling pathway critical for endodermal development	Higher	ns	Higher
DSG2 Desmoglein 2	An important component of desmosomes in epithelial cell type	Higher	ns	Higher
KRT8,19 Keratin 8, 19	The major intermediate filament proteins of epithelial cells	Higher	Higher	Higher
KRT18 Keratin 18	The major intermediate filament proteins of epithelial cells	Higher	ns	Higher

*Significantly increased mRNA expression between mutually compared stem cell types (fold change > 2; P value < 0.05). ns: not significant.

that neural ganglioside GD2(+)-sorted UC-MSCs showed increased expression of SSEA-4, OCT4, SOX2, and NANOG in comparison to unsorted or GD2-negative cells [70].

8. Transcriptomic Profile of UC-MSCs

In 2012, De Kock et al. studied the global gene expression profiles of four human mesoderm-derived stem cell populations. Human UC-MSCs showed significant enrichment in functional gene classes involved in liver and cardiovascular system development and function compared to MSCs derived from adipose tissue, bone marrow, and skin [12]. The most significant differences were found for genes presented in Table 3.

In 2010, Hsieh et al. published interesting data comparing the gene expression profiles of BM-MSCs and UC-MSCs. It was found that, for the two MSC types, there were no common genes among the top 50 known genes most strongly expressed! Top 10 for UC-MSCs included genes encoding somatostatin receptor 1, member 4 of immunoglobulin superfamily, gamma 2 smooth muscle actin, reticulon 1, natriuretic peptide precursor B, keratin 8, desmoglein 2, oxytocin receptor, desmocollin 3, and myocardin. The study also showed that genes related to cell proliferation (*EGF*), PI3K-NFkB signaling pathway (*TEK*), and neurogenesis (*RTN1*, *NPPB*, and *NRP2*) were upregulated in UC-MSCs compared to in BM-MSCs [71].

The UC-MSCs and BM-MSCs were also screened for their surface expression of HLA antigens, costimulatory factors, and immune tolerance molecules [9, 13]. It was found that the expression of MHCII molecules (HLA-DMA, -DRA, and -DPB1) in the BM-MSCs was 16-fold, 36-fold, and 4-fold higher, respectively, compared with the UC-MSCs. The expression levels of immune-related genes *TLR4*, *TLR3*, *JAG1*, *NOTCH2*, and *NOTCH3* in the BM-MSCs were 38-fold, 4-fold, 5-fold, 3-fold, and 4-fold higher, respectively, compared with the UC-MSCs [13]. These results promise successful future use of allogeneic UC-MSCs for clinical trials.

A more detailed comparative analysis of the UC-MSCs transcriptome is presented in the review by El Omar et al. [9].

9. The Multilineage Differentiation Potential of UC-MSCs

In vitro UC-MSCs showed very high differentiation capacity: these cells were able to differentiate into chondrocytes, adipocytes, osteoblasts, odontoblast-like cells, dermal fibroblasts, smooth muscle cells, skeletal muscle cells, cardiomyocytes, hepatocyte-like cells, insulin-producing cells, glucagon-producing cells, and somatostatin-producing cells, sweat gland cells, endothelial cells, neuroglia cells (oligodendrocytes), and dopaminergic neurons [8, 15, 21, 42, 72–75]. In 2014, it was found that under specific conditions UC-MSCs expressed markers of male germ-like cells and primordial-like germ cells; such a possibility had previously been shown only for embryonic stem cells (ESCs) or induced pluripotent stem cells [76, 77].

Comparison of the differentiation potential of UC-MSCs and MSCs from other sources (bone marrow and adipose tissue) is the subject of numerous studies presented in Table 4.

A number of studies have demonstrated the possibility of UC-MSCs' differentiation after genetic modification (transduction or transfection). UC-MSCs overexpressing hepatocyte growth factor (HGF) could differentiate into dopaminergic neuron-like cells secreting dopamine, tyrosine hydroxylase, and dopamine transporter [78] and promoted nerve fiber remyelination and axonal regeneration one week after transplantation in rats with collagenase-induced intracerebral hemorrhage [30]. After infection with adenovirus containing SF-1 cDNA, UC-MSCs had significantly higher expression of all steroidogenic mRNAs (including P450 side-chain cleavage enzyme, 3β-HSD, 17β-HSD type 3, LH-R, ACTH-R, P450c21, and CYP17), secreted significantly more steroidogenic hormones (including testosterone and cortisol), and had significantly higher cell viability than differentiated BM-MSCs [79].

Table 4: Comparison of the differentiation potential of UC-MSCs and MSCs from other sources.

Induction	Parameter	UC-MSCs	BM-MSCs	AT-MSCs	Reference
Osteogenic (35 days)	The average number of bone nodules from one well	19 ± 1.8	7.5 ± 1.3	11 ± 1.7	[13]
Adipogenic (21 days)	The ratio of differentiated adipocytes from the total cells	45 ± 1.5%	39 ± 1%	52 ± 3.2%	[13]
Neuronal (20 days)	The number of primary neurospheres	118 ± 5.2	80.4 ± 3.4	26 ± 3.12	[14]
	The average size of a primary neurosphere	175 ± 2.2 μm	100 ± 3.2 μm	57 ± 0.7 μm	
	The number of secondary neurospheres	47 ± 4.6	7 ± 1.2	Unable to form	
	The percentage of nestin+ cells	91.3 ± 2%	78 ± 1.2%	30.3 ± 6.4%	
	The percentage of β III tubulin+ cells	12.5 ± 0.7%	5.6 ± 0.4%	2.4 ± 0.4%	
Neuronal (9 days)	The percentage of β III tubulin+ cells	94.6 ± 1.3%	95 ± 1.2%	ND	[15]
	The percentage of cells expressing neuron-specific markers	c. 65%	c. 65%		
	The level of constitutively released dopamine	610 ± 21.7 pg/mL	559 ± 33.5 pg/mL		
	The level of ATP-stimulated release of dopamine	920 ± 45.6 pg/mL	813.5 ± 47.7 pg/mL		
Endothelial (12 days)	Flk-1 expression	17-fold increase	6-fold increase	ND	[16]
	vWF expression	13-fold increase	5-fold increase		
	VE-cadherin expression	16-fold increase	4.5-fold increase		
	Total tubule length of network in Matrigel angiogenesis assay	15 mm	11 mm		
Pancreatic (3 days)	Diameter of formed islet-like cell clusters	Larger (100–200 μm)	Smaller (<100 μm)	ND	[17]
	The percentage of differentiated cells expressing pancreatic-specific marker C-peptide	53.3%	30.9%		
	Insulin secretion on day 1 after differentiation	14 mIU/L	7 mIU/L		

Interestingly, the plasticity of UC-MSCs may depend on the conditions of pregnancy. UC-MSCs from preeclamptic patients were more committed to neuroglial differentiation: the protein expressions of neuronal (MAP-2) and oligodendrocytic (MBP) markers were significantly increased in cells from preeclampsia versus gestational age-matched controls [80]. At the same time, preterm birth had no effect on neuronal differentiation of UC-MSCs when compared to term delivery [81] but led to a decrease in osteogenic potential [82]. UC-MSCs obtained from gestational diabetes mellitus patients expressed similar levels of CD105, CD90, and CD73 when compared with UC-MSCs from normal pregnant women but showed decreased cell growth and earlier cellular senescence with accumulation of p16 and p53, displayed significantly lower osteogenic and adipogenic differentiation potentials, and, furthermore, exhibited low mitochondrial activity and significantly reduced expression of the mitochondrial function regulatory genes *ND2*, *ND9*, *COX1*, *PGC-1α*, and TFAM [83]. Thus, impaired metabolism of the maternal organism during pregnancy has a significant impact on the biological properties of neonatal MSCs. This fact should be taken into account when choosing a source of cells for clinical use.

10. Secretome of UC-MSCs

MSCs produce a variety of bioactive compounds that supply a paracrine mechanism for their therapeutic activity. However, UC-MSCs' secretome differs significantly from MSCs from other sources (bone marrow and adipose tissue). The most obvious dissimilarity is the almost complete absence of synthesis of the main proangiogenic factor VEGF-A: the level of secretion is 10^2 less than AT-MSCs and 10^3 less than BM-MSCs [59, 84, 85]. Wherein, transcription level of VEGF gene expression is detectable [85] and, according to some reports, is very similar to that of BM-MSC [57]. The production of some proangiogenic factors (including angiogenin and PLGF) by UC-MSCs is also reduced, and the production of some antiangiogenic factors (including thrombospondin-2 and endostatin) is increased compared with BM-MSCs and AT-MSCs [84, 85]. Contrariwise, UC-MSCs expressed higher levels of angiogenic chemokines such as CXCL1, CXCL,

CXCL5, CXCL6, and CXCL8 and angiogenic growth factors like HGF, bFGF, VEGF-D, PDGF-AA, TGF-β2, G-CSF, and TGF-β2 [59, 84, 86, 87]. Consequently, UC-MSCs realize their proangiogenic capacity by a VEGF-A-independent pathway [20, 85].

It has also been reported that UC-MSCs exhibited increased secretion of neurotrophic factors such as bFGF, nerve growth factor (NGF), neurotrophin 3 (NT3), neurotrophin 4 (NT4), and glial-derived neurotrophic factor (GDNF) compared to BM-MSCs and AT-MSCs [14]. Based on these and published data, the authors of the study believe that UC-MSCs could be precommitted to an ectodermal fate.

Additionally, UC-MSCs secrete significantly higher amounts of several important cytokines and hematopoietic growth factors, including G-CSF, GM-CSF, LIF, IL-1α, IL-6, IL-8, and IL-11, compared to BM-MSCs, and thus are better candidates for hematopoietic stem cells expansion [88].

11. The Immunomodulatory Properties of UC-MSCs

In 2008, Weiss et al. were the first to investigate the immunomodulatory properties of UC-MSCs. *In vitro* study supported five main conclusions:

(1) UC-MSCs suppressed the proliferation of Con-A-stimulated rat splenocytes (xenograft model) or activated human peripheral blood mononuclear cells (allogeneic model).

(2) UC-MSCs did not stimulate the proliferation of allogeneic or xenogeneic immune cells.

(3) UC-MSCs produced an immunosuppressive isoform of human leukocyte antigen HLA-G6 that inhibited the cytolytic activity of NK cells.

(4) UC-MSCs did not express immune response-related surface antigens CD40, CD80, and CD86, which participated in T lymphocytes activation.

(5) UC-MSCs produced anti-inflammatory cytokines, which provided their immunomodulatory properties [89].

It is currently believed that the immunomodulatory activity of UC-MSCs is provided by the paracrine mechanism. For example, UC-MSCs produce IL-6 that instructs dendritic cells to acquire tolerogenic phenotypes [90], prostaglandin E2 (PGE2) that suppresses NK cells cytotoxicity [91] and CD4+ and CD8+ T-cell proliferation [92], and indoleamine 2,3-dioxygenase (IDO) that inhibits the differentiation of circulating T follicular helper cells [93]. In contrast to BM-MSCs and AT-MSCs, UC-MSCs secrete anti-inflammatory cytokine IFN-α [84]. After exposure with proinflammatory cytokine IL-1β for 48 hours, UC-MSCs exhibited comparatively elevated expression of immunomodulatory molecules TGFβ1, IDO, TNF-stimulated gene 6 protein (TSG-6), and PGE2, when compared to MSCs from bone marrow or placenta [22]. PGE2 secreted by activated MSCs drives resident macrophages with M1 proinflammatory phenotype toward M2 anti-inflammatory phenotype and TSG-6 interacts with CD44 on resident macrophages to decrease TLR2/NFκ-B signaling and thereby decrease the secretion of proinflammatory mediators of inflammation. These findings place MSCs (and especially UC-MSCs due to their secretome) at the center of early regulators of inflammation [94].

Interestingly, culture conditions may influence the UC-MSCs' immunomodulatory properties: UC-MSCs-mediated suppression of T-cell proliferation in an allogeneic mixed lymphocyte reaction is more effective in xeno-free (containing GMP-certified human serum) and serum-free media than in standard fetal bovine serum-containing cultures. Therefore, the removal of xenogeneic components of the culture medium is important for future clinical study design in regenerative and transplant medicine [95].

12. Mitochondrial Transfer between UC-MSCs and Damaged Cells

About ten years ago the unexpected observation that MSCs can rescue cells with nonfunctional mitochondria by the transfer of either mitochondria or mitochondrial DNA was made [96]. The observation had broad implications for the therapeutic potentials of MSCs because failure of mitochondria is an initial event in many diseases, particularly with ischemia and reperfusion of tissues [97].

In a recent study, the capability of UC-MSCs to transfer their own mitochondria into mitochondrial DNA- (mtDNA-) depleted $\rho(0)$ cells was shown. The survival cells had mtDNA identical to that of UC-MSCs, whereas they expressed cellular markers identical to that of $\rho(0)$ cells. Importantly, these $\rho(0)$-plus-UC-MSC-mtDNA cells recovered the expression of mtDNA-encoded proteins and exhibited functional oxygen consumption and respiratory control, as well as the activity of electron transport chain (ETC) complexes I, II, III, and IV. In addition, ETC complex V-inhibitor-sensitive ATP production and metabolic shifting were also recovered. Furthermore, cellular behaviors including attachment-free proliferation, aerobic viability, and oxidative phosphorylation-reliant cellular motility were also regained after mitochondrial transfer by UC-MSCs. The therapeutic effect of UC-MSCs-derived mitochondrial transfer was stably sustained for at least 45 passages [98].

The transfer of mitochondria therefore provided a rational for the therapeutic use of UC-MSCs for ischemic injury or diseases linked to mitochondrial dysfunction.

13. Tumorigenic Potential of UC-MSCs

Perinatal stem cells possess the characteristics of both embryonic stem cells and adult stem cells as they possess pluripotency properties, as well as multipotent tissue maintenance; they represent a bridge between embryonic and adult stem cells [99]. Expression of markers of pluripotency in the UC-MSCs is higher than in BM-MSCs [8, 11, 72] but lower than in ESCs [41, 100]. Perhaps this explains the crucial difference between UC-MSCs and ESCs: UC-MSCs do not induce tumorigenesis, unlike ESCs. In one of the first works devoted to the subject, the tumor-producing capabilities of UC-MSCs were compared with human ESCs using the immunodeficient

mouse model. Animals that received human ESCs developed teratomas in 6 weeks (s.c. 85%; i.m. 75%; i.p. 100%) that contained tissues of ectoderm, mesoderm, and endoderm. No animal that received human UC-MSCs developed tumors or inflammatory reactions at the injection sites when maintained for a prolonged period (20 weeks) [101]. Moreover, it was shown that UC-MSCs could be immortalized by transduction with a lentiviral vector carrying *hTERT* (human telomerase reverse transcriptase) catalytic subunit gene but even then transfected UC-MSCs showed no transformation into tumors in nude mice [102].

In vitro model of cell culture transformation (cells were grown in the presence of breast and ovarian cancer cell conditioned medium for 30 days) demonstrated that no changes were observed in UC-MSCs' morphology, proliferation rates, or transcriptome compared to BM-MSCs that transformed into tumor-associated fibroblasts [103].

Therefore, human UC-MSCs, being nontumorigenic, have the potential for safe cell-based therapies.

14. Preclinical Studies regarding the Use of UC-MSCs

Promising results were obtained in recent preclinical studies regarding the use of UC-MSCs for the treatment of different diseases using animal models. Table 5 shows the most interesting data.

Reports from the early period of MSC-based cell therapy for tissue repair demonstrated that injected MSCs may survive, engraft, and differentiate into specific cell types and repair injured tissues. However, subsequent studies supported the notion that the level of UC-MSCs engraftment in the host organs of recipient animals was low after systemic administration and rather high after local administration. There is little evidence for the differentiation of UC-MSCs into relevant cells; it may be related to xenogeneic transplantation used in most of the studies. Presently, proposed mechanisms of UC-MSCs therapeutic activity include trophic and paracrine effects on cells of the immune system, remodeling of the extracellular matrix, angiogenesis, apoptosis, and stimulation of the migration and proliferation of resident progenitor cells [18, 19, 21–29, 31, 104]. All of the studies show amazing prospects for clinical use of UC-MSCs.

15. Clinical Studies regarding the Use of UC-MSCs

Currently, the FDA has registered dozens of clinical trials (phases 1–3) on the safety and efficacy of allogeneic unmodified UC-MSCs transplantation for the treatment of socially significant diseases. According to https://www.clinicaltrials.gov/ data [105] (search queries "wharton jelly msc" and "umbilical cord msc", results that contain "blood-derived" were excluded), UC-MSCs are used for the treatment of acute myocardial infarction, cardiomyopathies, critical limb ischemia, bronchopulmonary dysplasia in infants, HIV infection, diabetes mellitus types I and II, both acute and chronic liver diseases, autoimmune hepatitis, cirrhosis of various etiologies, ulcerative colitis, severe aplastic anemia, Alzheimer's disease, systemic lupus erythematosus, rheumatoid arthritis, myelodysplastic syndrome, hereditary ataxia, spinal cord injury, ankylosing spondylitis, osteoarthritis, multiple sclerosis, Duchenne muscular dystrophy, acute and resistant to steroid therapy "graft versus host" reactions, and other diseases. The diagrammatic representation of clinical applications of UC-MSCs is shown in Figure 3.

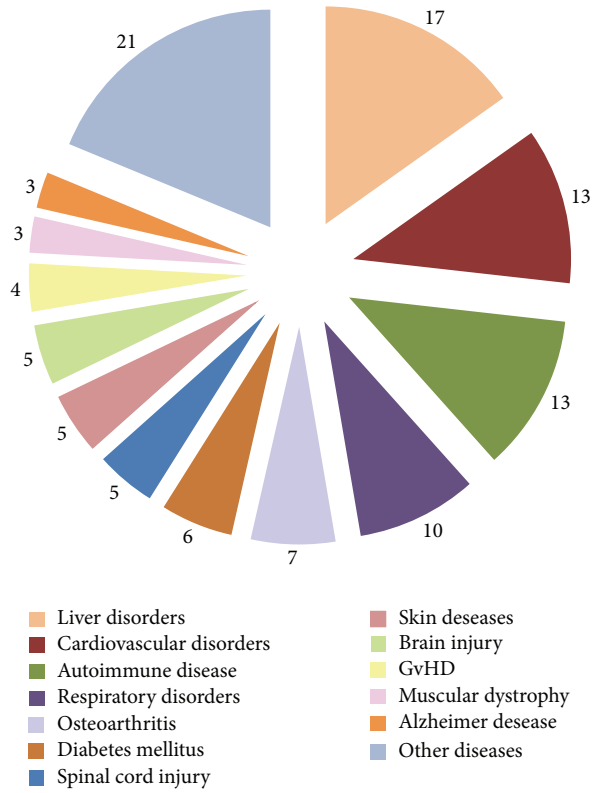

Figure 3: Number of clinical trials for UC-MSCs based therapy (https://ClinicalTrials.gov/).

At present, the results of only a small part of the clinical studies are published. Table 6 shows the most promising results of clinical trials (phases 2-3).

In all clinical studies UC-MSCs administration had no side-effects except for several cases of fever. In all clinical trials, only allogeneic transplantation of UC-MSCs is studied. This can be explained quite simply: UC-MSCs banking started a few years ago, so a set of recipient groups for autologous transplantation is not possible for the present. However, there is evidence that the efficacy of autologous and allogeneic MSCs transplantation is comparable [106–108].

The results of clinical trials using UC-MSCs are encouraging, particularly for treatment of autoimmune and endocrine diseases.

16. Requirements for the Standardization of Transplant Based on UC-MSCs

The main problem with comparing the results of experimental studies and clinical trials is the lack of a standardized protocol for the isolation, expansion, and cryopreservation

Table 5: Preclinical studies regarding the use of UC-MSCs.

Model	Animals	Treatment	Results	Cell fate	Reference
Neonatal lung injury	SCID beige mice	1×10^6 of human UC-MSCs, i.p.	The restoration of normal lung compliance, elastance, and pressure-volume loops (tissue recoil) associated with alveolar septal widening, suggestive of interstitial matrix modification	Cells tended to remain in the peritoneum or retroperitoneum, although eventually some were disseminated to and were retained in the lungs; differentiation into the relevant cells was not found	[18]
Subtotal liver resection (80% organ weight)	Sprague-Dawley rats	1×10^6 of rat UC-MSCs, intrasplenic injection	The stimulation of hepatocyte proliferation and liver weight restoration associated with more rapid recovery of mitochondria number and mitochondrial function of hepatocytes	Cells tended to remain in the spleen, although some part of them migrated to the liver; differentiation into the relevant cells was not studied	[19]
Hindlimb ischemia	BALB/c Slc-nu/nu mice	5×10^6 of human UC-MSCs predifferentiated into endothelial lineage, i.m.	The improvement of blood perfusion associated with increased blood vessel density	Some of transplanted cells were found adjacent to vessel walls; differentiation into the relevant cells was not found	[20]
Streptozotocin-induced diabetes mellitus	BALB/c mice	human UC-MSCs predifferentiated into islets like clusters, 10^3 clusters in a immunoisolatory capsule, i.p.	The reduction of hyperglycemia associated with increase of body weight	Cells survived and released insulin for 3 months of follow-up before terminating the experiment	[21]
Full skin excision wound	SCID mice	1×10^6 of human UC-MSCs seeded on decellularized amniotic membrane scaffold	The reduction of scar formation with hair growth and improved biomechanical properties of regenerated skin	Cells seeded on decellularized amniotic membrane were grafted onto the area of dermal injury; differentiation into the relevant cells was not studied	[22]
Excisional wound-splinting model	BALB/c nude mice	$0{,}8 \times 10^6$ of human UC-MSCs, intradermal injection, 0.2×10^6 of human UC-MSCs, applied to the wound bed	Accelerated wound healing associated with enhancing collagen deposition and angiogenesis	Engrafted cells did not express CD31 or differentiate into the typical cutaneous resident cells	[23]
Myocardial infarction	C57BL/6 mice	2×10^5 of human UC-MSCs, intramyocardial injection	The preservation of cardiac function associated with increased capillary density and decreased apoptosis in the injured tissue	Cells were not found to engraft the murine heart	[24]
Myocardial infarction	New Zealand white rabbits	5×10^6 of human UC-MSCs, subepicardial injection	Improved left ventricular ejection fraction and the percentage of fractional shortening, reduced amount of scar tissue	Some engrafted cells expressed troponin-I, F-actin, and connexin 43	[25]
Myocardial infarction	Guangxi Bama miniswines	40×10^6 of human UC-MSCs, intramyocardial injection	Improved myocardial perfusion and function associated with augmented vessel density and reduced cell apoptosis	Part of the engrafted cells differentiated into cardiomyocytes (cTNT+ cells) and vascular endothelia (vWF+ cells) 6 weeks after transplantation	[26]

Table 5: Continued.

Model	Animals	Treatment	Results	Cell fate	Reference
Radiation myelopathy	Sprague-Dawley rats	1×10^6 of human UC-MSCs, i.v., 4 transfusions at 1-week interval	Decreased forelimb paralysis and spinal cord histological damage, increased number of neurons in the anterior horn of the spinal cord, the endothelial cell density and the microvessel density in the white matter and gray matter of the spinal cord; increased relative magnitude of spinal cord blood flow; increased anti-inflammatory cytokine expression in the spinal cord	Cell engraftment and differentiation into the relevant cells were not studied	[27]
Dextran sulfate sodium induced acute colitis	NOD.CB_{17}-Prkdc^{scid}/J mice	2×10^6 of human UC-MSCs, i.v.	The diminution of the severity of colitis and histopathological score associated with decreased myeloperoxidase activity and the expression of cyclooxygenase 2 and iNOS in the colon	Cells were engrafted in the colon; differentiation into the relevant cells was not studied	[28]
Acute carrageenan-induced arthritis and chronic adjuvant induced arthritis models	Wistar rats	1.7×10^6 of human UC-MSCs, intraarticular	Faster remission of local and systemic arthritic manifestations associated with immunosuppression via a repression of T-cell proliferation and TGF-β-dependent paracrine promotion of iTreg conversion	Cell engraftment and differentiation into the relevant cells were not studied	[29]
Intracerebral hemorrhage	Sprague-Dawley rats	1×10^6 of human UC-MSCs overexpressing HGF, injection into the left ventricle	Motor function recovery associated with nerve fiber remyelination, reduced myelin-associated glycoprotein activity and higher reactivity in myelin basic protein and growth-associated protein-43	Cell engraftment and differentiation into the relevant cells were not studied	[30]
Sinonasal wound healing	New Zealand white rabbits	6×10^6 of human UC-MSCs overexpressing HGF, i.v.	Improved nasal wound healing recovery associated with reduced collagen deposition and decreased level of the fibrogenic cytokine TGF-β1	Cells migrated to the injured mucosa and epithelial layer; differentiation into the relevant cells was not found	[31]

Table 6: Clinical studies regarding the use of UC-MSCs.

Disease Number of clinical trials (NCT)	The number of recipients (age) The number of transplanted UC-MSCs The route of administration The frequency of administration	Main results	Reference
Type 1 diabetes mellitus NCT01219465	15 (≤25 years) $2{,}6 \pm 1{,}2 \times 10^6$ i.v. Twice, 4-week interval	(1) During the whole study (24 months), there was no statistical difference between treatment and control groups in mean fasting plasma glucose (FPG) and results of glutamic acid decarboxylase antibody (GADA) test In treatment group compared to control group: (2) Mean postprandial plasma glucose (PPG) levels and glycated hemoglobin HbA1c levels were lower since month 9 (3) Fasting C-peptide levels and mean C-peptide/glucose ratio (CPGR) levels were higher since month 6 (4) The dosage of insulin per day was progressively reduced since month 6. In 8 patients, the daily insulin dosage was reduced by more than 50% of the baseline, and in 3 patients insulin was discontinued. (5) No adverse reactions and no ketoacidosis appeared in treatment group, while in control group ketoacidosis appeared in 3 patients	[32]
Systemic lupus erythematosus NCT01741857	Six (15–60 years) 1×10^6 per 1 kg i.v. Once	One month after transplantation: (1) Serum indoleamine 2,3-dioxygenase (IDO) activity increased (2) Percentages of peripheral blood CD3+CD4+ T-cells decreased	[33]
Systemic lupus erythematosus NCT00698191	16 (17–55 years) 1×10^6 per 1 kg i.v. Once	(1) Significant improvements in the SLEDAI (Systemic Lupus Erythematosus Disease Activity Index) score in all patients 3 months after transplantation and in 2 patients 24 months after transplantation (2) In all patients with lupus nephritis ($n = 15$), proteinuria reduced 3 months after transplantation, 6 months after in 8 patients; 12 months after in 2 patients; 18 months after in 1 patient (3) In 13 patients with hypoproteinemia, serum albumin levels increased (4) In 6 patients with refractory cytopenias, the platelet count increased (5) The percentage of CD4+FoxP3+ T-cells (Treg cells) in peripheral blood increased (6) Serum levels of TGFβ increased, and serum levels of IL-4 decreased 3 months after transplantation (7) There was no significant difference in IL-10 levels between treatment and comparison groups	[34]
Bronchopulmonary dysplasia NCT01297205	Nine (preterm infants with birth weight of 630–1030 g) $10–20 \times 10^6$ per 1 kg Intratracheally Once	(1) There were no significant differences in the duration of intubation between treatment and comparison groups (2) BPD severity was lower in treatment group, regression coefficient 1.7 (3) In treatment group, levels of IL-1β, IL-6, IL-8, IL-10, MMP-9, TNFα, and TGFβ1 in tracheal aspirates at day 7 were significantly reduced compared with those at baseline or at day 3 posttransplantation	[35]

Table 6: Continued.

Disease Number of clinical trials (NCT)	The number of recipients (age) The number of transplanted UC-MSCs The route of administration The frequency of administration	Main results	Reference
HIV-1 NCT01213186	Seven (26–49 years) $0{,}5 \times 10^6$ per 1 kg i.v. Three transfusions at 1-month interval	(1) CD4 T-cell counts and CD4/CD8 ratio increased after 6 months of treatment compared with the individual baseline data as well as with controls (2) No significant alterations in counts of CD3 and CD8 T-cells, CD19+ B cells, CD3−CD56+ NK cells, CD3+CD56+NK T-cells, Lin-1−HLA-DR+CD11c+ mDCs, Lin-1−HLA-DR+CD123+ pDCs, and $\gamma\delta$T cells were observed (3) The percentages of naive and central memory T-cells subsets were gradually increased, whereas the effector memory and terminally differentiated effector T-cells subsets were gradually decreased (4) Significantly decreased PD-1 (programmed cell death 1) expression on total CD4, CD8 T-cells, and HIV-1-specific pentamer + CD8 T-cells at months 6, 9, and 12, and significantly increased BTLA (B-lymphocyte attenuator and T-lymphocyte attenuator) expression levels on total CD4 and CD8 T-cells were found at months 9 and 12 (5) Plasma levels of proinflammatory cytokines IFN-α2, TNF-α, IFN-γ, IL-9 (month 6), IL-1ra, IL-12p70, and IL-6 (months 6 and 12), chemokines MIP-1β, IP-10, IL-8, MCP-1, and RANTES (months 6 and 12), growth factors PDGF-BB (month 6), and G-CSF and VEGF (months 6 and 12) levels were significantly reduced	[36]
Primary biliary cirrhosis NCT01662973	Seven (33–58 years) $0{,}5 \times 10^6$ per 1 kg i.v. Three transfusions at 4-week interval	(1) There was a significant decrease in serum alkaline phosphatase and γ-glutamyltransferase levels at the end of the follow-up period (48 weeks) as compared with baseline (2) No significant changes were observed in serum alanine aminotransferase, aspartate aminotransferase, total bilirubin, albumin, prothrombin time activity, international normalized ratio, or immunoglobulin M levels	[37]
Acute-on-chronic liver failure NCT01218464	24 (24–59 years) $0{,}5 \times 10^6$ per 1 kg i.v. Three transfusions at 4-week interval	(1) The survival rates in patients were significantly increased during the 48-week follow-up period (2) There were increased levels of serum albumin and cholinesterase (12 weeks after the first transfusion), prothrombin activity (1 week after the first transfusion), hemoglobin level, and platelet counts (36 weeks after the first transfusion) (3) Serum total bilirubin (1 week after the first transfusion) and alanine aminotransferase (throughout the 48 weeks of follow-up) levels were significantly decreased	[38]
Myocardial infarction NCT01291329	58 (18–80 years) 6×10^6 Intracoronary infusion Once	(1) The absolute increase in the myocardial viability and perfusion within the infarcted territory was significantly greater than in the placebo group at four months. (2) The absolute increase in the global left ventricular ejection fraction at 18 months was significantly greater than that in the placebo group. (3) The absolute decreases in left ventricular end-systolic volumes and end-diastolic volumes at 18 months were significantly greater than those in the placebo group	[39]

of UC-MSCs [42] and of uniform requirements for the final product. The most complete published list of these requirements includes the following items:

(1) Tests for virology (HIV-1/2, HBV, HCV, HTLV-1/2, HPV, B-19, CMV, and EBV), syphilis, mycoplasma, and sterility being negative.

(2) Phenotype: the percentages of CD73+, CD90+, and CD105+ cells ≥ 98% and the percentages of CD34−, CD45−, HLA-DR−, CD14− or CD11b−, CD79a−, or CD19− ≤ 2%.

(3) Viability ≥ 80% after thawing.

(4) The content of endotoxin < 2 EU/mL and residual bovine serum albumin < 50 ng/package.

(5) No significant upregulation of transcriptase (*hTERT*) gene and oncogenes during large-scale expansion.

(6) No significant downregulation of tumor suppressor genes during large-scale expansion.

(7) Confirmed potency [109].

17. UC-MSCs Are Registered Trademark as UCX®

In the EU, UC-MSCs-based product was registered under the UCX trademark, manufactured by ECBio (Amadora, Portugal). Currently, UCX cells are being used as an active substance for the production of several off-the-shelf biopharmaceutical medicines at the point of initiating clinical trials. Research study for the UCX cells continues toward the use of these cells as an Advanced Therapy Medicinal Product (ATMP) [110].

18. UC-MSCs Banking for Clinical Use

Due to the properties demonstrated *in vitro* and *in vivo*, UC-MSCs have attracted the attention not only of the experimental groups but also of clinicians. It is no wonder that biobanks that had specialized previously only in umbilical cord blood storage introduced a new type of service, the storage of cultured MSCs from umbilical cord tissue. Among these biobanks, there are Cryo-Cell International, Inc. (Tampa Bay, USA), Precious Cells BioBank HQ (London, UK), Reliance Life Sciences (Navi Mumbai, India), Thai Health-Baby (Bangkok, Thailand), Cryosite (Granville, Australia), Pokrovsky Stem Cells Bank (Saint-Petersburg, Russia), and other biobanks. The only restriction is that biomaterial must be obtained by Caesarean section; the total number of stored samples exceeds tens of thousands [109]. It is considered that long-term cryopreservation does not change the biological properties of UC-MSCs [111]. From our point of view, the optimal solution in terms of future clinical use is simultaneous banking of cord blood (as a source of hematopoietic stem cells [4]) and cultured MSCs from umbilical cord tissue [112].

19. Conclusion

The human umbilical cord is a source of MSCs that have

(i) a unique combination of prenatal and postnatal MSCs properties;

(ii) no ethical problems with obtaining biomaterial;

(iii) significant proliferative and differentiation potential;

(iv) lack of tumorigenicity;

(v) karyotype stability;

(vi) high immunomodulatory activity.

Currently isolated and cultured umbilical cord MSCs are a promising storage object of the leading biobanks of the world, and the number of registered clinical trials on their use is currently growing.

Abbreviations

MSCs: Mesenchymal stem cells
BM-MSCs: Bone marrow-derived mesenchymal stem cells
UC-MSCs: Umbilical cord-derived mesenchymal stem cells
ISCT: International Society for Cellular Therapy
ESCs: Embryonic stem cells
AT-MSCs: Adipose tissue-derived mesenchymal stem cells.

Competing Interests

The authors declare that they have no competing interests.

Authors' Contributions

Irina Arutyunyan, Andrey Elchaninov, and Andrey Makarov drafted the paper. Timur Fatkhudinov and Irina Arutyunyan outlined, edited, and revised the paper and all authors read and approved the final paper.

Acknowledgments

This research was supported by Russian Science Foundation, Project no. 16-15-00281. The authors thank Irina Teveleva for final editing. They acknowledge Marina Tumkina for help with paper preparation.

References

[1] M. Crisan, S. Yap, L. Casteilla et al., "A perivascular origin for mesenchymal stem cells in multiple human organs," *Cell Stem Cell*, vol. 3, no. 3, pp. 301–313, 2008.

[2] A. Bongso and C.-Y. Fong, "Phenotype and differentiation potential of stromal populations obtained from various zones of human umbilical cord: an overview," *Stem Cell Reviews and Reports*, vol. 9, no. 2, pp. 226–240, 2013.

[3] "Anatomy and pathology of the umbilical cord," in *Pathology of the Human Placenta*, K. Benirschke, P. Kaufmann, and R. N. Baergen, Eds., pp. 380–451, Springer, New York, NY, USA, 2006.

[4] S. Knudtzon, "In vitro growth of granulocytic colonies from circulating cells in human cord blood," *Blood*, vol. 43, no. 3, pp. 357–361, 1974.

[5] K. D. McElreavey, A. I. Irvine, K. T. Ennis, and W. H. I. McLean, "Isolation, culture and characterisation of fibroblast-like cells derived from the Wharton's jelly portion of human umbilical cord," *Biochemical Society Transactions*, vol. 19, no. 1, article 29S, 1991.

[6] H.-S. Wang, S.-C. Hung, S.-T. Peng et al., "Mesenchymal stem cells in the Wharton's jelly of the human umbilical cord," *STEM CELLS*, vol. 22, no. 7, pp. 1330–1337, 2004.

[7] A. K. Batsali, M.-C. Kastrinaki, H. A. Papadaki, and C. Pontikoglou, "Mesenchymal stem cells derived from Wharton's jelly of the umbilical cord: biological properties and emerging clinical applications," *Current Stem Cell Research and Therapy*, vol. 8, no. 2, pp. 144–155, 2013.

[8] A. Can and S. Karahuseyinoglu, "Concise review: human umbilical cord stroma with regard to the source of fetus-derived stem cells," *STEM CELLS*, vol. 25, no. 11, pp. 2886–2895, 2007.

[9] R. El Omar, J. Beroud, J.-F. Stoltz, P. Menu, E. Velot, and V. Decot, "Umbilical cord mesenchymal stem cells: the new gold standard for mesenchymal stem cell-based therapies?" *Tissue Engineering—Part B: Reviews*, vol. 20, no. 5, pp. 523–544, 2014.

[10] C.-Y. Fong, M. Richards, N. Manasi, A. Biswas, and A. Bongso, "Comparative growth behaviour and characterization of stem cells from human Wharton's jelly," *Reproductive BioMedicine Online*, vol. 15, no. 6, pp. 708–718, 2007.

[11] U. Nekanti, V. B. Rao, A. G. Bahirvani, M. Jan, S. Totey, and M. Ta, "Long-term expansion and pluripotent marker array analysis of Wharton's jelly-derived mesenchymal stem cells," *Stem Cells and Development*, vol. 19, no. 1, pp. 117–130, 2010.

[12] J. De Kock, M. Najar, J. Bolleyn et al., "Mesoderm-derived stem cells: the link between the transcriptome and their differentiation potential," *Stem Cells and Development*, vol. 21, no. 18, pp. 3309–3323, 2012.

[13] X. Li, J. Bai, X. Ji, R. Li, Y. Xuan, and Y. Wang, "Comprehensive characterization of four different populations of human mesenchymal stem cells as regards their immune properties, proliferation and differentiation," *International Journal of Molecular Medicine*, vol. 34, no. 3, pp. 695–704, 2014.

[14] S. Balasubramanian, C. Thej, P. Venugopal et al., "Higher propensity of Wharton's jelly derived mesenchymal stromal cells towards neuronal lineage in comparison to those derived from adipose and bone marrow," *Cell Biology International*, vol. 37, no. 5, pp. 507–515, 2013.

[15] I. Datta, S. Mishra, L. Mohanty, S. Pulikkot, and P. G. Joshi, "Neuronal plasticity of human Wharton's jelly mesenchymal stromal cells to the dopaminergic cell type compared with human bone marrow mesenchymal stromal cells," *Cytotherapy*, vol. 13, no. 8, pp. 918–932, 2011.

[16] M.-Y. Chen, P.-C. Lie, Z.-L. Li, and X. Wei, "Endothelial differentiation of Wharton's jelly-derived mesenchymal stem cells in comparison with bone marrow-derived mesenchymal stem cells," *Experimental Hematology*, vol. 37, no. 5, pp. 629–640, 2009.

[17] L.-F. Wu, N.-N. Wang, Y.-S. Liu, and X. Wei, "Differentiation of Wharton's jelly primitive stromal cells into insulin-producing cells in comparison with bone marrow mesenchymal stem cells," *Tissue Engineering Part A*, vol. 15, no. 10, pp. 2865–2873, 2009.

[18] L. Liu, Q. Mao, S. Chu et al., "Intranasal versus intraperitoneal delivery of human umbilical cord tissue-derived cultured mesenchymal stromal cells in a murine model of neonatal lung injury," *American Journal of Pathology*, vol. 184, no. 12, pp. 3344–3358, 2014.

[19] A. V. El'chaninov, M. A. Volodina, I. V. Arutyunyan et al., "Effect of multipotent stromal cells on the function of cell mitochondria in regenerating liver," *Bulletin of Experimental Biology and Medicine*, vol. 158, no. 4, pp. 566–572, 2015.

[20] M. Choi, H.-S. Lee, P. Naidansaren et al., "Proangiogenic features of Wharton's jelly-derived mesenchymal stromal/stem cells and their ability to form functional vessels," *International Journal of Biochemistry and Cell Biology*, vol. 45, no. 3, pp. 560–570, 2013.

[21] S. S. Kadam and R. R. Bhonde, "Islet neogenesis from the constitutively nestin expressing human umbilical cord matrix derived mesenchymal stem cells," *Islets*, vol. 2, no. 2, pp. 112–120, 2010.

[22] V. Sabapathy, B. Sundaram, V. M. Sreelakshmi, P. Mankuzhy, and S. Kumar, "Human Wharton's jelly mesenchymal stem cells plasticity augments scar-free skin wound healing with hair growth," *PLoS ONE*, vol. 9, no. 4, Article ID e93726, 2014.

[23] R. Shohara, A. Yamamoto, S. Takikawa et al., "Mesenchymal stromal cells of human umbilical cord Wharton's jelly accelerate wound healing by paracrine mechanisms," *Cytotherapy*, vol. 14, no. 10, pp. 1171–1181, 2012.

[24] D. S. Nascimento, D. Mosqueira, L. M. Sousa et al., "Human umbilical cord tissue-derived mesenchymal stromal cells attenuate remodeling after myocardial infarction by proangiogenic, antiapoptotic, and endogenous cell-activation mechanisms," *Stem Cell Research and Therapy*, vol. 5, no. 1, article 5, 2014.

[25] M. Latifpour, S. N. Nematollahi-Mahani, M. Deilamy et al., "Improvement in cardiac function following transplantation of human umbilical cord matrix-derived mesenchymal cells," *Cardiology*, vol. 120, no. 1, pp. 9–18, 2011.

[26] W. Zhang, X. Liu, L. Yang et al., "Wharton's jelly-derived mesenchymal stem cells promote myocardial regeneration and cardiac repair after miniswine acute myocardial infarction," *Coronary Artery Disease*, vol. 24, no. 7, pp. 549–558, 2013.

[27] L. Wei, J. Zhang, X.-B. Xiao et al., "Multiple injections of human umbilical cord-derived mesenchymal stromal cells through the tail vein improve microcirculation and the microenvironment in a rat model of radiation myelopathy," *Journal of Translational Medicine*, vol. 12, no. 1, article 246, 2014.

[28] Y. Lin, L. Lin, Q. Wang et al., "Transplantation of human umbilical mesenchymal stem cells attenuates dextran sulfate sodium-induced colitis in mice," *Clinical and Experimental Pharmacology and Physiology*, vol. 42, no. 1, pp. 76–86, 2015.

[29] J. M. Santos, R. N. Bárcia, S. I. Simões et al., "The role of human umbilical cord tissue-derived mesenchymal stromal cells (UCX®) in the treatment of inflammatory arthritis," *Journal of Translational Medicine*, vol. 11, article 18, 2013.

[30] A. M. Liu, G. Lu, K. S. Tsang et al., "Umbilical cord-derived mesenchymal stem cells with forced expression of hepatocyte growth factor enhance remyelination and functional recovery in a rat intracerebral hemorrhage model," *Neurosurgery*, vol. 67, no. 2, pp. 357–365, 2010.

[31] J. Li, C.-Q. Zheng, Y. Li, C. Yang, H. Lin, and H.-G. Duan, "Hepatocyte growth factor gene-modified mesenchymal stem cells augment sinonasal wound healing," *Stem Cells and Development*, vol. 24, no. 15, pp. 1817–1830, 2015.

[32] J. Hu, X. Yu, Z. Wang et al., "Long term effects of the implantation of Wharton's jelly-derived mesenchymal stem cells from

the umbilical cord for newly-onset type 1 diabetes mellitus," *Endocrine Journal*, vol. 60, no. 3, pp. 347–357, 2013.

[33] D. Wang, X. Feng, L. Lu et al., "A CD8 T cell/indoleamine 2,3-dioxygenase axis is required for mesenchymal stem cell suppression of human systemic lupus erythematosus," *Arthritis & Rheumatology*, vol. 66, no. 8, pp. 2234–2245, 2014.

[34] L. Sun, D. Wang, J. Liang et al., "Umbilical cord mesenchymal stem cell transplantation in severe and refractory systemic lupus erythematosus," *Arthritis and Rheumatism*, vol. 62, no. 8, pp. 2467–2475, 2010.

[35] Y. S. Chang, S. Y. Ahn, H. S. Yoo et al., "Mesenchymal stem cells for bronchopulmonary dysplasia: phase 1 dose-escalation clinical trial," *Journal of Pediatrics*, vol. 164, no. 5, pp. 966–972.e6, 2014.

[36] Z. Zhang, J. Fu, X. Xu et al., "Safety and immunological responses to human mesenchymal stem cell therapy in difficult-to-treat HIV-1-infected patients," *AIDS*, vol. 27, no. 8, pp. 1283–1293, 2013.

[37] L. Wang, J. Li, H. Liu et al., "A pilot study of umbilical cord-derived mesenchymal stem cell transfusion in patients with primary biliary cirrhosis," *Journal of Gastroenterology and Hepatology*, vol. 28, supplement 1, pp. 85–92, 2013.

[38] M. Shi, Z. Zhang, R. Xu et al., "Human mesenchymal stem cell transfusion is safe and improves liver function in acute-on-chronic liver failure patients," *Stem Cells Translational Medicine*, vol. 1, no. 10, pp. 725–731, 2012.

[39] L. R. Gao, Y. Chen, N. K. Zhang et al., "Intracoronary infusion of Wharton's jelly-derived mesenchymal stem cells in acute myocardial infarction: double-blind, randomized controlled trial," *BMC Medicine*, vol. 13, article 162, 2015.

[40] M. Dominici, K. Le Blanc, I. Mueller et al., "Minimal criteria for defining multipotent mesenchymal stromal cells. The International Society for Cellular Therapy position statement," *Cytotherapy*, vol. 8, no. 4, pp. 315–317, 2006.

[41] X.-Y. Wang, Y. Lan, W.-Y. He et al., "Identification of mesenchymal stem cells in aorta-gonad-mesonephros and yolk sac of human embryos," *Blood*, vol. 111, no. 4, pp. 2436–2443, 2008.

[42] D.-R. Li and J.-H. Cai, "Methods of isolation, expansion, differentiating induction and preservation of human umbilical cord mesenchymal stem cells," *Chinese Medical Journal*, vol. 125, no. 24, pp. 4504–4510, 2012.

[43] D. Trivanović, J. Kocić, S. Mojsilović et al., "Mesenchymal stem cells isolated from peripheral blood and umbilical cord Wharton's Jelly," *Srpski Arhiv za Celokupno Lekarstvo*, vol. 141, no. 3-4, pp. 178–186, 2013.

[44] Y. Mori, J. Ohshimo, T. Shimazu et al., "Improved explant method to isolate umbilical cord-derived mesenchymal stem cells and their immunosuppressive properties," *Tissue Engineering Part C: Methods*, vol. 21, no. 4, pp. 367–372, 2015.

[45] P. Salehinejad, N. B. Alitheen, A. M. Ali et al., "Comparison of different methods for the isolation of mesenchymal stem cells from human umbilical cord Wharton's jelly," *In Vitro Cellular and Developmental Biology—Animal*, vol. 48, no. 2, pp. 75–83, 2012.

[46] Y.-F. Han, R. Tao, T.-J. Sun, J.-K. Chai, G. Xu, and J. Liu, "Optimization of human umbilical cord mesenchymal stem cell isolation and culture methods," *Cytotechnology*, vol. 65, no. 5, pp. 819–827, 2013.

[47] T. Margossian, L. Reppel, N. Makdissy, J.-F. Stoltz, D. Bensoussan, and C. Huselstein, "Mesenchymal stem cells derived from Wharton's jelly: comparative phenotype analysis between tissue and in vitro expansion," *BioMedical Materials and Engineering*, vol. 22, no. 4, pp. 243–254, 2012.

[48] I. Majore, P. Moretti, F. Stahl, R. Hass, and C. Kasper, "Growth and differentiation properties of mesenchymal stromal cell populations derived from whole human umbilical cord," *Stem Cell Reviews and Reports*, vol. 7, no. 1, pp. 17–31, 2011.

[49] J. Hua, J. Gong, H. Meng et al., "Comparison of different methods for the isolation of mesenchymal stem cells from umbilical cord matrix: proliferation and multilineage differentiation as compared to mesenchymal stem cells from umbilical cord blood and bone marrow," *Cell Biology International*, vol. 38, no. 2, pp. 198–210, 2014.

[50] F. V. Paladino, J. S. Peixoto-Cruz, C. Santacruz-Perez, and A. C. Goldberg, "Comparison between isolation protocols highlights intrinsic variability of human umbilical cord mesenchymal cells," *Cell and Tissue Banking*, vol. 17, no. 1, pp. 123–136, 2016.

[51] F. Hendijani, H. Sadeghi-Aliabadi, and S. Haghjooy Javanmard, "Comparison of human mesenchymal stem cells isolated by explant culture method from entire umbilical cord and Wharton's jelly matrix," *Cell and Tissue Banking*, vol. 15, no. 4, pp. 555–565, 2014.

[52] K. Bieback and I. Brinkmann, "Mesenchymal stromal cells from human perinatal tissues: from biology to cell therapy," *World Journal of Stem Cells*, vol. 2, no. 4, pp. 81–92, 2010.

[53] D. L. Troyer and M. L. Weiss, "Concise review: Wharton's jelly-derived cells are a primitive stromal cell population," *Stem Cells*, vol. 26, no. 3, pp. 591–599, 2008.

[54] C. T. Vangsness Jr., H. Sternberg, and L. Harris, "Umbilical cord tissue offers the greatest number of harvestable mesenchymal stem cells for research and clinical application: a literature review of different harvest sites," *Arthroscopy*, vol. 31, no. 9, pp. 1836–1843, 2015.

[55] T. K. Chatzistamatiou, A. C. Papassavas, E. Michalopoulos et al., "Optimizing isolation culture and freezing methods to preserve Wharton's jelly's mesenchymal stem cell (MSC) properties: an MSC banking protocol validation for the Hellenic Cord Blood Bank," *Transfusion*, vol. 54, no. 12, pp. 3108–3120, 2014.

[56] M. Badowski, A. Muise, and D. T. Harris, "Mixed effects of long-term frozen storage on cord tissue stem cells," *Cytotherapy*, vol. 16, no. 9, pp. 1313–1321, 2014.

[57] L.-L. Lu, Y.-J. Liu, S.-G. Yang et al., "Isolation and characterization of human umbilical cord mesenchymal stem cells with hematopoiesis-supportive function and other potentials," *Haematologica*, vol. 91, no. 8, pp. 1017–1026, 2006.

[58] A. Shaer, N. Azarpira, M. H. Aghdaie, and E. Esfandiari, "Isolation and characterization of human mesenchymal stromal cells derived from placental decidua basalis; umbilical cord wharton's jelly and amniotic membrane," *Pakistan Journal of Medical Sciences*, vol. 30, no. 5, pp. 1022–1026, 2014.

[59] H. Wegmeyer, A.-M. Bröske, M. Leddin et al., "Mesenchymal stromal cell characteristics vary depending on their origin," *Stem Cells and Development*, vol. 22, no. 19, pp. 2606–2618, 2013.

[60] S. Karahuseyinoglu, O. Cinar, E. Kilic et al., "Biology of stem cells in human umbilical cord stroma: in situ and in vitro surveys," *Stem Cells*, vol. 25, no. 2, pp. 319–331, 2007.

[61] Z.-B. Ruan, L. Zhu, Y.-G. Yin, and G.-C. Chen, "Karyotype stability of human umbilical cord-derived mesenchymal stem cells during in vitro culture," *Experimental and Therapeutic Medicine*, vol. 8, no. 5, pp. 1508–1512, 2014.

[62] G. Chen, A. Yue, Z. Ruan et al., "Human umbilical cord-derived mesenchymal stem cells do not undergo malignant transformation during long-term culturing in serum-free medium," *PLoS ONE*, vol. 9, no. 6, Article ID e98565, 2014.

[63] Z. Shi, L. Zhao, G. Qiu, R. He, and M. S. Detamore, "The effect of extended passaging on the phenotype and osteogenic potential of human umbilical cord mesenchymal stem cells," *Molecular and Cellular Biochemistry*, vol. 401, no. 1-2, pp. 155–164, 2015.

[64] S. S. Kadam, S. Tiwari, and R. R. Bhonde, "Simultaneous isolation of vascular endothelial cells and mesenchymal stem cells from the human umbilical cord," *In Vitro Cellular and Developmental Biology—Animal*, vol. 45, no. 1-2, pp. 23–27, 2009.

[65] T. Bakhshi, R. C. Zabriskie, S. Bodie et al., "Mesenchymal stem cells from the Wharton's jelly of umbilical cord segments provide stromal support for the maintenance of cord blood hematopoietic stem cells during long-term ex vivo culture," *Transfusion*, vol. 48, no. 12, pp. 2638–2644, 2008.

[66] D. Majumdar, R. Bhonde, and I. Datta, "Influence of ischemic microenvironment on human Wharton's Jelly mesenchymal stromal cells," *Placenta*, vol. 34, no. 8, pp. 642–649, 2013.

[67] C. Tantrawatpan, S. Manochantr, P. Kheolamai, Y. U-Pratya, A. Supokawe, and S. Issaragrisil, "Pluripotent gene expression in mesenchymal stem cells from human umbilical cord Wharton's jelly and their differentiation potential to neural-like cells," *Journal of the Medical Association of Thailand*, vol. 96, no. 9, pp. 1208–1217, 2013.

[68] K. Drela, A. Sarnowska, P. Siedlecka et al., "Low oxygen atmosphere facilitates proliferation and maintains undifferentiated state of umbilical cord mesenchymal stem cells in an hypoxia inducible factor-dependent manner," *Cytotherapy*, vol. 16, no. 7, pp. 881–892, 2014.

[69] F. Amiri, R. Halabian, M. D. Harati et al., "Positive selection of wharton's jelly-derived CD105+ cells by MACS technique and their subsequent cultivation under suspension culture condition: a simple, versatile culturing method to enhance the multipotentiality of mesenchymal stem cells," *Hematology*, vol. 20, no. 4, pp. 208–216, 2015.

[70] J. Xu, W. Liao, D. Gu et al., "Neural ganglioside GD2 identifies a subpopulation of mesenchymal stem cells in umbilical cord," *Cellular Physiology and Biochemistry*, vol. 23, no. 4–6, pp. 415–424, 2009.

[71] J.-Y. Hsieh, Y.-S. Fu, S.-J. Chang, Y.-H. Tsuang, and H.-W. Wang, "Functional module analysis reveals differential osteogenic and stemness potentials in human mesenchymal stem cells from bone marrow and Wharton's Jelly of umbilical cord," *Stem Cells and Development*, vol. 19, no. 12, pp. 1895–1910, 2010.

[72] Y. Han, J. Chai, T. Sun, D. Li, and R. Tao, "Differentiation of human umbilical cord mesenchymal stem cells into dermal fibroblasts in vitro," *Biochemical and Biophysical Research Communications*, vol. 413, no. 4, pp. 561–565, 2011.

[73] H. Wang, T. Zhao, F. Xu et al., "How important is differentiation in the therapeutic effect of mesenchymal stromal cells in liver disease?" *Cytotherapy*, vol. 16, no. 3, pp. 309–318, 2014.

[74] S. Yang, K. Ma, C. Feng et al., "Capacity of human umbilical cord-derived mesenchymal stem cells to differentiate into sweat gland-like cells: A Preclinical Study," *Frontiers of Medicine in China*, vol. 7, no. 3, pp. 345–353, 2013.

[75] Y. Chen, Y. Yu, L. Chen et al., "Human umbilical cord mesenchymal stem cells: a new therapeutic option for tooth regeneration," *Stem Cells International*, vol. 2015, Article ID 549432, 11 pages, 2015.

[76] N. Li, S. Pan, H. Zhu, H. Mu, W. Liu, and J. Hua, "BMP4 promotes SSEA-1$^+$ hUC-MSC differentiation into male germ-like cells *in vitro*," *Cell Proliferation*, vol. 47, no. 4, pp. 299–309, 2014.

[77] M. Latifpour, Y. Shakiba, F. Amidi, Z. Mazaheri, and A. Sobhani, "Differentiation of human umbilical cord matrix-derived mesenchymal stem cells into germ-like cells," *Avicenna Journal of Medical Biotechnology*, vol. 6, no. 4, pp. 218–227, 2014.

[78] J.-F. Li, H.-L. Yin, A. Shuboy et al., "Differentiation of hUC-MSC into dopaminergic-like cells after transduction with hepatocyte growth factor," *Molecular and Cellular Biochemistry*, vol. 381, no. 1-2, pp. 183–190, 2013.

[79] X. Wei, G. Peng, S. Zheng, and X. Wu, "Differentiation of umbilical cord mesenchymal stem cells into steroidogenic cells in comparison to bone marrow mesenchymal stem cells," *Cell Proliferation*, vol. 45, no. 2, pp. 101–110, 2012.

[80] M. Joerger-Messerli, E. Brühlmann, A. Bessire et al., "Preeclampsia enhances neuroglial marker expression in umbilical cord Wharton's jelly-derived mesenchymal stem cells," *Journal of Maternal-Fetal and Neonatal Medicine*, vol. 28, no. 4, pp. 464–469, 2015.

[81] M. Messerli, A. Wagner, R. Sager et al., "Stem cells from umbilical cord Wharton's jelly from preterm birth have neuroglial differentiation potential," *Reproductive Sciences*, vol. 20, no. 12, pp. 1455–1464, 2013.

[82] L. Penolazzi, R. Vecchiatini, S. Bignardi et al., "Influence of obstetric factors on osteogenic potential of umbilical cord-derived mesenchymal stem cells," *Reproductive Biology and Endocrinology*, vol. 7, article 106, 2009.

[83] J. Kim, Y. Piao, Y. K. Pak et al., "Umbilical cord mesenchymal stromal cells affected by gestational diabetes mellitus display premature aging and mitochondrial dysfunction," *Stem Cells and Development*, vol. 24, no. 5, pp. 575–586, 2015.

[84] P. R. Amable, M. V. T. Teixeira, R. B. V. Carias, J. M. Granjeiro, and R. Borojevic, "Protein synthesis and secretion in human mesenchymal cells derived from bone marrow, adipose tissue and Wharton's jelly," *Stem Cell Research and Therapy*, vol. 5, no. 2, article 53, 2014.

[85] P. Kuchroo, V. Dave, A. Vijayan, C. Viswanathan, and D. Ghosh, "Paracrine factors secreted by umbilical cord-derived mesenchymal stem cells induce angiogenesis in vitro by a VEGF-independent pathway," *Stem Cells and Development*, vol. 24, no. 4, pp. 437–450, 2015.

[86] P. R. Amable, M. V. Teixeira, R. B. Carias, J. M. Granjeiro, and R. Borojevic, "Gene expression and protein secretion during human mesenchymal cell differentiation into adipogenic cells," *BMC Cell Biology*, vol. 15, no. 1, article 46, 2014.

[87] S. Balasubramanian, P. Venugopal, S. Sundarraj, Z. Zakaria, A. S. Majumdar, and M. Ta, "Comparison of chemokine and receptor gene expression between Wharton's jelly and bone marrow-derived mesenchymal stromal cells," *Cytotherapy*, vol. 14, no. 1, pp. 26–33, 2012.

[88] R. Friedman, M. Betancur, L. Boissel, H. Tuncer, C. Cetrulo, and H. Klingemann, "Umbilical cord mesenchymal stem cells: adjuvants for human cell transplantation," *Biology of Blood and Marrow Transplantation*, vol. 13, no. 12, pp. 1477–1486, 2007.

[89] M. L. Weiss, C. Anderson, S. Medicetty et al., "Immune properties of human umbilical cord Wharton's jelly-derived cells," *Stem Cells*, vol. 26, no. 11, pp. 2865–2874, 2008.

[90] Y. Deng, S. Yi, G. Wang et al., "Umbilical cord-derived mesenchymal stem cells instruct dendritic cells to acquire tolerogenic phenotypes through the IL-6-mediated upregulation of

SOCS1," *Stem Cells and Development*, vol. 23, no. 17, pp. 2080–2092, 2014.

[91] D. Chatterjee, N. Marquardt, D. M. Tufa et al., "Role of gamma-secretase in human umbilical-cord derived mesenchymal stem cell mediated suppression of NK cell cytotoxicity," *Cell Communication and Signaling*, vol. 12, no. 1, article 63, 2014.

[92] M. Najar, G. Raicevic, H. I. Boufker et al., "Mesenchymal stromal cells use PGE2 to modulate activation and proliferation of lymphocyte subsets: combined comparison of adipose tissue, Wharton's Jelly and bone marrow sources," *Cellular Immunology*, vol. 264, no. 2, pp. 171–179, 2010.

[93] R. Liu, D. Su, M. Zhou, X. Feng, X. Li, and L. Sun, "Umbilical cord mesenchymal stem cells inhibit the differentiation of circulating T follicular helper cells in patients with primary Sjögren's syndrome through the secretion of indoleamine 2,3-dioxygenase," *Rheumatology*, vol. 54, no. 2, pp. 332–342, 2015.

[94] D. J. Prockop, "Concise review: two negative feedback loops place mesenchymal stem/stromal cells at the center of early regulators of inflammation," *Stem Cells*, vol. 31, no. 10, pp. 2042–2046, 2013.

[95] I. Hartmann, T. Hollweck, S. Haffner et al., "Umbilical cord tissue-derived mesenchymal stem cells grow best under GMP-compliant culture conditions and maintain their phenotypic and functional properties," *Journal of Immunological Methods*, vol. 363, no. 1, pp. 80–89, 2010.

[96] J. L. Spees, S. D. Olson, M. J. Whitney, and D. J. Prockop, "Mitochondrial transfer between cells can rescue aerobic respiration," *Proceedings of the National Academy of Sciences of the United States of America*, vol. 103, no. 5, pp. 1283–1288, 2006.

[97] D. J. Prockop and J. Y. Oh, "Medical therapies with adult stem/progenitor cells (MSCs): a backward journey from dramatic results in vivo to the cellular and molecular explanations," *Journal of Cellular Biochemistry*, vol. 113, no. 5, pp. 1460–1469, 2012.

[98] H.-Y. Lin, C.-W. Liou, S.-D. Chen et al., "Mitochondrial transfer from Wharton's jelly-derived mesenchymal stem cells to mitochondria-defective cells recaptures impaired mitochondrial function," *Mitochondrion*, vol. 22, pp. 31–44, 2015.

[99] R. R. Taghizadeh, K. J. Cetrulo, and C. L. Cetrulo, "Wharton's Jelly stem cells: future clinical applications," *Placenta*, vol. 32, supplement 4, pp. S311–S315, 2011.

[100] C.-Y. Fong, L.-L. Chak, A. Biswas et al., "Human Wharton's jelly stem cells have unique transcriptome profiles compared to human embryonic stem cells and other mesenchymal stem cells," *Stem Cell Reviews and Reports*, vol. 7, no. 1, pp. 1–16, 2011.

[101] K. Gauthaman, C.-Y. Fong, C.-A. Suganya et al., "Extra-embryonic human Wharton's jelly stem cells do not induce tumorigenesis, unlike human embryonic stem cells," *Reproductive BioMedicine Online*, vol. 24, no. 2, pp. 235–246, 2012.

[102] X.-J. Liang, X.-J. Chen, D.-H. Yang, S.-M. Huang, G.-D. Sun, and Y.-P. Chen, "Differentiation of human umbilical cord mesenchymal stem cells into hepatocyte-like cells by hTERT gene transfection in vitro," *Cell Biology International*, vol. 36, no. 2, pp. 215–221, 2012.

[103] A. Subramanian, G. Shu-Uin, K.-S. Ngo et al., "Human umbilical cord Wharton's jelly mesenchymal stem cells do not transform to tumor-associated fibroblasts in the presence of breast and ovarian cancer cells unlike bone marrow mesenchymal stem cells," *Journal of Cellular Biochemistry*, vol. 113, no. 6, pp. 1886–1895, 2012.

[104] R. Donders, M. Vanheusden, J. F. J. Bogie et al., "Human Wharton's jelly-derived stem cells display immunomodulatory properties and transiently improve rat experimental autoimmune encephalomyelitis," *Cell Transplantation*, vol. 24, no. 10, pp. 2077–2098, 2015.

[105] Database of publicly and privately supported clinical studies of human participants, http://www.clinicaltrials.gov/.

[106] L. Planka, P. Gal, H. Kecova et al., "Allogeneic and autogenous transplantations of MSCs in treatment of the physeal bone bridge in rabbits," *BMC Biotechnology*, vol. 8, article 70, 2008.

[107] Y. L. Kasamon, R. J. Jones, L. F. Diehl et al., "Outcomes of autologous and allogeneic blood or marrow transplantation for mantle cell lymphoma," *Biology of Blood and Marrow Transplantation*, vol. 11, no. 1, pp. 39–46, 2005.

[108] K. Ashfaq, I. Yahaya, C. Hyde et al., "Clinical effectiveness and cost-effectiveness of stem cell transplantation in the management of acute leukaemia: a systematic review," *Health Technology Assessment*, vol. 14, no. 54, pp. 1–172, 2010.

[109] L. Liang and Z. C. Han, "Regenerative medicine and cell therapy," in *Umbilical Cord Mesenchymal Stem Cells: Biology and Clinical Application*, J. F. Stoltz, Ed., pp. 62–70, IOS Press BV, Amsterdam, The Netherlands, 2012.

[110] J. P. Martins, J. M. Santos, J. M. de Almeida et al., "Towards an advanced therapy medicinal product based on mesenchymal stromal cells isolated from the umbilical cord tissue: quality and safety data," *Stem Cell Research and Therapy*, vol. 5, no. 1, article 9, 2014.

[111] K. Cooper and C. Viswanathan, "Establishment of a mesenchymal stem cell bank," *Stem Cells International*, vol. 2011, Article ID 905621, 8 pages, 2011.

[112] M. Secco, E. Zucconi, N. M. Vieira et al., "Mesenchymal stem cells from umbilical cord: do not discard the cord!," *Neuromuscular Disorders*, vol. 18, no. 1, pp. 17–18, 2008.

Hindawi Publishing Corporation
Stem Cells International
Volume 2016, Article ID 8414715, 10 pages
http://dx.doi.org/10.1155/2016/8414715

Research Article

Comparison of Osteogenesis between Adipose-Derived Mesenchymal Stem Cells and Their Sheets on Poly-ε-Caprolactone/β-Tricalcium Phosphate Composite Scaffolds in Canine Bone Defects

Yongsun Kim,[1] Seung Hoon Lee,[1] Byung-jae Kang,[2] Wan Hee Kim,[1] Hui-suk Yun,[3] and Oh-kyeong Kweon[1]

[1]*BK21 PLUS Program for Creative Veterinary Science Research, Research Institute for Veterinary Science and College of Veterinary Medicine, Seoul National University, Seoul 08826, Republic of Korea*
[2]*College of Veterinary Medicine and Institute of Veterinary Science, Kangwon National University, Chuncheon 24341, Republic of Korea*
[3]*Powder & Ceramics Division, Korea Institute of Materials Science, Changwon 51508, Republic of Korea*

Correspondence should be addressed to Oh-kyeong Kweon; ohkweon@snu.ac.kr

Received 16 May 2016; Revised 1 July 2016; Accepted 5 July 2016

Academic Editor: Marco Tatullo

Multipotent mesenchymal stem cells (MSCs) and MSC sheets have effective potentials of bone regeneration. Composite polymer/ceramic scaffolds such as poly-ε-caprolactone (PCL)/β-tricalcium phosphate (β-TCP) are widely used to repair large bone defects. The present study investigated the *in vitro* osteogenic potential of canine adipose-derived MSCs (Ad-MSCs) and Ad-MSC sheets. Composite PCL/β-TCP scaffolds seeded with Ad-MSCs or wrapped with osteogenic Ad-MSC sheets (OCS) were also fabricated and their osteogenic potential was assessed following transplantation into critical-sized bone defects in dogs. The alkaline phosphatase (ALP) activity of osteogenic Ad-MSCs (O-MSCs) and OCS was significantly higher than that of undifferentiated Ad-MSCs (U-MSCs). The *ALP, runt-related transcription factor 2, osteopontin,* and *bone morphogenetic protein 7* mRNA levels were upregulated in O-MSCs and OCS as compared to U-MSCs. In a segmental bone defect, the amount of newly formed bone was greater in PCL/β-TCP/OCS and PCL/β-TCP/O-MSCs/OCS than in the other groups. The OCS exhibit strong osteogenic capacity, and OCS combined with a PCL/β-TCP composite scaffold stimulated new bone formation in a critical-sized bone defect. These results suggest that the PCL/β-TCP/OCS composite has potential clinical applications in bone regeneration and can be used as an alternative treatment modality in bone tissue engineering.

1. Introduction

Synthetic bone substitutes such as collagen, hydroxyapatite (HA), β-tricalcium phosphate (β-TCP), and synthetic polymers are currently available for bone tissue regeneration. Ceramic scaffolds that consist of HA and β-TCP have been widely used to repair bone defects in clinical applications, since they have good biocompatibility and a microstructure similar to the mineral component of natural bone [1, 2]. Poly-ε-caprolactone (PCL), a type of polymer-based composite, has also been used for bone tissue engineering owing to its biodegradability, biocompatibility, and low inflammatory response [3, 4]. Some recent studies have examined the feasibility of using composite polymer/ceramic scaffolds such as PCL/β-TCP so as to combine the advantages of each material [4–6].

Cell-based tissue engineering is a promising alternative approach to bone regeneration. In particular, mesenchymal stem cells (MSCs) show great potential for therapeutic use in bone tissue engineering due to their capacity for osteogenic differentiation and regeneration [7]. However, transplanted single-cell suspensions do not attach, survive, or proliferate

on target tissues [8]. To overcome this limitation, cell sheet technology has been developed to enhance the regenerative capacity of tissue-engineered products [9, 10]. Cell sheets are beneficial for cell transplantation because they preserve cell-cell junctions as well as endogenous extracellular matrix (ECM), thereby ensuring homeostasis of the cellular microenvironment for the delivery of growth factors and cytokines that promote tissue repair over a prolonged period of time.

We hypothesized that combining polymer and ceramic scaffolds and MSCs or MSC sheets could accelerate and enhance bone regeneration in large bone defects. In this study, canine adipose-derived MSC (Ad-MSC) sheets were generated by cell sheet technology, and the osteogenic potential of Ad-MSCs and Ad-MSC sheets was investigated *in vitro*. In addition, composite PCL/β-TCP scaffolds seeded with Ad-MSCs or wrapped with osteogenic cell sheets were constructed and assessed for their osteogenic potential after transplantation into critical-sized bone defects in dogs.

2. Materials and Methods

2.1. Isolation and Culture of Canine Ad-MSCs. The study protocol was approved by the Institutional Animal Care and Use Committee of Seoul National University (SNU-140801-1). MSCs derived from canine hip adipose tissue were isolated and characterized [11]. The tissue was collected aseptically from the subcutaneous fat of a 2-year-old beagle dog under anesthesia, washed with Dulbecco's phosphate-buffered saline (DPBS; Thermo Fisher Scientific Inc., USA), minced, and then digested with collagenase type I (1 mg/mL; Sigma-Aldrich) at 37°C for 30–60 min with intermittent shaking. The suspension was filtered through a 100 μm nylon mesh and centrifuged to separate floating adipocytes from stromal cells. Preadipocytes in the stromal vascular fraction were plated at 8,000–10,000 cells/cm^2 in T175 culture flasks containing Dulbecco's modified Eagle's medium (Thermo Fisher Scientific Inc., USA) supplemented with 3.7 g/L sodium bicarbonate, 1% penicillin and streptomycin, 1.7 mM L-glutamine, and 10% fetal bovine serum (Thermo Fisher Scientific Inc., USA). Cells were incubated in a humidified atmosphere at 37°C and 5% CO_2. Unattached cells and residual nonadherent red blood cells were removed after 24 h by washing with PBS, and the culture medium was replaced every 2 days. Cells were used for experiments after the third passage.

2.2. Preparation of Osteogenic Cell Sheet (OCS) and Ad-MSC Cultures. OCS was prepared as previously described [9]. Briefly, Ad-MSCs were seeded at a density of 1×10^4 cells/cm^2 in a 100 mm culture dish and cultured in growth medium containing 0.1 μM dexamethasone (Sigma-Aldrich, USA) and 82 μg/mL L-ascorbic acid 2-phosphate (A2-P, Sigma-Aldrich, USA) for 10 days. As a positive control for Ad-MSCs induced to undergo osteogenic differentiation (O-MSCs), cells were seeded at the same density and cultured in growth medium containing 0.1 μM dexamethasone, 15 μg/mL A2-P, and 10 mM β-glycerophosphate (Sigma-Aldrich, USA) [12, 13]. Undifferentiated Ad-MSCs (U-MSCs, negative control) were cultured in unsupplemented growth medium for 10 days. Morphological changes in cells during culture were monitored under an inverted light microscope (Olympus Corp., Japan). The OCS was fixed in 4% paraformaldehyde, embedded in paraffin, sectioned at a thickness of 4 μm, and stained with hematoxylin and eosin (H&E).

2.3. Alkaline Phosphatase (ALP) Activity Measurement. Cells cultured in 100 mm dishes were used for measurement of ALP activity using an ALP assay kit (Takara Bio Inc., Japan) according to the manufacturer's instructions. Briefly, p-nitrophenyl phosphate (pNPP) solution was prepared by dissolving 24 mg pNPP substrate in 5 mL ALP buffer. Cells were scraped into 200 μL extraction solution, homogenized, and sonicated. The cleared supernatant was collected after centrifugation at 13,000 ×g and 4°C for 10 min. A 50 μL volume of cell lysate supernatant was mixed with 50 μL pNPP substrate solution and incubated at 37°C for 30 min. After adding 50 μL stop solution (0.5 N NaOH), absorbance was measured at 405 nm with a spectrophotometer.

2.4. Quantification of Mineralization. Alizarin Red S (ARS) staining was used to detect calcium mineralization. Cells cultured in 100 mm dishes for 10 days were washed twice with DPBS and fixed with 4% paraformaldehyde (Wako, Japan) at room temperature for 10 min. Cells were then washed three times with distilled water, and 3 mL of 40 mM ARS (Sigma-Aldrich, USA, pH 4.1–4.3) was added to each dish, followed by incubation at room temperature for 20 min with gentle shaking. Excess dye was removed by aspiration and cells were washed three times with distilled water. For quantification of staining, the ARS was solubilized in 2 mL cetylpyridinium chloride (Sigma-Aldrich, USA) for 1 h [14], and the absorbance at 570 nm was measured with a spectrophotometer.

2.5. Gene Expression Analysis. Total RNA was isolated from cells using the Hybrid-RTM RNA extraction kit (GeneAll Bio, Korea) according to the manufacturer's protocol. RNA concentration was determined by measuring optical density at 260 nm with a NanoDrop ND-1000 spectrophotometer (NanoDrop Technologies, USA). cDNA was synthesized from RNA using a commercially available cDNA synthesis kit (Takara Bio, Japan). Quantitative reverse transcription polymerase chain reaction (qRT-PCR) was carried out on an ABI 7300 Real-Time PCR system (Applied Biosystems, USA) and SYBR Premix Ex Taq (Takara Bio, Japan). Primer sequences are listed in Table 1. Expression levels of target genes were normalized to the level of glyceraldehyde 3-phosphate dehydrogenase (GAPDH) and quantitated with the $\Delta\Delta$Ct method [15].

2.6. Fabrication of PCL/β-TCP Scaffolds. PCL was dissolved in chloroform at 40°C. NaCl and β-TCP were ground and sieved, and granules between 25 and 33 μm were selected. β-TCP was prepared by calcination of nano-TCP (Merck, USA) at 1,000°C for 4 h. Selected NaCl granules were mixed

Table 1: Primers sequences used for quantitative reverse transcription PCR.

Target gene		Primer sequence (5′-3′)
RUNX2	Forward	TGTCATGGCGGGTAACGAT
	Reverse	TCCGGCCCACAAATCTCA
ALP	Forward	TCCGAGATGGTGGAAATAGC
	Reverse	GGGCCAGACCAAAGATAGAG
Osteopontin	Forward	GATGATGGAGACGATGTGGATA
	Reverse	TGGAATGTCAGTGGGAAAATC
Osteocalcin	Forward	CTGGTCCAGCAGATGCAAAG
	Reverse	GGTCAGCCAGCTCGTCACAGTT
BMP7	Forward	TCGTGGAGCATGACAAAGAG
	Reverse	GCTCCCGAATGTAGTCCTTG
AXIN	Forward	ACGGATTCAGGCAGATGAAC
	Reverse	CTCAGTCTGTGCCTGGTCAA
β-catenin	Forward	TACTGAGCCTGCCATCTGTG
	Reverse	ACGCAGAGGTGCATGATTTG
VEGF	Forward	CTATGGCAGGAGGAGAGCAC
	Reverse	GCTGCAGGAAACTCATCTCC
GAPDH	Forward	CATTGCCCTCAATGACCACT
	Reverse	TCCTTGGAGGCCATGTAGAC

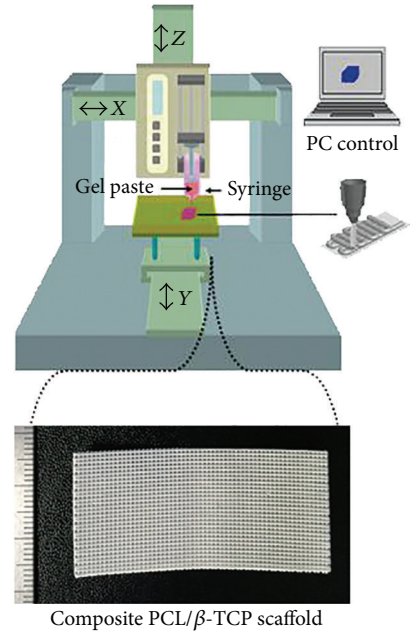

Figure 1: Photograph of a fabricated composite PCL/β-TCP scaffold. Sheet-type porous scaffolds (50 × 25 mm, five layers) were constructed by extruding the gel paste onto a substrate using a three-dimensional printing system.

with predetermined amounts of ceramic particles (1 : 1 = NaCl : PCL, 1.5 : 1 = ceramic : PCL, weight ratios). Combined powders were mixed with the PCL suspension to produce a homogeneous paste. Sheet-type porous scaffolds (50 × 25 mm, five layers) were constructed by extruding the gel paste onto a substrate using a three-dimensional (3D) printing system (Figure 1). The shapes and sizes of the PCL/β-TCP scaffold were designed using a computer system. NaCl was removed by immersing the scaffold in deionized water to produce macrosized pores in strut and the water was replaced every 2 h with fresh water at 30°C after sufficient drying of the scaffold.

2.7. Preparation of Scaffold with Ad-MSCs and Cell Sheet. Scaffolds were immersed in DPBS for 24 h. Ad-MSCs (~1 × 10^6) were seeded on the scaffolds in a 100 mm dish for the PCL/β-TCP/U-MSCs group. After 24 h of incubation, the medium was replaced with osteoinductive medium for the PCL/β-TCP/O-MSCs group. The culture was maintained for 10 days at 37°C and 5% CO_2, and the medium was changed every 48 h. For the PCL/β-TCP/OCS group, the scaffold was wrapped with four OCS after 10 days of culture. Cell-free scaffolds cultured in growth medium under the same conditions were used as controls.

2.8. Animal Experiments. Beagle dogs (n = 20, 2-3-year-old) weighing 8.7 ± 1.4 kg were used in the study. Dogs were handled in accordance with the animal care guidelines of the Institute of Laboratory Animal Resources, Seoul National University, Korea. The dogs were assigned to one of five groups (n = 4 in each): PCL/β-TCP (control), PCL/β-TCP/U-MSCs, PCL/β-TCP/O-MSCs, PCL/β-TCP/OCS, and PCL/β-TCP/O-MSCs/OCS. The Institutional Animal Care and Use Committee of Seoul National University approved the experimental design. Dogs were medicated and anesthetized with tramadol (4 mg/kg by intravenous (i.v.) injection; Toranzin; Samsung Pharmaceutical Co., Korea), propofol (6 mg/kg i.v.; Provive; Claris Lifesciences, Indonesia), and atropine sulfate (0.05 mg/kg by subcutaneous injection; Jeil Pharmaceutical Co., Korea). Anesthesia was maintained with isoflurane (Forane solution, Choongwae Pharmaceutical Co., Korea) at 1.5 minimum alveolar concentration throughout the procedure. Electrocardiography, pulse oximetry, respiratory gas analysis, and rectal temperature measurement were carried out using an anesthetic monitoring system (Datex-Ohmeda S/5; GE Healthcare, UK). Under sterile conditions, a craniomedial incision was made to the skin to expose the diaphysis of the left radius. To create a critical-sized segmental defect in the radial diaphysis, a 15 mm long segmental defect was made to the middle portion of the diaphysis using an oscillating saw (Stryker, USA) as previously described [16, 17]. Overlying periosteum was also resected from the defect area. Defects were surrounded by the experimental scaffold. A nine-hole, 2.7 mm dynamic compression plate (DePuy Synthes, Switzerland) was placed on the cranial aspect of the radius. The soft tissue was closed with 3-0 polydioxanone sutures (Ethicon, USA), and the skin was closed with 4-0 nylon sutures. All the animals were bandaged for 2 days after operation.

2.9. Microcomputed Tomography (CT) Bone Imaging. Dogs were sacrificed 12 weeks after implantation. The radius segment was excised, trimmed, and fixed in 10% formaldehyde. Samples were scanned using a micro-CT system (Skyscan;

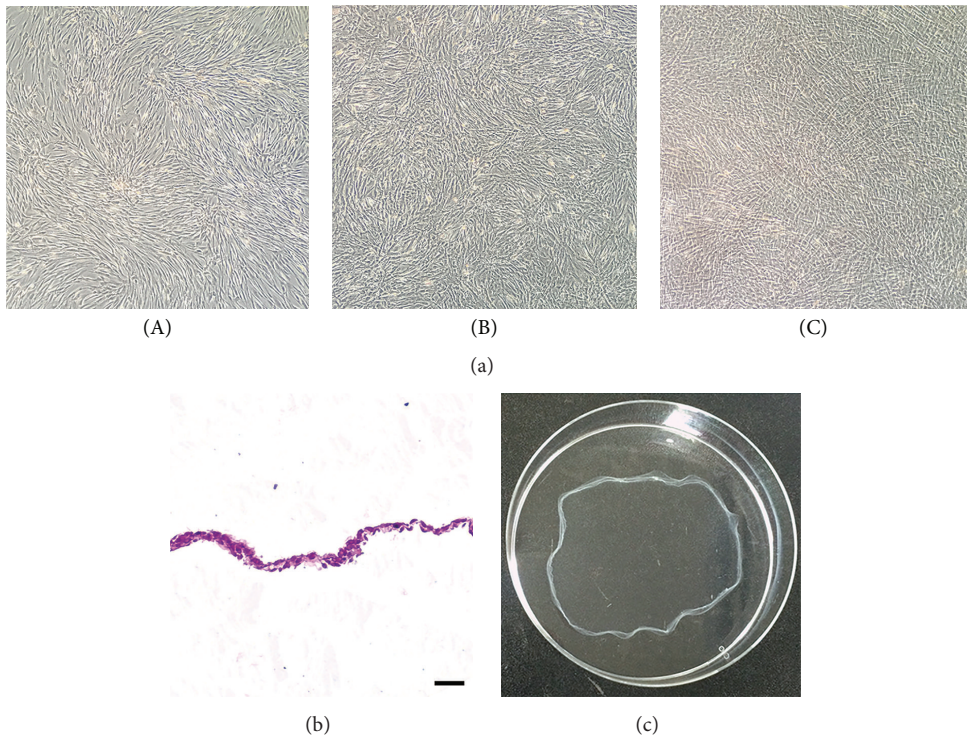

Figure 2: Morphological characteristics of the adipose-derived mesenchymal stem cells (Ad-MSCs) and Ad-MSC sheets. (a) (A) undifferentiated Ad-MSCs, (B) osteogenic Ad-MSCs, and (C) osteogenic Ad-MSC sheets observed under a phase contrast microscope. (b) OCS was composed of multiple layers of cells surrounded by ECM. (c) OCS was easily detached by cell scraper. Scale bars = 25 μm.

Bruker Corp., Belgium) and 3D images were reconstructed; the volume of newly formed bone within bone defects was calculated using the auxiliary software (Bruker Corp., Belgium).

2.10. Histological Analysis. After micro-CT measurement, specimens were decalcified in 10% ethylenediaminetetraacetic acid for 4 weeks at room temperature and then dehydrated through a graded series of alcohol, embedded in paraffin, sectioned at a thickness of 5 or 8 μm, and stained with H&E or Masson's trichrome according to standard protocols.

2.11. Statistical Analysis. Results are expressed as mean ± standard deviation. Statistical analysis was performed using SPSS v.21.0 software (IBM Corp., USA). Group means were compared with the Kruskal-Wallis tests followed by Mann-Whitney U tests. A P value of less than 0.05 was considered statistically significant.

3. Results

3.1. Cell Sheet Formation and Osteogenic Differentiation. U-MSCs and O-MSCs cultured for 10 days exhibited a spindle-shaped, fibroblast-like morphology with clearly delineated cell margins (Figures 2(a)(A) and 2(a)(B)). However, OCS appeared to overlap and were stacked on top of one another, with indistinguishable cell-cell boundaries (Figure 2(a)(C)). The OCS was composed of two to four layers of cells surrounded by ECM (Figure 2(b)), and it was easily detached by cell scraper (Figure 2(c)). ALP activity was higher in the O-MSCs and OCS than in the U-MSCs group ($P < 0.05$; Figure 3). After staining with ARS, calcium-rich granules were clearly visible in the O-MSCs group (Figure 4(a)(B)), whereas no nodules were observed in the U-MSCs and OCS groups (Figures 4(a)(A) and 4(a)(C)). The degree of ARS staining was also greater in the O-MSCs group (Figure 4(b)).

3.2. Expression of Osteogenic Differentiation Markers in Ad-MSCs and Matrix Cell Sheets. The expression of *runt-related transcription factor 2 (RUNX2), ALP, osteopontin, bone morphogenetic protein 7 (BMP7),* and *transforming growth factor beta (TGF-β)* mRNA was significantly upregulated in O-MSCs and OCS compared to the U-MSCs control ($P < 0.05$; Figure 5). *RUNX2* and *TGF-β* transcript levels were higher in OCS than in the O-MSCs group ($P < 0.05$). The involvement of the Wnt/β-catenin signaling pathway was investigated by evaluating *axis inhibition protein 2 (AXIN2)* and *β-catenin* expression. Both transcripts were upregulated in O-MSCs and OCS relative to U-MSCs ($P < 0.05$). The mRNA level of *vascular endothelial growth factor (VEGF)* tends to be downregulated in O-MSCs and OCS as compared to the U-MSCs group.

3.3. In Vivo Bone Regeneration in Canine Radial Defects. New bone was detected within defects at the bone margin. In the

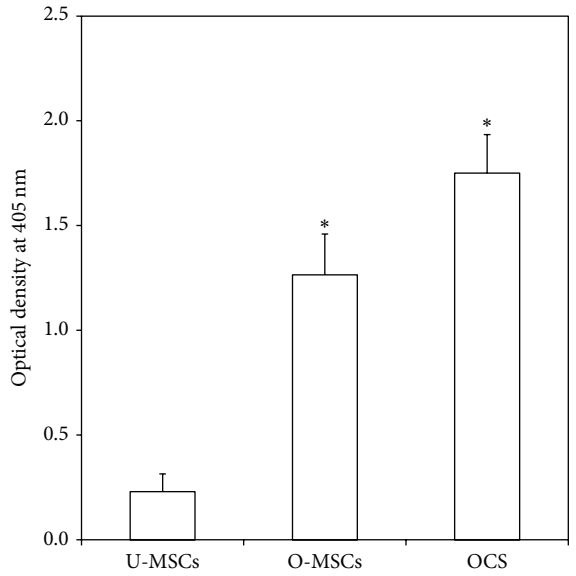

Figure 3: Quantification of alkaline phosphatase (ALP) activity. ALP activity was significantly higher in the O-MSCs and OCS than in the U-MSCs group ($^{*}P < 0.05$).

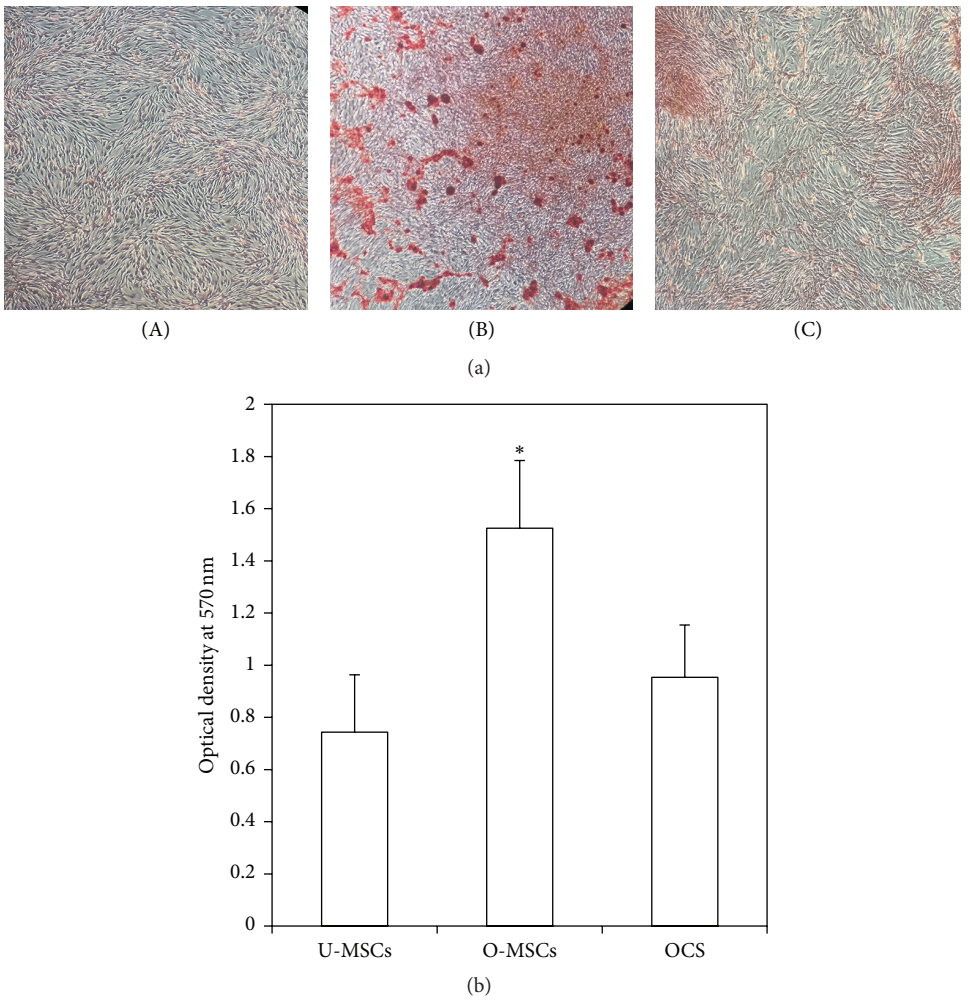

Figure 4: Alizarin Red S (ARS) staining. (a) (A) U-MSCs, (B) O-MSCs, and (C) OCS were stained using ARS solution. Calcium-rich granules were clearly visible in the O-MSCs group. (b) The degree of mineralization was greater in the O-MSCs group ($^{*}P < 0.05$).

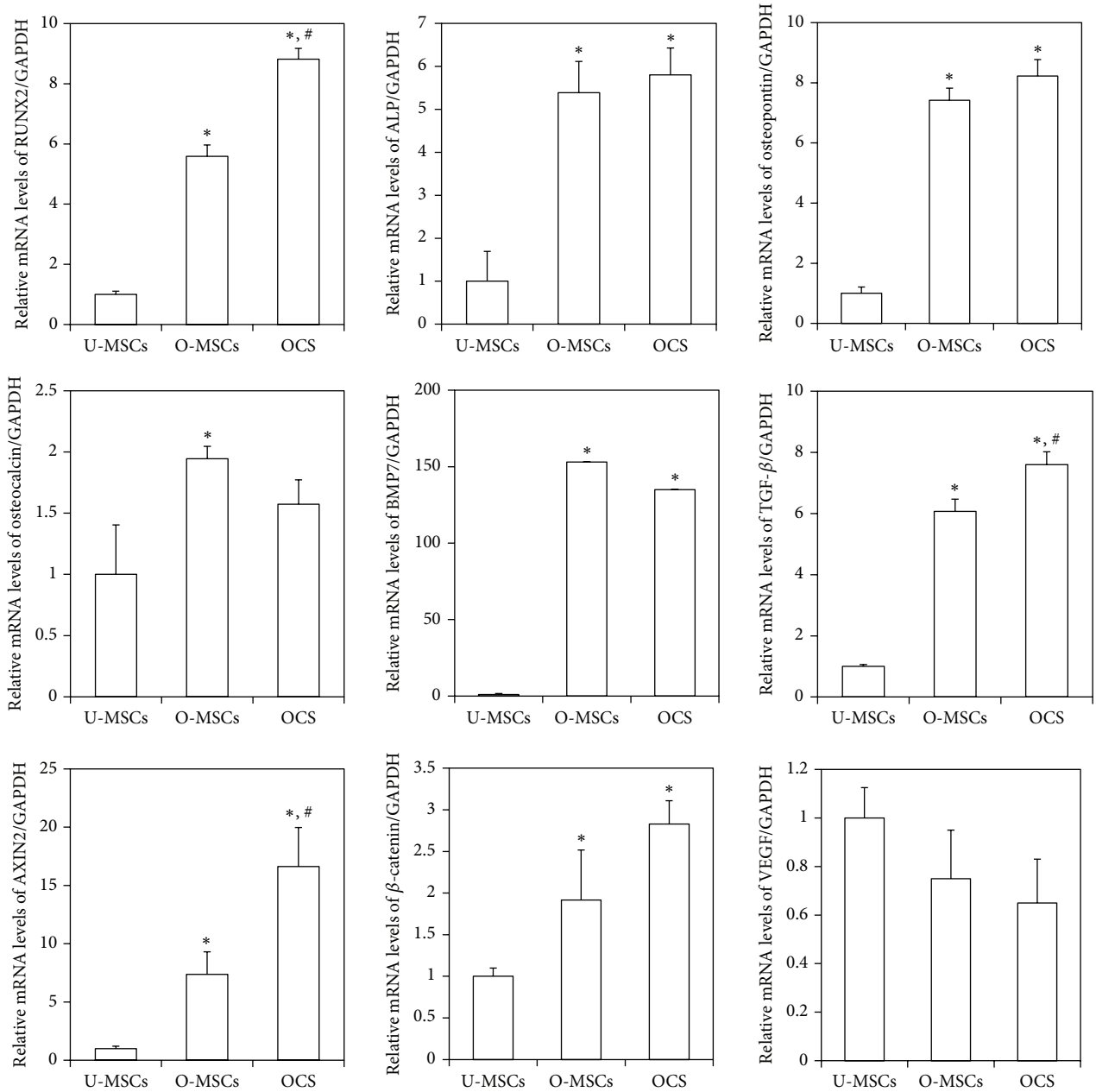

Figure 5: Expression of osteogenic differentiation markers. The expression of *RUNX2, ALP, osteopontin, BMP7*, and *TGF-β* mRNA was significantly upregulated in O-MSCs and OCS ($^{*}P < 0.05$). *RUNX2* and *TGF-β* transcript levels were higher in OCS than in the O-MSCs group ($^{\#}P < 0.05$). *AXIN2* and *β-catenin* mRNA expression was upregulated in O-MSCs and OCS ($^{*}P < 0.05$). ∗: compared to the U-MSCs group, #: compared to the O-MSCs group.

3D reconstructed image, the cone-shaped newly formed bone was visible (Figure 6(a)). From the sagittal view, the bone volume was discernible (Figure 6(b)), and a quantitative 3D micro-CT analysis revealed the following values for newly formed bone mass: PCL/β-TCP, $1.89 \pm 1.27\,cm^3$; PCL/β-TCP/U-MSC, $8.10 \pm 1.46\,cm^3$; PCL/β-TCP/O-MSC, $16.81 \pm 3.15\,cm^3$; PCL/β-TCP/OCS, $26.53 \pm 6.02\,cm^3$; and PCL/β-TCP/O-MSC/OCS, $28.11 \pm 5.5\,cm^3$ (Figure 6(c)). The amount of new bone formed was greater in all experimental groups than in the PCL/β-TCP group ($P < 0.05$). Moreover, groups with cell sheets (with or without O-MSCs) showed a greater volume of newly formed bone than the other groups ($P < 0.05$).

3.4. Histological Evaluation. At 12 weeks after implantation, decalcified paraffin sections were stained with H&E and Masson's trichrome to identify regenerated bone in defect areas. In all experimental groups, new bone was observed in longitudinal sections throughout the segmental defect and there was no obvious inflammation. Most of the defect areas

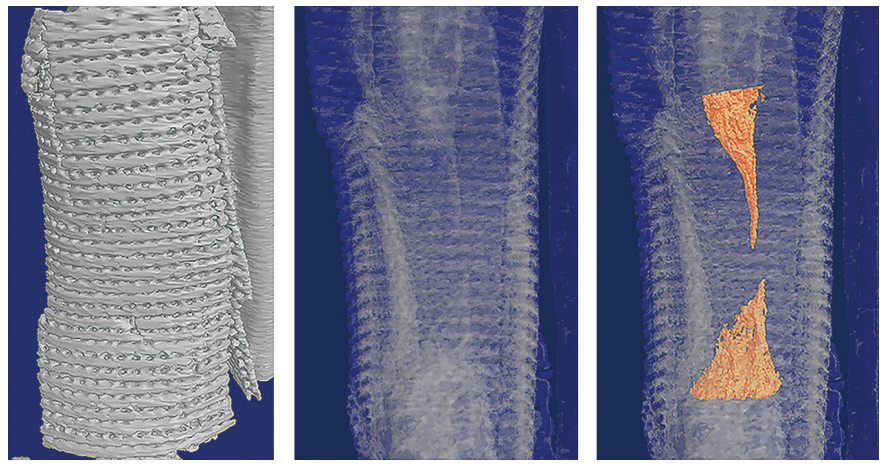

(a)

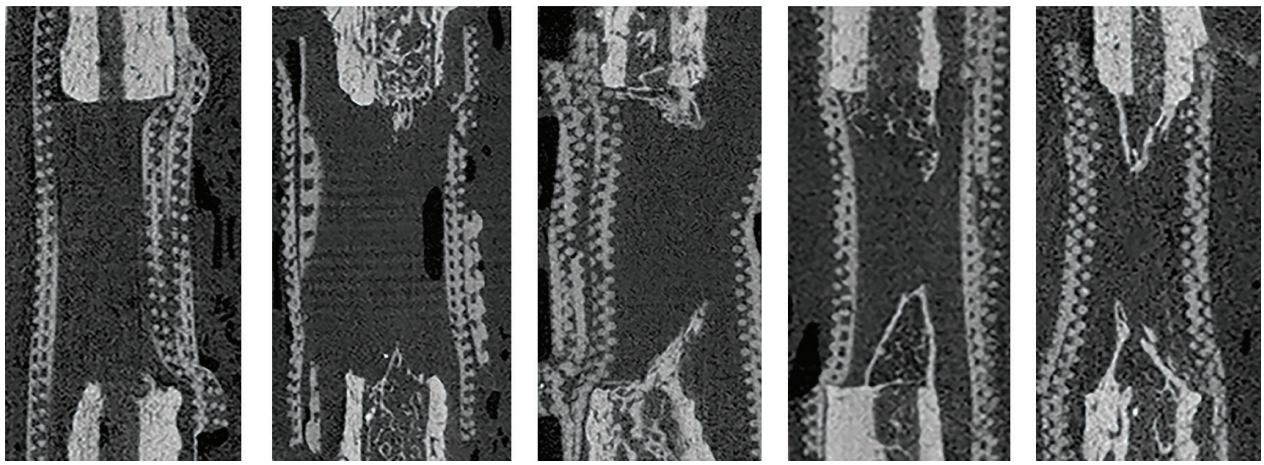

(b)

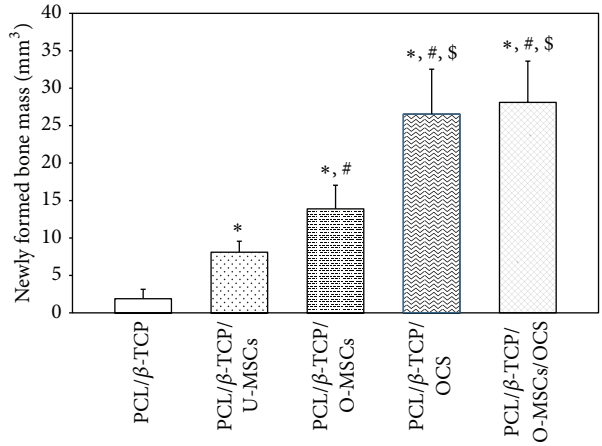

(c)

Figure 6: Bone regeneration in canine radial defects. (a) 3D reconstructed image and (b) sagittal view image showed that new bone formation was detected within defects at the bone margin. (c) Quantitative 3D micro-CT analysis revealed that groups with cell sheets (with or without O-MSCs) showed a greater volume of newly formed bone than the other groups ($^{*,\#,\$}P < 0.05$). ∗: compared to the PCL/β-TCP group, #: compared to the PCL/β-TCP/U-MSCs group, and \$: compared to the PCL/β-TCP/O-MSCs group.

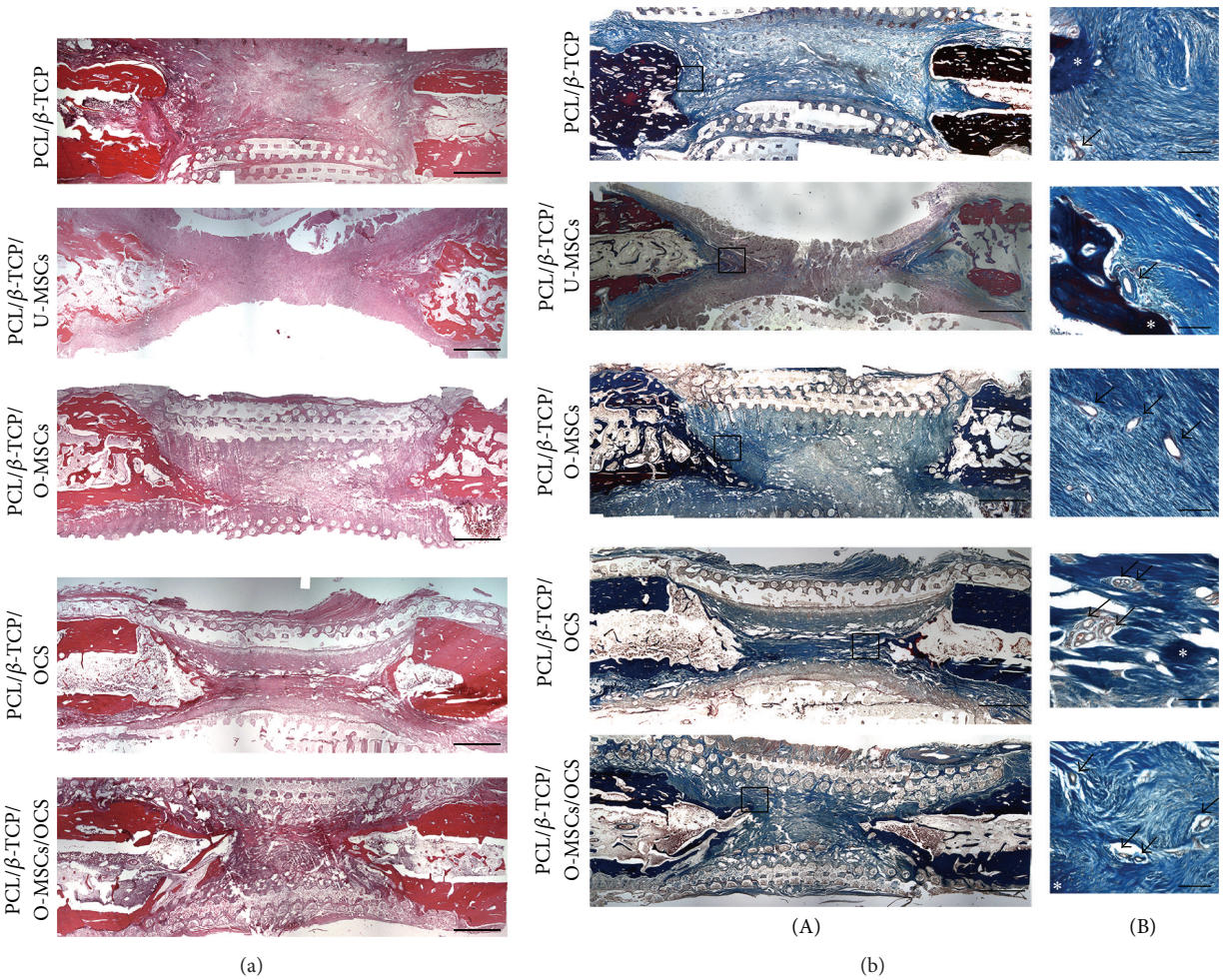

Figure 7: Histological analysis. (a) In hematoxylin and eosin staining, most of the defect areas were filled with fibrous connective tissue, and newly formed bone tissue had a woven, trabecular appearance. (b) Masson's trichrome staining revealed abundant collagenous tissue around the regenerated tissue. Vasculatures were observed inside and around the new bone. Asterisks and arrows indicate bone tissue and vasculatures, respectively. Scale bars = ((a), (b)(A)) 200 μm, ((b)(B)) 15 μm.

were filled with fibrous connective tissue and newly formed bone tissue had a woven, trabecular appearance (Figure 7(a)). Masson's trichrome staining revealed abundant collagenous tissue around the regenerated tissue (Figure 7(b)(A)). In addition, vasculatures were observed inside and around the new bone (Figure 7(b)(B)).

4. Discussion

The present study investigated the osteogenic potential of Ad-MSCs and Ad-MSC sheets, as well as that of composite PCL/β-TCP scaffolds seeded with Ad-MSCs or wrapped with OCS after their transplantation into critical-sized bone defects in dogs. MSCs have been reported to promote fracture repair; however, injection of single-cell suspensions leads to uneven distribution and weak adhesion of cells, which may ultimately result in cell death [8]. Additionally, the transplantation of isolated cells is impractical for bone regeneration in large-sized defects, which would require an adequate supply of cells. This is provided by cell sheets, which have intact cell-cell junctions and ECM that confer mechanical support and thereby maintain the integrity of the transplant [18]. In this study, we create a cell sheet using A2-P; the OCS had multiple layers of proliferating cells with ECM formation. A2-P is a stable form of ascorbic acid that plays a role in collagen biosynthesis and ECM deposition [19]. The OCS was readily detached from the culture dish using a scraper rather than a proteolytic agent such as trypsin, which preserved critical cell surface proteins such as ion channels, growth factor receptors, and cell-to-cell junction proteins.

MSCs are capable of producing multiple mesenchymal cell lineages under specific culture conditions [7, 12]. Differentiation into the osteoblastic lineage is induced by culturing in osteoinductive medium containing dexamethasone, vitamin C, and β-glycerophosphate. In this study, the O-MSCs and OCS showed strong osteogenic potential, as evidenced by upregulation of the osteogenic differentiation markers such as *RUNX2, ALP,* and *osteopontin* as well as the increase in ALP activity relative to undifferentiated Ad-MSCs. These

osteogenic effects of O-MSCs and OCS correspond well with those previously reported [20, 21]. In our *in vivo* study, the PCL/β-TCP/O-MSC group showed more extensive bone regeneration than the PCL/β-TCP/U-MSC group, likely due to the higher osteogenic potential of O-MSCs relative to U-MSCs. Moreover, there was more newly formed bone in the PCL/β-TCP/OCS and PCL/β-TCP/O-MSC/OCS groups than in those without OCS. The enhanced bone formation might be due to the delivery of osteogenic cells and ECM to the defect sites by MSC sheets.

As for the role of MSCs in bone tissue engineering, besides osteogenic differentiation, MSCs are thought to exert therapeutic effects via secretion of trophic factors that provide a supportive microenvironment for cell survival, renewal, and differentiation [22]. It has been suggested that wrapped cell sheets function as a tissue-engineered periosteum at bone defect sites. A biomimetic periosteum can maintain homeostasis of the cellular microenvironment by delivering growth factors. A previous study showed that paracrine factors of MSCs play a positive role in bone repair [23, 24]. During bone healing, the proliferation and osteoblastic differentiation of endogenous or exogenous MSCs are influenced by various growth factors, among which TGF-β and BMPs play a major role. Both are members of the TGF-β superfamily, a group of dimeric proteins, acting as growth and differentiation factors. The BMP/TGF-β signaling induces MSCs differentiation into osteoblast via activation of intracellular pathways such as SMAD and mitogen-activated protein kinase signaling [25, 26]. Wnt signaling is also crucial in bone regeneration. Wnt/β-catenin signaling pathway promotes osteoblastogenesis, activation of osteoblast activity, inhibition of osteoclast activity, and increase in bone mass [1, 27]. In the present study, OCS showed higher expression of *RUNX2*, *BMP7, TGF-β, AXIN2,* and *β-catenin*, suggesting that the induction of bone regeneration by OCS occurs via activation of the BMP/TGF-β and Wnt signal pathways.

Osteogenesis requires a well-developed vascular supply. It has been proposed that MSCs and cell sheets stimulate bone formation by inducing vascularization [7, 9, 21]. Neovascularization helps to overcome the hypoxic environment and facilitate bone formation. VEGF promotes angiogenesis and indirectly stimulates bone formation by inducing the ingress of osteoprogenitor cells. In the present study, U-MSCs, O-MSCs, and OCS expressed *VEGF*, which corresponded to the formation of a vascular network around newly formed bone tissue following transplantation of scaffolds into bone defects. This neovascularization may also have positive effects on the bone tissue regeneration.

In this study, we used a PCL/β-TCP composite as a scaffold for bone regeneration. PCL is a biodegradable polymer with a porous 3D structure [28]. This scaffold has approximately 500 μm sized pores and 70% of porosity; thus, it has large surface area. Ceramic powders such as β-TCP, which is an inorganic component of bone, may enhance the mechanical properties of the PCL scaffolds. Recent studies have shown that β-TCP has good osteoconductivity and biocompatibility and promotes MSCs adherence, survival, and osteogenic differentiation [29, 30]. Thus, in large bone defects, the PCL/β-TCP composite may provide structural and mechanical support and enhance interactions between scaffold and cells or cell sheets in a manner that is conducive to bone regeneration.

5. Conclusion

Our results demonstrate that osteogenic Ad-MSC sheets have strong osteogenic potential. Moreover, OCS combined with a PCL/β-TCP composite scaffold stimulated new bone formation to repair critical-sized bone defects in dogs. Ad-MSC sheets not only deliver osteogenic cells along with ECM, but also secrete trophic factors at defect sites for the bone regeneration. Our findings indicate that the PCL/β-TCP/OCS composite has a therapeutic potential for the treatment of bone defects and could be used to enhance current treatment practices.

Competing Interests

The authors state that there are no competing interests.

Acknowledgments

This work was supported by the National Research Foundation of Korea (NRF-2013R1A1A2004506, 2011-0017572).

References

[1] J. Guan, J. Zhang, H. Li et al., "Human urine derived stem cells in combination with β-TCP can be applied for bone regeneration," *PLoS ONE*, vol. 10, no. 5, Article ID e0125253, 2015.

[2] N. Kondo, A. Ogose, K. Tokunaga et al., "Bone formation and resorption of highly purified β-tricalcium phosphate in the rat femoral condyle," *Biomaterials*, vol. 26, no. 28, pp. 5600–5608, 2005.

[3] S. A. M. Ali, S.-P. Zhong, P. J. Doherty, and D. F. Williams, "Mechanisms of polymer degradation in implantable devices. I. Poly(caprolactone)," *Biomaterials*, vol. 14, no. 9, pp. 648–656, 1993.

[4] G. Wei and P. X. Ma, "Structure and properties of nano-hydroxyapatite/polymer composite scaffolds for bone tissue engineering," *Biomaterials*, vol. 25, no. 19, pp. 4749–4757, 2004.

[5] K. Fujihara, M. Kotaki, and S. Ramakrishna, "Guided bone regeneration membrane made of polycaprolactone/calcium carbonate composite nano-fibers," *Biomaterials*, vol. 26, no. 19, pp. 4139–4147, 2005.

[6] R. L. Simpson, F. E. Wiria, A. A. Amis et al., "Development of a 95/5 poly(L-lactide-co-glycolide)/hydroxylapatite and β-tricalcium phosphate scaffold as bone replacement material via selective laser sintering," *Journal of Biomedical Materials Research B: Applied Biomaterials*, vol. 84, no. 1, pp. 17–25, 2008.

[7] B.-J. Kang, H.-H. Ryu, S. S. Park et al., "Comparing the osteogenic potential of canine mesenchymal stem cells derived from adipose tissues, bone marrow, umbilical cord blood, and Wharton's jelly for treating bone defects," *Journal of Veterinary Science*, vol. 13, no. 3, pp. 299–310, 2012.

[8] M. Yamato and T. Okano, "Cell sheet engineering," *Materials Today*, vol. 7, no. 5, pp. 42–47, 2004.

[9] M. Akahane, A. Nakamura, H. Ohgushi, H. Shigematsu, Y. Dohi, and Y. Takakura, "Osteogenic matrix sheet-cell transplantation using osteoblastic cell sheet resulted in bone formation without scaffold at an ectopic site-," *Journal of Tissue Engineering and Regenerative Medicine*, vol. 2, no. 4, pp. 196–201, 2008.

[10] T. Long, Z. Zhu, H. A. Awad, E. M. Schwarz, M. J. Hilton, and Y. Dong, "The effect of mesenchymal stem cell sheets on structural allograft healing of critical sized femoral defects in mice," *Biomaterials*, vol. 35, no. 9, pp. 2752–2759, 2014.

[11] H.-H. Ryu, J.-H. Lim, Y.-E. Byeon et al., "Functional recovery and neural differentiation after transplantation of allogenic adipose-derived stem cells in a canine model of acute spinal cord injury," *Journal of Veterinary Science*, vol. 10, no. 4, pp. 273–284, 2009.

[12] M. Neupane, C.-C. Chang, M. Kiupel, and V. Yuzbasiyan-Gurkan, "Isolation and characterization of canine adipose-derived mesenchymal stem cells," *Tissue Engineering A*, vol. 14, no. 6, pp. 1007–1015, 2008.

[13] N. M. Vieira, V. Brandalise, E. Zucconi, M. Secco, B. E. Strauss, and M. Zatz, "Isolation, characterization, and differentiation potential of canine adipose-derived stem cells," *Cell Transplantation*, vol. 19, no. 3, pp. 279–289, 2010.

[14] C. A. Gregory, W. G. Gunn, A. Peister, and D. J. Prockop, "An Alizarin red-based assay of mineralization by adherent cells in culture: comparison with cetylpyridinium chloride extraction," *Analytical Biochemistry*, vol. 329, no. 1, pp. 77–84, 2004.

[15] K. J. Livak and T. D. Schmittgen, "Analysis of relative gene expression data using real-time quantitative PCR and the 2-ΔΔCT method," *Methods*, vol. 25, no. 4, pp. 402–408, 2001.

[16] T. L. Arinzeh, S. J. Peter, M. P. Archambault et al., "Allogeneic mesenchymal stem cells regenerate bone in a critical-sized canine segmental defect," *The Journal of Bone & Joint Surgery—American Volume*, vol. 85, no. 10, pp. 1927–1935, 2003.

[17] S. P. Bruder, K. H. Kraus, V. M. Goldberg, and S. Kadiyala, "The effect of implants loaded with autologous mesenchymal stem cells on the healing of canine segmental bone defects," *The Journal of Bone & Joint Surgery—American Volume*, vol. 80, no. 7, pp. 985–996, 1998.

[18] Q. Xie, Z. Wang, Y. Huang et al., "Characterization of human ethmoid sinus mucosa derived mesenchymal stem cells (hESMSCs) and the application of hESMSCs cell sheets in bone regeneration," *Biomaterials*, vol. 66, pp. 67–82, 2015.

[19] J. Yu, Y.-K. Tu, Y.-B. Tang, and N.-C. Cheng, "Stemness and transdifferentiation of adipose-derived stem cells using L-ascorbic acid 2-phosphate-induced cell sheet formation," *Biomaterials*, vol. 35, no. 11, pp. 3516–3526, 2014.

[20] M. Akahane, H. Shigematsu, M. Tadokoro et al., "Scaffold-free cell sheet injection results in bone formation," *Journal of Tissue Engineering and Regenerative Medicine*, vol. 4, no. 5, pp. 404–411, 2010.

[21] A. Nakamura, M. Akahane, H. Shigematsu et al., "Cell sheet transplantation of cultured mesenchymal stem cells enhances bone formation in a rat nonunion model," *Bone*, vol. 46, no. 2, pp. 418–424, 2010.

[22] R. C. Lai, S. S. Tan, B. J. Teh et al., "Proteolytic potential of the MSC exosome proteome: implications for an exosome-mediated delivery of therapeutic proteasome," *International Journal of Proteomics*, vol. 2012, Article ID 971907, 14 pages, 2012.

[23] Y.-E. Byeon, H.-H. Ryu, S. S. Park et al., "Paracrine effect of canine allogenic umbilical cord blood-derived mesenchymal stromal cells mixed with beta-tricalcium phosphate on bone regeneration in ectopic implantations," *Cytotherapy*, vol. 12, no. 5, pp. 626–636, 2010.

[24] M. Pensak, S. Hong, A. Dukas et al., "The role of transduced bone marrow cells overexpressing BMP-2 in healing critical-sized defects in a mouse femur," *Gene Therapy*, vol. 22, no. 6, pp. 467–475, 2015.

[25] G. Chen, C. Deng, and Y.-P. Li, "TGF-β and BMP signaling in osteoblast differentiation and bone formation," *International Journal of Biological Sciences*, vol. 8, no. 2, pp. 272–288, 2012.

[26] S. Vanhatupa, M. Ojansivu, R. Autio, M. Juntunen, and S. Miettinen, "Bone morphogenetic protein-2 induces donor-dependent osteogenic and adipogenic differentiation in human adipose stem cells," *Stem Cells Translational Medicine*, vol. 4, no. 12, pp. 1391–1402, 2015.

[27] T. Reya and H. Clevers, "Wnt signalling in stem cells and cancer," *Nature*, vol. 434, no. 7035, pp. 843–850, 2005.

[28] H.-S. Yun, S.-H. Kim, D. Khang, J. Choi, H.-H. Kim, and M. Kang, "Biomimetic component coating on 3D scaffolds using high bioactivity of mesoporous bioactive ceramics," *International Journal of Nanomedicine*, vol. 6, pp. 2521–2531, 2011.

[29] G. Marino, F. Rosso, G. Cafiero et al., "β-Tricalcium phosphate 3D scaffold promote alone osteogenic differentiation of human adipose stem cells: in vitro study," *Journal of Materials Science: Materials in Medicine*, vol. 21, no. 1, pp. 353–363, 2010.

[30] P. Müller, U. Bulnheim, A. Diener et al., "Calcium phosphate surfaces promote osteogenic differentiation of mesenchymal stem cells," *Journal of Cellular and Molecular Medicine*, vol. 12, no. 1, pp. 281–291, 2008.

Hindawi Publishing Corporation
Stem Cells International
Volume 2016, Article ID 3604203, 9 pages
http://dx.doi.org/10.1155/2016/3604203

Review Article

Recent Advances and Future Direction in Lyophilisation and Desiccation of Mesenchymal Stem Cells

Akalabya Bissoyi,[1] Awanish Kumar,[2] Albert A. Rizvanov,[3] Alexander Nesmelov,[3] Oleg Gusev,[3,4] Pradeep Kumar Patra,[5] and Arindam Bit[1]

[1]*Department of Biomedical Engineering, National Institute of Technology, Raipur 492010, India*
[2]*Department of Biotechnology, National Institute of Technology, Raipur 492010, India*
[3]*Institute of Fundamental Medicine and Biology, Kazan Federal University, Kazan 420000, Russia*
[4]*Preventive Medicine & Diagnosis Innovation Program (PMI), Division of Genomic Technologies, RIKEN, Yokohama 2300045, Japan*
[5]*Department of Biochemistry, Pt. JNM Medical College, Raipur 492001, India*

Correspondence should be addressed to Albert A. Rizvanov; albert.rizvanov@kpfu.ru and Arindam Bit; arinbit.bme@nitrr.ac.in

Received 18 April 2016; Accepted 3 July 2016

Academic Editor: Andrea Ballini

Mesenchymal Stem Cells (MSCs) are a promising mammalian cell type as they can be used for the reconstruction of human tissues and organs. MSCs are shown to form bone, cartilage, fat, and muscle-like cells under specific cultivation conditions. Current technology of MSCs cryopreservation has significant disadvantages. Alternative technologies of mammalian cells preservation through lyophilisation or desiccation (air-drying) are among the upcoming domains of investigation in the field of cryobiology. Different protectants and their combinations were studied in this context. Loading of the protectant in the live cell can be a challenging issue but recent studies have shown encouraging results. This paper deals with a review of the protectants, methods of their delivery, and physical boundary conditions adopted for the desiccation and lyophilisation of mammalian cells, including MSCs. A hybrid technique combining both methods is also proposed as a promising way of MSCs dry preservation.

1. Introduction

Mesenchymal Stem Cells (MSCs) are multipotent stromal cells able to differentiate into different cell types, including chondrocytes, adipocytes, and osteoblasts [1–3]. MSCs have potential utility in cell therapy and regenerative medicine, with applications relating to tissue engineering and as vehicles for gene therapy. Advantages of their usage include high plasticity, regenerative, and immunosuppressive properties and tropisms toward inflamed, hypoxic, and cancerous sites [2]. Additionally, the typical usage of MSCs for the patient was derived from autologous transplantation. It is biologically safe and free of any ethical issues associated with the source of cell.

The usage of MSCs requires their preservation in a way allowing them to be rapidly available for an application. The commonly used approach for MSCs storage is cryopreservation using liquid nitrogen [4]. This technology can ensure a high viability of stored cells but the storage, transfer, and prevention of contamination are complicated and relatively expensive. Lyophilisation (freeze-drying) and desiccation (air-drying) combined with the application of specific protective compounds emerge as a promising strategies for the storage of mammalian cells, including MSCs. As these technologies allow the storage of dried samples at ambient temperature, they can greatly simplify storage and distribution of samples, thereby decreasing the preservation cost. However, the usage of these technologies requires a revision of existing protocols in order to enhance the cell viability rates. For this purpose, we need an improved understanding of processes underlying the cell survival during water loss and in the dry state.

This paper discusses the fundamental principles, mechanisms, and advantages of the lyophilisation and desiccation usage for MSCs preservation. It also briefly describes an application and possible crosstalk of these technologies, usage

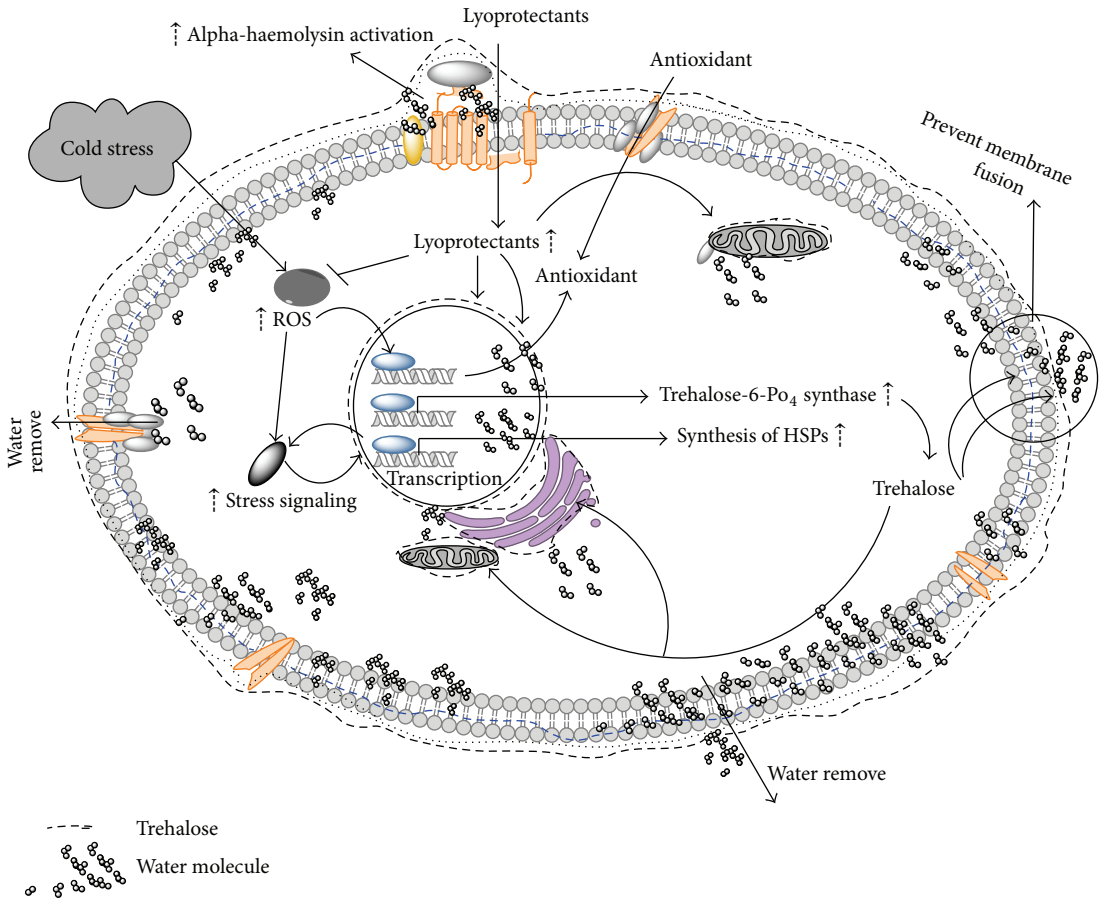

Figure 1: Molecular mechanics involved in cell lyophilisation.

of different lyoprotectants, and physiological factors involved in the cell response.

2. Lyophilisation and Desiccation

Lyophilisation is a process of drying of the frozen sample when frozen water is removed in two steps: primary drying (sublimation), followed by secondary drying (desorption). Since lyophilisation is performed at low temperature, it is used to stabilize and prolong shelf life of thermolabile products and those products which are otherwise unstable in aqueous state and hence need to be dried. The principle involved is sublimation of water at temperature and pressure below its triple point, that is, 611 Pascal and 0.0098 degree Celsius. Sublimation takes place after the sample is frozen by supplying heat through conduction or radiation or both. The driving force behind the sublimation or removal of water is the water vapour concentration gradient between the drying front and the condenser [5]. Similarly to the cryopreservation, different poly-hydroxy compounds such as sugars, polyalcohols, and their derivatives can be used in lyophilisation to protect the products that are sensitive to occurring dehydration. These compounds are called lyoprotectants and are reviewed below. The diagram summarizing the processes beyond the cell lyophilisation in the presence of nonreducing disaccharide trehalose is depicted on (Figure 1). Lyophilisation was reported to ensure the viability up to 70% of MSCs without addition of protectants [6].

Desiccation is a nature-driven process, widely used by plants and lower animals as a way to survive the water deficiency. In response to desiccation, such organisms switch to the specific state of suspended animation, anhydrobiosis, allowing them to revive when water returns [7]. Organisms capable of anhydrobiosis were found among a variety of taxa, including bacteria, yeast, invertebrates, and plants [8]. The common process underlying anhydrobiosis is an accumulation of sugars such as trehalose or sucrose [7]. In the dry state these sugars form a highly viscous glass-like medium that has been shown to be necessary for stabilization of cell components [9]. In addition, anhydrobiotes were shown to utilize a variety of protective proteins such as LEA (Late Embryogenesis Abandoned) and heat-shock proteins (HSPs), proteins of antioxidant system, or transport proteins [10]. Successful short-term storage of human fibroblast was achieved [11], but successful MSCs desiccation is not reported yet.

3. Protectants in Lyophilisation and Desiccation

A variety of protectants were tried for the dry preservation of mammalian cells. Among them, nonreducing disaccharides

trehalose and sucrose are the most popular because they are used by almost every anhydrobiotic animal. There are two main hypotheses explaining the protective effect of sugars in desiccation: (i) water-replacement hypothesis and (ii) vitrification hypothesis [9]. The water-replacement hypothesis proposes that sugars replace water interacting with polar or charged groups of biomolecules via direct hydrogen bonds. Thereby sugars stabilize the native structure of phospholipid membranes or proteins in the absence of water. The vitrification hypothesis assumes that sugars ensure a glass-like state of both cytoplasm and extracellular medium, preventing denaturation or mechanical disruption of membranes and cellular components. Proteins, such as LEA, can also play an important role in the formation of vitrified medium during desiccation [9]. Protectants naturally used by anhydrobiotic animals were successfully used for lyophilisation.

Nonreducing sugars were preferred as protectants for desiccated objects since they are less reactive than reducing monosaccharides or disaccharides like maltose. Maltose has proven to be an effective lyoprotectant for DNA [12], but its higher reactivity should be taken into account for the dry storage. Similarly, nonreducing disaccharide sucrose was shown to be more susceptible to hydrolysis into reducing monosaccharides than trehalose [7]. This indicates that trehalose might be a preferable over sucrose as a protectant in applications requiring the storage of dry samples. Interestingly, widely used cryoprotectants such as dimethyl sulfoxide (DMSO) or glycerol did not find a usage as protectants during desiccation, due to fundamental differences between these modes of preservation.

4. Advantages of Trehalose over Other Protectants

Trehalose is widely assumed as the protectant superior to others in the desiccation context. The hydration radius of trehalose is 2.5 times greater than that of sucrose, which implies that 2.5 times the concentration of sucrose is required to provide the same protein protection properties as trehalose [13]. Trehalose interacts more strongly with both water and proteins [14] and is able to displace water molecules which are bound to carbonyls at the phospholipid bilayer of cell membranes unlike to sucrose [15]. Trehalose has higher glass transition temperature (T_g) than sucrose which means that when a small amount of water is added, T_g for sucrose goes below the storage temperature and hence the sample dried with sucrose degrades more rapidly as compared to trehalose dried product (whose T_g remains above storage temperature). In addition, antioxidant effect of trehalose was shown [16]. Hence, due to all these properties of trehalose, it can be considered to be superior to the sucrose as an effective protectant for the dry storage (Table 1).

Table 1: Advantages of trehalose over sucrose as a lyoprotectant.

Sucrose	Trehalose
Vulnerable to hydrolysis under acidic conditions	Not prone to hydrolysis under acidic conditions
Smaller hydration radius; thus large amount of sucrose is required for lyophilisation	Hydration radius 2.5 times that of sucrose, thus requiring 2.5 times less trehalose for lyophilisation as compared to sucrose
Does not protect cells and proteins from oxidative damage	Protects cells and proteins from oxidative damage
Less interaction with water and hence does not displace water molecules bound to carbonyls at the phospholipid bilayer of the cell membrane	Interacts more strongly with water and thus able to displace water molecules bound to carbonyls at the phospholipid bilayer of cell membranes
Lower transition temperature	High transition temperature

5. Synergistic Enhancers

Different combinations of protective agents were tried for the desiccation of cells, since it is clear from existing studies that anhydrobiotic animals typically use the interplay of several mechanisms. Similarly to the case of trehalose, these combinations were mostly inspired by their naturally existing prototypes in different anhydrobiotic organisms. Study shows that more than 40 mM trehalose could effectively maintain the viability of MSC more than 92% for 7 days at 4°C storage temperature [17].

Expression of small heat-shock proteins (HSPs) is tightly linked to the stress tolerance, including the desiccation tolerance in African chironomid *Polypedilum vanderplanki* [18]. Probably, chaperone activity of these proteins can mitigate deleterious effects of water loss. Transfection of embryonic cells of human kidney with the gene Hsp26 protein coupled with trehalose application exhibits a sharp rise in survival after desiccation in comparison to trehalose alone [19]. This improved cell survival clearly demonstrates a useful synergy of trehalose and HSP for the recovery of cells undergoing desiccation and rehydration. Expression level of Hsp26 protein can be further increased in order to improve this method of cell drying [19].

Another promising way to improve desiccation tolerance of cells is the use of LEA proteins. LEA proteins stabilize vitrified sugar glasses which are important in the dried state [20] and protect desiccation-liable proteins from deactivation and aggregation [21]. Additionally, LEA proteins were shown to interact with biological membranes [22]; protein studied in this work was only afterwards identified as LEA protein [23]. Recently, LEA protein from African chironomid *Polypedilum vanderplanki* was reported to ensure the same level of protection as intracellular trehalose, as judged by membrane integrity after rehydration [24]. Since existing LEA proteins differ in their characteristics and localization [24, 25], their combination with each other or with other protectants is a promising way of engineering of cells tolerant to desiccation.

Combination of trehalose with other molecules has also been tested for an increase in cell viability compared to usage of trehalose alone. A study involving desiccation of bovine sperm using sorbitol as a substitute for trehalose proves

that in bovine sperm during dehydration it can be used as an excellent osmolyte and it also offers improvement in motility of sperm during desiccation. Sorbitol was found to be enhanced protection on permeating through the plasma membrane, whose mechanism is yet to understand properly [26]. Glycerol also has a significant role in combination with trehalose in achieving higher postrehydration membrane integrity in the desiccation of adipose tissue derived adult stem cells [27].

Recent studies involve the components of stress alleviating pathways such as chelators. For instance, sperm exhibited improved desiccation tolerance and enhanced survival rates when they were coupled with either sucrose or intracellular trehalose along with 1 mM Desferal to the desiccation buffer. Although sperm motility at postdrying stage did not show significant improvement, an increase in membrane integrity of sperm was observed [28]. Furthermore, recent study shows that sucrose, trehalose, and raffinose pretreatment improve postthaw viability of MSCs after cryopreservation [29].

Synergistic effect of trehalose and Arbutin (antioxidant) associated with an induction of HSPs in human MSCs was also shown [30]. These findings may highlight the correlation between the enhancer molecules and desiccation tolerance in mammalian cells which should be taken into account to derive a standard protocol.

6. Trehalose Delivery

Presence of protectants such as trehalose on both sides of the cell membrane is important for adequate protection of intracellular components and cell membrane. However, the key protectants trehalose and sucrose are not membrane permeable. In typical case, MSCs do not have transporters for those protectants. The possible use of native membrane pores such as P2X7 [35] is very limited because they are specific to only a few cell types. Human MSCs are also capable of loading trehalose from the extracellular space by a fluid-phase endocytosis [34] but this process is inefficient and cell type dependent [37]. Thus the presence of trehalose in the MSCs should be achieved artificially.

The number of proteins were shown to transport trehalose or other protective sugars into the cells, such as MalEFGK2, MAL11/AGT1, or TRET1 [38]. The advantages of TRET1 transporter are its high-capacity, specificity to the trehalose, neutral pH optimum, and expression from one gene [38]. Stable expression of TRET1 in Chinese hamster ovary (CHO) cells causes an astonishing increase by 170% of the cell viability after desiccation [38]. However, the use of this transporter may not be suitable for the MSCs preservation since this approach requires the genetic modification of the cells. The same reason may block the use of trehalose synthesis inside the cells despite of successful expression of trehalose producing genes in human fibroblast cells [32].

Direct methods of trehalose loading have also been used for the delivery of trehalose. Electropermeabilization was first tried as a trehalose delivery mechanism by Shirakashi et al. in mouse myeloma cells in isotonic trehalose substituted medium [31]. Microinjection was also successfully used for the trehalose loading in human oocytes, an attempt to improve their cryosurvival [39]. However, the poration of the cell membrane allows nonspecific transport of molecules and ions. Resulting alteration of transmembrane ionic balance may lead to significant cell damage.

A novel technique of trehalose loading involves the use of basic amino acid rich cell penetrating peptides (CPPs), such as peptide KRKRWHW [39]. This peptide was designed to deliver trehalose into mammalian cells on the base of molecular simulations. Trehalose, as a cargo coupled with the KRKRWHW peptide through hydrogen bond and π–π bond, was successfully loaded into the Mouse Embryonic Fibroblasts (MEFs) [36]. This CPP is able to efficiently deliver trehalose into mammalian cells with low cytotoxicity even at high concentrations. Therefore, this CPP may be very helpful for improving the tolerance of cells during desiccation. Similarly, Toner and his group used a genetically engineered mutant of *Staphylococcus aureus* α-hemolysin to create pores and to load trehalose into the cytoplasm of fibroblast cells [33]. In this study, trehalose was used as cryoprotectant.

Recently, a successful trehalose loading into cells was achieved through modification of its molecule [32]. Intracellular concentration of trehalose was sufficient for applications in biopreservation while the impact on cellular viability and function was negligible. Different ways of trehalose delivery into mammalian cells are summarized in Table 2.

7. Role of Physical Factors and Cell Culture Condition

The physical conditions of the macroenvironment and microenvironment of cells play a major role in the desiccation tolerance of desiccated cells. The beneficial aspect of this approach is an elimination of genetic engineering of the cells. A thorough study of the effects of various physical conditions should be carried out to make conclusions for optimization of favourable limits for all the physical parameters. Primarily, vacuum conditions improve the cell tolerance to desiccation in case of lyophilisation compared to air-drying. In case of MSCs, lyophilisation can ensure the cell viability up to 70% even without trehalose [6]. However, results of this study cannot be directly extrapolated to the cell storage because the cell viability was studied only at 2 h after lyophilisation.

Electromagnetic cryopreservation is undergoing a lot of research as a way of cryopreservation of MSCs, since static and oscillating electric fields and magnetic fields influence the ice formation [40]. Dental pulp stem cells preserved in a programmed freezer using magnetic field show around 70% viability when recovered, suggesting that magnetic freezing may be an alternate method for MSC preservation [41].

We have studied also the effect of drying rate on cell viability. Cultured cells were dried in tissue culture plates in the airflow of a biosafety cabinet. The drastically increased cell-death was observed in an absence of trehalose (data not shown). Ceasing laminar airflow caused a reduction of the rate of desiccation and an increase of cell recovery. Interestingly, clearly different cell viability was observed among different wells and within different areas of the same well. A better cell survival was observed at the well periphery,

Table 2: Different methods to deliver trehalose into cells.

Method	Explanation	Reference
Electroporation	Murine myeloma cells were loaded with trehalose by electroporation, then freeze-dried, and rehydrated	[31]
Genetically engineering the cells	Human primary fibroblasts were transfected with otsA and otsB genes from *E. coli*, encoding for trehalose synthase	[32]
Genetically engineered pores	Genetically engineered mutant of alpha-hemolysin from *Staphylococcus aureus* was used to create pores in the cellular membrane of 3T3 fibroblasts and human keratinocytes. Resulting nonselective pore is equipped with a metal-actuated switch that is sensitive to extracellular zinc concentrations, thus permitting controlled loading of trehalose	[33]
Fluid phase endocytosis	Human MSCs were loaded by trehalose up to 30 mM internal concentration at usual cultivation conditions for 24 h at 37°C in the presence of MSC medium with 0–125 mM trehalose	[34]
Endogenous cell surface receptor	TF-1 cells were permeabilized using an endogenous protein P2X7	[35]
Cell penetrating peptides (CPPs)	Trehalose was coupled with CPP and incubated with mouse embryonic fibroblast cells at usual cultivation conditions	[36]

whereas reverse occurred at the centre of the well (data not shown).

In a different set of experiments we demonstrated that MSC-like cells from third molar tooth germs maintained their biological properties, including expression of MSC surface antigens CD29, CD73, CD90, CD105, and CD166, expression of pluripotency associated genes, proliferation, and differentiation ability [42]. Importantly, cryopreserved cells displayed neuroprotective effects in a model of neuroblastoma SH-SY5Y cells exposed to oxidative and chemotherapeutic stress conditions.

Light causes deleterious effect on the cells during desiccation, probably because of the increase of the free radicals concentration. Fluorescence light was shown to generate free radicals within hamster of human cells, thereby facilitating oxidative DNA lesion and single-strand breaks. Therefore, cells desiccated and maintained at dark condition have greater viability than those exposed to the fluorescence light.

In order to optimize the ability of cell culture to withstand desiccation, the effects of desiccation temperature and cell culture confluency were also investigated. Optimal desiccation tolerance was found at higher cell density. Cell aggregation decreases their tolerance to desiccation. The temperature of operation for cell desiccation greatly influences the viability of cells, and the optimal survival point was found to be slightly lower than room temperature (20°). Recovery of desiccated cells was sufficient at this optimum temperature only. Therefore, it can be summarized that vacuum encapsulates the cells during the process of desiccation thereby improving the cell viability. Also, it had been found that cells can survive without addition of carbohydrates (or polyols) if the slow process of desiccation is followed by vacuum storage. A consistent outcome of the procedure can be obtained by defining a desiccation process which preserves cellular structures. Even in this case, gradual loss of viability may be found because of destruction with time of the desiccated state due to release of free radicals [11].

8. Application of Lyophilisation and Desiccation and Molecular Mechanism Involved

Survival of cells in dry and desiccated states is few of the most fascinating phenomena of nature and is lot to explore. The ability of MSCs to withstand these conditions for sustaining high degree of viability could have applications for wide spectrum of biological sciences, including tissue engineering. From above discussion it can be concluded that the lyophilisation and desiccation are two competing formulators for long-term storage of MSC. Both these technologies have been quite successfully applied in a wide range of fields including tissue engineering. Preservation of MSCs through desiccation in the dry state is used to meet the growing demand for MSCs storage and transport in regenerative medicine. Desiccation provides significant advantages over lyophilisation because of simplicity and higher energy efficiency. However desiccation may cause cell stress such as changes in cell volume, osmotic pressure, shrinkage of membrane/cell organelles, changes in activity of enzyme, metabolism downregulation, increased salt concentrations, cell viscosity changes, and stress protein production [43]. Lyophilisation seems to be more safe technology in this respect since it helps to avoid damage maintaining sample frozen throughout drying. Lower cell damage and loss of activity and higher degree of dehydration are the principle advantages of lyophilisation. Lyophilisation should be used when complete rehydration needed and product are heat liable, unstable, or high valuable. However, lyophilisation may also cause problems due to changes in liquid phase, solubility, and water freezing [44]. Thus, both processes have their own pros and cons and different application.

The potential of MSCs in regenerative medicine increases the importance of development of optimized protocols for their desiccation and lyophilisation. Uptake of protectants by MSCs is required for successful desiccation or lyophilisation.

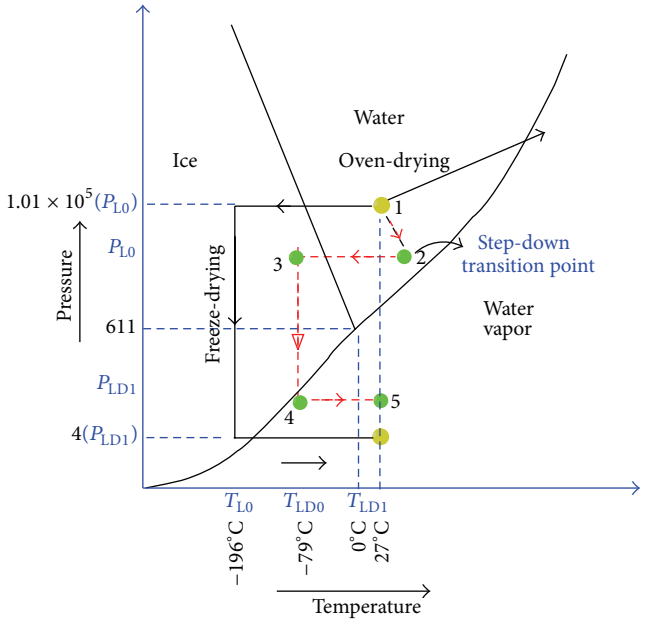

FIGURE 2: Phase diagram for cells under lyophilisation and desiccation.

However, uptake of protectant by cells can cause cellular response specific to the cell type. Since HSPs are able to improve the cell viability and protect cells from apoptosis during freeze-drying [19], some MSCs cells may be more resistant because of their ability to produce higher HSP levels. Similarly, MSCs can differ in antioxidant response to the activation of stress sensing mechanisms under desiccation or lyophilisation. Since antioxidants have protective potential for a dry storage [30], this difference should also be taken into account.

9. Crosstalk between the Process of Lyophilisation and Desiccation

Thermodynamic aspects of the above two processes of preservation of MSC are interestingly competitive. Each process can involve quantization of temperature and pressure for transition from one state to another in order to improve cellular viability. Figure 2 shows a typical thermodynamic diagram for fluidic matter (specifically extracellular and intracellular fluid).

In the figure, black arrowed path indicates the normal process of lyophilisation which involves vitrification followed by creation of extensive vacuum at a temperature of −79 degrees centigrade. This process is expensive as well as time consuming. On the other hand, desiccation involves greater cellular mortality due to rapid dehydration of cellular masses by overshooting the base temperature of the cellular medium to a higher point. A brief description of the heat transfer accounted during the process of lyophilisation is described below.

Bioheat equation for heat transfer in a system of suspended cells in ultrathin straw (UTS) undergoing for slow cooling or vitrification can be realised by zero-dimensional heat transfer equation and it is given as

$$\frac{1}{r}\frac{\partial}{\partial r}\left(\lambda r\frac{\partial T}{\partial r}\right)+\frac{\partial}{\partial z}\left(\lambda\frac{\partial T}{\partial z}\right)+\dot{q}=\rho c_p\frac{\partial T}{\partial t}, \tag{1}$$

where λ, c_p, and $\dot{q}$ refers to thermal conductivity, specific heat, and metabolic heat source, respectively. Latent heat thus released is considered as ineffective, because insignificant volume ratio of ice to the maximum crystallisable ice x is (1×10^{-3}). Since the diameter of cellular suspension is much smaller than the length of UTS, therefore, heat transfer along the axis can be neglected. Additionally, thermal property within the UTS can be assumed to be uniform and temperature-independent. Thus, the above equation can be simplified as

$$\frac{1}{r}\frac{\partial}{\partial r}\left(r\frac{\partial T}{\partial r}\right)=\frac{1}{\alpha}\frac{\partial T}{\partial t}, \tag{2}$$

where α is the thermal diffusivity.

Let the initial temperature of the suspension be T_0 and let the final temperature be T_∞. Let the dimensionless form of temperature be expressed as

$$\theta^* = \frac{T - T_\infty}{T_0 - T_\infty}. \tag{3}$$

Therefore, the transient temperature distribution can be written as

$$\theta^* = \sum_{n=1}^{\infty} C_n \exp\left(-\zeta_n^2 F_0\right) J_0\left(\zeta_n \frac{r}{r_0}\right), \tag{4}$$

where

$$F_0 = \frac{\alpha t}{r_0^2},$$
$$C_n = \frac{2}{\zeta_n}\left[\frac{J_1(\zeta_n)}{J_0^2(\zeta_n) + J_1^2(\zeta_n)}\right], \tag{5}$$

where J_0 and J_1 are Bessel functions and are positive roots of the transcendental equation defined by ζ_n:

$$\zeta_n \frac{J_1(\zeta_n)}{J_0(\zeta_n)} = \frac{2hr_0}{k}, \tag{6}$$

where heat transfer coefficient is denoted by "h" and often it evaluates the quality of the cryopreservation system.

The production of volume fraction of ice (x) is governed by the equation

$$\frac{dx}{dt} = \kappa a_1(x)(T_m - T)\exp\left(\frac{-Q}{RT}\right), \tag{7}$$

where

$$\kappa = \frac{L}{\pi\lambda^2 \nu T_m r_f},$$
$$a_1(x) = x^{2/3}(1 - x), \tag{8}$$

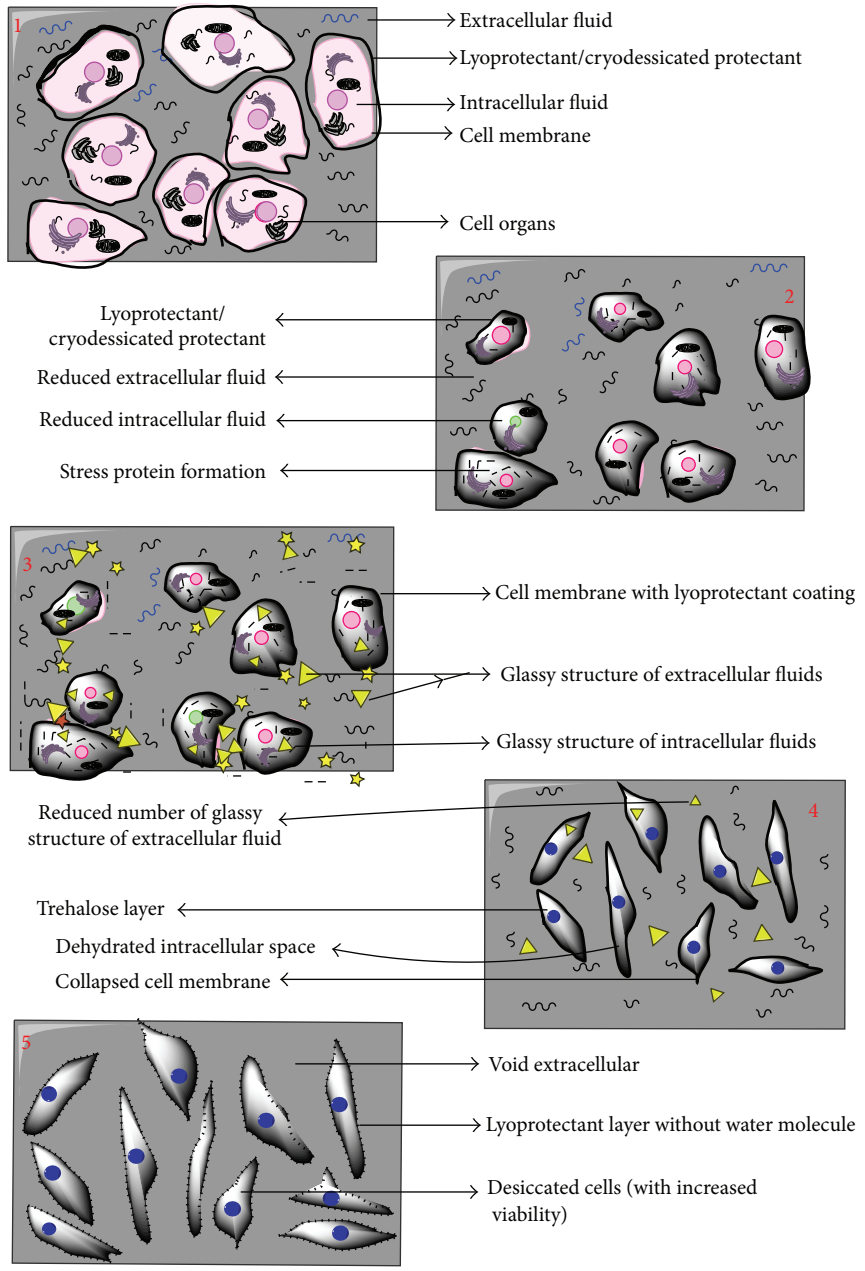

Figure 3: Hypothesized physiological changes being observed in cells following red path for desiccation-lyophilisation phase.

where T_m, Q, R, L, and r_f refer to temperature at the end of the freezing process, activation energy, gas constant, latent heat, and radius of ice when x is equal to 1, respectively. The thickness of transition layer between liquid and solid ("mushy zone") is λ, and n is the kinematic viscosity.

In view of the above thermodynamics describing processes of lyophilisation and desiccation, it has been observed that viability of cell is a vital issue. It results in a requirement of crosstalk between the above two mentioned processes. An approach of crosstalk has also been explained by the three-point thermodynamic diagram. Path defined by red colour as (1→2→3→4→5) is the projected path for the process of desiccation followed by lyophilisation. Sample is at room temperature at point 1; then, it is mildly heated with a gradual decrease in pressure to reach a state of point 2. Point 2 is defined as step-down transition point: slope and intercepts of this point are optimized in order to achieve maximum pressure drop, with minimum increase in temperature and maximum dehydration of the cell. Thus maximum cellular viability can be maintained. Once this state is achieved, the cell mass will be allowed to freezing state while maintaining the temperature to be constant, and point 3 will be reached. Point 3 is a critical point of freezing at low pressure when crystalline state of fluid present in intracellular and extracellular regions will be converted to glassy state. Then, desiccation will be followed by freeze-drying to reach point 4. Since vitrification of cell is done at lower pressure, it might happen that vitrification temperature

will be much higher than −80 degrees centigrade. Therefore, pressure drop required to achieve vapour state from freeze state is much higher, reducing the cost of the combined process. Last step is sample dehydration by rapid temperature increase (up to room temperature) at constant pressure to reach point 5. This entire path of crosstalk is able to ensure two vital aspects of preservation of cells: (i) enhancement of cellular viability and (ii) decreasing lyophilisation (freeze-drying) cost. The scheme of hypothesized processes in the cells undergoing desiccation-lyophilisation in accordance with proposed method is depicted in the following (Figure 3).

Cell preservation using crosstalk technique explained in the previous section can be achieved in a controlled chamber. Rate of dehydration of cell can be monitored continuously by a ultrasonic transducer measuring the humidity in the chamber. Cell viability can be continuously monitored by a droplet based remote microscopic system and real-time processing of obtained images. Output of this image-processing system can be used to control temperature and pressure in the chamber.

10. Conclusion

Enhanced measures of protection are required for successful anhydrobiotic engineering of MSCs since existing protocols are not able to ensure robust cell recovery. Although the lyophilisation and desiccation are found to be efficient in some cases, the limitations of individual methods impart certain rigidity of their implementation. At the same time, maintenance of the dried cells viability in long-term storage is another critical issue which needs to be addressed. Continuous monitoring and control of preservation process can ensure successful MSCs preservation, but optimization for all the physical parameters is also needed.

Competing Interests

The authors declare that there are no competing interests regarding the publication of this paper.

Authors' Contributions

All authors contributed equally in this paper. Akalabya Bissoyi and Awanish Kumar had made equal contribution to this work.

Acknowledgments

The authors are thankful to National Institute of Technology, Raipur (CG), India, for providing facility for this work. This study was supported by Russian Science Foundation grant for international group (14-44-00022) as well as National grant of Department of Science and Technology (YSS/2015/000618) New Delhi, India.

References

[1] A. I. Caplan and S. P. Bruder, "Mesenchymal stem cells: building blocks for molecular medicine in the 21st century," *Trends in Molecular Medicine*, vol. 7, no. 6, pp. 259–264, 2001.

[2] J. S. Park, S. Suryaprakash, Y.-H. Lao, and K. W. Leong, "Engineering mesenchymal stem cells for regenerative medicine and drug delivery," *Methods*, vol. 84, pp. 3–16, 2015.

[3] A. Bissoyi and K. Pramanik, "Role of the apoptosis pathway in cryopreservation-induced cell death in mesenchymal stem cells derived from umbilical cord blood," *Biopreservation and Biobanking*, vol. 12, no. 4, pp. 246–254, 2014.

[4] M. Haack-Sørensen and J. Kastrup, "Cryopreservation and revival of mesenchymal stromal cells," *Methods in Molecular Biology*, vol. 698, pp. 161–174, 2011.

[5] G. R. Nireesha, L. Divya, C. Sowmya et al., "Lyophilization/freeze drying—an review," *International Journal of novel Trends in Pharmaceutical Sciences*, vol. 3, no. 4, pp. 87–98, 2013.

[6] S.-Z. Zhang, H. Qian, Z. Wang et al., "Preliminary study on the freeze-drying of human bone marrow-derived mesenchymal stem cells," *Journal of Zhejiang University: Science B*, vol. 11, no. 11, pp. 889–894, 2010.

[7] J. H. Crowe, "Anhydrobiosis: an unsolved problem," *Plant, Cell and Environment*, vol. 37, no. 7, pp. 1491–1493, 2014.

[8] D. Keilin, "The leeuwenhoek lecture: the problem of anabiosis or latent life: history and current concept," *Proceedings of the Royal Society B: Biological Sciences*, vol. 150, no. 939, pp. 149–191, 1959.

[9] M. Sakurai, T. Furuki, K.-I. Akao et al., "Vitrification is essential for anhydrobiosis in an African chironomid, Polypedilum vanderplanki," *Proceedings of the National Academy of Sciences of the United States of America*, vol. 105, no. 13, pp. 5093–5098, 2008.

[10] O. Gusev, Y. Suetsugu, R. Cornette et al., "Comparative genome sequencing reveals genomic signature of extreme desiccation tolerance in the anhydrobiotic midge," *Nature Communications*, vol. 5, article 4784, 2014.

[11] I. Puhlev, N. Guo, D. R. Brown, and F. Levine, "Desiccation tolerance in human cells," *Cryobiology*, vol. 42, no. 3, pp. 207–217, 2001.

[12] S. G. L. Quaak, J. B. A. G. Haanen, J. H. Beijnen, and B. Nuijen, "Naked plasmid DNA formulation: effect of different disaccharides on stability after lyophilisation," *AAPS PharmSciTech*, vol. 11, no. 1, pp. 344–350, 2010.

[13] M. Sola-Penna and J. Roberto Meyer-Fernandes, "Stabilization against thermal inactivation promoted by sugars on enzyme structure and function: why is trehalose more effective than other sugars?" *Archives of Biochemistry and Biophysics*, vol. 360, no. 1, pp. 10–14, 1998.

[14] A. Lerbret, P. Bordat, F. Affouard, A. Hédoux, Y. Guinet, and M. Descamps, "How do trehalose, maltose, and sucrose influence some structural and dynamical properties of lysozyme? Insight from molecular dynamics simulations," *Journal of Physical Chemistry B*, vol. 111, no. 31, pp. 9410–9420, 2007.

[15] M. Del C Luzardo, F. Amalfa, A. M. Nuñez, S. Díaz, A. C. Biondi De Lopez, and E. A. Disalvo, "Effect of trehalose and sucrose on the hydration and dipole potential of lipid bilayers," *Biophysical Journal*, vol. 78, no. 5, pp. 2452–2458, 2000.

[16] M. B. França, A. D. Panek, and E. C. A. Eleutherio, "Oxidative stress and its effects during dehydration," *Comparative Biochemistry and Physiology—A Molecular and Integrative Physiology*, vol. 146, no. 4, pp. 621–631, 2007.

[17] G. Di, J. Wang, M. Liu, C.-T. Wu, Y. Han, and H. Duan, "Development and evaluation of a trehalose-contained solution formula to preserve hUC-MSCs at 4∘C," *Journal of Cellular Physiology*, vol. 227, no. 3, pp. 879–884, 2012.

[18] O. Gusev, R. Cornette, T. Kikawada, and T. Okuda, "Expression of heat shock protein-coding genes associated with anhydrobiosis in an African chironomid *Polypedilum vanderplanki*," *Cell Stress & Chaperones*, vol. 16, no. 1, pp. 81–90, 2011.

[19] X. Ma, K. Jamil, T. H. MacRae et al., "A small stress protein acts synergistically with trehalose to confer desiccation tolerance on mammalian cells," *Cryobiology*, vol. 51, no. 1, pp. 15–28, 2005.

[20] S. C. Hand, M. A. Menze, M. Toner, L. Boswell, and D. Moore, "LEA proteins during water stress: not just for plants anymore," *Annual Review of Physiology*, vol. 73, no. 1, pp. 115–134, 2011.

[21] R. Hatanaka, Y. Hagiwara-Komoda, T. Furuki et al., "An abundant LEA protein in the anhydrobiotic midge, PvLEA4, acts as a molecular shield by limiting growth of aggregating protein particles," *Insect Biochemistry and Molecular Biology*, vol. 43, no. 11, pp. 1055–1067, 2013.

[22] P. L. Steponkus, M. Uemura, R. A. Joseph, S. J. Gilmour, and M. F. Thomashow, "Mode of action of the COR15a gene on the freezing tolerance of Arabidopsis thaliana," *Proceedings of the National Academy of Sciences of the United States of America*, vol. 95, no. 24, pp. 14570–14575, 1998.

[23] M. J. Wise, "LEAping to conclusions: a computational reanalysis of late embryogenesis abundant proteins and their possible roles," *BMC Bioinformatics*, vol. 4, article 52, 2003.

[24] S. Li, N. Chakraborty, A. Borcar, M. A. Menze, M. Toner, and S. C. Hand, "Late embryogenesis abundant proteins protect human hepatoma cells during acute desiccation," *Proceedings of the National Academy of Sciences of the United States of America*, vol. 109, no. 51, pp. 20859–20864, 2012.

[25] R. Hatanaka, O. Gusev, R. Cornette et al., "Diversity of the expression profiles of late embryogenesis abundant (LEA) protein encoding genes in the anhydrobiotic midge *Polypedilum vanderplanki*," *Planta*, vol. 242, no. 2, pp. 451–459, 2015.

[26] R. Sitaula, A. Fowler, M. Toner, and S. Bhowmick, "A study of the effect of sorbitol on osmotic tolerance during partial desiccation of bovine sperm," *Cryobiology*, vol. 60, no. 3, pp. 331–336, 2010.

[27] S. Mittal and R. V. Devireddy, "Desiccation tolerance of adult stem cells in the presence of trehalose and glycerol," *The Open Biotechnology Journal*, vol. 2, no. 1, pp. 211–218, 2008.

[28] R. Sitaula, H. Elmoazzen, M. Toner, and S. Bhowmick, "Desiccation tolerance in bovine sperm: a study of the effect of intracellular sugars and the supplemental roles of an antioxidant and a chelator," *Cryobiology*, vol. 58, no. 3, pp. 322–330, 2009.

[29] Y. A. Petrenko, O. Y. Rogulska, V. V. Mutsenko, and A. Y. Petrenko, "A sugar pretreatment as a new approach to the Me2SO- and xeno-free cryopreservation of human mesenchymal stromal cells," *Cryo Letters*, vol. 35, no. 3, pp. 239–246, 2014.

[30] K. Jamil, J. H. Crowe, F. Tablin, and A. E. Oliver, "Arbutin enhances recovery and osteogenic differentiation in dried and rehydrated human mesenchymal stem cells," *Cell Preservation Technology*, vol. 3, no. 4, pp. 244–255, 2005.

[31] R. Shirakashi, C. M. Köstner, K. J. Müller, M. Kürschner, U. Zimmermann, and V. L. Sukhorukov, "Intracellular delivery of trehalose into mammalian cells by electropermeabilization," *Journal of Membrane Biology*, vol. 189, no. 1, pp. 45–54, 2002.

[32] N. Guo, I. Puhlev, D. R. Brown, J. Mansbridge, and F. Levine, "Trehalose expression confers desiccation tolerance on human cells," *Nature Biotechnology*, vol. 18, no. 2, pp. 168–171, 2000.

[33] A. Eroglu, M. J. Russo, R. Bieganski et al., "Intracellular trehalose improves the survival of cryopreserved mammalian cells," *Nature Biotechnology*, vol. 18, no. 2, pp. 163–167, 2000.

[34] A. E. Oliver, K. Jamil, J. H. Crowe, and F. Tablin, "Loading human mesenchymal stem cells with trehalose by fluid-phase endocytosis," *Cell Preservation Technology*, vol. 2, no. 1, pp. 35–49, 2004.

[35] G. D. Elliott, X. H. Liu, J. L. Cusick et al., "Trehalose uptake through P2X7 purinergic channels provides dehydration protection," *Cryobiology*, vol. 52, no. 1, pp. 114–127, 2006.

[36] Y. Wei, C. Li, L. Zhang, and X. Xu, "Design of novel cell penetrating peptides for the delivery of trehalose into mammalian cells," *Biochimica et Biophysica Acta (BBA)—Biomembranes*, vol. 1838, no. 7, pp. 1911–1920, 2014.

[37] A. Abazari, L. G. Meimetis, G. Budin, S. S. Bale, R. Weissleder, and M. Toner, "Engineered trehalose permeable to mammalian cells," *PLoS ONE*, vol. 10, no. 6, Article ID e0130323, 2015.

[38] N. Chakraborty, M. A. Menze, H. Elmoazzen et al., "Trehalose transporter from African chironomid larvae improves desiccation tolerance of Chinese hamster ovary cells," *Cryobiology*, vol. 64, no. 2, pp. 91–96, 2012.

[39] A. Eroglu, M. Toner, and T. L. Toth, "Beneficial effect of microinjected trehalose on the cryosurvival of human oocytes," *Fertility and Sterility*, vol. 77, no. 1, pp. 152–158, 2002.

[40] B. Wowk, "Electric and magnetic fields in cryopreservation," *Cryobiology*, vol. 64, no. 3, pp. 301–303, 2012.

[41] S.-Y. Lee, G.-W. Huang, J.-N. Shiung et al., "Magnetic cryopreservation for dental pulp stem cells," *Cells Tissues Organs*, vol. 196, no. 1, pp. 23–33, 2012.

[42] M. E. Yalvaç, M. Ramazanoglu, M. Tekguc et al., "Human tooth germ stem cells preserve neuro-protective effects after long-term cryo-preservation," *Current Neurovascular Research*, vol. 7, no. 1, pp. 49–58, 2010.

[43] M. Potts, S. M. Slaughter, F.-U. Hunneke, J. F. Garst, and R. F. Helm, "Desiccation tolerance of prokaryotes: application of principles to human cells," *Integrative and Comparative Biology*, vol. 45, no. 5, pp. 800–809, 2005.

[44] M. Tang, W. F. Wolkers, J. H. Crowe, and F. Tablin, "Freeze-dried rehydrated human blood platelets regulate intracellular pH," *Transfusion*, vol. 46, no. 6, pp. 1029–1037, 2006.